THE ROLE OF THE TUMOUR MICROENVIRONMENT COMPONENTS IN CANCER CELL BEHAVIOUR AND DRUG RESPONSE.

DIMAKATSO ALICE SENTHEBANE

SNTDIM001

Thesis presented for the degree of

DOCTOR OF PHILOSOPHY

In the division of

Medical Biochemistry and Structural Biology

Department of Integrative Biomedical Sciences in the faculty of Health Sciences at the University of Cape Town

Supervisor: Professor M. Iqbal Parker

Co-supervisor: Doctor Kevin Dzobo

October 2022

DEDICATION

The thesis is dedicated to my late parents, Mapaseka Senthebane and Moses Ndhlovu, for the beautiful foundations they have laid for my education. Also dedicated to my late brother, Thato Senthebane, whose joy for this degree has been my source of strength and motivation during times of discouragement.

I will carry you in my heart forever.

DECLARATION

I, **Dimakatso Alice Senthebane**, hereby declare that the content this thesis is based on my original work, except where acknowledgements indicate otherwise; and that neither the work nor any part has been, is being, or to be submitted for another degree in this or any other University. I am now submitting this thesis for academic examination towards the Degree of Doctor of Philosophy in Medical Biochemistry.

Signature of candidate: DA Senthebane Date: 05/10/2022

ACKNOWLEDGEMENTS

My supervisor Prof Iqbal Parker, thank you for everything you have done for me, for your support, guidance, patience and encouragement. For always for making sure that I have everything I need to complete my research.

My co-supervisor Dr Kevin Dzobo, for your continuous support and mentorship. Your love and passion for science has really inspired me. You were incredibly patient with me, and I learnt a lot from you. Thank you for all of your life advise and for always being there for me when I needed you.

Arielle Rowe, our previous lab technician, for always keeping the lab organized and making our work easier. Thank you.

Lizette Fick, thank you for providing me with the facilities and assistance I needed to conduct immunohistochemistry experiments.

Prof Dhiren Govender, Anatomical pathologist, for performing the histological analyses.

Susan Cooper and Prof Dirk Lang, for your assistance with the fluorescence microscope.

Mr Ronnie for the assistance with flow cytometry analysis. Thank you.

John Iradukunda, for your assistance with the Mass Spectrometry and Proteomics data analysis. Thank you for everything.

A special thank you to Dr Denver Hendricks, for editing my thesis and providing me with scientific advice.

I would like to acknowledge the SAMRC-Bongani Mayosi National Health Scholars Programme and UCT Vice Councillor Research Scholarship, for providing me with financial support.

I would like to say a heartfelt thank you to my parents, Mr Mooketsi and Mrs Nneheng Mogoe, for all the love and support. Thank you for always believing in me and encouraging me to follow my dreams. Without you, I would not have made it this far. Thank you for everything.

My siblings, Junior, Entle, Oabile Mogoe and the rest of my beautiful family, thank you for your continuous love, believing in me and your support.

Dr Mdu Gama and Dr Zanele Ditse, for your excellent mentorship and support. Thank you.

My best friend, Zukiswa Jiki, who walked this journey with me. I cannot appreciate you enough for your love and support. I've always been able to count on you to be there for me. I am really grateful for your friendship.

A special thanks to my friend Dr. Kamo Mamashela for the sleepless nights we spent on the phone during the final months of my thesis write-up. Thank you for your support. You made the journey so much more enjoyable.

My friends, Tsepo Ngwenyama, Katlego Ramahala, Lisa Mahlaba, Tlakale Mogebisa, Mathapelo Chaba, Loyiso Vuko, Siyavuya Fikamva and Liso Tshaka for your words of encouragement and continuous support. You guys are the best. Thank you for everything.

My labmates/friends, Bianca Abrahams, Gabrielja Wilensky, Caryn Rahj, Humaira Lambarey, Jammie Pillaye, Nonku Mkwanazi and Raabieah Gamieldien for making sure that the environment is healthy and friendly to work in. For laughter and moments outside the lab environment. Thank you for your help, advice, and support. You are all amazing.

Above all, I thank God for providing me with the resources and strength I required to complete this PhD. I thank Him for His abundant grace in guiding me through this process. I would not have had the wisdom or physical ability to do so without Him.

TABLE OF CONTENT

LIST OF TABLES

LIST OF FIGURES

ABBREVIATIONS

α-SMA	Smooth Muscle actin-alpha
ºC	Degree Celsius
Ab	Antibody
ABC	ATP Binding Cassette
ALDH1	Aldehyde Dehydrogenase 1
APS	Ammonium Persulphate
ATRA	All-trans Retinoic acid
BCA	Bicinchoninic acid
BMI1	B cell-specific Moloney murine leukaemia virus integration site 1
BMP-4	Bone morphogenic protein 4
BSA	Bovine Serum Albumin
CAFs	Cancer Associated Fibroblasts
CAM-DR	Cell-Adhesion-Mediated Drug Resistance
CAMs	Cancer Associated Microphages
CAR T	Chimeric antigen receptor
cd-ECM	Cancer-derived extracellular matrix
cDNA	Complementary deoxyribonucleic acid
CI	Confidence Interval
CK	Cytokeratin
CNS	Central Nervous System
CSCs	Cancer Stem Cells
C_T	Threshold cycle
DAPI	4',6-diamidino-2-phenylindole
DEPC	Diethylpyrocarbonate
DMEM	Dulbecco's modified Eagle's medium
DMSO	Dimethyl sulfoxide
dNTPs	Deoxynucleotide triphosphates
DTT	Dithiothreitol
ECM	Extracellular Matrix
EDTA	Ethylenediaminetetraacetic acid
EGF	Epidermal Growth Factor

EGFR	Epidermal Growth Factor Receptor
EMA	Epithelial Membrane Antigen
EMT	Epithelial-to-Mesenchymal Transition
EndMT	Endothelial-To-Mesenchymal Transition
EpCAM	Epithelial Cell Adhesion Molecule
ERK	Extracellular signal-regulated kinase
FAP	Fibroblast Activation Protein
FBS	Fetal Bovine Serum
FCS	Foetal Calf Serum
FGF	Fibroblast Growth Factor
FSP	Fibroblast Specific Protein
GAPDH	Glyceraldehyde-3-phosphate dehydrogenase
H&E	Haematoxylin and Eosin
HDACs	Histone deacetylases
HDMs	Histone demethylase
HEPES	4-(2-hydroxyethyl)-1-piperazieenthanesulfonic acid
HER2	Human Epidermal Growth Factor Receptor 2
HIF-1	Hypoxia inducible factor 1
HMTs	Histone Methyltransferase
HNSCC	Head and Neck Squamous Cell Carcinoma
HPV	Human Papilloma Virus
HRP	Horseradish peroxidase
IC_{50}	Antibody concentration able to reduce infection by 50%
IgG	Immunoglobulin G
IL	Interleukin
JAK	Janus Kinase
JNK	c-JUN N-terminal Kinase
KDa	Kilodalton
MAPK	Mitogen Activated Protein Kinase
MDR1	Multi-drug resistance 1
MMP	Matrix Metalloprotease
MSCs	Mesenchymal Stem Cells
MTT	3-(4,5-dimethylthiazol-2-yl)-2,5 diphenyltetrazolium
NFkB	Nuclear Factor kappa B

PBS	Phosphate Buffered Saline
PCR	Polymerase Chain Reaction
PD-1	Programmed Cell Death 1
PDGFR-α	Platelet derived growth factor receptor-alpha
PI	Protease Inhibitor
PTEN	Phosphatase and Tensin Homolog
qRT-PCR	Quantitative Real Time Polymerase Chain Reaction
Rb	Retinoblastoma protein
ROS	Reactive oxygen species
SD	Standard deviation
SDF-1	Stromal derived factor 1
SDS	Sodium Dodecyl Sulfate
SDS-PAGE	Sodium Dodecyl Sulfate Polyacrylamide Gel Electrophoresis
SEM	Standard Error of the mean
siRNA	Selective Inhibitor of Nuclear Export
SP	Side population
STAT	Signal Transducer and Activator of Transcription
TAMs	Tumour Associated Macrophages
TBS	Tris Buffered Saline
TBST	Tris Buffered Saline and Tween 20
TCR	T-cell Receptor
TEMED	Tetramethylethylenediamine
TGF-β	Transforming growth factor-beta
TIMP	Tissue Inhibitor of Metalloproteases
TME	Tumour Microenvironment
VEGF	Vascular Endothelial Growth Factor
WHO	World Health Organisation

ABSTRACT

Introduction

Cancer is a public health burden which continues to cause many deaths and an economic burden worldwide. New and improved ways of thinking about anti-cancer drug design and development are needed now and in future. Recent reports demonstrate the key role played by the tumour microenvironment (TME) in tumour progression and the development of drug resistance. This study investigated the interactions between cancer cells and the stroma within the TME, specifically fibroblasts, mesenchymal stem cells (MSC), cancer stem cells (CSCs) as well as the extracellular matrix (ECM), with the goal to develop an *in vitro* model that mimics solid tumours in terms of cellular characteristics and drug response.

Mesenchymal stem cells were investigated as potential sources of cancer-associated fibroblasts (CAFs) in solid tumours. The expression of CAFs markers, α-SMA and vimentin, increased significantly in MSCs co-cultured with oesophageal and breast cancer cells indicating conversion of MSCs into cell-like CAFs. WHCO1 (oesophageal) and MDA MB 231 (breast) cancer cells co-cultured with MSCs survived paclitaxel and cisplatin treatments better than cancer cells alone. To assess the prognostic value of CSCs, the expression and malignant behaviour of CSC markers were also examined in clinicopathologically-confirmed oesophageal cancer biopsies and *in vitro*. Oesophageal cancer biopsies stained strongly for the cancer stem cell markers, CD44 and ALDH1A1, demonstrating the presence of CSCs in these tumours. FACS-isolated side population cells exhibited high levels of cancer stem cell markers, self-renewal markers and drug resistance proteins and were associated with increased drug resistance versus cancer cells.

In order to measure how ECM proteins affect oesophageal cancer cell response to chemotherapeutic drugs, 3D cell-derived ECMs was used as a model. The analysis of ECM proteins using qRT-PCR in oesophageal cancer biopsies showed that collagens, fibronectin, and laminins were overexpressed in tumour tissue compared with adjacent normal tissues. The culture of cancer cells on decellularised ECMs reduced the effect of drugs on cancer cells compared to those plated on plastic (control). The reduction

of the effects of drugs was associated with significant activation of survival signalling pathways. Knockdown of collagen and fibronectin with siRNA combined with drugs resulted in increased sensitivity of cancer cells to drugs and lower colony formation and cancer cell migration. Lastly, this study utilized multi-cell tumour spheroids (MCTS) from WHCO1 and MDA MB 231 cells co-cultured with WI38 and CT1 fibroblasts to mimic tumour cell-stromal cell interactions as observed within the *in vivo* tumour microenvironment. The data show that spheroids were more resistant to drugs than monolayer cultures of the same cells. MCTS displayed characteristics similar to *in vivo* tumours in terms of response to drugs. Associated with these findings were increased levels of CSCs in MCTS compared to monolayer.

This study demonstrated that MSCs are a possible source of 'CAFs' *in vivo* and can support cancer cell growth. This study also demonstrated the presence of CSCs in tumours and that the targeting of these cells can shrink tumours and prevent potential metastasis and relapse of tumours. This study revealed that ECM proteins play major roles in the response of cancer cells to chemotherapy and suggest that targeting ECM proteins, especially type I collagen and fibronectin, can be an effective therapeutic strategy against chemoresistant tumours. MCTS, as shown in this study, is a valuable tool for the evaluation of the therapeutic effect of drugs. Overall, this study demonstrates the critical role played by the tumour microenvironment in tumour growth and metastasis and provides new insights into cancer treatment.

CHAPTER 1:

LITERATURE REVIEW

1.1 Cancer Burden

Cancer remains one of the largest causes of mortality and morbidity worldwide. Cancer develops when normal cells undergo genetic and epigenetic alterations, resulting in aberrant cell proliferation. There are over a hundred different forms of cancer, each with its own particular behaviour and treatment response [1]. Globally, more people die of cancer than that from HIV/AIDS, tuberculosis, or malaria put together [2, 3]. Significant strides have been recorded in the fight against cancer, with the development of many new chemotherapeutic agents, mainly targeted therapies against many cancers [4]. However, a major hurdle to successful cancer treatment is the development of therapy resistance and metastasis [5, 6]. Cancer cells display great plasticity, adaptive behaviour and tumour heterogeneity, requiring a diversity of treatments. Whilst several therapeutic strategies have been developed to target cancer cells, the main approaches remain those targeting DNA repair mechanisms and the replication machinery [7].

It is possible that over time cancer cells migrate and invade the surrounding tissues and enter circulation and metastasise to distant organs[8, 9]. Mutations in cancer cells to several oncogenes and tumour suppressor genes, including c-Myc, p53, and transforming growth factor- (TGF-), have been shown to play important roles in tumour migration, invasion, and metastasis in a variety of cancers, including oesophageal and breast cancer. [10]. In addition, most oncogenes and tumour suppressor genes also contribute toward therapy resistance [11].

Oesophageal cancer is among the least studied and most deadly types of cancer in the world [12]. Over the last decade, its incidence has been rising in western countries, making it the 7th most common cancer worldwide and the 6th leading cause of death, overall [13]. Squamous cell carcinoma (which occurs in the upper 2/3 of the oesophagus) and adenocarcinoma (which occurs in the lower region of the oesophagus) are the two most common types of oesophageal cancer (Figure 1.1) [14].

It is unclear how the latter develops. According to research, factors such as alcohol consumption, helicobacter poli, smoking, or gastro-oesophageal reflux, which cause inflammation, can promote the development of cancer [14].

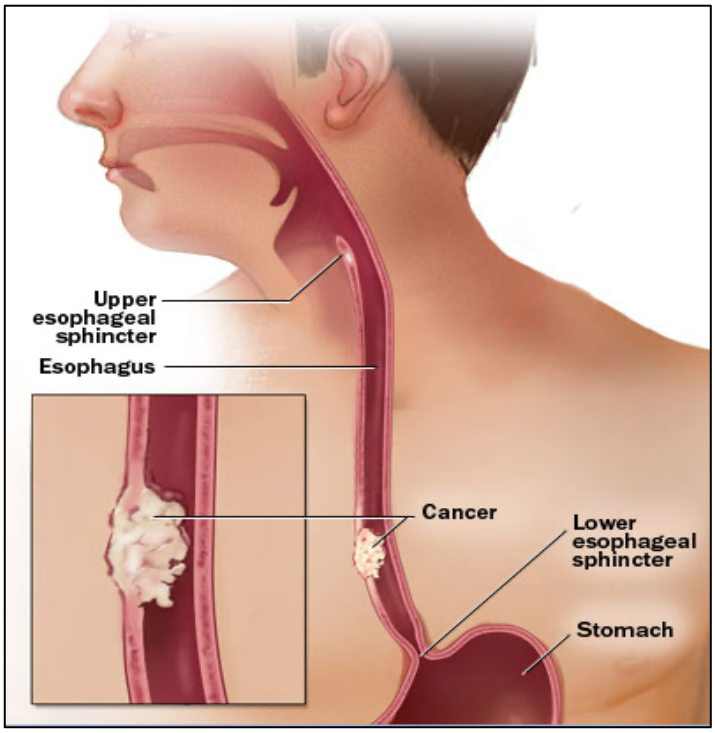

Figure 1. 1. Oesophageal cancer. Oesophageal cancer can be classified according to the type of cells that are involved. Oesophageal squamous cell carcinoma (OSCC) occurs in the upper and middle of the oesophagus. Oesophageal adenocarcinoma (OAC) occurs mainly in the lower third of the oesophagus. (Source: https://www.thocpa.com/specialties/esophageal-cancer/).

Although oesophageal cancer has been better diagnosed and treated, no significant improvements have been made in mortality rates. It is considered one of the most aggressive and refractory cancers with a 5-year survival rate of about 10% [15]. A wide variety of conventional oesophageal cancer treatments are used, and some are successful, however, about half of cases result in a cancer recurrence and patients succumb to the disease.[16]. The cellular and molecular mechanisms underlying the initiation and progression of oesophageal cancer, which is typically detected late, are poorly understood. Several recent studies have suggested that development of therapy-resistant cancer cells, as well as the absence of effective chemotherapy drugs that directly target cancer cells, is a major cause behind post-therapeutic recurrence and metastasis of oesophageal cancer. [17].

1.2 Treatment strategies for cancer

Most cancer patients present late for cancer treatment and current treatment options lead to a low survival rate, making cancer treatment extremely challenging. Cancer treatment depends on several factors including the type of cancer, the primary location of the tumour, metastatic region, patient's medical history, age and health status of the patient. The successful treatment of cancer must aim to prevent repetition of metastasis that might occur in the future and improve the long-term survival chances for the patient. Conventional cancer treatment includes surgery, radiation, and chemotherapy either alone or in combination.

1.2.1 Surgery

Surgery is often and generally the first line of approach for cancer treatment. Surgery involves the removal of tumour and the nearby tissues during an operation. For many cancer types, a biopsy is used as the main diagnostic tool for cancer. It can also be used for staging to determine the size of the tumour and if or where cancer has spread. Surgery is combined with other cancer therapies such as chemotherapy or radiation therapy for many cancer patients. These therapies may be administered before surgery (neoadjuvant) or after surgery (adjuvant). This is to help prevent cancer growth, metastasis and recurrence.

1.2.2 Radiotherapy

Radiotherapy is one of the three routine methods in conventional cancer therapy [27]. Radiotherapy is used when the tumour is localised and has not metastasized to other parts of the body. Although radiotherapy damages both normal cells and cancer cells, normal cells are able to recover from radiation damage faster than cancer cells [18]. It can be applied alone or in combination with other conventional methods such as surgery or chemotherapy to get better results for patients. In recent decades, advanced radiotherapy techniques have been developed, including 3D conformal radiotherapy (3DCRT), which employs computed tomography (CT) imaging to define target volumes, as well as the widespread use of computer-controlled treatment planning [19]. Intensity-modulated radiation therapy (IMRT), a form of high-precision conformal radiation therapy, specifies the intensity of radiation beams by calculating computer-driven optimization to ensure the desired dose distribution [19].

1.2.3 Chemotherapy

Chemotherapeutic drugs interfere with DNA synthesis by inhibiting cellular processes involved in the cell cycle, leading to programmed cell death. Alkylating agents are the first type of chemotherapeutic agents that have been used since the 1940s. Alkylating agents bind directly to DNA and proteins, interfering with replication and transcription and/or resulting in mutations. These agents induce DNA damage in cancers leading to apoptosis [20]. Alkylating agents can act at any point in the cell cycle. A subgroup of alkylating agents called the platinum-containing compounds, include Cisplatin, Carboplatin and Oxaliplatin [21].

Antimetabolites are another type of chemotherapeutic agent. Antimetabolites are classified as folic acid, pyrimidine, and purine analogues based on their structure and function. Antimetabolites interfere with DNA and RNA synthesis during the S phase of the cell cycle by acting as false metabolites that are incorporated into newly synthesised DNA and RNA or inhibit enzymes required for nucleic acid production. Methotrexate, 5-Fluorouracil, and Cytosine Arabinoside are some examples of antimetabolites [22]. Chemotherapeutic agents can be used in combination with other cancer treatments, such as surgery and radiation therapy. Cancer patients can be treated with different drugs simultaneously, where these drugs differ in their mechanism of action.

Taxanes are derived from naturally occurring chemicals found in the yew tree's bark and have been shown to have potent cytotoxic effects on a variety of tumour types [23, 24]. The classic mechanism of action underlying taxanes' antitumour activity has been attributed to their inherent ability to bind and stabilize the microtubules [24, 25]. As a result of taxane binding to β-tubulin, the microtubule assembly is promoted [24, 25] and this causes cell mitosis to be blocked, leading to apoptosis. Paclitaxel, docetaxel and cabazitaxel are example of taxane anticancer drugs that have been successfully used in chemotherapy for a variety of cancers [26].

Vinca alkaloids are naturally derived molecules found in the leaves of the Madagascar periwinkle Catharanthus roseus [27] and include vincristine, vinblastine, and vinorelbine. Vinca alkaloids are antimicrotubule agents, similar to taxanes, but instead of stabilizing the structure they bind to the β-tubulin subunit, preventing the molecule's

structure from being straightened, blocking the polymerization of the molecule with microtubular α-tubulin [25]. The vinca alkaloids have been generally included in combination chemotherapy regimens for medicinal treatment agents for testicular carcinoma and both Hodgkin and non-Hodgkin lymphomas [28].

1.2.4 New anti-cancer strategies

As a result of the sequencing of the human genome and advancements in genetic technology, we know more about cancer's genetic changes, initiation and proliferation, as well as therapeutic mechanisms and new treatment targets [29]. The core of modern medicine's approach to cancer therapy is understanding the pathophysiology of the disease, human genes, and discovering new molecular targets. Development of targeted therapies is one of the most promising cancer therapy strategies. By focusing on cancer cells, these targeted therapies cause less harm to healthy cells than conventional therapies [30]. As with chemotherapeutic drugs, these therapy agents are expected to target cell cycle, oncogenic pathways, and metastatic cells, but they are expected to kill only malignant cells and not normal ones [31].

The process of angiogenesis allows cancer cells to develop new blood vessels for growth. Various angiogenic factors are released during blood vessel formation, causing endothelial cells to proliferate, migrate, and invade in new vascular structures [32, 33]. Vascular endothelial growth factor (VEGF), basic fibroblast growth factor (bFGF), platelet-derived growth factor (PDGF), transforming growth factor (TGF), insulin-like growth factor and angiopoietin are examples of well-known pro-angiogenic factors that mediate the angiogenic switch [32, 34]. The development of anti-angiogenic therapies has recently mostly concentrated on inhibiting the activities of its receptors, including VEGF, FGF, PDGF, and TGF receptors [35].

Growth factors and their receptors are abundant in human tumours. One of the most commonly studied receptor families is the epithelial growth factor receptor (EGFR) [31]. A mutation in the EGFR gene can cause it to grow excessively, which can lead to cancer [36]. Gefitinib and erlotinib are EGFR inhibitors that can inhibit the signal EGFR that activates cells to grow rapidly [31, 37]. Targeting immune system properties provides a method for increasing the selectivity of anticancer treatment. There is a noticeable value to trastuzumab in patients with HER2-positive metastatic breast

cancer [38]. This humanised monoclonal antibody targets the HER-2 gene and stimulates the immune system, inhibiting the physiological activity of the HER2-signaling network [31]. It is known that breast cancers with an amplification of the HER-2 gene are more aggressive and have a worse prognosis [39].

A different approach to immunotherapy is adoption cell transfer (ACT) that involves isolating T-cells (T-lymphocytes) with the best anticancer activity, expanding them *ex vivo*, and rehydrating them. The development of genetically modified T cells through ACT, such as chimeric antigen receptor (CAR)-T, has made substantial progress in treating malignant tumours [40]. CAR-T cell therapy recognizes specific antigens expressed on cancer cells' surfaces using antibody fragments [40]. There are various methods for genetically modifying T-cells, including viral transduction, non-viral methods such as DNA-based transposons, CRISPR/Cas9, or other methods that transfer DNA or mRNA to the cells [41]. There has been evidence that CAR T-cell therapy for end-stage acute lymphocytic leukaemia patients led to a full recovery in up to 92% of patients [42].

Defective apoptotic cell death is a major barrier to effective treatment. A member of the BCL-2 family of proteins is responsible for regulating programmed cell death [43]. The pro-apoptotic members, Bak and Bax, effectively dissipate mitochondrial membrane potential when activated, allowing cytochrome release and activating caspases, which eventually leads to cell death [44]. Bcl-xl and Bcl-2, anti-apoptotic family members, bind to Bak and Bax and inhibit their activation [44]. New therapeutics have been developed that directly activate the apoptosis process, referred to as BH3-mimetics [43, 44]. Apoptosis in cancer cells is activated by BH3-mimetics that bind and inhibit BCL-2 family members that promote survival [44, 45]. ABT-737 is an experimental anticancer agent that works via this mechanism [45]. Co-administration of ABT-737 with doxorubicin, gemcitabine, and cisplatin results in a synergetic effect in dedifferentiated thyroid carcinoma cells of different histology origins [46].

1.3 Chemoresistance

The majority of cancer patients present in the late stages of the disease, when cancer has already evolved and progressed to an advanced stage with metastatic capabilities, is usually very aggressive, and does not respond to commonly prescribed radio and chemotherapeutic agents.

The treatment of oesophageal cancer by chemotherapy involves destroying or killing abnormally dividing cells by using various drugs. Through inducing apoptosis and inhibiting the progression of the cell cycle, these drugs kill cancer cells [47]. Despite this, cancer cells are able to acquire numerous strategies to compromise the efficacy of many therapeutic agents, resulting in chemoresistance [48]. Chemoresistance has been demonstrated to be mediated by a number of mechanisms, as shown in Figure 1.2. Enhancement of survival signalling pathways, inactivation of drugs, reduced uptake of drugs, DNA repair and inhibition of apoptosis are some examples [49]. Furthermore, recent studies have revealed that the tumour microenvironment contribute to resistance of drugs [48].

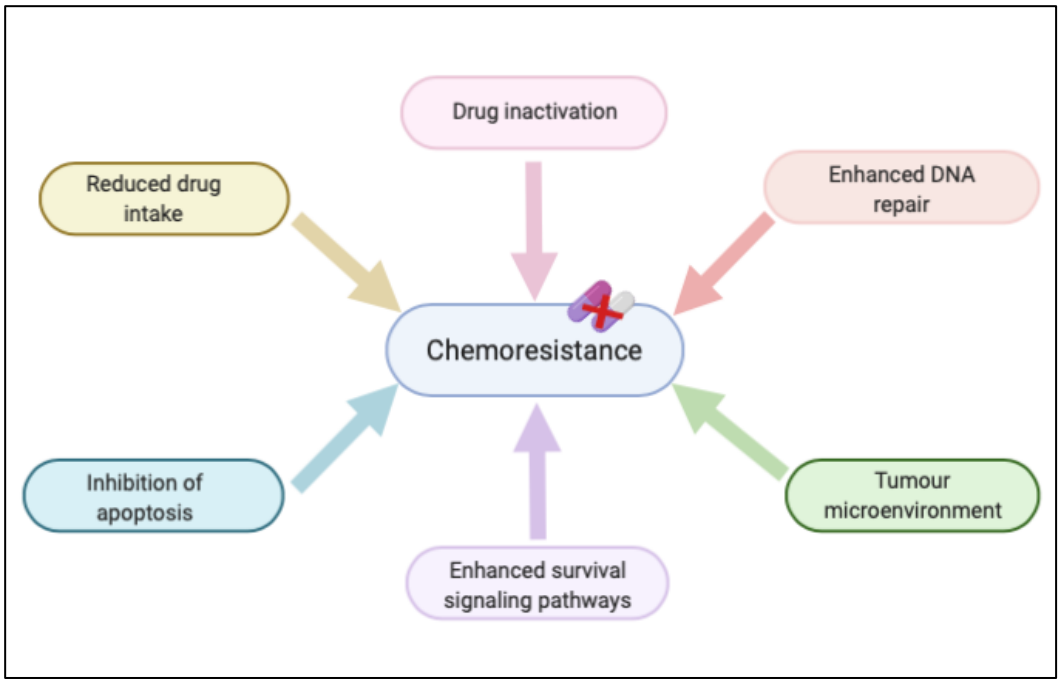

Figure 1. 2. A schematic diagram of the mechanisms involved in chemoresistance. Many signalling pathways that contribute to cell proliferation and cell survival are altered in cancer cells. By activated DNA repair pathways, these alterations contribute to drug resistance by increasing the expression of nuclear antiapoptotic and proliferation genes during the cell cycle. Due to their ability to increase efflux and inactivation of drugs, cancer cells have also been observed as being resistant to chemotherapy.

Many drug discovery assays are conducted using *in vitro* models that do not mimic the tumour microenvironment found *in vivo*. Our understanding of tumour behaviour in 3D environments is limited by lack of good *in vitro* models. Within the tumour microenvironment, immune cells, stromal cells and extracellular matrix form a dynamic biological repertoire. In many cases, this results in drug candidates being

misinterpreted as effective. To avoid such circumstances, drug candidates should be tested *in vitro* on models that mimic the in vivo tumour microenvironment.

1.4 The Tumour Microenvironment

In cancer patients, the tumour microenvironment (TME) is an important determinant in the proliferation and metastasis of cancer cells, as well as the effectiveness of anti-cancer drugs [50, 51]. There several stromal components in the TME such as endothelial cells, lymphocytes, macrophages, fibroblasts, mesenchymal stem cells (MSCs) cancer stem cells (CSCs), as well as the extracellular matrix (ECM) (Figure 1.3).

Resistance to anticancer drugs and apoptotic pathways can be influenced by the mechanics of interaction between stromal cells and tumour cells. This interaction involves growth factors, cytokines, and ECM. Hypoxia in the TME is associated to the activation of genes involved in cancer cell survival and angiogenesis, as well as chemoresistance in many cancer cells, because many chemotherapy agents generate free radicals that damage DNA in the presence of oxygen [52]. Hypoxia can cause drug resistance by increasing the expression of genes encoding P-glycoproteins, which are involved in drug inactivation [53]. Furthermore, the cytotoxicity of anticancer drugs can be influenced by the pH of the tumour microenvironment and many chemotherapeutic drugs can be inhibited by an acidic microenvironment. [54]. The distribution of many anticancer medications is influenced by the pressure gradient inside the microenvironment.

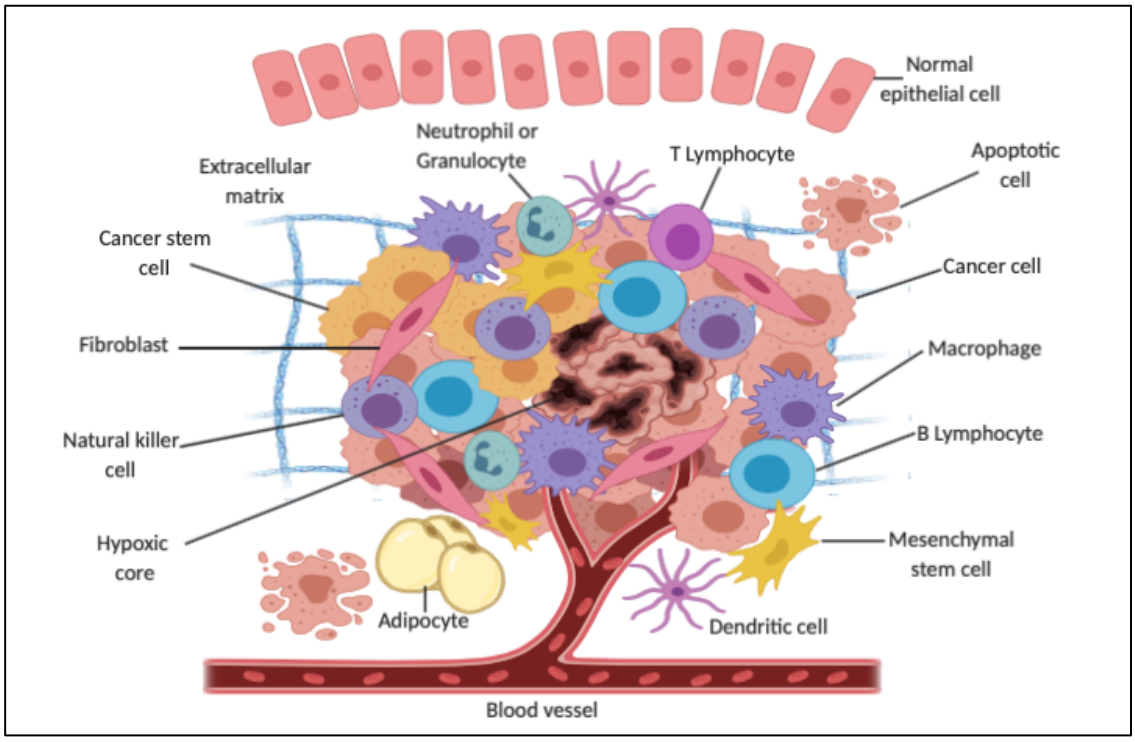

Figure 1. 3. The components of the tumour microenvironment. There several stromal components in the TME such as endothelial cells, lymphocytes, macrophages, fibroblasts, mesenchymal stem cells (MSCs) cancer stem cells (CSCs), as well as the extracellular matrix (ECM). Image created using Biorender (https://biorender.com/).

1.4.1 Cancer-associated Fibroblasts in the Tumour Microenvironment

One of the landmark publications by Virchow described fibroblasts as cells with a spindle shape and responsible for the synthesis of ECM proteins such as collagen [55]. Several other reports also show that fibroblasts are the dominant cells within the TME and can undergo transformation under conditions such as inflammation, fibrosis and wound healing [56]. Inflammation and fibrosis are major processes linked with cancer initiation and development, making fibroblasts critical players during these processes [57, 58].

Normal fibroblasts in a tumour mass can become activated over time and are therefore referred to as cancer-associated fibroblasts (CAFs) or tumour-associated fibroblasts (TAFs) (Figure 1.4) [56]. In the early stages of cancer formation, fibroblasts can be anti-tumourigenic, however, when activated to CAFs, these cells become pro-tumourigenic through several mechanisms that are not yet fully understood [59]. CAFs will eventually dominate the stromal cells within the TME and contribute to tumour progression by releasing various growth factors as well as synthesising the ECM. [60].

The source of CAFs is still clouded with controversy, with many reports showing that several stromal cells can become CAFs. The transformation of stromal cells leads to the formation of large spindle-shaped cells that display increased stress fibres and enhanced cellular-ECM connections [61]. In some cases, CAFs show similar characteristics to normal fibroblasts, with the exception that CAFs have increased ribosomes and rough endoplasmic reticulum (rER) [61]. Some of the markers used in the characterisation of CAFs include α-smooth muscle actin (α-SMA), vimentin and desmin [62]. Other significant differences between normal fibroblasts and CAFs include increased proliferation rate, migratory behaviour and ECM synthesis in CAFs [63]. In addition, the activities of CAFs within the TME result in remodelling of the TME, a process sometimes referred to as desmoplasia, associated with fibrosis and the stiffening of tissue [64].

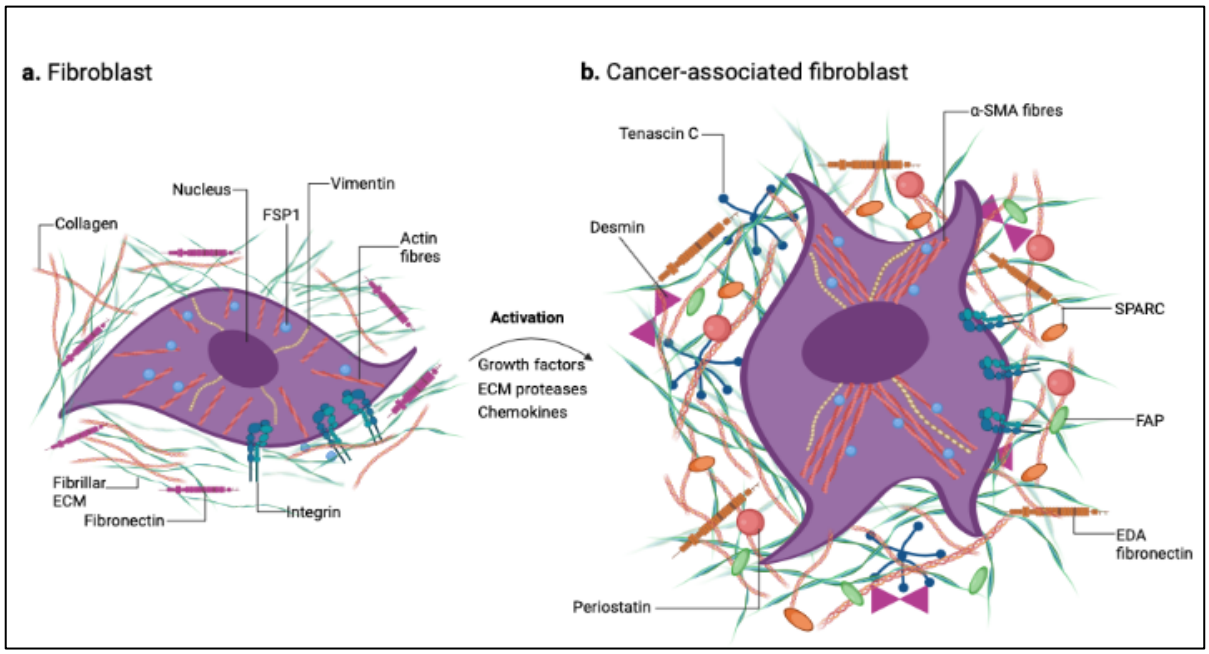

Figure 1. 4. A diagram of a normal and activated fibroblast. **(A)** Normal fibroblasts are the most common types of cells embedded within the ECM and are responsible for the synthesis of collagens and fibrillar proteins. Fibroblasts maintain tissue homeostasis and interact with the surrounding the microenvironment through integrins. Various growth factors such as TGF- β, PDGF and FGF, chemokines and ECM proteases mediate the activation of fibroblasts. **(B)** Once activated, fibroblasts undergo a phenotype change and become cancer-associated fibroblasts (CAFs) expressing several markers such as FSP1, periostin and α-SMA. The activated phenotype is also associated with enhanced proliferative activity and increased secretion of ECM proteins such as collagen I, fibronectin with the different domain an (EDA-fibronectin), tenascin C and SPARC (secreted protein acidic and rich in cysteine). Image created using Biorender (https://biorender.com/).

CAFs and desmoplasia are linked with cancer initiation and relapse and may contribute to cancer progression and resistance to therapy [65]. TME remodelling is linked with the presence of CAFs and other stromal cells such as cancer-associated

macrophages and endothelial cells [66]. CAFs create and maintain the TME as well as remodelling the ECM, whereas remodelling is also required for both generating and maintaining CAFs [66]. The equilibrium that exists between ECM synthesis and degradation is distorted by CAFs, with increased synthesis of ECM. High ECM proteins have been shown to block immune cells from infiltrating into the tumour, thus limiting an immune response to tumours [67]. The ECM provides an ideal environment for cancer cell-stromal-ECM interactions and allows angiogenesis [67].

CAFs also promote angiogenesis through the release of enzymes such as MMPs. MMPs are involved in remodelling the TME via degradation of the ECM, releasing the VEGF-A sequestered by the ECM during this process [68]. VEGF-A is known to promote vascularisation, which the growing tumour needs to exchange nutrients and toxic substances[68]. Many growth factors and cytokines are also released by CAFs, which regulate inflammation and promote tumour cell immune evasion [69]. A better knowledge of the source of CAFs and their role in the TME will result in the development of novel and better anti-cancer strategies [70, 71].

Many reports have suggested that CAFs may originate from stromal cells such as macrophages, endothelial cells and mesenchymal stem cells [56, 72]. It is not surprising, therefore, that CAFs demonstrate significant heterogeneity within the TME. Normal fibroblasts have been shown to be activated within the vicinity of the cancer cells, whilst other stromal cells, including MSC and macrophages, either infiltrate into the tumour or are recruited to the tumour. Other sources of CAFs include pericytes undergoing transdifferentiation, epithelial cells via the process of epithelial-mesenchymal transition (EMT) and endothelial cells through the process called endothelial to mesenchymal transition (EndMT) [73]. For example, fibrocytes from the bone marrow can be recruited via the circulation to the tumour and eventually transform into CAFs [74]. Other reports link MSCs to CAFs in several cancers [75]. For example, the presence of osteopontin has been shown to mediate TGF-β dependent transformation of MSCs into CAFs in breast cancer [76].

Furthermore, local and recruited MSCs can interact with cancer cells leading to their transformation into CAFs. In addition, liver and pancreatic stellate cells have also been shown to be activated and transform into CAFs [73, 77]. Increased ECM synthesis leading to fibrosis are shown to activate and transform epithelial cells within the vicinity

of cancer cells into CAFs [78]. Thus, epithelial cancers can also contain increased levels of CAFs that drive tumour progression. Endothelial cells have also been shown to become activated into CAFs through EndMT [79]. Due to their different potential sources, there are no universal markers for CAFs [78, 79].

Other stromal cells, including adipocytes and pericytes, undergo a transdifferentiation process leading to the formation of CAFs [80]. Thus, most cells localised near a growing tumour and those recruited to tumour sites can be transformed into pro-tumourigenic cells, including CAFs. The accurate picture of the involvement of stromal cells and the ECM in tumour initiation and progression is just beginning to become apparent, with a lot still to be revealed. In addition, detailed mechanisms involved in tumour formation and therapy resistance are also still emerging.

As a result, it is not surprising that CAFs are highly heterogeneous, with various subsets demonstrating diverse phenotypes and roles within the TME, and CAF heterogeneity varying depending on the stage of tumour formation and progression [81]. CAFs demonstrate DNA alterations, increased ROS generation and the presence of hypoxia, leading to CAFs evolving with cancer cells during tumour growth [59]. The ECM present within the TME also evolves over time as the cellular component of the TME changes. Therefore, the ECM within a growing tumour is synthesised by both stromal cells and cancer cells and is pro-tumourigenic compared to normal ECM [82].

Recent research on the presence of molecular and functional CAF heterogeneity in pancreatic ductal adenocarcinoma (PDAC) has uncovered three subtypes of CAFs. In There were two distinct CAF subtypes in PDAC, characterized by either myofibroblastic or inflammatory phenotypes involving transforming growth factor (TGF)-β and IL-1/1JAK-STAT signalling [83]. The myofibroblastic CAFs (myCAFs), located adjacent to the cancer cells and demonstrating high levels of α-SMA expression and low levels of inflammatory mediators [84]. They also described another subtype of CAFs as inflammatory CAFs (iCAFs), located more distantly from cancer cells, which have low expression of α-SMA and high expression of inflammatory mediators, such as interleukin-6 (IL-6) [84]. Additionally, a new population of CAFs, which express major histocompatibility complex (MHC) class II and CD74, allowing antigen-dependent T-cell receptor ligation in CD4+ T cells [85].

It is well established that distinct CAF subtypes can interconvert during cancer development, however, it is unclear how this occurs and which CAF subtype is associated with prognosis and therapeutic sensitivity. It has been reported that iCAFs in pancreatic cancer cells can transform into myCAFs when TGF-β signalling is activated or IL-1-induced JAK/STAT signalling is inhibited [86]. This indicates that both of these subtypes of cells are plastic. Additionally, the response of fibroblasts and the α-SMA promoter to extracellular cues, including substrate stiffness, suggests that the α-SMA-high, matrix-producing-high state can be reversed [87]. In order to improve our understanding of CAF plasticity, in-depth research on CAF subtypes is required.

1.4.1.1 Cancer-associated fibroblast markers

Subsets of different CAFs have been identified within the TME. These can be spatially distributed throughout the tumour, with distinct markers such as α-SMA, fibroblast activation protein-alpha (FAP) and PDGF receptor-β (PDGFR-β) expressed by subsets of CAFs [60]. Thus, two or more markers are usually used in CAF characterisation.

Several markers are used to identify CAFs, and one of the best-known markers is α-SMA, a marker also used to characterised of other cells such as smooth muscle cells and pericytes [59]. Cancers such as breast, pancreatic and liver cancers contain CAFs expressing enhanced levels of α-SMA [77]. Unfortunately, several other cells also express this marker, complicating its use in the characterisation of CAFs. α-SMA is involved in the maintenance of cell structure as well as in cell migration and contraction. Vimentin is another CAF marker that is highly upregulated in CAFs, for example, in breast and prostate cancers [88]. Some of the known functions of vimentin include promoting cellular migration and maintaining cellular integrity [89]. Another marker used in CAF characterisation is desmin which has been shown to be downregulated in CAFs [90].

Caveolin-1 (Cav-1) is a scaffold and structural protein involved in caveolae formation in cellular membranes. It is expressed throughout the body, with endothelial, epithelial, adipocyte, fibroblast, and CAF cells exhibiting the highest levels of Cav-1 [91]. It has been reported that high expression of Cav-1 facilitates tumourigenesis by inhibiting apoptosis, facilitating anchorage-independent growth, drug resistance, as well as facilitating metastasis [91]. In addition, clinical studies have shown that tumour

prognosis is poor when caveolin-1 is downregulated on stromal CAFs [92]. A decrease in Cav-1 protein expression in CAFs is associated with poor clinical outcomes, metastases, and tumour recurrence in breast cancer [93]. Other CAF markers that have been used recently include CD10 and G-protein-coupled receptor 77 (GPR77). These two markers are highly expressed in CAFs and promote cellular stemness and breast cancer chemoresistance [94]. A hindrance to the use of CD10 and GPR77 is the expression of these markers in other stromal cells and neutrophils [94].

Another marker used in CAF characterisation is a fibroblast-specific protein (FSP) or S100A4. FSP has been found to be expressed in fibroblasts and, through its serine protease activity, can remodel the TME [95]. Fibroblasts that express FSP also have the ability to synthesise large quantities of ECM and thus can hinder drugs from reaching cancer cells, contributing to chemoresistance. FSP-expressing stromal cells have been found to be highly malignant [96]. FSP is expressed both in cancer cells and CAFs in breast cancers [97]. Another marker expressed by CAFs is PDGFR-β [98]. A crucial role for PDGFR-β signalling is the activation of CAFs, which promote breast cancer growth and progression [99]. It has been shown that colorectal cancer cells can acquire PDGFR-β during EMT, and the activation of this receptor contributes to their ability to metastasise [100].

In conclusion, CAFs display significant heterogeneity with different cellular origins as well as many functions in tumours. One hindrance to the utilisation of CAFs in cancer treatment is the lack of reliable markers for CAFs that can be used in therapeutic targeting. Recent data demonstrates that the presence of CAF subsets increase the challenge encountered [59, 101]. Overall, regardless of origin and location within a tumour, CAFs are an important cell type in tumours, and markers must be found to identify and target these cells during cancer diagnosis and treatment.

1.4.1.2 Cancer-associated fibroblasts and Carcinogenesis

Several studies have demonstrated the critical role of TME in tumour progression and metastasis [67]. Most TME components start as anti-tumourigenic but with time become pro-tumourigenic via the synthesis and release of growth factors and deposition of excessive ECM [72, 82]. Normal stromal cells, including normal fibroblasts, display anti-tumourigenic behaviour on cancer cell growth *in vitro* [102].

PTEN expression by stromal cells plays a significant role in this inhibitory effect, especially on epithelial tumours [103]. Some of the known growth factors and cytokines released by stromal cells include VEGF, SDF-1, TGF-β and IL-6, which are involved in the remodelling of the TME [72]. Furthermore, hypoxia and the generation of ROS are also known to play a part in transforming of normal cells into pro-tumourigenic cells [104]. CAFs, for example, impact cancer cell proliferation, angiogenesis inflammation, migration, invasion, chemoresistance and immune evasion by releasing many growth factors and cytokines (Figure 1.5) [105].

Normal stromal cells can be induced to synthesise and release growth factors and other inflammatory proteins by cancer cells [106]. In addition, the hypoxic conditions present in tumours result in the generation of increased levels of ROS. Indeed, ROS generation has been shown to induce the release of hypoxia-inducible factor 1-α (HIF1-α) and CXC-chemokine ligand 12 by several stromal cells, leading to increased metabolic activity and migration [107]. Another important cytokine released by CAFs is IL-6, which activates the JAK-STAT signalling [108]. The activation of JAK-STAT signalling in CAFs can promote cancer cell invasive behaviour besides the JAK-STAT signalling cascade being important in maintaining the CAF phenotype [109].

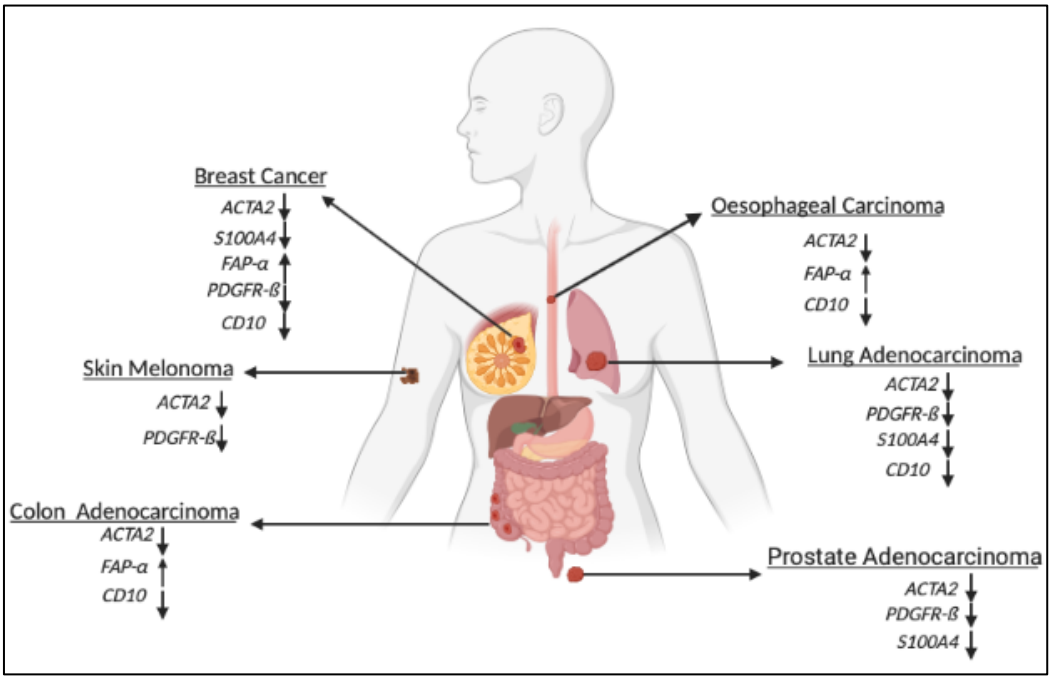

Figure 1. 5. Summary of differential CAF marker expression in different cancers. In several primary tumours, CAFs (heterogeneous cellular population) express several markers such as ACTA2, FAP, CD10, PDGFR-β and S100A4.

Several pieces of evidence demonstrate the symbiotic relationship between CAFs and cancer cells. CAFs express and release large amounts of TGF-β, and cancer cells respond to the TGF-β released by the CAFs [110]. CAFs are also responsible for synthesising and releasing increased amounts of MMPs and urokinase-type plasminogen activator (uPA) [111, 112]. MMPs released by CAFs influence the amount of ECM proteins present in a tumour, thus affecting cancer cell migration and invasion into the surrounding tissues. For example, increased amounts of collagen levels within the TME are associated with cancer cell invasiveness [113].

The degradation of ECM proteins by CAF-derived MMPs can also create the space needed by tumour cells to burrow through and invade new tissues and organs [71, 82]. Tumour growth and invasion require that new blood vessels be synthesised to sustain tumour growth with all the required nutrients and the removal of toxic substances [114]. As CAFs synthesise increased amounts of ECM proteins, they also impact ECM stiffness, influencing blood vessels and the flow of blood [82, 115]. Furthermore, the equilibrium between the expression of anti-angiogenic factors and pro-angiogenic factors determines the formation of blood vessels and, ultimately, tumour growth [116, 117]. Pro-angiogenic factors are upregulated during tumour formation resulting in dysregulated blood vessel formation [118]. CAFs, leukocytes, and macrophages are the major sources of pro-angiogenic factors, including VEGFA, PDGFC, FGF2, osteopontin and MMPs [119, 120].

1.4.1.3 Cancer-associated fibroblasts and Therapy Resistance

Cancer cells can be drug-resistant through several mechanisms. One of the mechanisms is intrinsic, mediated via the expression of several proteins, especially the transporter proteins, including the ABC proteins. In addition, genetic alterations can also impact drug uptake and export. Another mechanism is the evolution of cancer cells resulting in previously responsive tumours becoming unresponsive. The TME has emerged as a contributor to therapy resistance. The interaction between cancer cells, stromal cells, and the ECM is critical in the development of chemoresistance. CAFs have received increased attention as the dominant stromal cells within the TME. CAFs' increased synthesis of ECM proteins can prevent drugs from reaching cancer cells. High ECM proteins surrounding cancer cells can also limit blood vessels formation within the tumour [121].

Whilst limitation of blood vessel formation might appear anti-tumourigenic, high concentrations of drugs will not be able to reach cancer cells that are on the inside of the tumour mass. In addition, CAFs can bind to fibronectin in a process referred to as cell-adhesion-mediated drug resistance (CAM-DR), that has been implicated in drug resistance [122]. The versatile IL-6 cytokine has been implicated in resistance to chemotherapy in lung cancer [123]. Besides cancer cells being resistant to therapy, CAFs have demonstrated their ability to resist drugs such as gemcitabine in pancreatic cancer [124]. Cancer treatment itself has been shown to result in the transformation of cancer cells and stromal cells into therapy-resistant cells. For example, chemotherapy can cause DNA damage in stromal cells, causing the release of factors known to promote cancer cell survival [125]. Chemotherapy can also induce normal fibroblasts into CAF-like cells, and radiotherapy can induce ECM protein synthesis, causing increased survival of cancer cells [126, 127].

1.4.2.1 Mesenchymal stem cells in the Tumour Microenvironment

Mesenchymal stem cells (MSCs) are multipotent stromal stem cells with the ability to self-renew and differentiate into many cell lineages, including adipocytes, chondrocytes and osteoblasts [128]. MSCs are characterized by their expression of stromal cell markers CD73, CD105 and CD90 [129]. Studies have revealed that MSCs play a role in both tumourigenesis, metastasis and recurrence of tumours [130, 131]. They also play special roles as a resident component in the tumour microenvironment by developing into adult mesenchymal cells to support tumour parts. Moreover, several studies have demonstrated that MSCs can enhance the ability of tumour cells to metastasise by enhancing motility and invasiveness as well as creating metastatic niches within secondary tumour sites [132]. MSCs are recruited to injured areas or hypoxic tumour microenvironments [133]. During cancer progression, tumour cells secrete a variety of growth factors, cytokines, and chemokines such as interleukin 1 beta (IL1β), transforming growth factor-beta (TGF-β) and stromal cell-derived factor 1 alpha (SDF1α) [134, 135].These factors play crucial roles in recruiting MSCs to tumours, amd this is related to the enhancement of neoplastic properties in tumours cells [133]. In various cancer types, MSCs have been linked to tumour growth and progression, as well as aiding cancer spread by stimulating the epithelial to

mesenchymal transition (EMT)[136, 137]. The chemokine (C-C motif) ligand 5 (CCL5) released by MSCs, for example, was demonstrated to increase the invasion, migration, and metastasis of breast cancer cells [138].

MSCs undergo considerable phenotypic changes during differentiation, including morphological elongation, reduced adhesion, reduced cytoskeletal fibres, and increased migration [139]. The precise mechanisms underlying MSC to CAF differentiation have not yet been determined. However, there is emerging evidence that tumour-secreted factors promote MSCs differentiation into CAF phenotype by activating TGF-β /Smad signalling [140]. TGF-expression has been demonstrated to improve MSC differentiation into CAFs by increasing alpha-smooth muscle actin (-SMA) expression while decreasing gelsolin expression [141]. MSCs treated with tumour-conditioned medium increased the expression of CAF-associated genes and myofibroblast lineage markers, such as SMA, vimentin, and FSP1 [142]. Taken together, MSCs are affected by tumour-promoting factors secreted by tumour cells in the tumour stroma.

MSCs' multilineage potential provides a favourable milieu for tumour cells and increases the release of growth-promoting substances. MSCs enhanced the self-renewal ability of breast cancer stem cells by modulating cytokine networks that include C-X-C ligand 7 (CXCL7) and IL6 [143]. It has been shown that secreted of IL-6 by MSCs enhances sphere formation and tumour initiation in lung cancer cells by activating JAK2/STAT3 pathways [130]. Through levels of bone morphogenetic signalling, cancer associated MSCs (CA-MSCs) increase tumour cell proliferation and grow tumours [144]. In addition, activation of the WNT and TGF-β pathways in both cancer and stromal cells increased the number of CSCs in gastric cancer [131]. These results show MSCs support cancer cells progression by regulating the TME.

1.4.3 Cancer Stem Cells in the Tumour Microenvironment

Great strides have been made regarding cancer patient outcomes via the provision of improved therapies and the use of combinatorial treatment. However, many obstacles remain, including developing therapy resistance in general and chemoresistance in particular [72, 145]. Chemoresistance usually results in relapse and development of

metastatic disease [72, 82, 146]. One of the central heterogeneity of human malignancies is the presence of cancer stem cells (CSCs), a rare population of slow-cycling cells with the abilities of self-renewal, pluripotency, and chemo-resistance. [147, 148].

There are two hypotheses that have been proposed to explain the tumour heterogeneity seen in solid tumours: the ‘clonal evolution model’ and the ‘cancer stem cell hypothesis’. The first model is the clonal evolution model in 1967, which suggests that the majority of cancers are the result mutational acquisition that promotes clonal expansion and diversification [149]. According to this theory, cancer is an evolutionary process mediated by multiple stepwise mutations that happen in somatic cells, which are followed by natural selection that favours clones with the best phenotypic characteristics [145, 149]. In the CSC hypothesis, CSCs are a rare population of cells with stem cell-like properties that have the ability to self-renew and the capacity to give rise to non-CSC within the tumour mass [150]. Thus, CSCs can give rise to a primary tumour and form new tumours at distant sites [151]. The CSCs that escape the primary tumour site and start new tumours at distant sites, therefore, act as ‘seeds’ for the growth of secondary tumours [151].

CSCs demonstrate an incredible ability to withstand the harsh conditions when circulating through the body through various means, including increased expression of ABC transmembrane transporters and other detoxifying enzymes [152]. However, CSCs have been shown to resist therapy, including chemotherapy and radiotherapy, due to the increased expression of ABC drug transporters, quiescence and an efficient DNA repair mechanism [145]. Thus, to succeed in cancer treatment and overcome therapy resistance, novel strategies must be developed to target CSCs [153].

CSCs are also called tumour-initiating cells (TICs) due to their ability to form new tumours at new sites [154]. The discovery of CSCs in acute myeloid leukemia (AML) in 1994 has led to the possibility of the isolation of similar tissue-specific CSCs and progenitor cells from other tumours [154]. CSCs are present in many cancers, such as colon, lung and breast cancers. The use of Hoechst dye to obtain side population cells, antibody-based isolation, tumoursphere development, and ALDH enzyme activity have all been utilised to describe CSCs [155, 156]. Each of these CSC isolation

methods have its merits and demerits. For example, the side population cells isolated using the Hoechst stain show increased efflux abilities compared with normal cells due to enhanced expression of ATP-binding cassette (ABC) transporter proteins. However, this method is not very specific, and the isolated population may contain normal cancer cells with no self-renewal abilities. Thus, in many cases, a combination of these methods is used to improve the quality of CSCs.

Several signalling pathways are upregulated in CSCs. Thus, when it comes to cancer treatment, new drugs or therapies can target some of these signalling cascades that are dysregulated in CSCs. Conventional cancer therapies usually target fast-dividing cells and thus do not affect CSCs that are slow dividing (Figure 1.6) [145, 146]. The targeting of CSCs in tumours will largely depend on our ability to find new markers for CSCs and the in-depth characterisation of CSCs. Thus, as it stands, successful and durable cancer treatment might only come from targeting both cancer cells and CSCs.

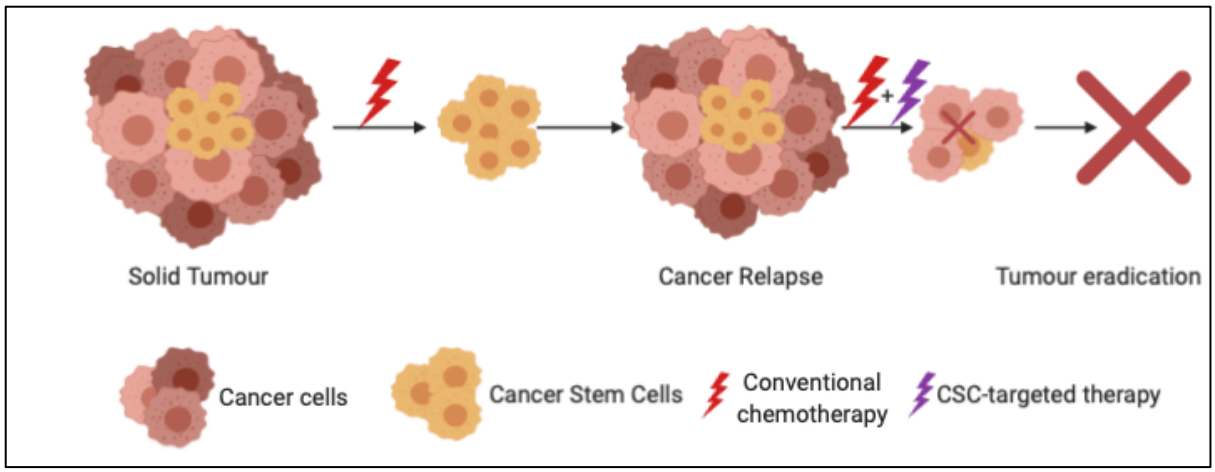

Figure 1. 6. CSCs can resist conventional therapies. When a solid tumour is treated with conventional chemotherapy, the bulk of the tumour will be eliminated. Due to intrinsic survival mechanisms and quiescent abilities of CSCs, these cells are able to circumvent the anti-proliferative effects of conventional cytotoxic therapies and thereby persist after treatment. Due to the reduction in overall tumour size, there is the general misconception that the cancer has been eradicated. This is however not the case, as months to years later, there is the reestablishment of a solid tumour after seemingly successful therapy. Ideally, the development of drugs targeting both CSCs and cancer cells should be sufficient in completely eradicating cancer. Image created using Biorender (https://biorender.com/).

1.4.3.1. Cancer Stem Cell Markers and Therapy resistance

Conventional therapies do not eliminate CSCs due to their ability to efflux drugs and other molecules faster than cancer cells [145]. CSCs are a subtype of cancer cell that has the ability to self-renew and differentiate[145, 157]. One of the challenges of

working with CSCs is isolating and characterising them. CD24, CD44, CD133, and ALDH are among the CSC markers targeted by antibodies (Table 1.1) [156]. In most cases, a combination of CSC markers is used in their characterisation, for example, lung CSCs are known to express markers such as CD133+, ALDH1+ and CD44+ [158]. CSCs from other cancers may display distinct markers such as melanoma CSCs are ABCB5+ whilst medulloblastoma CSCs are CD15+ (Table 1.1).

Table 1. 1. Cancer stem cells markers in different cancers

Cancer	CSC Markers	References
Gastric	CD133+, CD44+	[159]
Glioma	CD44+, CD133+, A2B5+, BCRP1+, SSEA-1+	[160]
Leukaemia	CD34+, CD38−, CD123+	[161, 162]
Prostate cancer	CD133+, CD44+, α2β1, ALDH	[163]
Pancreatic cancer	CD133+, CD44+, ABCG2, ALDH, EpCAM+	[164]
Melanoma	ABCB5+, CD20+	[165]
Head and neck cancer	CD44+, CD133+	[166]
Sarcoma	CD29+, CD117+, CD133+, Nestin+, Stro-1+	[167]
Cervical	CD133+, CD49f+, CK-17+	[168]
Oesophageal	CD44+, ALDH1+, Integrin α7+	[169]
Kidney	CD44+, CD24-, CD133+, CD105+	[170]
Lung cancer	CD133+, CD44+, ABCG2, ALDH, CD90+	[171]
Colon cancer	CD133+, CD44+, CD24+, EpCAM+, ALDH	[172]
Liver cancer	CD133+, CD44+, CD90+, ALDH, ABCG2, CD24+	[173, 174]
Breast cancer	CD133+, CD44+, CD24−, ALDH-1	[175]

To further complicate the treatment of many cancers, CSCs increase in tumours after treatment, demonstrating the enduring abilities of CSCs [176, 177]. They can also resist conventional therapies via enhanced adaptation to hypoxia and the activation of

survival signalling pathways (figure 1.6) [177]. Furthermore, CSCs have been observed to have immune evasion abilities, with an increased ability to undergo EMT as well as undergo metabolic adaptations to survive low nutrient conditions [145, 177].

In particular, ALDH superfamily and aldehyde dehydrogenase 1 (ALDH1) are detoxifying enzymes involved the in oxidation of aldehydes to carboxylic acids and retinol to retinoic acid [178]. Although they are expressed in normal and in cancer cells, ALDH1 is highly over expressed in CSCs [179], making ALDH1 one of the reliable markers for identifying of CSCs in several cancers. Several reports showed that ALDH1 is an independent prognostic marker for low survival in colorectal cancer patients [180], and enhanced ALDH1 activity can be used to identify TICs in prostate cancer [181]. In addition, other studies also showed that ALDH1 is a marker of cancer cells with self-renewal abilities in a human renal cell carcinoma cell line [182]. ALDH1 is highly overexpressed in breast CSCs [183], and cells expressing it can easily form xenograft tumours [183]. ALDH1 expression has also been linked to the development of chemoresistance [184], with some studies showing that inhibition of ALDH1 activity in CSCs sensitizes cells to chemotherapy [185].

CSCs also show enhanced expression of drug efflux proteins, including the ABC transporters (figure 1.7) [186]. Examples of members of this family include ABCB1, ABCG2, ABCB5, ABCC1, and multi-drug resistance 1 (MDR1) [187]. ABCB1 is highly expressed in breast CSCs and is linked to chemoresistance [188]. Inhibition of ABC transporters can successfully sensitize cancer cells to several drugs [189, 190].

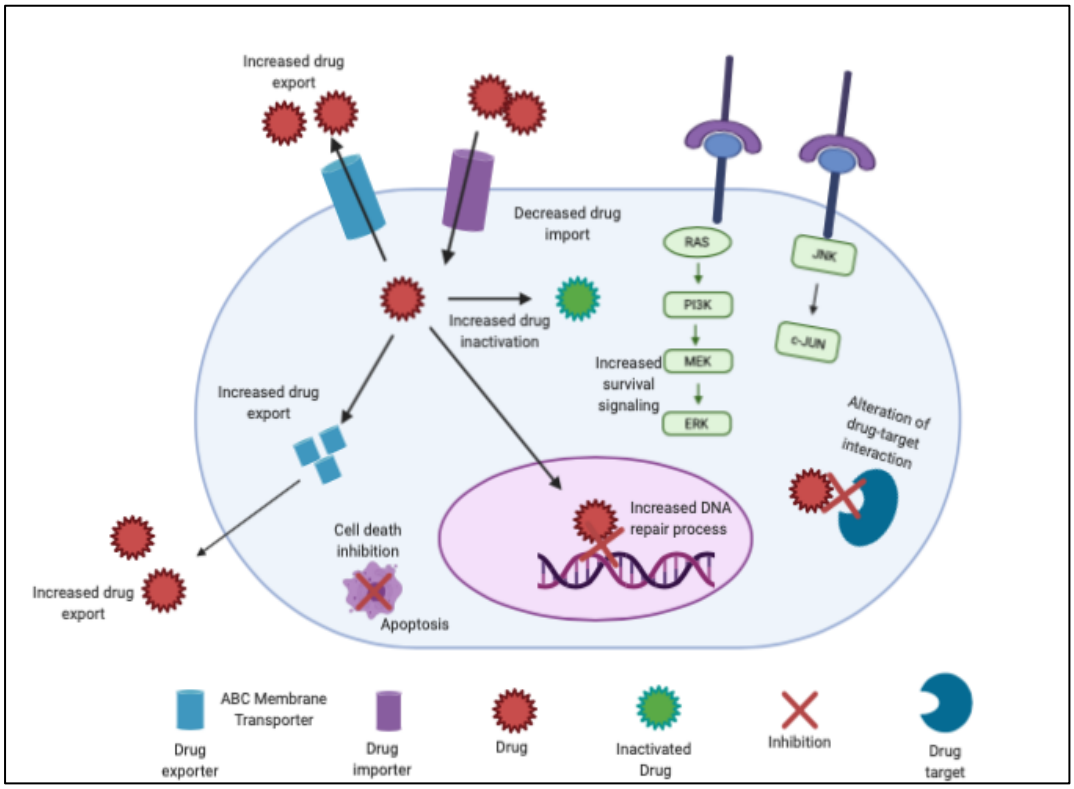

Figure 1. 7. Hallmarks of cancer stem cells include, enhanced survival signalling, increased expression of ABC membrane transporters, increased drug inactivation as well as increased DNA repair processes compared to cancer cells. These allow CSCs to survive conventional therapy, resulting in chemoresistance. Image created using Biorender (https://biorender.com/).

1.4.4. The Extracellular Matrix

One of the most important components of the TME is the extracellular matrix (ECM). The ECM forms the structural part of the TME and is located under the epithelial layer surrounding the connective tissue cells [191, 192]. The ECM comprises of several macromolecules, with the main classes being the collagens, proteoglycans, elastic fibres and glycoproteins [191]. In the human body, many cells are in contact with the ECM, and there is an interaction between the two. The composition of the ECM is in a constant state of flux and varies with the stage of development and pathological conditions [193]. Several cells synthesise the ECM components and these cells will continue to interact with their own ECM, and the ECM produced by other cells [191, 194]. One of the most studied forms of ECM is present in connective tissue and is composed of type I collagen. ECM consists of two types: interstitial connective tissue and basement membrane, which interact bidirectionally with cells and tissues to accomplish biological functions. Both interstitial connective tissue and basement membrane ECMs are capable of modulating functions such as cell proliferation, differentiation, angiogenesis, branching morphogenesis, wound healing, and

homeostasis [194, 195]. In some cases, basal lamina and basement membrane are sometimes used interchangeably, however, there is a difference between them. The basement membrane is composed of two layers, the basal lamina and the reticular lamina. The basal lamina is made up of multiple proteins that form a flexible bond with the underlying connective tissue to anchor epithelial cells.

The ECM of interstitial connective tissue ranges from soft, gel-like scaffolds made from collagen I, fibronectin, or cartilage proteoglycans to tough, dense sheets [196]. Integrins and other cell surface ECM receptors regulate intercellular and inter-tissue interactions within the interstitial connective tissue ECM. In contrast, the basement membrane is a highly specialised ECM that forms thin acellular layers beneath cells separating them from their interstitial matrix and connecting them to it [197]. A significant amount of basement membrane components are produced by tumours of epithelial origin. During metastasis, tumour cells are in contact with endothelial basement membrane. The spread of tumours is facilitated by the degradation of the basement membrane leading to the migration, and production of proteases by tumour cells [198]. The basement membrane is primarily composed of type IV collagen, laminin, entactin/nidogen, perlecan (heparan sulphate proteoglycan) and various growth factors [199]. These components interact with each other to form the matrix.

ECM, is known to influence cellular properties such as shape and movement. Indeed, the constant interaction between the cells and the ECM is the basis for tissue and organ structure and function [200]. In physiologically normal tissue, the ECM provides a stable physical environment required by cells, tissue and organs but undergoes a controlled turnover leading to structural remodelling needed for normal development. The ECM provides structural support to connective tissue, blood vessels, and cartilage, which is one of its most important functions. Collagen and fibronectin are primarily responsible for this support. Thus, the ECM in the body serves three key functions: providing tensile and compressive strength to tissues; physical protection of cells and tissues against changes in the microenvironment and water retention; and cell organisation and control through interactions with other proteins.

ECMs in different tissues and organs perform specialised functions. For example, the ECM of the bone and tooth enamel is mineralised to be able to withstand compression. Meanwhile, the ECM found in the eye has to be translucent so that light can pass

through. The ECM of tendons is very elastic. Through its action of tethering growth factors and other biomolecules, the ECM assumes a role in biological functions. Growth factors known to be tethered by the ECM include TGF-β, TNF-α, VEGF and IL-3 [201]. ECM proteins can generate cellular responses and activate signalling pathways. For example, type IV collagen has been shown to induce DNA synthesis in liver cells and fibronectin can inhibit the generation of new blood vessels in tumours [202]. The amount and type of ECM can also determine the induction of enzymes such as MMPs, whilst these enzymes, in are involved in regulating ECM turnover and other biological functions [203].

The ECM is mainly composed of collagens, fibronectin and vimentin interspersed with proteoglycans. The final composition of the ECM and other properties of its components determines its complexity and potential interactions within the ECM and between cells [204]. Fibroblasts are mostly responsible for the synthesis of the ECM, whilst a considerable amount of the ECM also comes from other mesenchymal cells. The equilibrium between ECM synthesis and degradation is important in the maintenance of homeostasis and any alterations to this balance can be deleterious to the ECM integrity. For instance, increased synthesis of the ECM can result in fibrosis, whilst decreased ECM synthesis can cause tissue wasting. Growth factors and cytokines are involved in regulating ECM synthesis and degradation, with several signalling pathways playing critical roles in maintaining the ECM synthesis/degradation balance in different tissues and organs.

Several studies aimed at understanding the interaction between cells and their environment or niche have utilised artificial matrices from purified proteins, including collagen, fibronectin and laminin [195, 205], while others have used cells grown on 2D rigid surfaces made of isolated ECM proteins, including fibronectin and type I collagen. Whilst these studies have vastly enhanced our knowledge about cell-ECM interactions, these do not adequately define mechanistic interactions between cells and ECM *in vivo* [206]. These researches have greatly expanded our understanding of the molecular contents and architectures of integrin receptors, focal adhesion complexes, and their interactions with the ECM. However, a 2D surface from isolated ECM proteins provides a rigid environment to cells and that in contrast to the ECM found in 3D surfaces of the *in vivo* niche [207, 208].

It is important that cells are studied in an environment that mimics their natural niche rather than the use of rigid 2D surfaces. Several reports have shown that 3D ECM can influence cellular behaviour and gene expression in different situations than 2D ECM. For example, different ECMs regulate different subsets of genes in monocytes [209]. In addition, different ECMs induce and activate different signalling pathways depending on ECM rigidity and elasticity, demonstrating that the biophysical and biochemical state of the ECM is important in tissue homeostasis [210].

Several conditions, including fibrosis, tumour development, invasion and metastasis, are associated with constant changes in ECM composition driven by synthesis, deposition and degradation of the ECM and, in the process altering the properties of the ECM. Alteration of the rigidity of the ECM influence the adhesion properties and structure of the ECM and ultimately determine the signalling cascades activated and eventual cellular phenotypes [211, 212]. Due to decreased receptor autophosphorylation, fibroblasts grown in a relaxed ECM have a lower proliferative capacity in response to PDGF than fibroblasts produced in monolayers.

In vivo-like 3-D culture systems such as tumour spheroids and organoids are able to recapitulate several *in vivo* biochemical and biophysical properties of cellular niches in *vivo*, whilst at the same time allowing opportunities for experimental manipulation [207]. When tumours invade the surrounding tissues, they degrade the basement membrane, allowing neoplastic epithelial cells to come into contact with adjacent mesenchymal compartments. Stromal cells are also known to aid tumour growth through the production of the ECM and growth factors. The eventual ‘altered’ ECM present within tumours is used by epithelial cells and the fibroblasts for growth and a pre-extravasation microenvironment. By providing the appropriate niche, *in vivo*-like mesenchymal ECM mimics *in vivo* microenvironments much better. As a result, such ECMs have several advantages over artificial ECMs in terms of assessing the physiological growth properties of both stromal and tumour cells.

In the TME, the ECM plays critical roles, including maintaining tissue structure and function and regulating cellular behaviour directly and indirectly [213]. As a result, several mechanisms involved in regulating ECM production, degradation and remodelling have been studied over the years [214]. Any disruption to these mechanisms may lead to diseases such as cancer, fibrosis and osteogenesis

imperfecta [213, 215].

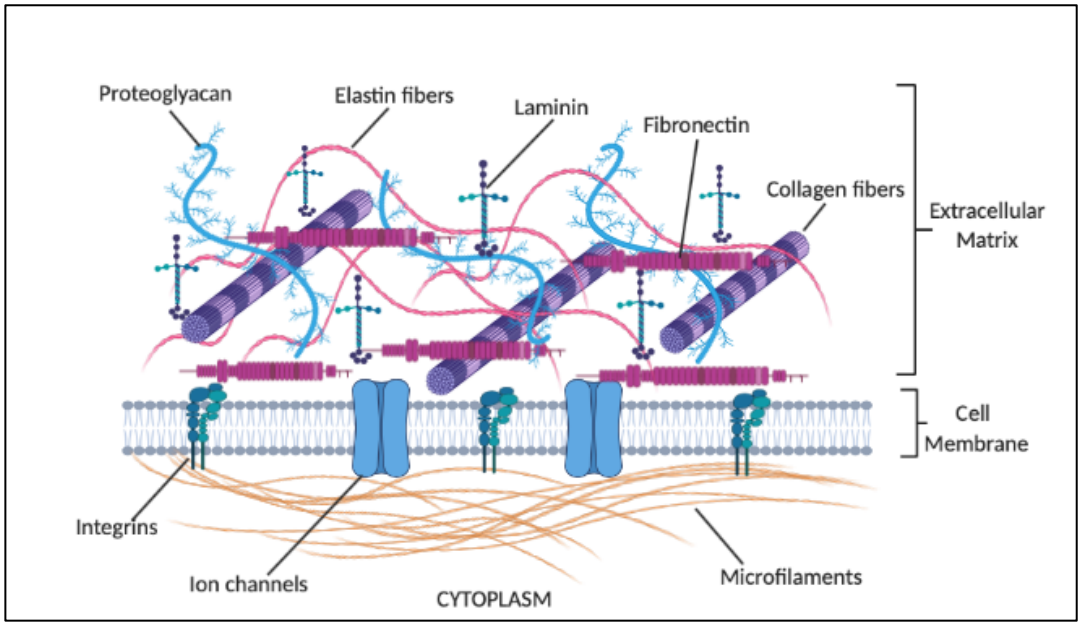

Figure 1. 8. The Extracellular matrix is made up of biochemical components that connect cells. Glycoproteins, proteins, proteoglycans, and polysaccharides are examples. Glycoproteins act as a ligand for cell surface proteins like integrins, allowing them to connect with one another. Protein networks are formed when ECM proteins such as fibronectin, collagen, elastin, and laminin form insoluble bundles. Image created using Biorender (https://biorender.com/).

1.4.4.1 The Extracellular Matrix in Tumour Progression

The ECM maintains tissue structure and function by acting as a scaffold and influence cellular proliferation and differentiation via biomolecules tethered to it [216]. The attachment of the ECM to cells via receptors allows it to influence cellular signalling and permit interactions between cells and their environment [217]. Many enzymes are involved in changing the ECM composition through remodelling, including lysyl oxidase (LOX), MMPs, cathepsins and tissue inhibitors of metalloproteinases (TIMPs) [215].

ECM elasticity and rigidity induce tumour progression and malignancy via integrin signalling [213]. The ECM's alteration also influences cancer cell growth, survival, migration and anticancer drug resistance [213]. One of the most abundant ECM proteins is collagen [213], providing structural support to cells and regulating cell adhesion, supporting chemotaxis and migration. Increased type I collagen synthesis can cause an increase in ECM stiffness, promoting tumour growth in the process [213]. In addition, MMPs-mediated ECM remodelling can lead to cell migration by creating pores allowing cancer cells to travel to distant tissues and organs [214]. For example,

Page-McCaw and colleagues demonstrated that increases in collagen synthesis and the resulting ECM stiffness induce integrin signalling, promoting tumour growth and survival [214].

1.4.4.2 The Extracellular Matrix and Chemoresistance

The ECM constitutes a physical barrier to drugs within the TME [218]. Tumour cells can acquire resistance to drugs through their interaction with the ECM [219], diffusion and pressure related to drug transport, as well as changes in ECM synthesis, result in ECM overproduction, which hinders and delays drug delivery [219].

The ECM contributes to the development of drug resistance by preventing drug passage and penetration into solid tumours. The TME is also compacted in such a way that tumour cells are surrounded mainly by stromal cells. Thus, cancer cells exist in regions where they experience hypoxia and low metabolic nutrients [220]. In addition, the ECM is known to induce survival signalling cascades in cancer cells, thereby promoting their survival [218]. Some of the survival pathways activated by the ECM include PI3K/AKT, p53, and MAPK [191, 192]. Increased deposition of collagen and overexpression of LOX can cause an increase in ECM stiffness in cancer, which upregulates the focal adhesion assembly and activate PIK3 signalling [221].

Studies have shown that the ECM plays an important role in tumour vascularisation [222]. Vascularisation is an indicator of tumour development and progression. Vascularisation decreases as matrix density increases in both the collagen and fibrin matrix. In addition to the physical barrier, a stiff matrix compresses micro blood vessels, making drugs more difficult to reach target tissues through the vasculature . ECM also affect vascularisation indirectly through hypoxia [222]. Overgrowth of cancer cells, as well as a structural and functional abnormality of ECM both, contributes to hypoxia of solid tumour [223]. In turn, hypoxia affects vascularisation via the activation of HIF-1α. The HIF-1α been implicated in chemoresistance, as well as in the activation of MDR1 expression in hypoxic colon cancer [224, 225].

The composition of the ECM also determines how effective the ECM limits drugs from reaching cancer cells. For example, collagen can bind and stabilise glycosaminoglycan as a member of the ECM, thereby influencing tumour cell resistance to drugs [226]. Furthermore, the ECM influences the toxicity of chemotherapeutic drugs by resisting apoptosis in small-cell lung cancer [227].

Regardless of the source of the ECM, the ECM protects tumour cells from drugs such as 5-fluorouracil [227]. The remodelling of the ECM and the resulting increase in several enzymes causes resistance to cisplatin [228]. These findings implicate the ECM in chemoresistance and require further investigation.

1.5. Modelling the Tumour Microenvironment

1.5.1 Decellularized Extracellular Matrix Model

In the process of initiation and progression of cancer, ECM plays an important role, which can be studied by 2D and 3D cultures [213, 215]. 2D monolayers are the most often utilized in cancer research, although they do not accurately represent cancer cell interaction with their environment, treatment efficacy, or resistance to drugs [215]. In contrast, 3D cultures are more representative of *in vivo* TME regarding the interaction of cancer cells with their microenvironment and is more representative of the effects of anticancer drugs [229]. It is also essential that 3D cultures systems can obtain a physiological orientation of extracellular receptors such as collagen receptors and integrins. Better cell-ECM interactions compared to 2D culture systems can promote important biological processes such as migration, adhesion, cell differentiation and cell proliferation [202].

The composition of ECM is complex and tissue-specific. The normal tissue stroma contains different cell types such as endothelial cells, fibroblasts, immune cells and MSCs. The communications and spatial arrangements of these cells are tissue-specific. For physiologically and therapeutically relevant tissue engineering and cancer investigations, recapitulating the native TME *in vitro* based on cell types within specific tissue matrices is critical [230]. To mimic the TME, decellularized ECM is used as an *in vitro* ECM model. Native ECM is obtained by removing the cellular components from native tissues or cultured cells.

Co-culturing different types of cells have now become common practice, and it contributes to our understanding of cell-cell interactions and signalling mechanisms. Fibroblasts and MSCs are common sources of 3D-ECM due to their ability to produce collagen-rich ECM. The use of cell-derived matrices eliminates allogenic or xenogenic

cellular antigens, as well as other immune responses including DNA replication [231]. Decellularized ECM from cells has been utilised to investigate the role of ECM in stem cell development, and it has been discovered that tumour cells have increased chemoresistance to 5-fluorouracil when exposed to decellularized ECM obtained from malignant tumour cells [232].

Also cell-derived decellularised ECM has several advantages, however, it is difficult to obtain cell-derived decellularised ECM with composition, mechanical properties, and microstructure that are the same as those found *in vivo* when analysing the comprehensive role played by ECM in cancer progression *in vitro*. Cell types and culture conditions affect the composition of ECM derived from cells and decellularized ECM can be influenced by the substrate used for its preparation.

1.5.2 Three dimensional (3D) Spheroids

In addition to the decellularized ECM system described above, 3D spheroids have recently been developed to mimic the TME and are widely used in cancer drug screening [233]. 3D spheroids possess several *in vivo* characteristics such as cell-cell interactions, drug penetration, production and deposition of the ECM [234]. As a result, cells grown in 2D monolayer cultures tend to lose their tissue-specific characteristics. Spheroids are aggregates of cells grown in suspension, which adhere to each other through adherens junction, tight junctions, or desmosomes [235]. Multicellular tumour spheroids (MCTS) are tumour spheroid models that have been employed in a variety of studies, including cell biology, tumour biology, epithelial morphogenesis, drug screening, and nanoparticle evaluation [236]. In biology and biomedical research, it has become increasingly recognised that MCTS show higher similarities to native tissues in terms of 3D structure, cell-microenvironment interactions, metabolism, and phenotypic features than 2D cultured cells. One of the advantages of MCTS over other 3D cell culture models is its well-defined, spherically symmetric geometry. Measurement of the spheroid morphology allows direct comparison of the effects of treatments on the cellular functions, making it ideal for screening therapeutic agents at high throughput.

The advantage of MCTS is that cancer cells in spheroids are more similar to cells *in vivo* than cells in 2D monolayers. Initially, tumour growth is characterized by exponential cell expansion. Then the proliferation rate of cells declines, and the

number of quiescent (non-proliferating) cells increases. Necrotic cells also accompany tumour growth (Figure 1.9) [237]. The organisation of cells in layers and diffusive gradients serve as microenvironmental stresses that force inner cells to adapt to their metabolism, resulting in the impaired therapeutic efficacy of anticancer drugs [237, 238]. As an example, cells in a hypoxic environment are resistant to drugs that promote cell death via reactive oxygen species (ROS). In contrast, the presence of necrotic and quiescent cells reduces the therapeutic efficacy of drugs against proliferating cells [238]. Furthermore, drugs generally effective in rapidly dividing cells do not demonstrate a significant therapeutic effect on the interior regions of spheroids as these are composed of senescent and necrotic cells [238].

A key feature of MCTS is the presence of a network of structural (collagen and elastin) and adhesive (fibronectin and laminin) ECM proteins rather than in the 2D culture [237]. In addition, spheroids' ECM-cell and cell-cell physical contacts form a barrier that limits the penetration and distribution of anticancer compounds in tumour mass [237]. The MCTS can reproduce the cellular heterogeneity of tumour tissues and should allow for a more accurate assessment of cancer cells' interactions with their microenvironment and their potential impact on therapy.

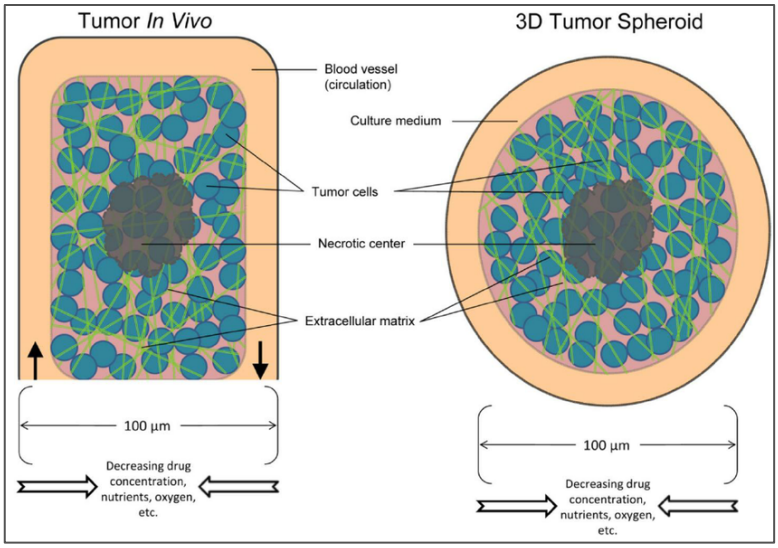

Figure 1. 9. Comparison of the components between *in vivo* tumours and *in vitro* tumour spheroid models. (Diagram from [239]).

The gene expression profiles of cancer cells in spheroids more closely resemble the *in vivo* gene expression profiles than those in 2D cultures [240]. One study examined and compared the expression patterns of 179 genes in 2D and 3D spheroid cultures of melanoma cells. The results showed that many genes are overexpressed in 3D

spheroids [241]. Signalling pathways activation in 3D cultured cells also differs from that in 2D cultured cells. For example, HER2 homodimers activate MAPK signalling in 3D cultures, while HER2/HER3 heterodimers activate PI3K signalling in 2D cultures [242].

A 3D culture with only a cancer cell line does not fully mimic the genetic heterogeneity of cells present in tumours. Cancer cells and stromal cells are co-cultured to overcome MCTS limitations [243]. For example, triple co-culture of pancreatic cancer cells, endothelial cells (Human umbilical vein endothelial cells, HUVEC) and fibroblasts (MRC-5) demonstrated that the presence of a complex microenvironment reduced the sensitivity of cancer cells to cancer drugs, therefore closely recapitulating the observed *in vivo* resistance to treatment [243]. A 3D co-culture of monocytes with pancreatic cells and fibroblasts was used to induce the production of immunosuppressive cytokines, which are known to enhance the polarisation of M2 like macrophages [244].

A short timeframe to produce MCTSs should be considered when choosing an approach for MCTS formation. MCTS are manufactured using clusters of cell aggregates or single cells in the suspension derived from *in vitro* cultured tumour cell lines [245, 246]. Several techniques are used to form spheroid structures, many of which are optimised to produce these structures on a large scale under highly reproducible conditions. They utilize surfaces or physical forces that resist cell attachment to stimulate cell-to-cell interactions and support 3D spheroid formation [237]. The liquid overlay method is a commonly used method for generating spheroids. The method is based on using non-adherent 96-well plates coated with poly-2-hydroxyethyl methacrylate (poly-HEMA) or agarose to prevent cell attachment [247, 248]. Various factors, including cell types, the initial number of cells, medium formulation, and static or dynamic culture conditions, affect the speed and uniformity of the spheroids [245]. The hanging-drop method is another beneficial technique for producing uniform spheres with a predetermined size. For the large-scale production of MCTS, rotary bioreactors are often used. The surfaces of spinner flasks and roller bottles are treated to reduce the adhesion of cells [248]. In contrast to static cultures, rotary cultures generate spheroids that are relatively uniform in size. As part of the spheroid fabrication, various supplements such as methylcellulose, engineered cellular linker, and various ECM components can be added [246].

MCTS have some limitations in that the cell type, the culture technique, the composition and volume of the medium, and the density of the cells all contribute to the variability in MCTS formation, thus leading to difficulties in reproducing spheroid formation. As spheroids grow and change in shape, cell culture systems tend to have diffusion gradients. As a result, the viability of cells may be compromised because of a lack of nutrients in the core of the spheroid.

1.5.3 Organoids

Recent reports indicate that organoid technology may be used to model the TME. Organoids are an advanced form of multicellular structure. They are grown from embryonic stem cells or induced pluripotent stem cells and consist of organ-specific cell types that self-organise through cell sorting and spatially restricted lineage commitment similar to *in vivo* [249]. Matrigel and various growth factors were used to develop the first long-term intestinal organoids that had both proliferative crypts and differentiated villus sections [250]. Organoids for various organs and tissues have been created using various biomaterials, such as silk-collagen for neural tissue and Matrigel for lung tissue [251]. Generated 3D organoids are advantageous over 2D and other current 3D culture models that use patient-derived xenografts (PDX) or cell lines. This is due to the accumulation of genetic changes in multiple-passaged cell lines that no longer represent the original primary tissue [230].

Organoid technology has provided a unique opportunity to improve primary and clinical cancer research with the intrinsic advantage of retaining the heterogeneity of the original tumours [252]. Normal organoids can be mutated into tumour organoids using gene-editing techniques to mimic genetic alterations that arise during cancer development and progression [253]. Several patient-derived organoids (PDTOs) have been developed [254]. Organoid technology has been extended as a model for personalised cancer treatment and drug screening [226]. The PDTOs showed different dose-dependent responses to sorafenib treatment in different patients [255]. The structure and function of organoids are influenced by some but not all of the characteristics of real organs. As a starting point, all organoids lack vasculature, which plays an essential role in transporting nutrients and wastes. In addition, some organoids may lack key types of cells found in the human body. Furthermore, the earliest stages of organ development are replicated only by some organoids [256].

1.6. Study Hypothesis

Chemotherapy resistance remains a challenge during cancer treatment, resulting in increased morbidity and mortality rates. Importantly, tumour cells exist in a complex microenvironment, comprised of various stromal cells and the ECM, and these contribute to tumorigenesis and the development of resistance to therapy.

Therefore, this study hypothesised that the dynamic interactions between cancer cells and their microenvironment, including stromal cells and ECM components, promote cancer cell proliferation, migration, and drug resistance, leading to cancer progression and metastases.

1.7 Project Aim and Objectives

1.7.2 Aim

This study investigated the role played by various components of the tumour microenvironment, namely CAFs, CSCs and the ECM, on cancer cell behaviour and drug response. Furthermore, the study developed a three-dimensional multi-cellular model with which to study the interaction between cancer cells and their stromal components and how this influence chemoresistance and migration.

1.7.3 Objectives

1) Investigate the origins of CAFs by using mesenchymal stem cells as a potential source of cancer-associated fibroblasts in tumours.
2) To identify and characterise cancer stem cells, as well as to investigate their functions in the progression of cancer and drug resistance
3) Investigate the effect of cell-derived extracellular matrix on cancer cell proliferation, migration and drug response.
4) To develop a 3D MCTS model to investigate the effect of the crosstalk between cancer cells and fibroblasts.

CHAPTER 2:

MESENCHYMAL STEM CELLS AS POSSIBLE SOURCE OF CANCER-ASSOCIATED FIBROBLASTS IN CANCER.

2.1 Introduction

Therapy resistance is still a problem in the treatment of cancer, which is in part due to the fact that the majority of the treatments currently available are designed to target the cells of the tumour rather than the surrounding components of the TME [257]. It is well known that the development of cancer is driven not only by the intrinsic properties of cancer cells but also by the makeup of the TME and the interactions between its cellular components and cancer cells. As a result, the complexity of the TME plays an important role in patient outcome [70]. For the development of novel biomarkers and therapeutic targets, it is therefore critical to understand the composition and role of TME and stromal cells. Cancer-associated fibroblasts (CAFs) are the major stromal cells in the TME in many tumours. Dvorak *et al.* proposed the theory that " a tumour is a wound that never heals" [258]. CAFs are similar to myofibroblasts in morphology, which display large spindle-shaped cells that are activated during wound healing [259]. During wound healing, activated fibroblasts decrease when the process has been completed [260]. CAFs, in wound healing do not undergo apoptosis or change their phenotype, unlike normal fibroblasts and myofibroblasts [261]. A variety of mechanisms can be used by CAFs to control cancer growth, progression, therapy resistance, and metastasis.

While fibroblasts have been shown to contribute to the population of CAFs in the TME, CAFs heterogeneity has also been attributed to other stromal cells (Figure 1.12). Several studies suggest that CAFs display complex heterogeneity [262, 263]. In addition, local fibroblasts within the tissue where the tumour is forming can be activated via their interaction with a remodelled ECM and tumour cells. Besides the activation of local fibroblasts, CAFs can also originate from cells such as fibrocytes and MSCs, pericytes, smooth muscle cells, adipocytes, epithelial cells, endothelial cells, and stellate cells (Figure 2.1) [77]. Increasing evidence suggests that MSCs may give rise to a significant subpopulation of CAFs.

It is well known that the cytokines released by cancer cells participate significantly in the transformation of MSCs into CAF. It was shown that breast cancer cells, like all other cells, produce SDF-1, PDGF, VEGF, IL-6, and TGF-β1, among others, that favour the differentiation of MSCs to CAFs and their subsequent activation [264]. In addition, cancer cells have been shown to produce chemokines and cytokines such as IL-6, CCL2 and SDF-1 during hypoxic conditions, leading to MSCs recruitment and activation [265]. Therefore, MSCs can stimulate cancer growth and metastasis directly or indirectly as they differentiate into CAFs.

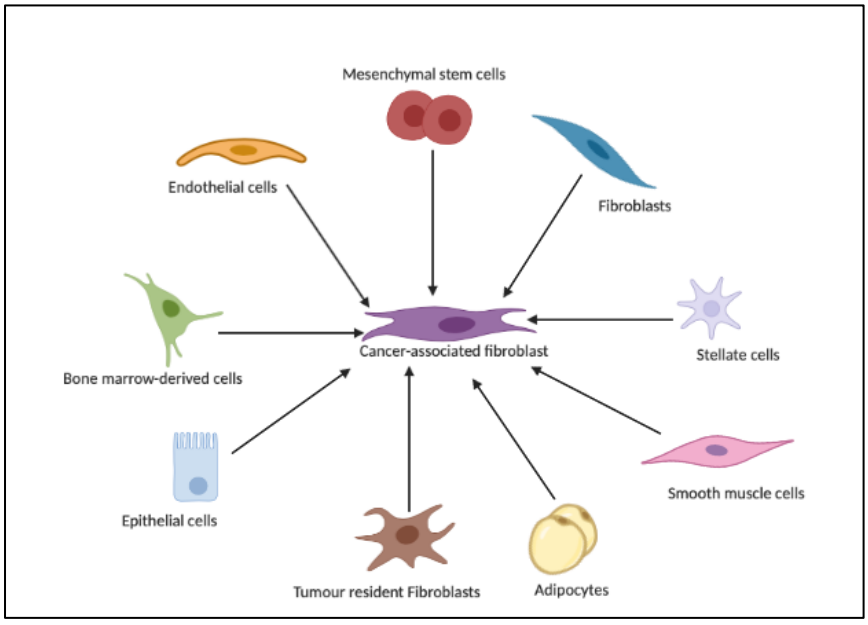

Figure 2.1. Potential origins of CAFs. CAFs can originate from various cell populations through several mechanisms. For example, CAFs can originate from cells such as fibrocytes and MSCs, pericytes, smooth muscle cells, adipocytes, epithelial cells, endothelial cells, and stellate cells.

Signalling mechanisms that regulate fibroblast activation include lysophosphatidic acid and TGF- β family ligands, which modulate the activities of serum response factor (SRF) and SMAD transcription factors, respectively, to promote the expression of the activated fibroblast marker α-SMA and vimentin [87]. Several biological markers have been utilised in the recent characterisation of CAFs, such as FAP, PDGFRα/β, tenascin C, desmin, CD90 and podoplanin (PDPN) (Table 2.1) [60]. Given the heterogeneity displayed by CAFs, it is not surprising that there is no universal marker for CAFs. In practice, these markers are used in combination to characterise CAFs. In turn, CAF heterogeneity may allow for more tailored and specific therapies to be developed for specific cancer types.

Table 2.1. Markers for cancer-associated fibroblasts

CAFs Marker	Description of protein
α-SMA	Actin isoform
Tenascin-C	Extracellular matrix glycoprotein
Vimentin	Type III intermediate filament protein
PDGFRα/β	Protein tyrosine kinase receptor
FAP	Membrane-bound gelatinase
Periostin	Secreted extracellular matrix protein
Thy-1	Glycophosphatidylinositol anchored protein
Caveolin-1	Scaffolding protein within caveolar membranes
Podoplanin	Mucin-type protein, heavily O-glycosylated glycoprotein

In this chapter, it is hypothesised that cancer cells secrete soluble factors that stimulate MSC to transform into CAFs-like cells that express αSMA and vimentin. This study show that Wharton's Jelly-derived MSCs cultured in media conditioned by WHCO1 cell (oesophageal cancer cell line) and MDA MB231 cells (a breast cancer cell line) expressed vimentin and αSMA. Thus, Wharton's Jelly-derived MSCs are converted to CAFs-like cells by factors present in cancer cell-conditioned medium. The co-culture of cancer cells and ‘CAFs’ derived from MSCs promoted cancer cell growth, proliferation, metastasis and drug resistance.

2.2 Results

2.2.1 Investigation of the expression of CAFs markers and MSC markers in several cancer types.

The expression of CAF and MSC markers was investigated in several cancer types using publicly available databases and bioinformatics techniques. This study then evaluated the correlation between CAFs markers and MSCs markers and drug resistance genes.

2.2.1.1 Evaluation of CAF and MSC marker expression in human tumours.

Several reports have indicated that CAFs and MSCs are recruited to develop tumours and act in a pro-tumourigenic by releasing several biomolecules such as growth factors and cytokines. As a pilot study, publicly available databases, such as The Cancer Genome Atlas (TCGA), Oncomine, and Tumour Immune Estimation Resource (TIMER), were used to assess the expression of different CAF and MSC marker mRNAs in normal and tumour tissues for a variety of malignancies (see Materials and Methods for description of databases). The use of publicly available databases allows the investigation of gene expression based on many normal and tumour tissues which were not available during this study.

The Oncomine database was used to analyse CAF mRNA levels in tumour tissues and normal tissues of various cancer types (Figure 2.2). CAF markers such as ACTA2, FAP, and S100A4 were found to be upregulated in several tumour tissues compared to adjacent normal tissues, including breast carcinoma (BRCA), oesophageal carcinoma (OSCA), head and neck (HNSC), and lymphoma tumours (Figure 2.2). Coincidentally, MSC markers such as CD73, CD90 and CD105 were also upregulated in several tumour tissues compared to normal tissues using the same databases (Figure 2.2).

To further investigate the expression of CAF and MSC markers in human cancers, CAF and MSC markers expression was investigated using RNA-seq data of multiple cancers in the TIMER database. The CAF marker (FAP) and MSC marker (CD90) expression levels were significantly upregulated in tumour tissues compared to normal

tissues of several cancers (Figure 2.3). In addition, genes associated with both CAFs and MSCs, including TGF-β and collagens, were also upregulated in several tumour tissues compared to normal tissues (Figure 2.2; Figure 2.3).

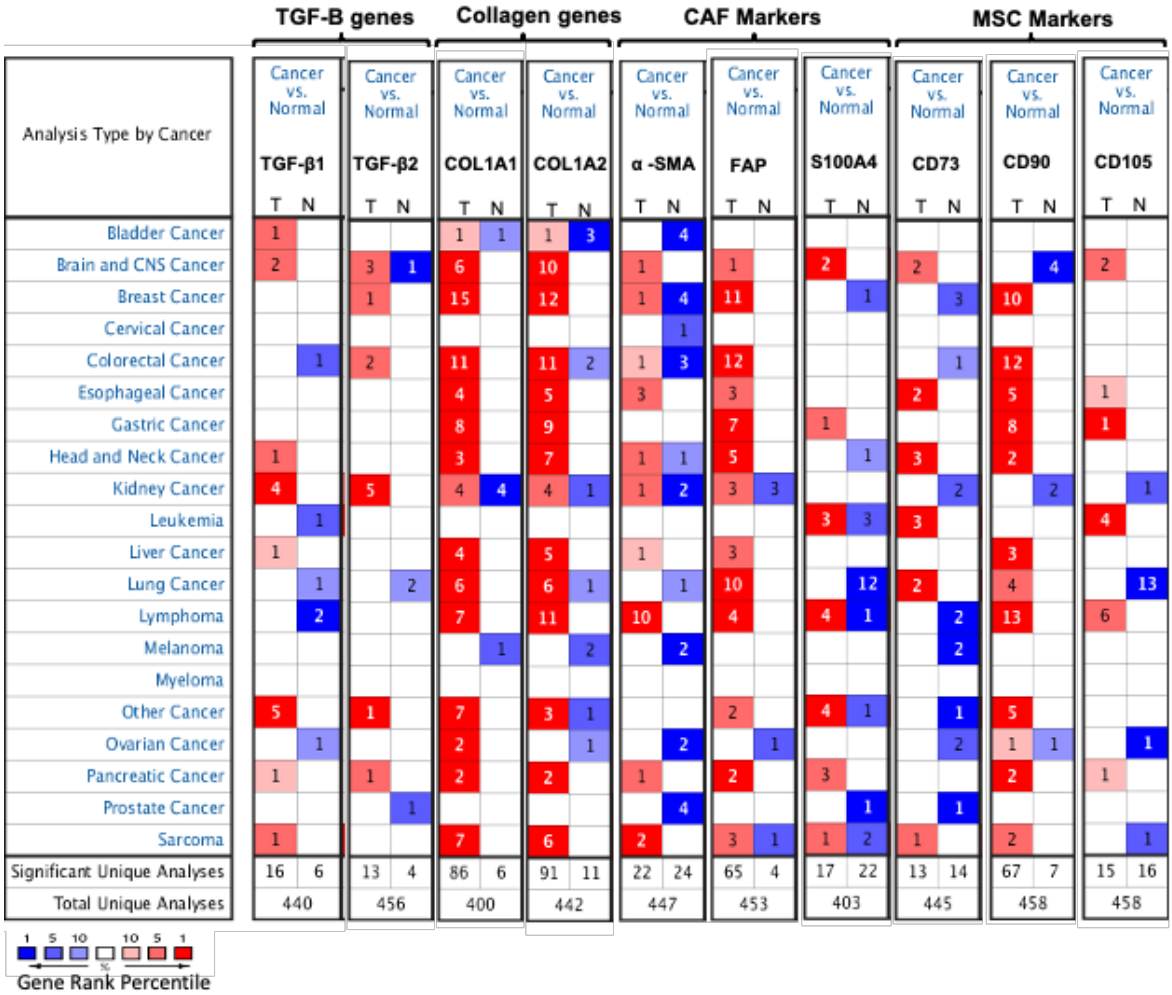

Figure 2.2. TGF-β1, TGF-β2, collagen genes, CAF and MSC marker gene expression in different human cancers and adjacent normal tissues. Gene expression of CAF markers, MSC markers, collagen gens and TGF-β in tumours versus normal tissues was based on data from the Oncomine database. P-value was set as $p < 0.001$; Fold change > 2; Gene rank was set at 10 %. The numbers shown in the Figure represent datasets with statistically significant mRNA levels, with red showing overexpression and blue as under-expression of genes in tumour samples compared to normal tissues. Colour intensity indicates the best rank of the gene in the analyses. The left column in each dataset represents tumour sample and the right is a representative of normal tissue. The number in each cell is the number of analyses that met our thresholds.

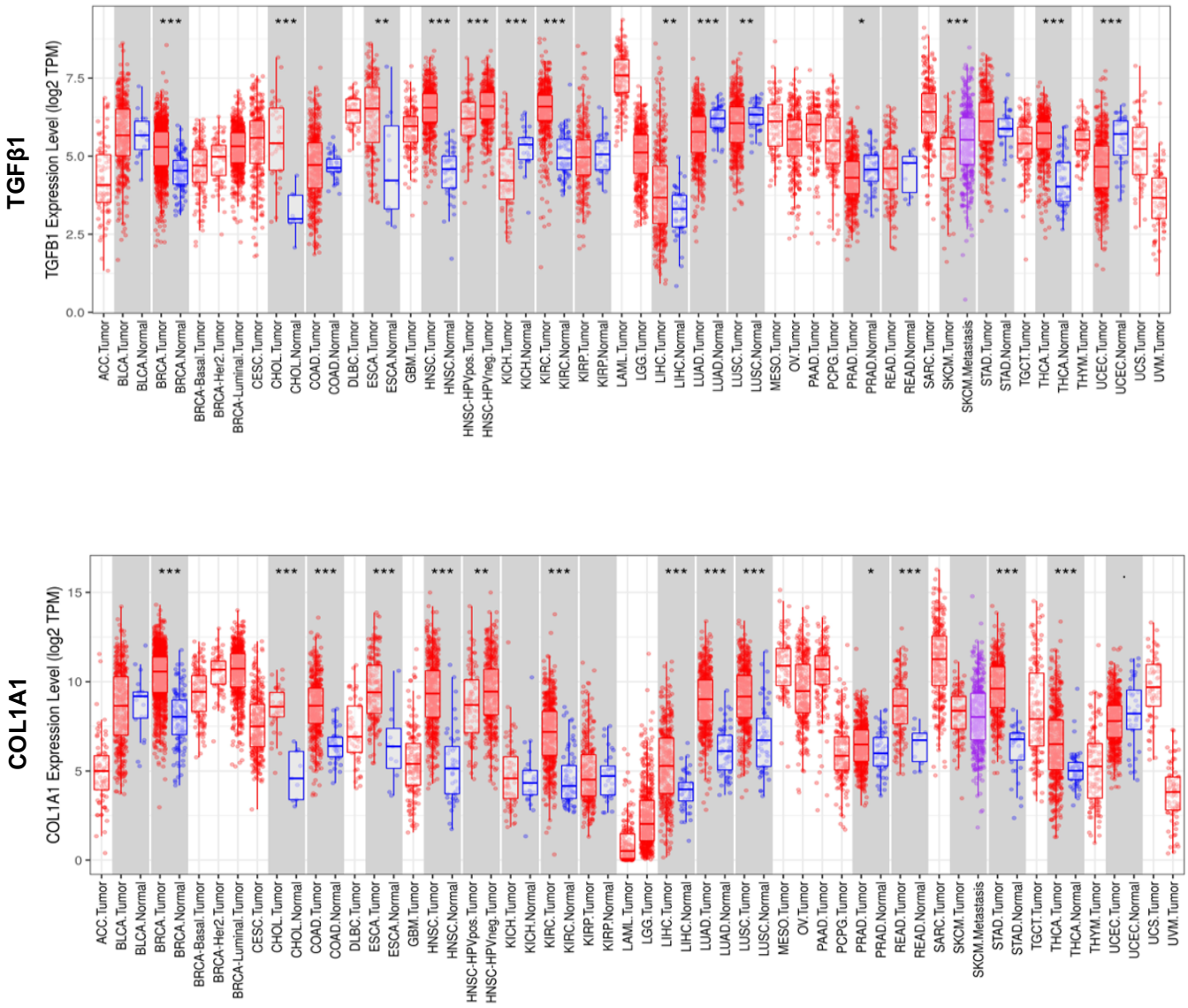

Figure 2. 3. TGF-B1, COL1A1, FAP and CD90 expression in different human tumours and adjacent normal tissues based on data from the TIMER database. Gene expression in tumours versus normal tissues was based on data from the Oncomine database. The expression of TGFβ1and COL1A1,was investigated in tumour samples Datasets with statistically significant gene expression, red showing overexpression and blue as under-expression of genes. Statistical significance of differential expression was evaluated using the Wilcoxon test (***p<0.001,**p<0.01, *p<0.05).

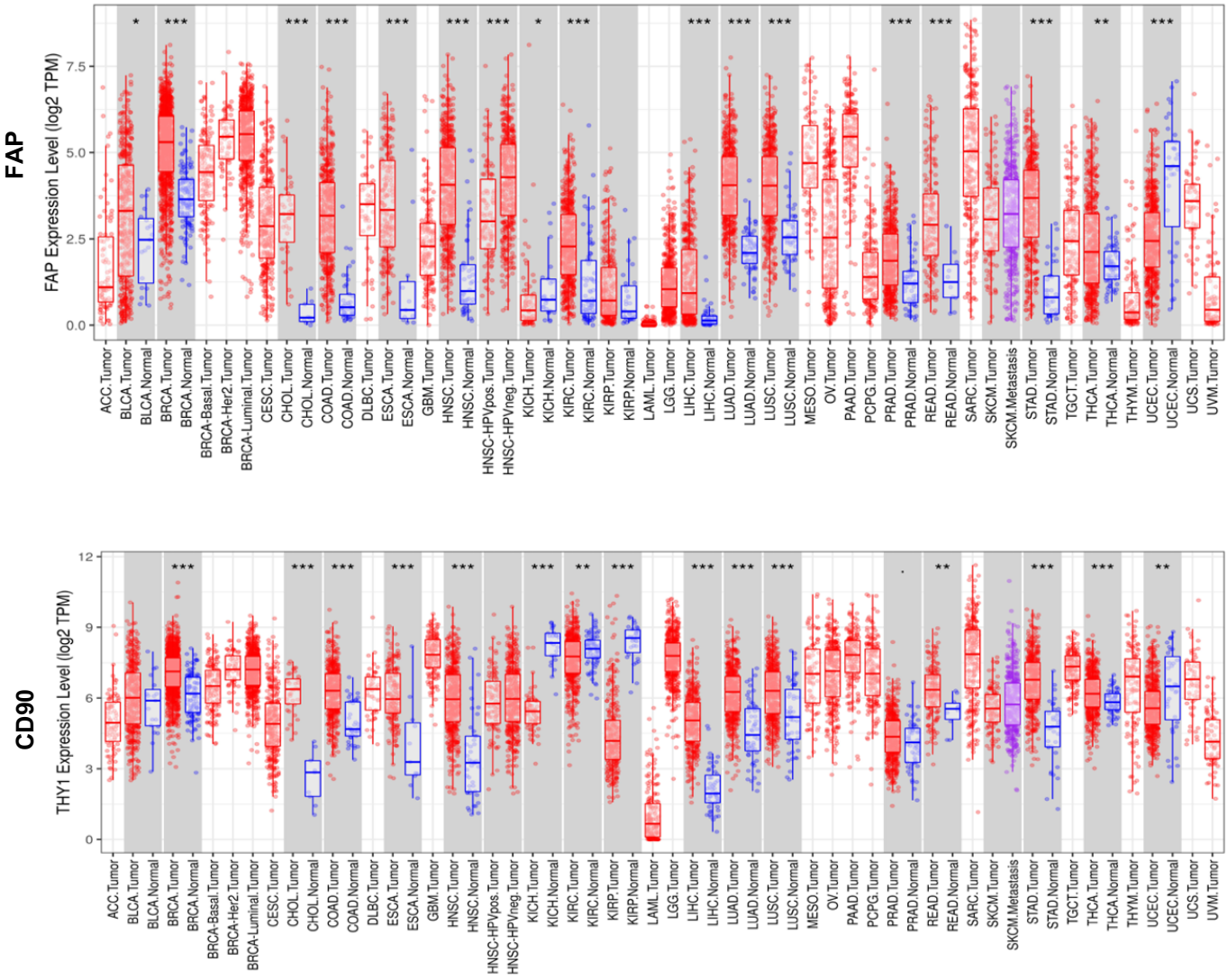

Figure 2.3 (continued). TGF-B1, COL1A1, FAP and CD90 expression in different human tumours and adjacent normal tissues based on data from the TIMER database. Gene expression in tumours versus normal tissues was based on data from the Oncomine database. The expression of FAP and CD90 was investigated in tumour samples Datasets with statistically significant gene expression, red showing overexpression and blue as under-expression of genes. Statistical significance of differential expression was evaluated using the Wilcoxon test (***p<0.001,**p<0.01, *p<0.05).

2.2.1.2 CAF markers expression is correlated with MSC markers expression in tumour tissues.

Many reports have suggested that MSCs recruited to tumours can be transformed into CAFs over time [140, 266]. In order to examine the correlation between CAF and MSC markers, a correlation analysis was conducted between CAF and the MSC markers via the TIMER database. The results show that CAF markers are significantly correlated with MSC markers in several cancers. Specifically, this study focused on BRCA (n = 1093) and OSCA (n = 184). The analysis showed that FAP is significantly correlated with CD73, CD90, CD105 and CD45 expression in BRCA (Figure 2.4, Table 2.2). The results suggested that FAP expression had a strong relationship with CD73 and CD90 in BRCA. In addition, FAP was significantly correlated with CD90, CD105 and CD45 expression in OSCA tumour, with CD90 showing a strong correlation while weakly correlated with CD105 and CD45 (Figure 2.4, Table 2.3). Furthermore, another CAF marker ACTA2, was significantly correlated with CD73, CD90 and CD105 expression in BRCA tumours (Figure 2.5, Table 2.2). ACTA2 was also significantly correlated with the expression of CD90, CD105 and CD45 in OSCA (Figure 2.5, Table 2). However, CAF markers FAP and ACTA2 were not significantly correlated with MSC marker CD73 in OSCA (Figure 2.4 & 2.5, Table 2.3).

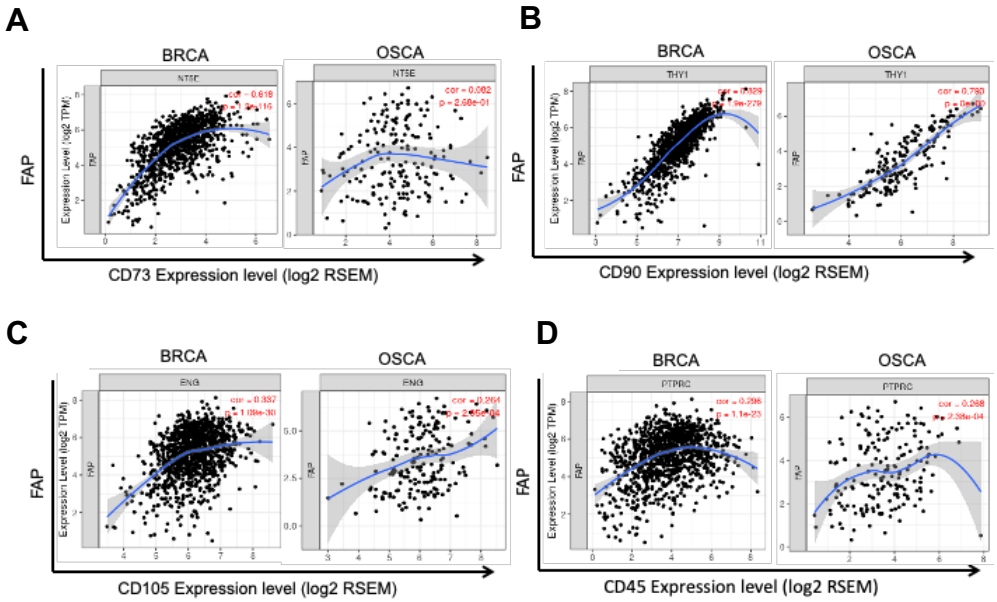

Figure 2. 4. Correlation analyses between expression of FAP and MSC markers. TIMER database was used to evaluate the correlation between CAF marker FAP and MSC markers in BRCA (n = 1093) and OSCA (n = 184). **(A)** Correlations between FAP expression and CD73 expression in BRCA and OSCA, **(B)** Correlations between FAP expression and CD90 expression in BRCA and OSCA, **(C)** Correlations between FAP expression and CD105 expression in BRCA and OSCA, **(D)** Correlations between FAP expression and CD45 expression in BRCA and OSCA.

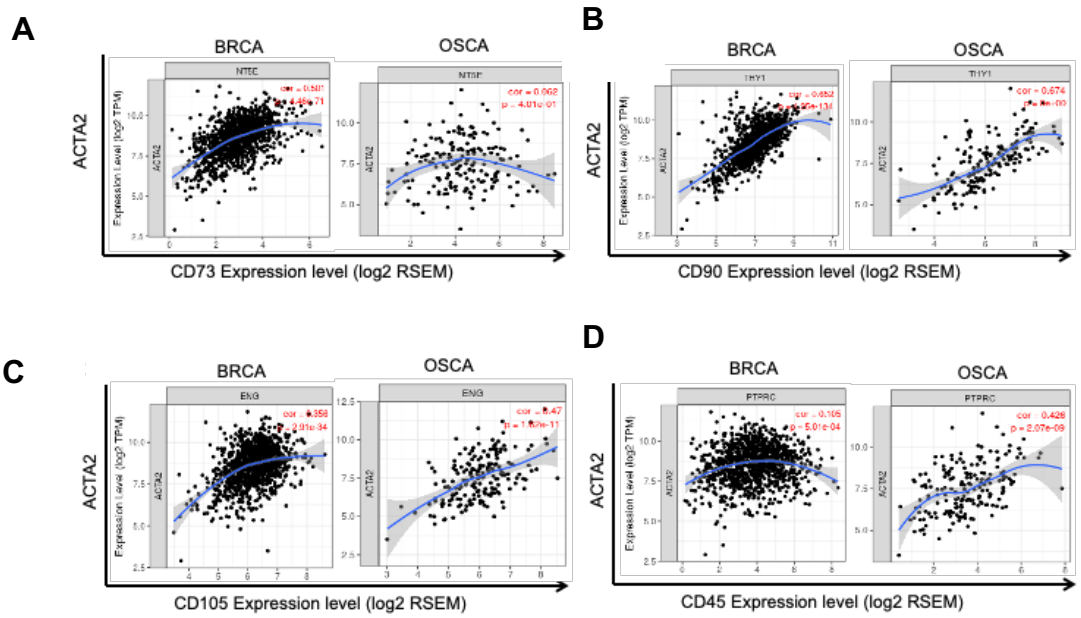

Figure 2. 5. Correlation analyses between expression of ATCA2 and MSC markers. The data analysis was done as described in figure 2.3 of section 2.2.1.2. **(A)** Correlations between ACTA2 expression and CD73 expression in BRCA and ESCA, **(B)** Correlations between ACTA2 expression and CD90 expression in BRCA and ESCA, **(C)** Correlations between ACTA2 expression and CD105 expression in BRCA and ESCA, **(D)** Correlations between ACTA2 expression and CD45 expression in BRCA and ESCA.

2.2.1.3. CAF marker expression correlation with Drug Resistance gene expression and Protein-Protein Interaction Network.

This study further investigated the association between CAF marker expression and drug resistance. The use of the TIMER database and samples from the TCGA, the analysis revealed that FAP is significantly correlated with the expression of drug resistance genes, ABCC1, ABCC2, ABCC3 and ABCB1 in BRCA (Figure 2.6, Table 1). In OSCA, a significant correlation was observed between FAP expression and ABCC1, ABCC2 and ABCC3 gene expression (Figure 2.6, Table 2). In addition, ACTA2 expression was significantly correlated with ABCC2, ABCC3 and ABCB1 gene expression in BRCA (Figure 2.7, Table 1). In OSCA, ACTA2 was significantly correlated with ABCC1 and ABCB1 gene expression (Figure 2.7, Table 2).

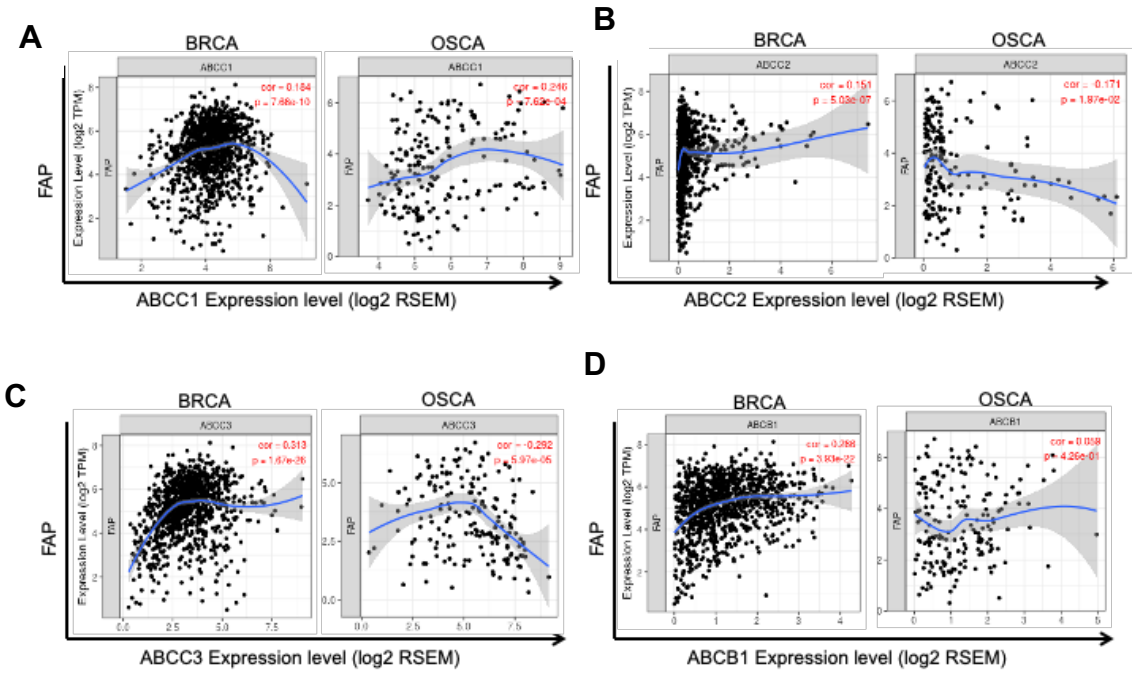

Figure 2. 6. Correlation analyses between expression of FAP and Drug Resistance markers. The data analysis was done as described in figure 2.3 of section 2.2.1.2. **(A)** Correlations between FAP expression and ABCC1 expression in BRCA and OSCA, **(B)** Correlations between FAP expression and ABCC2 expression in BRCA and OSCA, **(C)** Correlations between FAP expression and ABCC3 expression in BRCA and OSCA, **(D)** Correlations between FAP expression and ABCB1 expression in BRCA and OSCA.

Table 2. 2. Correlation analysis between CAF markers and MSC markers in Breast carcinoma based on data from TIMER.

Gene	Gene marker	Correlation	p-value
FAP	CD73	0.618	***
FAP	CD90	0.829	***
FAP	CD105	0.337	***
FAP	CD45	0.296	***
FAP	ABCC1	0.184	***
FAP	ABCC2	0.151	***
FAP	ABCC3	0.313	***
FAP	ABCB1	0.286	***
ACTA2	CD73	0.501	***
ACTA2	CD90	0.652	***
ACTA2	CD105	0.356	***
ACTA2	CD45	0.105	**
ACTA2	ABCC1	0.044	0.149
ACTA2	ABCC2	0.087	**
ACTA2	ABCC3	0.242	***
ACTA2	ABCB1	0.302	***

*p<0.05, **p<0.005, ***p<0.0005.

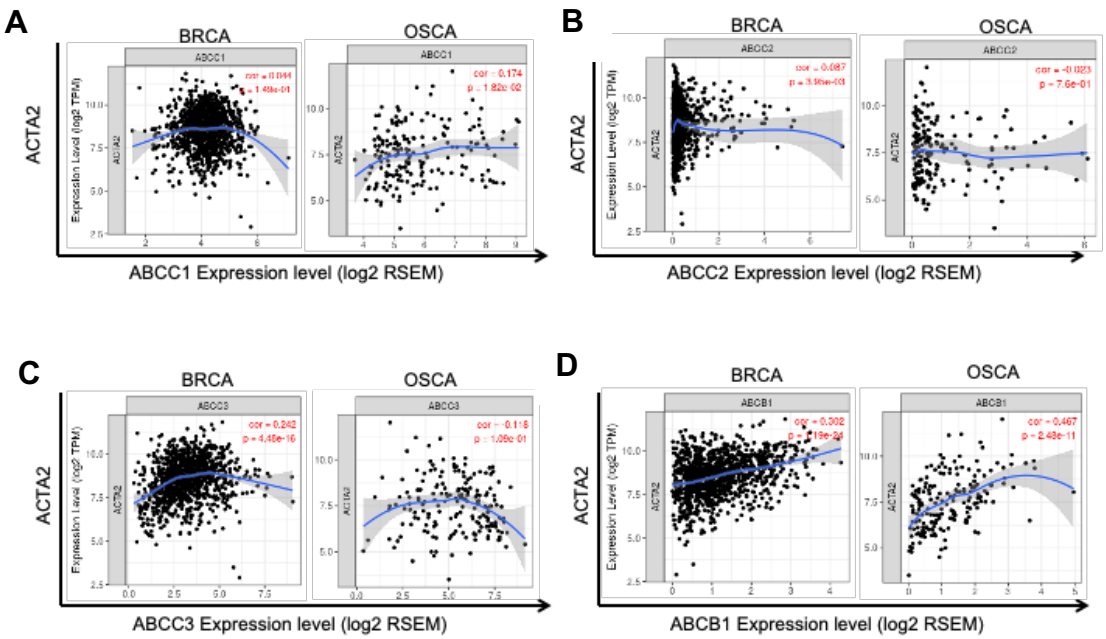

Figure 2. 7. Correlation analyses between expression of ATCA2 and Drug Resistance markers. The data analysis was done as described in figure 2.3 of section 2.2.1.2. **(A)** Correlations between ACTA2 expression and ABCC1 expression in BRCA and OSCA, **(B)** Correlations between ACTA2 expression and ABCC2 expression in BRCA and OSCA, **(C)** Correlations between ACTA2 expression and ABCC3 expression in BRCA and OSCA, **(D)** Correlations between ACTA2 expression and ABCB1 expression in BRCA and OSCA.

Table 2. 3. Correlation analysis between CAF markers and MSC markers in oesophageal carcinoma based on data from TIMER.

Gene	Gene marker	Correlation	p-value
FAP	CD73	0.082	0.268
FAP	CD90	0.793	***
FAP	CD105	0.264	**
FAP	CD45	0.268	**
FAP	ABCC1	0.246	**
FAP	ABCC2	0.171	*
FAP	ABCC3	0.292	***
FAP	ABCB1	0.059	0.426
ACTA2	CD73	0.062	0.401
ACTA2	CD90	0.674	***
ACTA2	CD105	0.470	***
ACTA2	CD45	0.426	***
ACTA2	ABCC1	0.174	*
ACTA2	ABCC2	0.023	0.760
ACTA2	ABCC3	0.118	0.109
ACTA2	ABCB1	0.467	***

*p<0.05, **p<0.005, ***p<0.0005.

It is important to identify proteins interacting with CAF markers as well as the functional information of the proteins. Protein-protein interaction (PPI) networks for CAF markers, FAP and ACTA2, were analysed using the GeneMANIA database. The analysis revealed that FAP interacts with several proteins, including collagen genes, CD90 (THY1) and other proteins such as DPP4 and DPP8 (Figure 2.8). Another CAF marker, ACTA2, interacts with several proteins including, MYOCD, MYH11 and CNN1 (Figure 2.8).

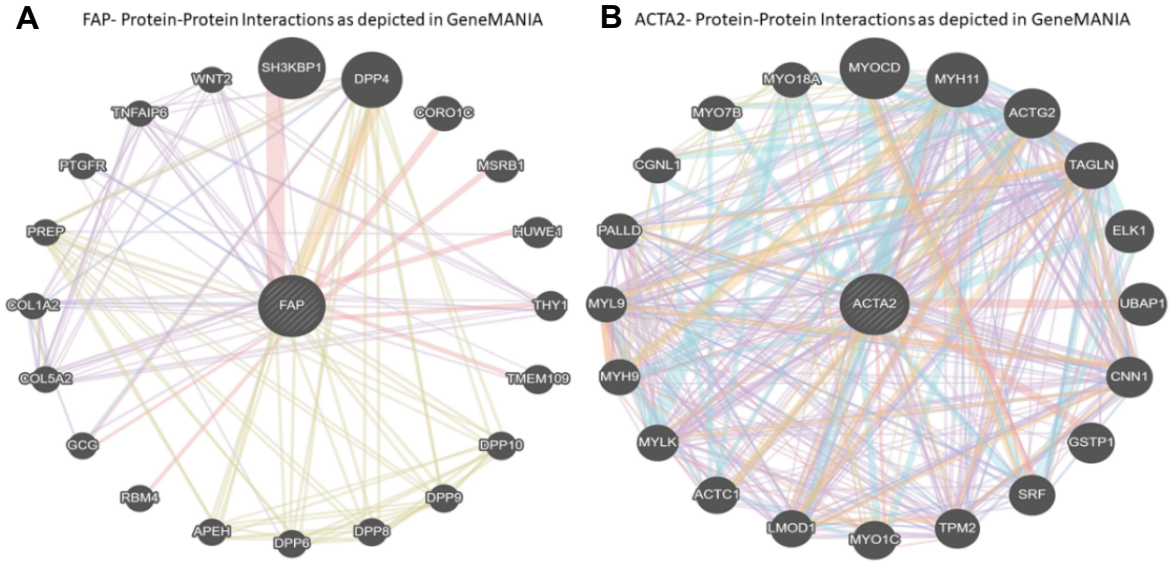

Figure 2. 8. CAF markers, FAP and ACTA2, protein-protein interaction networks. GeneMANIA database was used to analyse the protein-protein interaction networks for CAF markers. Representative PPI networks of **(A)** FAP and **(B)** ACTA2 as depicted in GeneMANIA.

2.2.2 The role of cancer cells in WJ-MSCs differentiation into CAFs

An examination of online databases revealed a significant relationship between CAF markers and several MSC markers. Thus, *in vitro* co-culture experiments of cancer cells and MSCs were conducted to study whether Wharton's Jelly-derived mesenchymal stem cells (WJ-MSCs) can be transformed into CAF-like cells

2.2.2.1 The effect of cancer cells on MSCs differentiation and their expression of levels of CAFs markers.

This study used a transwell co-culture system comprised of cancer cells (WHCO1 oesophageal and MDA MB231 breast cancer) and WJ-MSCs to establish an *in vitro* model that could better simulate the TME. Transwell assays are commonly used *in*

vitro to study the interaction of cancer cells and their stromal component. Therefore, co-culture experiments were performed to determine whether cancer cells (WHCO1 and MDA MB231 cells) play a role in triggering the differentiation of WJ-MSCs into CAF-like cells. After every co-culture experiment, a cell lysate from WJ-MSCs was collected for western blot analysis. RNA from WJ-MSCs was extracted for real-time quantitative polymerase chain reaction (RT-qPCR) analysis.

Western blot results showed a clear gradual increase of α-SMA and vimentin expressions in WJ-MSCs co-cultured with WHCO1 cancer cells up to a maximum of 16 days (Figure 2.9 A). The quantification of SMA and vimentin band intensities normalised to GAPDH from western blot analysis using densitometric analysis is shown in Figure 2.9 A. These results were substantiated with RT-qPCR analysis where the expression of Actin, alpha 2, smooth muscle aorta actin (ACTA2) (α-SMA gene) showed an increase in WJ-MSCs co-cultured with WHCO1 and MDA MB231 cancer cells over 24 days (Figure 2.9 B). After WHCO1 and MDA MB231 cancer cells were removed from the co-culture system, the expression of α-SMA and vimentin decreased (Figure 2.9 A).

This study has shown that cancer cells can possibly trigger WJ-MSC differentiation into cells that behave like CAF through the expression of α-SMA and vimentin. This study further investigated the role of TGF-β and 1 μM 5-azacytidine in the differentiation of WJ-MSCs. TGF-β has been proposed as a factor released by both cancer cells and stromal cells to influence their interaction, as well as an important molecule capable of inducing MSC differentiation into CAF-like cells [140]. Studies have shown that the silenced DNA can be demethylated by epigenetic modifiers such as 5-azacytidine. Through 5-azacytine treatment, MSCs can be transformed into myogenic lineages that also express α-SMA, FSP, and vimentin [142, 267].

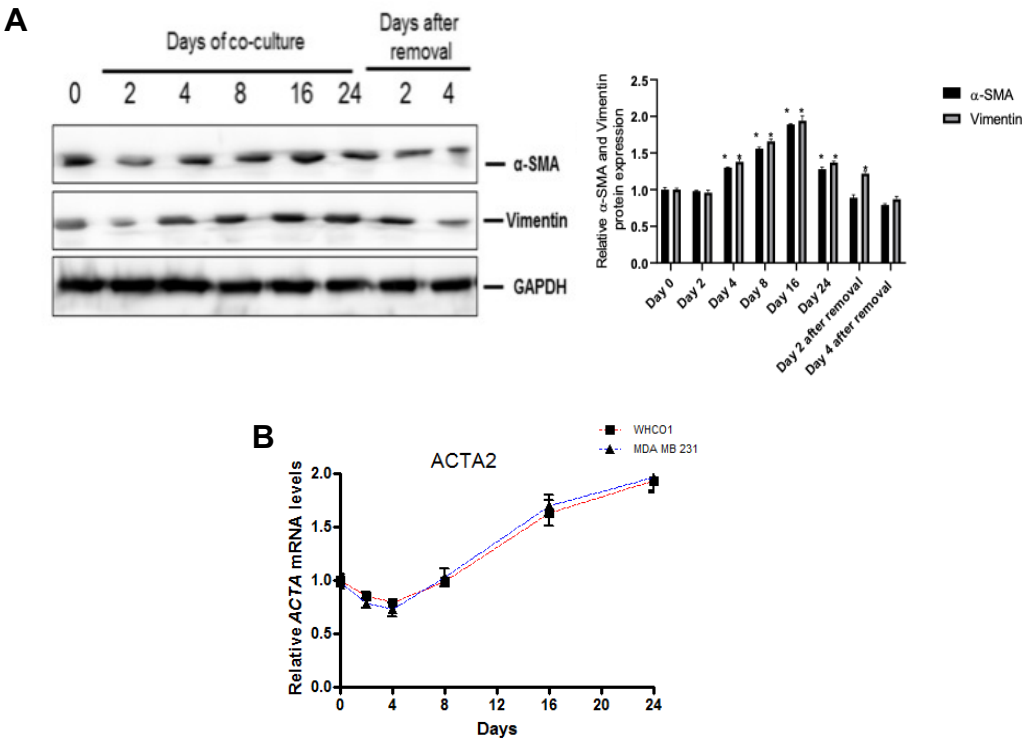

Figure 2. 9. The effect of cancer cells on MSCs differentiation and their expression of levels of CAFs markers. Cancer cells and WJ-MSCs were co-cultured in transwell plates, where 5 x 10^5 of WJ-MSC cells were cultured on the upper insert and cancer cells (WHCO1 or MDA MB231) were cultured on the lower compartment. **(A)** Western blot analysis of α-SMA and vimentin expression of lysate from WJ-MSCs co-cultured with WHCO1 cancer cells over an incubation period of 24 days. **(B)** RT-qPCR analysis of the ACTA2 expression in WJ-MSCs co-cultured with WHCO1 and MDA MB231 cancer cells. Densitometric analysis of α-SMA and vimentin relative GAPDH were normalised to day 0. Data shown are the mean ± SEM experiments performed in triplicates and repeated at least two independent times. *p≤ 0.05.

2.2.2.2 The effect of cancer cells, TGF-β and 1 μM 5-azacytidine on the differentiation of WJ-MSC.

WJ-MSCs (5 x 105) were co-cultured with cancer cell lines (WHCO1 and MDA MB231) (5 x 105) for up to 16 days to explore the involvement of TGF-β in MSCs differentiation, 5-azacytidine, and cancer cells in the differentiation of WJ-MSCs into CAFs through the expression of SMA and type I collagen. Treatment of MSCs with 5-azacytidine has been shown to reduce the methylation promoter, resulting in an increased gene expression and differentiation [267]. After 16 days of culture, cell lysates from MSCs were prepared for western blot analysis and RNA from MSCs was extracted for RT-qPCR analysis. In another experiment, WJ-MSCs cultured without cancer cells were treated with TGF-β and 5-azacytidine to final concentrations of 10 nM and 1 μM, respectively.

Western blot data showed that exposure of WJ-MSCs to WHCO1 oesophageal and MDA MB231 breast cancer cells resulted in increased expression of α-SMA and type I collagen in WJ-MSCs (Figure 2.10 A-D). Treatment with 10 nM TGF-β (Figure 2.10 A, B) and 1 μM 5-azacytidine (Figure 2.10 C, D) also resulted in increased expression of α-SMA and type I collagen for up to 48 hours. Western blot quantification by densitometric analysis using GAPDH as a loading control to quantify protein band intensities is shown (Figure 2.10 A-D). RT-qPCR results substantiated the western blot data, where it was observed that type I collagen and ACTA2 gene expression was upregulated in co-cultured WJ-MSCs or WJ-MSCs treated with 10 nM TGF-β and 1 μM 5-azacytidine (Figure 2.11 and Figure 2.12). In addition, this study evaluated the expression of Smad2 and Smad3 genes, structurally similar genes and thought to be equally important in mediating TGFβ signals [268]. This analysis showed that Smad2 (Figure 2.13 A, C) and Smad3 (Figure 2.13 B, D) was increased in WJ-MSCs co-cultured with WHCO1 cancer cells. The treatment of WJ-MSCs with 10 nM TGF-β (Figure 2.13 A, B) or 1 μM 5-azacytidine (Figure 2.13 C, D) also increased expression of Smad2 and Smad3 in WJ-MSCs.

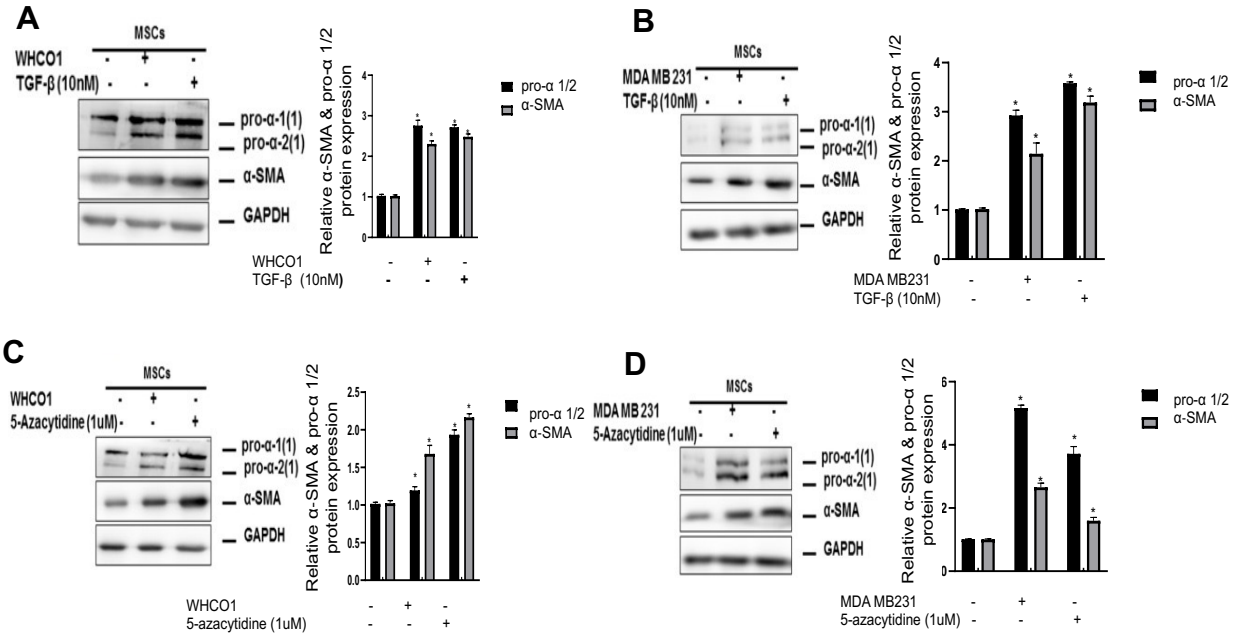

Figure 2. 10. The effect of cancer cells, TGF-β and 1 μM 5-azacytidine on the differentiation of WJ-MSCs. Cancer cells and WJ-MSCs were co-cultured in transwell plates, where WJ-MSC were cultured on the upper insert and cancer cells (WHCO1 or MDA MB231) were cultured on the lower compartment. **(A, C)** Western blot analysis of α-SMA and type I collagen expression levels from WJ-MSCs lysate co-cultured with WHCO1 and **(B, D)** MDA MB21 cancer cells for 16 days or after the addition of **(A, B)** 10 nM TGF-β and **(C, D)** 1 μM 5-azacytidine. Densitometric analysis of α-SMA and type I collagen relative to loading control (GAPDH) were normalised to WJ-MSC cultured alone. Data shown is the mean ± SEM experiments performed in triplicates and repeated at least three independent times. Statistical significance was determined by student paired t-test (*$p \leq 0.05$).

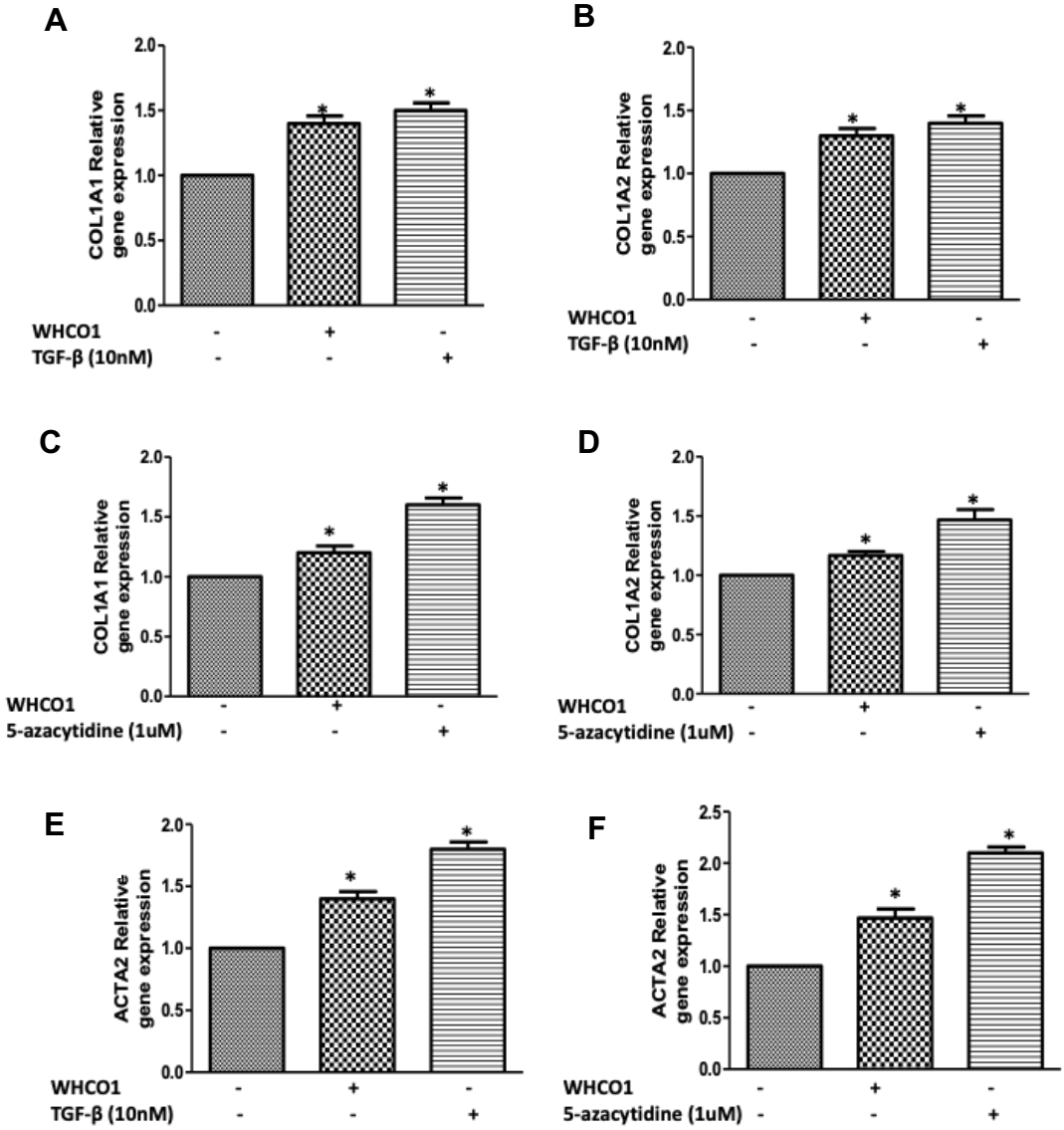

Figure 2. 11. The effect of cancer cells, TGF-β and 1 μM 5-azacytidine on the differentiation of WJ-MSCs. Cancer cells and WJ-MSCs were co-cultured in transwell plates, where WJ-MSC were cultured on the upper insert and WHCO1 cancer cells were cultured on the lower compartment. RT-qPCR analysis of **(A-D)** type I collagen and **(E, F)** ACTA2 gene expression levels from WJ-MSCs RNA co-cultured with WHCO1 cancer cells for 16 days. RT-qPCR analysis of type I collagen in WJ-MSCs after the addition of **(A, B)** 10 nM TGF-β and **(C, D)** 1 μM 5-azacytidine. RT-qPCR analysis of ACTA2 gene expression level in WJ-MSC treated with **(E)** 10 nM TGF-β and **(F)** 1 μM 5-azacytidine. The mean ± SEM experiments performed in triplicates and repeated at least three independent times are shown. Statistical significance was determined by student paired t-test (*$p \leq 0.05$).

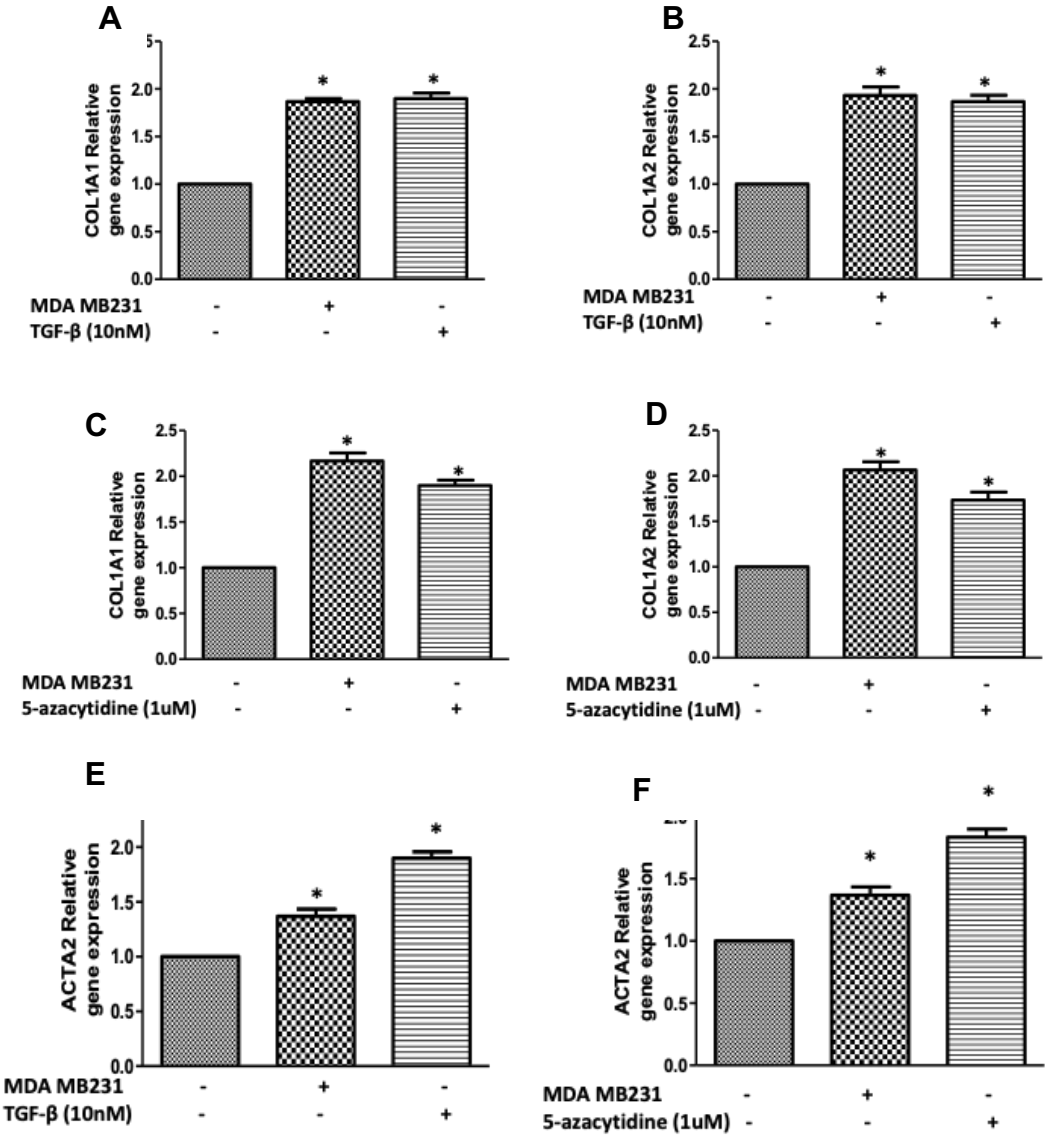

Figure 2. 12. The effect of cancer cells, TGF-β and 1 μM 5-azacytidine on the differentiation of WJ-MSCs. Cancer cells and WJ-MSCs were co-cultured in transwell plates, where WJ-MSC were cultured on the upper insert and MDA MB231 cells were cultured on the lower compartment. RT-qPCR analysis of **(A-D)** type I collagen and **(E, F)** ACTA2 gene expression levels from WJ-MSCs RNA co-cultured with MDA MB231 cancer cells for 16 days. RT-qPCR analysis of type I collagen in WJ-MSCs after the addition of (A, B) 10 nM TGF-β and **(C, D)** 1 μM 5-azacytidine. RT-qPCR analysis of ACTA2 gene expression level in WJ-MSC treated with **(E)** 10 nM TGF-β and **(F)** 1 μM 5-azacytidine. Data shown is the mean ± SEM experiments performed in triplicates and repeated at least three independent times. Statistical significance was determined by student paired t-test (*$p \leq 0.05$).

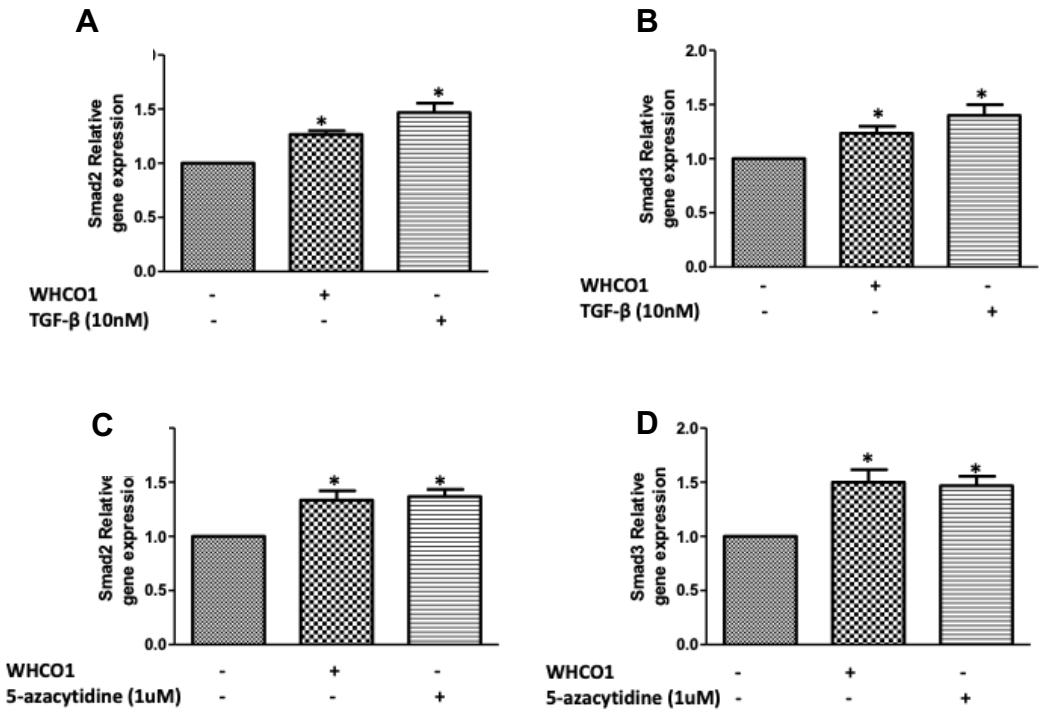

Figure 2. 13. The effect of cancer cells, TGF-β and 1 μM 5-azacytidine on the differentiation of WJ-MSCs. Cancer cells and WJ-MSCs were co-cultured in transwell plates, where WJ-MSC were cultured on the upper insert and MDA MB231 cells were cultured on the lower compartment. RT-qPCR analysis of **(A, C)** Smad2 and **(B, D)** Smad3 gene expression levels from WJ-MSCs RNA co-cultured with WHCO1 cancer cells for 16 days, or after the addition of **(A, B)** 10 nM TGF-β and **(C, D)** 1 μM 5-azacytidine. Data shown is the mean ± SEM experiments performed in triplicates and repeated at least three independent times. Statistical significance was determined by student paired t-test (*p≤ 0.05).

2.2.3 The effects of TGF-β inhibition on the differentiation of WJ-MSCs co-cultured with cancer cells.

TGF-β inhibitor SB431542 (10 nM) or TGF-β siRNA were added to the co-culture system to see if TGF- has a role in the expression of the CAF marker (α-SMA) in WJ-MSCs co-cultured with cancer cells. WJ-MSCs were cultured in the upper insert and cancer cells (WHCO1 or MDA MB231) were cultured in the lower compartment as described in the legend to figure 2.9. TGF-β inhibitor SB 431542 was added to the co-culture media to a final concentration of 10 μM and co-culture was continued for 16 days. Western blot analysis was used to determine the expression of α-SMA in co-cultured WJ-MSCs. Results show that the addition of SB431542 decreased the levels of α-SMA in WJ-MSCs exposed to WHCO1 or MDA MB231 cancer cells (Figure 2.14 A, B). The co-culture of WJ-MSCs and cancer cells was continued for 16 days after treatment with TGF-β siRNA at 100 nM concentration. Transfections were done every three days till the end of the experiment to sustain TGF-β knockdown in cells. The data show that inhibition of TGF-β expression in co-culture WJ-MSCs resulted in

decreased expression of α-SMA (Figure 2.14 C, D). In addition, it was observed that TGF-β knockdown in both WHCO1 and MDA MB231 cells during co-culture decreased the α-SMA protein levels (Figure 2.14 E, F). Quantification by densitometry of α-SMA band intensities normalised to GAPDH of western blot analysis is shown in Figure 2.14 (A-F).

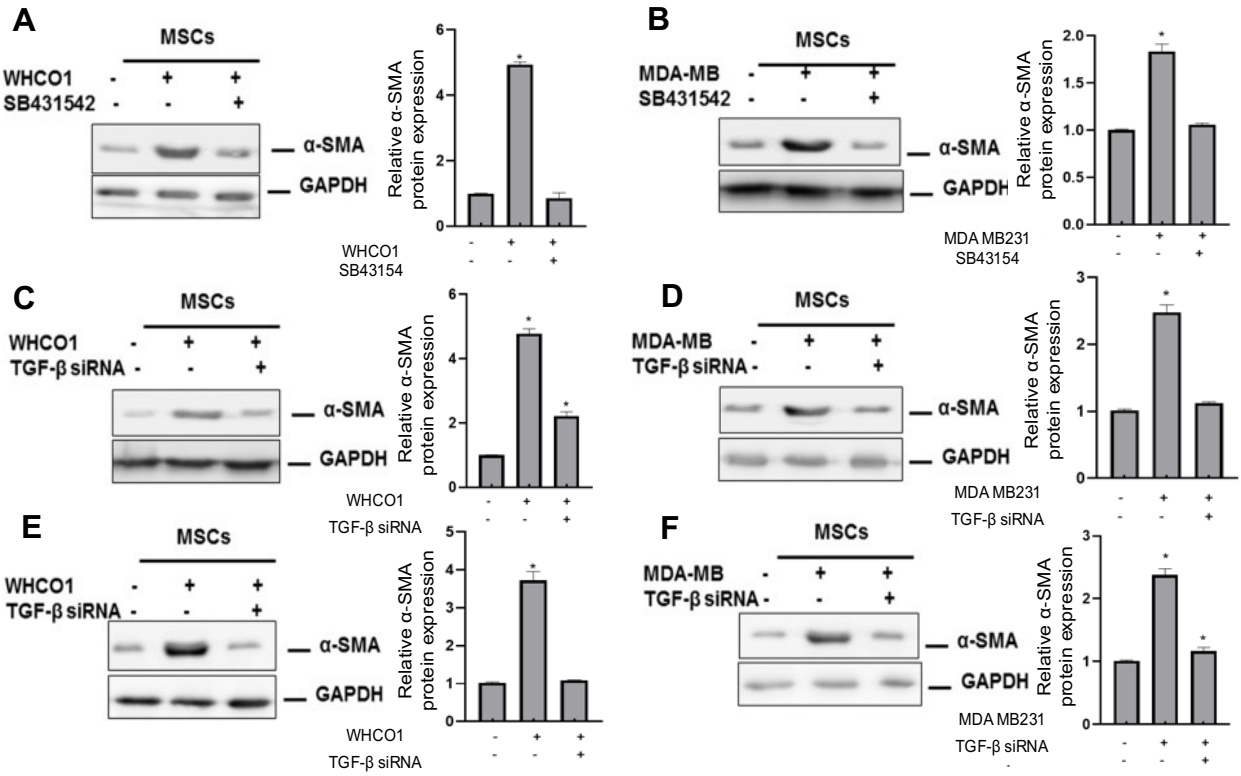

Figure 2. 14. Co-cultured WJ-MSCs showed reduced expression of α-SMA after inhibition of TGF- β. TGF-β inhibitor SB 431542 or TGF-β siRNA was added to the co-culture media and co-culture was continued for 16 days. Western blot analysis was used to determine the expression levels of α-SMA in co-cultured WJ-MCSs. **(A, B)** α-SMA expression levels in co-cultured WJ-MSCs after addition of TGF-β inhibitor SB431542. **(C, D)** The expression α-SMA in co-cultured WJ-MSCs after TGF- β siRNA addition. **(E, F)** The expression α-SMA in co-cultured WJ-MSCs following WHCO1 or MDA MB231 treatment with TGF- β siRNA. Quantification by densitometric analysis of α-SMA band intensities is normalised to GAPDH. Data shown is the mean ± SEM experiments performed in triplicates and repeated at least three independent times. *p≤ 0.05.

2.2.4. The response of cancer cells co-culture with WJ-MSCs to anticancer drugs.

This study shows that MSCs can be attracted to the tumour site by cancer cells and become part of the TME as CAF-like cells. CAFs or MSCs have been shown to play significant roles in cancer progression and cancer cell resistance to chemotherapy. Thus, this study investigated whether WHCO1 and MDA MB231 cancer cells co-

cultured with WJ-MSCs would respond differently to the anticancer drugs compared to cancer cells alone. Co-cultured WHCO1 and MDA MB231 cancer cells were then treated with increasing concentrations of cisplatin and paclitaxel for 48 hours. After 48 hours of treatment, cells were counted with a Countess Cell counter using Trypan Blue exclusion method. Cell survival was expressed as a percentage of cells treated with 0.1% DMSO (solvent) (control). Results showed that WHCO1 and MDA MB231 cells were slightly less sensitive to paclitaxel (Figure 2.15 A, C) and cisplatin (Figure 2.15 B, D) treatment when co-cultured with WJ-MSCs than WHCO1 (Figure 2.15 A, B) and MDA MB231(Figure 2.15 C, D) cells alone.

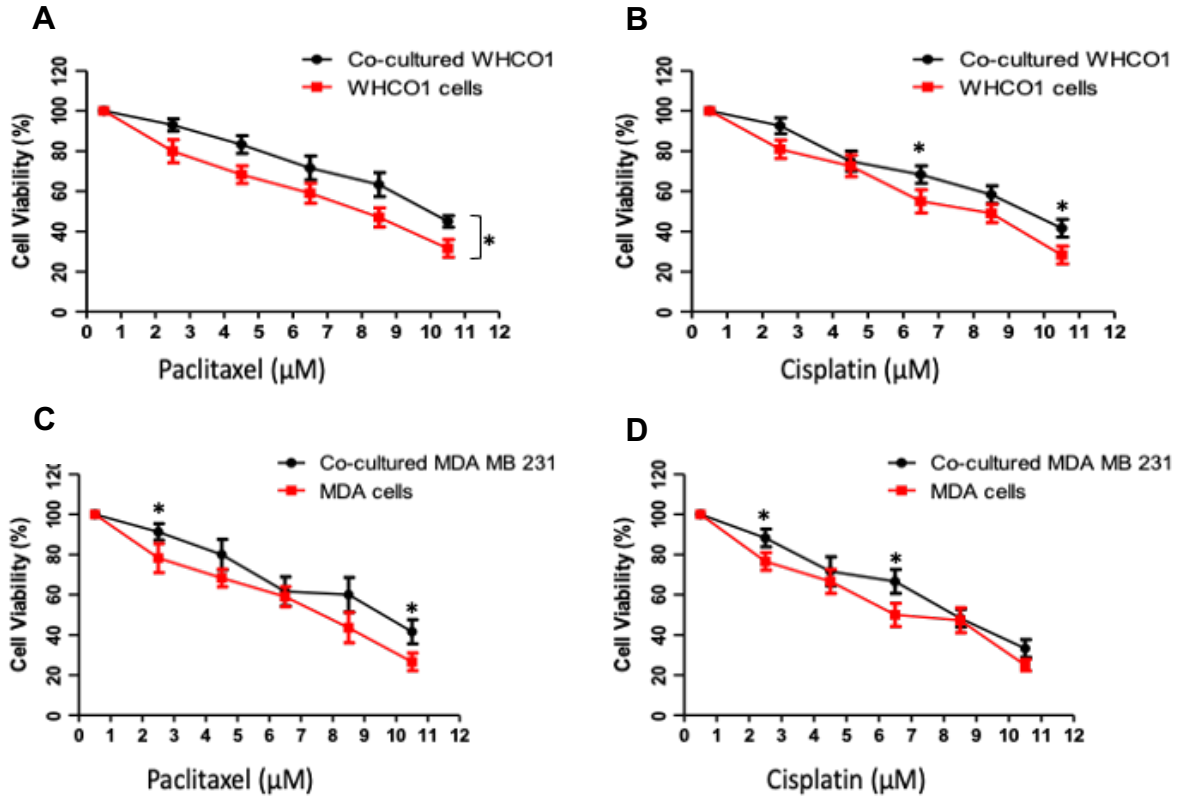

Figure 2. 15. The response of cancer cells co-culture with WJ-MSCs to anticancer drugs. Co-cultured **(A, B)** WHCO1 and **(C, D)** MDA MB231 cancer cells were treated with increasing concentrations of **(A, C)** paclitaxel and **(B, D)** cisplatin for 48 hours. Cell counting was done using Trypan Blue exclusion method. Shown are the mean ± SEM experiments performed in triplicates and repeated at least two independent times. *p≤ 0.05.

2.3 Discussion

This study reports the expression CAFs markers in several human cancers and their relationship with MSC markers. First, online public databases were used to determine the expression of CAF markers and MSC markers in different cancer. Then the study investigated the correlation between CAF markers and MSC markers.

In the tumour microenvironment, CAFs and MSCs play a crucial roles in the growth and metastasis of cancer, as well as the development of resistance to therapy. These cells have typically been identified using various markers. Based on the Oncomine database, this study found that CAF markers (ACTA2, FAP and S100A4), compared to normal tissues, were highly expressed in several cancers, including breast, oesophageal, head and neck and lymphoma tissues. A study by Schmidt-Hansen et al. (2004) showed that co-cultures of tumour cells with fibroblasts could stimulate the release of S100A4, which plays an extracellular role in tumours and fibroblasts [269]. In addition, S1004A is described to play a role as being an angiogenic factor and increases MMP expression [270]. On the other hand, ACTA2 (α-SMA gene) in lung adenocarcinomas patients is associated with increased distant metastasis and poor prognosis [271]. In another study by Jia et al. (2014), the expression of FAP was found to be significantly associated with poor outcomes in breast cancer patients [272]. Furthermore, this study showed that MSC markers are highly expressed in breast, oesophageal, head and neck and lymphoma tumours compared to normal tissues. A study in gastric cancer found that cells expressing CD73, CD90 and C105 are involved in the progression of the disease [273].

Furthermore, genes involved in CAFs and MSCs, such as TGF-β and collagen, are upregulated in several cancers compared to normal tissues. TGF-β induces the expression of growth factors, cytokines, and ECM proteins in CAFs, as well as playing a role in the differentiation of MSCs into CAFs [274, 275]. Yu et al. (2014), showed an increase in the aggressiveness of breast cancer through EMT, with increased cell-ECM adhesion, invasion and migration when CAFs with α-SMA expression secreted TGF-β 1 [276]. Thus, this study may help us understand the interaction between cancer cells and their stroma.

Using the Timer database, it was shown that MSC markers were correlated with CAF markers FAP in breast carcinoma, with ACTA2 correlated with CD73, CD90 and CD105. However, analysis of oesophageal carcinoma showed that FAP and ACTA2 expression were significantly correlated with CD45, CD90 and CD105. This may suggest that CAF markers FAP and ACTA2 marker might not be correlated with CD73 in OSCA and warrant further research on these markers in OSCA. This study is one of few studies to report the correlation between CAF markers and MSCs markers. However, in a study by Paunescu et al. (2011), CAFs and MSCs were found to share important similarities, including the presence of cell surface molecules and expression of proteins such as Vimentin and α-SMA [277]. Moreover, CAFs and other stromal cells also highly express genes associated with the mesenchymal subtype rather than cancer cells [278]. Combined with findings from this study, the evidence points to the possibility that CAFs can be derived from MSCs, which may suggest a genealogical relationship between them.

According to Jena et al. (2020), there is substantial evidence supporting the notion that CAFs mediate resistance of solid tumours to anticancer drugs [263]. The secretion of growth factors and cytokines by CAFs contributes to tumour growth, angiogenesis, and drug resistance. In many cellular settings, the occurrence of chemoresistance is mediated via increased efflux of the drug, which is induced by activating the ABC transporter [279]. The current study analysed the correlation between CAF marker expression and ABC transporter expression levels. A significant correlation was found between CAF markers (FAP or ACTA2) and ABC transporter genes (ABCC1-3 and ABCB1). In pancreatic cancer, the expression of ABCC1 was showed to be positively associated with that of TGF- β 1, ACAT2, FAP, or PDGFRB [280]. Furthermore, CAF derived IL-8 encourages chemoresistance in human gastric cancer by activating NF-κB and increasing ABCB1 expression [281]. These findings provide evidence suggesting that CAFs regulate drug sensitivity of cancer cells.

The CAF marker FAP interacts with proteolytic enzymes like as dipeptidyl peptidases (DPPs), which are suitable therapeutic targets for treating human diseases, according to analysis of the PPI networks [282, 283]. For example, the inhibition of DPP8/9 induces cell death in myeloma cells [283]. In addition, ACTA2 interacts with cancer-related genes such as MYH11, CNN1 and MYCOD, which have been linked to poor

prognoses for cancer patients [284-286]. These results indicate that CAF markers may be used as novel therapeutic targets for cancer treatment.

Many studies have shown that CAF interactions with cancer cells play an important role in tumour growth, however, the precise origin and function of CAFs are still unclear. This study investigated whether WJ-MSC exposed to cancer cells will differentiate into CAFs and express CAF markers. The role of differentiated WJ-MSCs in cancer cell drug response was investigated using co-culture systems.

The effects of oesophageal WHCO1 and breast MDA MB231 cancer cells on Wharton's Jelly-derived mesenchymal stromal/stem cell (WJ-MSC) gene expression were investigated over 24 days of culture. Long term culture of cancer cells with WJ-MSCs triggers WJ-MSC differentiation into CAF-like cells via the expression of the CAF markers, α-SMA and vimentin. These results are in agreement with a previous study that showed that long term exposure of MSCs to tumour conditioned medium from breast cancer cells induced a phenotype that resembles myofibroblast-like features in CAFs and increased expression of vimentin, α-SMA and FAP [287]. TGF-β is one of the growth factors secreted by cancer cells in order to evade immune detection and it has been shown to increase the expression of CAF markers. TGF-β plays a role in the activation of fibroblasts by inducing intracellular signalling pathways. One member of the TGF-β superfamily, Nodal, converts normal fibroblasts to CAFs together with TGF-β signalling pathway activation in fibroblasts [288]. Treatment of MSCs with TGF-β or 5-azacytidine has been shown to induce MSCs differentiation into CAFs. These findings are in agreement with our study that showed that treatment of naïve MSCs with exogenous TGF-β and treatment of naïve MSCs with 5-azacytidine for up to 48 hours resulted in increased expression of α-SMA and type I collagen similar to MSCs co-cultured with these cells for 16 days.

When MSCs were co-cultured with oesophageal or breast cancer cells, differentiation and expression of myofibroblast lineage markers were observed. Furthermore, an increased expression of α-SMA was observed following incubation of WJ-MSCs treated with TGF-β for up to 48 hours. It is possible that the addition of TGF-β to the co-culture system may have accelerated phenotypic changes in the WJ-MSC and the

expression of α-SMA in comparison to WJ-MSCs cultured alone. A further investigation of CAFs markers on WJ-MSCs cultured alone was not performed in this study. However, a study showed that, when treated to tumour conditioned medium for short to longer days, MSCs exhibited increasing amounts of vimentin, α-SMA, and FSP, indicating that these cells were developing into myofibroblasts as opposed to MSCs alone, which expressed decreasing amounts of each protein [142]. Furthermore, another study showed that α-SMA and FAP in co-culture group significantly increased relative to MSCs culture alone [289]. Therefore, these findings support the hypothesis that co-culturing cancer cells with MSCs might enable MSCs to develop the CAFs phenotype.

Many studies have shown that ACTA2 (α-SMA) gene transcription is regulated by interacting with several signalling pathways [271, 290]. To substantiate these results, TGF-β inhibitor SB 431542 was added to the co-culture media. The addition of a TGF-β inhibitor resulted in the decreased expression of α-SMA in MSCs exposed to cancer cells. Knockdown of TGF-β in WJ-MSCs or cancer cells using TGF-β siRNA resulted in decreased α-SMA protein levels in MSCs exposed to cancer cells. Research has shown that activation of the TGF-β receptor complex initiates several of downstream cascades like the Smad2/3 signalling pathways [291]. Similarly, this study also observed increased expression of Smad2/3 in WJ-MSCs co-cultured with cancer cells or treated with TGF-β or 5-azacytidine. These results show that the TGF-β/Smad signalling pathway is involved in the differentiation of MSCs into CAFs and that TGF-β is probably secreted by both MSCs and cancer cells. Interestingly, results from this study are consistent with those of a study showing that human bone marrow MSCs transduced with lentiviral vectors inhibiting TGF-β/Smad signalling have a reduced expression of CAF markers when co-cultured with cancer cells or treated with tumour-conditioned medium [292].

Moreover, this study suggests that factors secreted by tumour cells can recruit MSCs and influence them to become part of the TME. Importantly, when WHCO1 and MDA MB231 are co-cultured with “cancer cell activated” WJ-MSCs, they marginally survived treatment with paclitaxel and cisplatin better than WHCO1 and MDA MB231 cancer

cells alone. It is evident that the presence of WJ-MSCs, possibly through the secretion of growth factors, protected the cancer cells from the effect of the drugs used.

In summary, this study showed that CAF and MSC markers were upregulated in several cancer types compared to normal tissues. The study also showed that there is a relationship between CAF markers and MSC markers. Functional and correlative analyses of patient material indicate that targeting CAFs may lead to improved treatment strategies. The CAF markers also interacted with drug resistance genes as well as genes associated with poor prognosis. This study demonstrated that co-culturing cancer cells and WJ-MSCs holds great promise for providing an approach in which the interaction between stromal and tumour cells can be studied. This study developed a cell culture method for generating cancer-associated fibroblasts, a key component of tumour stroma. A better model for understanding the interplay between different stroma cells and cancer cells within the tumour microenvironment will be important in the development of strategies for improving tumour therapy.

CHAPTER 3:

CANCER STEM CELLS ENHANCE CHEMORESISTANCE, AND METASTATIC BEHAVIOUR IN HUMAN OESOPHAGEAL CANCER.

3.1 Introduction

There are many factors that determine prognosis for cancer, including tumour stage and differentiation [145, 146, 293, 294]. However, these clinical criteria are frequently insufficient for risk stratification, resulting in incorrect clinical prognosis predictions. A reliable prognostic factor that can accurately predict clinical prognosis is urgently needed for cancers that are not well studied, such as oesophageal cancer. Cancer stem cells have varying predictive value depending on the type of cancer and histological subtype [295-297]. Several studies have demonstrated the existence of therapy-resistant cancer stem-like cells as a probable mechanism for the recurrence and spread of oesophageal cancer after treatment [15, 145, 146]. Patients with oesophageal cancer may become chemoresistent to 5-fluorouracil and cisplatin by expressing high levels of miR-200 and CSC-related proteins [298, 299]. Furthermore, tissue samples from individuals resistant to neoadjuvant treatment with 5-fluorouracil, doxorubicin, and cisplatin showed elevated expression of the multidrug resistance protein 2 (MRP2) [300, 301].

Tumours are a heterogeneous population of cells with different phenotypes [145, 146]. Recent data suggest that tumours contain a subset of cells called cancer stem cells that have stem cell-like features (CSCs) [145, 146, 154]. Melanoma, glioma, breast, ovarian, and head and neck cancers have all been identified to have CSCs. [145, 302-304]. CSCs have been found to alter neoplastic cell behaviour, aggressiveness, and therapeutic responsiveness, in addition to being crucial in the initiation, maintenance, and relapse of tumours. CSCs are rare cancer cells that have the capacity to self-renew and proliferate over a long time. Additionally, they can resist chemotherapy and radiotherapy [145, 305, 306]. They are capable of forming tumour spheres *in vitro*, and their ability to create xenograft tumours in immunocompromised SCID mice has indicated that they contain tumourigenic cells [307, 308]. Cell sorting technology has

been used to isolate CSCs that use antibodies against various surface markers, including cluster of differentiation 44 (CD44), CD133, CD24, and CD166 [309-311]. The CD44+/CD24- phenotype has been linked to a considerably worse prognosis in several malignancies, including breast cancer, according to various studies [312, 313]. Other markers, such as aldehyde dehydrogenase 1 (ALDH1) and p63, have also been demonstrated to be useful in this regard [314, 315]. CSCs can also be identified and isolated through side population technique. With dual-wavelength FACS analysis, side population cells can be isolated and identified in tumours as a small subpopulation of cancers have stem cells-like properties [316, 317]. In several cancers, it has been shown that the side population cells are enriched with CSCs and can be isolated using Hoechst 33342 dye [316, 318]. In cancer therapy, CSCs are a promising target and any therapy that targets CCs may improve cancer treatment and survival. However, there are not a lot of studies that describe the relationship between OSCC prognosis and CSC markers.

In this study, it was hypothesised that cancers contain a small subset of cancer cells called cancer stem cells (CSCs) which can be isolated via the side population (SP) technique. These CSCs have stem-cell properties, are responsible for tumour initiation, growth, migration, and resistance to chemotherapy. To test this hypothesis, the presence of CSCs markers in oesophageal tumour biopsies was investigated as well as studied in isolated FACS-sorted OSCC and breast cancer side population cells. Overall, this study provides evidence that CSCs are present in OSCC biopsies and the SP cells are an enriched source of tumour promoting, migratory, and drug resistant cells in human cancers. This suggests that CSCs-specific genes and signalling pathways may be a potential target for effective cancer therapies.

3.2 Results

3.2.1 Marker expression in oesophageal squamous cell carcinoma.

RT-qPCR and immunohistochemistry were used to evaluate the expression of CSC and proliferation markers in OSCC biopsies. This section focuses mainly on oesophageal cancer.

3.2.1.1 Immunohistochemical staining analysis of CSC and proliferation marker expression in clinical OSCC samples.

The expression of CSCs markers was analysed in biopsy samples from patients with histopathologically confirmed OSCC. The clinicopathological characteristics of the patients are shown in Table 3.1 [319]. ALDH1A1 expression extended outward from the basement membrane occupied by stem cells in normal tissue resections, whereas robust expression was observed in tumour tissue (Figure 3.1). Immunohistochemical staining of OSCC tumour tissues showed that CD44 expression was significantly higher in tumour tissues than in normal tissue from the same patient (Figure 3.1). CD44 expression showed a disorderly pattern characteristic of dysplastic tissue architecture commonly observed in neoplastic lesions. CD44 expression was observed in normal tissues along with the basal epithelial layer, a region well known to contain normal oesophageal stem cells (Figure 3.1). The expression of CD44 was closely associated with the degree of cellular differentiation in oesophageal cancer patient samples. Possible keratin pearl structures were observed at 40x magnification of the oesophageal squamous cell carcinoma tissues. The keratin structures usual are present when cells undergo terminal differentiation.

In addition to CD44, CD133 was investigated as a possible marker that could be used to stratify oesophageal CSCs. Although CD133 co-expressed with CD44 [320], no CD133 expression was observed in both normal and OSCC tumour tissues (Figure 3.1). The expression of the proliferation marker, Ki67, was also assessed in normal and tumour tissues. In normal tissues, Ki67 expression was observed in specific cells along the basal epithelial layer extending to the apical surface of the oesophageal mucosa. In tumour tissues, Ki67 expression was more widely dispersed and observed in more cells, correlating with the expression level of CD44 (Figure 3.1).

Table 3. 1. Clinicopathological characteristics of OSCC samples from patients used in the study.

Biopsy Number	Histology	Sex	Age	Tumour Differentiation (Grade)	Tumour Site ICD-10	Invasive or infiltrating
543	OSCC	M	55	ND	C15.4	Infiltrating
547	OSCC	F	30	Moderate	C15.5	Invasive
551	OSCC	M	47	Moderate	C15.5	Invasive
556	OSCC	F	54	Moderate	C15.4	Invasive
561	OSCC	M	58	Moderate	C15.9	Keratinizing
563	OSCC	M	52	Moderate	C15.5	Infiltrating
569	OSCC	F	79	Poor	C15.4	Invasive
571	OSCC	F	48	Moderate	C15.3	Keratinizing
573	OSCC	F	41	ND	C15.3	Infiltrating
591	OSCC	M	47	Moderate	C15.4	Invasive
596	OSCC	F	67	Moderate	C15.4	Invasive
601	OSCC	M	59	ND	C15.4	Infiltrating
607	OSCC	F	48	Moderate	C15.4	ND
613	OSCC	M	54	Moderate	C15.9	Invasive
618	OSCC	F	60	Moderate	C15.4	Keratinizing
619	OSCC	M	57	Moderate	C15.4	Infiltrating
621	OSCC	F	64	Moderate	C15.4	Invasive
622	OSCC	F	83	ND	C15.4	Infiltrating
627	OSCC	M	52	Moderate	ND	ND
634	OSCC	F	57	Moderate	C15.4	Keratinizing
635	OSCC	M	57	Moderate	C15.4	Keratinizing

OSCC: Oesophageal squamous cell carcinoma
M: Male
F: Female
ND: Not determined

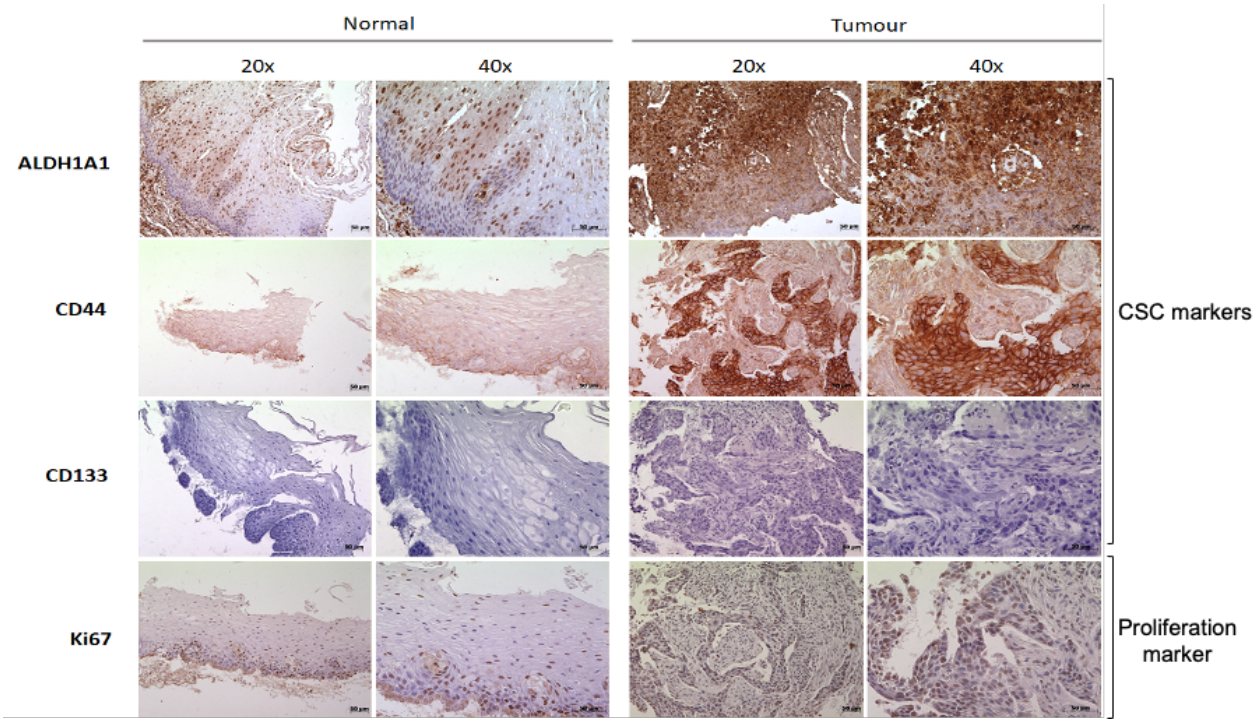

Figure 3.1. Representative expression of CSC and proliferation markers OSCC biopsies. Both normal and OSCC tumour tissues were stained with CSC markers (ALDH1A1, CD44 and CD133) and proliferation marker (Ki67) using immunohistochemical staining. Scale bar: 50 µm.

3.2.1.2 RT-qPCR analysis of CSC and proliferation marker expression in OSCC samples.

RT-qPCR using total RNA extracted from 21 matched normal and tumour biopsies from oesophageal cancer patients substantiated the increased expression of CD44 and ALDH1A1 in patient tumour samples versus normal tissues (Figure 3.2 A). There were significantly reduced CD24 and CD133 mRNA levels in tumour tissues (Figure 3.2 A). CSCs are known to have elevated expression of several self-renewal markers such as Oct3/4, Sox2, Nanog and p63. The statistical analysis of RT-qPCR data showed significantly increased expression of Oct3/4, Sox2, Nanog and p63 in tumour tissues versus normal tissues (Figure 3.2 B). Results also showed that the expression of CK5/6, a sensitive marker for squamous differentiation, was low in tumour biopsies compared to normal biopsies.

Individual tumours are known to exhibit high heterogeneity of the major chromatin protein linker histone H1.0, with cells capable of self-renewal and tumour-initiating abilities showing significantly reduced expression of the protein [321]. Non-tumour

promoting cells, on the contrary, express significantly higher levels of the histone H1.0, one of multiple histone H1 variants. The H1F0 gene is encoded by H1.0. Therefore, the levels of the H1F0 gene and other H1 variants (*HISTH1A, HISTH1B and HISTH1C*) were evaluated in oesophageal cancer clinical samples from patients. RT-qPCR showed that *HIF0, HISTH1A, HISTH1B* and *HISTH1C* were expressed at deficient levels in OSCC tumour tissue samples relative to normal tissue samples from the same patient (Figure 3.2 C). In addition, the expression of several ABC transporter proteins was also evaluated. The data showed that ABCB1, ABCG2, MDR-1 and MGMT mRNA levels were significantly higher in tumour tissue samples compared to normal tissue samples (Fig 3.2 D). Overall, the data confirmed the expression of markers associated with stem cell-like tumour cells in several epithelial cancers.

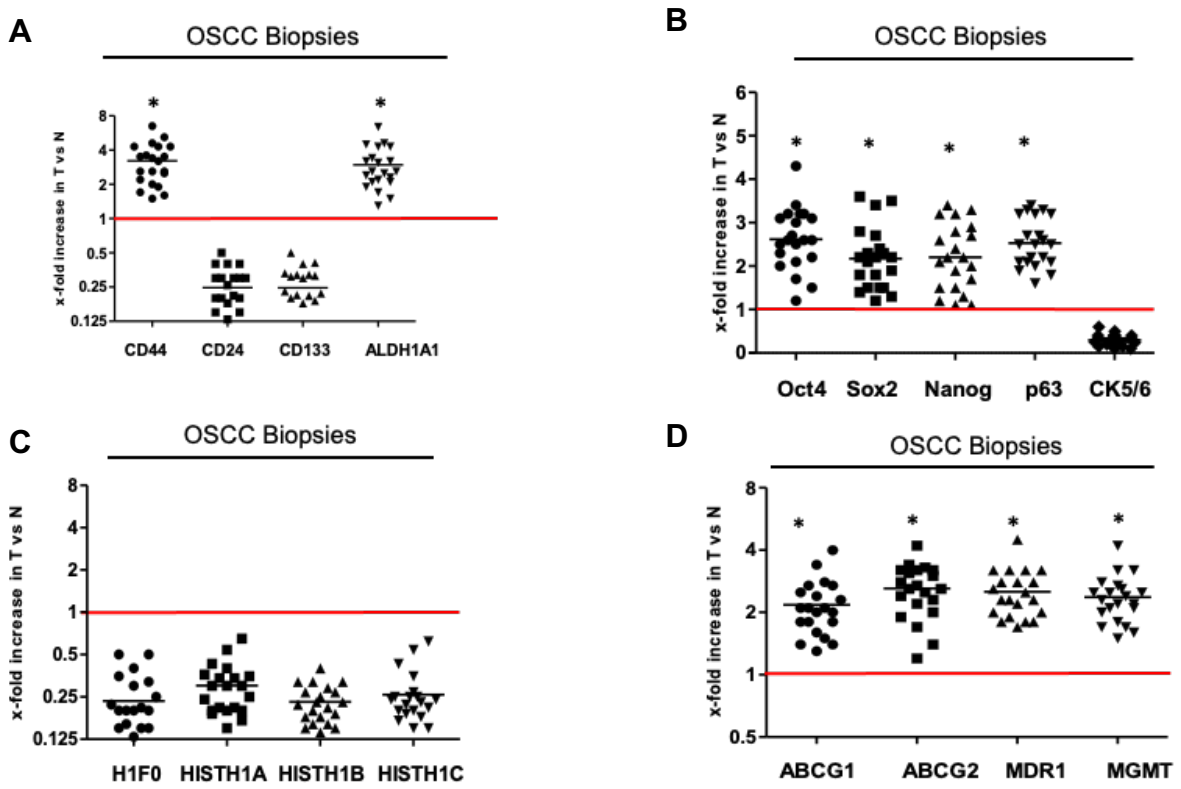

Figure 3.2. Expression of markers associated with CSCs in normal and tumour biopsies. RT-qPCR analysis of total RNA extracted from both normal and OSCC biopsies (n=21) to investigate the expression of **(A)** CSC markers, **(B)** self-renewal markers, **(C)** histone family genes and **(D)** drug resistant genes. The data shown is the mean ± SEM experiments performed in triplicate and repeated at least two independent times. (*p<0.05).

3.2.2 Characterisation of isolated side population cells from cancer cell lines.

Side population (SP) cells were isolated, enriched with CSCs, from cancer cell lines using two FACS based methods. These methods include the antibody-based method and the use of Hoechst stain. In addition, the tumour initiating behaviour of isolated side population cells as well as their response to chemotherapeutic drugs were investigated.

3.2.2.1 Isolation of CSCs from WHCO1 and MDA MB 231 cell lines.

Two fluorescent activated cell sorting (FACS)-based methods are generally used to isolate CSCs from cancer cells. These methods isolate the SP cells by either using antibodies against CSC markers or Hoechst stain. Preliminary analysis of the two methods showed that both methods isolated cells that expressed significantly high levels of CSC markers such as CD44, ALDH1A1 and ABCG2 (data not shown). Therefore, this study opted to continue with the Hoechst side population technique for this study (Figure 3.3 A, B). The isolation of CSCs using the Hoechst SP technique is based on the dye efflux ability of CSCs through ATP-binding cassette (ABC) transporters. In addition SP cells were isolated from both WHC01 oesophageal (Figure 3.3 A) and MDA MB 231 breast cancer cell lines (Figure 3.3 B). SP (gated P4) and cells (gate P5) were sorted separately for further analysis (Figure 3.3 A, B).

Western blot analysis was done to evaluate the expression of CSC markers and drug resistant genes in SP cells versus cancer cells. SP cells showed significantly increased levels of CD44, ALDH1A1, ABCG2 and MDR-1 compared to WHCO1 cells (Figure 3.3 C). Additionally, the breast cancer cell line MDA MB 231 was included in the analyses to confirm the specificity of the antibodies used and for comparative purposes. MDA MB 231 is one of the most malignant breast cancer lines known and has been shown to express high levels of CSC markers [322]. SP cells obtained from MDA MB 231 cell line showed similarly high levels of CSC markers and drug resistance proteins (Figure 3.3 D). Furthermore, qRT-PCR analysis of SP cells from several cancer cell lines supported western blot data for CSC markers, self-renewal markers, and drug resistance genes. (Figure 3.3 E). MDA MB 231 CSCs showed increased CD133 expression compared to MDA MB 231 cancer cells. Similar proliferative profiles and expression of CSC markers were obtained for WHCO1 OSCC

cell line, therefore, WHCO1 cells were chosen for further analyses. Where possible, other OSCC cell lines are also used to confirm the results.

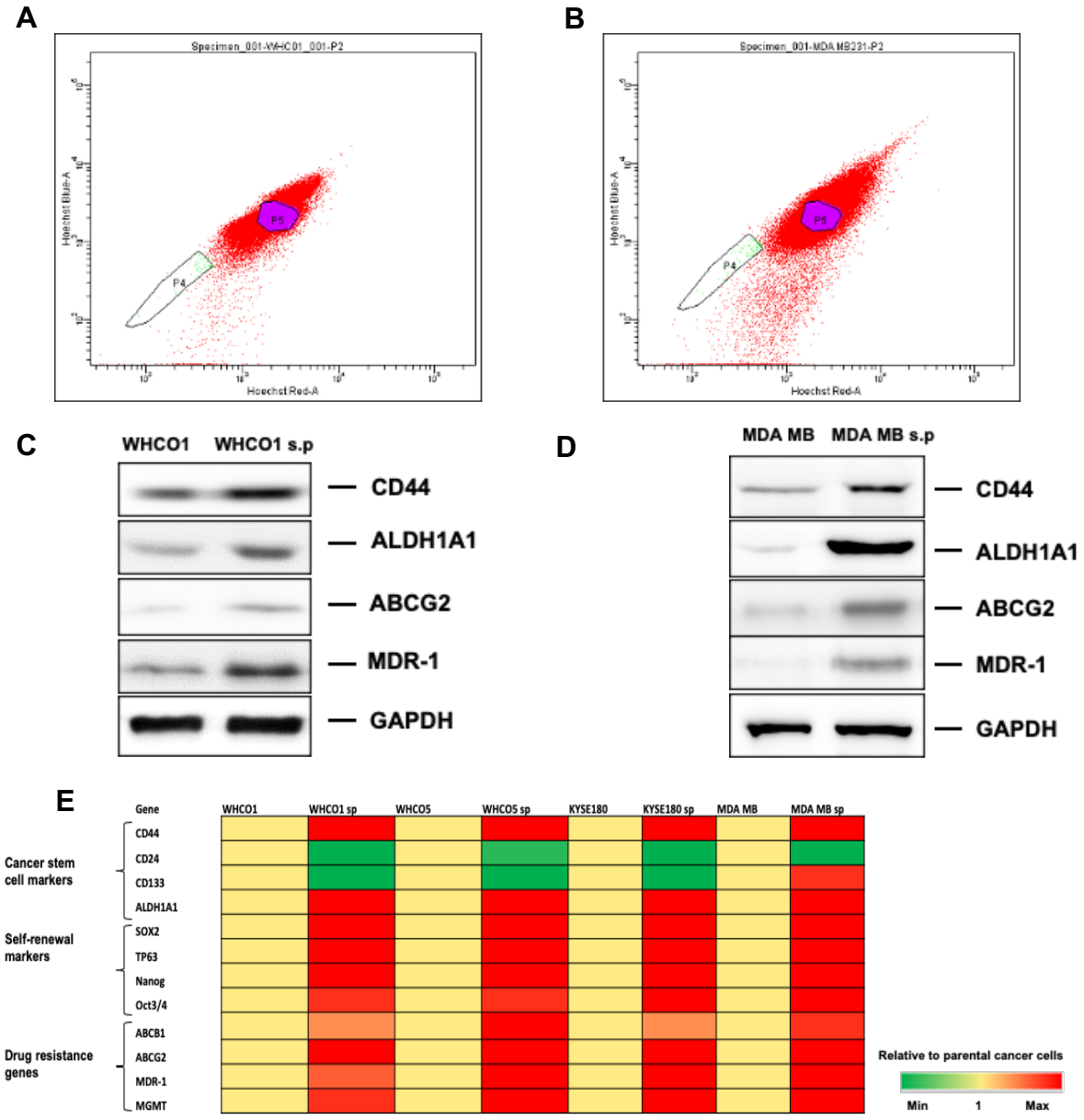

Figure 3.3. Isolation and characterisation of SP cells. SP and cancer cells were isolated by FACS sorting followed by propagation in tissue culture as described in Materials and Methods (section 7.2.4). **(A, B)** Representative flow cytometry profiles showing the sorted SP cells, Gate P4, and the cancer cells, Gate P5. The expression of CSC markers and drug resistance proteins were examined in **(C)** WHCO1 **(D)** and MDA MB231 SP and cancer cells using western blot analysis. GAPDH was used as a loading control. The results shown are representative of western blot analysis done three independent times. **(E)** RT-qPCR analysis of cancer cells and their corresponding side population cells evaluating CSC markers, self-renewal markers and drug resistance genes. Cancer cells were normalised and compared to the corresponding SP cells. The results are based on at least two independent experiments.

3.2.2.2 Morphological differences between WHCO1 and SP cells.

The morphological differences between OSCC cell lines and their corresponding side population cells using immunofluorescence using Phalloidin stain to bind to polymeric filament actin were investigated. WHCO1 cells and isolated SP cells were treated with 4.2 μM cisplatin for 24 hours and compared with untreated cells. At the end of the experiment, cells were stained with Phalloidin (green) and DAPI (blue) for the nucleus. No major morphological differences were found between untreated WHCO1 cells and their isolated SP cells (Figure 3.4). However, distinct morphological differences were observed between treated WHCO1 cells and isolated SP cells, with isolated SP cells appearing smaller and more rounded than cancer cells (Figure 3.4).

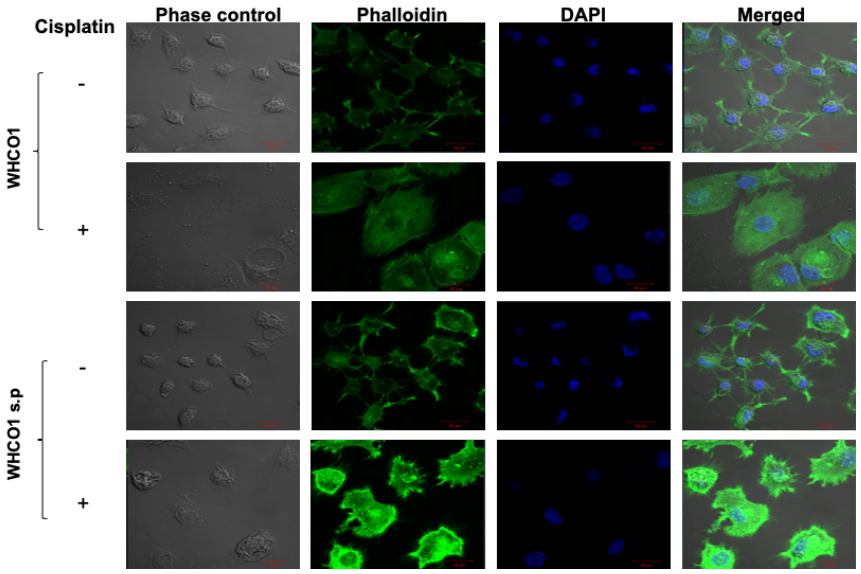

Figure 3. 4. Morphological differences between WHCO1 cells and their corresponding side population cells. WHCO1 cells and SP cells were cultured on glass coverslips and treated with 4.2 μM cisplatin for 24 hours as described in section 7.2.15. Cells were stained with FITC-conjugated Phalloidin (green) for F-actin and nuclei were stained with DAPI (blue). Representative immunofluorescent images of WHCO cancer and their isolated SP cells stained with Phalloidin (green) for F-actin and DAPI (blue). Scale bar= 20 μm. Results are representative of at least two independent experiments.

3.2.2.2 Isolation of SP cells and formation of tumourspheres.

Tumoursphere formation is commonly used to test for stem cell-like phenotype. WHCO1 cells and isolated SP cells were cultured in low attachment dishes to allow anchorage-independent growth. Culture of cells was continued for up to 16 days and fresh media was added every two days. The results showed that both oesophageal cancer cell lines, WHCO1 (Figure 3.5 A, C) and KYSE180 (Figure 3.5 B, D), and their

corresponding SP cells were able to form tumourspheres after 4 days. However, cancer cells formed tumourspheres that were smaller and loose, whilst tumourspheres formed by isolated SP cells were much larger and compact. Further analysis of WHCO1 cells, isolated CSCs and tumourspheres using western blot (Figure 3.5 E) and RT-qPCR (Figure 3.5 G) demonstrated that CSC markers and self-renewal markers are upregulated in tumourspheres compared to isolated SP cells. Quantification using densitometric analysis of CSCs and self-renewal marker band intensities are shown in Figure 3.5 F.

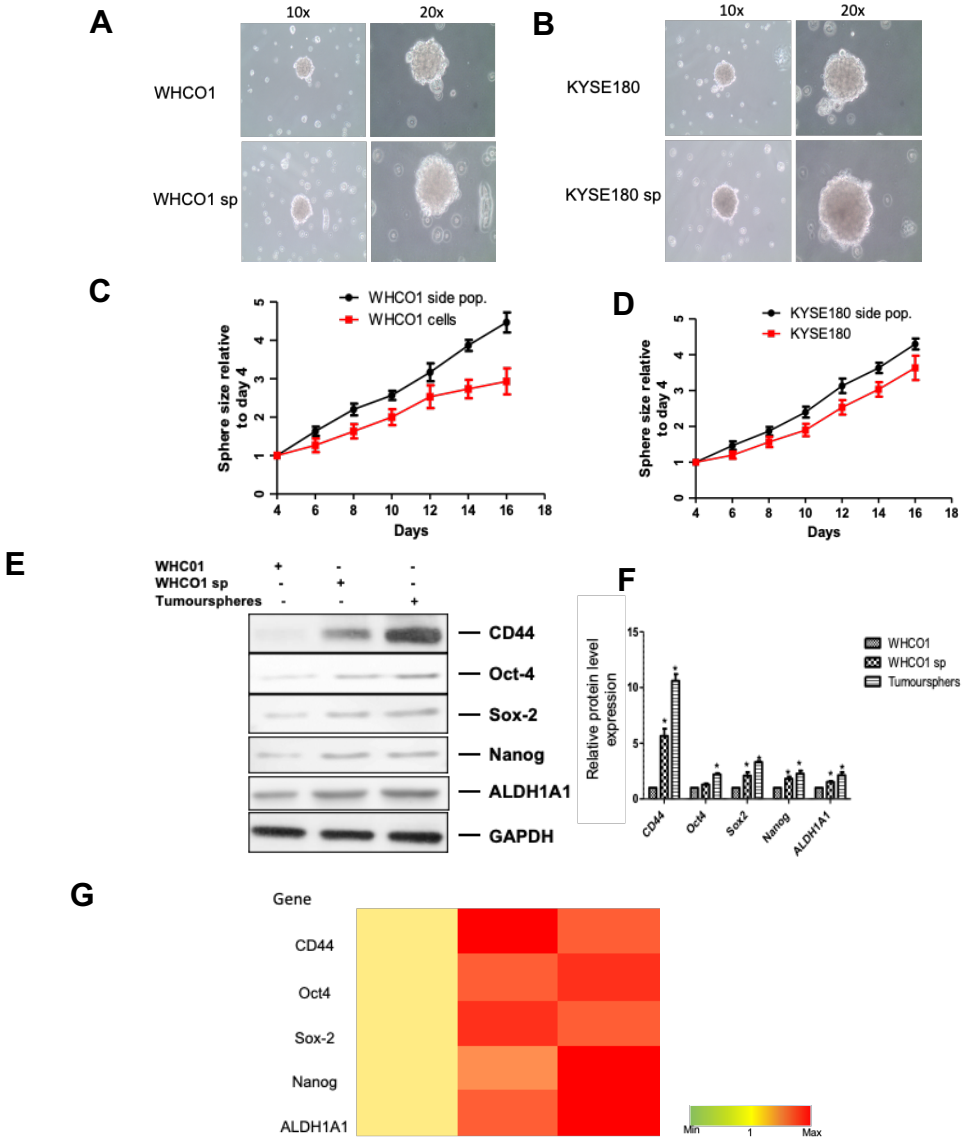

Figure 3. 5. The ability of isolated SP cells to form tumourspheres. Images representative of tumourspheres formed by **(A)** WHCO1 cells and isolated SP cells, **(B)** KYSE 180 cells and isolated SP cells after 16 days of culture. Sphere size analysis of **(C)** WHCO1 cells and **(D)** KYSE 180 cells. Sphere sizes were analysed relative to day 4. **(E)** Western blot and **(G)** RT-qPCR analyses were performed on WHCO1 cells, isolated CSCs and tumourspheres formed by SP cells. CSCs markers and self-renewal markers were upregulated in tumourspheres compared to isolated SP and WHCO1 cells. GAPDH was used as a loading control. **(F)** Densitometric analysis of band intensities relative to GAPDH was normalised to WHCO1 cells. Data shown are the mean ± SEM experiments performed in triplicates and repeated at least three independent times. (*p<0.05).

3.2.3 The effect of chemotherapeutic drugs on WHCO cells and their isolated SP cells.

In this section, the cytotoxicity of different drugs in different OSCC cell lines was determined. In addition, the effect of drugs on cell viability, colony formation, cell cycle progression, apoptosis and migration on WHCO1 cells and isolated SP cells was investigated.

3.2.3.1 Determination of the cytotoxicity of different drugs

The MTT assay was used to determine the concentration at which paclitaxel, cisplatin and 5-Fluorouracil kill 50% of viable cells as described in section 7.2.9.2. This concentration is referred to as the IC_{50}. Cells were treated with increasing concentration of drugs for 24 hours and viable cells were monitored using the MTT assay. The IC_{50} values with confidence intervals were calculated from the dose response curves cell viability for WHCO1 and KYSE180 using GraphPad Prism Software (Figure 3.6). Table 3.2 shows the IC_{50} values of all the drugs for WHCO1 and KYSE cells. The IC_{50} values of paclitaxel at 24 hours were 3.77 µM and 4.42 µM for WHCO1 and KYSE180, respectively (Table 2.2). Cisplatin's IC_{50} values for WHCO1 and KYSE180 at 24 hours were 19.46 µM and 17.08 µM for WHCO1 and KYSE180 respectively (Table 3.2). Furthermore, the IC_{50} values WHCO1 and KYSE180 for 5-fluorouracil were 18.97 µM and 16.68 µM, respectively (Table 3.2). Therefore, for the purpose of this study, 1.5 µM, 9 µM and 8 µM of paclitaxel, cisplatin and 5-fluorouracil, respectively, were chosen to treat OSCC cells.

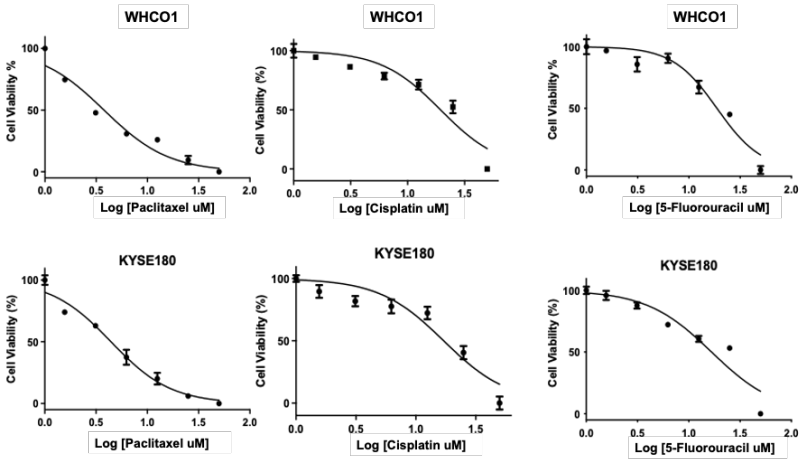

Figure 3. 6. IC_{50} determination for drugs in WHCO1 and KYSE180 OSCC cells. Oesophageal cancer cells were treated with increasing concentrations (µM) of paclitaxel, cisplatin and 5-fluorouracil for 24 hours. MTT assay was done after 24 hours, and absorbance was read at 595nm. GraphPad Prism software was used to determine the IC_{50} values. The results shown are representative of the mean ± SD experiments performed in triplicates and repeated at least two independent times.

Table 3. 2. IC_{50} values (μM) with 95% confidence interval of drugs in WHCO1 and KYSE180.

	WHCO1		KYSE180	
Drugs	**IC50 Values**	**Confidence Interval**	**IC50 Values**	**Confidence Interval**
Paclitaxel	3.7 μM	0.03 μM	4.42 μM	0.02 μM
Cisplatin	19.46 μM	1.3 μM	17.08 μM	2.2 μM
5-Fluorouracil	18.79 μM	2.1 μM	16.68 μM	1.1 μM

3.2.3.2 The effect of chemotherapeutic drugs on cell viability.

The viability of WHCO1 cells and isolated SP cells was investigated in response to the effects of several chemotherapeutic drugs used as frontline drugs in OSCC treatment, including paclitaxel, cisplatin, 5-fluorouracil, and epirubicin. WHCO1 cells and isolated SP cells were treated with 0.1% DMSO (control), paclitaxel, cisplatin, and 5-fluorouracil at the increasing concentration for 24 hrs and proliferation was monitored using the MTT assay. Treatment of WHCO1 and isolated SP cells with increasing concentrations of the above drugs showed that isolated SP cells were generally more resistant than the WHCO1 cells (Figure 3.7 A-C).

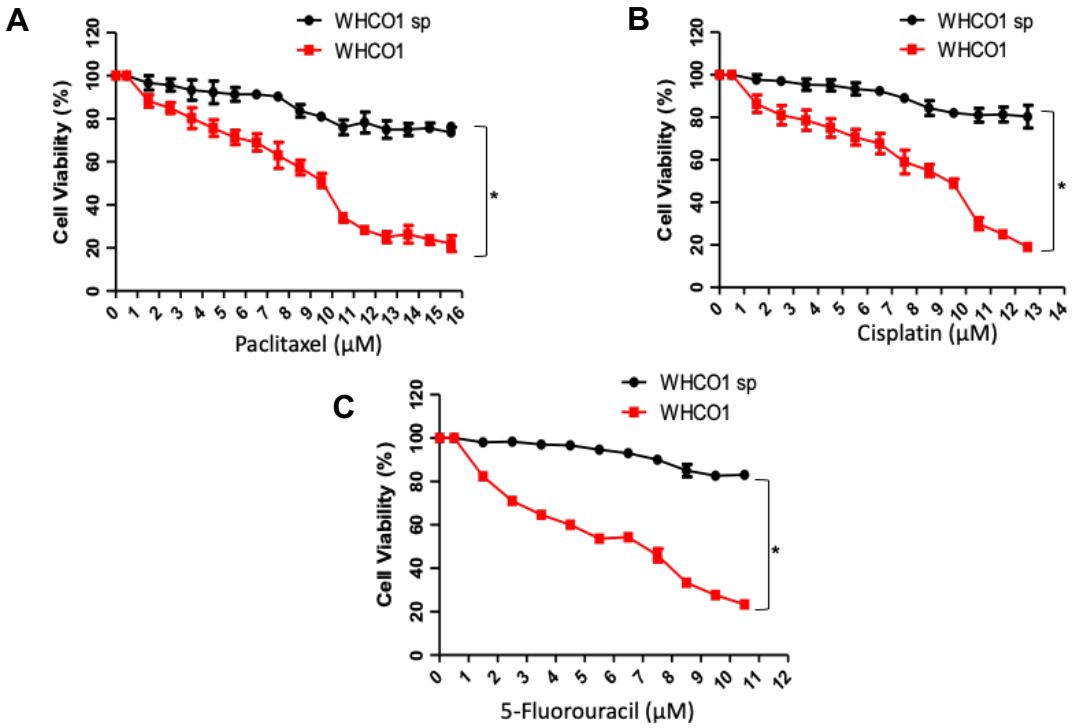

Figure 3. 7. The effect of chemotherapeutic drugs on parent and isolated SP cell viability. WHCO1 cells and CSCs were plated in a 96 well plate followed by treatment with different concentrations of **(A)** Paclitaxel, **(B)** Cisplatin, **(C)** 5-Fluorouracil and 0.1% DMSO (vehicle control) for 24 hours. MTT was used to monitor the cell viability of cells. Data shown are the mean ± SEM experiments performed in triplicates and repeated at least two independent times. *p <0.05.

3.2.3.3 The effect of drugs on colony formation of OSCC cells and their isolated SP cells

The *in vitro* colony-forming assay demonstrates the capacity of a single cell to self-renew into a colony of cells [323]. Having shown that isolated SP cells survived the effect of drugs better than cancer cells, the ability of WHCO1 and KYSE180 cells and their isolated SP to form colonies was investigated. Experiments were set up as described in section 7.2.15. Cells were grown for 10 days, media were changed every two days, followed by treatment with chemotherapeutic drugs or DMSO (control) for 24 hours. After 10 days of culture, cells were fixed with methanol and stained with 0.5% crystal violet. The number of colonies formed were counted using the ImageJ software. Isolated SP cells from WHCO1 (Figure 3.8 A, B) and KYSE180 cells (Figure 3.9 A, B) formed more colonies than WHCO1 and KYSE180 cells in the absence of drugs. The addition of paclitaxel, cisplatin and 5-fluorouracil reduced the total number of colonies formed, but isolated SP cells still formed significantly more colonies than cancer cells (Figure 3.8). In comparison to colonies formed by WHCO1 and KYSE180 cells, KYSE180 cells displayed a greater increase in colony formation. Furthermore, the colonies formed by the CSCs were different size and irregular in shape.

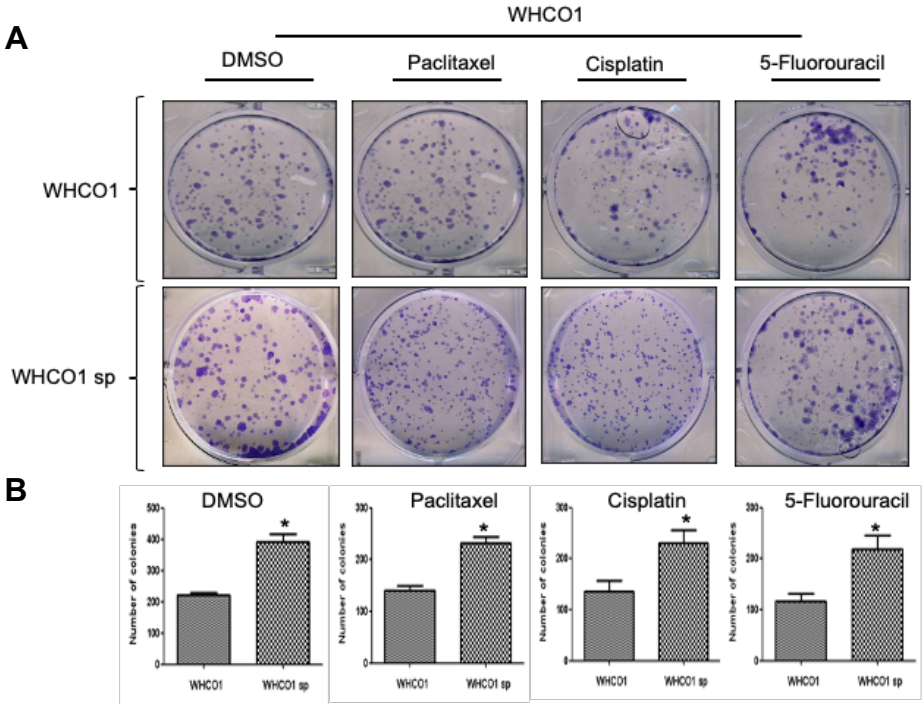

Figure 3.8. Isolated SP cells formed more colonies than WHCO1 cells. WHCO1 cells and their isolated SP cells were treated with different drugs and DMSO, allowed to form colonies. **(A)** Photographed images of colonies formed by WHCO1 cells and their isolated SP cells. **(B)** Graphs represent the number of colonies, comparing WHCO1 cells with isolated SP cells. Data shown are the mean ± SEM experiments performed in triplicates and repeated at least two independent times. Student paired t-test was used to determine statistical significance. (*$p<0.05$)

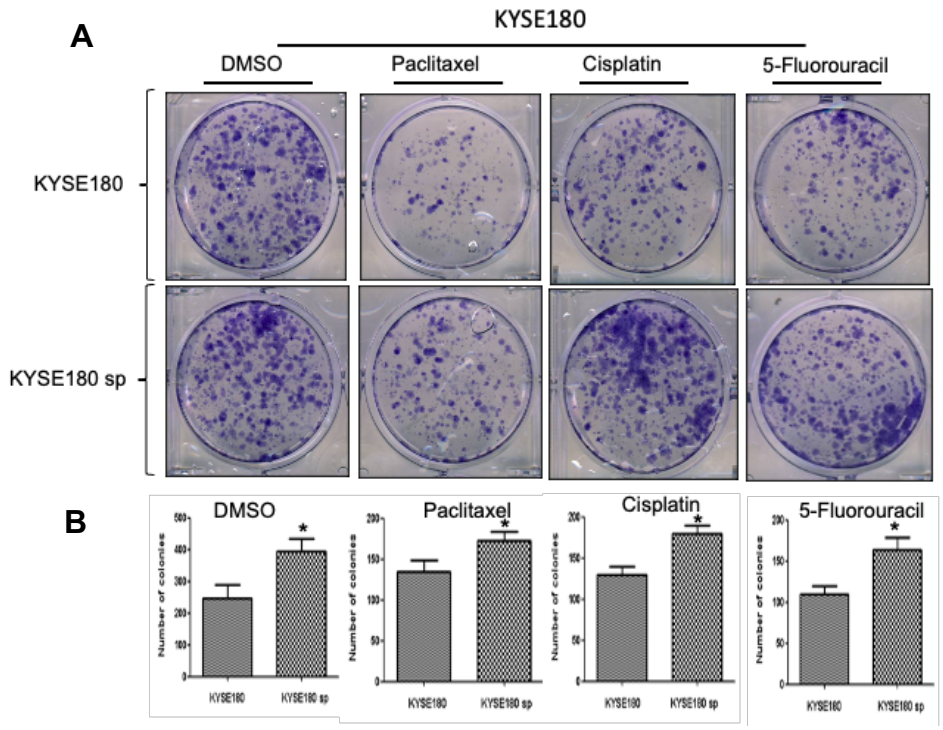

Figure 3.9. Isolated SP cells formed more colonies than KYSE180 cells. KYSE180 cells and their isolated SP cells were treated with different drugs and DMSO, allowed to form colonies. **(A)** Photographed images of colonies formed by KYSE180 cells and their isolated SP cells. **(B)** Graphs represent the number of colonies, comparing KYSE180 cells with isolated SP cells. Data shown are the mean ± SEM experiments performed in triplicates and repeated at least two independent times. Student paired t-test was used to determine statistical significance. (*p<0.05)

3.2.3.4 The effect of chemotherapeutic drugs on apoptosis and cell cycle arrest

Flow cytometry using propidium iodide was used to determine whether chemotherapeutic drugs will affect the cell progression of WHCO1 cells and isolated SP cells. DMSO-treated WHCO1 cells and isolated SP cells showed similar cell cycle profiles (Figure 3.10 A, B). The addition of Paclitaxel and cisplatin increased the percentage of WHCO1 cells in G2/M phases compared to isolated SP cells, as well as an increased number of cells undergoing apoptosis (Figure 3.10 A, B). In both WHCO1 cells and isolated SP cells, 5-fluorouracil induced a G1 cell cycle arrest, with an increase in the WHCO1 cells compared to isolated SP cells (Figure 3.10 A, B).

Cancer can be treated by controlling or eliminating the uncontrolled growth of cells. However, most successful treatments target apoptosis. CSCs have been shown to display increased resistance to drug-induced apoptosis. One of the methods widely used to monitor apoptosis is Annexin V, a protein with a strong calcium-dependent affinity for phosphatidylserine (PS). Therefore, cellular apoptosis was assessed using

Annexin V/Propidium Iodide double staining followed by flow cytometry. DMSO-treated WHCO1 cells showed a slight increase in cells undergoing early apoptosis (Q2) compared to isolated SP cells (Figure 3.10 C, D). Furthermore, there was a 2.2-, 1.1- and 2.1-fold in late apoptosis (Q3) induction in WHCO1 cells treated with paclitaxel, cisplatin and 5-fluorouracil, respectively, compared to isolated SP cells (Figure 3.10 C, D). Together, the results suggest that isolated SP cells from WHCO1 cells have the ability to resist both drug-induced cell cycle arrest and apoptosis.

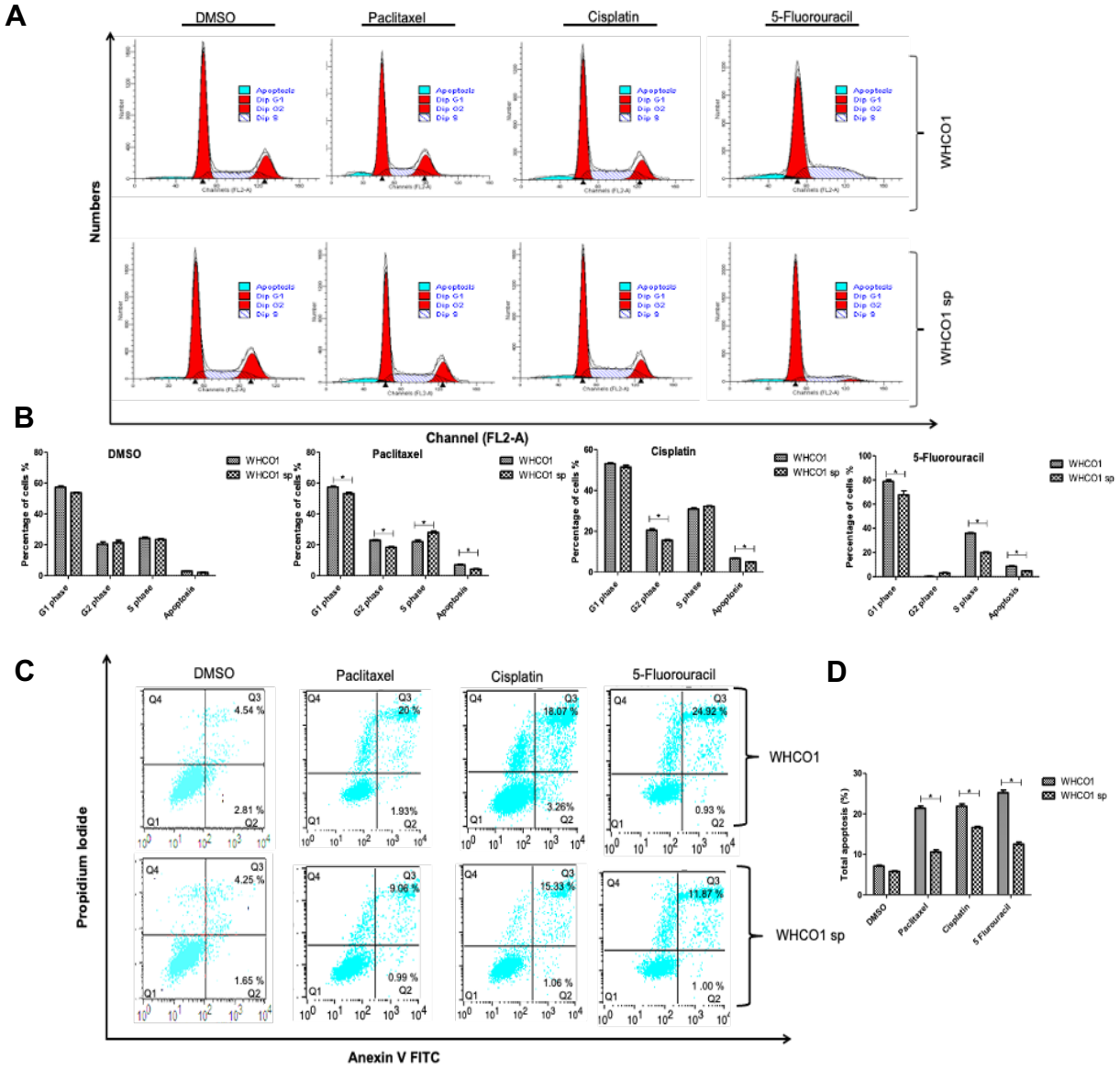

Figure 3. 10. WHCO1 isolated SP cells exhibit an increased ability to resist drug-induced cell cycle arrest and apoptosis. Flow cytometry was used to analyse the effects of chemotherapeutic drugs on WHCO1 and isolated SP **(A)** cell cycle and **(C)** cell apoptosis. **(B, D)** Graphs represent the percentage of cells in each phase and total apoptosis, respectively. Data shown are the mean ± SEM experiments performed in triplicates and repeated at least two independent times. Student paired t-test was used to determine statistical significance. (*p<0.05).

3.2.3.5. Comparison of the metastatic behaviour of untreated and treated WHCO1 cells and isolated SP cells.

A hallmark of cancer is its ability to invade surrounding tissue and grow at distant sites. It is proposed that CSCs are responsible for tumour development, invasion, metastasis, and recurrence [324]. The poor prognosis of OSCC is primarily due to cancer cells' invasiveness and metastatic abilities. Having shown that isolated SP cells survived the treatment of drugs, this study then investigated whether isolated SP cells might be involved in the metastatic ability of OSCC cells. In addition, the effect of chemotherapeutic drugs on the migration of WHCO1 cells versus isolated SP cells was investigated.

The wound-healing assay, a standard *in vitro* assay for determining cell migration in two dimensions, was performed, as described in section 7.2.21. After allowing cells to reach confluence, serum starvation was done for 16 hours before making the "wound" scratch *in vitro* to eliminate cell proliferation during migration. The ‘wound” scratch was created by a single scrape using a yellow pipette tip (200 µl). Images of the migration into the gap were taken at 0 and 15 hours. After 15 hours, it was observed that isolated SP cells had migrated to close the wound whilst a gap was still visible in the WHCO1 cells (Figure 3.11). Isolated SP cells also migrated to close the wound after 15 hours in the presence of paclitaxel, cisplatin or 5-fluorouracil. However, WHCO1 cells showed reduced migratory in the presence of drugs (Figure 3.11). This data demonstrated that isolated SP cells migrated to close the wound even in the presence of drugs compared to WHCO1 cells.

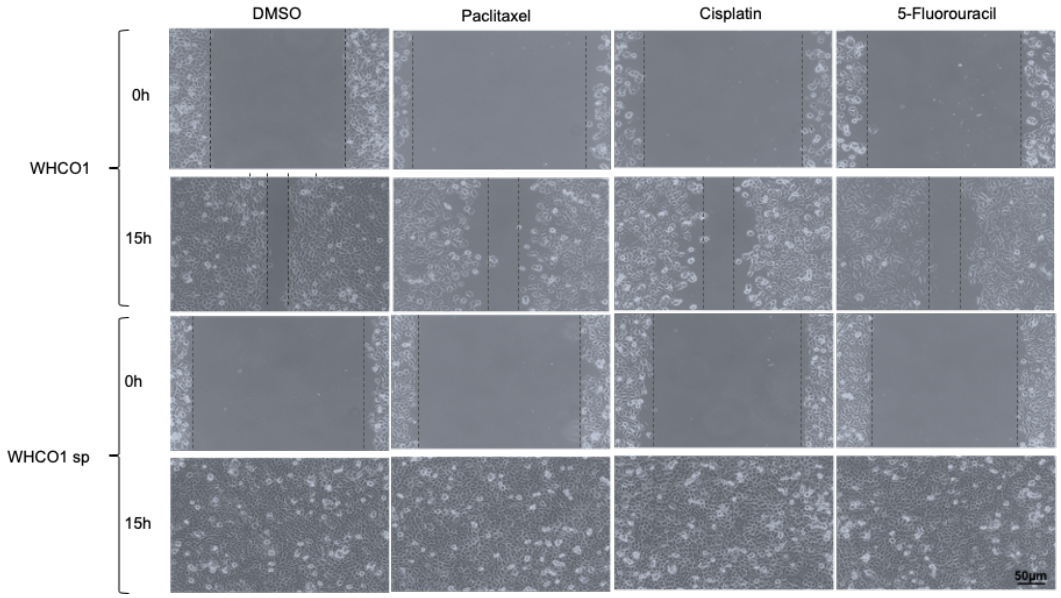

Figure 3. 11. Comparison of the metastatic behaviour of untreated and treated parental WHCO1 cells and isolated SP cells. A wound-healing assay was used to determine the metastatic behaviour of WHCO1 cells and isolated SP cells. The effect of chemotherapeutic drugs on the migratory abilities of WHCO1 cells versus isolated SP cells was also investigated. Isolated SP cells migrated to close the wound even in the presence of drugs. Data shown represent experiments performed at least two independent times. Scale bar = 50 µm.

3.2.3.6. The expression of genes involved in epithelial-to-mesenchymal transition (EMT) and metastasis.

To further investigate the role played by CSCs on cancer cell migration, genes involved in EMT, and metastasis were investigated using western blot analysis and zymography. Western blot analysis of the expression of FOXM1, MMP2 and MMP9 in EMT and metastasis showed increased expression of these genes in isolated SP cells compared to WHCO1 and KYSE180 cells (figure 3.12 A, B). Quantification by densitometric analysis of band intensities was relative to GAPDH (Figure 3.12 C, D). Densitometric values of isolated SP cells were normalised to that of WHCO1 and KYSE180 cells. Furthermore, gelatin Zymographic analysis of culture media showed that MMP2 and MMP9 activities were upregulated in isolated SP cells compared to OSCC cells suggesting that secreted MMPs may contribute towards the metastatic capabilities of isolated SP cells (Figure 3.12 E). In addition, this study assessed the expression of interleukin-6 (IL6) and interleukin-8 (IL-8) in isolated SP cells compared to WHCO1 and KYSE180 cells. Both IL6 and IL8 were upregulated in isolated CSCs compared to WHCO1 and KYSE180 cells (Figure 3.12 A, B). These results suggest that isolated CSCs may play a role in cancer migration by secreting EMT-associated metastatic genes and cytokines.

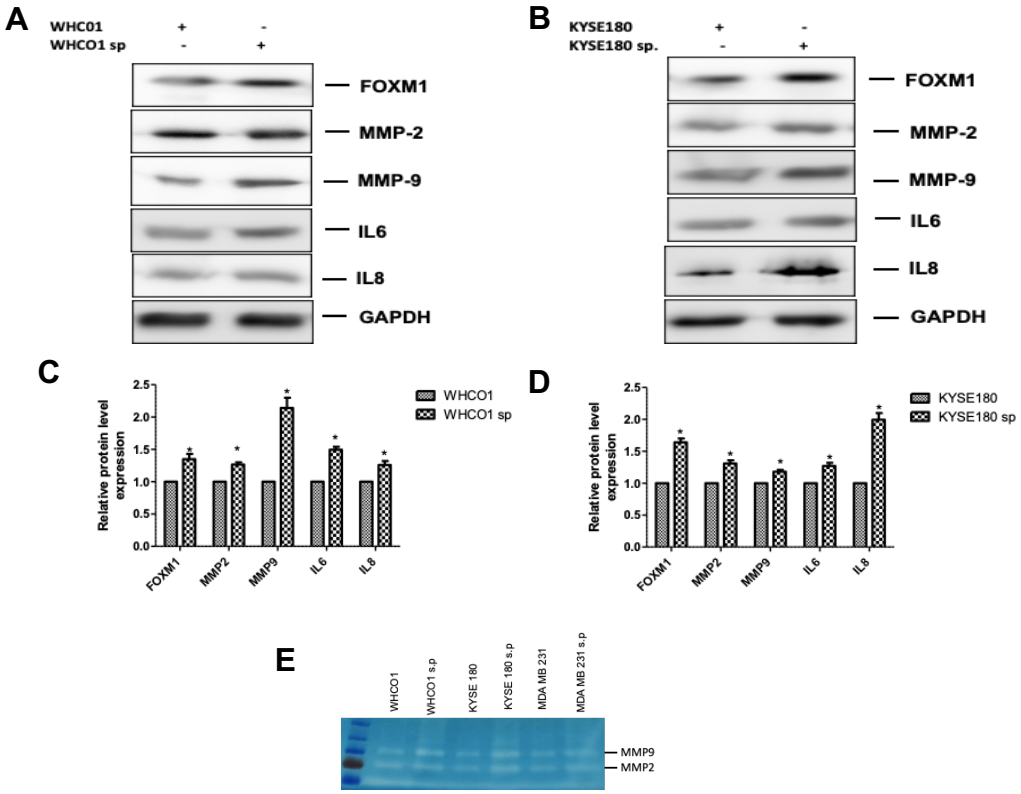

Figure 3. 12. The expression of genes involved in EMT and metastasis. **(A, B)** Western blot analysis of OSCC and isolated SP cells was used to evaluate the expression of genes involved in EMT and metastasis. **(C, D)** Densitometric analysis of protein band intensities relative to GAPDH. **(E)** Gelatin Zymography was performed on media samples to evaluate the MMP2 and MMP9 activities. The data shown are the mean ± SEM experiments performed in triplicate and repeated at least two independent times. (*p<0.05).

3.2.4 Survival pathways were elevated in SP-derived tumourspheres.

The activation of many survival pathways, including MEK-ERK, PI3K/Akt, and NF-k signalling pathways, was examined to learn more about the mechanisms of chemoresistance used by the isolated side population cells. A comparison of the differences between WHCO1 cells, isolated SP cells and tumourspheres showed that MEK-ERK, PI3K/ Akt and NF-kβ expression were significantly elevated in isolated SP and SP-derived tumourspheres compared to WHCO1 cells (Figure 3.13 A). Densitometric analysis was done to quantify MEK-ERK, PI3K/Akt and NF-kβ band intensities (Figure 3.13 B).

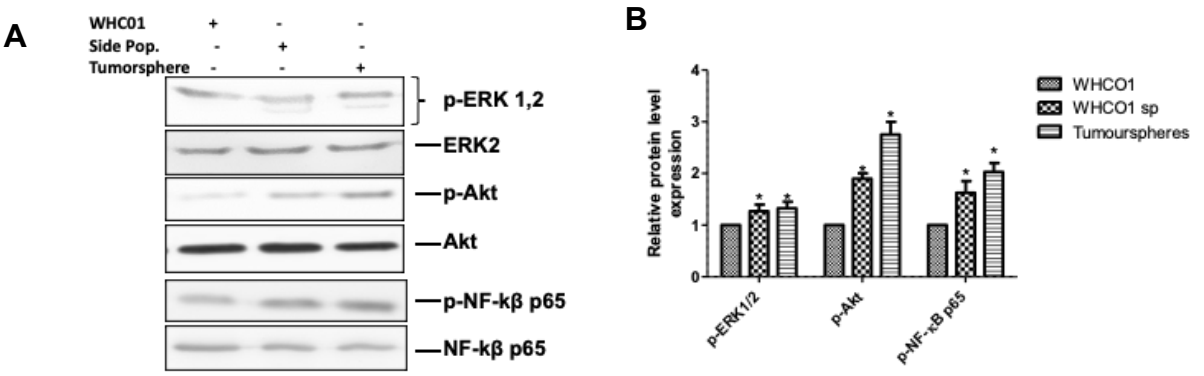

Figure 3.13. Survival pathways were elevated in SP-derived tumourspheres. (A) The data represent western blot analysis of survival pathways such as MEK-ERK, PI3K/Akt, JNK and NF-kβ signalling pathways in WHCO1 cells, SP cells and tumourspheres. **(B)** Densitometric analysis of MEK-ERK, PI3K/Akt, JNK and NF-kβ band intensities. Densitometric values of isolated SP and tumourspheres were normalised to that of parent WHCO1 cells. Data shown is the mean ± SEM experiments performed in triplicate and repeated at least two independent times. (*p<0.05).

3.3. Discussion

While cancer therapies eliminate most tumour cells, advanced tumours can develop drug resistance [325]. Most therapies, according to the CSC theory, fail to prevent relapse in part because of the presence of a tiny minority of cells known as cancer stem cells [145, 154, 326]. CSCs reside in the TME and may contribute to the development of drug resistance and tumour relapse. Developing novel strategies against drug-resistant cancer cells, including CSCs, remains a significant challenge and there is a need for novel drugs or therapies. Several scientific findings have shown the presence of a subset of cancer cells with stem cell-like properties that are responsible for tumour progression, development of chemoresistance and tumour relapse implicated in metastasis [145, 327].

In this investigation, CSC marker expression in biopsy samples and isolated side population cancer cells were evaluated. Immunohistochemical analysis showed that CSC markers, CD44 and ALDH1A1, were elevated in OSCC patient tumour samples compared to normal tissues. Ginestier et al. (2007) demonstrated that ALDH1A1 expression was correlated with poor patient prognosis [328]. In addition, ALDH1A1 appear to be associated with poor patient survival [329]. CD44 has also been used as a CSC marker to predict poor prognosis in ovarian cancer [330, 331]. Overall, the data suggest that ALDH1A1 and CD4 CSC markers may be used to predict the prognosis of OSCC. Several methods have been used to isolate and identify CSCs, with the use

of cell surface markers and the SP cells being two of the common ones [316, 332]. The use of antibodies against cell surface markers such as CD44 and CD133 is an expensive method for the isolating and identifying of CSCs. On the other hand, based on the exclusion of Hoechst 33342, the side population technique is a cheap and relatively easy technique used to isolate CSCs [310].

This study also demonstrated that CSCs from oesophageal cancer cell lines exhibited stem cell-like properties by expressing CD44 and ALDH1A as well as self-renewal markers. Their colony formation capability, proliferation rate, cell cycle profile, drug resistance, apoptosis, and migration were analysed and compared. Compared with cancer cells, isolated SP cells expressing CD44 and ALDH1A1 had more significant colony formation potential. CD44 positive subpopulation cells were found to have increased colony formation [333]. One way to enrich cells for CSCs is through the tumoursphere formation assay [334]. The isolated CSCs were able to form tumourspheres *in vitro* that expressed higher levels of CSC and self-renewal markers. The ability of CSC-like cells to form tumourspheres *in vitro* has been shown to initiate tumours *in vivo*. These results suggest that CSC markers may play a role in OSCC colony formation and proliferation. Knocking down CD44 in CSCs found to prevent the formation of colonies and inhibit tumourigenesis in xenograft models [335]. Kim et al. (2011) reported that Oct4-high cells formed more tumourspheres and expressed elevated levels of CSC markers [336].

In addition to isolated CSCs forming colonies and tumourspheres, less apoptosis and more resistance to drug-induced cell apoptosis were observed. A recent study reported that CD44 is involved in prostate cancer metastasis and resistance to drugs [337]. CD44 positive cells were also found to express higher levels of the anti-apoptotic protein Bcl-2 in breast cancer cells [338]. Our results are consistent with other studies showing increased expression of ALDH1A1 in drug resistant cancer cell lines [339]. ABC transporter, ABCG2, and MDR-1 are some of the key factors contributing to the chemoresistance of CSCs. This study showed that isolated SP cells had increased the expression of these genes. Overall, these results suggest that markers associated with CSCs can be useful in predicting drug resistance to cancers.

The migration of tumour cells from the primary tumour is a crucial step in the metastatic cascade, and CSCs are likely to promote this migration. In adult tissues, some aspect of this migration capability is maintained through a process known as epithelial to mesenchymal transition (EMT). Moreover, it is suggested that the activation of migration by CSC may be through the process of EMT [340]. In Gastric cancer, CSCs are associated with cancer invasion and metastasis through EMT [339]. Immunoblot and RT-PCR analysis showed that proteins such as MMPs and FOXM1 associated with the EMT process are significantly upregulated in isolated CSCs compared to cancer cells. EMT process occurs in migrating and invading cells and is an integral part of metastasis [341, 342]. MMPs are known to dock on CD44 and degrade the basement membrane, promoting cancer cell invasion and migration [343]. Notably MMP9 localises to the tip of migrating cells to degrade matrix proteins such as collagen [344]. Metastasis is a complex process and cannot be explained solely through the EMT process [345, 346].

The present study demonstrated that isolated CSCs expressed significant amounts of several signalling pathway genes, including MEK-ERK, PI3K/Akt and NF-kβ. All these signalling pathways are involved in the mediation of cellular survival by preventing apoptosis [347, 348]. Indeed, both NF-kβ and MEK-ERK signalling pathways have been associated with the recurrence of several cancer types [147, 349]. The activation of these three signalling pathways in human oesophageal cancer could be used as a diagnostic for treatment resistant CSCs. Overall, the study showed that *in vitro*, CSC markers are essential in promoting invasion and metastasis. They do so through the process of EMT and induction of survival pathways in oesophageal cancer stem cells. Drugs commonly used for OSCC treatment, such as paclitaxel, cisplatin, 5-fluorouracil and epirubicin, cannot eradicate CSCs [350]. This might explain the high occurrence of the development of drug-resistant disease and relapse [351]. These results may also apply to other solid cancers where these drugs are used. Therefore, new drugs must target CSCs. Moreover, targeting a single CSC marker such as CD44 might not be sufficient to eliminate OSCC. OSCC could be eradicated more effectively by using anti-CSC therapy combined with chemotherapeutic agents.

The use of monoclonal antibodies is one of the new strategies to treat chemo-resistant cancers [352, 353]. Due to their specificity, monoclonal antibodies represent a

promising method for interfering with a single target molecule with high selectivity [354]. All the CSC markers used in this study have been shown to be expressed by side population cells in several cancers [332, 355]. Several CSC and self-renewal markers have been associated with poor prognosis in many cancers such as cervical, breast and colon cancer [356, 357]. High proliferation marker Ki67 expression has been correlated with poor overall patient survival in many cancers [358, 359]. This study shows that the expression of Ki67 in OSCC biopsy samples follows the same trend as that of CSC markers. This is in agreement with a study that showed CSC marker to associated with high expression of Ki67 [360]. The use of CD133 as a prognostic marker in OSCC is controversial, with some studies showing its usefulness whilst others show that it is not a good prognostic marker [361, 362].

Compared to CSCs isolated from cancer cells, this study showed that tumourspheres expressed significantly higher levels of CSC and markers of self-renewal. It is possible to speculate that tumourspheres contain more CSCs than both isolated CSCs and OSCC cells based on their expression of CSC and self-renewal markers. Together our data supported our hypothesis that CSC markers are present in OSCC biopsies and isolated CSCs. In addition, our results suggest that CSCs may play an important role in regulating growth, migration and drug resistance of cancer cells. However, there may be other markers of CSCs that contribute to the maintenance of CSC characteristics in OSCC. CSC markers could be used to predict the prognosis and drug resistance. Investigating more of these markers and their roles might provide insight into OSCC prognosis and drug resistance.

CHAPTER 4:

EXTRACELLULAR MATRIX PROTECTS CANCER CELLS FROM THE EFFECTS OF DRUGS.

4.1 Introduction

The ECM is a crucial component of all tissues and organs, acting as both a physical scaffold for cells and playing critical roles in several biochemical processes needed to maintain tissue and organ structure and function. The ECM is also important in the maintenance of tissue homeostasis. When the proteins that make up the ECM are defective, several pathophysiological conditions may arise [363, 364]. Different tissues and organs have different ECM components, but in most cases, the ECM is made up of proteins such as collagens, fibronectin, laminins, polysaccharides and water [365]. Recent reports indicate that the ECM in the same tissue is in constant state of flux, depending on several factors such as stage of development and presence or absence of disease [365].

Several reports have shown great interest in the developing 3D micro-physiological models that can recapitulate both normal and disease conditions *in vitro* [249, 366]. Furthermore, most drug discovery investigations are conducted using *in vitro* tumour microenvironment models that do not replicate the *in vivo* tissue microenvironment present during development, morphogenesis, and disease state [367, 368]. The lack of true *in vitro* models limits our understanding of the interaction between tissue components such as cells, biomolecules and the ECM [369, 370]. The same scenario is observed in modelling tumours, with most models used to date lack their replication of the tumour microenvironment. Cells such as macrophages, fibroblasts, endothelial cells, pericytes, and the ECM would make up the full complement of TME components. [371, 372]. The reductionist approach of using individual components of the tumour microenvironment can lead to conclusions regarding to the interactions between TME components and the effectiveness of drugs. Recent reports using newer models such as tumour spheroids and organoids that better mimic the *in vivo* tumour microenvironment has allowed scientists to get a clearer picture of the TME [373, 374].

The ECM is a meshwork of tethered biomolecules, proteins and glycosaminoglycans [373, 375]. The function of the ECM is mainly to provide mechanical and biochemical support to cells, allowing adhesion and migration [365, 376]. Furthermore, the ECM also acts as a relay of extracellular cues by interacting with cell receptors. The ECM has been shown to recruit and sequester biomolecules such as growth factors and cytokines, thereby influencing cell growth and signalling [377, 378]. The ECM is produced mainly by fibroblasts within the TME, with contributions from other stromal cells such as MSCs, pericytes, macrophages and endothelial cells [379, 380]. The main cellular component of the stroma is fibroblasts, commonly called tumour-associated fibroblasts (TAFs) or cancer-associated fibroblasts (CAFs) [381, 382]. These activated fibroblasts grow much faster than normal fibroblasts and synthesise increased amounts of the ECM [383, 384].

Drug resistance continues to be a major challenge in the treatment of OSCC, with many patients succumbing to the disease [385, 386]. Our knowledge of the pathways involved in tumour start and development is currently limited. In addition, there is a dearth of information regarding tumour relapse and metastasis. While genetic alterations may initiate cellular transformation, the interaction between tumour cells and stromal cells, as well as the ECM, is crucial in tumour initiation and progression. Recent reports also show that tumour stroma cell interaction influence the response of cancer cells to therapy. Notably, the development of therapy resistance in general and chemoresistance, in particular, has been shown to be influenced by the tumour microenvironment [387-389].

Through the synthesis and release of many biomolecules, stromal cells play an important role in cancer angiogenesis and epithelial to mesenchymal transition [390, 391]. ECM proteins like collagen and fibronectin have been found to be elevated in a variety of cancers [375, 392]. For example, tumours are known to ‘harden’ due to increased synthesis and deposition of ECM proteins such as collagens, laminins and fibronectin [392, 393]. Thus, ECM proteins can influence several cancer cell properties from proliferation to invasion. Several reports utilising purified ECM proteins have shown that interaction between ECM and cancer cells is crucial in cancer cell behaviour [372, 394, 395]. Decellularised cell-derived ECMs contain native ECM proteins, are easy to acquire, and are cost-effective, according to recent studies [372,

394, 395]. Despite the fact that CAFs are an integral part of the TME, fibroblast-derived decellularised ECM would replicate the desmoplastic milieu of the tumour [396].

Compared to 2D cultures in monolayer, the use of 3D cultures has made it possible to mimic an *in vitro* microenvironment closer to the tumour. These recent advances have made it possible to reassemble the ECM *in vitro* by using a decellularized ECM (dECM) to a better understanding of cancer cell-ECM interactions. This chapter is based on the hypothesis that the ECM plays a critical role in tumour progression and migration, as well as act as a physical barrier to therapy effectiveness by activating survival pathways. To test this hypothesis, this study first evaluated ECM gene expression in oesophageal tumour tissues compared to their adjacent normal tissue, as well as in cell lines. Secondly, cell-derived ECM were used to investigate cancer cell behaviour and drug response, compared to cancer cells on plastic dishes. Furthermore, knockdown studies were done to investigate the relationship between specific ECM proteins and drug resistance as well as migratory capacity of cancer cells.

4.2 Results

4.2.1 The expression of ECM genes, integrins and MMPs in OSCC tumours and cell lines.

The expression of ECM genes, integrins and matrix metalloproteases (MMPs) in tumour samples and cell lines was investigated using RT-qPCR.

4.2.1.1 ECM, integrins and MMP mRNA levels in OSCC biopsies.

Biopsies were collected from confirmed OSCC cancer patients and used to evaluate the expression of the ECM and associated genes (see Table 3.1, Chapter 3). ECM mRNA levels were determined via comparative qRT-PCR of tumour tissues versus adjacent normal tissue for each patient using GAPDH as a normalizer. The expression of collagens, fibronectin and laminins were significantly upregulated in OSCC tumour tissues compared to normal tissue (Figure 4.1 A, B).

The TME is constantly being remodelled, thus, the quantity and nature of proteins and other biomolecules are constantly fluctuating. Matrix metalloproteases (MMPs) and cathepsins are involved in remodelling the ECM. MMPs such as MMP1, MMP2, MMP9 and MT1-MMP are known to degrade various ECM proteins, and this study showed the levels of MMP-1, MMP2, MMP3 and MMP9 mRNA were higher in tumours than in normal tissues (Figure 4.1C). The expression of some integrin genes in OSCC tumour tissues versus normal tissues was compared to determine the levels of ECM protein receptors. The data show that integrins gene expression was higher in tumour and normal tissues (Figure 4.1D). Following the determination of EMC proteins in biopsy samples using RT-qPCR, immunohistochemical staining using OSCC biopsy specimen to stain for type I collagen was performed. Anti-type I collagen staining in both tumour and normal biopsy specimens demonstrated that type I collagen was increased in tumour specimens compared to normal biopsy specimens (Figure 4.1 E).

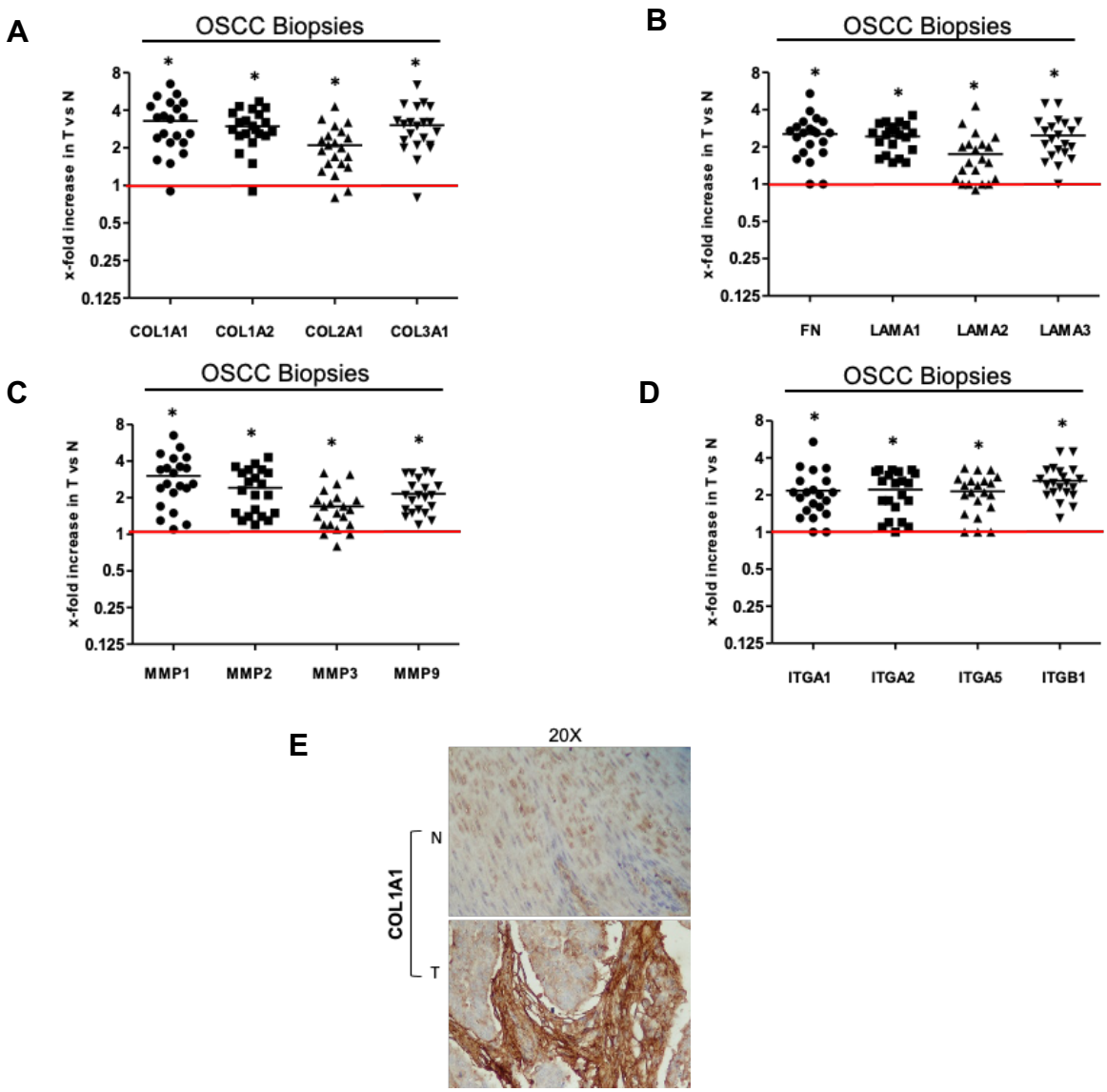

Figure 4. 1. ECM, integrins and MMP mRNA levels in OSCC biopsies. The gene expression of ECM genes, MPPs and integrins was evaluated in tumour samples and compared to normal tissues. qRT-PCR was used to evaluate the gene expression levels of **(A)** collagen, **(B)** fibronectin and laminin, **(C)** MMPs and **(D)** integrins in OSCC tumour samples (T) versus adjacent normal tissue (N) for each patient. Normal tissue was taken as 1 and GAPDH was used as a housekeeping gene to normalise target gene expression. **(E)** Immunohistochemical staining of type I collagen in OSCC specimen. Statistical analysis to determine the significant difference of gene expression in tumour versus normal sample was done using a 2-tailed non-parametric Mann-Whitney test. * $p < 0.05$.

4.2.1.2 The expression of ECM components in cell lines.

ECM within the TME is produced by both tumour cells and stromal cells, including CAFs. Therefore, this study evaluated the expression of ECM proteins in fibroblasts and OSCC cell lines using qRT-PCR analysis. Comparison of the CT1, WI38 and FG_0 fibroblast cell lines and the WHCO1, WHCO5, WHCO6, KYSE180, KYSE450, KYSE520 OSCC cell lines indicated that CT1 cells had elevated ECM protein synthesis compared to WI18 and FG_0 fibroblasts (Figure 4.2 A-E). Conversely, cancer

cells showed reduced ECM protein synthesis of about 30–50% compared to normal fibroblasts (Figure 4.2 A-E). The expression of α-smooth muscle actin (α -SMA), a marker for activated fibroblasts, was evaluated in both western blot and qRT-PCR assays. The transformed CT1 fibroblasts had significantly elevated α-SMA expression than normal fibroblasts (WI38 and FG0) (Figure 4.3 A, B). Furthermore, the CT1 fibroblasts displayed spindle-shaped morphological features, typical of fibroblasts found within tumours (Figure 4.3 C).

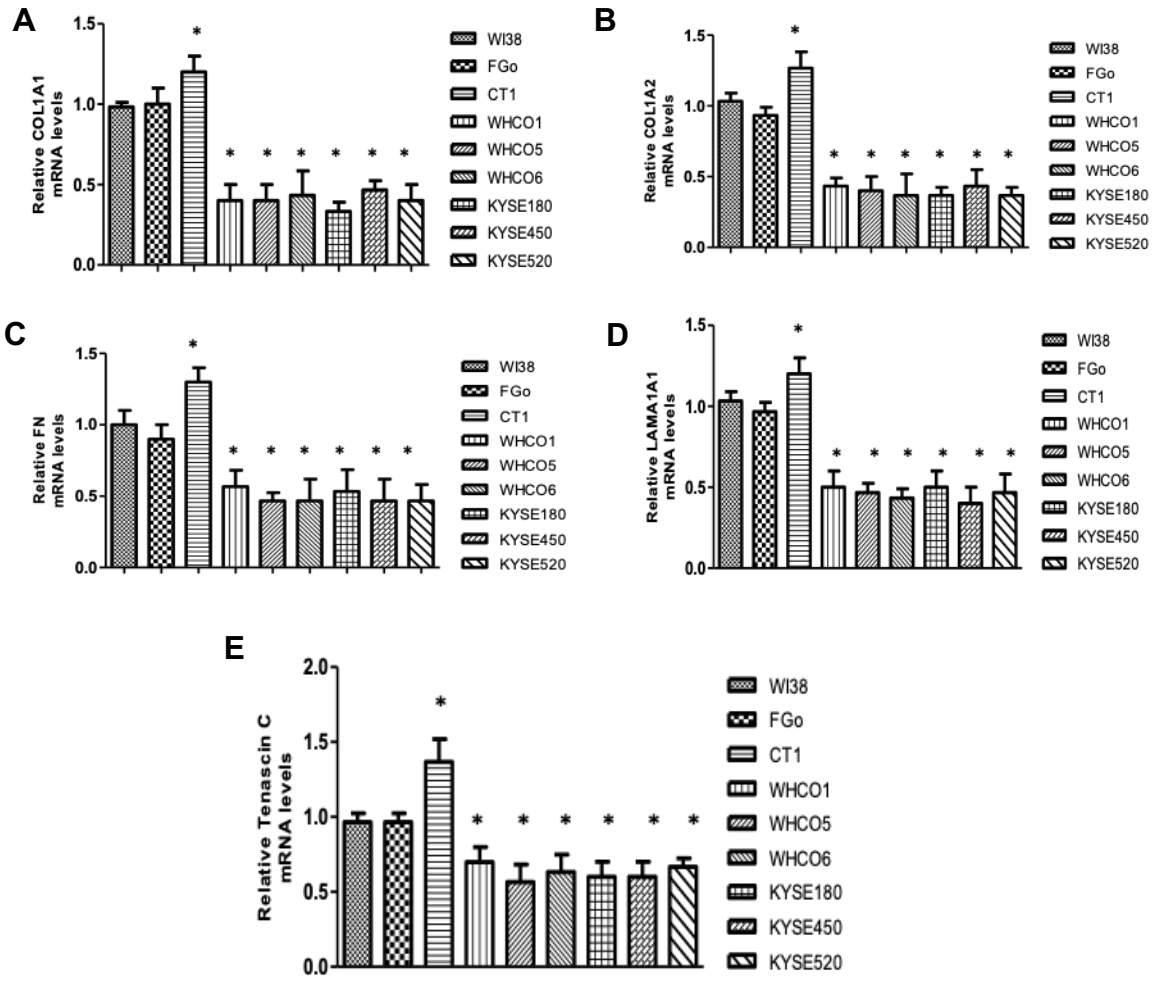

Figure 4. 2. The expression of ECM proteins in OSCC and fibroblast cell lines. qRT-PCR analysis was used to evaluate the expression of; **(A)** collagen, type 1, alpha 1 (COL1A1), **(B)** COL1A2, **(C)** fibronectin (FN), **(D)** laminin 1 alpha 1 (LAMA1A1) and **(E)** Tenascin C in OSCC and fibroblast cell lines. The values of all the OSCC, CT1 and FG0 were normalized to that of WI38. GAPDH was used as a housekeeping gene to normalise target gene expression. The results shown are representative of the mean ± SEM experiments performed in triplicates and repeated at least two independent times. Statistical significance was done using one way ANOVA. * $p < 0.05$.

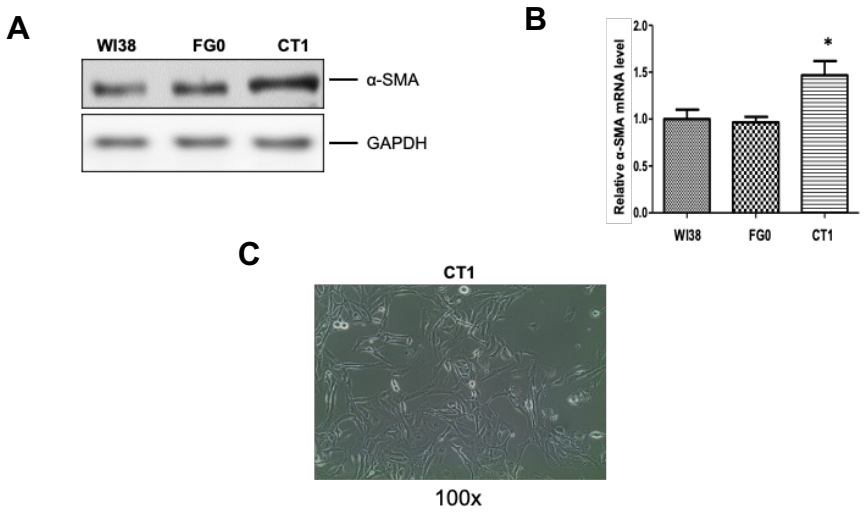

Figure 4. 3. Elevated expression levels of α-SMA in CT1 fibroblast cells. **(A)** Western blot analysis was done to determine the expression of α-SMA in WI38, FG_0 and CT1 fibroblasts cell lines. **(B)** Evaluation of α-SMA mRNA expression was done using qRT-PCR analysis relative to GAPDH. **(C)** Images of CT1 fibroblasts cells were captured using a phase-contrast image. Results shown are the mean ± SEM of experiments performed at least two independent times. *p<0.05.

4.2.2 Isolation and characterisation of decellularised ECMs

Several reports have shown that fibroblasts are a vital component of various tissues and the main stromal cell type responsible for the synthesis of the ECM [397]. Various other reports have utilized a fibroblast-derived ECM to study cancer cell and mesenchymal stem cell interactions [229]. Fibroblasts within tumours are often referred to as cancer-associated fibroblasts. Cell-derived 3D culture models were utilized for this section, which involved culturing cancer cell lines on these models. As illustrated in Figure 4.4 A, this investigation used decellularised ECMs made by fibroblasts (CT1 fibroblasts; tfd-ECM), OSCC cell lines (cd-ECM), and a combination of fibroblasts and cancer cells (combi-ECM).

Since all the OSCC cell lines used in this study had similar gene expression profiles, the WHCO1 cell line was used in all subsequent experiments unless indicated otherwise. The γ-radiation transformed WI-38 human lung fibroblast cell line, (CT1) represented our “transformed fibroblasts”. CT-1 fibroblasts produced an ECM (tfd-ECM) displaying a more highly linearized pattern than the ECM produced by WHCO1 cells (cd-ECM) and a mixture of CT-1 fibroblasts and WHCO1 cells (combi-ECM) (Figure 4.4 A, right column). Matrigel and Fibronectin, two commonly used synthetic and solubilized ECMs, do not form linearized ECMs. It is hypothesised that

linearisation, or lack thereof, influences how cancer cells respond to chemotherapeutic drugs and may better represent the *in vivo* ECM than these purified ECM components.

An important step in studying cell-ECM interactions is the need to analyse the detailed composition of the ECM being used. Therefore, ECMs were decellularized using 0.5% Triton X-100 and 0.1 M NH4OH as described in section 7.2.20.1. The composition of the several ECMs utilised (tfd-ECM, cd-ECM, and combi-ECM) was examined in this study utilising gel electrophoresis, Alcian blue staining for proteoglycan, and a proteomics pipeline combining liquid chromatography with tandem mass spectrometry (LC-MS/MS) (Figure 4.4 B). SDS-PAGE and Alcian blue staining results revealed that decellularised ECMs were generally made up of identical ECM proteins and proteoglycans, with differences in protein and proteoglycan amounts observed in each ECM (Figure 4.4 C).

The Q-Exactive MS instrument acquired MS1 and MS2 data for all samples. All samples had a Total Ion Chromatogram (TIC) in the same range to maximise peptide loading into the LC/MS/MS (Figure 4.5 A-C). MaxQuant analysis of the spectra and comparison with the Uniprot Human protein database was conducted to identify protein groups. This analysis allowed the identification of the different peptides and proteins from the ECMs (Figure 4.5 A-C). Similar proteins were found in the three decellularised ECMs. A total of 24 glycoproteins, including fibronectin, laminin and tenascin C, were identified (Table 4.1). Of the 20 collagens identified, collagen type alpha 1 and 2 chains were also detected (Table 4.1). In addition, 18 ECM regulators, 9 proteoglycans, and 9 secreted factors were also identified (Table 4.1).

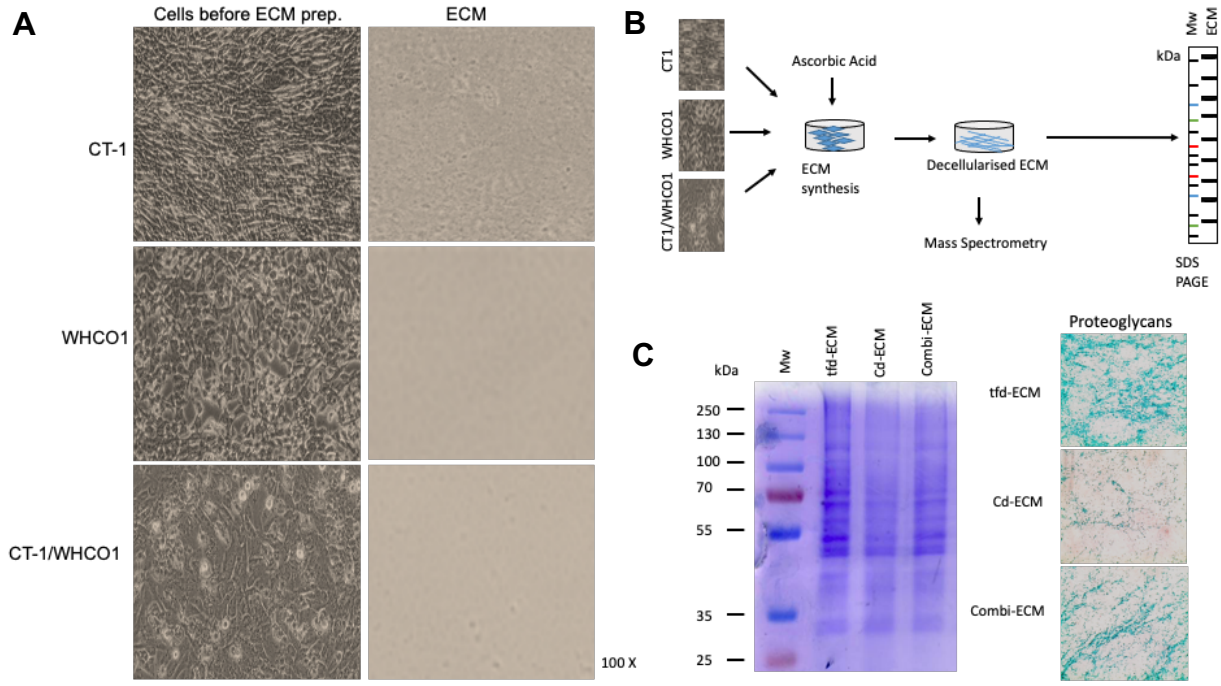

Figure 4. 4. Analysis of decellularised ECM. Mass spectrometric characterisation of ECM produced by fibroblasts and cancer cells. **(A)** Phase-contrast microscope images of fibroblasts and cancer cells before and after the decellularisation procedure. **(B)** Diagrammatic representation of decellularised ECMs preparation and evaluation using SDS PAGE and mass spectrometry. **(C)** Images showing SDS PAGE analysis and Coomassie Blue staining of decellularised ECMs (left panel). Alcian Blue staining for proteoglycans within decellularised ECMs (right panel). Representative images are shown. Images were taken at 100× magnification.

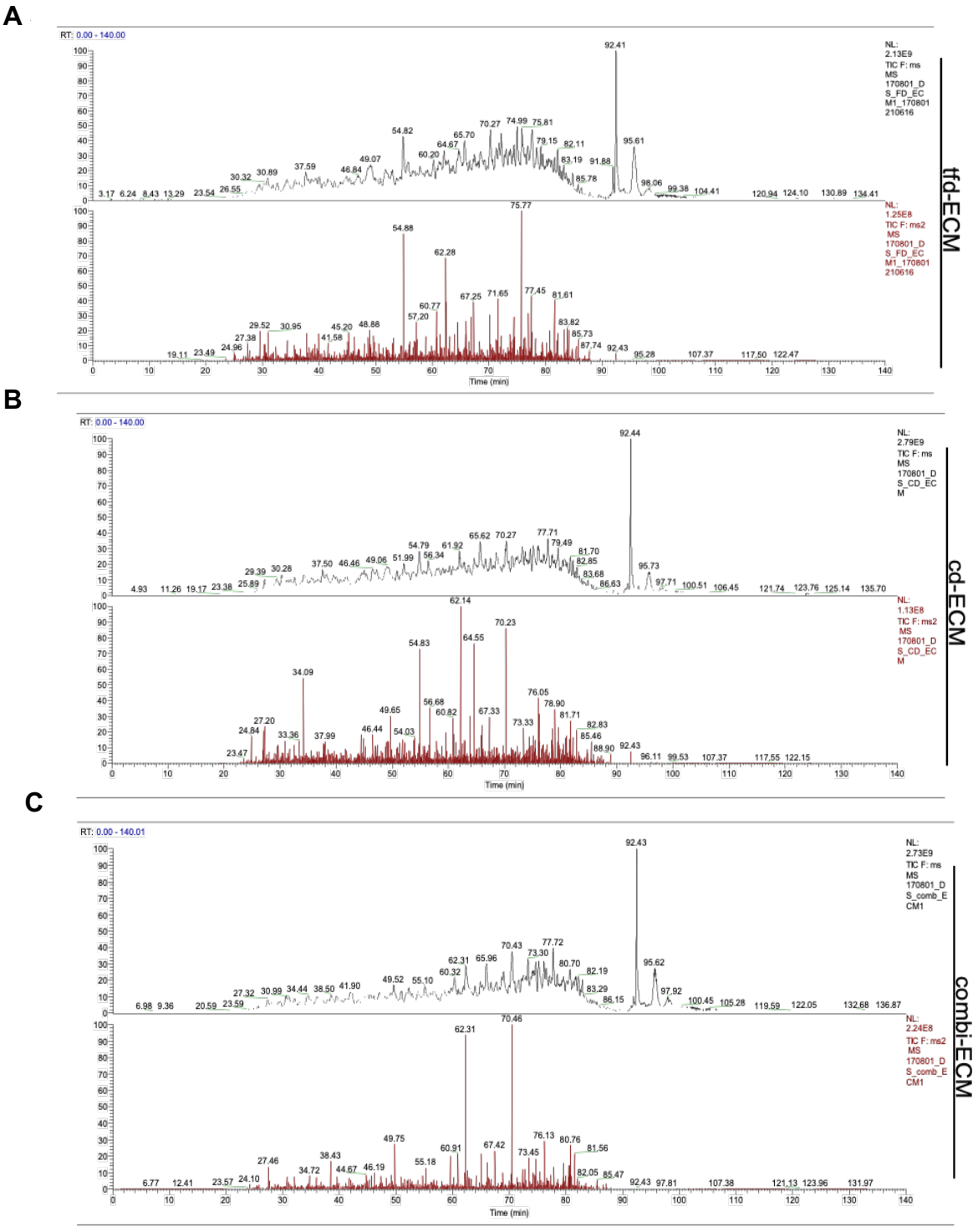

Figure 4. 5. Representative mass spectrometric chromatogram of decellularized ECMs. A representative TIC generated from a 140-minute linear LC gradient was used to analyse the label-free, **(A)** tfd-ECM, (B) cd-ECM and **(C)** combi-ECM samples. Upper panel: MS1 ion chromatogram; Lower pane: MS2 ion chromatogram. MaxQuant software was used to analyze the raw files to identify of proteins. Major ECM proteins identified are summarised in Table 4.1.

Table 4. 1. A summary of ECM proteins was identified from MaxQuant analysis.

Glycoproteins	Collagens	ECM Regulators	ECM Affiliated Proteins	Secreted Factors	Proteoglycans
FN1	COL1A1	TGM2	LGALS1	S100A13	HSPG2
LAMA3	COL1A2	HTRA1	FREM2	EGFL7	BGN
LAMA5	COL6A3	CSTB	ANXA2	IGF2	DCN
FBN1	COL3A1	LOXL2	FREM1	S100A11	LUM
TGFB1	COL12A1	LOXL1	ANXA6	S100A6	ASPN
TNC	COL6A1	SERPINH1	ANXA5	S100A13	OGN
EMILIN1	COL4A2	CTSB	COLC12	CXCL12	PRELP
LAMC1	COL6A2	LOX	CLEC3B	CCL25	VCAN
LAMB2	COL4A5	ITH5	LGALS3	PF4	
FBLN2	COL4A4	ADAM10	LGALS8	FGF2	
LAMA2	COL5A2	ADAMTSL1	SEMA3C	INSL5	
TNXB	COL7A1	PLG	CLEC14A	ANGPTL2	
POSTN	COL11A1	PZP	ANXA9	S100A9	
THBS1	COL4A1	CTSK	ANXA1		
FBN2	COL5A1	ADAMTSL5	PLXDC2		
FBLN1	COL5A3	SERPINA1A	SFTPA1		
LAMB3	COL14A1	SERPINA3K	CSPG4		
LAMA4	COL16A1	PLOD1	SFTPD		
AGRN	COL18A1				
FGB	COL15A1				
LAMC2					
VWF					
HMCN1					
LTBP4					

4.2.3 The effects of ECMs and drugs on WHCO1 cancer cell behaviour.

While this study was able to show ECM protein composition from the cell-derived ECMs, this suggested that ECM proteins play major roles in cancer cell progression, migration and drug resistance. To test this hypothesis, cells were cultured on plastic and on the cell-derived ECMs and the response to several chemotherapeutic drugs was examined through analyzing proliferation, apoptosis, colony formation, MMP activity, signaling pathways and migration.

4.2.3.1. Determination of IC_{50} of WHCO1 cells plated on plastic and ECMs.

Common therapeutic drugs used to treat of WHCO1 cancer cells include cisplatin, 5-fluorouracil and epirubicin. WHCO1 cells were treated with 0.1% DMSO as a control or various amounts of chemotherapeutic medicines to meet the study's goal. The MTT assay was used to determine the concentration at which paclitaxel, cisplatin and 5-Fluorouracil kill 50% of viable cells as described in section 7.2.9.2. Cells were treated with increasing concentration of drugs for 24 hours and viable cells were monitored using the MTT assay. The IC_{50} values with confidence intervals were calculated from the dose response curves cell viability for WHCO1 and KYSE180 using GraphPad Prism Software. The IC50 values for WHCO1 cells cultivated on ECM were greater than those for cells cultured on plastic, according to MTT data (Table 4.2). In order to study gene expression in response to the drugs, cells were treated with concentrations of drugs that were lower than their determined IC_{50} values for 24 hrs. This study used 4.2 μM cisplatin, 3.5 μM 5-fluorouracil and 2.5 μM epirubicinWHCO1 cells were plated on plastic or ECMs and treated with the above drugs for 24 hours. Morphological analysis displayed no differences between cells on plastic or on ECM, whether in the absence or presence of drugs (Figure 4.6). The IC_{50} obtained for cells plated on plastic and treated for 24 hours are in the same range as those obtained in the previous chapter.

Table 4. 2. Determination of IC_{50s} of cells cultured on plastic and on ECMs.

Drug	**Plastic**	**tfd-ECM**	**cd-ECM**	**combi-ECM**
Cisplatin (IC_{50} ± S.D. (μM))	18.5 ± 6.4	23.8 ± 3.2	22.4 ± 4.5	25.7 ± 3.2
5-FU (IC_{50} ± S.D. (μM))	14.1 ± 3.8	19.1 ± 2.6	20.6 ± 2.2	21.9 ± 1.8
Epirubicin (IC_{50} ± S.D. (μM))	12.8 ± 2.3	17.3 ± 4.5	18.5 ± 1.9	27.8 ± 5.3

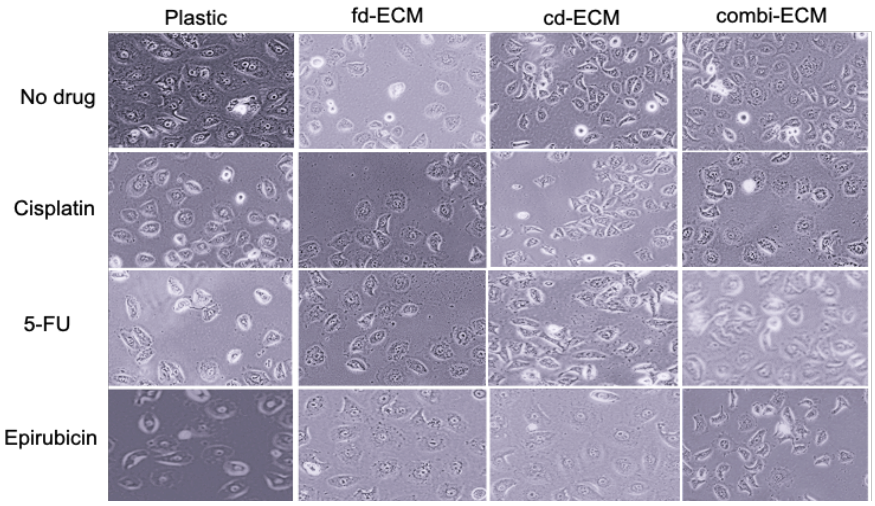

Figure 4.6. Morphology of WHCO1 cells plated on plastic versus cell-derived ECMs. WHCO1 cells were plated on plastic and ECMs, then treated with 4.2 μM cisplatin, 3.5 μM 5-fluorouracil and 2.5 μM epirubicin for 24 hours. Images were photographed using a phase-contrast image with an Olympus SC30 camera. The images were taken at 20 x magnification.

4.2.3.2 ECMs Protect WHCO1 Cells from the Effects of Anticancer Drugs

To determine the effect of cell-derived ECM on cellular proliferation on treated WHCO1 cells, MTT assays or cell counting were done. The proliferation of cells was monitored over 72 hours by trypsinisation and counting cells using the countess cell counter or using the MTT assay at each time period. The proliferation results showed that in the absence of drugs, no significant differences in cancer cell proliferation were observed between cells grown on plastic and those on ECMs (Figure 4.7 A). In contrast, cisplatin caused a significant decrease in cell proliferation on plastic compared to those on the ECM (Figure 4.7 B). A similar trend was obtained for cancer cell proliferation when cells were treated with 5-fluorouracil or epirubicin (Figure 4.7 C, D). On the other hand, the culture of cancer cells on ECMs reduced the cytotoxic effect of the drugs used in the study. This study also evaluated the effect of drugs on cell doubling time when grown on plastic or on ECM (Table 4.3). In addition to cell proliferation assays, the doubling time of cells plate on plastic or ECM was investigated. Doubling time is defined by the time it takes for WHCO1 cancer cells to double. In the absence of drugs, similar doubling times were obtained for cells grown on plastic and ECMs. However, the doubling times for cells grown in the presence of drugs and on ECM were lower than for cells grown on plastic and drugs (Table 4.3).

To further delineate the effect of drugs and-ECMs on the proliferation of WHCO1 cells, the expression of cell proliferation markers (Ki67 and PCNA) showed no significant change in Ki67 and PCNA expression in untreated WHCO1 cells plated on either plastic or ECM (Figure 4.8 A). In the presence of drugs, however, the expression of Ki67 and PCNA increased significantly in WHCO1 cells plated on EC (Figure 4.8 B-D). Furthermore, analysis of immunoblot band intensities, as illustrated in Figure 4.8. Overall, the results suggest that ECMs reduce the drugs' effect on WHCO1 cell proliferation, most probably through the expression of Ki67 and PCNA.

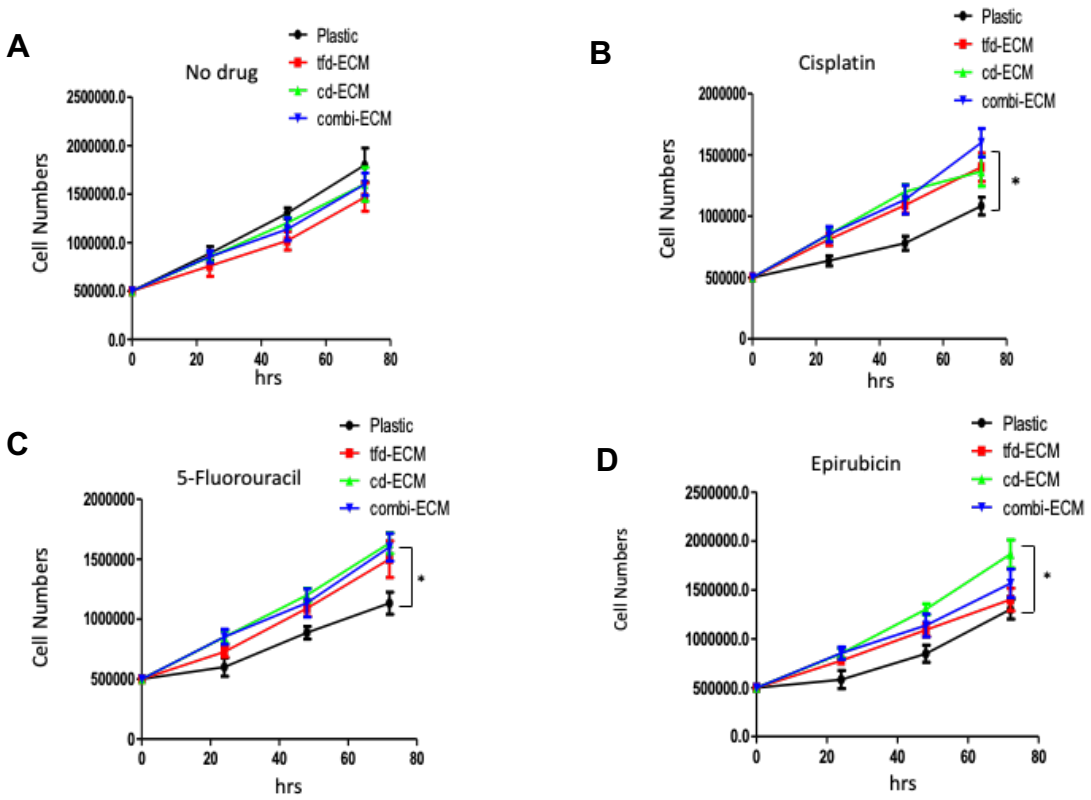

Figure 4. 7. Influence of decellularised ECMs on WHCO1 cell proliferation. 5 x 10^5 WHCO1 cells were plated on culture dishes with or without the cell-derived ECMs. Cellular proliferation of WHCO1 cells, **(A)** untreated, or treatment with **(B)** 4.2 µM cisplatin, **(C)** 3.5 µM 5-fluorouracil and **(D)** 2.5 µM epirubicin, was monitored for the indicated time (24, 48, and 72 hrs). Cell counting was performed as described in (section 7.2.8.1). The results shown are the mean ± SEM of experiments performed at least two independent times.

Table 4. 3. Doubling times of cells grown on plastic and on d-ECMs, with or without drugs.

	Plastic	**tfd-ECM**	**cd-ECM**	**combi-ECM**
No Drug (hours)	33.6 ± 3.3	38.6 ± 5.7	37.1 ± 4.2	36.8 ± 4.5
Cisplatin (hours)	55.3 ± 9.4	39.5 ± 4.3	36.9 ± 3.8	36.7 ± 5.8
5-FU (hours)	56.2 ± 5.1	39.5 ± 3.6	32.6 ± 4.6	31.9 ± 3.8
Epirubicin (hours)	58.3 ± 2.5	34.7 ± 3.5	30.7 ± 4.9	32.1 ± 3.8

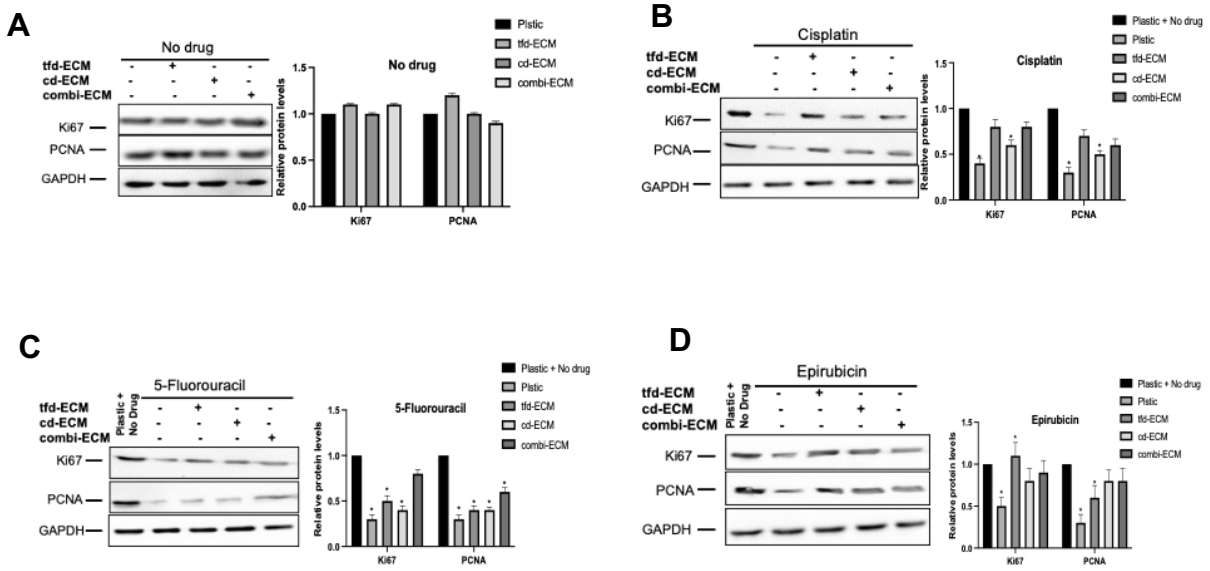

Figure 4. 8. Decellularised ECMs increase the expression of Ki67 and PCNA in the presence of drugs. Western blot analysis was done to evaluate the effects of ECMs on the expression of Ki67 and PCNA in WHCO1 cancer cells. WHCO1 cells were cultured on plastic or on ECMs and treated with drugs as indicated for 24 hours. **(A)** Expression of Ki67 and PCNA in WHCO1 cells in the absence of drugs or treated with **(B)** 4.2 μM cisplatin, **(C)** 3.5 μM 5-fluorouracil and **(D)** 2.5 μM epirubicin. Densitometric analysis of Ki67 and PCNA was relative to GAPDH, and the values were normalised to either plastic or plastic + no drug. Data show western blot (left panel) and densitometric analysis (right panel). Results shown are the mean ± SD of experiments performed in at least two independent experiments. *p < 0.05.

4.2.3.3 Effects of ECMs and drugs on WHCO1 cell cycle.

Flow cytometry using propidium iodide was performed to study whether ECM plays a role in the cell cycle progression of WHCO1 cells. WHCO1 cells were treated with 4.2 μM cisplatin, 3.5 μM 5-fluorouracil or 2.5 μM epirubicin for 24 hours, followed by cell cycle analysis. In the absence of drugs, the cell cycle profiles between cells grown on ECM compared to those grown on plastic were similar (Figure 4.9 A). Cisplatin resulted in G2 phase cell cycle arrest in WHCO1 cells cultured on plastic, and the effect of cisplatin was reduced in cells cultured on ECM, with cd-ECM and combi-ECM reducing the drug effectiveness more than the tfd-ECM (Figure 4.9 B). The addition of 5-fluorouracil caused a G1 phase cell cycle arrest and the drug effect was reduced in cells cultured on ECM (Figure 4.9 C). In addition, WHCO1 cells cultured on combi-ECM displayed similar profiles to cells cultured on plastic without of drugs (Figure 4.9 C). The addition of epirubicin resulted in a relative insignificant G2 phase cell cycle arrest on plastic and in the presence of combi-ECM (Figure 4.9 D).

Having observed that ECMs abrogated the effect of drugs on WHCO1 cell cycle, the effects of ECMs on cell cycle regulatory proteins such as cyclin D1 and p21 were investigated (Figure 4.10). In the absence of drugs, no significant effect was observed on the expression of cyclin D1, although there was a significantly decreased expression of p21 in WHCO1 cells plated on ECM (Figure 4.10 A). The expression of cyclin D1 and p21 protein was increased in the presence of drugs in WHCO1 cells cultured on ECM compared to those on plastic (Figure 4.10 B-D). The band intensities of at least two immunoblot gels normalized to GAPDH (Figure 4.10, right panel) suggest that ECMs reduce drug-induced cells cycle arrest through increased expression of cell cycle regulatory proteins.

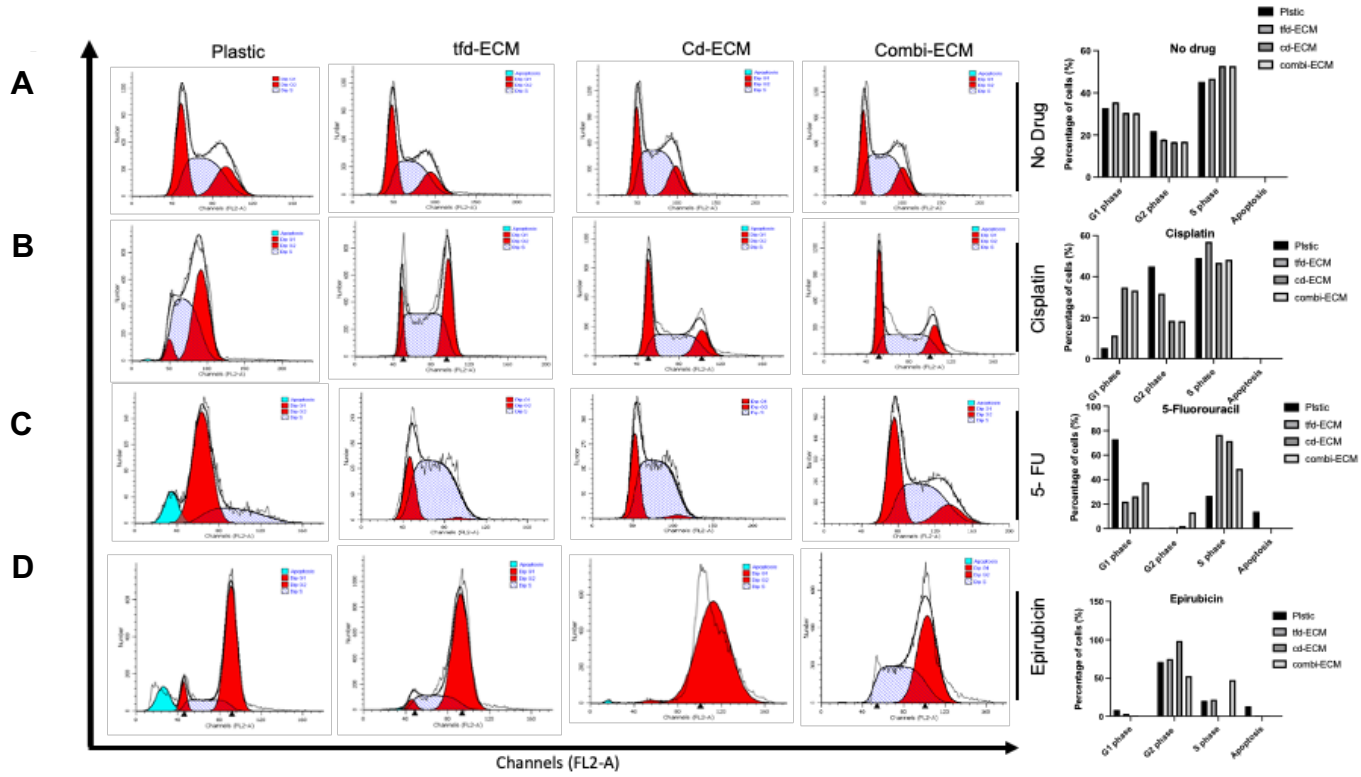

Figure 4.9. ECM abrogates drug-induced cell cycle arrest. Cell cycle analysis of **(A)** 5 x 10^5 Untreated WHCO1 cells, **(B)** WHCO1 cells treated with 4.2 µM cisplatin, **(C)** 3.5 µM 5-fluorouracil and **(D)** 2.5 µM epirubicin, grown on plates with or without ECMs, was carried out by flow cytometry using propidium staining. The percentage of cells in each cell cycle phase was analysed using Modfit LT software (Verity Software House) as described in section 7.2.13.1. Results shown representative of experiments done in triplicate and repeated at least three independent times.

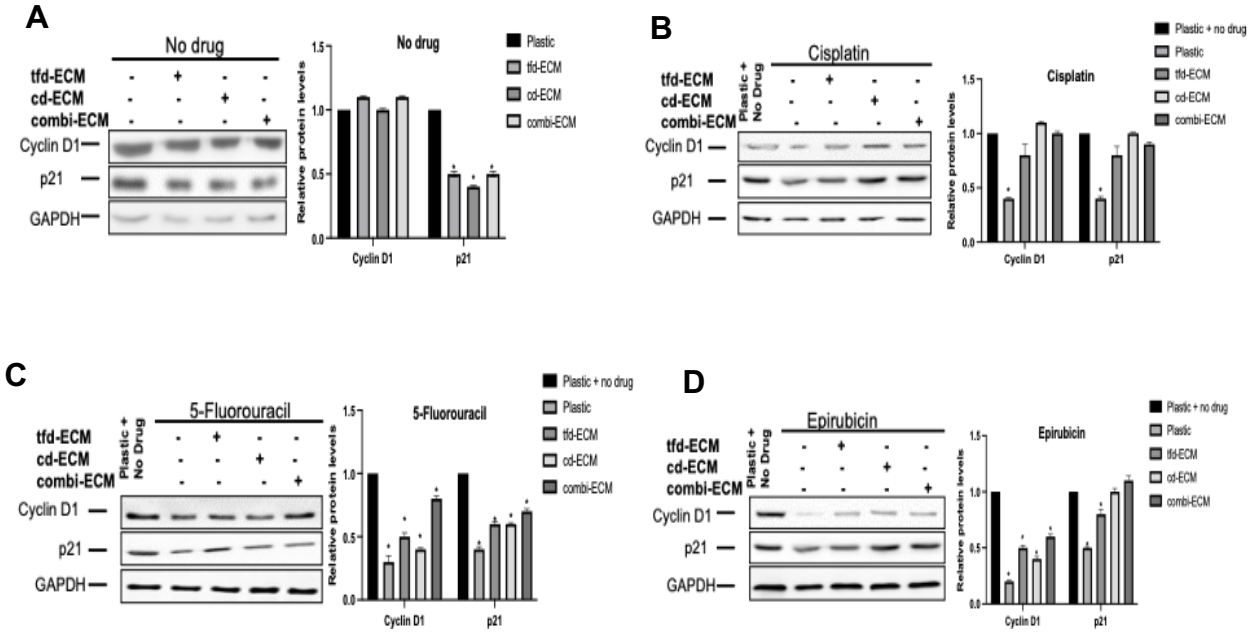

Figure 4. 10. ECMs increase the expression levels of cell cycle regulatory proteins. 10 cm plates with or without ECMs were used to grow **(A)** 5 x 10^5 Untreated WHCO1 cells, **(B)** 5 x 10^5 WHCO1 cells treated with 4.2 μM cisplatin, **(C)** 3.5 μM 5-fluorouracil and **(D)** 2.5 μM epirubicin for 24 hours. Western blot analysis was done to evaluate the expression of cell cycle regulatory proteins. Densitometric analysis of cyclin D1 and p21 are shown relative to GAPDH and the results were normalised either to plastic or to plastic plus no drug. Data show western blot (left panel) and densitometric analysis (right panel). Results shown are the mean ± SEM of experiments performed at least two independent times. * $p < 0.05$.

4.2.3.4 Effects of ECMs and drugs on WHCO1 apoptosis.

In order to evaluate whether the protective effect of the ECM was due to inhibition of apoptosis, Annexin V/Propidium Iodide double staining was used to determine cellular apoptosis (Figure 4.11). In the absence of drugs apoptosis was observed whether WHCO1 cells were plated on plastic or ECM (Figure 4.11 A, Q2 + Q3). Cisplatin-induced major apoptosis on WHCO1 cells plated on plastic (20% total apoptosis) and the presence of ECM reduced the drug-induced apoptosis (Figure 4.11 B, Q2 + Q3). The same results were observed in the presence of 5-Fluorouracil, with 16% total apoptosis in WHCO1 cells plated on plastic that was decreased in the presence of ECM (Figure 4.11 C, Q2 + Q3). Treatment with epirubicin resulted in 6% total apoptosis for WHCO1 grown on plastic and the effect was reduced in WHCO1 cells plated on all three ECMs (Figure 4.11 D, Q2 + Q3). Further analysis of Bcl-2 and Bcl-xL protein levels (antiapoptotic proteins) by western blot analysis revealed increased levels of these proteins when untreated or treated WHCO1 cells were cultured on ECMs (Figure 4.12, A-B), which is consistent with the above results. Using

densitometric analysis, the band intensities of at least two immunoblot gels were normalized to GAPDH (Figure 4.12, right panel). These results suggest that drug-induced apoptosis resistance may be caused by a combination of reduced ECM effects and increased antiapoptotic protein expression.

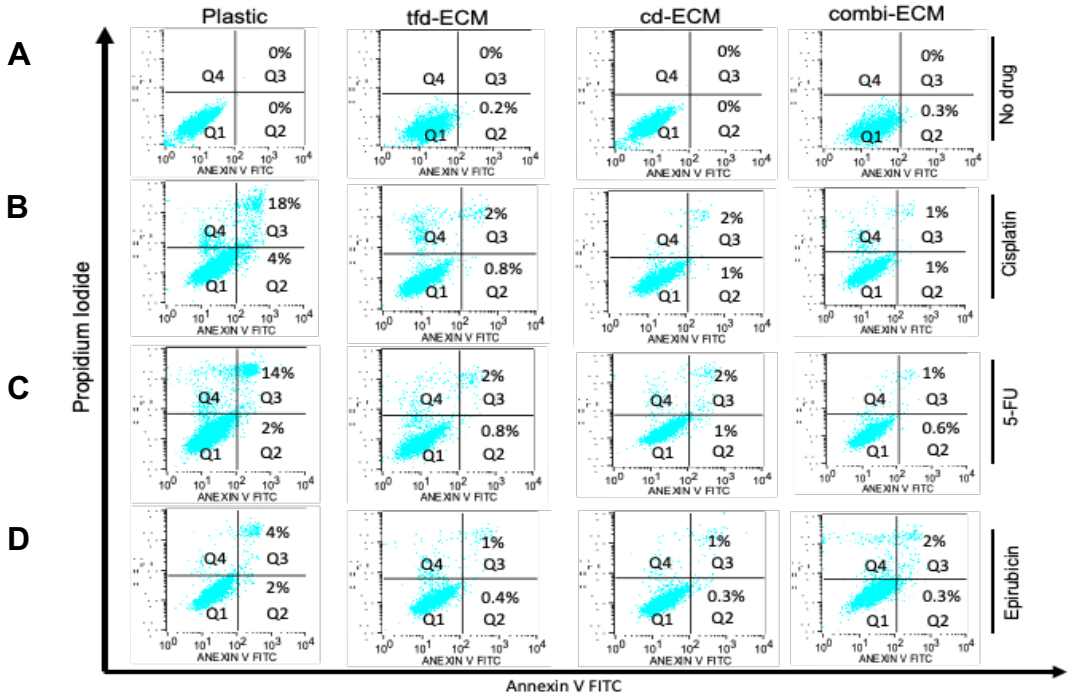

Figure 4. 11. Effect of ECM on cellular apoptosis in WHCO1 cells. Apoptosis analysis of **(A)** Untreated WHCO1 cells, WHCO1 cells treated with **(B)** 4.2 µM cisplatin, **(C)** 3.5 µM 5-fluorouracil and **(D)** 2.5 µM epirubicin, grown on plates with or without ECMs, was carried out by flow cytometry using Annexin V/Propidium Iodide double staining. Data acquisition was performed using the Cellquest software (Version 5.1, Becton Dickinson, Franklin Lakes, NJ, USA) as described in section 7.2.13.2. Results shown are representative of experiments done in triplicate and repeated at least three independent times.

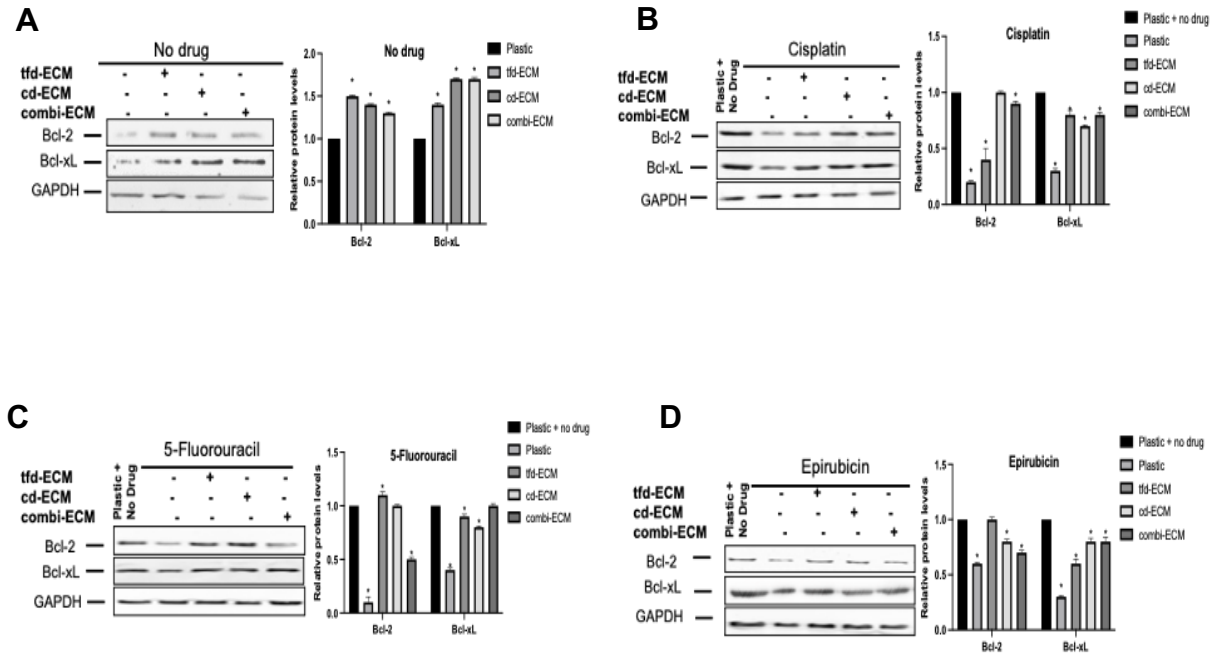

Figure 4.12. Increased antiapoptotic protein expression levels due to ECMs. WHCO1 cells were grown in 10 cm dishes with or without ECMs according to the following conditions: **(A)** 5 x 10^5 untreated WHCO1 cells, 5 x 10^5 WHCO1 cells treated with **(B)** 4.2 μM cisplatin, **(C)** 3.5 μM 5-fluorouracil and **(D)** 2.5 μM epirubicin. The expression levels of antiapoptotic proteins were evaluated using Western blot analysis. Bcl-2 and Bcl-xL densitometric analysis was performed relative to GAPDH and normalized to plastic or plastic plus no drug. Data show western blot (left panel) and densitometric analysis (right panel). Results shown are the mean ± SEM of experiments performed at least two independent times. * $p < 0.05$.

4.2.3.4 ECM increases the colony formation in the presence of anticancer drugs.

Given the significant increase in the proliferation, reduced drug-induced cell cycle arrest and apoptosis, the effects of ECM on colony formation of WHCO1 cells treated with drugs were investigated. Then, WHCO1 cells were grown in 6-well plates with or without the ECM and incubated for 10 days as described in the material and methods section (section 7.2.14). WHCO1 cells were treated with cisplatin, 5-fluorouracil and epirubicin for 24hours. After fixing, the cells were stained with 0.5% crystal violet and images of colonies were taken. In the absence of drugs, WHCO1 cells grown on ECM showed significantly increased colony formation compared to those plated on plastic (Figure 4.13 A). In the presence of drugs, the colony formation of WHCO1 cells increased compared to WHCO1 cells grown on plastic (Figure 4.13 A).

The previous chapter showed that cancer stem cells (CSCs) are present within tumours and play key roles in the development of drug resistance. This chapter investigated the effect of ECM on colony formation of WHCO1 cancer stem cells. The

side population technique was used to isolate WHCO1 CSCs, as described in Chapter 3 and Figure 4.13 B, C. Isolated WHCO1 SP cells formed more colonies on ECMs than on plastic (Figure 4.13 B). In addition, this study compared the effect of various ECMs on colony formation of WHCO1 and SP cells treated with 4.2 μM cisplatin. Both treated WHCO1 cells plated on ECM formed more colonies than those on plastic, with SP cells generating more colonies than parental WHCO1 cells (Figure 4.13 C). Overall, the ECM influences the formation colonies of WHCO1 cells and SP cells even in the presence of cisplatin, indicating that ECM has a significant influence on WHCO1 and SP cells colony formation, even when cisplatin is present.

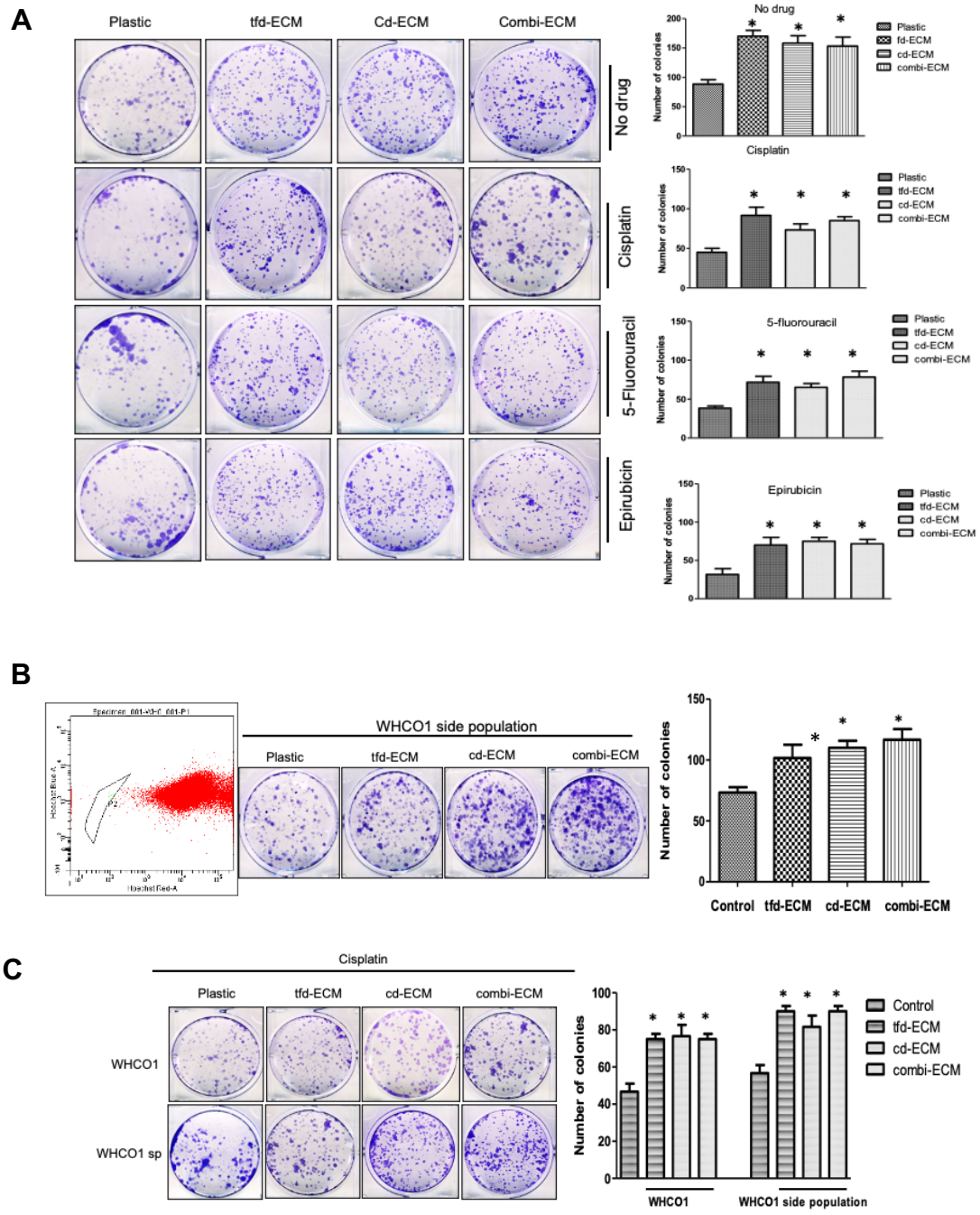

Figure 4. 13. ECMs increased colony formation in WHCO1 cancer cells. Cells were grown in 6-well plates with or without the ECM and incubated for 10 days and treated with drugs cisplatin, 5-fluorouracil or epirubicin. Cells were fixed and then stained with 0.5% crystal violet. **(A)** Images of colonies formed by WHCO1 cells on plastic or ECMs in the presence of cisplatin, 5-fluorouracil or epirubicin. **(B)** Images were obtained of WHCO1 SP sorting and colony formation of SP cells on plastic or ECM. **(C)** Representatives images of colonies from parental WHCO1 cells and SP cells on plastic or ECMs in the presence of cisplatin. The bar graphs on the right panel represent the quantification of colonies formed. Results shown are the mean ± SEM of experiments performed at least two independent times. * $p < 0.05$.

4.2.3.5 The ECM upregulates matrix metalloprotease gene expression in WHCO1 cells

Tumours rely on MMP-driven ECM degradation to move through the ECM and eventually invade and metastasise. This study, therefore, assessed the effects of ECM on the levels of MMPs using western blot analysis and their activity via Zymography. Western blot analysis revealed that WHCO1 cells had elevated levels of MMP-2 and MMP9 when plated on ECMs compared to plastic (Fig 4.14 A). The addition of cisplatin, 5-fluorouracil or epirubicin did not affect the expression of MMPs (Fig 4.14 B-D). The band intensities of immunoblot gels were normalized to GAPDH using densitometric analysis (Figure 4.14 A-B, right panel). The zymographic analysis confirmed increased MMP2 and MMP9 activity WHCO1 cells are plated on ECMs compared to plastic (Fig 4.14 A, lower panel). The elevated MMP2 and MMP9 activities were maintained in the WHCO1 cells grown on ECM when treated with cisplatin (Fig 4.14 B, lower panel). However, the presence of 5-fluorouracil and epirubicin, did not result in any change in MMP activity in cells grown on either plastic or ECM (Fig 4.14 C, D, lower panel). This could be due to 5-fluorouracil and epirubicin affecting the activation of the MMPs (Fig 4.14 C, D). Together these results provide evidence for the role of ECMs in the activation of MMPs in cancer cells.

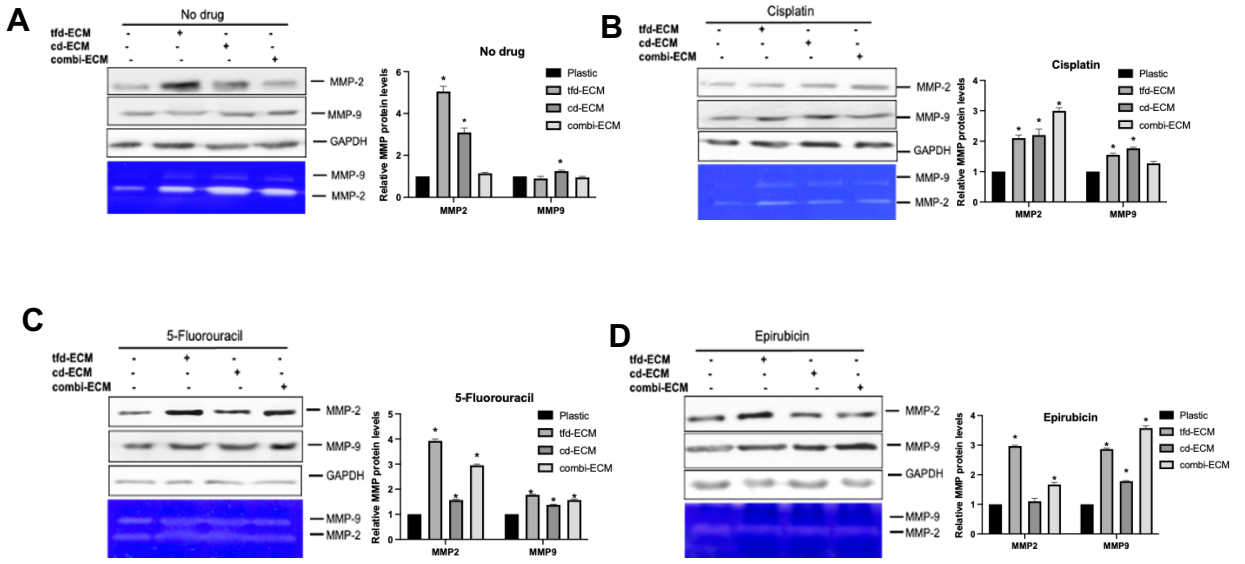

Figure 4. 14. The presence of ECMs affects the expression and activity of MMP9 and MMP2. WHCO1 cells **(A)** untreated and treated with **(B)** 4.2 μM cisplatin, **(C)** 3.5 μM 5-fluorouracil, or **(D)** 2.5 μM epirubicin for 24 hours, were grown on plates with or without ECM. Western blot analysis was used to determine the protein expression of MPPs (upper panel), and MMP activity was determine by gelatin Zymography of conditioned media (lower panel). The densitometric analysis of MMP9 and MMP2 expression was performed relative to GAPDH and normalized to plastic or plastic plus no drug. The left panel shows a western blot and the right panel a densitometric analysis. The results shown are representative of at least two independent experiments.

4.2.3.6 The ECM increases the expression of integrins in WHCO1 cells.

In addition to providing structural support, the ECM allows cell-to-cell and cell-to-matrix communication and can provide both mechanical and chemical stimulation to cells, resulting in diverse intracellular signals. Surface adhesion receptors have been shown to mediate many cell-ECM interactions, specifically, integrin-mediated signalling pathways are responsible for integrating signals from extracellular matrix components to control cellular development. Since the ECM protected WHCO1 cells from drug effects, this study investigated the effects of ECMs and drugs on integrin-mediated signalling to identify components responsible for this protective effect. The levels of adhesion receptors, including integrin α2, α3, α11 and β1, were assessed in WHCO1 cells using western blot analysis. In the absence of drugs, ITGα2 and ITGβ1 were increased in WHCO1 cells plated on cd-ECM and combi-ECM compared to those on plastic, while ITGα3 was significantly upregulated WHCO1 plated on all 3 ECMs (Figure 4.15 A). WHCO1 cells plated on ECMs and treated with cisplatin showed increased expression levels of ITGα2, ITGα3 and ITGβ1 compared to plastic. ITGα11 was elevated in WHCO1 cells plated on combi-ECM compared to cells on plastic (Figure 4.15 B). Treatment with 5-fluorouracil and epirubicin resulted in differential integrin expression in WHCO1 cells plated on both plastic and ECM (Figure 4.15 C,D).

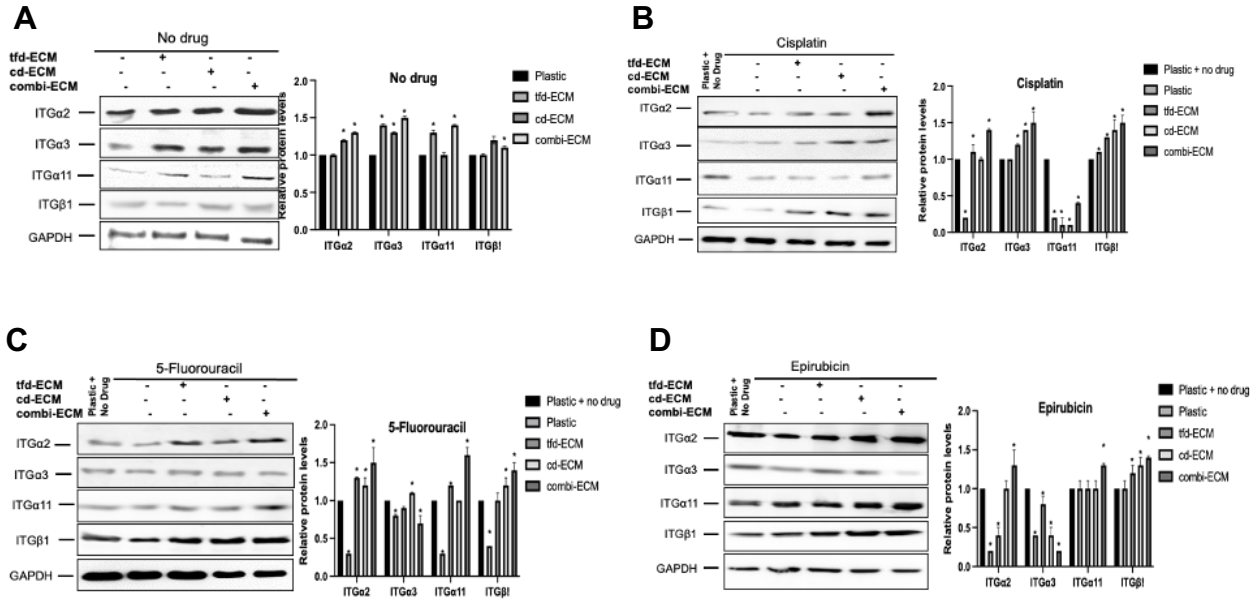

Figure 4.15. ECM increases the expression of integrins in WHCO1 cells. Western blot analysis of total lysate extracted from WHCO1 cells grown on either plastic, tfd-ECM), cd-ECM or combi-ECM was used to determine the level of integrins. The expression levels of integrin were evaluated in **(A)** untreated WHCO1 cells and WHCO1 cells treated with **(B)** cisplatin, **(C)** 5-fluorouracil or **(D)** epirubicin. Densitometric analysis of band intensities was done relative to GAPDH and normalized to plastic or plastic plus no drug. The left panel shows a western blot and the right panel a densitometric analysis. Results shown are the mean ± SEM of experiments performed at least two independent times. * $p < 0.05$.

4.2.3.7 ECM induces MEK/ERK and PI3K/Akt signalling in WHCO1 cells.

Integrins activate a variety of signalling pathways, including MEK/ERK, PI3K/Akt, that mediate most of the biological effects of ECM. Activation of pathways has been shown to enhance the growth, survival, and metabolism of cancer cells. To determine whether ECMs activate survival pathways in WHCO1 cells treated with drugs, MEK/ERK and PI3K/Akt levels were determined using western blot analysis (Figure 4.16). Phosphorylated EKR 1,2 (p-ERK 1,2) levels were elevated in untreated WHCO1 cells grown on three different ECMs, while p-Akt levels did not differ significantly from WHCO1 cells cultured on plastic (Figure 4.16 A). However, in the presence of drugs, both p-ERK1,2 and p-Akt levels were more pronounced in WHCO1 cells grown on cell-derived ECMs (Figure 4.16 B-D). Figure 4.16 A-D shows the quantification of band intensities using densitometric analysis (right panel). Overall, these results suggest that ECM activated the MEK-ERK and PI3k-Akt signalling pathways in WHCO1 cells.

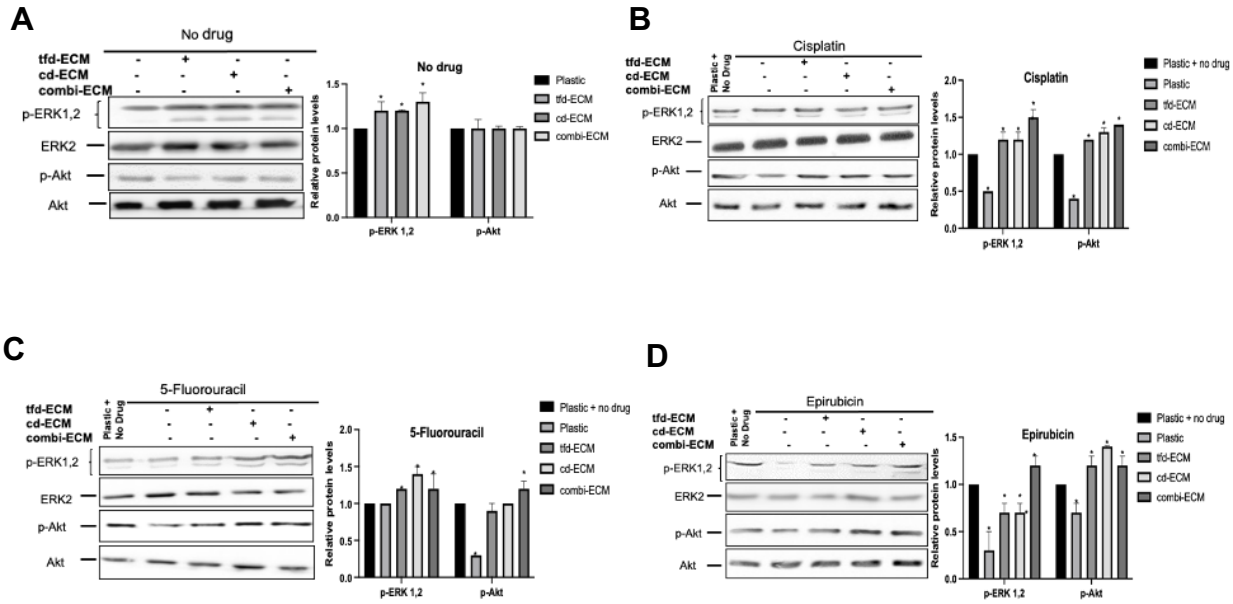

Figure 4.16. ECM induced MEK/ERK and PI3K/Akt activation in WHCO1 cells. Total lysate extracted from WHCO1 cells grown on either plastic, tfd-ECM, cd-ECM or combi-ECM was analysed using western blot. The effects of ECMs on the activation of signalling pathways was evaluated in **(A)** untreated WHCO1 cells, **(B)** WHCO1 cell treated with cisplatin, **(C)** with 5-fluorourail or **(D)** with epirubicin. Densitometric analysis of band intensities was done relative to GAPDH and normalized to plastic or to plastic plus no drug. The left panel shows a western blot and the right panel a densitometric analysis. Results shown are the mean ± SEM of experiments performed at least two independent times. * $p < 0.05$.

4.2.4. The effect of ECM proteins on drug-induced apoptosis and migration.

ECM proteins are involved in cellular survival, migration and invasion. Two major ECM proteins within the tumour microenvironment are type I collagen and fibronectin. This study showed that our cell-derived ECM consists of several ECM proteins, including type I collagen and fibronectin (section 4.2.2). This study investigated whether these two proteins played any role in WHCO1 cell apoptosis and migration by transient knockdown of type I collagen and fibronectin in CT1 fibroblasts and WHCO1 cells. Western blot analysis revealed that siRNAs successfully reduced type I collagen and fibronectin levels in CT-1 fibroblasts and WHCO1 cells (Figure 4.17 A, B). These cells were then used to prepare cell-derived ECMs to investigate the effect of collagen- or fibronectin-deficient ECMs on colony formation. Knockdown of type I collagen and fibronectin in addition to WHCO1 cells treated with cisplatin resulted in fewer colonies versus cells cultured on normal ECMs (Figure 4.17 C).

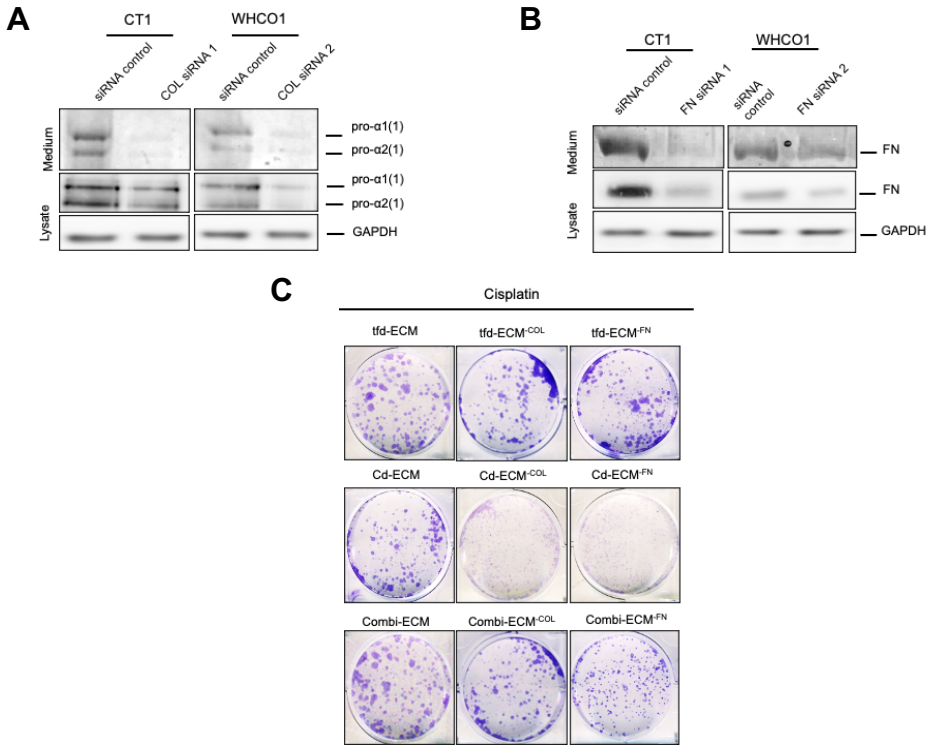

Figure 4. 17. Knockdowns of type I collagen and fibronectin in ECM synthesis. CT1 fibroblasts and WHCO1 cells were transfected with siRNA targeting type I collagen and Fibronectin. Knockdown of ECM proteins, **(A)** type I collagen and **(B)** Fibronectin using siRNA were evaluated via western blot analysis. Cell-derived ECMs were synthesised as described in section 7.2.3 with subsequent fibronectin siRNA and type I collagen siRNA. **(C)** Cells were grown in 6-well plates with ECM or protein-deficient ECMs and incubated for 10 days then treated with cisplatin. Cells were fixed and then stained with 0.5% crystal violet and images of colonies formed by WHCO1 cells were taken. Results shown are representative of at least two independent experiments.

Using Annexin V/Propidium iodide double staining, the effects of collagen- or fibronectin-deficient ECMs on drug-induced apoptosis were also investigated. Treatment with cisplatin induced increased apoptosis in WHCO1 cells cultured on type I collagen- and fibronectin-deficient ECMs than on normal ECMs (Figure 4.18 A). Western blot analysis of antiapoptotic proteins, Bcl-2 and Bcl-xL demonstrated decreased expression levels in the absence of type I collagen and fibronectin (Figure 4.18 B). The band intensities of immunoblot gels were normalized to GAPDH using densitometric analysis (Figure 4.18 B, right panel).

Using collagen- or fibronectin-deficient ECMs, the migratory capabilities of WHCO1 cells were investigated. To achieve this, cellular foci of 4 µl containing a total of 2 x 10^4 WHCO1 cells were added to culture dishes with or without the ECMs, as described in section 7.2.19. Images of cell migration were taken at times 0 hours and 24 hours. The results demonstrated that WHCO1 cells grown on normal ECMs migrated further than those cultured on plastic or type I collagen deficient ECMs (Figure 4.19 A, B). Integrins also function as cell-cell adhesion molecules, aiding the cells to attach to other cells and with the proteins of the ECM. Our studies focused on the functional role of α2β1 integrin, a major type I collagen receptor, in WHCO1 cell migration. The monoclonal antibody MAB1998 was used to block the activity of α2β1 integrin in WHCO1 cell suspension. The differences in migration of cells when plated on normal combi-ECM or collagen-deficient combi-ECM were investigated. Blocking α2β1 integrin antibody together with type I collagen knockdown synergistically abrogated WHCO1 cell migration on combi-ECM (Figure 4.17 C). Overall, the results suggest that ECM proteins, including type I collagen and fibronectin, may be mediators of cell survival and migration and that knockdown of specific ECM proteins may boost chemotherapeutic effects and suppress cancer development.

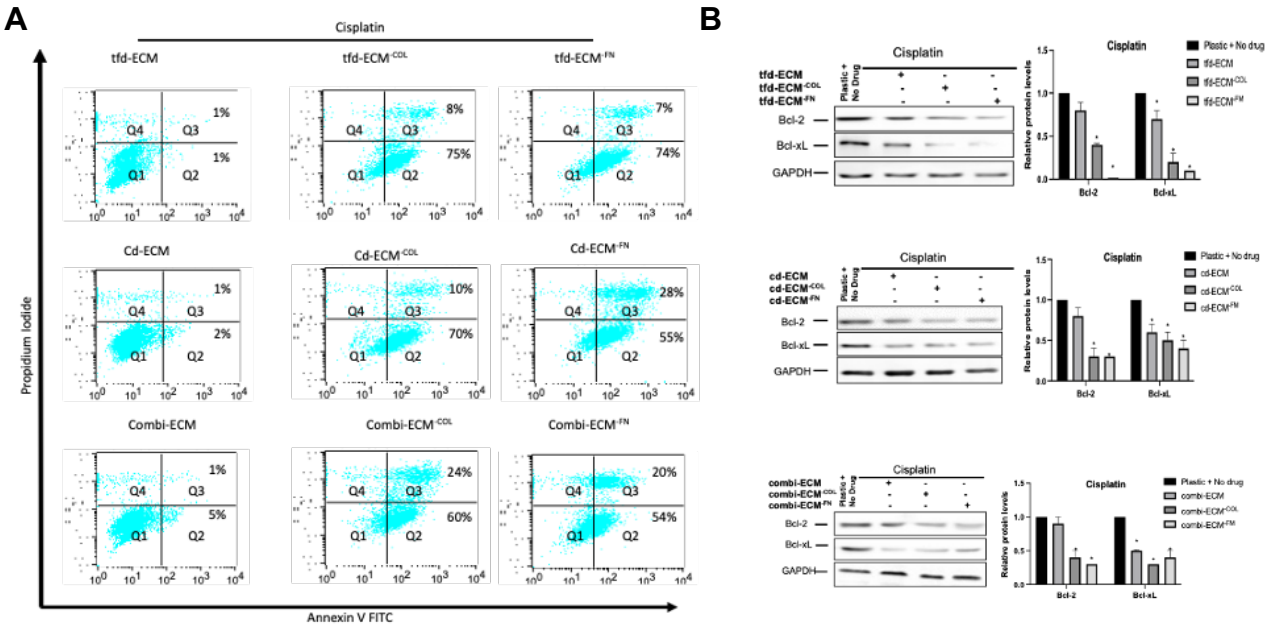

Figure 4. 18. Knockdowns of type I collagen and fibronectin resulted in increased apoptosis in WHCO1 cells. WHCO1 cells were plated on dishes with normal ECMs or protein-deficient ECMs and then treated with cisplatin. **(A)** Apoptosis analysis of WHCO1 cells was carried out by flow cytometry using Annexin V/Propidium Iodide double staining. Data acquisition was performed using the Cellquest as described in section 7.2.13.2. **(B)** Western blotting was used to evaluate the levels of Bcl-2 and Bcl-xL antiapoptotic proteins. Bcl-2 and Bcl-xL densitometric analysis was performed relative to GAPDH. Data show western blot (left panel) and densitometric analysis (right panel). The results shown are the mean ± SEM of experiments performed at least two independent times. * $p < 0.05$.

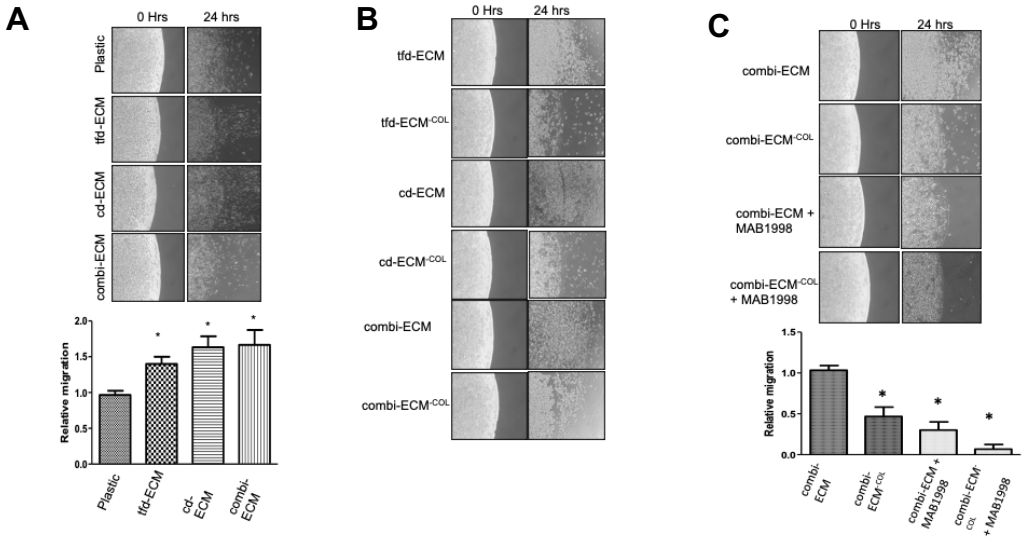

Figure 4. 19. Decreased cellular migration due to type I collagen and fibronectin knockdown in ECMs. WHCO1 cells were added to culture dishes with or without the ECMs in 4 µl cellular foci, as described in section 7.2.19. The cellular migration of WHCO1 cells was measured after 24 hours. **(A)** Representative images (top panel) showing migration of plated on plastic or normal ECMs. Quantification of distance migration was done using Image J, shown on the lower panel. **(B)** Representative images showing WHCO1 cell migration plated on ECMs following type I collagen and fibronectin knockdown. **(C)** Representative images showing WHCO1 cells migration after α2β1 integrin-blocking and knockdown of type I collagen in combi-ECM. The number of WHCO1 cells that have migrated following the type I collage knockdown and α2β1 integrin-blocking were quantified using Image J. Results shown are the mean ± SEM of experiments performed at least two independent times. * $p < 0.05$.

4.3 Discussion

The tumour microenvironment (TME) is key to the initiation and progression of different cancers [229, 391]. The TME is dynamic and comprises cancer cells, stromal cells, the ECM, biomolecules including growth factors and cytokines and immune cells [398, 399]. Within the TME, cancer-associated fibroblasts (CAFs) are the main cell types that have been shown to play crucial roles in influencing cancer growth as well as the synthesis of the ECM [11]. Several pieces of evidence point to CAFs and other stromal cells as the key to tumour growth via synthesis of ECM proteins and aiding in metastasis [400, 401]. Targeting the products of stromal cells such as the ECM may offer efficacy in controlling cancer development, chemoresistance and metastasis. Currently, few studies have focused on the ECM as a component of the tumour microenvironment. This is partly due to the fact that the ECM is constantly changing within the TME and may be difficult to define at any particular stage of cancer development.

This study determined novel targets from within the TME by investigating how ECM proteins affect cancer cell response to drugs. The study found that both type I collagen and fibronectin is involved in oesophageal cancer cell survival, migration and chemoresistance. These two proteins are also increased in oesophageal tumour samples versus adjacent normal tissue. ECM proteins have been reported to be linked to poor prognosis and chemoresistance [402, 403]. Previous reports have also linked type I collagen and fibronectin with cancer cell migration [404, 405]. This study showed that the removal of both type I collagen and fibronectin influenced oesophageal cancer cell survival, migration and chemoresistance. Type I collagen and fibronectin have been shown to promote the migration of breast cancer cells [406]. Many of the ECM proteins present in it could determine a tumour's ability to progress and become invasive. This study showed that MMPs and integrins were elevated in tumour samples. By binding to the ECM, integrins can activate the synthesis of MMPs and upregulate their expression. The activation of MMPs by integrins promotes oral squamous carcinoma cell proliferation and metastasis *in vivo* [407], suggesting that MMPs and integrins play critical roles in tumour development. As a result, the analysis of ECM proteins, integrin and MMPs present in the stroma of OSCC could advance our understanding of the interaction of OSCC cells with their stromal component.

To study the features of the *in vivo* tumour microenvironment [408, 409], various combinations of ECM proteins, cancer cells and stromal components in one culture system have been explored [410]. The role of different ECM members in chemotherapeutic resistance has not been studied in detail. This study aims to elucidate the mechanism by which the ECM can contribute to drug resistance in cancer cells. Most cancer cell cultures employed in various studies lack cell-cell and cell-ECM interactions Models utilizing ECM components have improved our understanding of how tumour cells interact with one another and ECM. Tumour cells grown in monolayers and on ECM proteins show apparent differences in morphology, expression of genes and proteins, growth rate, and invasive properties [411, 412]. *In vivo*, cancer cells are surrounded by many tumour components that restrict the movement of anticancer drugs throughout the tumour. In contrast, on 2D surfaces, cancer drugs can reach cancer cells without encountering physical barriers. For example, the doxorubicin sensitivity of breast cancer cells grown in a 3D-ECM model is altered compared with 2D monolayer culture [413]. In 2D and 3D grown colorectal cancer cells, 5 fluorouracil and erlotinib, an EGFR inhibitor, were discovered to have distinct drug sensitivities [414]. In addition to preventing drugs from physically accessing cancer cells, our study showed that the decellularized ECMs could also upregulate genes related to cell proliferation (Ki67 and PCNA) and antiapoptotic genes such as Bcl-2 and Bcl-xL. Decellularized ECMs can influence cellular biological processes through increasing the expression of these genes. This could be an adaptive mechanism by cancer cells use when exposed to new environments.

Natural decellularised ECMs were utilised instead of purified ECM proteins to better simulate the *in vivo* tumour microenvironment, as the combination of cancer cells and fibroblasts best represents the ECM milieu present in TME [373]. Collagen type I and II, fibronectin, proteoglycans such as biglycan and decorin, and major basement membrane components such as lamin, POSTN, and perlecan are among the decellularized ECMs produced in this study. They all play important roles in cancer cell proliferation, differentiation, adhesion, migration, and survival. [415, 416]. Many studies have shown a link between changes in deposition and amounts of collagens, including type I collagen, with impaired development and development of cancers [417, 418]. Collagens found within the ECM in normal tissues can be highly uniform in orientation, whilst in pathological conditions, the orientation is varied [419, 420].

Overall, the number of different collagens in the ECM influences its properties, such as elasticity and biomolecule availability, such as growth factors and chemokines [365, 376]. Collagens within the ECM also play other important roles within the body. For example, collagens are essential within basement membranes where they contribute to the separation of different layers of tissues. Increased collagen deposition within basement membranes can lead to membrane stiffening, disrupting regular exchange of biomolecules and movement of cells [421]. In many pathological conditions such as cancer, basement membranes are thinner than normal tissues. This has been attributed to less deposition of collagens including, type IV, type XV and type XIX collagens [422, 423]. Indeed, several *in vitro* studies have also shown that collagen knockdown can enhance the migration of cancer cells [319, 424, 425].

In addition, glycoproteins are actively involved in regulating processes including proliferation, migration and adhesion [426, 427]. The glycosaminoglycan chains of proteoglycans are also negatively charged, allowing proteoglycans to impact the organisation of other ECM constituents [427]. The negative charge on proteoglycans also allows the ECM as a whole to sequester growth factors and other biomolecules [428, 429]. Due to their size and structure, proteoglycans can also participate in binding ligands to receptors, allowing cells, including cancer cells, to respond to various changes in extracellular cues. Several signalling pathways, including the MEK-ERK and the PI3-Akt pathways, have been shown to be activated through the participation of proteoglycans in bonding to various receptors [430, 431]. Most well-known glycoproteins include fibronectin, fibrinogen, vitronectin, laminin, thrombospondins, periostin and osteopontin. Among the well-known proteoglycans are decorin, aggrecan and perlecan. Several glycoproteins and proteoglycans were discovered by mass spectrometric analysis of the ECMs used in this investigation. Various cancer cell behaviours, such as growth, proliferation, invasion and drug response, are influenced by the physical structure of the ECM in the TME [432]. Decellularised ECMs promoted the migration of WHCO1 cells. In agreement with these findings, ECM components were found to be crucial for cell invasion in bladder cancer [433]. These results provide insight into aspects that should be considered when developing a 3D model that can accurately mimic the TME to develop successful new therapies.

Chemoresistance can increase through multiple mechanisms. One of these mechanisms is cell growth promotion. We have examined how different ECMs affect WHCO1 oesophageal cancer cells' respond to drugs such as cisplatin, 5-fluorouracil, and cisplatin. These chemotherapeutic drugs have been shown to activate cell cycle checkpoints resulting in the cell cycle arrest in cancer cells [434]. The findings of this study are similar with previous research, indicating that medicines can cause cell cycle arrest in cells cultured on plastic, and that this effect was reduced in decellularised ECMs. Various reports support this observation. For example, it has been shown that ECM proteins activate β1 integrin to protect small cell lung cancer cells from cell cycle arrest and apoptosis induced by the DNA damaging agents [435]. In this study, cancer cell- and stromal cell-derived ECMs were able to promote or induce resistance to the chemotherapeutic drugs in WHCO1 cancer cells. Similarly, *in vivo*, it is possible that many ECM components as part of the TME work in concert to enable cancer cells to grow and develop resistance to drugs. This study showed that the ECMs encouraged the capability of a single cancer cell to form more colonies compared to cells plated on plastic. These observations are in agreement with a study by Lai Y et al. (2010) that showed that MSCs plated on ECMs formed more colonies than those plated on plastic [436]. These findings suggest that the ECM may influence both the development and progression of cancer.

One of the major receptors for ECM-cell interactions is integrins. Integrins are heterodimers involved in transmitting extracellular cues into cellular signalling [437]. During development and in some pathological conditions, specific integrins are expressed and these influence specific cellular activities such as migration, proliferation, and adhesion [438, 439]. Importantly, the binding of various integrins, including αvβ1, αvβ3 and α4β1, to ECM molecules has been linked with tumour cell invasion during tumourigenesis [440]. Furthermore, the specific expression of certain integrins may be linked to the promotion of tumourigenesis, drug resistance and metastasis [441]. The enhanced expression of α5β1 and its binding to ECM molecule fibronectin has been linked to reduced drug efficacy in models of cancers [442, 443]. Overall, the involvement of integrins in development and in pathological conditions such as cancers depends on the type of integrin, ECM molecules and cell type [444, 445]. In this study, we observed that WHCO1 cells cultured on ECM migrate more

readily along the direction of the ECM fibres, whereas WHCO1 cells grown on plastic showed a decrease in migration.

Certain survival pathways are activated when cancer cells adhere to specific ECM proteins, enhancing the chemoresistance of the cancer cells. This study showed that when WHCO1 cells were cultured on the different ECMs, significant upregulation of the MEK-ERK pathway and PI3K/Akt was observed. When cisplatin was added, the MEK-ERK signalling pathway in WHCO1 cells plated on all ECMs remained upregulated compared to plastic. When WHCO1 on the ECMs was plated with 5-fluorouracil and epirubicin, both MEK-ERK and PI3K/Akt remained elevated compared to plastic. ECM-tethered growth factors may be responsible for activating these pathways. When cancer cells bind to ECM, several signalling pathways are activated, such as PI3K/Akt, MEK-ERK and Rho/ROCK [446, 447]. Resistance to 5-fluorouracil, epirubicin, and cyclophosphamide in breast cancer has been demonstrated to be largely dependent on the protein composition of the stromal ECM [448]. The MEK-ERK and PI3K-RAF signalling pathways are known to induce the expression of several cell cycle-associated proteins, including cyclin D1. As a result of activating these Ras-mediated pathways, proteins such as cyclin D1 are protected from degradation. In this study it was observed that the addition of 5-fluorouracil and epirubicin decreased the doubling time. This could be due to the use of drug concentration much lower than the actual IC50's, not meant to kill the cells. The presence of the low drug concentration and the 'physically blocking' ECMs may have promoted the activation of survival pathways in cancer cells. This might promote cancer cell proliferation as observed in this study for 5-fluorouracil and epirubicin. Whilst stromal cells and tumour cells both can release growth factors and chemokines and thus influence signalling, the ECM can enhance or decrease the resulting signalling via the release of sequestered growth factors and chemokines and sequestering synthesised factors, respectively [449, 450]. In addition, the stiffness of the ECM can influence integrin-based signalling during normal development and in diseases [451, 452]. Reports indicate that signalling cascades, including the MEK-ERK and the JNK signalling cascades can be activated by ECM stiffening in various conditions [453, 454]. Other signalling cascades also respond to ECM composition and stiffness. Thus, targeting these signalling cascades, together with ECM composition and stiffness are plausible strategies to control tumour progression and metastasis. The findings of this study showed that treatments

inhibiting the production of certain ECM components, such as type I collagen and fibronectin, can help deliver drugs to cancer cells more effectively. This study found that the ECM is a limiting factor on drug efficacy and suggested that combination therapy, including drugs that target the ECM components as well as cancer cells be used. Overall, both the cd-ECM and combi-ECM promoted cancer proliferation and migration more than the tdf-ECM. Based on data from this study, the cd-ECM and combi-ECM may contain cancer-specific sequested growth factors and proteins that activate survival pathways in cancer cells more than tdf-ECM. More studies comparing the three dECM are required. For example, long term studies are needed to elucidate the role played by transformed fibroblasts in cancer cell growth and migration. As a results, it would be important and interesting to do further studies to compare the three cell-derived ECM on how they promote cancer cell growth.

CHAPTER 5:
USE OF 3D MULTICELLULAR TUMOUR SPHEROIDS CULTURE TO INVESTIGATE DRUG SENSITIVITY IN CANCER CELLS.

5.1 Introduction

A tumour mass comprises cancer cells, stromal cells, ECM and biomolecules; a complexity that has presented multiple challenges of replicating *in vitro* experiments [262, 455]. [456, 457]. The three-dimensional (3D) multicellular tumour spheroids (MCTS) model has become an integral part of cancer research as a tool to bridge the gap between 2D monolayer cultures and *in vivo* solid tumours [458, 459]. MCTS are cell clusters formed through self-assembly or forced growth starting from single-cell suspensions. MCTs can be obtained from cancer cells or co-cultures of cancer cells and various stromal cells such as fibroblasts, endothelial cells, or immune cells [460]. In terms of morphology, MCTS are influenced by cell type, cell density, culture media and culture method [461]. Classically, MCTS can be grouped as compact spheroids, tight aggregates, or loose aggregates of cells. Importantly, MCTS show various features of avascular tumours such as the external proliferating zone, an internal quiescent zone, and a necrotic core (Figure 5.1) [462]. Cells within MCTS are closely packed in high density into spheroids. Thus, the cells within MCTS can interact with each other and other components and maintain complex communications with the ECM [461]. Various reports have shown that MCTs recapitulate *in vivo* solid tumours in different aspects, including resembling the heterogeneous architecture of tumours, growth factor distribution, limited oxygen, necrotic area and nutrients gradients across the tumour [463]. Importantly, MCTs demonstrate similar growth properties to tumours [464, 465]. In addition, cancer cells and stromal cells within MCTS show cell-to-cell and cell-to-ECM interactions as in solid tumours [240]. Similarities between solid tumours and MCTS allow the various biological properties of solid tumours to be studied *in vitro* and can also be applied to other applications such as drug discovery and studying drug efficacy [457, 466]. However, the clinical relevance of MCTS is still under evaluation.

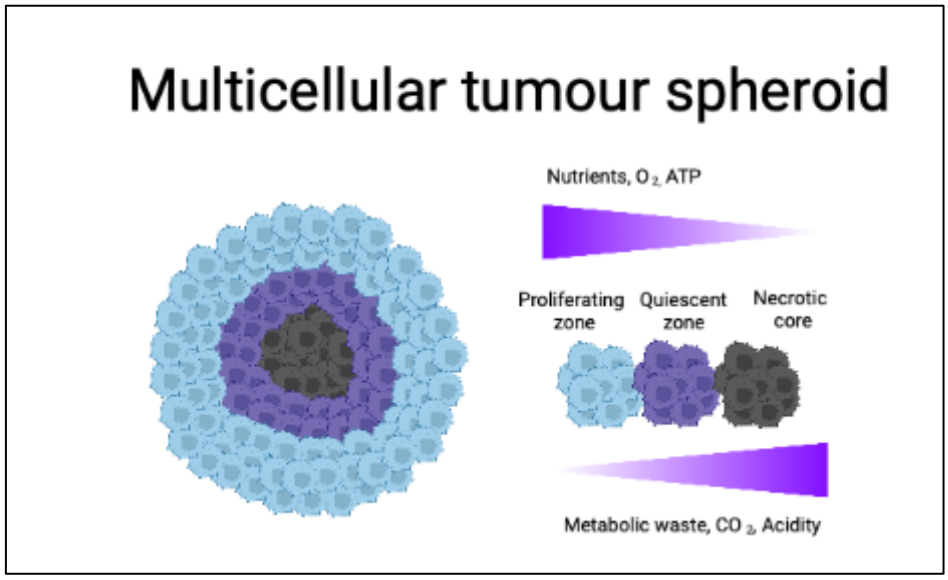

Figure 5. 1. Schematic representation of the *in vitro* 3D multicellular tumour spheroid. Cellular aggregates called multicellular tumour spheroids (MCTS) are created by seeding cells on low adhesive or agarose-coated culture plates. The MCTS mimics the *in vivo* microenvironment of solid tumours in terms of nutrients, oxygen, pH gradients, and zone formation. *In vitro*, MCTS provides a platform for investigating cell-cell and cell-ECM interactions. Figure created using Biorender (https://biorender.com/).

Various methods have been derived to form MCTS, with the major method incorporating the use of a 3D scaffold and the other involving scaffold-free conditions [467, 468]. The 3D scaffold method involves seeding cells on an acellular 3D artificial matrix that mimics ECM architecture [469, 470]. Currently, various matrices are in use, including, ECM proteins such as collagen, Matrigel and laminin [471]. In the scaffold-free method, cells are seeded in a liquid overlay or hanging drops [461, 472]. In the hanging drop method, a cell suspension is placed on a lid of a culture dish, and the surface tension and gravity allow the formation of spheroids [473]. This method has a high reproducibility compared to other methods as changes in cell density can be controlled to give rise to MCTS of different sizes [470]. Once formed, spheroids can then be transferred to low attachment plates or culture dishes. Low adhesive culture dishes can also be used, causing cells to aggregate in the liquid overlay method [469, 474]. Advances in technologies have seen the advent of new methods for MCTS formation involving microfluidic systems and 3D bio-printing [475].

This chapter is primarily focused on MCTS formation and its application in cancer biology. First, the MCTS model was used to determine how cancer cells and their stromal components interact to influence chemoresistance and migration.

5.2. Results

5.2.1. Multi-cellular tumour spheroid culture optimization and characterisation

The progression of cancer is partly promoted by the presence of stromal cells such as fibroblasts and immune cells. WHCO1 (oesophageal) and MDA MB 231 (breast) cells were utilized to investigate their ability to form tumour spheroids *in vitro* when cultured alone and with normal (WI38) and transformed (CT1) fibroblasts. In order to enable spheroid formation, 96-well round-bottom low attachment plates were used to prevent cell adhesion to the well bottom and allow the formation of spheroids in suspension. This allowed cell-to-cell interaction, leading to spherical formation within a short period of time. The diameter and circularity of spheroids were measured to monitor the growth of spheroids. Our analysis demonstrated that 3000-5000 cells at day 3 formed spheroids of about the same size (Figure 5.2 A) and were optimum for the formation of spherical structures and not loose cell aggregates. Both WHCO1 and MDA MB 234 cancer cells were able to form tumour spheroids within a day (Figure 5.2 B). However, the growth kinetics of the spheroids formed by cancer cells alone and in co-culture with fibroblasts were different. Tumour spheroids formed by both WHCO1 and MDA MB 234 cancer cells alone increased in size at a faster rate over the 7 days of culture compared to co-cultured cells, as demonstrated by the spheroid diameter measurements (Figure 5.2 C).

The addition of WI38 and CT1 fibroblasts to cancer cells resulted in spheroids growing at a slow rate and the formation of slightly smaller and more compact tumour spheroids compared to cancer cells alone (Figure 5.2 B, C). Tumour spheroids formed by cancer cells alone and in co-culture with fibroblasts can be maintained over 7 days. There were no observable differences in spheroid circularity over 7 days of culture for both cancer cells alone and in co-culture with fibroblasts (Figure 5.2 D). These results indicate that 96-well round-bottom low attachment plates were sufficiently non-adherent and promoted compact spheroid formation.

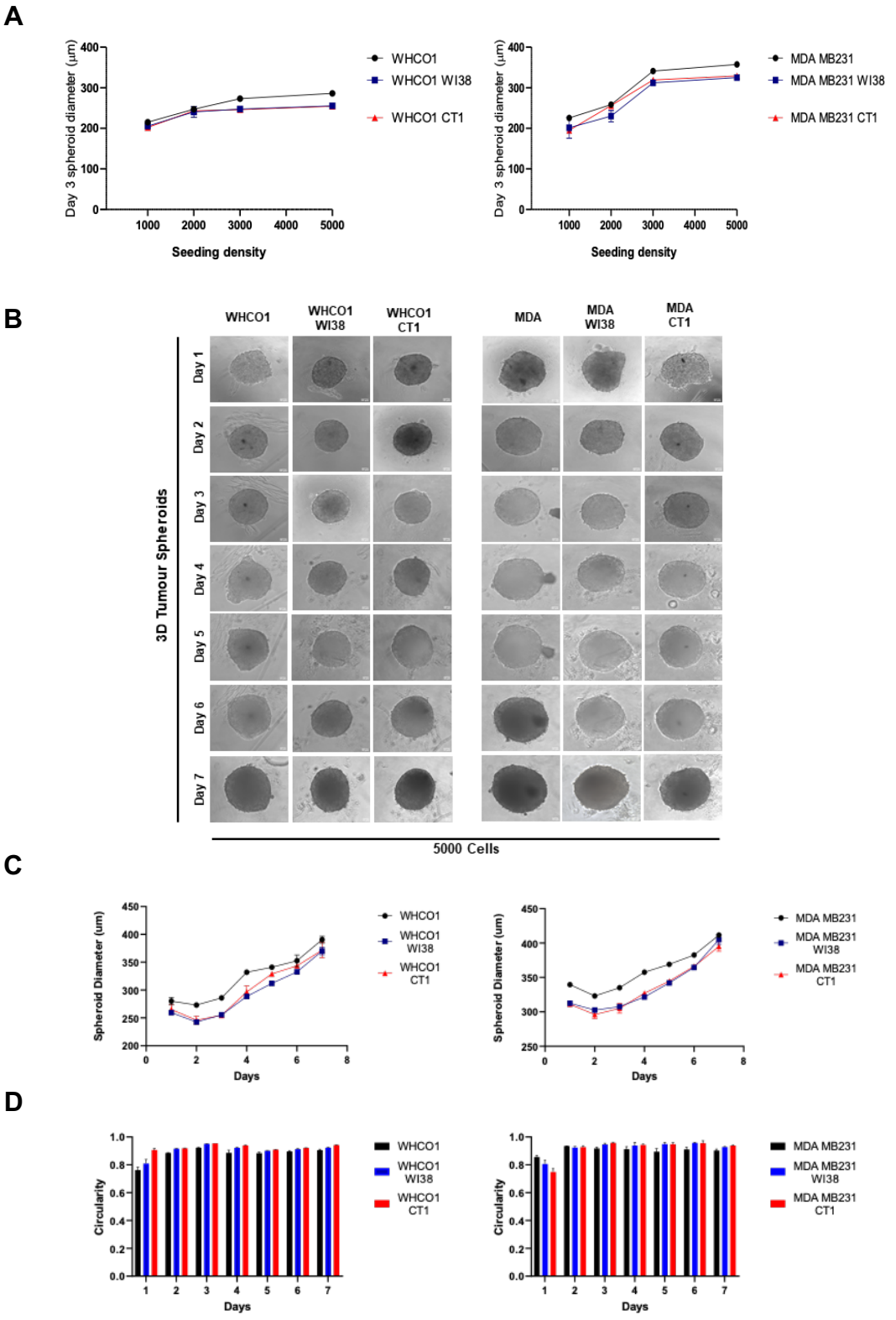

Figure 5. 2. Tumour spheroids morphology and growth characterisation. WHCO1 and MDA MB231 cancer cells cultured alone or with Wi38 or CT1 fibroblast at a 1:1 ratio were used to form tumour spheroids in 96-well low attachment plates. **(A)** Diameter of day 3 spheroids obtained after seeding cells at different densities per well (1000-5000 cells). **(B)** Tumour spheroids representative images cultured were at 5000 cells per well from day 1 to 7. Scale bar: 50 µm. **(C)** Spheroid diameter, for both WHCO1 and MDA MB 234 cells alone and co-cultured with CT-1 and WI38 cells, overtime for the 7 days used in the study after seeding 5000 cells /dish. **(D)** Change in circularity over 7 days in spheroids from WHCO1 and MDA MB 234 cells, alone or co-cultured with fibroblasts at a 1:1 ratio (n =3). The results shown are the mean ±SEM of experiments performed in triplicate and repeated at least two times.

5.2.2 WHCO1 and MDA MB 231 spheroid growth properties over days

To further study the characteristics of spheroids formed when cancer cells and fibroblasts are co-cultured, cells were cultured at a ratio of 1:1 and spheroid structures were observed over 3 days. In order to distinguish between the different cells, cancer cells were stained with Blue CMAC and fibroblasts with Texas Red to track the localization of cells within the spheroids by fluorescence imaging. Immediately after culturing cells in low attachment dishes, spherical structures started forming at day 0 (Figure 5.3 A, B). Importantly, both WHCO1 and MDA MB 231 cells, when co-cultured with WI38 and CT1 cells, displayed heterogeneous shapes at day 0, with the two cell types distributed equally throughout the spheroids (Figure 5.3 A, B). By day 1, spheroidal structure was obvious, but the cancer cells and fibroblasts were started segregating. On day 3, intra-spheroid localisation of cells showed cancer cells occupying the centre of the spheroid with fibroblasts on the outside (Figure 5.3 A, B). Various reports have suggested that the body uses this mechanism to isolate cancer cells from normal tissue [319, 403]. The fibroblasts on the periphery of the spheroid are known to synthesise large quantities of extracellular matrix proteins that form a capsule, isolating tumour cells in the process.

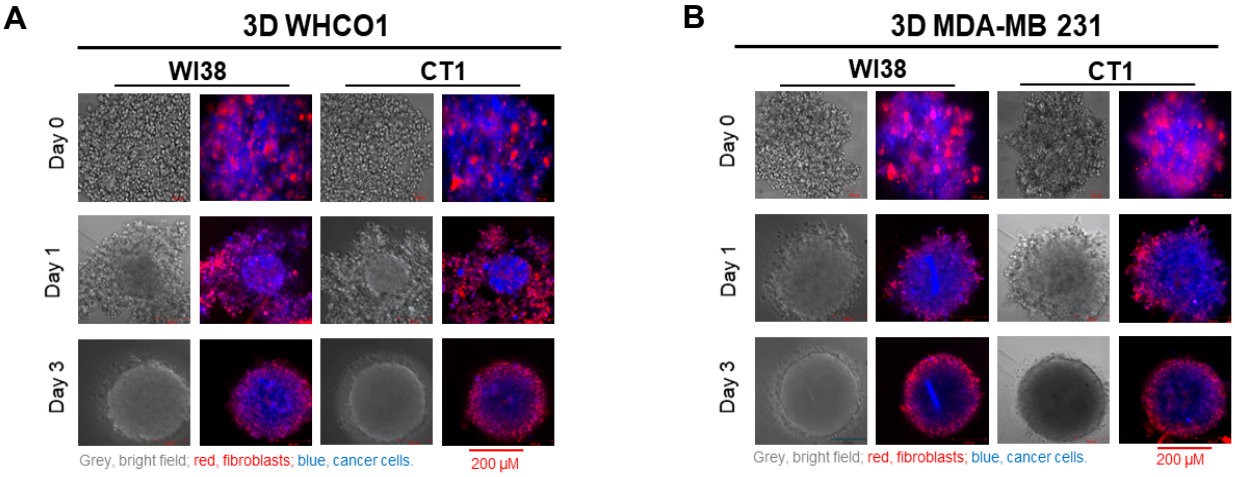

Figure 5. 3. Localisation of cancer cells and fibroblasts in spheroids generated over 3 days. WHCO1 and MDA MB231 cells were co-cultured with WI38 or CT1 fibroblasts at 5000 cell density in a ratio of 1:1. The cells were stained with Blue CMAC Texas red. **(A)** Representative images of spheroids generated using WHCO1 co-cultured with fibroblasts over 3 days showing the location of fibroblasts (red) and WHCO1 cells (blue). **(B)** Representative images of co-cultured fibroblasts (red) and MDA MB 231 cancer cells (blue) over a period of 3 days. Scale: the bar represents 200 µm. Experiments were performed at least two independent times.

5.2.3 Cisplatin, Epirubicin drug cytotoxicity studies in 2D and 3D cultures

Since co-culture of WHCO1 and MDA MB 231 with WI38 and CT1 fibroblasts has not been done before, it was necessary to establish dose-response curves for these cells in 2D and 3D cultures. Cisplatin and epirubicin are drugs commonly used in the treatment of oesophageal and breast cancer and were chosen for this study. The parameters used to determine of the dose-response curves were cell viability and metabolic activity of cells measuring ATP levels. In order to exclude the possibility of spheroid size influencing response to drugs, 3 days was chosen as the endpoint of the assays. Therefore, 3D spheroids and 2D cultures were treated with increasing drug concentrations for 72 hours. Viability was assessed using the CellTiter-Glo luminescent-based assay. The intensity of the luminescence signals was plotted as dose-responses curves using a GraphPad prism from which the IC_{50} was calculated (Figure 5.4). The representative IC_{50} values and their confidence intervals are shown in Table 5.1. The results indicated that cisplatin and epirubicin showed a 2.4- and 1.3-fold increased drug concentration needed for the same cytotoxicity, respectively, in 3D WHCO1 spheroids compared to 2D WHCO1 cells. On the other hand, cisplatin and epirubicin displayed 1.3- and 1.4-fold increased drug concentration needed for the same cytotoxicity, respectively, in 3D MDA MB231 spheroids compared to 2D cells. These findings demonstrated that 3D spheroids are less sensitive to the effects of both cisplatin and epirubicin. For the purpose of this study, 3.5 µM cisplatin was chosen for future experiments.

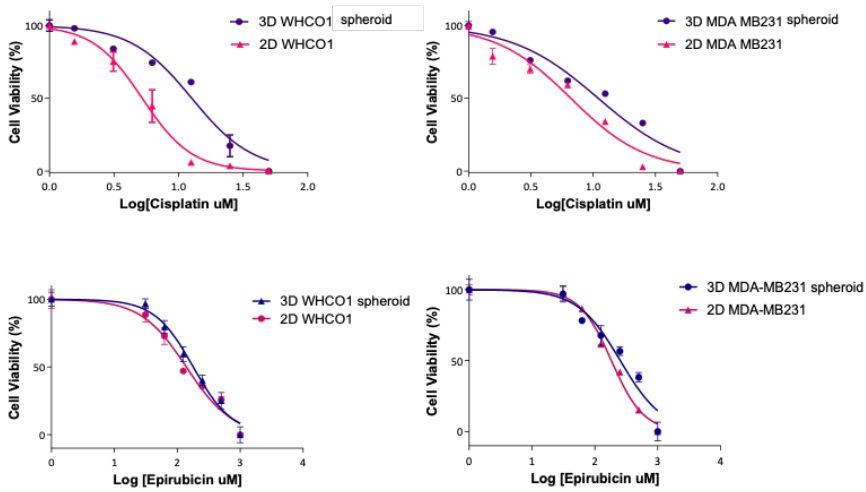

Figure 5. 4. Dose-response curves to determine IC_{50} values of cisplatin and epirubicin in both 2D and 3D cultures. 2D and 3D cultures of WHCO1 and MDA MB231 cells were treated with increasing concentration of cisplatin and epirubicin for 72 hours and subjected to CellTiter-Glo luminescent-based assay as described in section 7.2.9.3. Transformed log [cisplatin/ epirubicin] was used to determine the IC_{50} values of each culture. Results shown are the mean ±SEM of experiments performed in triplicate and repeated at least three times.

Table 5. 1. IC_{50} values for cisplatin and epirubicin.

	Cisplatin	Epirubicin
Culture	Mean IC_{50} ± SD µM 72 hours	Mean IC_{50} ± SD µM 72 hours
2D WHCO1	5.24 ± 0.80	0.140 ± 1.84
3D WHCO1 spheroids	12.66 ± 1.85	0.180 ± 1.88
2D MDA	6.62 ± 0.06	0.184 ± 1.95
3D MDA spheroids	8.71 ± 0.01	0.255 ± 1.80

5.2.4 Cell viability analysis of WHCO1 and MDA MB 231 2D, 3D and 3D co-cultures.

The metabolic activity of 2D, 3D and 3D co-cultures was investigated. WHCO1 and MDA MB231 cells were cultured as 2D or 3D cultures and co-cultured with WI38 or CT1 fibroblast cells at a 1:1 ratio for 72 hours. All cell cultures were incubated with 3.5 µM cisplatin for 72 hours. Metabolic activity was determined using the CellTiter-Glo luminescent-based assay. When 2D and 3D cancer cells or co-cultured with both WI38 and CT1 fibroblasts were treated with cisplatin, metabolic activity analysis demonstrated a decrease in activity when compared to control cells. (Figure 5.5 A, B). When compared to 2D and 3D cultures in WHCO1, 3D co-cultures including WI38 and CT1 fibroblasts were considerably less susceptible to 3.5 µM cisplatin and showed enhanced metabolic activity (Figure 5.5 A). A similar result was obtained when MDA MB 234 cells were investigated (Figure 5.5 B). In both WHCO1 and MDA MB231 cells, fibroblasts offered protection to cancer cells from the effect of the drugs. This is not surprising given that fibroblasts were found on the spheroids' periphery by day 3 and cancer cells were found in the centre. Furthermore, transformed fibroblasts (CT1) appear to offer better protection to cancer cells compared to normal fibroblasts (WI38) (Figure 5.5). These findings show that fibroblasts in 3D co-cultures conferred some form of protection to the cancer cells against cisplatin compared to 2D and 3D cultures.

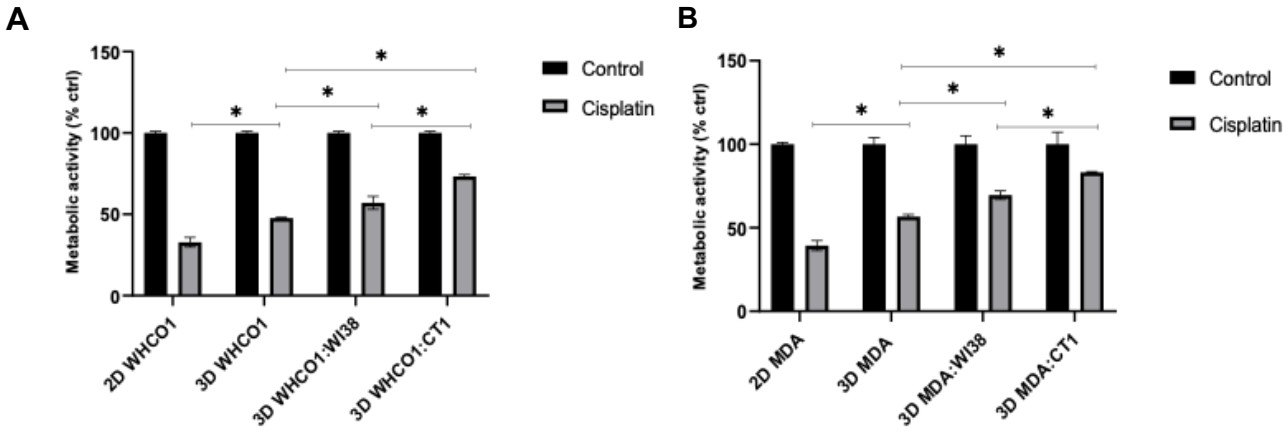

Figure 5. 5. Metabolic activity analysis of WHCO1 and MDA MB 231 2D, 3D and 3D co-cultures after treatment with cisplatin. 2D, 3D and 3D co-cultures of cancer cells and fibroblasts were treated with 3.5 μM cisplatin for 72 hours. Metabolic activity was determined using the CellTiter-Glo luminescent-based assay. Metabolic activity for 2D, 3D and 3D co-cultures in **(A)** WHCO1 and **(B)** MDA MB231 r cells after 72 hours of treatment with cisplatin. Results shown are the mean ±SEM of experiments performed in triplicate and repeated at least three times. A student t-test was used for the statistical analysis was performed using GraphPad Prism comparing cisplatin-treated cultures, *p < 0.05.

5.2.5 Analysis of apoptosis in 2D, 3D and 3D co-cultures.

To confirm the data as shown by the metabolic activity analysis as well as to determine the mechanism of growth inhibition, cell viability and apoptosis analyses were done for cells in 2D, 3D and 3D co-cultures. WHCO1 and MDA MB231 cells cultured as 2D, 3D or co-cultured with WI38 or CT1 fibroblasts were treated with 3.5 μM cisplatin for 72 hours. All cells were dissociated with 0.25% trypsin-EDTA and double-stained with Annexin V and PI as described in section 7.2.14.2. Flow cytometry analysis was used to evaluate apoptosis. Quantification was done using FlowJo software version 10.8. Cisplatin-induced 23.63% apoptosis in 2D WHCO1 cells, while 12.26% in 3D WHCO1 spheroids (Q2+Q3, early and late apoptosis, Figure 5.6 A). Furthermore, decreased apoptosis was observed in WHCO1 cells co-cultured with WI38 (10,85% total apoptosis) or CT1 (11.59% total apoptosis) in 3D cultures compared to 2D and 3D cultures. (Figure 5.6 A). Treatment with 3.5 μM cisplatin-induced total apoptosis of 12.35% and 9.51% in 2D and 3D MDA MB231 cultures, respectively (Figure 5.6 B). A decrease in apoptosis was also observed in the 3D co-culture of MDA MB231 with WI38 (9.51%) and CT1 (6.91%) compared to 2D cultures (Figure 5.6 B). MDA MB 231 cells in 2D show higher apoptosis levels than MDA MB 231 cells in 3D and those co-cultured with fibroblasts (Figure 5.6 B).

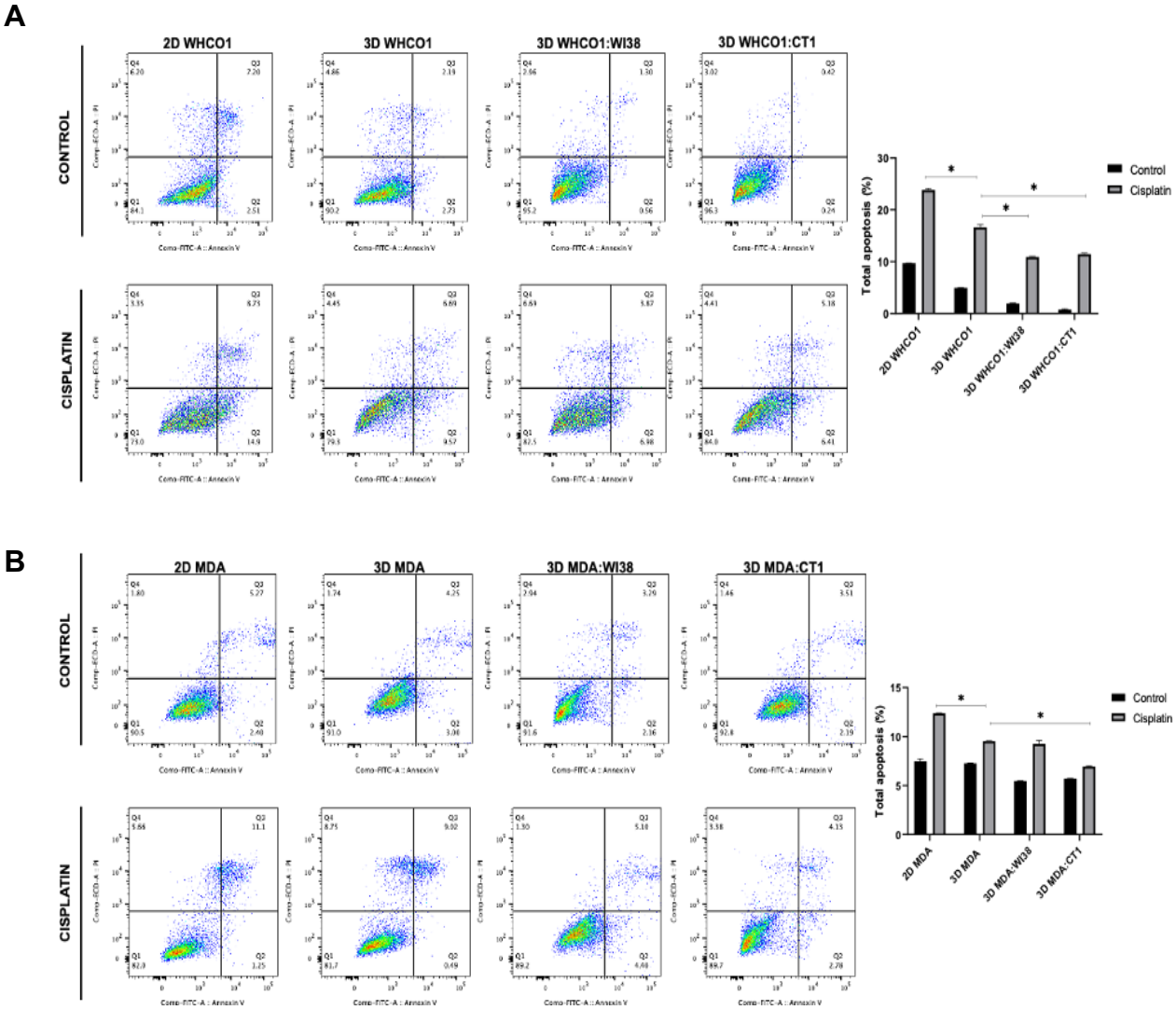

Figure 5. 6. Decreased apoptosis in 3D and 3D co-culture of cancer cells and fibroblasts. WHCO1 and MDA MB231 cells were cultured as 2D, 3D cultures or co-cultured with WI38 or CT1 fibroblasts and treated with 3.5 μM cisplatin for 72 hours. After treatment, double staining of Annexin V and PI was used to analyse apoptosis in **(A)** WHCO1 and **(B)** MDA MB231 cultures. Quantification of the number of cells undergoing apoptosis was measured using FlowJo software. Results shown are the mean ±SEM of experiments performed in triplicate and repeated at least two times. (*p<0.05).

5.2.6 Cell viability within 3D and 3D co-culture spheroids using Live/Dead staining.

The Viability of cells in 3D cultures and the co-cultures was also investigated using the Live/Dead assay Kit by fluorescent microscope. In this assay, Calcein AM fluorescence demonstrated metabolically viable cells (green fluorescence), and ethidium homodimer-1 fluorescence indicated dead cells (red fluorescence). Control dishes for WHCO1 cells had less cell death, with most cells staining as live (Figure 5.7 A). Cisplatin-treated dishes showed increased cell death. As measured by relative mean fluorescence intensity, WCHO1 cells alone in 3D treated with cisplatin showed

cell death of around 15.5% (Figure 5.7). WHCO1 cells co-cultured with fibroblasts showed cell death of 7.5 % (WI38) and 7.2 % (CT1), which is significantly lower than for WHCO1 cells alone (Figure 5.7 A). As measured by relative mean fluorescence intensity, MDA MB 231 cells alone in 3D treated with cisplatin showed cell death of around 18.6 % (Figure 5.7 B). MDA MB 231 cells co-cultured with fibroblasts showed cell death of 6.7 % (WI38) and 6.5 % (CT1), which is significantly lower than for MDA MB231 cells alone in 3D (Figure 5.7 B). Together, these results again demonstrated that fibroblasts in spheroids protect cancer cells.

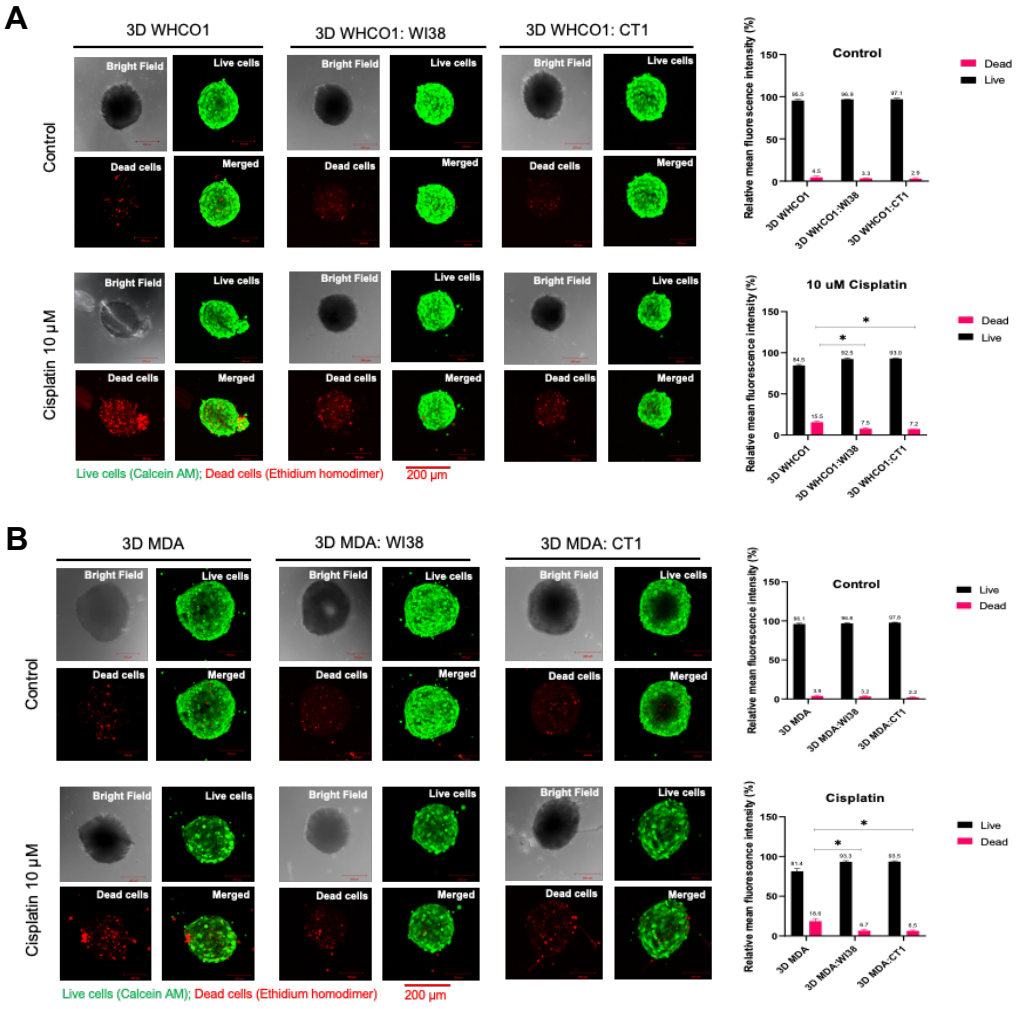

Figure 5. 7. Decreased apoptosis in 3D and 3D co-culture of cancer cells and fibroblasts. WHCO1 and MDA MB 231 were cultured as 2D or 3D cultures and co-cultured with WI38 or CT1 fibroblasts, and treated with 3.5 µM cisplatin for 72 hours. The Live/Dead assay Kit measured the cell viability in **(A)** WHCO1 and **(B)** MDA MB 231 cells using a fluorescent microscope. Calcein AM demonstrated live cells (green fluorescence), and ethidium homodimer-1 indicated dead cells (red fluorescence). Image J was used to quantify the mean fluorescence intensity. Scale bar= 200 µm. Results shown are the mean ±SEM of experiments performed in triplicate and repeated at least two times. (*p<0.05).

5.2.7 Invasive migration of cells out of 3D and 3D co-culture spheroids.

The MCTS model addresses critical cellular processes in tumour progression, such as invasion into the ECM. The invasive behaviour of the spheroids formed by cancer cells alone (WHCO1 and MDA MB 231) and in co-culture with fibroblasts (WI38 and CT1) was investigated using type I collagen, an ECM component commonly used for this assay. We established 3D spheroids of WHCO1 and MDA MB231 cells alone or in co-culture with WI38 or CT1 fibroblast cells using 96-well round-bottom low attachment plates for 72 hours. Spheroids were embedded into the type I collagen matrix as described in section 7.2.22 and treated with 3.5 μM cisplatin. On day 1, the data show that cells had started migrating out of the 3D spheroids in both control and cisplatin-treated WHCO1 cells alone and co-cultures (Figure 5.8 A, B). However, over time, there was enhanced cell migration out of the 3D co-culture spheroids. Cell migration out of mixed-cell spheroids showed a radial invasion into the surrounding matrix producing a characteristic “starburst” invasion pattern in a time-dependent manner (Figure 5.8). In the presence of cisplatin, there was higher cell migration out of the spheroids in the co-cultured spheroids than from WHCO1 alone-spheroids (Figure 5.8 A, B, left panel). Similar results were obtained for MDA MB 231 generated spheroids over the 3 days (Figure 5.8 A, B, right panel). As expected, co-culture of spheroids with fibroblasts demonstrated increased cancer cell migration in both control and cisplatin-treated conditions for MDA MB 234 cells over the 3 days of culture (Figure 5.8 A, B). ImageJ was used to measure the area occupied by invading cells (Figure 5.8 C, D). The spheroids with cancer cells and transformed CT1 fibroblast cells exhibited stronger invasive behaviour than those with WI38 in WHCO1 and MDA MB231 cells. The results suggest that the interaction between cancer cells and fibroblasts significantly facilitated WHCO1 and MDA MB231 invasion in MCTS.

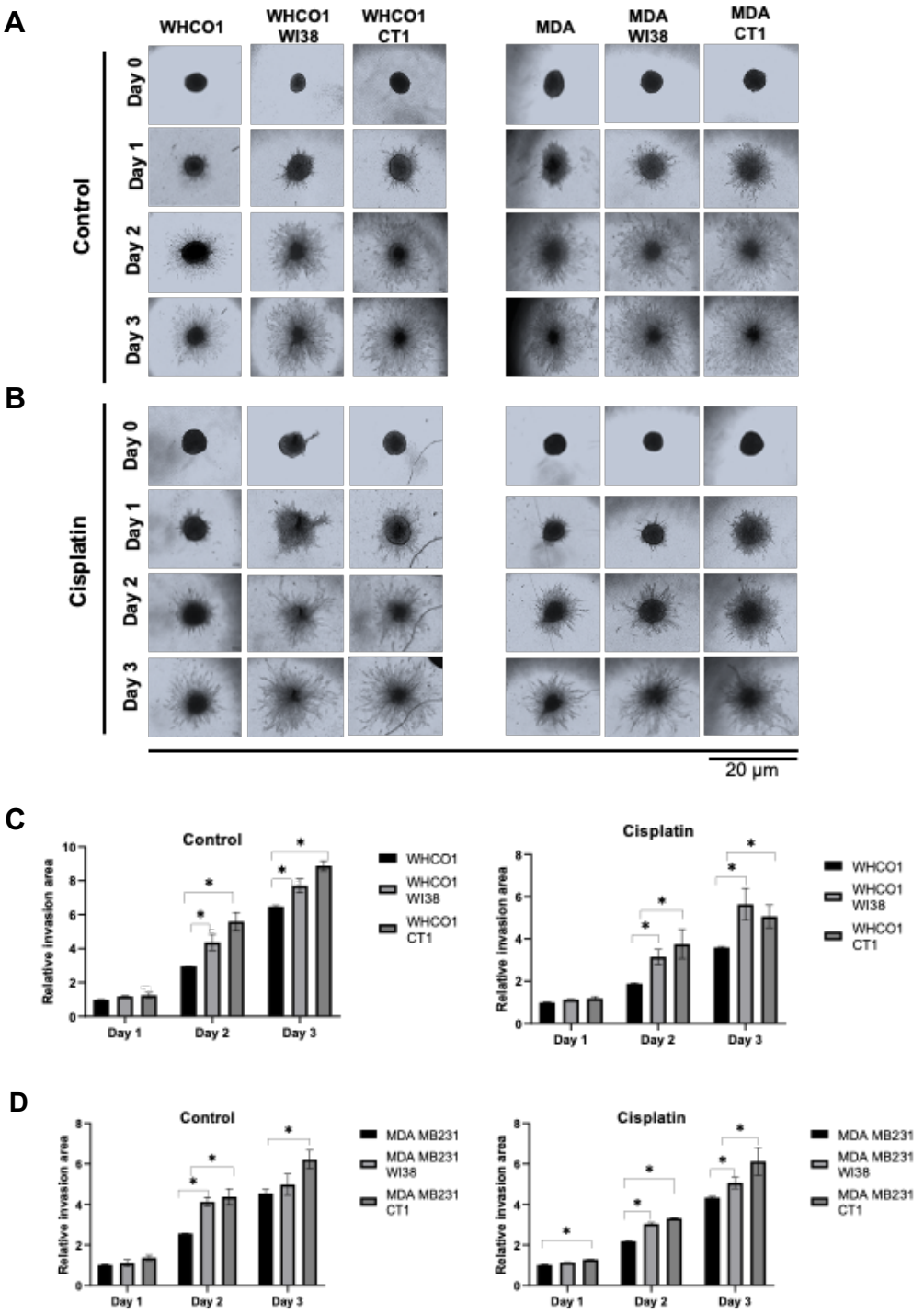

Figure 5. 8. Invasive migration of cells out of 3D and 3D co-culture spheroids. WHCO1 and MDA MB 234 3D and 3D co-culture cell invasion were measured by the 'Starburst formation' assay. Day 3 tumour spheroids were embedded in each well of the 96-well flat-bottomed plates containing type I collagen. **(A)** Representative images of control (no drug) WHCO1 and MDA MB 234 spheroids migrating through the matrix over 3 days of culture. **(B)** Representative images of cisplatin-treated WHCO1 and MDA MB 234 spheroids over 3 days show migration of cells through the matrix. **(C)** Quantification of control and cisplatin-treated WHCO1 spheroids invasion over 3 days of culture. **(D)** Control and cisplatin-treated MDA MB 234 spheroids invasion, over 3 days of culture, were quantified using ImageJ. Results shown are the mean ±SEM of experiments performed in triplicate and repeated at least two times. (*$p<0.05$).

5.2.8. 3D culture of WHCO1 and MDA MB 231 induced CSC markers gene expression.

Our earlier studies showed the presence of CSCs in WHCO1 and MDA MB231 by virtue of their expression of CD44 and ALDH1A1. Tumour spheroids have been reported to enrich CSCs [476]. Thus, in this study, the expression of cancer stem cell markers was investigated in 3D and 3D co-culture spheroids compared to 2D culture. Cancer stem cell markers ALDH1A1, CD44 and self-renewal markers SOX2 and OCT4 were chosen for this analysis. Western blot analysis showed that 3D and 3D co-culture spheroids from WHCO1 cells expressed high levels of ALDH1A1 and CD44 compared to their 2D cultures (Figure 5.9 A). qRT-PCR showed correspondingly increased levels of both ALDH1A1 and CD44 mRNA in 3D and 3D co-cultures of WHCO1 spheroids compared to 2D WHCO1 cells (Figure 5.9 C). The increase in both ALDH1A1 and CD44 was more pronounced in co-cultured spheroids than in WHCO1 alone spheroids. Similar results were obtained for MDA MB 231 cells (Figure 5.9 B, D). Quantification using densitometric analysis of ALDH1A1 and CD44 band intensities is shown in Figure 5.9 A, B (right panel).

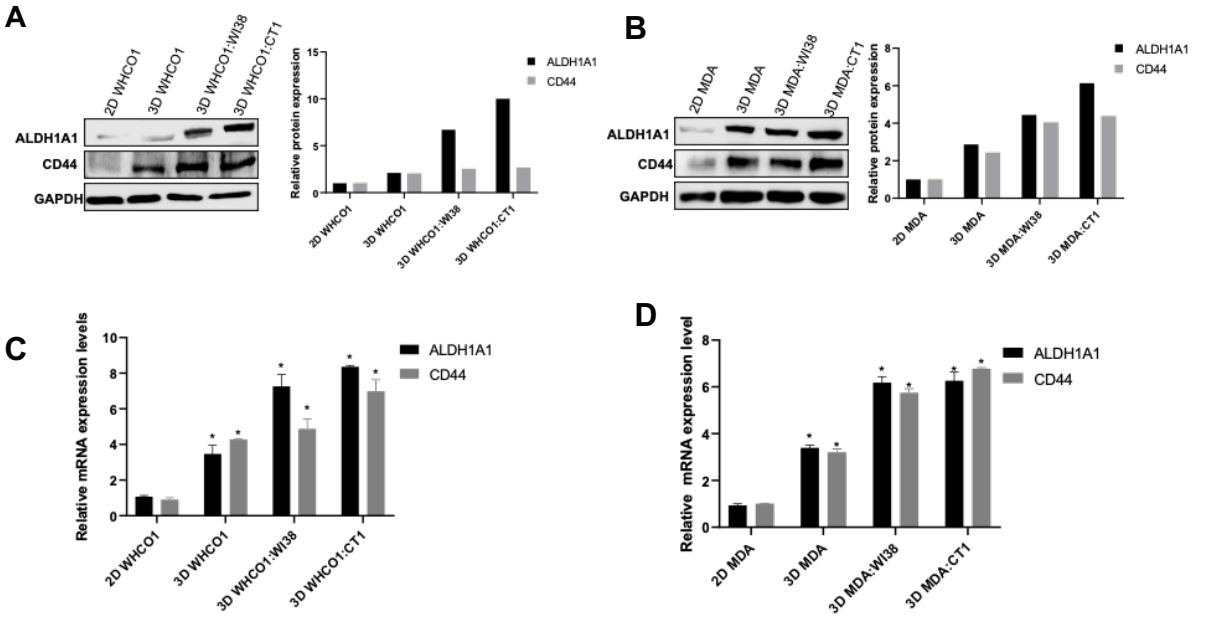

Figure 5. 9. 3D culture of WHCO1 and MDA MB 231 induced cancer stem cell gene expression. Expression of ALDH1A1 and CD44 in WHCO1 and MDA MB 234 2D and 3D cultures were investigated. Western blot analysis was used to determine ALDH1A1 and CD44 protein expression levels in **(A)** WHCO1 and **(B)** MDA MB231 2D, 3D and 3D co-cultures after 72 hrs of culture. Densitometric quantification of ALDH1A1 and CD44 protein expressions as shown (right panel). qRT-PCR was used to measure ALDH1A1 and CD44 mRNA levels in **(C)** WHCO1 and **(D)** MB231 2D, 3D and 3D co-cultures. The results shown are the mean ± SEM of experiments performed in triplicate and repeated at least two times. (*p<0.05).

OCT4 and SOX2 are transcription factors implicated in maintaining pluripotency by preventing differentiation and promoting self-renewal in CSCs [477]. Immunofluorescence and qRT-PCR were used to investigate the levels of SOX2 and OCT4 in 2D, 3D and 3D co-cultures (Figure 5.10). Immunofluorescence staining reveals that both SOX2 and OCT4 protein levels were increased in 3D and 3D co-cultures of WHCO1 cells compared to the respective 2D cultures (Figure 5.10 A). Using qRT-PCR analysis, the mRNA levels of SOX2 and OCT4 were elevated in 3D and 3D co-cultures compared to 2D cultures (Figure 5.10 C). ImageJ software was used to measure the relative mean fluorescence intensity. The same results were obtained using MDA MB 231 cells (Figure 5.10 B, D). Because of their enhanced multipotency and expression of pluripotency regulators, these findings suggest that 3D spheroids have a high level of flexibility. These findings support the theory that these spheroids are enriched with cells with stem cell characteristics.

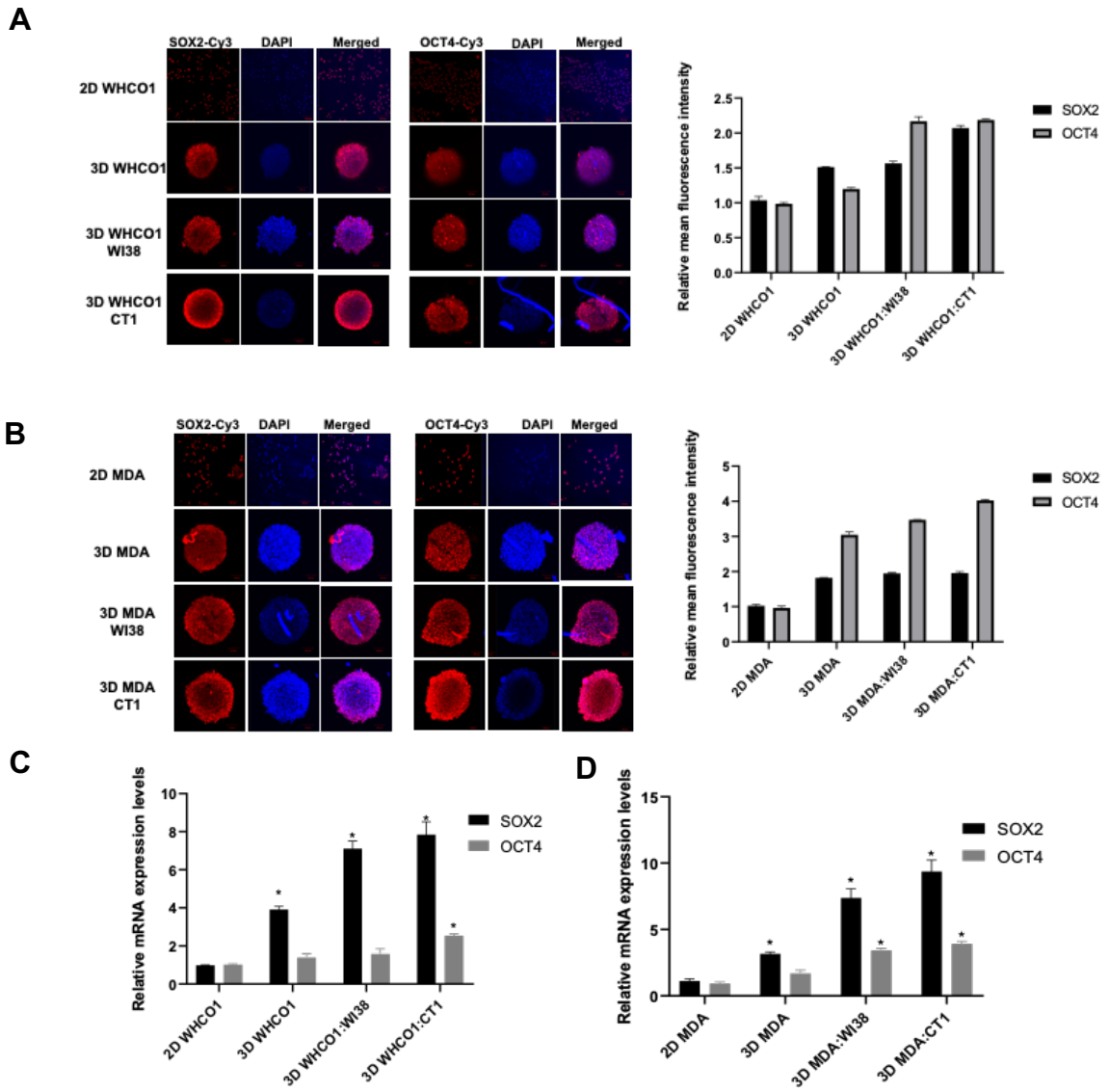

Figure 5. 10. Expression of SOX2 and OCT4 in WHCO1 and MDA MB 234 2D and 3D cultures. Representative immunofluorescence images of **(A)** WHCO1 and **(B)** MDA MB231 cells cultured as 2D cells on glass coverslips and as 3D or co-culture with fibroblasts on 96-well round bottoms, showing the expression levels of Cy3 labelled SOX2 and OTC4 (red fluorescence). DAPI was used to stain for the nuclei (blue fluorescence). Scale bar= 200 µm. Fluorescence intensity was measured using Image J (right panel). qRT-PCR was used to determine ALDH1A1 and CD44 mRNA levels in **(C)** WHCO1 and **(D)** MB231 2D, 3D and 3D co-cultures. Results shown are the mean ±SEM of experiments performed in triplicate and repeated at least two times. (*p<0.05).

5.3. Discussion

Tumour heterogeneity and plasticity present a challenge to the development of effective therapies. Whilst there is a great deal of tumour-stromal interactions, a lot is still to be done to overcome the problem of chemoresistance. The lack of suitable models that can recapitulate the *in vivo* tumour microenvironment for *in vitro* studies is a major challenge in studying tumours *in vitro*. One possibility is the development of spheroids composed of tumour cells and stromal cells to produce multicellular tumour spheroids (MCTS). As MCTS models allow the analysis of cellular responses that more closely mimic those that occur *in vivo*. Using both oesophageal WHCO1 and breast MDA MB 231 cancer cells alone or in co-culture with CT1 and WI38 fibroblasts, this study successfully established 3D spheroids that can be used to study *cancer in vitro*. In the 3D cultures, normal WI38 and CT1 transformed fibroblast cells were used to mimic the stromal compartment of tumours. The spheroids were used to study drug sensitivity, tumour cell growth, and migration. Importantly, the spheroids derived from the multi-cell culture of cancer cells and fibroblasts were able to mimic *in vivo* tumour behaviour in various ways. Firstly, we observed that tumour cells and stromal cells, such as fibroblasts, occupy specific regions of tumours with stromal cells on the outside and tumour cells on the inside of the solid tumour. Reports have shown that there is a stiffening of the surrounding tissue, during tumour formation, during which stromal cells surround and synthesize large quantities of ECM proteins to try and isolate the tumour cells [82, 403]. This has the effect of providing protection to tumour cells during drug treatment. Thus, our data show that 3D spheroids were less sensitive to drugs than 2D monolayers. Cancer cells and fibroblasts were mixed at a ratio of 1:1 to try to mimic the physiological conditions in the human body. Secondly, the spheroids generated showed a necrotic centre as expected of these structures. Various reports show that both cancer cells and stromal cells can be activated by low oxygen levels in tissues [478, 479]. This has the net effect of promoting drug resistance through the expression of growth factors and chemokines by stromal cells [480].

Investigating cell viability and apoptosis revealed that spheroids derived from cancer cells co-cultured with fibroblasts were more resistant to both cisplatin and epirubicin. In addition, normal WI38 fibroblasts demonstrate a different effect on cancer cells compared to transformed CT1 fibroblasts. Cancer cells demonstrate enhanced drug resistance as shown by decreased apoptosis and dead cells via the live-dead assay

when co-cultured with transformed CT1 fibroblasts compared to normal WI38 fibroblasts. Similarly, normal fibroblasts are transformed into CAFs in solid tumours and CAFs have been shown to promote drug resistance [481, 482]. Furthermore, transformed CT1 fibroblasts also promoted increased cell migration compared to normal WI38 fibroblasts.

Several reports have successfully used 3D spheroids to study cancer cell invasion [483, 484]. CAFs have also been implicated in migrating and invading colorectal cancer cells in 3D co-cultures [485]. In tumours, the secretion of ECM proteins such as collagen by CAFs can cause changes in the ECM rigidity, which promotes tumour growth and invasion [486]. This study, utilized type I collagen to mimic cancer cell invasion. Various other ECM proteins and glycoproteins, such as Matrigel, laminin and fibronectin have been used to study cancer cell migration and invasion [487, 488]. Importantly, we confirmed that co-culturing of tumour cells with fibroblasts could modulate cell invasion in MCTS. The interaction between tumour cells and fibroblasts effectively facilitated spheroid cell invasion when embedded on a type I collagen matrix. In another study, 3D hepatocellular carcinoma co-cultures with stromal cells were reported to have increased expression of type I collagen and cell invasion [489]. We suggest that mostly cancer cells are the ones migrating, however we cannot rule out that fibroblast can also migrate. The reason why there is an increased of cancer cell migrating in co-cultures may be due to pro-tumour-promoting factors from fibroblasts. In a co-culture, it was shown that fibroblasts are always the leading cell as stromal fibroblasts and carcinoma cells invade collectively, and carcinoma cells migrate in a pattern in the ECM behind the fibroblast [490]. Invasion of carcinoma cells required both protease- and force-mediated matrix remodelling to be facilitated by fibroblasts [490].

Interestingly, the majority of fibroblasts were localised in the periphery of the MCTS. In contrast, a study reported that mixed spheroids of fibroblasts and colorectal cancer cell lines result in the localisation of fibroblasts in central region [414]. A study in colorectal cancer observed that fibronectin expression in co-culture tumour spheroids of cancer cells and fibroblast was observed in the periphery region of the spheroids [491]. Furthermore, this study observed a decrease in apoptosis in the cisplatin treated co-cultured spheroid with fibroblasts. Possibly, this effect is caused by the deposition

of ECM by fibroblasts, which provides a physical barrier to prevent drug diffusion. A study observed that upregulation of one of the ECM component, fibronectin, coincided with the reduced uptake of DOX at higher concentration in co-cultured tumour spheroids of cancer cells and fibroblasts [489]. In light of our findings, this model may be useful for investigating CAF-induced drug resistance by using cancer cell-fibroblast interactions within 3D co-cultured spheroids.

CSCs are rare subpopulations of cells within tumours, have been proposed as supporting tumour aggressiveness and heterogeneity. Furthermore, CSCs play an important role in resistance to chemotherapy. Hence, the characterisation of CSCs is crucial for the development of more effective cancer treatments. Multiple studies have shown a subpopulation of cells in oesophageal and breast tumours that express particular markers and possess certain CSC traits, such as accelerated self-renewal, differentiation, and tumour-initiating ability, despite the fact that the CSC concept is controversial [492, 493]. Data from several studies revealed that it is possible to use spheroid cultures to enrich and identify CSCs [494, 495]. Our 3D spheroids of both oesophageal and breast cancer cells had high expression levels of CD44 and ALDH1A1 CSC markers compared to 2D cultures. A study by Reynolds and colleagues confirmed that CSC markers are expressed predominantly in spheroids of MDA MB231 breast cancer compared to adherent cells [495]. Similarly, our study showed that the expression of the stem cell-related genes, SOX2 and OCT4, increased in our 3D cultures. SOX2 has been associated with poor survival outcomes in breast cancer patients since it is an important transcription factor involved in embryonic stem cell self-renewal [496]. It has been proposed that a niche for CSC exists and that interactions with it contribute to the development of a self-renewing population of tumour cells. It is possible that CSCs may use the niche already created by CAFs or ECM components for colony expansion [497]. In addition, CAFs are able to induce stemness markers, promote sphere formation, and increase self-renewal and expansion of CSCs in breast and lung cancer [498, 499]. In our current study, we were able to identify the expression of CSC markers or self-renewal markers in the 3D co-culture of cancer cells and fibroblasts compared to 3D spheroids of cancer cells alone. The spheroids in our model appear to behave like cancer *in vivo* in that they show drug resistance and high migratory and invasion capabilities. Therefore,

understanding the role of CAFs in the environment and the origin of CSC niches are fundamental for developing effective anti-cancer drugs.

In summary, we utilised the MCTS model to study the interactions of cancer cells and their stromal components on 96-well round-bottom plates. WHCO1 and MDA MB231 cancer cells were able to form compact spheroids whether cultured alone or with normal WI38 or transformed CT1 fibroblasts. We were able to replicate the tumour microenvironment *in vivo* through the integration of fibroblasts. In our 3D co-cultured spheroids, we noticed a decreased sensitivity to cisplatin compared to 3D spheroids and cells grown as monolayers. By measuring drug resistance and invasion, we confirmed the similarity of 3D co-culture spheroids to *in vivo* tumours. Through the use of MCTS, we can better understand the dynamics of CSC populations in their expression of markers that can be used to come up with effective therapeutic drugs for CSCs. We also demonstrate that fibroblasts offer some protection to cancer cells in the presence of drugs. This could be because fibroblasts produce ECM proteins that could act as a physical barrier for drugs. Given the complexity of tumours *in vivo*, it may be possible to develop tumour models incorporating stromal components to study cell-cell and cell-ECM interactions, examine the role that CSCs play in cancer progression and evaluate potential agents to overcome drug resistance and tumour invasion.

CHAPTER 6:

GENERAL DISCUSSION AND CONCLUSION

6.1 Overall Discussion

The process of tumour initiation, development and eventual metastasis is a complex and dynamic process involving the interplay between many components of tissues, including cells, the ECM and biomolecules [261, 305]. Besides cancer cells, tumours contain stromal cells and several proteins and proteoglycans making up the ECM [70]. In addition, various biomolecules released by cancer cells and stromal cells are present within the TME. The success of the tumourigenesis process is determined by the interaction between the ECM, cells within the tissue, and biomolecules [118, 166]. Stromal cells within the tumour microenvironment, such as CAFs, myofibroblasts and immune cells, all play crucial roles in tumour progression [146, 157, 262]. This thesis presents new data on the involvement of various components of the TME in the formation of tumours and during the development of chemoresistance during chemotherapy.

In summary, this thesis demonstrates that MSCs may be recruited to tumours and transformed into cells that may assist cancer cells in growing. This study shows that cells such as MSCs, CAFs and CSCs are part of the ‘machinery’ required by cancer cells to develop into solid tumours fully and to metastasise. These stromal cells work in concert with other TME components such as the ECM and growth factors in promoting cancer cell proliferation, growth, invasion, metastasis, and drug resistance [72, 82]. The purpose of this thesis was to look into the involvement of TME, including acellular and cellular components, in tumour genesis, growth, and chemoresistance. There is a subpopulation of cells, including CAFs and CSCs, that contribute to tumour progression and the development of chemoresistance. CSCs that stain positively for several stem cell markers such as CD44 and ALDH1A1 are present in oesophageal tumour biopsies. Most importantly, these CSCs are not sensitive to commonly used drugs such as cisplatin and paclitaxel, possibly explaining why oesophageal cancer always ends up relapsing.

Within the TME, CAFs have been shown in various studies to be crucial to tumour growth and metastasis [87, 105]. This study investigated the possibility that MSCs are

a source of CAFs. This notion is based on the fact that CAFs display great heterogeneity and that MSCs can differentiate into cells of various lineages [140, 142]. One obvious source of CAFs within the TME are the resident fibroblasts. Therefore, this study investigated the possibility that MSC recruited to the TME might be the source of CAFs. In addition, MSCs may contribute to the process of tumour progression and chemoresistance through the release of various growth factors, chemokines and cytokines [130]. Indeed, data from this study clearly show that MSCs recruited from different tissues to the TME may be transformed into CAFs-like cells through their interactions with cancer cells. This is in agreement with a report demonstrating that long-term culture of MSCs with tumour conditioned medium from breast cancer cells induces a phenotype that resembles CAFs [142]. Most importantly, the release of growth factors such as TGF-β plays a key role in the transformation MSCs into CAFs-like cells, including increased expression of α-SMA. The source of the TGF-β was shown to be from both cancer cells and the MSCs. Therefore, TGF-β is acting in a paracrine as well as an autocrine manner. The expression of α-SMA was elevated following incubation of MSCs derived from bone marrow with a conditioned medium from human colorectal cancer cells or with TGF-β [500]. In addition, CAFs may play a role in remodelling the extracellular matrix through the secretion of MMPs and growth factors that are important in angiogenesis, such as VEGF [112]. Importantly, CAFs have been shown to release cytokines and chemokines that are important for cancer progression and the development of chemoresistance [123]. This study suggests that MSCs contribute to CAF production within the TME and may play key roles in the development of chemoresistance.

Most cancer therapies fail to prevent relapse due to the presence subpopulation of cells known as CSCs with the ability to self-renew as well as the potential to differentiate into new cancer cells [303, 310]. Over the years, many studies have postulated that CSCs are ‘seeds’ for the growth of secondary tumours [164, 304]. In this study, we utilized both oesophageal and breast cancer cell lines to study how CSCs may contribute to tumour growth and chemoresistance. Cells positive for CSC markers including CD44 and ALDH1A1 were found in immunohistochemical staining of oesophageal samples. These markers have been identified to be correlated with poor prognosis in breast, lung and pancreatic cancers [158, 164, 293].

This study utilized two methods to isolate cancer stem cells: (i) through the use of antibodies and (ii) using side population cells after flow cytometry. The CSCs isolated from oesophageal cancer cells demonstrated increased expression of CSC markers, increased ability to form colonies, drug resistance as well as reduced apoptosis. *In vitro,* clonogenic assays have shown that only a small proportion of tumour cells in solid tumours are capable of forming colonies [329, 335]. Possibly, only a small portion of cells with very distinct phenotypes have the capacity to proliferate and form new tumours, but they do so very effectively. The ability of CSCs to initiate the formation of cancer as well as increase the expression of self-renewal markers *in vitro* was established in this study through increased production of tumour spheroids using side population cells. In colorectal cancers, the overexpression of CD44 characterises a population of cells able to form tumour spheres, suggesting anchorage-independent proliferation of these cells [501]. In severe combined immunodeficiency mice, a knock-down of CD44 reduced sphere formation and decreased tumour growth in gastric cancers [502]. Thus, this study, through using side population cells, demonstrates that CSCs are able to form new tumours compared to cancer cells. Results from this study also agree with other results that show that CD44 expression correlates with increased drug resistance and increased cancer metastasis [324, 338]. Furthermore, the expression of ALDH1A1 correlates with drug resistance in various cancers [329, 339]. Interestingly, in clinical sample studies and cell culture models, it has been found that ALDH1A1-positive lung cancer stem cells are more resistant to EGFR-TKI (gefitinib) and anticancer chemotherapy drugs (cisplatin, etoposide, and fluorouracil) than ALDH1A1-negative cells [503]. Typically, chemotherapeutic agents induce apoptosis in the proliferating cells, however, CSCs have the ability to arrest the cell cycle (quiescent state), which gives them the ability to become resistant to chemotherapy [176]. While successful cancer therapy eliminates most of the cancer cells, a subset of cancer stem cells can survive and promote cancer relapse due to their increased invasiveness and resistance to chemotherapies. For instance, a study has shown that temozolomide, the most commonly used anti-glioma chemotherapy, consistently expands the pool of glioma stem cells (GSCs) over time in both patient-derived and established glioma cell lines [504]. This was demonstrated to be due to interconversion between differentiated tumour cells and GSCs based on phenotypic and functional interactions. CSCs are also protected against DNA damaging radiation therapy and chemotherapy by mechanisms that regulate cell cycle and promote DNA damage

repair [505]. According to Bao et al. 2006, CD133+ glioma stem cells are more resistant to ionizing radiation than CD133- gliomas and can be enriched following radiation therapy [506]. Consistent with these reports, cell cycle and apoptosis analyses in the present study showed that isolated CSCs showed reduced cell cycle arrest and apoptotic cells compared to cancer cells.

Furthermore, data from this study also showed that genes associated with invasion and metastasis, such as MMPs and FOXM1, were upregulated in CSCs compared to cancer cells. Several signalling pathways, such as PI3K/Akt, c-Myc and MER-ERK, and transcriptional regulators such as OCT4, Nanog, and SOX2, are also commonly activated in CSCs to regulate their self-renewal and differentiation state [336, 389]. Importantly, this study showed that isolated CSCs expressed high levels of several signalling pathway genes such as MEK-ERK and the PI3K-Akt. These pathways are involved in mediating several cellular processes, such as survival and prevention of apoptosis. This study utilized commonly used drugs such as paclitaxel, cisplatin and epirubicin in the treatment of oesophageal cancer and breast cancer. Based on the results obtained in this study, the presence of CSCs may explain the high occurrence of drug resistance in various cancers, including oesophageal cancer. New strategies involving targeting both cancer cells and CSCs may result in better patients outcomes. Overall data from this study show that markers associated with CSCs were upregulated and that such cells may promote relapse via drug resistance.

The infiltration of cells from the epithelial cells into the tumour and the interaction between transforming cells and the ECM play a key role during the process of tumour progression and chemoresistance. In addition, as the tumour continues to grow, cancer cells are exposed to both cancer-derived and stromal-cell derived extracellular matrices. The ECM is a dynamic and complex component of the tumour microenvironment that contributes physical, mechanical, and biochemical qualities to the tumour microenvironment's overall character [223]. Besides the proteins and proteoglycans of the ECM, the ECM sequesters several biomolecules, such as growth factors, chemokines and cytokines. In addition, these substances can be released at any time and facilitate tumour development and chemoresistance [227]. To study the role of the ECM, this study utilized cell-derived extracellular matrix produced by the removal of cells and other biomolecules. The cell-derived ECMs have been utilized in

several assays to study their contribution to the development of chemoresistance [227, 410]. This study utilized both stromal-derived extracellular matrix as well as cancer-derived extracellular matrix and showed that in the presence of cell derived extracellular matrices, WHCO1 cells are able to resist similar concentrations of drugs compared to cells that were plated on plastic. This study postulate that the ECM contributes to the development of chemoresistance through the physical prevention of drugs accessing the cancer cells and the ECM sequestering some of the drugs so that the eventual concentration of drugs reaching cancer cells is reduced. Interestingly, interactions between cells and their ECM play a fundamental role in cancer cell behaviour and homeostasis, especially in response to environmental changes and stresses.

According to studies, less than 5% of drugs tested *in vitro* reach patients, demonstrating that the presence of ECM is critical to studying cancer cell behaviour *in vitro* as it increases drug efficacy in patients [223]. This study demonstrated that the extracellular matrix influences tumour progression, metastasis, and chemoresistance by several assays, including as proliferation, migration, and apoptosis. Furthermore, this study demonstrates that the ECM protected cancer cells from the drug-induced apoptosis through increased expression of antiapoptotic genes compared to cells plated on 2D or plastic. This is supported by a study reporting that the protective effect of stromal-derived ECM on colon cancer was associated with increased expression of Bcl-2 and Bcl-xL [227]. In addition, cell-derived ECM may also suppress apoptosis by activating signalling pathways according to the integrin-mediated cell attachment, as this study demonstrates. Cancer cells can use the ECM to activate intracellular signalling pathways necessary to promote their proliferation and migration during progression. In Chapter 2, we showed that cancer cells secrets TGF-β to facilitate the transformation of MSCs to CAFs-like cells. Interestingly, the mechanical properties of the ECM also influence the activity and availability of TGF-β. TGF-β is stored as a latent complex in the ECM, and integrins are the primary activators of latent TGF-β *in vivo*. Furthermore, the current study found activation of integrins in cancer cells plated on the CD-ECM, which might indicate activation of latent TGF-β, as previously observed in this study.

Several ECM proteins are known to play a key role in promoting the growth of cancer cells, drug resistance and the migration. For instance, type IV collagen increases migration of breast cancer cells compared to no ECM control [507]. In this study, knockdown of type I collagen and fibronectin demonstrated that the removal of these two ECM components sensitises WHCO1 cells to the effect of drugs. Moreover, the removal of these ECM components resulted in reduced cell migration. This means that these two ECM components play critical roles in the development of chemoresistance and migration. An effective method of remodelling ECM is to remove one or more of its components. However, the degradation of ECM components allows the normal ECM to be gradually destroyed and replaced by tumour-derived ECM. Furthermore, ECM degradation may serve as an important driver of cancer cell motility. Remodelling of the ECM by MMPs has been associated with cancer cells migration. An earlier study revealed cancer cells could also degrade the ECM by recruiting MMPs to focal adhesion sites [203].

Recent studies have shown that 3D MCTS are a good intermediate step between *in vitro* and *in vivo* models, and they do offer better biological relevance in various research areas. MCTS models are made up of cellular aggregates from single cells to become tightly packed together and therefore communicate strongly with one another [246]. In addition, cells within the tumour interact with the ECM in a much stronger way. Thus, MCTS recapitulate the *in vivo* solid tumour features, including nutrient distribution, oxygen distribution and structural organization. Various studies have shown that MCTS display similar growth kinetics and resistance to tremors similar to *in vivo* solid tumours [246, 414]. Therefore, this study utilized the 3D MCTS model to study the interaction between cancer cells and fibroblasts to reveal how this relationship influences cancer cell response to drugs. To study the growth kinetics of tumour spheroids, the shape of the tumourspheres was evaluated using microscopy and the shape of the spheroid. Interesting to note, slightly smaller spheroid sizes were observed in the 3D co-cultures than in their respective 3D cultures.

In this study liquid overlay technique using low attachment, dishes was used to prevent cell adhesion and promote the formation of cellular aggregates, that formed spheroids over time. This technique has several benefits, including the ability to generate a single-per well spheroid naturally by gravity and optimal culture conditions, metabolic

activity, and morphological and localisation of cells within the spheres were determined. The data obtained in this study showed that the 3D structure of spheroids formed within 24 hours. In order to mimic the physiological situation of *in vivo* tumours, WHCO1 cells and fibroblasts were mixed at a ratio of 1 to 1. Similar culture conditions for spheroid formation have been observed in several studies [414]. The data from this study showed that spheroids from WHCO1 cells co-cultured with fibroblasts resisted drugs more than WHCO1 cells alone, as exemplified by the decrease in apoptotic cells and dead cells compared to normal fibroblasts. It is known that the fibroblasts *in vivo* conditions promote tumour cell invasion [259]. The co-culture of transformed CT1 fibroblasts and WHCO1 cells appears to enhance the resistance of cancer cells to drugs and invasion of cells into the matrix. CAFs influence the signalling pathways involved in CRC cell migration and invasion in 3D co-cultures [485]. In addition to chemoresistance and cell invasion, 3D co-cultures showed high levels of CSC and self-renewal markers. CAFs have been shown to be capable of secreting factors that have been implicated in regulating the growth of CSCs [499]. This study developed a 3D tumour spheroid model that can be used to study various cancers. The findings reveal that *in vitro* spheroids made up of multicellular components can mimic different aspects of solid tumours *in vivo.*

6.2 Conclusion

Cancer treatment's future success lies partly in a precise understanding of the interaction between different components of the tumour microenvironment, especially the interaction between cancer cells, stromal cells such as fibroblasts, and the extracellular matrix. Understanding these interactions makes it possible to identify and target specific components and associated signalling pathways to treat cancer and prevent the development of chemoresistance. Recent studies indicate that interfering with processes such as the epithelial to mesenchymal transition and with the interaction between cancer cells and fibroblasts may help in destroying cancer cells by removing the support system needed for tumour growth. In addition, the targeting of stromal components such as the extracellular matrix may allow drugs to reach cancer cells and to be more effective and prevent the development of chemoresistance. Targeting tumour stroma is an appealing strategy as these components do not harbour genetic mutations similar to cancer cells. There is a need

for further studies, however, as targeting stromal cells may negatively affect other tissues and organs. Therefore, a combination of drugs targeting both cancer cells and some stromal components appear to be one of the various possible strategies to control cancer.

This study showed that stromal cells that are recruited to tumours play a crucial role in tumour initiation and further development of tumours and chemoresistance. By interfering with the relationship or interaction between cancer cells and fibroblasts could prevent the release of various growth factors, such as chemokines and cytokines, which are required by cancer cells to grow, which can result in tumour shrinkage. However, further studies are required before this is possible side effects can occur.

Another strategy that can be taken is targeting the extracellular matrix to prevent cancer growth as well as to overcome chemoresistance. The dense extracellular matrix of solid tumours prevents drugs from reaching cancer cells and therefore aids the development of chemoresistance. This study shows that targeting extracellular matrix proteins such as collagen and proteoglycans such as fibronectin may help achieve better outcomes through effective drug delivery to tumours. This points to the effectiveness of targeting cancer cells as well as stromal cells and stromal components such as the extracellular matrix. This study enhances our understanding of the interaction between cancer cells and the extracellular matrix and has shown that targeting the ECM components and cancer cells is a viable option during cancer treatment.

In conclusion, this study demonstrates that three-dimensional multicellular tumour spheroids made up of cancer cells and fibroblasts mimic various features of *in vivo* solid tumours. This provides a dynamic analysis of cells during treatment. Furthermore, the study provides evidence of the utility of 3D multicellular spheroids as a good model for studying various cancers. Taken together, this data show that various components of the tumour microenvironment play significant roles in the process of traumatic genesis and development of tumours as well as in chemoresistance.

6.3 Limitations and recommendations

1. This study describes the associated of only single MSC marker with fibroblast markers. Comparing multiple markers at the same time might show a stronger association with fibroblast lineage. Future studies using two or more marker would be important to reveal a possible stronger association between MSC markers and fibroblasts.
2. Studies have shown that *in vitro* CSCs can be enriched using tumoursphere forming methods. Therefore, future studies may include the possible use of enriched-CSCs from tumourspheres as an *in vitro* model to study CSCs biology further.
3. The 24 hour time point used in this study clearly demonstrate that ECM does influence cancer cell growth and migration. In order to reflect medication use in the clinic future studies will need to/will extend this period of time to encompass extended incubation times and drug concentrations. To this effect starting with animal studies would be good.
4. Based on the results from this study, it is clear that most of the cells migrating out of the spheroids could be cancer cells. However, fibroblast are also able to migration, but a lower rate than cancer cells. Given the 3 days of co-culture, it is possible most of the migration is done by cancer cells. A limitation of the study is the lack of using dyes to differentiate the cells. Future studies will use specific dye for cancer cells and fibroblasts to determine the cells migrating, studying the differences in morphology and different markers.

CHAPTER 7:

MATERIALS AND METHODS

7.1 Materials

7.1.1 Clinical Tissue Collection

Biopsy samples were collected over a period of 1 year at Groote Schuur Hospital, Cape Town, South Africa. All Patients attended the oncology clinic of Groote Schuur Hospital. Oesophageal squamous cell carcinoma (OSCC) biopsy samples were confirmed by pathologist, Prof Govender, through immunohistochemistry. World Health Organisation criteria was used to determine the histological parameters. Ethical approval (Ref number: 040/2005) was obtained from the Research Ethics Committee of the Health Sciences Faculty (University of Cape Town, South Africa) and informed consent acquired from all patients according to institutional guidelines. The Declaration of Helsinki guidelines (DOH 2004) were used [508]. OSCC biopsies as well as corresponding adjacent normal tissue samples were taken from each patient. The biopsies were stored in RNAlater solution (Qiagen, Hilden, Germany) at -80°C. Tumour samples containing at least 50% of tumour cells were used in this study. OSCC patient clinicopathological characteristics are shown in section 3 (Table 3.1).

7.1.2 Cell lines

The cell lines used in this study were the following:
Human oesophageal cancer cell lines WHCO1, WHCO5, WHCO6 were originally established from South African patient biopsy samples of oesophageal squamous cell carcinoma [509].
KYSE180 was established from well differentiated oesophageal squamous carcinoma resected from middle intra-thoracic oesophageal of a 53-year old Japanese man prior to treatment [510].
The MDA-MB-231 cell line is an epithelial, triple negative human breast cancer cell line, obtained from a pleural effusion of a 51-year-old Caucasian female with a metastatic mammary adenocarcinoma [511].

Human embryonic lung fibroblasts, (WI38) (ATCC CCL-75) (Manassas, VA, USA).
γ-radiation transformed WI38 human lung fibroblast, CT-1 fibroblast (gift from DR M. Nambia (Tokyo, Japan) [512].
Wharton's Jelly-derived mesenchymal stromal/stem cells (WJ-MSCs) were established from human umbilical cords collected from full-term births at the University of Pretoria, South Africa [229].

7.2. Methods

7.2.1 Maintenance of cells in culture

Cancer cells were cultured at 37°C in a humidified atmosphere of 5% CO_2 in Dulbecco's modified Eagle's (DMEM) supplemented with 10% heat inactivated fetal bovine serum (FBS), 100 U/ml penicillin and 100 µg/ml streptomycin. WJ-MSCs were maintained in KnockOut DMEM supplemented with 10% FBS, FGF, 100 U/ml penicillin and 100 µg/ml streptomycin. Sorted cells were then cultured and maintained in serum-free medium composed of DMEM/F12 medium supplemented with, 100 U/ml penicillin and 100 µg/ml streptomycin, 20 ng/ml recombinant epidermal growth factor, 20 ng/ml human recombinant basic fibroblast growth factor, 1% GlutaMax and 2% B27 supplement. Cells were cultured at 70% confluent and cells were trypsinised with 0.05% trypsin-EDTA. The media was changed three times a week.

7.2.2. Thawing/Freezing of cells.

Frozen cells were collected from long-term storage in liquid nitrogen and thawed in a 37°C water bath. The vials were wiped with 70% ethanol, cells were transferred to 12 ml falcon tubes, containing 5 ml of fresh growth media. and centrifuged at 500 x G for 3 minutes. The supernatant was aspirated, and the cell pellet were then resuspended in fresh complete medium and plated in a 100 mm dish containing 10ml of complete medium.

For long term storage, cells were harvested by incubation with 0.5% trypsin-EDTA for 2-3 minutes at 37°C. Once cells had detached, the trypsin-EDTA was inactivated by

adding an equal volume of the complete DMEM. Cells were pelleted by centrifugation at 500 x G for 5 minutes and resuspended in freezing down media (70% DMEM, 20 % FBS and 10% DMSO) (v/v) by gentle pipetting action. The cells were aliquoted into 2 ml cryotubes (1 ml containing about10^6 cells) and stored at -80°C for 48 hours before being transferred to liquid nitrogen.

7.2.3 Mycoplasma test

Cells were regularly checked for mycoplasma contamination. Cells were cultured in pen/strep free DMEM media for 3 days on coverslips. The cells were fixed with ice cold methanol and distilled water was used to rinse off the methanol. The cover slips were then incubated with Hoechst stain, DNA-binding stain, for no longer that 30 seconds. The Hoechst was rinsed off using distilled water and the cover slips were mounted on a microscope slide using mowiol. Cells were visualised using a Zeiss Axiovert fluorescent microscope (Carl Zeiss, Jena Germany).

7.2.4. Preparation of cell-derived ECM

Confluent cells (WHCO1 and CT-1 transformed fibroblasts) were split in 0.5% trypsin-EDTA and cells were cultured in 100 mm tissue culture dishes. The cells were grown in DMEM supplemented with 10% heat inactivated FBS, 100 U/ml penicillin and 100 µg/ml streptomycin at 37°C in a humidified incubator and 5% CO_2. Fresh ascorbic acid was added every alternative day to a final concentration of 50 µg/ml according to established protocols [410]. Cells were grown to 8 days post confluence after which the medium was aspirated, the cell were rinsed with PBS and lysed by adding 1 ml of freshly prepared 20 mM ammonium hydroxide for one minute [410, 513]. The resulting matrix was treated with DNase. The matrix was washed three times with PBS, fixed to the dish with a 50% ethanol rinse, air dried and sterilised overnight under UV light in a tissue culture cabinet. The matrices were checked using an inverted phase contrast microscope to check that all the had been lysed and that a cell-free 3D matrix remained attached to the culture dish. Matrix-coated dishes were stored at 4°C and used within two weeks after preparation. Extracellular matrix protein integrity is stable under these storage conditions [410]. Before use, the matrix-coated dishes were

rinsed with sterile PBS followed by one rinse with tissue culture medium. CT1 fibroblast cells were used to prepare the transformed fibroblast-derived ECM (tfd-ECM) while WHCO1 cancer cells were used for the cancer-derived ECM (cd-ECM). Co-culture of CT1 and WHCO1 cells produced combinatorial ECM (combi-ECM). For the production of cell-derived ECM without fibronectin (ECM^{-fn}) and without type I collagen (ECM^{-col1}), CT1 and WHCO1 cells were transfected with either fibronectin siRNA or type I collagen siRNA and grown on tissue culture dishes. Cell-derived ECM was done as described above with subsequent fibronectin siRNA and type I collagen siRNA added after two days. In order to characterise the cell-derived ECM, the ECM was dissolved in 5 M Guanidine-HCL in buffer and analysed by SDS-Page as described in Section 7.2.20. Total protein was stained with Ponceau stain and Coomassie stain. Human fibronectin and type I collagen were also loaded to serve as markers. To evaluate proteoglycan composition within the ECMs, the ECM was prepared on coverslips and fixed using 3% paraformaldehyde solution. ECMs were incubated with 1% Alcian Blue for 20 minutes and washed three times with PBS. Images were observed and photographed using a light microscope (Olympus CKX41 with SC30 camera).

7.2.5. Side-population (SP) analysis and sorting

Side population cells were isolated based as described by Goodell et all (2005). Confluent WHCO1, WHCO5, WHCO6, KYSE 180 and MDA MB 23 cells were split using 0.05% trypsin-EDTA and centrifuged at 500 x G for 5 minutes. Cells were resuspended at 1 x 10^6 cell/ml in pre-warmed DMEM supplemented with 2% FBS, 10 mM HEPES, 1% penicillin/streptomycin and Hoechst 33342 dye to a final concentration of 5 µg/ml and mixed well by gentle inversion. Tubes were incubated for 90 minutes at 37°C with intermittent mixing. After 90 minutes cells were pelleted at 500 x G for 5 minutes and resuspended in ice-cold HBSS supplemented with 2% FBS and 10 mM HEPES. Propidium iodide (PI) was added at a concentration of 5 µg/ml for dead cell discrimination. Samples were kept at 4°C to until analysis. Cells were filtered through a 50 µm nylon mesh prior to analysis.

Forward Scatter (FSC) and PI were displayed using a dot plot to exclude dead cells and the remaining live cells were analysed. Propidium iodide fluorescence was also excited at 351 to 364 nm and measured through the 675 EFLP. A second dot plot region representing Side Scatter (SSC) and Hoechst 33342 blue cells was used to include all live cells. Side Scatter (SSC) and Hoechst 33342 red was displayed using a third dot plot to set the emission for determining DNA labelling in live cells. Dichroic mirror short-pass (DMSP) of 610-nm was used to separate the emission wavelengths. In addition, low SSC and low FSC events, which enriched in SP cells, were considered. The SP and non-SP of each cell line was sorted with a cell sorter. Sorted cells were then cultured and maintained in serum-free DMEM/F12 medium supplemented with, 100 U/ml penicillin and 100 µg/ml streptomycin, 20 ng/ml recombinant epidermal growth factor, 20 ng/ml human recombinant basic fibroblast growth factor, 1% GlutaMax and 2% B27 supplement.

7.2.6. Immunophenotyping

WHCO1 and MDA MB 231 cancer cells were washed twice with PBS, trypsinised with 0.05% trypsin-EDTA and centrifuged at 500 x G for 3 minutes at 4°C. Cells were resuspended in PBS containing 5% FBS to a final concentration of 1 x 10^6 cells/ml. and stained with anti-CD44-PE (Abcam, ab269300) and anti-CD24-FITC (Abcam, ab30350) at 1:50 dilution. Samples were incubated with antibodies for 40 minutes at 4°C in the dark, washed with cold PBS and followed by FACS buffer (45 ml of 1X PBS and add 5ml of 10% BSA). The cells were compared to negative controls that were incubated with isotype-specific IgG1-FITC (Santa Cruz). The number of cells staining positive for a marker was determined by the percentage of cells present within a gate established using the FITC-conjugated isotype-matched control. At least 50 000 events were acquired on FACScan cell sorter (BD Bioscience, CA, USA).

7.2.7. Coculture assay

Cells were co-cultured in 6 welled transwell plates (size of pore 4 µm, Polycarbonate membrane, Costar, Corning, Cambridge, USA). WJ-MSCs (5 x 10^5 cells) were cultured in the upper insert and WHCO1 or MDA MB 231 cells (5 x 10^5 cells) were placed in the lower compartment of the 6-well plates. The control group had empty inserts (no cells) containing a 1:1 mixture of WJ-MSCs in Knockout DMEM supplemented with 10% FBS, FGF, 100 U/ml penicillin and 100 µg/ml streptomycin and cancer cell in DMEM complete medium. For longer incubation periods, the medium was changed every 3 days and fresh TGF-β and reagents were added. At specific time points or at the end of the experiment, cancer cells and WJ-MSCs were harvested for analyses. For the drug treatment assay, WHCO1 and MDA MB 231 cancer (5 x10^5) were cultured or co-cultured with WJ-MSCs for 16 days. Empty inserts were used for control group (no WJ-MSCs) and a 1:1 mixture of Knockout DMEM supplemented with 10% FBS, FGF, pen/strep and DMEM supplemented with 10% FBS and pen/strep was used. Medium was changed every 3 days for longer incubation periods. At the end of the same number of WHCO1 and MDA MB 231 cancer cells were treated with increasing concentrations of paclitaxel or cisplatin for 48 hours. After 48 hours, cells were counted in a Countess Cell counter (Invitrogen) using the Trypan Blue exclusion method. DMSO control (0.1%) was used to calculate percentages of cells. Each experiment was performed in triplicates and three independent experiments were performed.

7.2.8. 3D Tumoursphere formation

To recapitulate the 3D structure of the tumours *in vivo,* spheroids were created using different methods. Single cell suspension of parental cells and side population cells from cancer cells (WHCO1) were used to from tumour spheroids *in vitro* in low-attachment dishes. Cells were plated in serum-free DMEM/F12 (1:1 volume) media supplemented with B27 (to promote growth with differentiation), 20 ng/ml EGF and bFGF and 10 ng/ml HGF. The media was refreshed with growth factors twice a week until floating aggregates were formed. Cells were allowed to grow for up to 16 days in attachment dishes, to prevent cell attachment, and images of tumourspheres were observed by microscopy. For passaging, tumourspheres were collected by gently

centrifugation at 500 x G, counted and dissociated into single cells through the use of 0.05% trypsin-EDTA. Mechanical dissociation was also done using by pipetting up and down until all spheroids were dissociated in single cells. In some experiments, tumourspheres were passaged every 6-8 days after reaching a diameter of around 100 µm. The diameter of the spheroids was measured using Image J software. Tumourspheres were also treated with chemotherapeutic drugs for the indicated time periods.

7.2.9. Multicellular Tumour Spheroid formation (MCTS)

Frozen cells (WHCO1, Wi38, CT1) were thawed in a 37°C water bath. The vials were wiped with 70% ethanol, cells were transferred to 12 ml falcon tubes and centrifuged at 500 x G for 3 minutes. The supernatant was aspirated, and the pellet was resuspended in complete DMEM supplemented with 10% FBS and pen/strep. Cells were counted with a Countess Cell counter using the Trypan Blue exclusion method. Cells were grown at a density of 5 x 10^3 cells/100 µl per well in Nunclon™ Sphera™ 96-well, U-shaped-bottom microplates (Thermo Scientific, Waltham, MA, USA) and allowed to grow for 72 hours in humidified atmosphere with 5 % CO_2 at 37°C. 3D co-cultures were obtained by mixing 2 x 10^5 of WHCO1 or MDA MB231 cancer cells and 2 x 10^5 of CT1 or Wi38 fibroblast cells to a total of 5 x 10^3 per well. Spheroid growth was measured using spheroid diameter and metabolic activity as an indicator of cell viability. For spheroid culture treatment, freshly prepared medium containing the required drug concentrations were added to the spheroids. The cultures were then incubated for 3 days prior to performing the cell cytotoxicity assays, flow cytometric assays, western blot and immunofluorescence. Inverted Leica DMi1 microscope equipped with digital camera Leica MC120 HD was used to take images with phase-contrast optics. The images of the were analysed using Image J (version 1.52g, National Institutes of Health Bethesdda, MD, USA) to measure cell diameter and circularity.

7.2.10. Cell Viability assay

7.2.10.1. Trypan blue exclusion protocol

Cell proliferation rates after plating cancer cells with/without drugs was determined using the trypan blue exclusion method. Briefly, cancer cells (5 x 10^5) were plated on dishes with or without cell-derived ECM and/or with/without drugs for the indicated time periods. Cell layers were rinsed with PBS, trypsinised with 0.05 % trypsin-EDTA and centrifuged at 1800 rmp for 5 minutes. Cell were resuspended in DMEM supplemented with 10% FBS 100 U/ml penicillin and 100 µg/ml streptomycin and 10 µl of the cell suspension was mixed with 10 µl of Trypan Blue. Cell counting was done using the Countess Cell Counter (Invitrogen). Cell numbers were plotted against time and the cell proliferation rate was measured and compared to that of control cells. This experiment was performed in three replicates and in three independent experiments.

7.2.10.2. MTT assay

The MTT assay was used to measure cell death by quantifying the viability of metabolically active cells. The MTT assay was carried out by plating 2 x 10^3 in 96-well plates with or without cell-derived ECM, in a final volume of 100 µl DMEM supplemented with 10% FBS 100 U/ml penicillin and 100 µg/ml streptomycin per well. After the indicated incubation period, cells were washed with PBS and incubated in fresh medium containing 10 µl (final concentration of 0.5 mg/ml) of 3-(4,5-dimethylthiazol-2-yl)-2,5-diphenyltetrazolium bromide (MTT) at 37°C for 4 hours. The formazan produced in the reaction, was dissolved by adding 200 µl of 10% sodium lauryl sulphate (SLS) for 16 hours at 37°C. The absorbance of each sample was measured at 595 nm using a microtiter plate reader (Model 680, Biorad). The IC_{50} and the confidence interval were derived from quadruplicate data retrieved from a microtiter plate reader (Model 680, Biorad). The data was analysed using GraphPad Prism 5.0 software (2006). The values obtained from the absorbance readings were presented as mean ± SEM, log transformed and fitted onto a non-linear regression log (inhibitor) vs. response equation in order to construct a sigmoidal dose response curve.

7.2.10.3. Metabolic activity assay for spheroids

Metabolic activity assays were performed on WHCO1 and MDA MB231 cells grown in 2D, 3D or 3D co-cultured. Post-treatment cell viability was measured using luminescent-based cell metabolic activity assay CellTiter-Glo® (G9681, Promega) according to the manufacturer's instructions. The reagent was thaw overnight at 4°C followed by placing the reagent in 22°C water bath prior to use for 30 minutes. 100 µl of the CellTiter-Glo® reagent was added to 100 µl of medium containing cells in a 96-well plate. The content was mixed for 5 minuted to induce cell lysis then the plate was incubated at room temperature for 25 minutes. The intensity of the luminescence signal at 420 nm wavelength was detected using Veritas microplate luminometer (Promega). The absorbance was calculated using GraphPad Prism 5.0 software.

7.2.11. Cell Cytotoxicity assay

7.2.11.1. IC50 Determination

The IC50 of the drugs on WHCO1 cells were determined by plating 2 x 10^2 cells/well in 96-well plates and cells were allowed to attach overnight. Cells were then treated with varying concentrations of drugs or vector alone (0.1% DMSO). Cells were incubated with drugs for 24, 48 or 72 hours at 37°C after which 10 µl MTT reagent (Sigma Aldrich, USA) was added to a final concentration of 0.5 mg/ml and cells were incubated for 4 hours at 37°C. The SLS solution was added to the cells and the plates were incubation overnight followed by measuring the absorbance at 595 nm using a Biotek microplate spectrophotometer (Winooski, VT, USA). For IC50 determination of spheroids, CellTiter-Glo® reagent was used as described above (section 7.2.9.3). The IC50 and 95% confidence intervals (CI) were derived from quadruplicate data and data was analysed using GraphPad Prism 5.0 software (2006). The data were presented as mean (± SEM), log transformed, and fitted into a non-linear regression log(inhibitor) vs response equation to make a dose response curve.

7.2.12. Quantitative Real Time PCR (qRT-PCR)

7.2.12.1. RNA isolation of cells

Total RNA isolation was done according to the procedure of Chomczynski and Sacchi (1983) using Trizol reagent (Invitrogen Corporation, California, USA). Cells were seeded in 35mm or 100 mm dishes, after 24 hours the medium was changed to fresh DMEM supplemented with 10% FBS 100 U/ml penicillin and 100 µg/ml streptomycin and cells were incubated with or without drugs for different time points as indicated. The medium was aspirated, cells were washed with cold PBS and lysed by adding 1 ml of Trizol reagent. The cell lysate was scraped off the dish and pipetted into 1.5ml Eppendorf tubes. The homogenous samples were incubated for 5 minutes at room temperature with intermittent shaking to ensure complete dissociation of nucleoprotein complexes. Chloroform (200 µl per 1 ml of Trizol) was added to each sample and the samples were shaken vigorously for 15 seconds followed by incubation at room temperature for 3 minutes. The samples were then centrifuged at 14 000 rpm for 15 minutes at 4°C to separate the phases. The upper aqueous phase was transferred to a fresh tube and the RNA was precipitated by the addition 500 µl isopropyl alcohol per 1 ml Trizol. Samples were shaken vigorously for 15 seconds and incubated at room temperature for 10 minutes. The samples were centrifuged at 14 00 rpm for 30 minutes at 4°C to pellet the RNA. The supernatant was carefully removed. The RNA was rinsed once with 1 ml of 75% ethanol and vortexed at low speed for 5-10 seconds followed by centrifugation at 7500 rpm for 5 minutes at 4°C. The supernatant was removed and the pellet air-dried for 10 minutes at room temperature. The RNA was dissolved in 30-50 µl DEPC-water by heating at 55°C for 5 minutes and stored at -80°C. The concentration of the extracted RNA was determined using a Nanodrop spectrophotometer 2000 (Thermo Fischer Scientific, USA). The absorbance was measured at 260 nm and 280 nm, RNA that had A_{260}/A_{280} ratio between 1.8 - 2.0 was considered pure.

7.2.12.2. RNA extraction of spheroids

In 2 ml Eppendorf tubes, 50 spheroids were lysed with 250 µl of Trizol reagent and incubated for 5 minutes at room temperature. To the sample, 50 µl of chloroform was added, samples were shaken vigorously for 15 seconds, and incubated at room

temperature for 5 minutes. The samples were then centrifuged at 14 000 rpm for 15 minutes at 4°C to separate the phases. In new Eppendorf tubes, 100 µl of each aqueous phase was transferred, followed by the addition of 125 µl isopropanol, vortexing and incubation for at room temperature for 10 minutes. The samples were centrifuged at 14 00 rpm for 30 minutes at 4°C to pellet the RNA. The supernatant was removed and in each tube, the RNA pellets were washed with 75% ethanol. Samples were the vortexed allowed by centrifugation at 7500 rpm for 5 minutes at 4°C. The supernatant was removed, and the pellet air-dried for 10 minutes at room temperature. The RNA was dissolved in 30 µl of DEPC-water by heating at 55°C. The concentration of the extracted RNA was determined using a Nanodrop spectrophotometer 2000 (Thermo Fischer Scientific, USA).

7.2.12.3. RNA extraction of biopsy samples

RNA from Biopsy Tissue Samples was extracted using the Qiagen AllPrep DNA/RNA/miRNA Kit (QIAGEN, Venlo, The Netherlands) . The RNA extraction was carried out as described by the manufacturer. Normal tissue adjacent to tumour and tumour samples in RNAlater were used for RNA extraction. Tissue samples were washed twice with PBS. 30 mg of tissue was dissected into several smaller pieces using a sterile scalpel blade and pieces were then placed in a 1.5 ml microfuge tube. For tissue disruption and homogenisation, 300 µl of Buffer RLT containing β-mercaptoethanol was added then the tissue was homogenised at room temperature in a tissue-rupture by placing the tip of the pestle probe into the tube at full speed until the tissue lysate is uniformly homogeneous. The lysate was centrifuged at 14 000 rpm for 10 minutes at room temperature. The supernatant was transferred to an AllPrep DNA spin column placed in a 2ml collection tube and centrifuged at 14 000 rpm for 30 seconds. 300 µl of RLT buffer was added to the spin column and centrifuged at 14 000 rpm for 30 seconds. The flow through was transferred to a 2 ml microfuge tube and RNA clean-up was carried out using the RNeasy mini kit (QIAGEN, Venlo, TheNetherlands). The RNA clean-up was carried out as described by the manufacturer. Following the dissolution of the RNA in DEPC water, the volume was adjusted to 100 µl using RNAse free water. RNA was precipitated with a Qiashredder (QIAGEN, Venlo, The Netherlands) and washed with 70% ethanol using the RTL buffer. The RNA was then eluted from the column with RNAse-free water. The

concentration of the extracted RNA was determined using a Nanodrop spectrophotometer 2000 (Thermo Fischer Scientific, USA).

7.2.12.4. Synthesis of cDNA

Complementary DNA (cDNA) was synthesised using 2 µg RNA and 50 µM oligo $(dT)_{15}$ primer and Impromp II reverse transcriptase (Promega Inc, Madison, WI, USA) in the presence of dNTPs and $MgCl_2$, following the manufacturer's instructions. Briefly, the following were added to a nuclease-free microcentrifuge tube:

50µM oligo $(dT)_{15}$ primer	1 µl
5µg total RNA	X µl
Distilled water (DEPC-dH_2O)	Y µl
Total volume	9 µl

(X = depends on the concentration of the RNA and Y = add up to a final volume of 9 µl). The volume of the RNA varied as it was dependent on the concentration of the RNA sample and the total reaction was kept constant for each sample by addition of DEPC treated dH_2O to reach a final volume of 9 µl

The above mixture was heated at 70°C for 10 minutes to break up any secondary structure and ensure strand separation, as well as annealing of oligo (dT). The PCR tube containing the mixture was spun by brief centrifugation for 4 seconds and placed on ice immediately. For each sample, 11 µl of the following master mix was added to make a final volume of 20 µl per sample:

cDNA synthesis master mix

5 x First strand buffer	5 µl
dNTP mix	1 µl
RNase inhibitor	1 µl
$MgCl_2$	2 µl
Impromp II reverse transcriptase	1 µl
Nuclease-free water	1 µl
Total volume	11 µl

The final mixture was mixed well, centrifuged briefly and incubated or 2 hours at 42°C. The resulting cDNA was stored at -20°C.

7.2.12.5. Quantitative real time PCR

Quantitative real time (RT) polymerase chain reaction (PCR) was performed, to measure the relative changes in RNA levels, using KAPA SYBR® FAST qPCR Universal Kit (KAPA Biosystems, S.A) and LightCycler® 480 II (Roche). The qRT-PCR was done in 96 well plates by adding 2 µl of cDNA, forward primer, reverse primer (see appendix b), dH_2O and KAPA SYBR® FAST qPCR Universal Master Mix as shown below:

qRT-PCR reaction mixture:

KAPA SYBR® Fast Master Mix	12.5 µl
Forward Primer	1 µl
Reverse Primer	1 µl
Water	8.5 µl
cDNA or Water (control)	2 µl
Total volume	25 µl

Every qRT-PCR plate had a negative control and reactions were done in triplicate. Glyceraldehyde-3-phosphate dehydrogenase (GAPDH) was used as an internal control.

7.2.12.5. Analysis of qRT-PCR data

Real Time PCR data were analysed using the comparative $2^{-\Delta\Delta CT}$ method for relative quantification. The gene of interest was normalised against the reference gene, GAPDH, and expressed as fold induction.

7.2.13. Western Blot Analysis

7.2.13.1. Protein extraction

Cells or spheroids were plated in 100 mm or 96-well culture dishes in complete DMEM supplemented with 10% FBS 100 U/ml penicillin and 100 µg/ml streptomycin for 24 or 72 hours before treatment with chemotherapeutic drugs. At the end of each experiment cells were washed with cold PBS and lysed with 1 x RIPA supplemented with protease inhibitors then incubated with for 5 minutes in ice. A cell scraper was used to harvest the cells, which were transferred to a 1.5 ml Eppendorf tubes and sonicated for 10 seconds on ice (Heat System-Ultrasonic, Inc, Plainview, New York). The cell lysate was centrifuged at 10 000 rpm for 10 minutes at 4°C and the supernatant was transferred to a fresh tube. Protein quantification was done using the BCA (Bicinchoninic Acid) Assay (Pierce® Bradford Protein Assay kit, Thermo Fischer Scientific, USA) according to the manufacturer's protocol. Protein concentration was measured using a standard curve from a serial dilution of bovine serum albumin (BSA) standards concentrations ranging from 0 to 2000 µg/ml. Protein concentrations were determined by diluting 5 µl of the lysate with 25 µl of dH_2O in a 96-well plate, followed by the addition of 200 µl of the BCA working reagent and incubated at 37°C for 30 minutes. Absorbance was measured in a Multiskan FC microplate photometer (Thermo Scientific, USA) at 595 nm.

7.2.13.2. SDS-Polyacrylamide Gel Electrophoresis

7.2.13.2.1. Preparation and electrophoresis of gels

Proteins were separated by sodium dodecyl sulphate polyacrylamide gel electrophoresis (SDS-PAGE). using a 10% separating and a 4% stacking gel as detailed in Table 7.1. The separating gel was added first into BioRad Mini protein system overlayed with water to create a level between separating and the stacking gel. Once the separating gel had set, the water was decanted followed by adding the stacking gel and the insertion of combs in each gel to create loading wells. Combs were removed once the gel had polymerised and the wells were rinsed with 1 x running buffer. 50 µg protein was mixed with 4 x loading dye and water to a total volume of 40 µl. The samples were heated for 5 minutes at 95°C to ensure the denaturation of proteins. In each gel, 6 µl of molecular weight marker, (PageRuler^{TM} Plus Prestained Protein Ladder, Thermo Scientific, USA), was loaded and followed by 40 µl of the protein sample into the next well. Gel was run at 150 V for 1 hour to separate the proteins.

Table 7. 1. Reagents and volumes used to prepare separating and stacking gels for western blot.

Reagents	**Stacking Gel**	**Separating Gels**
	4%	10%
Distilled water	3.65 ml	2.75
Tris Buffer	0.625 ml	3.75
30% Acrylamide	0.650 ml	3.35
10% SDS	50 μl	100
10% APS	60 μl	200
TEMED	6 μl	20

7.2.13.2.2. Transfer of protein to nitrocellulose membranes

The separated proteins were transferred to nitrocellulose membrane (BioRad, USA) using the BioRad mini gel transfer system. Whatman 3M filter paper, nitrocellulose

membrane and sponges were cut into the size of the gel and soaked in 1 x transfer buffer (see Appendix X) for 15 minutes. The sandwich was assembled in the inner black side of the transfer system cassette. The cassette was then placed in the transfer apparatus and the transfer was carried out at 100V for 70 minutes at 4°C.

7.2.13.2.3. Immunoblotting

The nitrocellulose membrane was removed from the transfer apparatus and place a container with 5% (w/v) fat-free milk dissolved in 1 x Tris-Buffered Saline (TBS) containing 0.1% Tween 20 (Sigma Aldrich, USA) (TBST). The nitrocellulose membrane was blocked for 1 hour on a shaker at room temperature then incubated overnight with diluted antibody at 4°C on a shaker. The list of antibodies used and their dilutions are shown on Table 7.2. The membrane was washed 3 times with TBST for 5 minutes followed by incubation of horseradish peroxide (HRP)-conjugated secondary antibodies diluted in 5% fat-free milk solution for 1 hour at room temperature on a shaker. After the incubation, the membrane was washed 3 times with TBST for 5 minutes.

7.2.13.2.4. Visualisation

The protein bands of interest were detected using chemiluminescent LumiGLO Substrate (KPL, USA) as per the manufacturer's instructions and visualised on a Bio-spectrum (UVP) detection system (BioSpectrumTM 500 imaging System, Upland, CA, USA) with VisionWorks LS Image Acquisition and Analysis Software (Version 6.8). The bands in the image captured by UVP CCD camera were quantified using ImageJ software.

7.2.13.2.5. Stripping a blot

To probe the same membrane with a secondary antibody, the first was stripped off by washing with 1M glycine pH 2.5 by shaking at room temperature for 10 minutes and neutralised by the addition of 1M Tris pH 7.5 for 5 minutes. Membrane was incubated with the blocking solution for 1 hour followed by the probing of a different primary antibody.

Table 7. 2. Antibody concentrations and incubation conditions.

Primary Antibody	Primary Antibody Conditions	Secondary Antibody	Secondary Antibody Conditions	Substrate
GAPDH [Santa Cruz Biotechnology]	1:5000 in 5% Milk TBST	Goat anti-Rabbit [Bio-Rad]	1:5000 in 5% Milk TBST	LumiGlo® chemiluminescent
α-SMA [Santa Cruz Biotechnology]	1:500 in 5% Milk TBST	Goat anti-Mouse [Bio-Rad]	1:5000 in 5% Milk TBST	LumiGlo® chemiluminescent
Vimentin [Santa Cruz Biotechnology]	1:500 in 5% Milk TBST	Goat anti-Mouse [Bio-Rad]	1:1000 in 5% Milk TBST	LumiGlo® chemiluminescent
Type I collagen [Abcam]	1:1000 in 5% Milk TBST	Goat anti-Rabbit [Bio-Rad]	1:5000 in 5% Milk TBST	LumiGlo® chemiluminescent
CD44 [Santa Cruz Biotechnology]	1:500 in 5% Milk TBST	Goat anti-Mouse [Bio-Rad]	1:5000 in 5% Milk TBST	LumiGlo® chemiluminescent
ALDH1A1 [Santa Cruz Biotechnology]	1:500 in 5% Milk TBST	Goat anti-Mouse [Bio-Rad]	1:5000 in 5% Milk TBST	LumiGlo® chemiluminescent
ABCG2 [Santa Cruz Biotechnology]	1:1000 in 5% Milk TBST	Goat anti-Mouse [Bio-Rad]	1:1000 in 5% Milk TBST	LumiGlo® chemiluminescent
MDR1 [Santa Cruz Biotechnology]	1:500 in 5% Milk TBST	Goat anti-Mouse [Bio-Rad]	1:5000 in 5% Milk TBST	LumiGlo® chemiluminescent
Oct4 [Abcam]	1:200 in 5% BSA	Goat anti-Rabbit [Bio-Rad]	1:5000 in 5% Milk TBST	LumiGlo® chemiluminescent
Sox2 [Abcam]	1:200 in 5% BSA	Goat anti-Rabbit [Bio-Rad]	1:5000 in 5% Milk TBST	LumiGlo® chemiluminescent
Nanog [Abcam]	1:1000 in 5% BSA	Goat anti-Rabbit [Bio-Rad]	1:5000 in 5% Milk TBST	LumiGlo® chemiluminescent
FOXM1 [Santa Cruz Biotechnology]	1:500 in 5% Milk TBST	Goat anti-Mouse [Bio-Rad]	1:5000 in 5% Milk TBST	LumiGlo® chemiluminescent
MMP2 [Cell Signalling	1:500 in 5% Milk TBST	Goat anti-Rabbit [Bio-Rad]	1:1000 in 5% Milk TBST	LumiGlo® chemiluminescent
MMP9 [Cell Signalling]	1:500 in 5% Milk TBST	Goat anti-Rabbit [Bio-Rad]	1:1000 in 5% Milk TBST	LumiGlo® chemiluminescent
IL6 [Santa Cruz Biotechnology	1:500 in 5% Milk TBST	Goat anti-Mouse [Bio-Rad]	1:5000 in 5% Milk TBST	LumiGlo® chemiluminescent
IL8 [Santa Cruz Biotechnology]	1:500 in 5% Milk TBST	Goat anti-Mouse [Bio-Rad]	1:5000 in 5% Milk TBST	LumiGlo® chemiluminescent
p-ERK 1,2 [Cell Signalling	1:500 in 5% BSA	Goat anti-Mouse [Bio-Rad]	1:1000 in 5% BSA	LumiGlo® chemiluminescent
ERK2 [Santa Cruz Biotechnology]	1:1000 in 5% Milk TBST	Goat anti-Rabbit [Bio-Rad]	1:1000 in 5% Milk TBST	LumiGlo® chemiluminescent
p-Akt [Cell Signalling]	1:500 in 5% Milk TBST	Goat anti-Rabbit [Bio-Rad]	1:5000 in 5% Milk TBST	LumiGlo® chemiluminescent
Akt [Cell Signalling]	1:500 in 5% Milk TBST	Goat anti-Rabbit [Bio-Rad]	1:5000 in 5% Milk TBST	LumiGlo® chemiluminescent
Ki67 [Santa Cruz Biotechnology	1:500 in 5% Milk TBST	Goat anti-Mouse [Bio-Rad]	1:5000 in 5% Milk TBST	LumiGlo® chemiluminescent

Table 7.2. Antibody concentrations and incubation conditions (continued).

Primary Antibody	Primary Antibody Conditions	Secondary Antibody	Secondary Antibody Conditions	Substrate
PCNA [Santa Cruz Biotechnology	1:500 in 5% Milk TBST	Goat anti-Mouse [Bio-Rad]	1:5000 in 5% Milk TBST	LumiGlo® chemiluminescent
Cyclin D1 [Santa Cruz Biotechnology]	1:500 in 5% Milk TBST	Goat anti-Mouse [Bio-Rad]	1:1000 in 5% Milk TBST	LumiGlo® chemiluminescent
p-p21 [Santa Cruz Biotechnology]	1:500 in 5% Milk TBST	Goat anti-Rabbit [Bio-Rad]	1:5000 in 5% Milk TBST	LumiGlo® chemiluminescent
Bcl-2 [Cell signalling]	1:500 in 5% Milk TBST	Goat anti-Mouse [Bio-Rad]	1:5000 in 5% Milk TBST	LumiGlo® chemiluminescent
Bcl-xL [Cell signalling]	1:1000 in 5% Milk TBST	Goat anti-Rabbit [Bio-Rad]	1:5000 in 5% Milk TBST	LumiGlo® chemiluminescent
Integrin α1 [Santa Cruz Biotechnology]	1:500 in 5% Milk TBST	Goat anti-Mouse [Bio-Rad]	1:1000 in 5% Milk TBST	LumiGlo® chemiluminescent
Integrin α2 [Santa Cruz Biotechnology]	1:500 in 5% Milk TBST	Goat anti-Mouse [Bio-Rad]	1:1000 in 5% Milk TBST	LumiGlo® chemiluminescent
Integrin α5 [Santa Cruz Biotechnology]	1:5000 in 5% Milk TBST	Goat anti-Mouse [Bio-Rad]	1:1000 in 5% Milk TBST	LumiGlo® chemiluminescent
Integrin β1 [Santa Cruz Biotechnology]	1:500 in 5% Milk TBST	Goat anti-Mouse [Bio-Rad]	1:5000 in 5% Milk TBST	LumiGlo® chemiluminescent

7.2.14. Gelatin Zymography

Zymographic analysis of protease activity was done as described by Healary *et al* (2005). Cells were grown in serum-free DMEM overnight, washed with PBS and fresh serum-free DMEM followed by the treatment with chemotherapeutic drugs. After the end of the treatment the serum-free DMEM was harvested and total proteins in the medium were quantified using the BCA (Bicinchoninic Acid) assay as described above. Polyacrylamide gels containing 1 mg/ml gelatin in a buffered solution consisting of 5 ml 1.5 M Tris-HCl pH 8.8, 200 µl 10% SDS, 8 ml 30% Acrylamide and 5 ml distilled water were prepared. Stacking gels contained 4% polyacrylamide in 0.125 M Tris-HCl pH 6.8. Gels were polymerised by adding 50 µl of 10% ammonium persulfate and 10 µl of TEMED. 2 x of the loading buffer (non-reducing) was added to the sample and electrophoresis was done at 25 mA for 2 hours. Followed by washing gels twice for 30 minutes each in 200 ml of 2.5% Triton X-100 with constant stirring and incubated in incubation buffer (50 mM Tris-HCl pH 7.5, 5 mM $CaCl_2$, 0.2 M NaCl and 0.02% Brij-35) for 18 hours at 37°C. Gels were washed then stained with Coomassie brilliant blue dissolved in 20% methanol and destained with 15% acetic acid, 10% methanol. Gelatinolytic activity was shown as transparent zones in the blue

gels. The areas of the cleared zones were analysed with a Fluor-S Multimager (BioRad, USA).

7.2.15. Flow cytometry

7.2.15.1. Cell cycle analysis

Cells plated on the ECM or treated with chemotherapeutic drugs were subjected to FACS analysis after staining the DNA with PI. Briefly, 5 x 10^5 cell were plated on either 100 mm plates with or without ECMs and allowed to grow overnight at 37°C. Cells were then treated with drugs for 24 hours. Following the treatment, the cells were collected (including floating cells) with 0.5% trypsin-EDTA and centrifuged at 4000 rpm for 5 minutes. The cells were washed twice with ice cold PBS and fixed with 70% ethanol for 30 minutes at -20°C. After washing step, cells were incubated with 50 μg/ml ribonuclease A (RNase A) (Roche, Indianapolis, IN, USA) in PBS for 30 minutes at 37°C. Followed by the incubation, cells were stained with PI solution (1 mg/ml) and analysed with FACS cell sorter (BD Biosciences, Franklin Lakes, NJ, USA). The cell population was identified and gated on a forward scatter (FSC) vs. side scatter (SSC) dot plot in acquisition mode. Fluorescent Channel 2(FL2) at 575nm was used for Propidium Iodide detection. A dot plot of FL2A(area) vs FL2W(width) was used to identify single cells and thus eliminating doublets. A histogram plot of FL2A was used to enumerate G1/G0, s-phase and G2 populations. The combined parameters FSC, SSC,FL2A and FL2W display the results. A threshold of 52 on the FSC channel was set to remove sample debris. Nile Red Fluorescent particles were used for instrument standardization, stability and reproducibility. Analysis and results obtained of acquired data was done with Modfit version 3.3, software.

7.2.15.2. Annexin V/Propidium Iodide Assay for Apoptosis

Apoptosis was determined by double staining with Annexin V conjugated to Fluorescein isothiocyanate (FITC) and Propidium Iodide (PI). Briefly, cells were plated in culture dishes with/without ECM at a density of 5 x 10^5 cell/plate and treated with either chemotherapeutic drugs or with 0.1% DMSO (control) for 24 hours. Post treatment, cells were harvested, washed twice with cold PBS and resuspended in 1 X

Binding Buffer at a concentration of 1 x 10^6 cells/ml. 100 µl of solution (1x 10^5 cells) was transferred to a 5 ml culture tube and stained with Annexin V conjugated with FITC and PI according to the manufacturer's instructions (FITC Annexin V Apoptosis Detection Kit I, BD Bioscience, USA). Tubes were vortexed gently and incubated for 15 minutes at room temperature in the dark. Flow cytometric analysis was done using a Beckman Coulter Flow Cytometer (Beckman Coulter, Life Sciences, Indianapolis, IN, USA). Data acquisition (2 × 104 events per treatment condition) was performed using the Cellquest software (Version 5.1, Becton Dickinson, Franklin Lakes, NJ, USA).

7.2.16. Colony Formation Assay

Plates containing cells that were 80-90% confluent were washed with PBS and incubated with 0.05% trypsin-EDTA solution for 2-5 minutes at 37°C. The trysin was neutralized with complete DMEM and the cells pelleted by centrifugation at 1800 rpm for 5 minutes. Cells were suspended in DMEM supplemented with 10% FBS 100 U/ml penicillin and 100 µg/ml streptomycin and counted using a Countess Cell Counter (Invitrogen) using the Trypan Blue exclusion method. 500 cells were cultured in 6-well plates with or without the ECM and incubated for 10 days. Cells were treated with drugs for 24 hours. Methanol (100%) was added to fix the colonies and staining was done using 0.05% crystal violet. Digital images of colonies were obtained using a scanning device or a camera and colonies were counted using ImageJ. The experiments were performed at least 3 times.

7.2.17. CellTracker and Live/Dead staining in spheroids

The co-cultured cells were stained with CellTracker in order to follow the spheroid localisation of the cells in time. Briefly, prior to seeding cells, cancer cells, CT1 and Wi38 fibroblast cells were washed with PBS. Cancer cells were incubated with serum free DMEM supplement 40 µM blue CMAC (C2110, Life Technologies,) and CT1 and Wi38 fibroblast were incubated with serum free DMEM supplemented with 10 µM Red CMTPX (C34552, Life Technologies) for 20 minutes at 37°C. Following the staining, 3D co-cultures were established, and fluorescence imaging was done.

Live-dead double staining was done on 3D and 3D co-culture spheroids. The spheroids were established as described in section 7.2.8 for 3 days and the spheroids were treated for 72 hours with chemotherapeutic drugs. After treatment, the spheroids were washed with once with PBS and stained with 4 µM Calcien AM (17783-1MG, sigma) and 10 µM ethidium homodimer (46043-1MG-F, sigma) for 45 minutes. Fluorescence imaging was performed. All steps were done with spheroids inside the 96 well plates.

Fluorescence imaging was done at 10x using Zeiss Axiovert 200M fluorescence microscope with AxioVision 4.8 Zeiss software and an Axioam HRm (Carl Zeiss, Jena Germany). Fluorescence signal images were obtained for CellTracker and Live/Dead stained cells. Using focus stacking, a Z-stack of each spheroid was taken, and a Z-projection obtained.

7.2.18. Immunofluorescence

2D cells were plated on glass coverslips in 6-well plates and 3D spheroid were established in Nunclon™ Sphera™ 96-well, U-shaped-bottom microplates. 2D and 3D cultures were washed twice with ice cold PBS after for 72 hours of treatment. Cells were fixed using 4% PFA (Paraformaldehyde) in PBS for 15 minutes at room temperature. The cells were washed twice with PBS and 0.25% Triton X-100 in PBS was used to permeabilise the cells for 15 minutes at room temperature. Cells were washed twice with PBS and blocked with 1% BSA in PBST with 0.3M glycine for 30 minutes. Cells were incubated with primary antibody (Table 7.3) diluted in 1% BSA in PBST overnight at 4°C. PBS was used to wash off the primary antibody. Secondary antibody was diluted in 1% BSA in PBST and added to the cells for 1 hour at room temperature in the dark. Secondary antibody was washed twice with PBS for 5 minutes intervals. DAPI (200 µg/ml) diluted to 1:400 in PBS was added to the cell for 5 minutes and was rinsed with PBS. All the steps for 3D cultures were done with spheroids inside the 96 U-bottom well plate. 2D cells on coverslips were mounted using Mowiol (Sigma-Aldrich, USA). Fluorescence imaging was done at 10x using Zeiss Axiovert 200M fluorescence microscope with AxioVision 4.8 Zeiss software and an Axioam HRm

(Carl Zeiss, Jena Germany). Each spheroid was used to create a Z-stack and a Z-projection using focus stacking. ImageJ software was used to measure fluorescence intensity.

Table 7. 3. Antibody concentrations and conditions for immunofluorescence microscope

Primary Antibody	Primary Antibody Conditions	Secondary Antibody	Secondary Antibody Conditions
Sox2 [Ab92494, Abcam]	1:100 1% BSA in PBST	Cy3 Goat anti Rabbit [Jackson ImmunoResearch]	1:300 1% BSA in PBST
Oct4 [Ab208907, Abcam]	1:100 1% BSA in PBST	Cy3 Goat anti Rabbit [Jackson ImmunoResearch]	1:300 1% BSA in PBST

7.2.19. Phalloidin staining

For immunofluorescence analysis, parental and side population cells from WHCO1 and MDA MB231 cells were cultured on glass cover slips. After 24 hours of culturing, cells were fixed in 4% paraformaldehyde for 20 minutes at room temperature. Permeabilisation of cell membranes was achieved using 0.1% Triton X-100 in PBS for 5 minutes at room temperature. Cells were then blocked with 1% BSA in PBS for 30 minutes. The cytoskeleton was stained using 50 ng/ml FITC-conjugated Phalloidin (Sigma-Aldrich, USA) by shaking for 1 hour at room temperature. Cells were then washed three times with PBS followed by counterstaining the nuclei with DAPI (200 μg/ml) (Sigma-Aldrich, USA). Glass cover slips were mounted using Mowiol (Sigma-Aldrich, USA). The slides were then stored in the dark at room temperature for the mowiol to set and then stored in the dark at 4°C until viewing. Stained cells were visualized using Zeiss Anxiovert 200 inverted fluorescent microscope (Carl Zeiss, Jena, Germany).

7.2.20. Immunohistochemistry

Sections oesophageal tumour and normal samples were formalin-fixed paraffin embedded and used in the evaluation of expression of ALDH1A1, CD133, CD44 and Ki67. Sections were cut to a 4 µm thickness and standard histological analyses were performed. Briefly, slides were heat-fixed at 60°C overnight and deparaffinized in xylene and rehydrated through a decreasing ethanol gradient. Endogenous peroxidase was inactivated with 3% hydrogen peroxide in water for 15 minutes and antigen retrieval was performed with slides heated in 0.01 M citrate buffer in a pressure cooker (97°C) for 20 minutes. Slides were allowed cool off in tap water and PBS-T (1 x PBS + 0.1% Tween) was used to wash in between steps. Slides were incubated with 100 µl primary antibodies against human ALDH1A1, CD133, CD44 and Ki67 for 1 hour (Table 7.4). Sections were rinsed with PBS-T and incubated with Envision+ System-Horseradish peroxidase (HRP) labelled polymer anti-mouse (Dako #K4001) for 30 minutes. Slide were washed with PBS-T and diaminobenzidine tetrachloride (DAB) substrate solution was used for 8 minutes to develop peroxidase colour. Haematoxylin was used as a counter stain and dehydrated through increasing ethanol gradient before being placed in xylene and mounting of the slides. Results were obtained using a light microscope and the samples were assessed and scored and confirmed by a pathologist.

Table 7. 4. Antibody conditions for immunohistochemistry

Primary Antibody	Conditions	Source
ALDH1A1 [ab134188, Abcam]	1:50	Mouse monoclonal
CD44 [ab9524, Abcam]	1:200	Mouse monoclonal
CD133 [ab216323, Abcam]	1:100	Rabbit monoclonal
Ki67 [ab92742, Abcam]	1:250	Rabbit monoclonal

7.2.21. siRNA Transfection Assay

Transfectin reagent (BioRad, Munich Germany) was used in the transient transfection assays. Short interfering RNAs (siRNAs) were purchased from Santa Cruz Biotechnology (Santa Cruz, CA, USA). 4 µl (0.5 µg) of 10 µM siRNA was dissolved in transfection diluent (6 µl) according to manufacturer's protocols. WHCO1 and CT1 cells were transfected with alpha type 1 collagen (COL1A1) and Fibronectin siRNAs using the Transfectin reagent and incubated for 6 hours. After 6 hours the medium was changed and ECM synthesis was continued for indicated period. To maintain knockdown efficiency subsequent transfections were carried out every 2 days for the duration of the ECM synthesis. In a different experiment, COL1A1 knockdown was accomplished by omitting ascorbic acid from the medium and ECM synthesis was continued for the duration indicated above. Cells were plated in 6-well plates with or without ascorbic acid and the ECM synthesis was continued for the indicated duration. Immunoblot and SDS-PAGE analysis was used to confirm COL1A1 and Fibronectin knockdowns.

7.2.22. Migration assay

To determine the influence ECMs have on cellular migration, confluent cells were trypsinised with 0.05% trypsin and neutralised by adding complete DMEM. Centrifugation was done at 1800 rpm for 5 minutes at room temperature and cells were resuspended in DMEM. Cells were counted in a Countess Cell Counter and diluted to a final density of 5000 cells per microliter. Cellular foci of 4 µl containing a total of 2×10^4 cells were added to culture dishes with or without the ECMs. An extra 100 µl of DMEM media was added to the cellular foci to prevent evaporation of media and incubation continued for 2 hours. An addition of 3 ml of complete DMEM was added and incubation was continued for 24 hours. Images were taken at time 0 hours and at 24 hours under 10 X magnification. To measure the area of migrating mass of cells, ImageJ software was used. Migration of cells on ECMs was normalized to that on plastic dishes.

Migration of parental and side population cells was determined using the wound healing assay. Briefly, 5×10^5 cells were plated in 6-well culture dishes and allowed to grow to confluency. For cell proliferation to be eliminated during migration, serum

starvation 16 hours after one-third confluence was applied before making the "wound" in vitro. Yellow plastic tip (p200) was used to make a scratch wound, the plated were rinsed with PBS to remove debris and fresh media was added to the cells. Images at 0 hours of the scratch wound were taken. Cells were then treated with chemotherapeutic drugs for the indicated time periods. At the end of each time period, the wound was observed by phase contrast using an Olympus CKX41 inverted microscope analysed with AnalySIS getIT software (Olympus, Tokyo, Japan).

7.2.23. 3D Invasion assay

Cells were grown at a density of 5 x 10^3 cells/100 µl per well in Nunclon™ Sphera™ 96-well, U-shaped-bottom microplates (Thermo Scientific, Waltham, MA, USA) and allowed to grow for 72 hours in humidified atmosphere with 5 % CO_2 at 37°C, to establish 3D spheroids. After 72 hours, spheroids were washed twice with PBS and embedded into a 70 µl of 1.5 mg/ml collagen type I rat tail matrix (Gibco, 41048301, Thermo Fisher Scientific, USA). 100 µl of complete DMEM with or without drugs was added to the wells with 3D spheroids. 3D cell invasion was observed using Inverted Leica DMi1 microscope equipped with digital camera Leica MC120 HD and images were taken at 0, 24, 48 and 72 hours. The area of the cell invasion was measured using ImageJ software.

7.2.24. Mass Spectrometry

7.2.24.1 ECM Preparation

Mass spectrometry was used to assess the proteomic profiles of the 3D-ECMs. The analysis was performed in triplicate ECM samples. 3D-ECMs were prepared using the method mentioned above with some modifications and following the protocol published by Adam Harvey, et al 2013. Briefly, confluent cells (WHCO1 and CT1) were split using 0.05% trypsin-EDTA and centrifuged at 1800 rpm for 5 mins. Cells were plated in DMEM supplemented with 10% FBS and 100 U/ml penicillin/streptomycin. The ascorbic acid was added to a final concentration of 50 µg/ml every second day and cells were maintained up to several days post confluence. After a thorough rinsing, the cells were lysed from the ECM using 5 ml of 0,5% Triton X-100 (Sigma-Aldrich, USA) for 10 minutes at room temperature. Followed by slowly adding 5 ml of 0.1 M

NH_4OH to the plates followed by three rinses with PBS. After the ECM had been prepared, the ECM was solubilized 5% SDS, 50 mM Tris-HCL, pH 6.8 and the ECM was scraped with a cell scraper. The SDS-lysate was collected into 1.5 ml centrifuge tubes and incubated at 95°C for 5 minutes. The samples were centrifuged at 14 000 rpm for 10 mins the supernatants called SDS-soluble ECM proteins were collected and placed on ice. ECM protein concentration was measured using BCS Protein Assay Kit following the protocol mentioned above.

7.2.24.2. Sample Preparation- FASP

After quantification, 100 µg samples were prepared by filter aided sample preparation (FASP) according to Ostasiewicz P. et al., 2010 [514]. The samples were added to a filter, diluted with 8M urea and centrifuged at 14 000 rpm for 15 minutes. 100 mM dithiothreitol (DTT) was added to the filter, mixed and incubated at room temperature for 30 minutes in the dark. Followed by centrifugation at 14 000 rpm for 15 minutes addition of 8M urea was added to the filter and centrifugation at 14 000 rpm for 15 minutes. 50 mM Iodoacetamide (IAA) was added to the filter, incubated in the dark at room temperature and centrifuged at 14 000 rpm for 15 minutes. 8M urea was added to the filter and centrifuged for 15 minutes at 14 000 rpm, this step was repeated twice. Then 50 mM ammonium bicarbonate (ABC) was added to the filter and centrifuged at 14 000 rpm for 15 minutes. The filter was transferred to a new collection tube, the proteins were digested using trypsin (1:50) and incubated for 16 hours in a wet chamber at 37°C. After incubation, the filter was centrifuged at 14 000 rpm for 10 minutes and 50 mM ABC was added followed by centrifugation at 14 000 rpm for 10 minutes. The resulting tryptic peptides were acidified in 0.1% formic acid and desalted using in-house C18 stage tips. The samples were dried in vacuum concentrator and reconstituted in 2% acetonitrile with 0.1% formic acid prior to LC-MS/MS analysis.

7.2.24.3. Q-Exactive

Thermo Scientific Dionex Ultimate 3000 UHPLC (Thermo Fisher Scientific, Waltham, MA, USA) coupled to a Thermo Scientifc Q-Exactive hybrid quadrupole Orbitrap mass spectrometer was used to analyse the samples. The Q Exactive was ran in data-dependent mode, with full scan MS spectra (m/z 300–1750) acquired in the Orbitrap

analyser after accumulation to an AGC target of 3e6 or an injection time of 250 MS at a resolution of 70,000.

7.2.24.4. Data Analysis

Label-free quantification was done using MaxQuant version 1.2.7.429 (Computational Systems Biochemistry, Martinsried, Germany) was used to process the raw files. MS/MS spectra were searched against Uniprot human protein database. A maximum of 1% peptide and 1% protein false discovery rate was applied to the run. Enzyme specificity was set to trypsin with a maximum of two missed cleavages. Carbamidomethylation of cysteine was set as a fixed modification, and oxidation of methionine and protein N-terminal acetylation were selected as variable modifications. The minimum peptide length was set to seven amino acids. Protein intensity values were normalized automatically using the LFQ algorithm to identify differentially expressed proteins. Perseus v.1.2.7.4 software was used to perform bioinformatic analyses of the data. Reverse and “only identified by site” entries were excluded. LFQ intensity values were log2 transformed, and the dataset was filtered to contain only entries with two minimum valid values in at least one group. Statistical significance was assessed using Student’s *t*-test to identify differentially expressed proteins between the groups.

7.2.25. Databases and RNA -seq/gene expression analysis

Several public databases were consulted for this study, including The Cancer Genome Atlas (TCGA) (https://cancergenome.nih.gov), Oncomine database (https://www.oncomine.org), Tumour Immune Estimation Resource (TIMER) database (https://cistrome.org/TIMER/), and the Human Protein Atlas (www.proteinatlas.org). Whole-genome messengers RNA expression levels of several CAF and MSC markers were examined in tumour and normal adjacent tissues. In Oncomine database, a large collection of cancer gene expression microarrays has been used to identify cancer-related genes and pathways [515]. By using Oncomine database, the expression level of genes was examined in thousands of 32 cancer types and the results were determined based on the following parameters: P-value < 0.001, fold change > 1.5, and gene ranking overall. TIMER provides access to

systematic analysis of immune infiltrates in cancers [516]. Therefore, gene expression in different cancers using RNA-seq data was assessed across all TCGA tumours with Wilcoxon tests in TIMER with statistical significance (P-value < 0.05). TIMER database analysis revealed a correlation between CAFs expression level and MSC markers in different cancer types, with a significance level of P<0.05. Using the Human Protein Atlas (HPA), researchers were able to study protein expression and localisation in human cells [517]. HPA database was used to detect the protein expression levels of genes. GeneMANIA (https://genemania.org) was used to construct protein-protein networks and determine the function of interactive genes [518]. The GeneMANIA database provides information about genes that are co-expressed, colocalized, and physically interact with CAFs.

7.2.26. Statistical Analysis

Statistical analysis was performed using GraphPad Prism version 5 software (GraphPad software, San Diego, California, USA). Experiments were performed in triplicates or quadruplets and expressed as means $\pm$ SEM. Paired Student's t test and one way ANOVA with a post hoc were used to analyse the data where a p-value of <0.05 was considered statistically significant. Data analysis was also done using non-parameter Mann-Whitney U test where a p-value of <0.05 was considered statistically significant.

REFERENCES

1. Wilson, T.R., D.B. Longley, and P.G. Johnston, *Chemoresistance in solid tumours.* Ann Oncol, 2006. 17 Suppl 10: p. x315-24.
2. Lemoine, M., et al., *In the shadow of HIV/AIDS: forgotten diseases in sub-Saharan Africa: global health issues and funding agency responsibilities.* J Public Health Policy, 2012. 33(4): p. 430-8.
3. Levitt, N.S., et al., *Chronic noncommunicable diseases and HIV-AIDS on a collision course: relevance for health care delivery, particularly in low-resource settings--insights from South Africa.* Am J Clin Nutr, 2011. 94(6): p. 1690s-1696s.
4. Philips, G.K. and M. Atkins, *Therapeutic uses of anti-PD-1 and anti-PD-L1 antibodies.* Int Immunol, 2015. 27(1): p. 39-46.
5. Gupta, V.K., et al., *Metastasis and chemoresistance in CD133 expressing pancreatic cancer cells are dependent on their lipid raft integrity.* Cancer Lett, 2018. 439: p. 101-112.
6. Zheng, X., et al., *Epithelial-to-mesenchymal transition is dispensable for metastasis but induces chemoresistance in pancreatic cancer.* Nature, 2015. 527(7579): p. 525-530.
7. Rastogi, N. and D.P. Mishra, *Therapeutic targeting of cancer cell cycle using proteasome inhibitors.* Cell division, 2012. 7(1): p. 26.
8. Friedl, P., et al., *Classifying collective cancer cell invasion.* Nature cell biology, 2012. 14(8): p. 777-783.
9. Sahai, E., *Mechanisms of cancer cell invasion.* Current opinion in genetics & development, 2005. 15(1): p. 87-96.
10. Stemmermann, G., et al., *The molecular biology of esophageal and gastric cancer and their precursors: oncogenes, tumor suppressor genes, and growth factors.* Human pathology, 1994. 25(10): p. 968-981.
11. Hanahan, D. and R.A. Weinberg, *Hallmarks of cancer: the next generation.* Cell, 2011. 144(5): p. 646-74.
12. Enzinger , P.C. and R.J. Mayer *Esophageal Cancer.* New England Journal of Medicine, 2003. 349(23): p. 2241-2252.

13. Jemal, A., et al., *Selected cancers with increasing mortality rates by educational attainment in 26 states in the United States, 1993-2007.* Cancer Causes Control, 2013. 24(3): p. 559-65.
14. Runge, T.M., J.A. Abrams, and N.J. Shaheen, *Epidemiology of Barrett's Esophagus and Esophageal Adenocarcinoma.* Gastroenterol Clin North Am, 2015. 44(2): p. 203-31.
15. Maugeri-Sacca, M., P. Vigneri, and R. De Maria, *Cancer stem cells and chemosensitivity.* Clin Cancer Res, 2011. 17(15): p. 4942-7.
16. Oppedijk, V., et al., *Patterns of Recurrence After Surgery Alone Versus Preoperative Chemoradiotherapy and Surgery in the CROSS Trials.* Journal of Clinical Oncology, 2014. 32(5): p. 385-391.
17. Maugeri-Sacca, M., A. Zeuner, and R. De Maria, *Therapeutic targeting of cancer stem cells.* Front Oncol, 2011. 1: p. 10.
18. Baskar, R., et al., *Cancer and radiation therapy: current advances and future directions.* International journal of medical sciences, 2012. 9(3): p. 193-199.
19. Ling, T.C., et al., *Analysis of Intensity-Modulated Radiation Therapy (IMRT), Proton and 3D Conformal Radiotherapy (3D-CRT) for Reducing Perioperative Cardiopulmonary Complications in Esophageal Cancer Patients.* Cancers (Basel), 2014. 6(4): p. 2356-68.
20. Siddik, Z.H., *Mechanisms of Action of Cancer Chemotherapeutic Agents: DNA-Interactive Alkylating Agents and Antitumour Platinum-Based Drugs*, in *The Cancer Handbook*. 2005, In The Cancer Handbook, M.R. Alison (ED).
21. Coluccia, M. and G. Natile, *Trans-platinum complexes in cancer therapy.* Anticancer Agents Med Chem, 2007. 7(1): p. 111-23.
22. Tiwari, M., *Antimetabolites: established cancer therapy.* J Cancer Res Ther, 2012. 8(4): p. 510-9.
23. Huizing, M.T., et al., *Taxanes: a new class of antitumor agents.* Cancer Invest, 1995. 13(4): p. 381-404.
24. Schiff, P.B., J. Fant, and S.B. Horwitz, *Promotion of microtubule assembly in vitro by taxol.* Nature, 1979. 277(5698): p. 665-7.
25. Jordan, M.A. and L. Wilson, *Microtubules as a target for anticancer drugs.* Nat Rev Cancer, 2004. 4(4): p. 253-65.
26. Ojima, I., et al., *Taxane anticancer agents: a patent perspective.* Expert Opin Ther Pat, 2016. 26(1): p. 1-20.

27. Moudi, M., et al., *Vinca alkaloids.* Int J Prev Med, 2013. 4(11): p. 1231-5.
28. Coufal, N. and L. Farnaes, *The Vinca Alkaloids*, in *Cancer Management in Man: Chemotherapy, Biological Therapy, Hyperthermia and Supporting Measures*, B.R. Minev, Editor. 2011, Springer Netherlands: Dordrecht. p. 25-37.
29. Turanli, B., et al., *A Network-Based Cancer Drug Discovery: From Integrated Multi-Omics Approaches to Precision Medicine.* Curr Pharm Des, 2018. 24(32): p. 3778-3790.
30. Ke, X. and L. Shen, *Molecular targeted therapy of cancer: The progress and future prospect.* Frontiers in Laboratory Medicine, 2017. 1(2): p. 69-75.
31. Kifle, Z.D., et al., *A recent development of new therapeutic agents and novel drug targets for cancer treatment.* SAGE Open Med, 2021. 9: p. 20503121211067083.
32. Shibuya, M., *Vascular Endothelial Growth Factor (VEGF) and Its Receptor (VEGFR) Signaling in Angiogenesis: A Crucial Target for Anti- and Pro-Angiogenic Therapies.* Genes Cancer, 2011. 2(12): p. 1097-105.
33. Leenders, W.P., B. Küsters, and R.M. de Waal, *Vessel co-option: how tumors obtain blood supply in the absence of sprouting angiogenesis.* Endothelium, 2002. 9(2): p. 83-7.
34. Melincovici, C.S., et al., *Vascular endothelial growth factor (VEGF) - key factor in normal and pathological angiogenesis.* Rom J Morphol Embryol, 2018. 59(2): p. 455-467.
35. Yadav, L., et al., *Tumour Angiogenesis and Angiogenic Inhibitors: A Review.* J Clin Diagn Res, 2015. 9(6): p. Xe01-xe05.
36. Zhong, L., et al., *Small molecules in targeted cancer therapy: advances, challenges, and future perspectives.* Signal Transduction and Targeted Therapy, 2021. 6(1): p. 201.
37. Merla, A. and S. Goel, *Novel Drugs Targeting the Epidermal Growth Factor Receptor and Its Downstream Pathways in the Treatment of Colorectal Cancer: A Systematic Review.* Chemotherapy Research and Practice, 2012. 2012: p. 387172.
38. Nieto, C., M.A. Vega, and E.M. Martín Del Valle, *Trastuzumab: More than a Guide in HER2-Positive Cancer Nanomedicine.* Nanomaterials (Basel), 2020. 10(9).

39. Gajria, D. and S. Chandarlapaty, *HER2-amplified breast cancer: mechanisms of trastuzumab resistance and novel targeted therapies.* Expert Rev Anticancer Ther, 2011. 11(2): p. 263-75.
40. Zhang, Y. and Z. Zhang, *The history and advances in cancer immunotherapy: understanding the characteristics of tumor-infiltrating immune cells and their therapeutic implications.* Cellular & Molecular Immunology, 2020. 17(8): p. 807-821.
41. McCune, J.S., *Rapid Advances in Immunotherapy to Treat Cancer.* Clin Pharmacol Ther, 2018. 103(4): p. 540-544.
42. Miliotou, A.N. and L.C. Papadopoulou, *CAR T-cell Therapy: A New Era in Cancer Immunotherapy.* Curr Pharm Biotechnol, 2018. 19(1): p. 5-18.
43. Alam, M., et al., *B Cell Lymphoma 2: A Potential Therapeutic Target for Cancer Therapy.* Int J Mol Sci, 2021. 22(19).
44. Delbridge, A.R.D. and A. Strasser, *The BCL-2 protein family, BH3-mimetics and cancer therapy.* Cell Death & Differentiation, 2015. 22(7): p. 1071-1080.
45. Perini, G.F., et al., *BCL-2 as therapeutic target for hematological malignancies.* J Hematol Oncol, 2018. 11(1): p. 65.
46. Wei, H. and M.T. Harper, *Comparison of putative BH3 mimetics AT-101, HA14-1, sabutoclax and TW-37 with ABT-737 in platelets.* Platelets, 2021. 32(1): p. 105-112.
47. Zahreddine, H. and K.L. Borden, *Mechanisms and insights into drug resistance in cancer.* Front Pharmacol, 2013. 4: p. 28.
48. Tredan, O., et al., *Drug resistance and the solid tumor microenvironment.* J Natl Cancer Inst, 2007. 99(19): p. 1441-54.
49. Kerbel, R.S., et al., *Multicellular resistance: a new paradigm to explain aspects of acquired drug resistance of solid tumors.* Cold Spring Harb Symp Quant Biol, 1994. 59: p. 661-72.
50. Sung, S.Y., et al., *Tumor microenvironment promotes cancer progression, metastasis, and therapeutic resistance.* Curr Probl Cancer, 2007. 31(2): p. 36-100.
51. Whatcott, C.J., et al., *Targeting the tumor microenvironment in cancer: why hyaluronidase deserves a second look.* Cancer Discov, 2011. 1(4): p. 291-6.
52. Garcia-Maceira, P. and J. Mateo, *Silibinin inhibits hypoxia-inducible factor-1alpha and mTOR/p70S6K/4E-BP1 signalling pathway in human cervical and*

hepatoma cancer cells: implications for anticancer therapy. Oncogene, 2009. 28(3): p. 313-24.

53. Jing, X., et al., *Role of hypoxia in cancer therapy by regulating the tumor microenvironment.* Molecular cancer, 2019. 18(1): p. 157-157.
54. Mahoney, B.P., et al., *Tumor acidity, ion trapping and chemotherapeutics. I. Acid pH affects the distribution of chemotherapeutic agents in vitro.* Biochem Pharmacol, 2003. 66(7): p. 1207-18.
55. Virchow, R., *Die Cellularpathologie in ihrer Begründung auf physiologische und pathologische Gewebelehre*. Vol. 1. 1871: Hirschwald.
56. Kalluri, R. and M. Zeisberg, *Fibroblasts in cancer.* Nature Reviews Cancer, 2006. 6(5): p. 392.
57. Dvorak, H.F., *Tumors: wounds that do not heal.* New England Journal of Medicine, 1986. 315(26): p. 1650-1659.
58. Hanahan, D. and R.A. Weinberg, *Hallmarks of cancer: the next generation.* cell, 2011. 144(5): p. 646-674.
59. Öhlund, D., E. Elyada, and D. Tuveson, *Fibroblast heterogeneity in the cancer wound.* Journal of Experimental Medicine, 2014. 211(8): p. 1503-1523.
60. Kalluri, R., *The biology and function of fibroblasts in cancer.* Nature Reviews Cancer, 2016. 16(9): p. 582.
61. De Wever, O., et al., *Stromal myofibroblasts are drivers of invasive cancer growth.* International Journal of Cancer, 2008. 123(10): p. 2229-2238.
62. Lazard, D., et al., *Expression of smooth muscle-specific proteins in myoepithelium and stromal myofibroblasts of normal and malignant human breast tissue.* Proceedings of the National Academy of Sciences, 1993. 90(3): p. 999-1003.
63. Saadi, A., et al., *Stromal genes discriminate preinvasive from invasive disease, predict outcome, and highlight inflammatory pathways in digestive cancers.* Proceedings of the National Academy of Sciences, 2010. 107(5): p. 2177-2182.
64. Kalli, M. and T. Stylianopoulos, *Defining the Role of Solid Stress and Matrix Stiffness in Cancer Cell Proliferation and Metastasis.* Front Oncol, 2018. 8: p. 55.
65. Tsujino, T., et al., *Stromal myofibroblasts predict disease recurrence for colorectal cancer.* Clinical cancer research, 2007. 13(7): p. 2082-2090.

66. Calvo, F., et al., *Mechanotransduction and YAP-dependent matrix remodelling is required for the generation and maintenance of cancer-associated fibroblasts.* Nature Cell Biology, 2013. 15: p. 637.
67. Cukierman, E. and D.E. Bassi. *Physico-mechanical aspects of extracellular matrix influences on tumorigenic behaviors*. in *Seminars in cancer biology*. 2010. Elsevier.
68. Baeriswyl, V. and G. Christofori. *The angiogenic switch in carcinogenesis*. in *Seminars in cancer biology*. 2009. Elsevier.
69. Yang, X., et al., *FAP promotes immunosuppression by cancer-associated fibroblasts in the tumor microenvironment via STAT3–CCL2 signaling.* Cancer research, 2016. 76(14): p. 4124-4135.
70. Bussard, K.M., et al., *Tumor-associated stromal cells as key contributors to the tumor microenvironment.* Breast Cancer Res, 2016. 18(1): p. 84.
71. Glentis, A., et al., *Cancer-associated fibroblasts induce metalloprotease-independent cancer cell invasion of the basement membrane.* Nature communications, 2017. 8(1): p. 924.
72. Senthebane, D.A., et al., *The role of tumor microenvironment in chemoresistance: to survive, keep your enemies closer.* International journal of molecular sciences, 2017. 18(7): p. 1586.
73. Omary, M.B., et al., *The pancreatic stellate cell: a star on the rise in pancreatic diseases.* The Journal of clinical investigation, 2007. 117(1): p. 50-59.
74. Barth, P.J., et al., *CD34+ fibrocytes in invasive ductal carcinoma, ductal carcinoma in situ, and benign breast lesions.* Virchows Archiv, 2002. 440(3): p. 298-303.
75. Jung, Y., et al., *Recruitment of mesenchymal stem cells into prostate tumours promotes metastasis.* Nature communications, 2013. 4: p. 1795.
76. Weber, C.E., et al., *Osteopontin mediates an MZF1-TGF-beta1-dependent transformation of mesenchymal stem cells into cancer-associated fibroblasts in breast cancer.* Oncogene, 2015. 34(37): p. 4821-33.
77. Yin, C., et al., *Hepatic stellate cells in liver development, regeneration, and cancer.* The Journal of clinical investigation, 2013. 123(5): p. 1902-1910.
78. Iwano, M., et al., *Evidence that fibroblasts derive from epithelium during tissue fibrosis.* The Journal of clinical investigation, 2002. 110(3): p. 341-350.

79. Zeisberg, E.M., et al., *Discovery of endothelial to mesenchymal transition as a source for carcinoma-associated fibroblasts.* Cancer research, 2007. 67(21): p. 10123-10128.
80. Jotzu, C., et al., *Adipose tissue derived stem cells differentiate into carcinoma-associated fibroblast-like cells under the influence of tumor derived factors.* Cellular oncology, 2011. 34(1): p. 55-67.
81. Huelsken, J. and D. Hanahan, *A subset of cancer-associated fibroblasts determines therapy resistance.* Cell, 2018. 172(4): p. 643-644.
82. Senthebane, D., et al., *The role of tumor microenvironment in chemoresistance: 3D extracellular matrices as accomplices.* International journal of molecular sciences, 2018. 19(10): p. 2861.
83. Biffi, G., et al., *IL1-Induced JAK/STAT Signaling Is Antagonized by TGFβ to Shape CAF Heterogeneity in Pancreatic Ductal Adenocarcinoma.* Cancer Discov, 2019. 9(2): p. 282-301.
84. Öhlund, D., et al., *Distinct populations of inflammatory fibroblasts and myofibroblasts in pancreatic cancer.* J Exp Med, 2017. 214(3): p. 579-596.
85. Elyada, E., et al., *Cross-Species Single-Cell Analysis of Pancreatic Ductal Adenocarcinoma Reveals Antigen-Presenting Cancer-Associated Fibroblasts.* Cancer Discov, 2019. 9(8): p. 1102-1123.
86. Sebastian, A., et al., *Single-Cell Transcriptomic Analysis of Tumor-Derived Fibroblasts and Normal Tissue-Resident Fibroblasts Reveals Fibroblast Heterogeneity in Breast Cancer.* Cancers (Basel), 2020. 12(5).
87. Sahai, E., et al., *A framework for advancing our understanding of cancer-associated fibroblasts.* Nature Reviews Cancer, 2020. 20(3): p. 174-186.
88. Vuoriluoto, K., et al., *Vimentin regulates EMT induction by Slug and oncogenic H-Ras and migration by governing Axl expression in breast cancer.* Oncogene, 2011. 30(12): p. 1436.
89. Wang, N. and D. Stamenovic, *Mechanics of vimentin intermediate filaments.* Journal of Muscle Research & Cell Motility, 2002. 23(5-6): p. 535-540.
90. Eyden, B., *The myofibroblast: phenotypic characterization as a prerequisite to understanding its functions in translational medicine.* Journal of cellular and molecular medicine, 2008. 12(1): p. 22-37.

91. Kaya, S., et al., *Differences in the expression of caveolin-1 isoforms in cancer-associated and normal fibroblasts of patients with oral squamous cell carcinoma.* Clin Oral Investig, 2021. 25(10): p. 5823-5831.
92. Guido, C., et al., *Metabolic reprogramming of cancer-associated fibroblasts by TGF-β drives tumor growth: connecting TGF-β signaling with "Warburg-like" cancer metabolism and L-lactate production.* Cell cycle, 2012. 11(16): p. 3019-3035.
93. Simpkins, S.A., et al., *Clinical and functional significance of loss of caveolin-1 expression in breast cancer-associated fibroblasts.* The Journal of pathology, 2012. 227(4): p. 490-498.
94. Su, S., et al., *CD10+ GPR77+ cancer-associated fibroblasts promote cancer formation and chemoresistance by sustaining cancer stemness.* Cell, 2018. 172(4): p. 841-856. e16.
95. Zhang, J., et al., *Fibroblast-specific protein 1/S100A4–positive cells prevent carcinoma through collagen production and encapsulation of carcinogens.* Cancer research, 2013. 73(9): p. 2770-2781.
96. Wang, X.M., et al., *Fibroblast activation protein increases apoptosis, cell adhesion, and migration by the LX-2 human stellate cell line.* Hepatology, 2005. 42(4): p. 935-945.
97. Orimo, A., et al., *Stromal fibroblasts present in invasive human breast carcinomas promote tumor growth and angiogenesis through elevated SDF-1/CXCL12 secretion.* Cell, 2005. 121(3): p. 335-348.
98. Pietras, K., et al., *Functions of paracrine PDGF signaling in the proangiogenic tumor stroma revealed by pharmacological targeting.* PLoS medicine, 2008. 5(1): p. e19.
99. Pinto, M.P., et al., *Malignant stroma increases luminal breast cancer cell proliferation and angiogenesis through platelet-derived growth factor signaling.* BMC Cancer, 2014. 14: p. 735.
100. Steller, E.J., et al., *PDGFRB promotes liver metastasis formation of mesenchymal-like colorectal tumor cells.* Neoplasia, 2013. 15(2): p. 204-17.
101. Öhlund, D., et al., *Distinct populations of inflammatory fibroblasts and myofibroblasts in pancreatic cancer.* Journal of Experimental Medicine, 2017. 214(3): p. 579-596.

102. Stoker, M., M. SHEARER, and C. O'NEILL, *Growth inhibition of polyoma-transformed cells by contact with static normal fibroblasts.* Journal of cell science, 1966. 1(3): p. 297-310.
103. Trimboli, A.J., et al., *Pten in stromal fibroblasts suppresses mammary epithelial tumours.* Nature, 2009. 461(7267): p. 1084.
104. Ryan, H.E., et al., *Hypoxia-inducible factor-1α is a positive factor in solid tumor growth.* Cancer research, 2000. 60(15): p. 4010-4015.
105. Wang, L., et al., *Cancer-associated fibroblasts enhance metastatic potential of lung cancer cells through IL-6/STAT3 signaling pathway.* Oncotarget, 2017. 8(44): p. 76116.
106. Erez, N., et al., *Cancer-Associated Fibroblasts Are Activated in Incipient Neoplasia to Orchestrate Tumor-Promoting Inflammation in an NF-κB-Dependent Manner.* Cancer Cell, 2010. 17(2): p. 135-147.
107. Toullec, A., et al., *Oxidative stress promotes myofibroblast differentiation and tumour spreading.* EMBO molecular medicine, 2010. 2(6): p. 211-230.
108. Albrengues, J., et al., *Epigenetic switch drives the conversion of fibroblasts into proinvasive cancer-associated fibroblasts.* Nature communications, 2015. 6: p. 10204.
109. Tan, H.-X., et al., *TGFβ1 is essential for MSCs-CAFs differentiation and promotes HCT116 cells migration and invasion via JAK/STAT3 signaling.* OncoTargets and therapy, 2019. 12: p. 5323.
110. Calon, A., D. Tauriello, and E. Batlle. *TGF-beta in CAF-mediated tumor growth and metastasis*. in *Seminars in cancer biology*. 2014. Elsevier.
111. Deryugina, E.I. and J.P. Quigley, *Tumor angiogenesis: MMP-mediated induction of intravasation- and metastasis-sustaining neovasculature.* Matrix Biology, 2015. 44-46: p. 94-112.
112. Taguchi, A., et al., *Matrix metalloproteinase (MMP)-9 in cancer-associated fibroblasts (CAFs) is suppressed by omega-3 polyunsaturated fatty acids in vitro and in vivo.* PLoS One, 2014. 9(2): p. e89605.
113. Provenzano, P.P., et al., *Collagen density promotes mammary tumor initiation and progression.* BMC medicine, 2008. 6(1): p. 11.
114. Carmeliet, P. and R.K. Jain, *Molecular mechanisms and clinical applications of angiogenesis.* Nature, 2011. 473(7347): p. 298.

115. Egeblad, M., M.G. Rasch, and V.M. Weaver, *Dynamic interplay between the collagen scaffold and tumor evolution.* Current opinion in cell biology, 2010. 22(5): p. 697-706.
116. Morrissey, C., et al., *Differential expression of angiogenesis associated genes in prostate cancer bone, liver and lymph node metastases.* Clinical & experimental metastasis, 2008. 25(4): p. 377-388.
117. Monsky, W.L., et al., *Role of host microenvironment in angiogenesis and microvascular functions in human breast cancer xenografts: mammary fat pad versus cranial tumors.* Clinical Cancer Research, 2002. 8(4): p. 1008-1013.
118. Bergers, G. and L.E. Benjamin, *Angiogenesis: tumorigenesis and the angiogenic switch.* Nature reviews cancer, 2003. 3(6): p. 401.
119. Zhang, L., et al., *CXCL12 overexpression promotes the angiogenesis potential of periodontal ligament stem cells.* Sci Rep, 2017. 7(1): p. 10286.
120. Crawford, Y., et al., *PDGF-C mediates the angiogenic and tumorigenic properties of fibroblasts associated with tumors refractory to anti-VEGF treatment.* Cancer Cell, 2009. 15(1): p. 21-34.
121. Zhao, J., et al., *Simultaneous inhibition of hedgehog signaling and tumor proliferation remodels stroma and enhances pancreatic cancer therapy.* Biomaterials, 2018. 159: p. 215-228.
122. Damiano, J.S., L.A. Hazlehurst, and W.S. Dalton, *Cell adhesion-mediated drug resistance (CAM-DR) protects the K562 chronic myelogenous leukemia cell line from apoptosis induced by BCR/ABL inhibition, cytotoxic drugs, and gamma-irradiation.* Leukemia, 2001. 15(8): p. 1232-9.
123. Shintani, Y., et al., *IL-6 secreted from cancer-associated fibroblasts mediates chemoresistance in NSCLC by increasing epithelial-mesenchymal transition signaling.* Journal of Thoracic Oncology, 2016. 11(9): p. 1482-1492.
124. Richards, K.E., et al., *Cancer-associated fibroblast exosomes regulate survival and proliferation of pancreatic cancer cells.* Oncogene, 2017. 36(13): p. 1770.
125. Huber, R.M., et al., *DNA damage induces GDNF secretion in the tumor microenvironment with paracrine effects promoting prostate cancer treatment resistance.* Oncotarget, 2015. 6(4): p. 2134-47.
126. Eke, I. and N. Cordes, *Radiobiology goes 3D: how ECM and cell morphology impact on cell survival after irradiation.* Radiotherapy and Oncology, 2011. 99(3): p. 271-278.

127. Barker, H.E., et al., *The tumour microenvironment after radiotherapy: mechanisms of resistance and recurrence.* Nature reviews Cancer, 2015. 15(7): p. 409-425.
128. Le Blanc, K. and D. Mougiakakos, *Multipotent mesenchymal stromal cells and the innate immune system.* Nature Reviews Immunology, 2012. 12(5): p. 383-396.
129. Dominici, M., et al., *Minimal criteria for defining multipotent mesenchymal stromal cells. The International Society for Cellular Therapy position statement.* Cytotherapy, 2006. 8(4): p. 315-317.
130. Hsu, H.S., et al., *Mesenchymal stem cells enhance lung cancer initiation through activation of IL-6/JAK2/STAT3 pathway.* Lung Cancer, 2012. 75(2): p. 167-77.
131. Nishimura, K., et al., *Mesenchymal stem cells provide an advantageous tumor microenvironment for the restoration of cancer stem cells.* Pathobiology, 2012. 79(6): p. 290-306.
132. Nabha, S.M., et al., *Bone marrow stromal cells enhance prostate cancer cell invasion through type I collagen in an MMP-12 dependent manner.* Int J Cancer, 2008. 122(11): p. 2482-90.
133. Rattigan, Y., et al., *Interleukin 6 mediated recruitment of mesenchymal stem cells to the hypoxic tumor milieu.* Exp Cell Res, 2010. 316(20): p. 3417-24.
134. Gao, H., et al., *Activation of signal transducers and activators of transcription 3 and focal adhesion kinase by stromal cell-derived factor 1 is required for migration of human mesenchymal stem cells in response to tumor cell-conditioned medium.* Stem cells, 2009. 27(4): p. 857-865.
135. Tu, S., et al., *Overexpression of interleukin-1β induces gastric inflammation and cancer and mobilizes myeloid-derived suppressor cells in mice.* Cancer cell, 2008. 14(5): p. 408-419.
136. Martin, F., et al., *Potential role of mesenchymal stem cells (MSCs) in the breast tumour microenvironment: stimulation of epithelial to mesenchymal transition (EMT).* Breast cancer research and treatment, 2010. 124(2): p. 317-326.
137. Xue, Z., et al., *Mesenchymal stem cells promote epithelial to mesenchymal transition and metastasis in gastric cancer though paracrine cues and close physical contact.* Journal of cellular biochemistry, 2015. 116(4): p. 618-627.

138. Karnoub, A.E., et al., *Mesenchymal stem cells within tumour stroma promote breast cancer metastasis.* Nature, 2007. 449(7162): p. 557-563.
139. McGrail, D.J., et al., *Differential mechanical response of mesenchymal stem cells and fibroblasts to tumor-secreted soluble factors.* PLoS One, 2012. 7(3): p. e33248.
140. Barcellos-de-Souza, P., et al., *Mesenchymal Stem Cells are Recruited and Activated into Carcinoma-Associated Fibroblasts by Prostate Cancer Microenvironment-Derived TGF-β1.* Stem Cells, 2016. 34(10): p. 2536-2547.
141. Kojima, Y., et al., *Autocrine TGF-β and stromal cell-derived factor-1 (SDF-1) signaling drives the evolution of tumor-promoting mammary stromal myofibroblasts.* Proceedings of the National Academy of Sciences, 2010. 107(46): p. 20009-20014.
142. Mishra, P.J., et al., *Carcinoma-associated fibroblast-like differentiation of human mesenchymal stem cells.* Cancer Res, 2008. 68(11): p. 4331-9.
143. Liu, S., et al., *Breast cancer stem cells are regulated by mesenchymal stem cells through cytokine networks.* Cancer research, 2011. 71(2): p. 614-624.
144. McLean, K., et al., *Human ovarian carcinoma–associated mesenchymal stem cells regulate cancer stem cells and tumorigenesis via altered BMP production.* J Clin Invest, 2011. 121(8): p. 3206-19.
145. Dzobo, K., et al., *Cancer Stem Cell Hypothesis for Therapeutic Innovation in Clinical Oncology? Taking the Root Out, Not Chopping the Leaf.* Omics, 2016. 20(12): p. 681-691.
146. Dzobo, K., et al., *Not Everyone Fits the Mold: Intratumor and Intertumor Heterogeneity and Innovative Cancer Drug Design and Development.* Omics, 2018. 22(1): p. 17-34.
147. Fu, Y., H. Li, and X. Hao, *The self-renewal signaling pathways utilized by gastric cancer stem cells.* Tumour Biol, 2017. 39(4): p. 1010428317697577.
148. Humphries, H.N., et al., *Characterization of Cancer Stem Cells in Colon Adenocarcinoma Metastasis to the Liver.* Frontiers in Surgery, 2018. 4(76).
149. Nowell, P.C., *The clonal evolution of tumor cell populations.* Science, 1976. 194(4260): p. 23-8.
150. Visvader, J.E., *Cells of origin in cancer.* Nature, 2011. 469(7330): p. 314-22.
151. Paget, S., *The distribution of secondary growths in cancer of the breast.* The Lancet, 1889. 133(3421): p. 571-573.

152. Oskarsson, T., E. Batlle, and J. Massagué, *Metastatic stem cells: sources, niches, and vital pathways.* Cell stem cell, 2014. 14(3): p. 306-321.
153. Turdo, A., et al., *Meeting the Challenge of Targeting Cancer Stem Cells.* Front Cell Dev Biol, 2019. 7: p. 16.
154. Lapidot, T., et al., *A cell initiating human acute myeloid leukaemia after transplantation into SCID mice.* Nature, 1994. 367(6464): p. 645-8.
155. Agliano, A., A. Calvo, and C. Box, *The challenge of targeting cancer stem cells to halt metastasis.* Seminars in Cancer Biology, 2017. 44: p. 25-42.
156. Nguyen, L.V., et al., *Cancer stem cells: an evolving concept.* Nature Reviews Cancer, 2012. 12(2): p. 133-143.
157. Dzobo, K., *Taking a Full Snapshot of Cancer Biology: Deciphering the Tumor Microenvironment for Effective Cancer Therapy in the Oncology Clinic.* Omics, 2020.
158. MacDonagh, L., et al., *Lung cancer stem cells: The root of resistance.* Cancer letters, 2016. 372(2): p. 147-156.
159. Zhang, C., et al., *Identification of CD44+ CD24+ gastric cancer stem cells.* Journal of cancer research and clinical oncology, 2011. 137(11): p. 1679.
160. Beier, D., et al., *CD133+ and CD133− glioblastoma-derived cancer stem cells show differential growth characteristics and molecular profiles.* Cancer research, 2007. 67(9): p. 4010-4015.
161. Wang, J.C. and J.E. Dick, *Cancer stem cells: lessons from leukemia.* Trends in cell biology, 2005. 15(9): p. 494-501.
162. Hope, K.J., L. Jin, and J.E. Dick, *Acute myeloid leukemia originates from a hierarchy of leukemic stem cell classes that differ in self-renewal capacity.* Nature immunology, 2004. 5(7): p. 738-743.
163. Collins, A.T. and N.J. Maitland, *Prostate cancer stem cells.* European journal of cancer, 2006. 42(9): p. 1213-1218.
164. Lee, C.J., J. Dosch, and D.M. Simeone, *Pancreatic cancer stem cells.* Journal of clinical oncology, 2008. 26(17): p. 2806-2812.
165. La Porta, C., *Cancer stem cells: lessons from melanoma.* Stem Cell Reviews and Reports, 2009. 5(1): p. 61-65.
166. Chinn, S.B., et al., *Cancer stem cells: mediators of tumorigenesis and metastasis in head and neck squamous cell carcinoma.* Head & neck, 2015. 37(3): p. 317-326.

167. Veselska, R., J. Skoda, and J. Neradil, *Detection of cancer stem cell markers in sarcomas.* Klin Onkol, 2012. 25 Suppl 2: p. 2s16-20.
168. Ortiz-Sánchez, E., et al., *Characterization of cervical cancer stem cell-like cells: phenotyping, stemness, and human papilloma virus co-receptor expression.* Oncotarget, 2016. 7(22): p. 31943.
169. Ming, X.-Y., et al., *Integrin α7 is a functional cancer stem cell surface marker in oesophageal squamous cell carcinoma.* Nature communications, 2016. 7(1): p. 1-14.
170. Peired, A.J., A. Sisti, and P. Romagnani, *Renal cancer stem cells: characterization and targeted therapies.* Stem cells international, 2016. 2016.
171. MacDonagh, L., et al., *Lung cancer stem cells: The root of resistance.* Cancer Lett, 2016. 372(2): p. 147-56.
172. Fan, F., et al., *The requirement for freshly isolated human colorectal cancer (CRC) cells in isolating CRC stem cells.* British journal of cancer, 2015. 112(3): p. 539-546.
173. Yang, Z.F., et al., *Significance of CD90+ cancer stem cells in human liver cancer.* Cancer cell, 2008. 13(2): p. 153-166.
174. Kimura, O., et al., *Characterization of the epithelial cell adhesion molecule (EpCAM)+ cell population in hepatocellular carcinoma cell lines.* Cancer science, 2010. 101(10): p. 2145-2155.
175. Al Faraj, A., et al., *Specific targeting and noninvasive imaging of breast cancer stem cells using single-walled carbon nanotubes as novel multimodality nanoprobes.* Nanomedicine (Lond), 2016. 11(1): p. 31-46.
176. Miyoshi, N., et al., *Cancer stem cells in relation to treatment.* Jpn J Clin Oncol, 2019. 49(3): p. 232-237.
177. Toh, T.B., J.J. Lim, and E.K. Chow, *Epigenetics in cancer stem cells.* Mol Cancer, 2017. 16(1): p. 29.
178. Ioannou, M., et al., *ALDH1B1 is a potential stem/progenitor marker for multiple pancreas progenitor pools.* Dev Biol, 2013. 374(1): p. 153-63.
179. Vassalli, G., *Aldehyde dehydrogenases: not just markers, but functional regulators of stem cells.* Stem cells international, 2019. 2019.
180. Vogler, T., et al., *The expression pattern of aldehyde dehydrogenase 1 (ALDH1) is an independent prognostic marker for low survival in colorectal tumors.* Experimental and molecular pathology, 2012. 92(1): p. 111-117.

181. van den Hoogen, C., et al., *High aldehyde dehydrogenase activity identifies tumor-initiating and metastasis-initiating cells in human prostate cancer.* Cancer research, 2010. 70(12): p. 5163-5173.
182. Ueda, K., et al., *Aldehyde dehydrogenase 1 identifies cells with cancer stem cell-like properties in a human renal cell carcinoma cell line.* PloS one, 2013. 8(10).
183. Ginestier, C., et al., *ALDH1 is a marker of normal and malignant human mammary stem cells and a predictor of poor clinical outcome.* Cell stem cell, 2007. 1(5): p. 555-567.
184. Tanei, T., et al., *Association of breast cancer stem cells identified by aldehyde dehydrogenase 1 expression with resistance to sequential Paclitaxel and epirubicin-based chemotherapy for breast cancers.* Clinical cancer research, 2009. 15(12): p. 4234-4241.
185. Yip, N., et al., *Disulfiram modulated ROS–MAPK and NFκB pathways and targeted breast cancer cells with cancer stem cell-like properties.* British journal of cancer, 2011. 104(10): p. 1564-1574.
186. Locher, K.P., *Mechanistic diversity in ATP-binding cassette (ABC) transporters.* Nat Struct Mol Biol, 2016. 23(6): p. 487-93.
187. Paredes Lario, A., et al., *[Expression of proteins associated with multidrug resistance and resistance to chemotherapy in lung cancer].* Arch Bronconeumol, 2007. 43(9): p. 479-84.
188. Wright, M.H., et al., *Brca1 breast tumors contain distinct CD44+/CD24- and CD133+ cells with cancer stem cell characteristics.* Breast Cancer Res, 2008. 10(1): p. R10.
189. Marcelletti, J.F., et al., *Leukemic blast and natural killer cell P-glycoprotein function and inhibition in a clinical trial of zosuquidar infusion in acute myeloid leukemia.* Leuk Res, 2009. 33(6): p. 769-74.
190. Tang, R., et al., *Zosuquidar restores drug sensitivity in P-glycoprotein expressing acute myeloid leukemia (AML).* BMC Cancer, 2008. 8: p. 51.
191. Dzobo, K., V.D. Leaner, and M.I. Parker, *Feedback regulation of the alpha2(1) collagen gene via the Mek-Erk signaling pathway.* IUBMB Life, 2012. 64(1): p. 87-98.
192. Dzobo, K., V.D. Leaner, and M.I. Parker, *Absence of feedback regulation in the synthesis of COL1A1.* Life Sci, 2014. 103(1): p. 25-33.

193. Stupack, D.G. and D.A. Cheresh, *ECM remodeling regulates angiogenesis: endothelial integrins look for new ligands.* Science's STKE, 2002. 2002(119): p. pe7-pe7.
194. Larsen, M., et al., *The matrix reorganized: extracellular matrix remodeling and integrin signaling.* Current opinion in cell biology, 2006. 18(5): p. 463-471.
195. Lu, P., et al., *Extracellular matrix degradation and remodeling in development and disease.* Cold Spring Harbor perspectives in biology, 2011. 3(12): p. a005058.
196. DeSimone, D.W. and R.P. Mecham, *Extracellular matrix in development*. 2013: Springer.
197. Timpl, R. and J.C. Brown, *Supramolecular assembly of basement membranes.* Bioessays, 1996. 18(2): p. 123-32.
198. Banerjee, S., et al., *Multiple roles for basement membrane proteins in cancer progression and EMT.* European Journal of Cell Biology, 2022. 101(2): p. 151220.
199. Yurchenco, P.D., *Basement membranes: cell scaffoldings and signaling platforms.* Cold Spring Harb Perspect Biol, 2011. 3(2).
200. Stetler-Stevenson, W.G., S. Aznavoorian, and L.A. Liotta, *Tumor cell interactions with the extracellular matrix during invasion and metastasis.* Annual review of cell biology, 1993. 9(1): p. 541-573.
201. Mann, B.K., R.H. Schmedlen, and J.L. West, *Tethered-TGF-β increases extracellular matrix production of vascular smooth muscle cells.* Biomaterials, 2001. 22(5): p. 439-444.
202. Ruoslahti, E. and E. Koivunen, *Integrin-binding peptides*. 1999, Google Patents.
203. Jabłońska-Trypuć, A., M. Matejczyk, and S. Rosochacki, *Matrix metalloproteinases (MMPs), the main extracellular matrix (ECM) enzymes in collagen degradation, as a target for anticancer drugs.* Journal of enzyme inhibition and medicinal chemistry, 2016. 31(sup1): p. 177-183.
204. Katz, B.-Z., et al., *Physical state of the extracellular matrix regulates the structure and molecular composition of cell-matrix adhesions.* Molecular biology of the cell, 2000. 11(3): p. 1047-1060.

205. Fukuda, K., et al., *Inhibition of matrix metalloproteinase-3 synthesis in human conjunctival fibroblasts by interleukin-4 or interleukin-13.* Investigative ophthalmology & visual science, 2006. 47(7): p. 2857-2864.
206. Nelson, C.M. and M.J. Bissell, *Of extracellular matrix, scaffolds, and signaling: tissue architecture regulates development, homeostasis, and cancer.* Annu. Rev. Cell Dev. Biol., 2006. 22: p. 287-309.
207. Beacham, D.A. and E. Cukierman, *Stromagenesis: the changing face of fibroblastic microenvironments during tumor progression.* Semin Cancer Biol, 2005. 15(5): p. 329-41.
208. Wozniak, M.A., et al., *Focal adhesion regulation of cell behavior.* Biochim Biophys Acta, 2004. 1692(2-3): p. 103-19.
209. Chung, A.S. and W.J. Kao, *Fibroblasts regulate monocyte response to ECM-derived matrix: The effects on monocyte adhesion and the production of inflammatory, matrix remodeling, and growth factor proteins.* Journal of Biomedical Materials Research Part A: An Official Journal of The Society for Biomaterials, The Japanese Society for Biomaterials, and The Australian Society for Biomaterials and the Korean Society for Biomaterials, 2009. 89(4): p. 841-853.
210. Stegemann, J.P., H. Hong, and R.M. Nerem, *Mechanical, biochemical, and extracellular matrix effects on vascular smooth muscle cell phenotype.* Journal of applied physiology, 2005. 98(6): p. 2321-2327.
211. Khatiwala, C.B., et al., *ECM compliance regulates osteogenesis by influencing MAPK signaling downstream of RhoA and ROCK.* Journal of bone and mineral research, 2009. 24(5): p. 886-898.
212. Ulrich, T.A., E.M. de Juan Pardo, and S. Kumar, *The mechanical rigidity of the extracellular matrix regulates the structure, motility, and proliferation of glioma cells.* Cancer research, 2009. 69(10): p. 4167-4174.
213. Lu, P., V.M. Weaver, and Z. Werb, *The extracellular matrix: a dynamic niche in cancer progression.* J Cell Biol, 2012. 196(4): p. 395-406.
214. Page-McCaw, A., A.J. Ewald, and Z. Werb, *Matrix metalloproteinases and the regulation of tissue remodelling.* Nat Rev Mol Cell Biol, 2007. 8(3): p. 221-33.
215. Cox, T.R. and J.T. Erler, *Remodeling and homeostasis of the extracellular matrix: implications for fibrotic diseases and cancer.* Dis Model Mech, 2011. 4(2): p. 165-78.

216. Kass, L., et al., *Mammary epithelial cell: influence of extracellular matrix composition and organization during development and tumorigenesis.* Int J Biochem Cell Biol, 2007. 39(11): p. 1987-94.
217. Pece, S., et al., *Biological and molecular heterogeneity of breast cancers correlates with their cancer stem cell content.* Cell, 2010. 140(1): p. 62-73.
218. Holle, A.W., J.L. Young, and J.P. Spatz, *In vitro cancer cell-ECM interactions inform in vivo cancer treatment.* Adv Drug Deliv Rev, 2016. 97: p. 270-9.
219. Morin, P.J., *Drug resistance and the microenvironment: nature and nurture.* Drug Resist Updat, 2003. 6(4): p. 169-72.
220. Grantab, R., S. Sivananthan, and I.F. Tannock, *The penetration of anticancer drugs through tumor tissue as a function of cellular adhesion and packing density of tumor cells.* Cancer Res, 2006. 66(2): p. 1033-9.
221. Levental, K.R., et al., *Matrix crosslinking forces tumor progression by enhancing integrin signaling.* Cell, 2009. 139(5): p. 891-906.
222. Campbell, N.E., et al., *Extracellular Matrix Proteins and Tumor Angiogenesis.* Journal of Oncology, 2010. 2010: p. 586905.
223. Cox, T.R., *The matrix in cancer.* Nat Rev Cancer, 2021. 21(4): p. 217-238.
224. Rohwer, N. and T. Cramer, *Hypoxia-mediated drug resistance: novel insights on the functional interaction of HIFs and cell death pathways.* Drug Resist Updat, 2011. 14(3): p. 191-201.
225. Lv, Y., et al., *Hypoxia-inducible factor-1α induces multidrug resistance protein in colon cancer.* Onco Targets Ther, 2015. 8: p. 1941-8.
226. Vincent, T. and N. Mechti, *Extracellular matrix in bone marrow can mediate drug resistance in myeloma.* Leukemia & lymphoma, 2005. 46(6): p. 803-811.
227. Kouniavsky, G., et al., *Stromal extracellular matrix reduces chemotherapy-induced apoptosis in colon cancer cell lines.* Clin Exp Metastasis, 2002. 19(1): p. 55-60.
228. Sherman-Baust, C.A., et al., *Remodeling of the extracellular matrix through overexpression of collagen VI contributes to cisplatin resistance in ovarian cancer cells.* Cancer Cell, 2003. 3(4): p. 377-86.
229. Dzobo, K., et al., *Wharton's Jelly-Derived Mesenchymal Stromal Cells and Fibroblast-Derived Extracellular Matrix Synergistically Activate Apoptosis in a p21-Dependent Mechanism in WHCO1 and MDA MB 231 Cancer Cells In Vitro.* Stem Cells Int, 2016. 2016: p. 4842134.

230. Rijal, G. and W. Li, *Native-mimicking in vitro microenvironment: an elusive and seductive future for tumor modeling and tissue engineering.* Journal of biological engineering, 2018. 12: p. 20-20.
231. Kutys, M.L., A.D. Doyle, and K.M. Yamada, *Regulation of cell adhesion and migration by cell-derived matrices.* Experimental Cell Research, 2013. 319(16): p. 2434-2439.
232. Hoshiba, T. and M. Tanaka, *Optimization of the tissue source, malignancy, and initial substrate of tumor cell-derived matrices to increase cancer cell chemoresistance against 5-fluorouracil.* Biochemical and Biophysical Research Communications, 2015. 457(3): p. 353-357.
233. Zanoni, M., et al., *3D tumor spheroid models for in vitro therapeutic screening: a systematic approach to enhance the biological relevance of data obtained.* Sci Rep, 2016. 6: p. 19103.
234. Minchinton, A.I. and I.F. Tannock, *Drug penetration in solid tumours.* Nat Rev Cancer, 2006. 6(8): p. 583-92.
235. Saias, L., et al., *Cell-Cell Adhesion and Cytoskeleton Tension Oppose Each Other in Regulating Tumor Cell Aggregation.* Cancer Res, 2015. 75(12): p. 2426-33.
236. Nath, S. and G.R. Devi, *Three-dimensional culture systems in cancer research: Focus on tumor spheroid model.* Pharmacology & Therapeutics, 2016. 163: p. 94-108.
237. Lazzari, G., P. Couvreur, and S. Mura, *Multicellular tumor spheroids: a relevant 3D model for the in vitro preclinical investigation of polymer nanomedicines.* Polymer Chemistry, 2017. 8(34): p. 4947-4969.
238. Costa, E.C., et al., *3D tumor spheroids: an overview on the tools and techniques used for their analysis.* Biotechnol Adv, 2016. 34(8): p. 1427-1441.
239. Phung, Y.T., et al., *Rapid generation of in vitro multicellular spheroids for the study of monoclonal antibody therapy.* J Cancer, 2011. 2: p. 507-14.
240. LaBarbera, D.V., B.G. Reid, and B.H. Yoo, *The multicellular tumor spheroid model for high-throughput cancer drug discovery.* Expert opinion on drug discovery, 2012. 7(9): p. 819-830.
241. Ghosh, S., et al., *Three-dimensional culture of melanoma cells profoundly affects gene expression profile: a high density oligonucleotide array study.* J Cell Physiol, 2005. 204(2): p. 522-31.

242. Pickl, M. and C.H. Ries, *Comparison of 3D and 2D tumor models reveals enhanced HER2 activation in 3D associated with an increased response to trastuzumab.* Oncogene, 2009. 28(3): p. 461-468.
243. Lazzari, G., et al., *Multicellular spheroid based on a triple co-culture: A novel 3D model to mimic pancreatic tumor complexity.* Acta Biomaterialia, 2018. 78: p. 296-307.
244. Kuen, J., et al., *Pancreatic cancer cell/fibroblast co-culture induces M2 like macrophages that influence therapeutic response in a 3D model.* PLoS One, 2017. 12(7): p. e0182039.
245. Cui, X., Y. Hartanto, and H. Zhang, *Advances in multicellular spheroids formation.* Journal of The Royal Society Interface, 2017. 14(127): p. 20160877.
246. Lu, H. and M.H. Stenzel, *Multicellular Tumor Spheroids (MCTS) as a 3D In Vitro Evaluation Tool of Nanoparticles.* Small, 2018. 14(13): p. e1702858.
247. Friedrich, J., et al., *Spheroid-based drug screen: considerations and practical approach.* Nat Protoc, 2009. 4(3): p. 309-24.
248. Lin, R.Z. and H.Y. Chang, *Recent advances in three-dimensional multicellular spheroid culture for biomedical research.* Biotechnol J, 2008. 3(9-10): p. 1172-84.
249. Dzobo, K., et al., *Three-Dimensional Organoids in Cancer Research: The Search for the Holy Grail of Preclinical Cancer Modeling.* Omics, 2018. 22(12): p. 733-748.
250. Sato, T., et al., *Single Lgr5 stem cells build crypt-villus structures in vitro without a mesenchymal niche.* Nature, 2009. 459(7244): p. 262-5.
251. Chen, Y.W., et al., *A three-dimensional model of human lung development and disease from pluripotent stem cells.* Nat Cell Biol, 2017. 19(5): p. 542-549.
252. Fatehullah, A., S.H. Tan, and N. Barker, *Organoids as an in vitro model of human development and disease.* Nat Cell Biol, 2016. 18(3): p. 246-54.
253. Fan, H., U. Demirci, and P. Chen, *Emerging organoid models: leaping forward in cancer research.* Journal of Hematology & Oncology, 2019. 12(1): p. 142.
254. Fumagalli, A., et al., *Genetic dissection of colorectal cancer progression by orthotopic transplantation of engineered cancer organoids.* Proc Natl Acad Sci U S A, 2017. 114(12): p. E2357-e2364.
255. Saito, Y., et al., *Establishment of Patient-Derived Organoids and Drug Screening for Biliary Tract Carcinoma.* Cell Rep, 2019. 27(4): p. 1265-1276.e4.

256. Fang, Y. and R. Eglen, *Three-Dimensional Cell Cultures in Drug Discovery and Development.* SLAS DISCOVERY: Advancing Life Sciences R&D, 2017. 22: p. 456-472.
257. Baghban, R., et al., *Tumor microenvironment complexity and therapeutic implications at a glance.* Cell Communication and Signaling, 2020. 18(1): p. 59.
258. Dvorak, H.F., *Tumors: wounds that do not heal. Similarities between tumor stroma generation and wound healing.* N Engl J Med, 1986. 315(26): p. 1650-9.
259. De Wever, O., et al., *Stromal myofibroblasts are drivers of invasive cancer growth.* Int J Cancer, 2008. 123(10): p. 2229-38.
260. Tomasek, J.J., et al., *Myofibroblasts and mechano-regulation of connective tissue remodelling.* Nat Rev Mol Cell Biol, 2002. 3(5): p. 349-63.
261. Li, H., X. Fan, and J. Houghton, *Tumor microenvironment: the role of the tumor stroma in cancer.* J Cell Biochem, 2007. 101(4): p. 805-15.
262. Dzobo, K. and C. Dandara, *Broadening Drug Design and Targets to Tumor Microenvironment? Cancer-Associated Fibroblast Marker Expression in Cancers and Relevance for Survival Outcomes.* Omics, 2020. 24(6): p. 340-351.
263. Jena, B.C., et al., *Cancer associated fibroblast mediated chemoresistance: A paradigm shift in understanding the mechanism of tumor progression.* Biochimica et Biophysica Acta (BBA) - Reviews on Cancer, 2020. 1874(2): p. 188416.
264. Giorello, M.B., et al., *Cancer-Associated Fibroblasts in the Breast Tumor Microenvironment.* Journal of Mammary Gland Biology and Neoplasia, 2021. 26(2): p. 135-155.
265. Hill, B.S., et al., *Tumor-educated mesenchymal stem cells promote pro-metastatic phenotype.* Oncotarget, 2017. 8(42): p. 73296-73311.
266. Jung, Y., et al., *Recruitment of mesenchymal stem cells into prostate tumours promotes metastasis.* Nature communications, 2013. 4: p. 1795-1795.
267. Zhou, G.-S., et al., *5-Azacytidine facilitates osteogenic gene expression and differentiation of mesenchymal stem cells by alteration in DNA methylation.* Cytotechnology, 2009. 60(1-3): p. 11-11.
268. Massagué, J., J. Seoane, and D. Wotton, *Smad transcription factors.* Genes & development, 2005. 19(23): p. 2783-2810.

269. Schmidt-Hansen, B., et al., *Functional significance of metastasis-inducing S100A4 (Mts1) in tumor-stroma interplay.* Journal of Biological Chemistry, 2004. 279(23): p. 24498-24504.
270. Schmidt-Hansen, B., et al., *Extracellular S100A4(mts1) stimulates invasive growth of mouse endothelial cells and modulates MMP-13 matrix metalloproteinase activity.* Oncogene, 2004. 23(32): p. 5487-5495.
271. Lee, H.W., et al., *Alpha-smooth muscle actin (ACTA2) is required for metastatic potential of human lung adenocarcinoma.* Clin Cancer Res, 2013. 19(21): p. 5879-89.
272. Jia, J., et al., *FAP-α (Fibroblast activation protein-α) is involved in the control of human breast cancer cell line growth and motility via the FAK pathway.* BMC Cell Biology, 2014. 15(1): p. 16.
273. Numakura, S., et al., *Mesenchymal Stem Cell Marker Expression in Gastric Cancer Stroma.* Anticancer Res, 2019. 39(1): p. 387-393.
274. Bierie, B. and H.L. Moses, *Tumour microenvironment: TGFbeta: the molecular Jekyll and Hyde of cancer.* Nat Rev Cancer, 2006. 6(7): p. 506-20.
275. Tan, H.-X., et al., *TGFβ1 is essential for MSCs-CAFs differentiation and promotes HCT116 cells migration and invasion via JAK/STAT3 signaling.* OncoTargets and therapy, 2019. 12: p. 5323-5334.
276. Yu, Y., et al., *Cancer-associated fibroblasts induce epithelial–mesenchymal transition of breast cancer cells through paracrine TGF-β signalling.* British journal of cancer, 2014. 110(3): p. 724-732.
277. Paunescu, V., et al., *Tumour-associated fibroblasts and mesenchymal stem cells: more similarities than differences.* Journal of cellular and molecular medicine, 2011. 15(3): p. 635-646.
278. Isella, C., et al., *Stromal contribution to the colorectal cancer transcriptome.* Nat Genet, 2015. 47(4): p. 312-9.
279. Gottesman, M.M., T. Fojo, and S.E. Bates, *Multidrug resistance in cancer: role of ATP-dependent transporters.* Nat Rev Cancer, 2002. 2(1): p. 48-58.
280. Wei, L., et al., *Cancer-associated fibroblasts-mediated ATF4 expression promotes malignancy and gemcitabine resistance in pancreatic cancer via the TGF-β1/SMAD2/3 pathway and ABCC1 transactivation.* Cell Death & Disease, 2021. 12(4): p. 334.

281. Zhai, J., et al., *Cancer-associated fibroblasts-derived IL-8 mediates resistance to cisplatin in human gastric cancer.* Cancer Letters, 2019. 454: p. 37-43.
282. Yu, D.M., et al., *The dipeptidyl peptidase IV family in cancer and cell biology.* Febs j, 2010. 277(5): p. 1126-44.
283. Sato, T., et al., *DPP8 is a novel therapeutic target for multiple myeloma.* Scientific Reports, 2019. 9(1): p. 18094.
284. Nie, M.-J., et al., *Clinical and prognostic significance of MYH11 in lung cancer.* Oncology letters, 2020. 19(6): p. 3899-3906.
285. Zhao, B., et al., *Identification of Potential Key Genes and Pathways in Early-Onset Colorectal Cancer Through Bioinformatics Analysis.* Cancer control : journal of the Moffitt Cancer Center, 2019. 26(1): p. 1073274819831260-1073274819831260.
286. Liu, Y., et al., *CALD1, CNN1, and TAGLN identified as potential prognostic molecular markers of bladder cancer by bioinformatics analysis.* Medicine, 2019. 98(2): p. e13847-e13847.
287. Mishra, P.J., et al., *Carcinoma-associated fibroblast-like differentiation of human mesenchymal stem cells.* Cancer research, 2008. 68(11): p. 4331-4339.
288. Li, Z., et al., *Nodal Facilitates Differentiation of Fibroblasts to Cancer-Associated Fibroblasts that Support Tumor Growth in Melanoma and Colorectal Cancer.* Cells, 2019. 8(6): p. 538.
289. Pan, C., et al., *Bone marrow mesenchymal stem cells in microenvironment transform into cancer-associated fibroblasts to promote the progression of B-cell acute lymphoblastic leukemia.* Biomed Pharmacother, 2020. 130: p. 110610.
290. Weiser-Evans, M.C.M., *Smooth Muscle Differentiation Control Comes Full Circle: The Circular Noncoding RNA, circActa2, Functions as a miRNA Sponge to Fine-Tune α-SMA Expression.* Circulation research, 2017. 121(6): p. 591-593.
291. Derynck, R. and Y.E. Zhang, *Smad-dependent and Smad-independent pathways in TGF-beta family signalling.* Nature, 2003. 425(6958): p. 577-84.
292. Shangguan, L., et al., *Inhibition of TGF-β/Smad Signaling by BAMBI Blocks Differentiation of Human Mesenchymal Stem Cells to Carcinoma-Associated Fibroblasts and Abolishes their Protumor Effects.* STEM CELLS, 2012. 30(12): p. 2810-2819.

293. Riaz, N., et al., *Expression of Androgen Receptor and Cancer Stem Cell Markers (CD44(+)/CD24(-) and ALDH1(+)): Prognostic Implications in Invasive Breast Cancer.* Transl Oncol, 2018. 11(4): p. 920-929.
294. Yang, Z., et al., *Identification of LETM1 as a marker of cancer stem-like cells and predictor of poor prognosis in esophageal squamous cell carcinoma.* Hum Pathol, 2018. 81: p. 148-156.
295. Dong, C., et al., *Cancer stem cell associated eight gene-based signature predicts clinical outcomes of colorectal cancer.* Oncol Lett, 2019. 17(1): p. 442-449.
296. Mohamed, H., et al., *The expression and prognostic value of stem cell markers Bmi-1, HESC5:3, and HES77 in human papillomavirus-positive and -negative oropharyngeal squamous cell carcinoma.* Tumour Biol, 2019. 41(3): p. 1010428319840473.
297. Wang, J.H., et al., *Combined prognostic value of the cancer stem cell markers CD47 and CD133 in esophageal squamous cell carcinoma.* Cancer Med, 2019. 8(3): p. 1315-1325.
298. Zhang, C., et al., *A novel 5-fluorouracil-resistant human esophageal squamous cell carcinoma cell line Eca-109/5-FU with significant drug resistance-related characteristics.* Oncol Rep, 2017. 37(5): p. 2942-2954.
299. Hamano, R., et al., *Overexpression of miR-200c induces chemoresistance in esophageal cancers mediated through activation of the Akt signaling pathway.* Clin Cancer Res, 2011. 17(9): p. 3029-38.
300. Vulsteke, C., et al., *Genetic variability in the multidrug resistance associated protein-1 (ABCC1/MRP1) predicts hematological toxicity in breast cancer patients receiving (neo-)adjuvant chemotherapy with 5-fluorouracil, epirubicin and cyclophosphamide (FEC).* Ann Oncol, 2013. 24(6): p. 1513-25.
301. Yang, H., et al., *Stemness and chemotherapeutic drug resistance induced by EIF5A2 overexpression in esophageal squamous cell carcinoma.* Oncotarget, 2015. 6(28): p. 26079-89.
302. Almanaa, T.N., M.E. Geusz, and R.J. Jamasbi, *A new method for identifying stem-like cells in esophageal cancer cell lines.* J Cancer, 2013. 4(7): p. 536-48.
303. Cabrera, M.C., R.E. Hollingsworth, and E.M. Hurt, *Cancer stem cell plasticity and tumor hierarchy.* World J Stem Cells, 2015. 7(1): p. 27-36.

304. Kise, K., Y. Kinugasa-Katayama, and N. Takakura, *Tumor microenvironment for cancer stem cells.* Adv Drug Deliv Rev, 2016. 99(Pt B): p. 197-205.
305. Bodenstine, T.M., et al., *Plasticity underlies tumor progression: role of Nodal signaling.* Cancer Metastasis Rev, 2016. 35(1): p. 21-39.
306. Cortina, C., et al., *A genome editing approach to study cancer stem cells in human tumors.* EMBO Mol Med, 2017. 9(7): p. 869-879.
307. Ishizawa, K., et al., *Tumor-initiating cells are rare in many human tumors.* Cell Stem Cell, 2010. 7(3): p. 279-82.
308. Schatton, T., et al., *Identification of cells initiating human melanomas.* Nature, 2008. 451(7176): p. 345-9.
309. Ricci-Vitiani, L., et al., *Identification and expansion of human colon-cancer-initiating cells.* Nature, 2007. 445(7123): p. 111-5.
310. Britton, K.M., et al., *Cancer stem cells and side population cells in breast cancer and metastasis.* Cancers (Basel), 2011. 3(2): p. 2106-30.
311. Boesch, M., et al., *The side population of ovarian cancer cells defines a heterogeneous compartment exhibiting stem cell characteristics.* Oncotarget, 2014. 5(16): p. 7027-39.
312. Kobayashi, T., et al., *Nucleostemin expression in invasive breast cancer.* BMC Cancer, 2014. 14: p. 215.
313. Takahashi, R.U., et al., *Cancer stem cells in breast cancer.* Cancers (Basel), 2011. 3(1): p. 1311-28.
314. Zhang, G., et al., *Esophageal cancer tumorspheres involve cancer stem-like populations with elevated aldehyde dehydrogenase enzymatic activity.* Mol Med Rep, 2012. 6(3): p. 519-24.
315. Gangavarapu, K.J., et al., *Aldehyde dehydrogenase and ATP binding cassette transporter G2 (ABCG2) functional assays isolate different populations of prostate stem cells where ABCG2 function selects for cells with increased stem cell activity.* Stem Cell Res Ther, 2013. 4(5): p. 132.
316. Richard, V., et al., *Side population cells as prototype of chemoresistant, tumor-initiating cells.* Biomed Res Int, 2013. 2013: p. 517237.
317. Haraguchi, N., et al., *Cancer stem cells in human gastrointestinal cancers.* Hum Cell, 2006. 19(1): p. 24-9.
318. Haraguchi, N., et al., *Characterization of a side population of cancer cells from human gastrointestinal system.* Stem Cells, 2006. 24(3): p. 506-13.

319. Senthebane, D.A., et al., *The Role of Tumor Microenvironment in Chemoresistance: 3D Extracellular Matrices as Accomplices.* Int J Mol Sci, 2018. 19(10).
320. Wang, C., et al., *Evaluation of CD44 and CD133 as cancer stem cell markers for colorectal cancer.* Oncol Rep, 2012. 28(4): p. 1301-8.
321. Torres, C.M., et al., *The linker histone H1.0 generates epigenetic and functional intratumor heterogeneity.* Science, 2016. 353(6307).
322. Fillmore, C.M. and C. Kuperwasser, *Human breast cancer cell lines contain stem-like cells that self-renew, give rise to phenotypically diverse progeny and survive chemotherapy.* Breast Cancer Research, 2008. 10(2): p. R25.
323. Neering, S.J., et al., *Leukemia stem cells in a genetically defined murine model of blast-crisis CML.* Blood, 2007. 110(7): p. 2578-85.
324. Li, F., et al., *Beyond tumorigenesis: cancer stem cells in metastasis.* Cell research, 2007. 17(1): p. 3-14.
325. Chan, D., et al., *Expression of Insulin-Like Growth Factor Binding Protein-5 (IGFBP5) Reverses Cisplatin-Resistance in Esophageal Carcinoma.* Cells, 2018. 7(10).
326. Dzobo, K., *Epigenomics-Guided Drug Development: Recent Advances in Solving the Cancer Treatment "jigsaw puzzle".* Omics, 2019. 23(2): p. 70-85.
327. Curtarelli, R.B., et al., *Expression of Cancer Stem Cell Biomarkers in Human Head and Neck Carcinomas: a Systematic Review.* Stem Cell Rev, 2018. 14(6): p. 769-784.
328. Ginestier, C., et al., *ALDH1 is a marker of normal and malignant human mammary stem cells and a predictor of poor clinical outcome.* Cell Stem Cell, 2007. 1(5): p. 555-67.
329. Leinung, M., et al., *Expression of ALDH1A1 and CD44 in primary head and neck squamous cell carcinoma and their value for carcinogenesis, tumor progression and cancer stem cell identification.* Oncology letters, 2015. 10(4): p. 2289-2294.
330. Sillanpää, S., et al., *CD44 Expression Indicates Favorable Prognosis in Epithelial Ovarian Cancer.* Clinical Cancer Research, 2003. 9(14): p. 5318-5324.
331. Zhou, J., et al., *CD44 Expression Predicts Prognosis of Ovarian Cancer Patients Through Promoting Epithelial-Mesenchymal Transition (EMT) by*

Regulating Snail, ZEB1, and Caveolin-1. Frontiers in oncology, 2019. 9: p. 802-802.

332. Niess, H., et al., *Side population cells of pancreatic cancer show characteristics of cancer stem cells responsible for resistance and metastasis.* Target Oncol, 2015. 10(2): p. 215-27.
333. Wang, C., et al., *Evaluation of CD44 and CD133 as cancer stem cell markers for colorectal cancer.* Oncology reports, 2012. 28(4): p. 1301-1308.
334. Lee, C.H., et al., *Tumorsphere as an effective in vitro platform for screening anti-cancer stem cell drugs.* Oncotarget, 2016. 7(2): p. 1215-26.
335. Du, L., et al., *CD44 is of Functional Importance for Colorectal Cancer Stem Cells.* Clinical Cancer Research, 2008. 14(21): p. 6751-6760.
336. Kim, R.J. and J.S. Nam, *OCT4 Expression Enhances Features of Cancer Stem Cells in a Mouse Model of Breast Cancer.* Lab Anim Res, 2011. 27(2): p. 147-52.
337. Hao, J.L., et al., *CD147/EMMPRIN and CD44 are potential therapeutic targets for metastatic prostate cancer.* Curr Cancer Drug Targets, 2010. 10(3): p. 287-306.
338. Madjd, Z., et al., *CD44+ cancer cells express higher levels of the anti-apoptotic protein Bcl-2 in breast tumours.* Cancer Immun, 2009. 9: p. 4.
339. Januchowski, R., et al., *Inhibition of ALDH1A1 activity decreases expression of drug transporters and reduces chemotherapy resistance in ovarian cancer cell lines.* Int J Biochem Cell Biol, 2016. 78: p. 248-259.
340. Shiozawa, Y., et al., *Cancer stem cells and their role in metastasis.* Pharmacology & therapeutics, 2013. 138(2): p. 285-293.
341. Jolly, M.K., et al., *EMT and MET: necessary or permissive for metastasis?* Mol Oncol, 2017. 11(7): p. 755-769.
342. Vincent, C.T. and J. Fuxe, *EMT, inflammation and metastasis.* Semin Cancer Biol, 2017. 47: p. 168-169.
343. Pramanik, K.K., et al., *Glycogen synthase kinase-3beta mediated regulation of matrix metalloproteinase-9 and its involvement in oral squamous cell carcinoma progression and invasion.* Cell Oncol (Dordr), 2018. 41(1): p. 47-60.
344. Stamenkovic, I. and Q. Yu, *Merlin, a "magic" linker between extracellular cues and intracellular signaling pathways that regulate cell motility, proliferation, and survival.* Curr Protein Pept Sci, 2010. 11(6): p. 471-84.

345. Gomez-Cuadrado, L., et al., *Mouse models of metastasis: progress and prospects.* Dis Model Mech, 2017. 10(9): p. 1061-1074.
346. Lambert, A.W., D.R. Pattabiraman, and R.A. Weinberg, *Emerging Biological Principles of Metastasis.* Cell, 2017. 168(4): p. 670-691.
347. Asati, V., D.K. Mahapatra, and S.K. Bharti, *PI3K/Akt/mTOR and Ras/Raf/MEK/ERK signaling pathways inhibitors as anticancer agents: Structural and pharmacological perspectives.* Eur J Med Chem, 2016. 109: p. 314-41.
348. Martinelli, E., et al., *Cancer resistance to therapies against the EGFR-RAS-RAF pathway: The role of MEK.* Cancer Treat Rev, 2017. 53: p. 61-69.
349. House, C.D., et al., *NFkappaB Promotes Ovarian Tumorigenesis via Classical Pathways That Support Proliferative Cancer Cells and Alternative Pathways That Support ALDH(+) Cancer Stem-like Cells.* Cancer Res, 2017. 77(24): p. 6927-6940.
350. Tu, C.C. and P.K. Hsu, *The frontline of esophageal cancer treatment: questions to be asked and answered.* Ann Transl Med, 2018. 6(4): p. 83.
351. Wang, X., et al., *Stem cell autocrine CXCL12/CXCR4 stimulates invasion and metastasis of esophageal cancer.* Oncotarget, 2017. 8(22): p. 36149-36160.
352. Cremolini, C., et al., *Negative hyper-selection of metastatic colorectal cancer patients for anti-EGFR monoclonal antibodies: the PRESSING case-control study.* Ann Oncol, 2017. 28(12): p. 3009-3014.
353. Lambert, J.M. and C.Q. Morris, *Antibody-Drug Conjugates (ADCs) for Personalized Treatment of Solid Tumors: A Review.* Adv Ther, 2017. 34(5): p. 1015-1035.
354. Purow, B. and K. Staveley-O'Carroll, *Targeting of vaccinia virus using biotin-avidin viral coating and biotinylated antibodies.* J Surg Res, 2005. 123(1): p. 49-54.
355. Wang, M., Y. Wang, and J. Zhong, *Side population cells and drug resistance in breast cancer.* Mol Med Rep, 2015. 11(6): p. 4297-302.
356. Jiang, X.D., et al., *[Expression of Oct4 and Sox2 and their clinical significance in tongue squamous cell carcinoma].* Zhonghua Kou Qiang Yi Xue Za Zhi, 2017. 52(1): p. 27-33.

357. Li, L., et al., *Expression of seven stem-cell-associated markers in human airway biopsy specimens obtained via fiberoptic bronchoscopy.* J Exp Clin Cancer Res, 2013. 32: p. 28.
358. Luo, Z.W., et al., *Increased expression of Ki-67 is a poor prognostic marker for colorectal cancer patients: a meta analysis.* BMC Cancer, 2019. 19(1): p. 123.
359. Jurikova, M., et al., *Ki67, PCNA, and MCM proteins: Markers of proliferation in the diagnosis of breast cancer.* Acta Histochem, 2016. 118(5): p. 544-52.
360. Ali, H.R., et al., *Cancer stem cell markers in breast cancer: pathological, clinical and prognostic significance.* Breast Cancer Research, 2011. 13(6): p. R118.
361. Okamoto, K., et al., *Expression status of CD44 and CD133 as a prognostic marker in esophageal squamous cell carcinoma treated with neoadjuvant chemotherapy followed by radical esophagectomy.* Oncol Rep, 2016. 36(6): p. 3333-3342.
362. Lu, L., et al., *Clinicopathological and prognostic significance of cancer stem cell markers CD44 and CD133 in patients with gastric cancer: A comprehensive meta-analysis with 4729 patients involved.* Medicine (Baltimore), 2016. 95(42): p. e5163.
363. Birkedal-Hansen, H., *Proteolytic remodeling of extracellular matrix.* Current opinion in cell biology, 1995. 7(5): p. 728-735.
364. Reddi, A. and K.A. Piez, *Extracellular matrix biochemistry*. 1984: Elsevier New York.
365. Hay, E.D., *Cell biology of extracellular matrix*. 2013: Springer Science & Business Media.
366. Fong, E.L., et al., *Heralding a new paradigm in 3D tumor modeling.* Biomaterials, 2016. 108: p. 197-213.
367. Pomo, J.M., R.M. Taylor, and R.R. Gullapalli, *Influence of TP53 and CDH1 genes in hepatocellular cancer spheroid formation and culture: a model system to understand cancer cell growth mechanics.* Cancer Cell Int, 2016. 16: p. 44.
368. Skardal, A., et al., *A reductionist metastasis-on-a-chip platform for in vitro tumor progression modeling and drug screening.* Biotechnol Bioeng, 2016. 113(9): p. 2020-32.
369. Holliday, D.L., *A three-dimensional in vitro model of breast cancer: Toward replacing the need for animal experiments.* Altern Lab Anim, 2010. 38 Suppl 1: p. 41-4.

370. Priwitaningrum, D.L., et al., *Tumor stroma-containing 3D spheroid arrays: A tool to study nanoparticle penetration.* J Control Release, 2016.
371. Pavlov, K. and C.C. Maley, *New models of neoplastic progression in Barrett's oesophagus.* Biochem Soc Trans, 2010. 38(2): p. 331-6.
372. Tan, P.H., et al., *Three-dimensional porous silk tumor constructs in the approximation of in vivo osteosarcoma physiology.* Biomaterials, 2011. 32(26): p. 6131-7.
373. Hoshiba, T. and M. Tanaka, *Decellularized matrices as in vitro models of extracellular matrix in tumor tissues at different malignant levels: Mechanism of 5-fluorouracil resistance in colorectal tumor cells.* Biochim Biophys Acta, 2016. 1863(11): p. 2749-2757.
374. Sholoqu, N., et al., *Recreating complex pathophysiologies in vitro with extracellular matrix surrogates for anticancer therapeutics screening.* Drug Discov Today, 2016. 21(9): p. 1521-31.
375. Aguado, B.A., et al., *Extracellular matrix mediators of metastatic cell colonization characterized using scaffold mimics of the pre-metastatic niche.* Acta Biomater, 2016. 33: p. 13-24.
376. Frantz, C., K.M. Stewart, and V.M. Weaver, *The extracellular matrix at a glance.* Journal of cell science, 2010. 123(24): p. 4195-4200.
377. Bachman, H., et al., *Utilizing Fibronectin Integrin-Binding Specificity to Control Cellular Responses.* Adv Wound Care (New Rochelle), 2015. 4(8): p. 501-511.
378. Belair, D.G., N.N. Le, and W.L. Murphy, *Design of growth factor sequestering biomaterials.* Chem Commun (Camb), 2014. 50(99): p. 15651-68.
379. Kim, S.H., et al., *Human lung cancer-associated fibroblasts enhance motility of non-small cell lung cancer cells in co-culture.* Anticancer Res, 2013. 33(5): p. 2001-9.
380. Uchinaka, A., et al., *Laminin alpha2-secreting fibroblasts enhance the therapeutic effect of skeletal myoblast sheets.* Eur J Cardiothorac Surg, 2016.
381. Catteau, X., et al., *Expression of the glucocorticoid receptor in breast cancer-associated fibroblasts.* Mol Clin Oncol, 2016. 5(4): p. 372-376.
382. Zhou, L., et al., *Targeted deactivation of cancer-associated fibroblasts by beta-catenin ablation suppresses melanoma growth.* Tumour Biol, 2016.

383. Akrish, S.J., et al., *Cancer associated fibroblasts are an infrequent finding in the microenvironment of proliferative verrucous leukoplakia associated squamous cell carcinoma.* J Oral Pathol Med, 2016.
384. Domogauer, J.D., S.M. de Toledo, and E.I. Azzam, *A Mimic of the Tumor Microenvironment: A Simple Method for Generating Enriched Cell Populations and Investigating Intercellular Communication.* J Vis Exp, 2016(115).
385. Chi, J., et al., *Clinical significance and prognostic value of TRIM24 expression in esophageal squamous cell carcinoma.* Aging (Albany NY), 2016. 8(9): p. 2204-2221.
386. Liu, S., et al., *Clinical and Biological Prognostic Factors for Locoregional Recurrence in Patients With Thoracic Esophageal Squamous Cell Carcinoma Treated With Radical 2-field Lymph Node Dissection: Results From Long-term Follow-up.* Int J Radiat Oncol Biol Phys, 2016. 96(2s): p. E175.
387. Ohashi, S., et al., *Recent Advances From Basic and Clinical Studies of Esophageal Squamous Cell Carcinoma.* Gastroenterology, 2015. 149(7): p. 1700-15.
388. Xi, R., et al., *HPV16 E6-E7 induces cancer stem-like cells phenotypes in esophageal squamous cell carcinoma through the activation of PI3K/Akt signaling pathway in vitro and in vivo.* Oncotarget, 2016.
389. Zhang, H.F., et al., *The PI3K/AKT/c-MYC Axis Promotes the Acquisition of Cancer Stem-Like Features in Esophageal Squamous Cell Carcinoma.* Stem Cells, 2016. 34(8): p. 2040-51.
390. Saito, S., et al., *Stromal fibroblasts are predictors of disease-related mortality in esophageal squamous cell carcinoma.* Oncol Rep, 2014. 32(1): p. 348-54.
391. Wang, J., et al., *The role of cancer-associated fibroblasts in esophageal cancer.* J Transl Med, 2016. 14: p. 30.
392. Fang, M., et al., *Collagen as a double-edged sword in tumor progression.* Tumour Biol, 2014. 35(4): p. 2871-82.
393. Zhu, J., et al., *Integrated extracellular matrix signaling in mammary gland development and breast cancer progression.* Histol Histopathol, 2014. 29(9): p. 1083-92.
394. Hussein, K.H., et al., *Three dimensional culture of HepG2 liver cells on a rat decellularized liver matrix for pharmacological studies.* J Biomed Mater Res B Appl Biomater, 2016. 104(2): p. 263-73.

395. Scherzer, M.T., et al., *Fibroblast-Derived Extracellular Matrices: An Alternative Cell Culture System That Increases Metastatic Cellular Properties.* PLoS One, 2015. 10(9): p. e0138065.
396. Kalluri, R. and M. Zeisberg, *Fibroblasts in cancer.* Nature Reviews Cancer, 2006. 6(5): p. 392-401.
397. Grinnell, F., *Fibroblasts, myofibroblasts, and wound contraction.* The Journal of cell biology, 1994. 124(4): p. 401-404.
398. Brechbuhl, H.M., et al., *Fibroblast subtypes regulate responsiveness of luminal breast cancer to estrogen.* Clin Cancer Res, 2016.
399. Chia, P.L., et al., *Targeting the vasculature: anti-angiogenic agents for malignant mesothelioma.* Expert Rev Anticancer Ther, 2016.
400. Wintzell, M., et al., *Protein markers of cancer-associated fibroblasts and tumor-initiating cells reveal subpopulations in freshly isolated ovarian cancer ascites.* BMC Cancer, 2012. 12: p. 359.
401. Ohlund, D., et al., *Distinct populations of inflammatory fibroblasts and myofibroblasts in pancreatic cancer.* J Exp Med, 2017. 214(3): p. 579-596.
402. Bourguignon, L.Y., M. Shiina, and J.J. Li, *Hyaluronan-CD44 interaction promotes oncogenic signaling, microRNA functions, chemoresistance, and radiation resistance in cancer stem cells leading to tumor progression.* Adv Cancer Res, 2014. 123: p. 255-75.
403. Senthebane, D.A., et al., *The Role of Tumor Microenvironment in Chemoresistance: To Survive, Keep Your Enemies Closer.* Int J Mol Sci, 2017. 18(7).
404. Clementz, A.G. and A. Harris, *Collagen XV: exploring its structure and role within the tumor microenvironment.* Mol Cancer Res, 2013. 11(12): p. 1481-6.
405. Cox, T.R., et al., *LOX-mediated collagen crosslinking is responsible for fibrosis-enhanced metastasis.* Cancer Res, 2013. 73(6): p. 1721-32.
406. Nolan, J., et al., *Collagen and fibronectin promote an aggressive cancer phenotype in breast cancer cells but drive autonomous gene expression patterns.* Gene, 2020. 761: p. 145024.
407. Li, X., et al., *Alphavbeta6-Fyn signaling promotes oral cancer progression.* J Biol Chem, 2003. 278(43): p. 41646-53.
408. Alemany-Ribes, M. and C.E. Semino, *Bioengineering 3D environments for cancer models.* Adv Drug Deliv Rev, 2014. 79-80: p. 40-9.

409. Imamura, Y., et al., *Comparison of 2D- and 3D-culture models as drug-testing platforms in breast cancer.* Oncol Rep, 2015. 33(4): p. 1837-43.
410. Serebriiskii, I., et al., *Fibroblast-derived 3D matrix differentially regulates the growth and drug-responsiveness of human cancer cells.* Matrix Biol, 2008. 27(6): p. 573-585.
411. Priwitaningrum, D.L., et al., *Tumor stroma-containing 3D spheroid arrays: A tool to study nanoparticle penetration.* J Control Release, 2016. 244(Pt B): p. 257-268.
412. Aihara, A., et al., *Novel 3-D cell culture system for in vitro evaluation of anticancer drugs under anchorage-independent conditions.* Cancer Sci, 2016. 107(12): p. 1858-1866.
413. Lovitt, C.J., T.B. Shelper, and V.M. Avery, *Doxorubicin resistance in breast cancer cells is mediated by extracellular matrix proteins.* BMC Cancer, 2018. 18(1): p. 41.
414. Zoetemelk, M., et al., *Short-term 3D culture systems of various complexity for treatment optimization of colorectal carcinoma.* Sci Rep, 2019. 9(1): p. 7103.
415. Ahmed, N., et al., *Role of integrin receptors for fibronectin, collagen and laminin in the regulation of ovarian carcinoma functions in response to a matrix microenvironment.* Clin Exp Metastasis, 2005. 22(5): p. 391-402.
416. Chen, X.D., et al., *The small leucine-rich proteoglycan biglycan modulates BMP-4-induced osteoblast differentiation.* Faseb j, 2004. 18(9): p. 948-58.
417. Cox, T.R. and J.T. Erler, *Molecular pathways: connecting fibrosis and solid tumor metastasis.* Clin Cancer Res, 2014. 20(14): p. 3637-43.
418. Hastings, J.F., et al., *The extracellular matrix as a key regulator of intracellular signalling networks.* British journal of pharmacology, 2019. 176(1): p. 82-92.
419. Provenzano, P.P., et al., *Collagen reorganization at the tumor-stromal interface facilitates local invasion.* BMC Med, 2006. 4(1): p. 38.
420. Amatangelo, M.D., et al., *Stroma-derived three-dimensional matrices are necessary and sufficient to promote desmoplastic differentiation of normal fibroblasts.* Am J Pathol, 2005. 167(2): p. 475-88.
421. Candiello, J., et al., *Biomechanical properties of native basement membranes.* The FEBS journal, 2007. 274(11): p. 2897-2908.

422. Amenta, P.S., et al., *Loss of types XV and XIX collagen precedes basement membrane invasion in ductal carcinoma of the female breast.* J Pathol, 2003. 199(3): p. 298-308.
423. Tosios, K., N. Kapranos, and S. Papanicolaou, *Loss of basement membrane components laminin and type IV collagen parallels the progression of oral epithelial neoplasia.* Histopathology, 1998. 33(3): p. 261-268.
424. Jolly, L.A., et al., *Fibroblast-mediated collagen remodeling within the tumor microenvironment facilitates progression of thyroid cancers driven by BrafV600E and Pten loss.* Cancer research, 2016. 76(7): p. 1804-1813.
425. Madsen, C.D., *Pancreatic cancer is suppressed by fibroblast-derived collagen I.* Cancer Cell, 2021. 39(4): p. 451-453.
426. Iozzo, R.V. and L. Schaefer, *Proteoglycan form and function: A comprehensive nomenclature of proteoglycans.* Matrix Biol, 2015. 42: p. 11-55.
427. Hardingham, T.E. and A.J. Fosang, *Proteoglycans: many forms and many functions.* Faseb j, 1992. 6(3): p. 861-70.
428. Ishihara, J., et al., *Laminin heparin-binding peptides bind to several growth factors and enhance diabetic wound healing.* Nature Communications, 2018. 9(1): p. 2163.
429. Broekelmann, T.J., N.K. Bodmer, and R.P. Mecham, *Identification of the growth factor–binding sequence in the extracellular matrix protein MAGP-1.* Journal of Biological Chemistry, 2020. 295(9): p. 2687-2697.
430. Bohaumilitzky, L., et al., *A Trickster in Disguise: Hyaluronan's Ambivalent Roles in the Matrix.* Front Oncol, 2017. 7: p. 242.
431. Price, Z.K., N.A. Lokman, and C. Ricciardelli, *Differing roles of hyaluronan molecular weight on cancer cell behavior and chemotherapy resistance.* Cancers, 2018. 10(12): p. 482.
432. Goetz, J.G., et al., *Biomechanical remodeling of the microenvironment by stromal caveolin-1 favors tumor invasion and metastasis.* Cell, 2011. 146(1): p. 148-163.
433. Alfano, M., et al., *Linearized texture of three-dimensional extracellular matrix is mandatory for bladder cancer cell invasion.* Scientific Reports, 2016. 6(1): p. 36128.

434. Shapiro, G.I. and J.W. Harper, *Anticancer drug targets: cell cycle and checkpoint control.* The Journal of clinical investigation, 1999. 104(12): p. 1645-1653.
435. Hodkinson, P.S., et al., *ECM overrides DNA damage-induced cell cycle arrest and apoptosis in small-cell lung cancer cells through β1 integrin-dependent activation of PI3-kinase.* Cell Death & Differentiation, 2006. 13(10): p. 1776-1788.
436. Lai, Y., et al., *Reconstitution of marrow-derived extracellular matrix ex vivo: a robust culture system for expanding large-scale highly functional human mesenchymal stem cells.* Stem cells and development, 2010. 19(7): p. 1095-1107.
437. Dzobo, K., *Integrins Within the Tumor Microenvironment: Biological Functions, Importance for Molecular Targeting, and Cancer Therapeutics Innovation.* Omics, 2021. 25(7): p. 417-430.
438. Conway, J.R.W. and G. Jacquemet, *Cell matrix adhesion in cell migration.* Essays Biochem, 2019. 63(5): p. 535-551.
439. Zhang, Y., G. Reif, and D.P. Wallace, *Extracellular matrix, integrins, and focal adhesion signaling in polycystic kidney disease.* Cell Signal, 2020. 72: p. 109646.
440. Hamidi, H. and J. Ivaska, *Every step of the way: integrins in cancer progression and metastasis.* Nature Reviews Cancer, 2018. 18(9): p. 533-548.
441. Samaržija, I., et al., *Integrin crosstalk contributes to the complexity of signalling and unpredictable cancer cell fates.* Cancers, 2020. 12(7): p. 1910.
442. Varner, J.A., D.A. Emerson, and R.L. Juliano, *Integrin alpha 5 beta 1 expression negatively regulates cell growth: reversal by attachment to fibronectin.* Molecular biology of the cell, 1995. 6(6): p. 725-740.
443. Stoeltzing, O., et al., *Inhibition of integrin α5β1 function with a small peptide (ATN-161) plus continuous 5-FU infusion reduces colorectal liver metastases and improves survival in mice.* International journal of cancer, 2003. 104(4): p. 496-503.
444. Jin, H. and J. Varner, *Integrins: roles in cancer development and as treatment targets.* British journal of cancer, 2004. 90(3): p. 561-565.
445. Weis, S.M. and D.A. Cheresh, *αV integrins in angiogenesis and cancer.* Cold Spring Harbor perspectives in medicine, 2011. 1(1): p. a006478.

446. Bommert, K., R.C. Bargou, and T. Stühmer, *Signalling and survival pathways in multiple myeloma.* Eur J Cancer, 2006. 42(11): p. 1574-80.
447. Mei, D., et al., *The Role of CTHRC1 in Regulation of Multiple Signaling and Tumor Progression and Metastasis.* Mediators Inflamm, 2020. 2020: p. 9578701.
448. Farmer, P., et al., *A stroma-related gene signature predicts resistance to neoadjuvant chemotherapy in breast cancer.* Nat Med, 2009. 15(1): p. 68-74.
449. Brown, Y., S. Hua, and P.S. Tanwar, *Extracellular matrix-mediated regulation of cancer stem cells and chemoresistance.* The international journal of biochemistry & cell biology, 2019. 109: p. 90-104.
450. Pietilä, E.A., et al., *Co-evolution of matrisome and adaptive adhesion dynamics drives ovarian cancer chemoresistance.* Nature Communications, 2021. 12(1): p. 1-19.
451. Mocanu, M.M., et al., *Associations of ErbB2, beta1-integrin and lipid rafts on Herceptin (Trastuzumab) resistant and sensitive tumor cell lines.* Cancer Lett, 2005. 227(2): p. 201-12.
452. Guo, W., et al., *Beta 4 integrin amplifies ErbB2 signaling to promote mammary tumorigenesis.* Cell, 2006. 126(3): p. 489-502.
453. Nguyen, T.V., et al., *Sorafenib resistance and JNK signaling in carcinoma during extracellular matrix stiffening.* Biomaterials, 2014. 35(22): p. 5749-5759.
454. Keely, P.J., *Mechanisms by which the extracellular matrix and integrin signaling act to regulate the switch between tumor suppression and tumor promotion.* Journal of mammary gland biology and neoplasia, 2011. 16(3): p. 205-219.
455. Dzobo, K., *Taking a Full Snapshot of Cancer Biology: Deciphering the Tumor Microenvironment for Effective Cancer Therapy in the Oncology Clinic.* Omics, 2020. 24(4): p. 175-179.
456. Mehta, G., et al., *Opportunities and challenges for use of tumor spheroids as models to test drug delivery and efficacy.* Journal of controlled release, 2012. 164(2): p. 192-204.
457. Rodrigues, T., et al., *Emerging tumor spheroids technologies for 3D in vitro cancer modeling.* Pharmacology & therapeutics, 2018. 184: p. 201-211.
458. Arab-Bafrani, Z., et al., *Enhanced radiotherapy efficacy of breast cancer multi cellular tumor spheroids through in-situ fabricated chitosan-zinc oxide bio-*

nanocomposites as radio-sensitizing agents. International Journal of Pharmaceutics, 2021. 605: p. 120828.

459. Ranjbar-Mohammadi, M., et al., *Multi-cellular tumor spheroids formation of colorectal cancer cells on Gelatin/PLCL and Collagen/PLCL nanofibrous scaffolds.* European Polymer Journal, 2019. 115: p. 115-124.
460. Hirschhaeuser, F., et al., *Multicellular tumor spheroids: an underestimated tool is catching up again.* Journal of biotechnology, 2010. 148(1): p. 3-15.
461. Timmins, N.E. and L.K. Nielsen, *Generation of multicellular tumor spheroids by the hanging-drop method*, in *Tissue engineering*. 2007, Springer. p. 141-151.
462. Lu, H. and M.H. Stenzel, *Multicellular tumor spheroids (MCTS) as a 3D in vitro evaluation tool of nanoparticles.* Small, 2018. 14(13): p. 1702858.
463. Riffle, S. and R.S. Hegde, *Modeling tumor cell adaptations to hypoxia in multicellular tumor spheroids.* Journal of Experimental & Clinical Cancer Research, 2017. 36(1): p. 1-10.
464. Han, S.J., S. Kwon, and K.S. Kim, *Challenges of applying multicellular tumor spheroids in preclinical phase.* Cancer Cell International, 2021. 21(1): p. 1-19.
465. Hamilton, G. and B. Rath, *Applicability of tumor spheroids for in vitro chemosensitivity assays.* Expert opinion on drug metabolism & toxicology, 2019. 15(1): p. 15-23.
466. Kim, S.M., P.H. Faix, and J.E. Schnitzer, *Overcoming key biological barriers to cancer drug delivery and efficacy.* Journal of Controlled Release, 2017. 267: p. 15-30.
467. Gong, X., et al., *Generation of multicellular tumor spheroids with microwell-based agarose scaffolds for drug testing.* PloS one, 2015. 10(6): p. e0130348.
468. Kapałczyńska, M., et al., *2D and 3D cell cultures–a comparison of different types of cancer cell cultures.* Archives of medical science: AMS, 2018. 14(4): p. 910.
469. Sant, S. and P.A. Johnston, *The production of 3D tumor spheroids for cancer drug discovery.* Drug Discovery Today: Technologies, 2017. 23: p. 27-36.
470. Costa, E.C., et al., *3D tumor spheroids: an overview on the tools and techniques used for their analysis.* Biotechnology advances, 2016. 34(8): p. 1427-1441.
471. Kamatar, A., G. Gunay, and H. Acar, *Natural and synthetic biomaterials for engineering multicellular tumor spheroids.* Polymers, 2020. 12(11): p. 2506.

472. Zhao, L., et al., *A 3D printed hanging drop dripper for tumor spheroids analysis without recovery.* Scientific reports, 2019. 9(1): p. 1-14.
473. Amaral, R.L., et al., *Comparative analysis of 3D bladder tumor spheroids obtained by forced floating and hanging drop methods for drug screening.* Frontiers in physiology, 2017. 8: p. 605.
474. Raghavan, S., et al., *Comparative analysis of tumor spheroid generation techniques for differential in vitro drug toxicity.* Oncotarget, 2016. 7(13): p. 16948.
475. Sabhachandani, P., et al., *Generation and functional assessment of 3D multicellular spheroids in droplet based microfluidics platform.* Lab on a Chip, 2016. 16(3): p. 497-505.
476. Herheliuk, T., et al., *Investigation of multicellular tumor spheroids enriched for a cancer stem cell phenotype.* Stem Cell Investig, 2019. 6: p. 21.
477. Liu, A., X. Yu, and S. Liu, *Pluripotency transcription factors and cancer stem cells: small genes make a big difference.* Chin J Cancer, 2013. 32(9): p. 483-7.
478. Close, D.A. and P.A. Johnston, *Detection and impact of hypoxic regions in multicellular tumor spheroid cultures formed by head and neck squamous cell carcinoma cells lines.* SLAS Discov, 2021.
479. Eguchi, T., et al., *Cancer extracellular vesicles, tumoroid models, and tumor microenvironment.* Semin Cancer Biol, 2022.
480. Shi, Y.F., et al., *Hypoxia induces the activation of human hepatic stellate cells LX-2 through TGF-beta signaling pathway.* FEBS Lett, 2007. 581(2): p. 203-10.
481. Zhang, H., et al., *CAF secreted miR-522 suppresses ferroptosis and promotes acquired chemo-resistance in gastric cancer.* Mol Cancer, 2020. 19(1): p. 43.
482. Wei, L., et al., *Cancer-associated fibroblasts promote progression and gemcitabine resistance via the SDF-1/SATB-1 pathway in pancreatic cancer.* Cell Death Dis, 2018. 9(11): p. 1065.
483. Takai, A., et al., *Three-dimensional Organotypic Culture Models of Human Hepatocellular Carcinoma.* Sci Rep, 2016. 6: p. 21174.
484. Song, Y., et al., *Activated hepatic stellate cells play pivotal roles in hepatocellular carcinoma cell chemoresistance and migration in multicellular tumor spheroids.* Sci Rep, 2016. 6: p. 36750.
485. Knuchel, S., et al., *Fibroblast surface-associated FGF-2 promotes contact-dependent colorectal cancer cell migration and invasion through FGFR-SRC*

signaling and integrin αvβ5-mediated adhesion. Oncotarget, 2015. 6(16): p. 14300-17.

486. Tilghman, R.W., et al., *Matrix rigidity regulates cancer cell growth by modulating cellular metabolism and protein synthesis.* PLoS One, 2012. 7(5): p. e37231.
487. Anguiano, M., et al., *The use of mixed collagen-Matrigel matrices of increasing complexity recapitulates the biphasic role of cell adhesion in cancer cell migration: ECM sensing, remodeling and forces at the leading edge of cancer invasion.* PLoS One, 2020. 15(1): p. e0220019.
488. Blaha, L., et al., *A microfluidic platform for modeling metastatic cancer cell matrix invasion.* Biofabrication, 2017. 9(4): p. 045001.
489. Khawar, I.A., et al., *Three Dimensional Mixed-Cell Spheroids Mimic Stroma-Mediated Chemoresistance and Invasive Migration in hepatocellular carcinoma.* Neoplasia, 2018. 20(8): p. 800-812.
490. Gaggioli, C., et al., *Fibroblast-led collective invasion of carcinoma cells with differing roles for RhoGTPases in leading and following cells.* Nat Cell Biol, 2007. 9(12): p. 1392-400.
491. Jeong, S.Y., et al., *Co-Culture of Tumor Spheroids and Fibroblasts in a Collagen Matrix-Incorporated Microfluidic Chip Mimics Reciprocal Activation in Solid Tumor Microenvironment.* PLoS One, 2016. 11(7): p. e0159013.
492. Wu, Q., et al., *Cancer stem cells in esophageal squamous cell cancer.* Oncology letters, 2019. 18(5): p. 5022-5032.
493. Song, K. and M. Farzaneh, *Signaling pathways governing breast cancer stem cells behavior.* Stem Cell Research & Therapy, 2021. 12(1): p. 245.
494. Goričan, L., B. Gole, and U. Potočnik, *Head and Neck Cancer Stem Cell-Enriched Spheroid Model for Anticancer Compound Screening.* Cells, 2020. 9(7): p. 1707.
495. Reynolds, D.S., et al. *Breast Cancer Spheroids Reveal a Differential Cancer Stem Cell Response to Chemotherapeutic Treatment*. Scientific reports, 2017. 7, 10382 DOI: 10.1038/s41598-017-10863-4.
496. Leis, O., et al., *Sox2 expression in breast tumours and activation in breast cancer stem cells.* Oncogene, 2012. 31(11): p. 1354-1365.
497. Sneddon, J.B. and Z. Werb, *Location, location, location: the cancer stem cell niche.* Cell stem cell, 2007. 1(6): p. 607-611.

498. Su, S., et al., *CD10(+)GPR77(+) Cancer-Associated Fibroblasts Promote Cancer Formation and Chemoresistance by Sustaining Cancer Stemness.* Cell, 2018. 172(4): p. 841-856.e16.
499. Huang, M., et al., *Breast cancer stromal fibroblasts promote the generation of CD44+CD24- cells through SDF-1/CXCR4 interaction.* J Exp Clin Cancer Res, 2010. 29(1): p. 80.
500. Emura, M., et al., *Development of myofibroblasts from human bone marrow mesenchymal stem cells cocultured with human colon carcinoma cells and TGF beta 1.* In Vitro Cell Dev Biol Anim, 2000. 36(2): p. 77-80.
501. Manhas, J., et al., *Characterization of cancer stem cells from different grades of human colorectal cancer.* Tumour Biol, 2016. 37(10): p. 14069-14081.
502. Takaishi, S., et al., *Identification of gastric cancer stem cells using the cell surface marker CD44.* Stem Cells, 2009. 27(5): p. 1006-20.
503. Huang, C.P., et al., *ALDH-positive lung cancer stem cells confer resistance to epidermal growth factor receptor tyrosine kinase inhibitors.* Cancer Lett, 2013. 328(1): p. 144-51.
504. Auffinger, B., et al., *Conversion of differentiated cancer cells into cancer stem-like cells in a glioblastoma model after primary chemotherapy.* Cell Death Differ, 2014. 21(7): p. 1119-31.
505. Ahmad, G. and M.M. Amiji, *Cancer stem cell-targeted therapeutics and delivery strategies.* Expert Opin Drug Deliv, 2017. 14(8): p. 997-1008.
506. Bao, S., et al., *Glioma stem cells promote radioresistance by preferential activation of the DNA damage response.* Nature, 2006. 444(7120): p. 756-60.
507. Wishart, A.L., et al., *Decellularized extracellular matrix scaffolds identify full-length collagen VI as a driver of breast cancer cell invasion in obesity and metastasis.* Science Advances, 2020. 6(43): p. eabc3175.
508. World Medical, A., *World Medical Association Declaration of Helsinki. Ethical principles for medical research involving human subjects.* Bulletin of the World Health Organization, 2001. 79(4): p. 373-374.
509. Veale, R.B. and A.L. Thornley, *Increased single class low-affinity EGF receptors expressed by human oesophageal squamous carcinoma cell lines.* S. Afr. J. Sci., 1989. 85: p. 375-379.
510. Shimada, Y., et al., *Characterization of 21 newly established esophageal cancer cell lines.* Cancer, 1992. 69(2): p. 277-84.

511. Cailleau, R., M. Olivé, and Q.V. Cruciger, *Long-term human breast carcinoma cell lines of metastatic origin: preliminary characterization.* In Vitro, 1978. 14(11): p. 911-5.
512. Namba, M., K. Nishitani, and T. Kimoto, *Characteristics of WI-38 cells (WI-38 CT-1) transformed by treatment with Co-60 gamma rays.* Gann = Gan, 1980. 71(3): p. 300-307.
513. Green, J.A. and K.M. Yamada, *Three-dimensional microenvironments modulate fibroblast signaling responses.* Adv Drug Deliv Rev, 2007. 59(13): p. 1293-8.
514. Ostasiewicz, P., et al., *Proteome, phosphoproteome, and N-glycoproteome are quantitatively preserved in formalin-fixed paraffin-embedded tissue and analyzable by high-resolution mass spectrometry.* J Proteome Res, 2010. 9(7): p. 3688-700.
515. Rhodes, D.R., et al., *Oncomine 3.0: Genes, Pathways, and Networks in a Collection of 18,000 Cancer Gene Expression Profiles.* Neoplasia, 2007. 9(2): p. 166-180.
516. Li, T., et al., *TIMER: A Web Server for Comprehensive Analysis of Tumor-Infiltrating Immune Cells.* Cancer Research, 2017. 77(21): p. e108-e110.
517. Thul, P.J. and C. Lindskog, *The human protein atlas: A spatial map of the human proteome.* Protein science : a publication of the Protein Society, 2018. 27(1): p. 233-244.
518. Warde-Farley, D., et al., *The GeneMANIA prediction server: biological network integration for gene prioritization and predicting gene function.* Nucleic Acids Res, 2010. 38(Web Server issue): p. W214-20.

APPENDIX A

SOLUTIONS

10 % Ammonium persulfate (APS)

100 mg APS

1 ml dH2O, store at 4°C

1% BSA in PBST

1g BSA

100 ml PBST

1% BSA in PBST + 0.3 M Glycine

0.5 g BSA

1.126 g Glycine

Up to 50 ml PBS-T

Colony fixation solution (160 ml)

Acetic acid (20 ml)

Methanol (140 ml)

Complete Media

450 ml DMEM

50 ml FBS (10%)

5 ml Pen/Strep (1%)

Coomassie staining solution

0.5 g Coomassie brilliant blue

200 ml methanol

100 ml acetic acid

400 ml dH2O

Crystal violet 0.5% solution (200 ml)

1 g crystal violet

50 ml methanol

150 ml dH2O

DEPC dH2O

100 µl DEPC

1 L dH2O

75 % DEPC- Ethanol

75 ml absolute ethanol

25 ml DEPC-dH2O

Destaining solution

100 ml acetic acid,

100 ml methanol

800 ml dH2O

0.5 M EDTA (pH 8.0)

37.22 g Na2EDTA-2H2O

140 ml dH2O

Adjust to pH 8.0 with NaOH

Make up to 200 ml with dH2O

Freezing down media

70% FBS

20% DMEM media

10% DMSO

MTT (5 mg/ml)

100 mg MTT

20 ml of 1x PBS at pH 7.4

Wrap in foil and store at 4°C for up to a month

5 M NaCl

58.44 g NaCl

Up to 200 ml dH2O

4% Paraformaldehyde

20 g Paraformaldehyde

Up to 400 ml PBS

Stir on a heating blocking at 60 °C

Add 1 M NaOH dropwise until the solution clears

Filter sterilise

Adjust the volume to 500 ml with PBS

10X PBS

40 g NaCl

1 g KCl

1 g KH2PO4

5.75 g Na2HPO4.2H2O

2.1 g KH2PO4

Up to 500 ml with dH2O

Calibrated to a pH of 7.4

Autoclave

0.1% PBS-T

500 ml 1 X PBS

500 µl Tween-20

4 X Protein loading dye

2.5 ml 1 M Tris at pH 6.8,

3 ml 20 % SDS,

0.5 ml 0.1 % Bromophenol blue and

4 ml Glycerol

50 µl β-mercaptoethanol

RIPA Solution

150 mM NaCl

1 % Triton X-100

0.1 % SDS

25 mM Tris, pH 7.4

1 % sodium deoxycholate

10 X Running buffer

29 g Tris

144 g Glycine

10 g SDS

Up to 1 L with dH2O

1 X Running buffer

100 ml 10 X Running buffer

900 ml dH2O

10 % SDS

10 g SDS

100 ml dH2O (stir on low heat)

10% Separating gel

2.75 ml dH2O

3.75 ml 1 M Tris pH 6.8,

3.35 ml 30 % Acrylamide

100 µl 10% SDS

200 µl 10% APS

20 µl TEMED

10% Solubilisation reagent: Sodium Lauryl sulphate (SLS)

25 g SLS

76.6 µl concentrated HCl

Up to 250 ml with dH2O

4% Stacking gel

3.65 ml dH2O

0.625 ml 1 M Tris pH 6.8,

0.65 ml 30 % Acrylamide

50 µl 10% SDS

60 µl 10% APS

6 µl TEMED

Stripping buffer

37.54 g Glycine

Up to 500 ml with dH2O

pH 2.5

10 X TBS

24.23 g Tris

80.06 g NaCl

Up to 1 L dH2O

pH 7.6

1 X TBS-Tween

100 ml 10 X TBS

900 ml dH2O

500 µl Tween-20

Make up to 1 L with dH2O

10 X Transfer buffer

144 g glycine

38 g Tris

Make up to 1 L dH2O

1 X Transfer buffer

100 ml 10 x Transfer buffer

200 ml Methanol

700 ml dH2O

1 M Tris

121 g Tris base to 800 ml dH2O,

Adjust the pH to 6.8, 7.5 or 8.8

Make up to 1 L with dH2O, then autoclave.

0.25% Triton X 100 in PBS (250 ml)

250 1 X PBS

625 µl Triton X 100

Trypsin

0.5 g trypsin powder

0.2 g EDTA powder

Up to 1 L with PBS buffer

The pH 7.4 and the

Filter sterilise

APPENDIX B

PRIMERS SEQUENCES

Gene symbol	Forward Primer (5' – 3')	Reverse Primer (5' – 3')	Temperature (°C)
GAPDH	GCTCTCCAGAACATCATCC	GCCTGCTTCACCACCTTC	60
COL1A1	GATTGAGACCCTTCTTACTCCTGAA	TTTGTATTCAATCACTGTCTTGC	60
COL1A2	GATTGAGACCCTTCTTACTCCTGAA	GGGTGGCTGAGTCTCAAGTCA	60
COL2A1	GTCCCAGGATGAGGTCAAGA	TGGCAAGCTCATTGTAGTCG	60
COL3A1	AAGGTCCAGCTGGGATACCT	CACCCTTTAATCCAGGAGCA	60
Smad2	CGGAGATTCTAACAGAACTG	TGCTTGAGCATCGCACTGAA	
Smad3	AGCACACAATAACTTGGACC	TAAGACACACTGGAACAGCGGATG	60
ACTA2	AGCGTGGCTATTCCTTCGT	CCATCAGGCAACTCGTAACTC	60
CD44	GAGCATCGGATTTGAGA	CATACTGGGAGGTGTTGG	
CD24	TGCTCCTACCCACGCAGATT	GGCCAACCCAGAGTTGGAA	
CD133	AAGCATTGGCATCTTCTATGG	AAGCACAGAGGGTCATTGAGA	57
ALDH1A1	TTGGAATTTCCCGTTGGTTA	CGTTAGGCCCATAACCAGGA	55
Oct3/4	CTTGCTGCAGAAGTGGGTGGAGGAA	CTGCAGTGTGGGTTTCGGGCA	60
SOX2	CCCAGCAGACTTCACATGT	CCTCCCATTTCCCTCGTTTT	60
Nanog	GCTTGCCTTGCTTTGAAGCA	TTCTTGACTGGGACCTTGTC	60
p63	GAAAGCAGCAAGTTTCGGAC	TTTCATAAGTCTCACGGCCC	60
CK5/6	ATCGCCACTTACCGCAAGCTGCTGGAGGG	AAACACTGCTTGTGACAACAGAG	60
H1F0	CTGGCTGCCACGCCCAAGAA	CGGCCCTCTTGGCACTGGAC	60
HISTH1A	CTCCTCTAAGGAGCGTGGTG	GAGGACGCCTTCTTGTTGAG	57
HISTH1B	GTCAAAAAGGTGGCGAAGAG	CTTGGCCTTTGCAGCTTTAG	55
HISTH1C	ACACCGAAGAAAGCGAAGAA	GCTTGACAACCTTGGGCTTA	55
ABCB1	GCCTGGCAGCTGGAAGACAAATAC	ATGGCCAAAATCACAAGGGTTAGC	60
ABCG2	TTGGTGGGCAACTGCATCG	GTTGGTTTCCATTTCAGATGACATCCG	60
MDR1	CCCATCATTGCAATAGCAGG	TGTTCAAACTTCTGCTCCTGA	60
MGMT	GCTGAATGCCTATTTCCACCA	CACAACCTTCAGCAGCTTCCA	60
Fibronectin	AGCAGACCCAGCTTAGAGTT	GCAGAAGTGTTTGGGTGACT	60
Laminin α1	GTCAGCGACTCAGAGTGTTTG	AACTTGGGTGAAAGATCGTCAG	60

Laminin α2	GAACCCGCAGTGTCGAATCT	GGGGAGTTAGCTGCCTTCA	60
Laminin α3	TAGACTTTGGAAGCACCTACTCA	GTTTATCAAGGACACCACAACCT	60
MMP1	GCTGGGAGCAAACACATCTGACCT	TGAGCCGCAACACGATGTAAGTTG	60
MMP2	CCGCCTTTAACTGGAGCAAA	TTTGGTTCTCCAGCTTCAGG	60
MMP3	CTGGGCCAGGGATTAATGGAG	GCTTCAGTGTTGGCTGAGTG	60
MMP9	GAGACAGCATGGCCAAATTA	CTCTAGAAACTGCTGAGGGC	60
Integrin α1	GGTGCTTATTGGTTCTCCGTTAG	TTCTCCTTTACTTCTGTGACATTGG	58
Integrin α2	GACCTATCCACTGCCACATGTGAAAAA	CCACAGAGGACCACATGTGAGAAAA	58
Integrin α5	TGCAGTGTGAGGCTGTGTACA	GTGGCCACCTGACGCTCT	58
Integrin β1	GAAGGGTTGCCCTCCAGA	GCTTGAGCTTCTCTGCTGTT	58
Tenascin C	ACCATGCTGAGATAGATGTTCCAAA	CTTGACAGCAGAAACACCAATCC	58

PUBLICATIONS

1. **Senthebane DA**, Jonker T, Rowe A, Thomford NE, Munro D, Dandara C, Wonkam A, Govender D, Calder B, Soares NC, Blackburn JM, Parker MI, Dzobo K. The Role of Tumour Microenvironment in Chemoresistance: 3D Extracellular Matrices as Accomplices. Int J Mol Sci. 2018 Sep 20;19(10).

2. **Senthebane DA**, Rowe A, Thomford NE, Shipanga H, Munro D, Mazeedi MAMA, Almazyadi HAM, Kallmeyer K, Dandara C, Pepper MS, Parker MI, Dzobo K. The Role of Tumour Microenvironment in Chemoresistance: To Survive, Keep Your Enemies Closer. Int J Mol Sci. 2017 Jul 21;18(7).

International Journal of
Molecular Sciences

MDPI

Article

The Role of Tumor Microenvironment in Chemoresistance: 3D Extracellular Matrices as Accomplices

Dimakatso Alice Senthebane [1,2], Tina Jonker [1,2], Arielle Rowe [2], Nicholas Ekow Thomford [3], Daniella Munro [3], Collet Dandara [3], Ambroise Wonkam [3], Dhirendra Govender [4], Bridget Calder [5], Nelson C. Soares [5], Jonathan M. Blackburn [5], M. Iqbal Parker [1] and Kevin Dzobo [1,2,*]

1 Division of Medical Biochemistry and Institute of Infectious Disease and Molecular Medicine, Faculty of Health Sciences, University of Cape Town, Anzio Road, Observatory, Cape Town 7925, South Africa; SNTDIM001@myuct.ac.za (D.A.S.); tyjonker@gmail.com (T.J.); iqbal.parker@uct.ac.za (M.I.P.)
2 International Centre for Genetic Engineering and Biotechnology (ICGEB), Cape Town Component, Wernher and Beit Building (South), UCT Campus, Anzio Road, Observatory, Cape Town 7925, South Africa; arielle.rowe@icgeb.org
3 Pharmacogenetics Research Group, Division of Human Genetics, Department of Pathology and Institute of Infectious Diseases and Molecular Medicine, Faculty of Health Sciences, University of Cape Town, Anzio Road, Observatory, Cape Town 7925, South Africa; Nicholas.thomford@uct.ac.za (N.E.T.); MNRDAN002@myuct.ac.za (D.M.); collet.dandara@uct.ac.za (C.D.); Ambroise.wonkam@uct.ac.za (A.W.)
4 Division of Anatomical Pathology, Faculty of Health Sciences, University of Cape Town, NHLS-Groote Schuur Hospital, Cape Town 7925, South Africa; dhiren.govender@uct.ac.za
5 Division of Chemical and Systems Biology, Department of Integrative Biomedical Sciences, Faculty of Health Sciences, Institute of Infectious Disease and Molecular Medicine, University of Cape Town, Cape Town 7925, South Africa; bridget.calder@uct.ac.za (B.C.); nelson.dacruzsoares@uct.ac.za (N.C.S.); jonathan.blackburn@uct.ac.za (J.M.B.)
* Correspondence: kd.dzobo@uct.ac.za; Tel.: +27-21-404-7689; Fax: +27-21-406-6060

Received: 1 September 2018; Accepted: 18 September 2018; Published: 20 September 2018

Abstract: Background: The functional interplay between tumor cells and their adjacent stroma has been suggested to play crucial roles in the initiation and progression of tumors and the effectiveness of chemotherapy. The extracellular matrix (ECM), a complex network of extracellular proteins, provides both physical and chemicals cues necessary for cell proliferation, survival, and migration. Understanding how ECM composition and biomechanical properties affect cancer progression and response to chemotherapeutic drugs is vital to the development of targeted treatments. Methods: 3D cell-derived-ECMs and esophageal cancer cell lines were used as a model to investigate the effect of ECM proteins on esophageal cancer cell lines response to chemotherapeutics. Immunohistochemical and qRT-PCR evaluation of ECM proteins and integrin gene expression was done on clinical esophageal squamous cell carcinoma biopsies. Esophageal cancer cell lines (WHCO1, WHCO5, WHCO6, KYSE180, KYSE 450 and KYSE 520) were cultured on decellularised ECMs (fibroblasts-derived ECM; cancer cell-derived ECM; combinatorial-ECM) and treated with 0.1% Dimethyl sulfoxide (DMSO), 4.2 μM cisplatin, 3.5 μM 5-fluorouracil and 2.5 μM epirubicin for 24 h. Cell proliferation, cell cycle progression, colony formation, apoptosis, migration and activation of signaling pathways were used as our study endpoints. Results: The expression of collagens, fibronectin and laminins was significantly increased in esophageal squamous cell carcinomas (ESCC) tumor samples compared to the corresponding normal tissue. Decellularised ECMs abrogated the effect of drugs on cancer cell cycling, proliferation and reduced drug induced apoptosis by 20–60% that of those plated on plastic. The mitogen-activated protein kinase-extracellular signal-regulated kinase (MEK-ERK) and phosphoinositide 3-kinase-protein kinase B (PI3K/Akt) signaling pathways were upregulated in the presence of the ECMs. Furthermore, our data show that concomitant addition

of chemotherapeutic drugs and the use of collagen- and fibronectin-deficient ECMs through siRNA inhibition synergistically increased cancer cell sensitivity to drugs by 30–50%, and reduced colony formation and cancer cell migration. Conclusion: Our study shows that ECM proteins play a key role in the response of cancer cells to chemotherapy and suggest that targeting ECM proteins can be an effective therapeutic strategy against chemoresistant tumors.

Keywords: esophageal cancer; 3D extracellular matrix; stroma; type I collagen; fibronectin; chemoresistance; signaling cascade; targeted therapy

1. Introduction

Great interest has been generated in developing microphysiological systems that can best mimic normal and pathological human conditions in vitro. Most drug discovery assays are performed using in vitro models that do not recapitulate the in vivo tumor microenvironment present during tumor growth, development and treatment [1–6]. The lack of good in vitro tumor models limits our understanding of the functional interplay between tumor cells and the tumor microenvironment [7–10]. The dynamic full in vivo biological repertoire of the tumor microenvironment include many cells such as fibroblasts, endothelial cells, immune cells and the ECM [7–16]. This ultimately leads to incorrect and misleading claims when it comes to the efficacy of drug candidates. Such scenarios can be avoided by employing in vitro models that better recapitulate the in vivo tumor microenvironment [3,17–23]. One important constituent of the tumor microenvironment is the extracellular matrix, a meshwork of proteins and glycosaminoglycans [3,17,18,20]. The ECM provides both mechanical and biochemical support for cellular adhesion and migration and acts as a conduit for extracellular cues via its interaction with cell surface receptors. It is known to sequester growth factors and cytokines and these will affect cellular growth and signaling [24–30]. Thus the ECM is the "theatre" where most cues or signals from diverse sources are integrated into a "specific" message that is relayed to cells. The ECM is synthesised mostly by fibroblasts with the contribution of other cells such as mesenchymal stem cells, macrophages and endothelial cells [31–36]. Fibroblasts are the main cellular components of tumor stroma [37–44]. Activated or transformed fibroblasts have a high proliferation rate and generate huge amounts of extracellular matrix [38,39,45–49].

Esophageal cancer is one of the most highly malignant neoplasms and can be classified into two main subtypes, esophageal adenocarcinomas and esophageal squamous cell carcinomas (ESCC), with the majority of deaths from ESCC occurring in developing countries [50–52]. ESCC is the third most common cancer in South African men [53,54]. Although promising progress has been attained in treating esophageal cancer, it responds poorly to chemotherapeutic drugs and the mortality still remains high [51,55–59]. Surgery, chemotherapy and radiotherapy are the most widely-used treatment methods but about half of advanced esophageal cancer cases result in recurrence and patients normally succumb to resistant disease [60–64]. There is a lack of understanding of the mechanisms driving the initiation, progression and the occurrence of refractory disease. Besides the gradual accumulation over time of genetic mutations in epithelial cells due to carcinogen exposure, the initiation, progression and response to chemotherapy of many tumors including esophageal cancer depends on the interplay between the stroma and tumor cells. Recent data suggest that the development of chemoresistant disease is beyond cancer cell autonomous mechanisms with the tumor microenvironment emerging as a key player in this phenomenon [50–52,65–70]. Several reports have shown the involvement of stromal fibroblasts in esophageal cancer angiogenesis and differentiation through the release of biomolecules and ECM synthesis [71–77]. The expression of several ECM proteins has been shown to be upregulated in many tumors [17,78–80]. The so-called 'hardening of the tumor' is in fact the deposition and crosslinking of thick fibres mainly made up of collagen and fibronectin [80–85]. ESCC stroma is fibrotic due to desmoplasia. Huge amounts of the ECM are deposited during ESCC

development. Thus the constituents of the ECM can have a lasting effect on cancer cells. Different types of ECMs have been used to study cancer cell-ECM interactions, with most ECM proteins being purified proteins [3,6–8,10,16,18,20,86]. Decellularised cell-derived ECMs contain native ECM proteins, and are cost-effective and easily obtainable [3,10,18,20,87–90]. Fibroblast-derived decellularised ECM would mimic the desmoplastic microenvironment of the ESCC.

This study investigated the effect of three different cell-derived ECMs on the response of esophageal cancer cells to chemotherapeutic drugs. We reproduced the native ECM microenvironment by employing decellularised ECMs synthesised by fibroblasts and cancer cells. Our data show that fibroblast- and cancer cell-derived ECMs contain similar ECM proteins, though in differing amounts. We report that decellularised ECMs, regardless of origin, induce chemoresistance to cisplatin, 5-fluorouracil and epirubicin. Survival pathways such as the MEK-ERK and PI3K-Akt pathways were activated in the presence of decellularised ECMs. Remarkably, we show that the use of type I collagen- and fibronectin-deficient ECMs and drugs have a synergistic negative effect on esophageal cancer cell proliferation, colony formation and migration. These results suggest that components of the tumor microenvironment underlie aspects of chemoresistance, and are therefore potential drug targets.

2. Results

2.1. ECM Proteins and Matrix Metalloproteases Expression in Clinical Esophageal Squamous Cell Carcinoma Tissues

Twenty-one biopsy samples were collected from histopathologically-confirmed ESCC patients and were used to evaluate the expression profiles of ECM and associated genes. The clinicopathological characteristics of the 21 ESCC patients are shown in Table 1. The age range of the patient cohort is 30–83 years with a median age of 55 years. Patients were nearly evenly distributed between male and females. Among the patient cohort, with the exception of one patient with a poorly differentiated tumor and four esophageal tumors which were not graded, all other esophageal tumors were moderately differentiated. To determine the importance of ECM proteins in ESCC, we determined the mRNA levels of several ECM proteins in primary esophageal cancer tumor tissue compared to normal tissue. Real time quantitative reverse transcription polymerase chain reaction (qRT-PCR) analysis of RNA extracted from matched ESCC patients' tumor and adjacent normal tissues, was performed. GAPDH was used as a normaliser. Our statistical analysis of the resultant data show that the expression of collagens, fibronectin and laminins was significantly upregulated in ESCC tumor tissues compared to the corresponding normal tissue (Figure 1A,B). Immunohistochemical staining of tumor and normal biopsy specimens using anti-type I collagen antibody showed significantly upregulated type I collagen in tumor specimens compared to normal biopsy specimens (Supplemental Figure S1A). The source of the ECM within the tumor microenvironment is both cancer cells and stromal cells including cancer-associated fibroblasts. Real time qRT-PCR analysis of RNA from normal fibroblasts (WI38, FG_0), transformed CT1 fibroblasts and several ESCC cell lines (WHCO1, WHCO5, WHCO6, KYSE 180, KYSE 450, KYSE 520) show that transformed CT1 fibroblasts express significantly higher ECM proteins than normal fibroblasts (Supplemental Figure S1B–D; Supplemental Figure S2A,B). ESCC cell lines express significantly lower ECM proteins, about 30–50%, compared to normal fibroblasts (Supplemental Figure S1B–D; Supplemental Figure S2A,B).

The tumor microenvironment is not constant, with levels of ECM proteins always fluctuating. Changes in the levels of ECM proteins within tumors can be brought about by matrix metalloproteases (MMPs). Among the MMPs, MMP1, MMP2, MMP9 and MT1-MMP produced by both stromal and tumor cells degrade and migrate through the ECM. Our data show significantly upregulated levels of MMP-1, MMP2, MMP3 and MMP9 mRNA in ESCC tumor tissues compared to the adjacent normal tissues (Figure 1C). Increased expression of ECM proteins might also be accompanied by the over-expression of their receptors, which are responsible for relaying extracellular cues between tumor cells and the tumor microenvironment. Indeed, integrins gene expression in the

clinical ESCC tumor tissues show significant higher levels of integrin α-1 (ITGA1), ITGA2, ITGA5 and ITGB1 mRNA compared to normal tissue from the same patient (Figure 1D).

Table 1. Clinicopathological characteristics of 21 ESCC samples from patients used in the study.

Biopsy Number	Histology	Sex	Age	Tumor Differentiation (Grade)	Tumor Site ICD-10	Invasive or Infiltrating
543	ESCC	M	55	ND	C15.4	Infiltrating
547	ESCC	F	30	Moderate	C15.5	Invasive
551	ESCC	M	47	Moderate	C15.5	Invasive
556	ESCC	F	54	Moderate	C15.4	Invasive
561	ESCC	M	58	Moderate	C15.9	Keratinizing
563	ESCC	M	52	Moderate	C15.5	Infiltrating
569	ESCC	F	79	Poor	C15.4	Invasive
571	ESCC	F	48	Moderate	C15.3	Keratinizing
573	ESCC	F	41	ND	C15.3	Infiltrating
591	ESCC	M	47	Moderate	C15.4	Invasive
596	ESCC	F	67	Moderate	C15.4	Invasive
601	ESCC	M	59	ND	C15.4	Infiltrating
607	ESCC	F	48	Moderate	C15.4	ND
613	ESCC	M	54	Moderate	C15.9	Invasive
618	ESCC	F	60	Moderate	C15.4	Keratinizing
619	ESCC	M	57	Moderate	C15.4	Infiltrating
621	ESCC	F	64	Moderate	C15.4	Invasive
622	ESCC	F	83	ND	C15.4	Infiltrating
627	ESCC	M	52	Moderate	ND	ND
634	ESCC	F	57	Moderate	C15.4	Keratinizing
635	ESCC	M	57	Moderate	C15.4	Keratinizing

ESCC: Esophageal squamous cell carcinoma; M: Male; F: Female; ND: Not done.

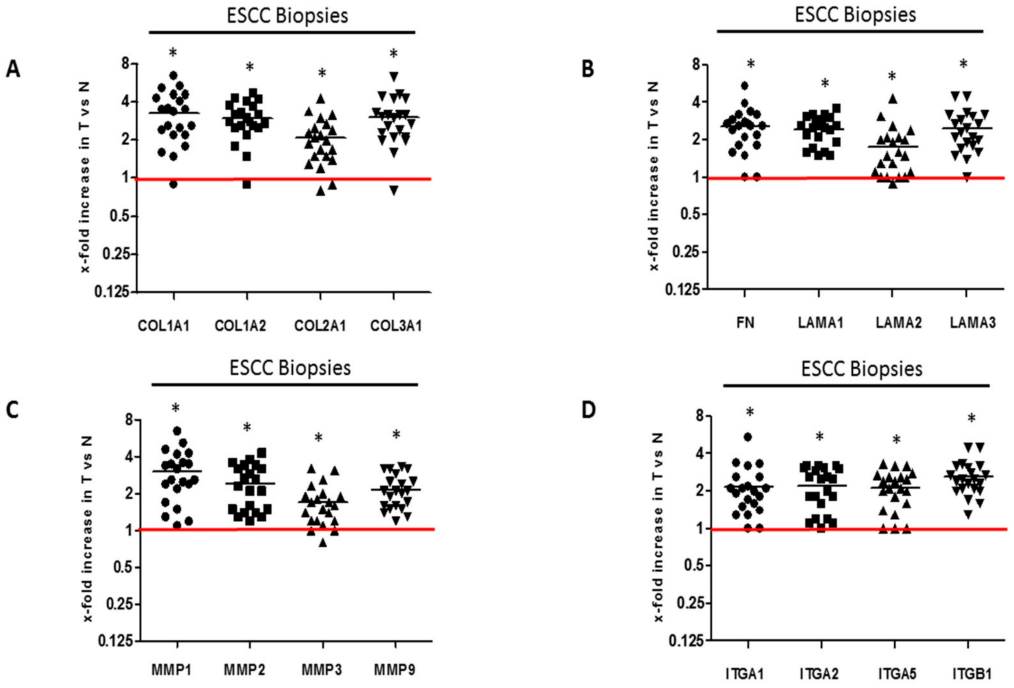

Figure 1. Gene expression profile of ECM proteins and associated proteins in ESCC samples: (**A**) qRT-PCR analysis of collagens mRNA expression in human ESCC samples; (**B**) Fibronectin and laminins mRNA expression in human ESCC samples. (**C**) qRT-PCR analysis of MMPs mRNA expressions in human ESCC samples; (**D**)'qRT-PCR analysis of integrins mRNA expression in human ESCC samples. Each ESCC tumor (T) mRNA was quantified relative to the corresponding normal sample (N) from the same patient, which is taken as one. GAPDH is the normaliser. Statistical analysis to determine significance difference of gene expression in tumor versus normal sample was done using a 2-tailed non-parametric Mann-Whitney test. * $p < 0.05$.

2.2. Detailed Analysis of Decellularised ECMs Used in the Study

Fibroblasts are the major stromal cell type responsible for ECM production and we previously utilised the fibroblast-derived ECM as a model to investigate cancer cell and mesenchymal stem cells interactions [88]. In the context of the tumor, fibroblasts within the tumor or surrounding the tumor are called cancer-associated fibroblasts. We utilised cell-derived 3D culture models involving plating ESCC lines on decellularised ECMs produced by transformed CT1 fibroblasts (fd-ECM), ESCC cell lines (cd-ECM) and a combination of transformed CT1 fibroblasts and WHCO1 cancer cells (combi-ECM) (Figure 2A). Our data show that the transformed CT1 fibroblasts express significantly more upregulated α-smooth muscle actin than normal fibroblasts WI38 and FG0 and show the spindle-shaped morphological features typical of CAFs found within tumors (Supplemental Figure S2C,D). We therefore used transformed CT1 fibroblasts, obtained by transforming WI38 fibroblasts through γ-radiation [91] as our "transformed fibroblasts". Transformed CT-1 fibroblasts produced an ECM (tfd-ECM) that is much more highly linearized than the ECM produced by WHCO1 cells (cd-ECM) and a mixture of CT-1 fibroblasts and WHCO1 cells (combi-ECM) (Figure 2A, right column). It is important to note that most synthetic and solubilised ECMs used in most experiments such as Matrigel and Fibronectin do not form a linearized ECM. This could have a huge impact on WHCO1 cancer cell response to drugs and probably mimic the in vivo ECM better than these purified ECMs.

In order to study cancer cell-ECM interactions, it is necessary to obtain a detailed composition of the decellularised ECMs. To analyse the composition of the tfd-ECM, cd-ECM and combi-ECM obtained after synthesis, we employed a proteomics pipeline using chromatography combined with tandem mass spectrometry (LC-MS/MS) to identify the peptides and proteins (Figure 2B). Our data showed that all decellularised ECMs generally contain similar ECM proteins and proteoglycans, with obvious differences in the quantities of ECM proteins and proteoglycans identified within tfd-ECM and combi-ECMs compared to cd-ECMs (Figure 2C; Supplemental Figure S3A–C). Mass spectrometric analysis identified well-known ECM proteins within the decellularised ECMs such as collagens, laminins and fibronectin (Table 2). As expected, tfd-ECM and combi-ECM showed higher amounts of ECM proteins such as type I collagen and fibronectin and glycoproteins than cd-ECM (Figure 2C).

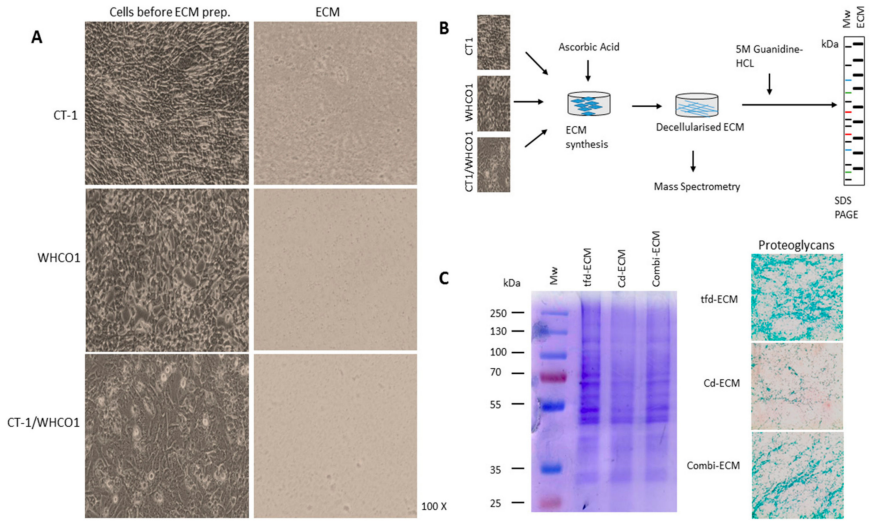

Figure 2. Characterisation of CT1 fibroblasts and WHCO1 cancer cells and their ECMs. (**A**) Phase contrast images of CT1 and WHCO1 cells prior to decellularization (left panel) and phase contrast microscopy of decellularised ECMs (right panel). Scheme of the ECM analysis workflow. Images were taken at 100× magnification. (**B**) Schematic representation of decellularised ECMs synthesis and analysis via SDS PAGE and mass spectrometry. (**C**) Representative image showing SDS PAGE and Coomassie Blue staining of decellularised ECMs (left panel). Representative Alcian Blue staining for proteoglycans in decellularised ECMs. Images were taken at 100× magnification.

Table 2. Major ECM proteins and associated entities identified in decellularised ECMs by mass spectrometric analysis.

Glycoproteins	Collagens	ECM Regulators	ECM Affiliated Proteins	Secreted Factors	Proteoglycans
			Gene Name		
FN1	*COL1A1*	*TGM2*	*LGALS1*	*S100A13*	*HSPG2*
LAMA3	*COL1A2*	*HTRA1*	*FREM2*	*EGFL7*	*BGN*
LAMA5	*COL6A3*	*CSTB*	*ANXA2*	*IGF2*	*DCN*
FBN1	*COL3A1*	*LOXL2*	*FREM1*	*S100A11*	*LUM*
TGFB1	*COL12A1*	*LOXL1*	*ANXA6*	*S100A6*	*ASPN*
TNC	*COL6A1*	*SERPINH1*	*ANXA5*	*S100A13*	*OGN*
EMILIN1	*COL4A2*	*CTSB*	*COLC12*	*CXCL12*	*PRELP*
LAMC1	*COL6A2*	*LOX*	*CLEC3B*	*CCL25*	*VCAN*
LAMB2	*COL4A5*	*ITH5*	*LGALS3*	*PF4*	
FBLN2	*COL4A4*	*ADAM10*	*LGALS8*	*FGF2*	
LAMA2	*COL5A2*	*ADAMTSL1*	*SEMA3C*	*INSL5*	
TNXB	*COL7A1*	*PLG*	*CLEC14A*	*ANGPTL2*	
POSTN	*COL11A1*	*PZP*	*ANXA9*	*S100A9*	
THBS1	*COL4A1*	*CTSK*	*ANXA1*		
FBN2	*COL5A1*	*ADAMTSL5*	*PLXDC2*		
FBLN1	*COL5A3*	*SERPINA1A*	*SFTPA1*		
LAMB3	*COL14A1*	*SERPINA3K*	*CSPG4*		
LAMA4	*COL16A1*	*PLOD1*	*SFTPD*		
AGRN	*COL18A1*				
FGB	*COL15A1*				
LAMC2					
VWF					
HMCN1					
LTBP4					

2.3. Decellularised ECMs Protect WHCO1 Cancer Cells from the Effect of Drugs

We sought to study the proliferation and migration of WHCO1 cancer cells on the underlying decellularised ECMs and to determine how the presence of the ECMs affect the response of WHCO1 cancer cells to chemotherapeutic drugs. Many drugs are used in ESCC chemotherapies, including cisplatin, 5-flurouracil and epirubicin. Cells were treated with 0.1% DMSO (control), cisplatin (M_W 300.05; CAS 15663-27-1; Sigma Aldrich, Steinheim, Germany), 5-fluorouracil (M_W 130.08 g/mol; CAS 51-21-8; Sigma Aldrich, Steinheim, Germany), epirubicin (M_W 579.98 g/mol; CAS 56390-09-1; Sigma Aldrich, Steinheim, Germany) at the indicated concentrations for different time periods. Drugs concentrations used were lower than half of reported and determined IC_{50} values, as determined by the MTT assay, as we were interested in studying the gene response of the WHCO1 cells to these chemotherapeutic drugs and not interested in actually killing the cells. IC_{50} values were measured in WHCO1 cancer cells over 24 h and were determined as the concentration of drugs needed to kill 50% of cells. As shown in Table 3, IC_{50} values for drugs were higher when cancer cells were plated on ECMs compared to plastic. No major morphological changes were observed between WHCO1 cancer cells plated on plastic and those plated on decellularised ECMs, with or without drugs (data not shown).

Table 3. Cytotoxicity quantification. Oesophageal cancer cells, WHCO1, were treated with drugs as indicated and the effect was evaluated by the MTT assay. The IC_{50} was determined as the concentration of drug needed to kill 50% of cells over 24 h treatment. Values of the IC_{50} are shown as mean ± S.D. of three independent determinations.

Drug	Plastic	tfd-ECM	cd-ECM	combi-ECM
Cisplatin (IC_{50} ± S.D. (μM))	18.5 ± 6.4	23.8 ± 3.2	22.4 ± 4.5	25.7 ± 3.2
5-FU (IC_{50} ± S.D. (μM))	14.1 ± 3.8	19.1 ± 2.6	20.6 ± 2.2	21.9 ± 1.8
Epirubicin (IC_{50} ± S.D. (μM))	12.8 ± 2.3	17.3 ± 4.5	18.5 ± 1.9	27.8 ± 5.3

With no drug present, there were no significant differences in cell proliferation between WHCO1 cells on plastic and those on decellularised ECMs (Figure 3A). Cisplatin caused a significant decrease in WHCO1 cell proliferation on plastic compared to those on the decellularised ECMs (Figure 3B).

The same trend is observed in WHCO1 cell proliferation in the presence of 5-fluorouracil and epirubicin (Figure 3C,D). The presence of the decellularised ECMs appears to protect WHCO1 cells and reduce the effect of drugs on WHCO1 cancer cell growth. The effect of drugs and ECMs on WHCO1 cancer cell doubling time is shown in Table 4. For the no-drug experiment, the doubling times are similar for both plastic and ECMs, whilst the doubling times for drug and ECMs are lower than those for plastic and drugs (Table 4). Immunoblot analysis substantiated these results with Ki67 and PCNA protein levels mostly upregulated in the presence of decellularised ECMs and drugs compared to plastic dishes and drugs (Figure 3A–D; Supplemental Table S1). Thus the ECMs reduce the effect of the chemotherapeutic drugs on WHCO1 cancer cell proliferation.

Table 4. Average esophageal cancer cells, WHCO1, population doubling times were calculated as described in Materials and Methods. Doubling times are presented as mean ± S.D of three independent determinations.

	Plastic	tfd-ECM	cd-ECM	combi-ECM
No Drug (hours)	33.6 ± 3.3	38.6 ± 5.7	37.1 ± 4.2	36.8 ± 4.5
Cisplatin (hours)	55.3 ± 9.4	39.5 ± 4.3	36.9 ± 3.8	36.7 ± 5.8
5-FU (hours)	56.2 ± 5.1	39.5 ± 3.6	32.6 ± 4.6	31.9 ± 3.8
Epirubicin (hours)	58.3 ± 2.5	34.7 ± 3.5	30.7 ± 4.9	32.1 ± 3.8

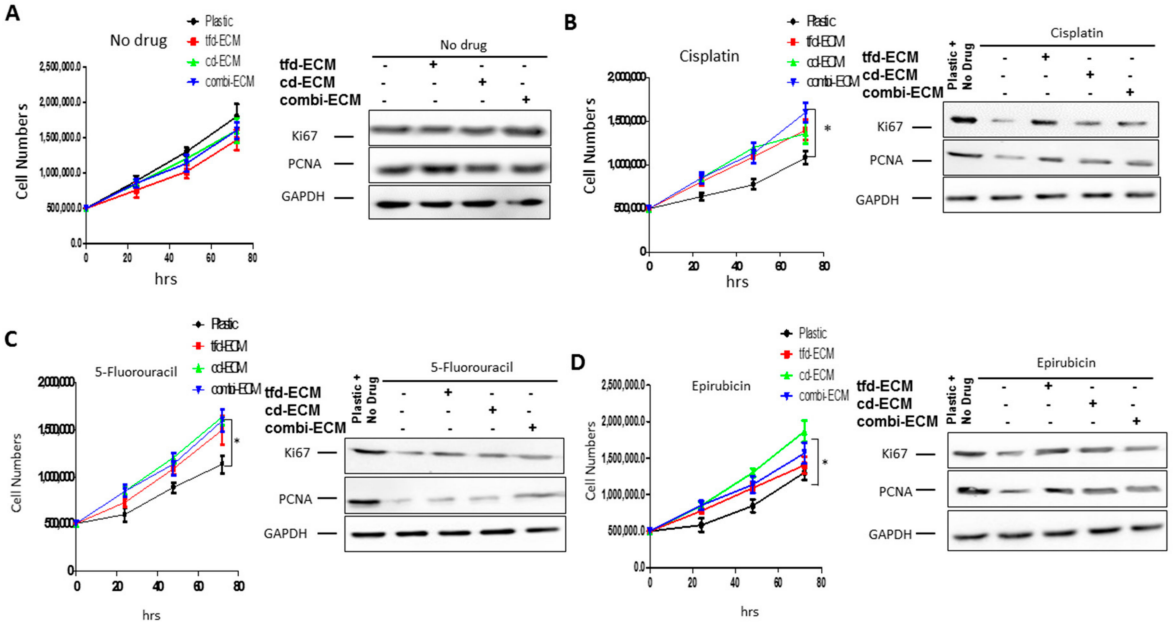

Figure 3. Effect of decellularised ECMs on WHCO1 cancer cell proliferation in response to cisplatin, 5-fluorouracil and epirubicin. WHCO1 cancer cells were cultured on plastic and on ECMs and treated with drugs as indicated for 24 h. Cell counting was done using the Countess Cell Counter. Total proteins (50 µg) were loaded on SDS PAGE gels and immunoblot analysis performed. (**A**) Effect of decellularised ECMs on WHCO1 cancer cell proliferation in the absence of drugs. (**B**) Effect of decellularised ECMs on WHCO1 cancer cell proliferation in response to cisplatin. (**C**) Effect of decellularised ECMs on WHCO1 cancer cell proliferation in response to 5-fluorouracil (**D**) Effect of decellularised ECMs on WHCO1 cancer cell proliferation in response to epirubicin. Data show cell counting (left panel) and immunoblot analysis (right panel). * $p < 0.05$.

2.4. Decellularised ECMs Reduce Drug-Induced Cell Cycle Arrest and Apoptosis in WHCO1 Cancer Cells

An assessment of the influence of decellularised ECMs on the effect of chemotherapeutic drugs on WHCO1 cell cycle progression and apoptosis by flow cytometry was done. With no drug present, our data indicate that the cell cycle profiles between cells on the ECMs compared to cells on plastic

are the same (Figure 4A; Supplemental Table S2). Addition of cisplatin caused a G2 phase cell cycle arrest in WHCO1 cells on plastic which was abrogated by the culture of cells on decellularised ECM, with cd-ECM and combi-ECM reducing drug effect more than the tfd-ECM (Figure 4A; Supplemental Table S2). Addition of 5-flurouracil resulted in G1 phase cell cycle arrest and this effect is reduced by the presence of decellularised ECMs with WHCO1 cells cultured on combi-ECM having similar profiles as cells cultured on plastic with no drug present (Figure 4A; Supplemental Table S2). Epirubicin induced a G2 phase cell cycle arrest in WHCO1 cells on plastic and this is slightly abrogated by the presence of combi-ECM (Figure 4A; Supplemental Table S2). Immunoblot analysis of cell cycle-associated proteins show increased cyclin D1 protein levels in the presence of drugs in WHCO1 cells cultured on ECMs compared to those on plastic (Figure 4B; Supplemental Table S3).

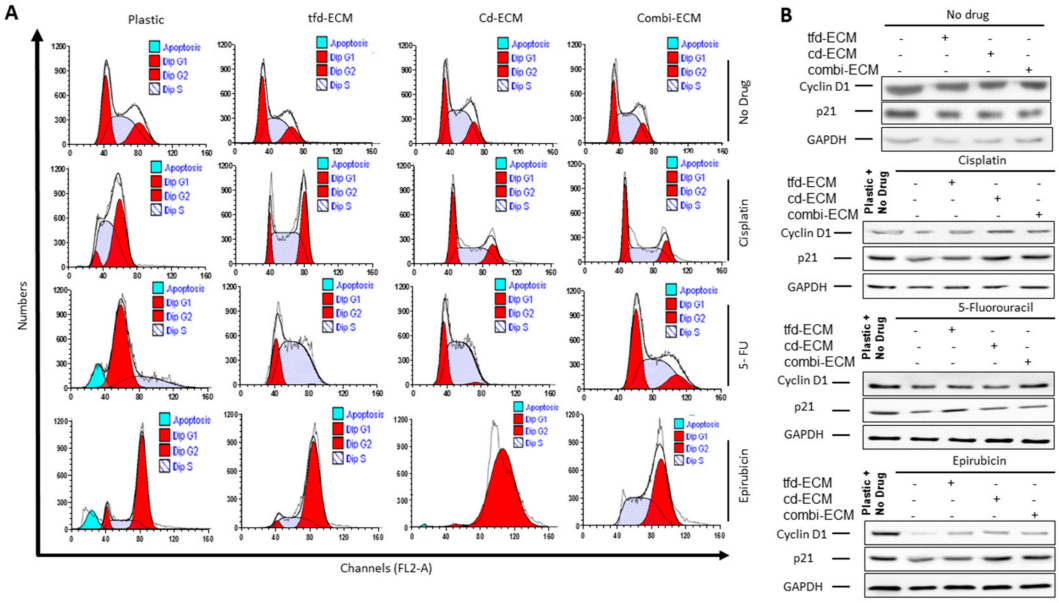

Figure 4. Decellularised ECMs abrogate drug-induced cell cycle arrest in WHCO1 cancer cells. (**A**) Effect of decellularised ECMs on WHCO1 cancer cell cycle progression in the presence of cisplatin, 5-fluorouracil and epirubicin. (**B**) Effect of decellularised ECMs on Cyclin D1 and p21 protein levels in WHCO1 cancer cells in response to the presence of cisplatin, 5-fluorouracil and epirubicin.

To determine whether the observed protective effect of the decellularised ECMs on WHCO1 cells was due to inhibition of apoptosis, cellular apoptosis was evaluated by Annexin V/Propidium Iodide double staining followed by flow cytometry. Culture of WHCO1 cells on decellularised ECMs reduced the number of apoptotic cells in the presence of drugs compared to cells grown on plastic (Figure 5A, shown in Q2 + Q3). Immunoblot analysis of anti-apoptotic proteins such as Bcl-2 and Bcl-xL showed an upregulation of these proteins in the presence of decellularised ECMs (Figure 5B; Supplemental Table S4). Culture of WHCO1 cells on decellularised ECMs in the presence of drugs resulted in more colonies being formed than those cultured on plastic in the presence of drugs (Figure 6A,B). A key subpopulation of tumor cells that has been found to play important roles in chemoresistance is the cancer stem cell population. We isolated cancer stem cell-like cells from cancer cells via the side population technique (Supplemental Figure S4A). We found that isolated CSC-like cells formed more colonies on ECMs and when challenged with drugs than normal cancer cells. (Supplemental Figure S4A–D). Thus, decellularised ECMs appear pro-tumorigenic.

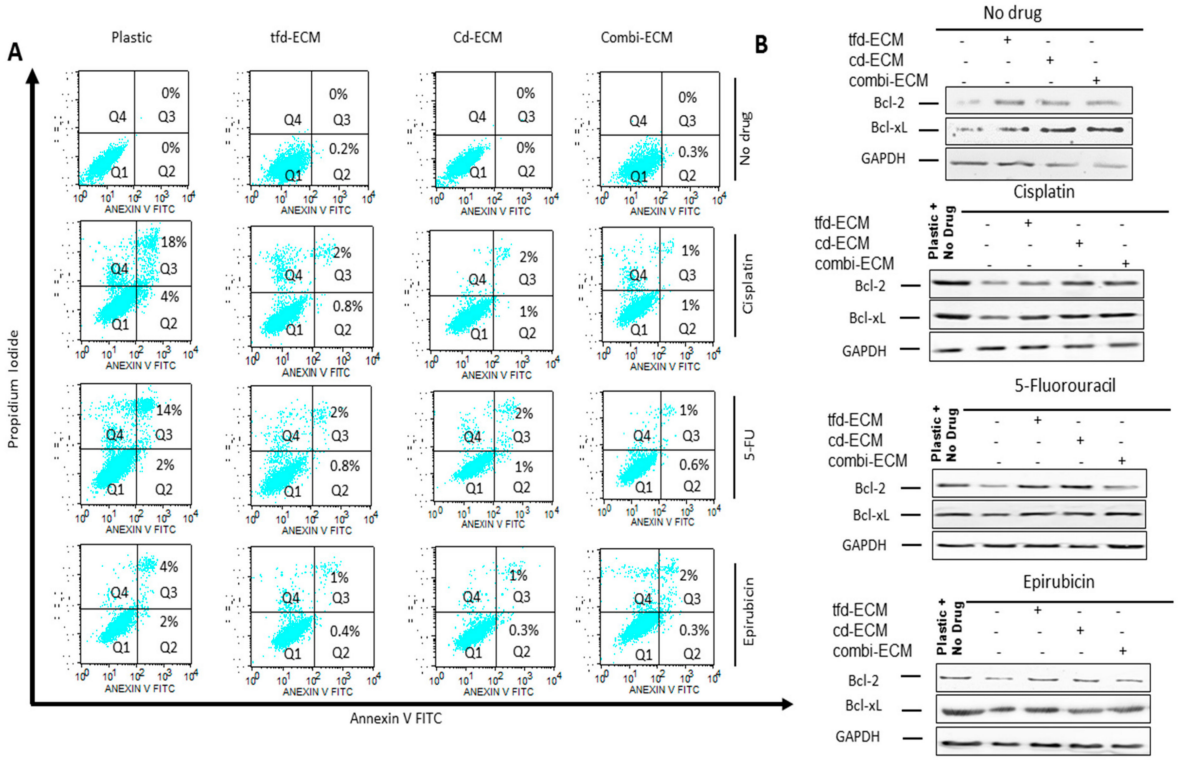

Figure 5. Decellularised ECMs reduce drug-induced apoptosis in WHCO1 cancer cells. (**A**) Effect of decellularised ECMs on drug-induced apoptosis in WHCO1 cancer cells (% apoptotic cells shown in quadrant Q2 and Q3). (**B**) Effect of decellularised ECMs on Bcl-2 and Bcl-xL protein levels in WHCO1 cancer cells in response to the presence of cisplatin, 5-fluorouracil and epirubicin.

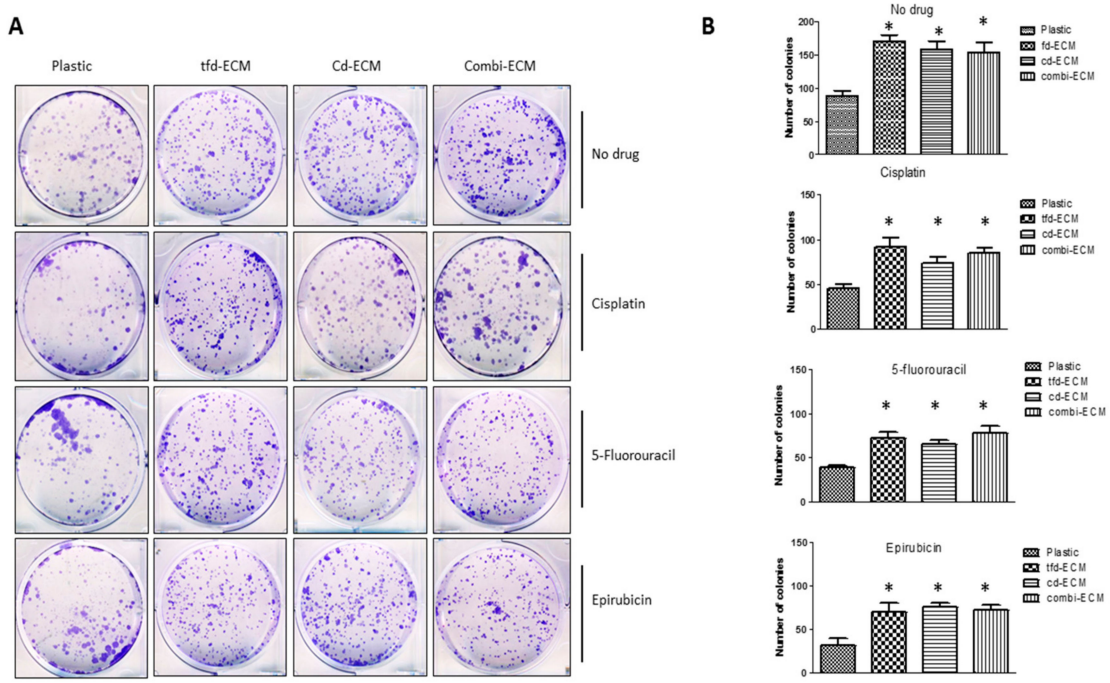

Figure 6. Decellularised ECMs reduce the effect of drugs on WHCO1 cancer cell colony formation. (**A**) Representative images of colony formation assay that was performed using WHCO1 cells cultured on either plastic or ECMs in the presence of cisplatin, 5-fluorouracil or epirubicin. (**B**) Quantification of colonies formed when WHCO1 cells were cultured either on plastic or ECMs in the presence of cisplatin, 5-flurouracil or epirubicin. * $p < 0.05$.

2.5. Decellularised ECMs Upregulates Several Survival Pathways in WHCO1 Cancer Cells

Cell surface adhesion receptors mediate most cancer cell-ECM interactions. These adhesion molecules are also responsible for transmitting extracellular initiated signaling to the cell. The levels of integrin α2, α3, α11 and β1 were assessed using immunoblot analysis. Decellularised ECMs and chemotherapeutic drugs caused differential integrin gene expression in WHCO1 cells (Figure 7A–D; Supplemental Table S5) with integrin α2 and α3 mostly upregulated compared to those on plastic and treated with drugs. These integrins are known to bind to several ECM proteins such as laminin, fibronectin, type I collagen, vitronectin and tenascin. The ECM is known to influence cellular behaviour through adhesion signaling. In addition, signal transduction pathways can be triggered by integrins resulting in the activation of several pathways affecting cancer cell proliferation, gene expression and invasion. To unravel the signaling pathways activated in cancer cells cultured on the ECMs and in response to the presence of drugs, we analysed the MEK-ERK and PI3K signaling pathways. Our data showed decellularised ECM-mediated upregulation of the MEK-ERK signaling pathway irrespective of the presence of drugs (Figure 8A–D; Supplemental Table S6). The PI3K-Akt pathway appears activated only in the presence of drugs. This is expected as PI3K-Akt signaling is one of the major survival pathways, likely activated as cancer cells respond to the presence of drugs.

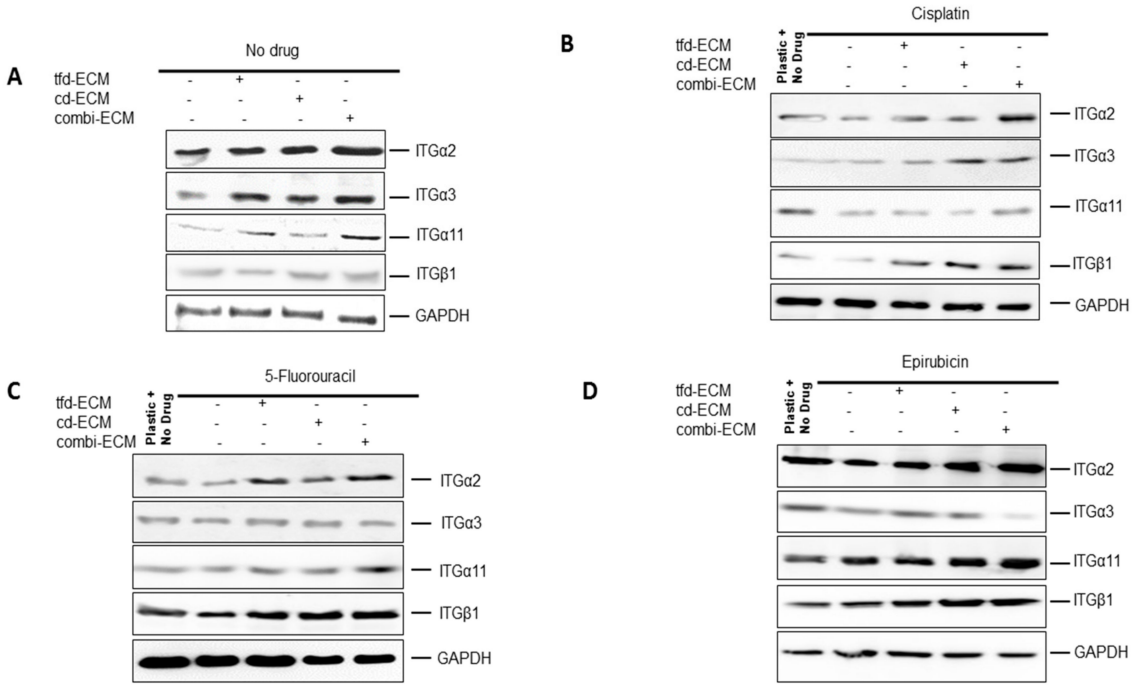

Figure 7. Increased integrin expression in WHCO1 cancer cells cultured on ECMs in comparison with those cultured on plastic. (**A**) Effect of decellularised ECMs on integrin α2, α3, α11 and β1 protein expression in the absence of drugs. (**B**) Effect of decellularised ECMs on integrin α2, α3, α11 and β1 protein expression in the presence of cisplatin. (**C**) Effect of decellularised ECMs on integrin α2, α3, α11 and β1 protein expression in the presence of 5-fluorouracil. (**D**) Effect of decellularised ECMs on integrin α2, α3, α11 and β1 protein expression in the presence of epirubicin GAPDH which was used as a loading control. Experiments were performed in triplicates and repeated twice.

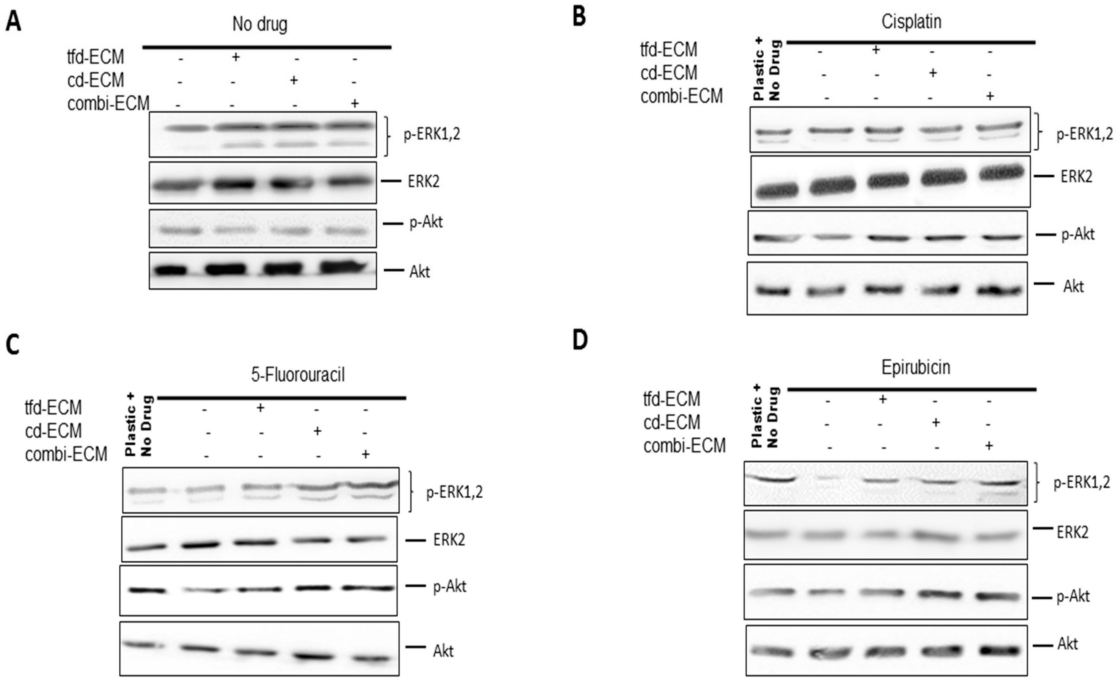

Figure 8. Decellularised ECMs increase both MEK-ERK and PI3K-Akt signaling activation (**A**) Influence of decellularised ECMs on MEK-ERK and PI3K-Akt signaling activation in the absence of drugs. (**B**) Influence of decellularised ECMs on MEK-ERK and PI3K-Akt signaling activation in the presence of cisplatin. (**C**) Influence of decellularised ECMs on MEK-ERK and PI3K-Akt signaling activation in the presence of 5-fluorouracil. (**D**) Influence of decellularised ECMs on MEK-ERK and PI3K-Akt signaling activation in the presence of epirubicin.

2.6. Type I Collagen and Fibronectin Play Key Roles in WHCO1 Cancer Cell Survival and Migration In Vitro

Several studies have shown that ECM proteins are involved in the survival, migratory behaviour and the invasiveness of cancer cells. Chief among these ECM proteins are type I collagen and fibronectin. This study show that type I collagen and fibronectin are major decellularised ECM proteins and are upregulated in ESCC patient samples. Our immunohistochemical staining of ESCC samples, qRT-PCR and mass spectrometric analysis of ECMs unequivocally showed the presence of high levels of type I collagen and fibronectin. To study the role that ECM proteins play in cancer cell migration, we performed transient type I collagen and fibronectin knockdowns in transformed CT1 fibroblasts and WHCO1 cancer cells during ECM synthesis using two siRNA for each ECM protein. Both type I collagen and fibronectin knockdown through the use of siRNA showed decreased levels of both collagen and fibronectin in the media and cell lysates compared to control in transformed CT1 fibroblasts and WHCO1 cells (Supplemental Figure S5A,B).

Type I collagen and fibronectin knockdown did not affect either fibroblasts or WHCO1 cell proliferation and morphology (data not shown). Beside the use of siRNA, the absence of ascorbic acid achieved the same knockdown of Type I collagen (data not shown). Drug-induced apoptosis is higher in cells cultured on collagen- and fibronectin-deficient ECMs than on normal decellularised ECMs (Figure 9A). Anti-apoptotic proteins such as Bcl-2 and Bcl-xL are downregulated in the absence of type I collagen and fibronectin (Figure 9B; Supplemental Table S7). Knockdown of type I collagen and fibronectin combined with challenging the cells with cisplatin resulted in less colony formation compared to cells on normal ECMs (Supplemental Figure S5C). WHCO1 cells plated on normal ECMs migrated further than those on plastic and those plated on collagen-deficient ECMs migrated slower than those on normal ECMs (Supplemental Figure S6A,B). The addition of anti-α2 blocking antibody in combination with type I collagen knockdown synergistically reduced WHCO1 cancer cell migration on combinatorial-ECM (Supplemental Figure S6C). Knockdown of fibronectin reduced migration of

WHCO1 cells by around 30–50% (data not shown). This study suggests that ECM proteins such as collagen and fibronectin are mediators of cancer cell survival and migration. These results, together with the observation that WHCO1 cancer cells plated on decellularised ECMs express increased levels of both fibronectin- and type I collagen-binding integrins (ITGα2, ITGα3, ITGα5 and ITGβ1), point to the matrix as a possible therapeutic target for drugs to inhibit cancer cell growth and metastasis. Collectively our data suggest that knocking down certain ECM proteins may be effective in suppressing cancer development and enhancing chemotherapeutic effects.

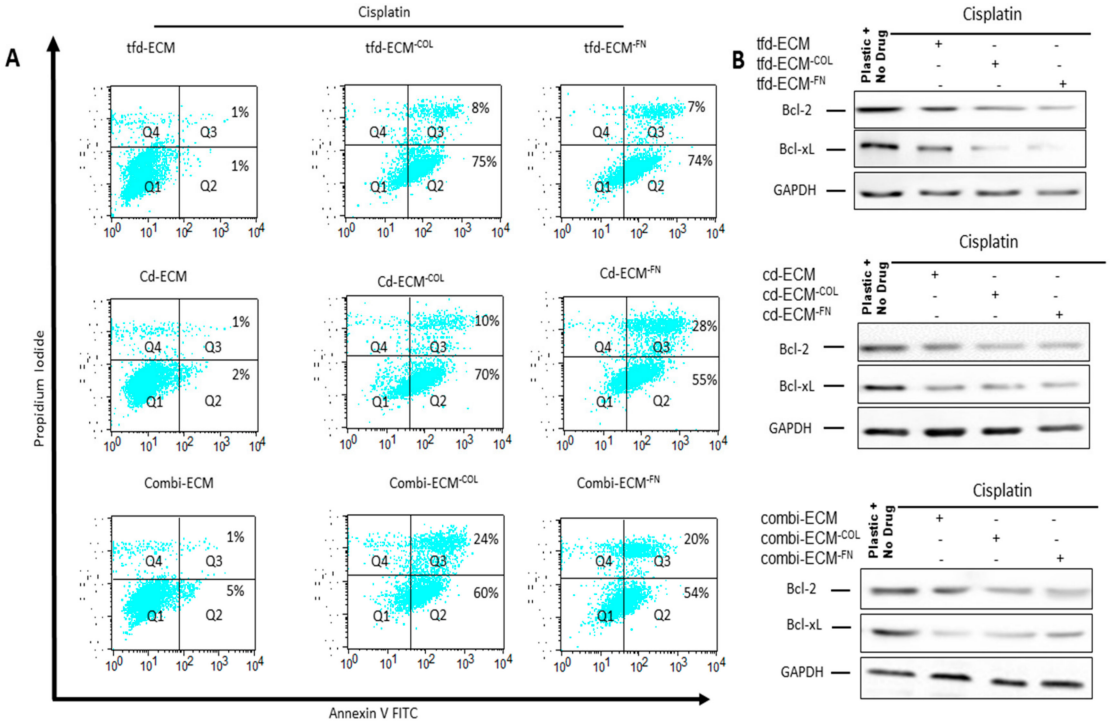

Figure 9. Collagen and fibronectin knockdown increase cisplatin-induced apoptosis. (**A**) Effect of collagen- and fibronectin-deficient ECMs on cisplatin-induced apoptosis in WHCO1 cancer cells (percentage of apoptotic cells shown in quadrant Q2 and Q3). (**B**) Effect of collagen- and fibronectin-deficient ECMs on Bcl-2 and Bcl-xL protein levels in the presence of cisplatin.

3. Discussion

It has now been established that the tumor microenvironment plays a huge role in determining the initiation and progression of cancer [9,11,14,38,72,75–77,88,92,93]. The tumor microenvironment is a dynamic and ever-changing environment comprised of many components including cancer cells, fibroblasts, immune cells, endothelial cells and the ECM [38,46,47,94–98]. Cancer-associated fibroblasts or tumor-associated fibroblasts (CAFs or TAFs) are the major cellular component of this environment and they play a role in modulating cancer progression [99–102]. Accumulating evidence suggests that CAFs play a crucial role in tumor development and metastasis by synthesising ECM proteins. Targeting CAFs is hindered by the fact that CAFs are heterogeneous, with different subpopulations having specific phenotypes and roles during tumor development and metastasis [103,104]. Thus, targeting CAFs is challenging. Targeting the ECM proteins synthesised by resident cells within the tumor microenvironment might be an effective method to control cancer development, chemoresistance and metastasis. However, to date, few studies have included important components of the tumor microenvironment such as the ECM in their experimental setup to evaluate the interactions between cancer cells and the tumor microenvironment ECM.

In our bid to identify potential therapeutic targets within the ESCC tumor microenvironment, we evaluated how ECM components would affect the response of WHCO1 esophageal cancer cells

to drugs. The first key finding of this study is that ECM proteins such as collagen and fibronectin play important roles in esophageal cancer cell survival, migration and chemoresistance. Importantly, these two ECM proteins are upregulated in esophageal tumor compared to normal tissue. The increased expression of ECM proteins including collagens, fibronectin and laminins in tumor biopsies is in contrast to the decreased expression of these ECM proteins by esophageal cancer cell lines. Thus, the increased expression of ECM proteins in tumor biopsies could be from both cancer cells and stromal cells known to be present in tumors. Several studies have shown that cancer-associated fibroblasts and macrophages synthesise increased levels of ECM proteins and these ECM proteins are associated with poor prognosis and chemoresistance in several cancer types [18,79,105–112]. Our data is in agreement with these recent studies illustrating the important role the ECM plays in the tumor microenvironment and in chemoresistance. Indeed, ECM proteins such as collagen and fibronectin have been associated with cancer cell migration before [79,113–122]. Our data show that knockdown of both collagen and fibronectin reduces esophageal cancer cell survival, migration and chemoresistance. Our data also show that MMP2 and MMP9 play a huge role in the migration of cancer cells. Several integrins were also found to be upregulated in tumor samples compared to normal samples. These ECM proteins, among other proteins, are potential chemotherapeutic targets. Several of these ECM proteins have been associated with survival pathways such as the MEK-ERK and Akt [79,123–126]. We have to appreciate that tumors are real ecosystems harbouring several cell types and non-cellular components such as the ECM. Our data suggest that the microenvironment is a shelter for cancer cells and aid their resistance to chemotherapy. Thus, the microenvironment plays a huge role in the development of chemoresistance.

Our analysis of the ECM proteins and integrins present in the stroma of the ESCC advance our understanding of the ESCC stroma and will allow future studies to focus on these proteins. The development of ESCC involves changes in the type and origin of the ECM present. Through the use of these cell-derived 3D ECMs we show that differences in the composition of different cell-derived ECMs and how this affects cancer cell response to chemotherapeutic drugs. Many features of the in vivo tumor microenvironments have been studied with many 3D tumor models having been made [127–133]. These models have attempted to include ECM proteins, cancer and stromal cells with the relevant biochemical and biophysical cues, into one system [2,3,90,93,134,135]. Many studies have been undertaken and have decisively shown that cells such as fibroblasts and mesenchymal stem cells are important contributors to cancer cell growth and possibly chemotherapeutic resistance [1,7,13,20,88,136,137]. Very few studies however have focused on the role the extracellular matrix play in chemotherapeutic resistance. The development of anti-stromal treatment, especially those targeting the stable ECM, which can be used together with chemotherapy, is a major advance in the treatment of several cancers.

3D ECM models have advanced our understanding of how cells interact with each other and with the ECM during tumor growth and invasion. These models have shown that cells in 3D environments show different cellular morphology and gene expression compared to those in 2D environments [9,20,88,90,93,134]. Cancer cells on 2D surfaces are normally exposed to uniform environments and concentrations of chemotherapeutic drugs whereas cells in 3D environments are exposed to gradients of biological signals and drug concentrations. Anti-cancer drugs added to cancer cells on 2D surfaces reach cancer cells without encountering physical barriers whereas cancer cells in vivo are surrounded by many tumor components and this restricts the movement of cancer drugs throughout the tumor. Earlier studies have shown that MDA MB 231 cells in 3D silk fibroin scaffolds require a higher drug dosage compared with the same cells on 2D cultures [138]. Ovarian cancer cells also show increased chemoresistance when grown as 3D spheroids compared to 2D culture [139–142]. It has now been established that 3D scaffolds generally better imitate the in vivo tumor microenvironment necessary for modelling cancer cell-ECM interactions and also for cancer cell-drug screening assays [136,143–147]. The interaction between cancer cells and their surrounding microenvironment plays a significant role in the acquisition of drug resistance in many cancers. The present study shows that besides physically inhibiting drugs from accessing

cancer cells, the decellularised ECMs can upregulate anti-apoptotic genes such as Bcl-2 and Bcl-xL. The upregulation of these genes could be an adaptation mechanism employed by cancer cells in new environments. Thus, the decellularised ECMs influence cellular biological processes.

Our study utilised natural decellularised ECMs instead of purified ECM proteins in a bid to better mimic the in vivo tumor microenvironment [148]. In drug discovery, decellularization of cell-derived ECMs and tissues has been used as an important tool to study the interactions between the ECM and cells [18,149,150]. Done properly, decellularization can be used to successfully preserve the biochemical composition of the ECM and native tissues. By combining both cancer cells and fibroblasts we hope this will best represent the ECM milieu present in the tumor microenvironment. In addition, we also evaluated how the different ECMs affect the WHCO1 esophageal cancer cells response to commonly used drugs cisplatin, 5-fluorouracil and epirubicin. To profile early transcriptional gene expression changes, less than half of the reported IC_{50} concentrations of the drugs were used. Cisplatin is known to interfere with DNA replication, which kills mostly cancer cells as they are fast growing cells. Cisplatin-induced DNA damage activates several cellular processes culminating in the activation of cell cycle checkpoints. This results in the induction of G2/M cell cycle arrest. Our data is in agreement with literature in showing that cisplatin induces G2/M cell cycle arrest. 5-Fluorouracil is known to mediate apoptosis and induce G1/S cell cycle phase arrest. Again, our data is in agreement with this. Epirubicin acts by intercalating DNA strands and has been reported to cause both G1 and G2/M cell cycle arrest. Several reports including those using the same concentration of epirubicin as we did in this study, have shown that epirubicin induces G1 and G2/M cell cycle arrest. Our data show that epirubicin induces G2/M cell cycle arrest in WHCO1 cells. That the tumor microenvironment and the ECM are as important as the genotype of cells is becoming clearer with recent data showing the importance of the ECM in breast cancers [151–157]. The three ECMs used in this study were observed to be able to promote or induce resistance to chemotherapeutic drugs in esophageal cancer cell lines. It is possible that in vivo many components of the tumor microenvironment act synergistically to induce resistance to drugs and enable cancer cells to growth. That the microenvironment plays a huge role in the development of cancer might explain why certain individuals are cancer-free yet harbour oncogenic mutations. The dynamics of the relationship between cancer cells and their microenvironment will determine whether oncogenic genes and mutations will exert their function.

It has also been shown that integrin signaling driven by cell-matrix adhesion play a huge role in the development of resistance against chemotherapy-induced apoptosis and that a combination of integrin signaling inhibition and chemotherapy can lead to an improvement in cytotoxic response [158–169]. It has been shown that the interaction between ECM proteins and integrins can enhance the resistance of multiple myeloma and small cell lung cancer cells to chemotherapy [170,171]. Blocking of integrins such as β1 has been shown to sensitise breast cancer cells to treatment [172–179]. Binding of integrins to the ECM has been show to influence cell cycle progression. Several studies have shown that the binding of integrins to the ECM influence DNA repair mechanisms, with binding causing increased DNA damage repair, leading to a stable genome and cellular survival [180–182]. Previous studies have shown that fibroblasts-secreted type I collagen, often upregulated in tumor microenvironments, can decrease chemotherapeutic drug uptake in cancer cells thus affecting the response of the cancer cells to the drugs [183,184]. Upregulation of fibronectin was found to increase human ovarian cancer cell migration and invasion [185–187]. Several studies have shown that the presence of fibronectin promotes therapeutic reagents resistance in vitro [158,159,188,189]. Indeed, these studies have shown the mechanisms through which fibronectin influence carcinogenesis and chemoresistance. The source of these ECM proteins could be both tumor cells and stromal cells present within the tumor microenvironment. Small peptides that directly target the biosynthesis of ECM proteins such as fibronectin have been developed [190]. When cancer cells adhere to certain ECM proteins it has been shown they acquire chemoresistance through activation of certain survival pathways [191–194].

Our data show that the MEK-ERK and the PI3K/Akt pathways were significantly upregulated when WHCO1 cells were cultured on the different ECMs. In the presence of cisplatin, however,

the MEK-ERK signaling pathway remained significantly upregulated in WHCO1 cells plated on all ECMs compared to plastic. In the presence of 5-flurouracil and epirubicin, both MEK-ERK and PI3K/Akt remained upregulated in the WHCO1 plated on the ECMs compared to plastic. Many signaling pathways such as PI3K/Akt, MEK-ERK, and the Rho/ROCK pathways have been shown to be activated when cancer cells bind to the ECM [191,195–198]. The activation of these signaling pathways could be a result of growth factors tethered on the ECMs. In breast cancer it has been shown that resistance to 5-flurouracil, epirubicin and cyclophosphamide is largely dependent on the protein composition of the stromal ECM [199]. Several cell cycle-associated proteins such as cyclin D1 are known to be induced through the activation of the MEK-ERK and PI3K-Raf signaling pathways. The activation of these Ras-mediated pathways induce the transcription of proteins such as cyclin D1 and protect it from proteolytic degradation and also export from the nucleus. Our data show the activation of the MEK-ERK and PI3K-Raf signaling pathways in the presence of ECMs. Thus, cyclin D1 might be protected from degradation by the same pathways, resulting in its presence through the G1/S/G2 cell cycle phases. The consequential effect being the protection of WHCO1 cancer cells plated on ECMs from drug-induced apoptosis as opposed to those on plastic.

Therapies that target the ECM provide a promising approach to overcome chemoresistance either by preventing ECM-conferred chemoresistance or by altering the ECM such that current therapies can overcome physical treatment limits [200–204]. It has been shown that the dense ECM can inhibit therapeutic drug penetration, diffusion and transport, thus the ECM acts as a barrier to drug delivery [205–211]. A key finding of this study is that treatments that inhibit some ECM components production such as fibronectin and type I collagen can help to achieve better drug delivery. In our study, the ECM is clearly acting as a limiting factor on drug effectiveness and we suggest combination therapy for cancer patients with one drug targeting the ECM components to aid in the diffusion of cancer drugs. Future studies should use larger patient cohorts to strengthen the results. In conclusion, we have advanced our understanding of cancer cell-ECM interaction through identifying that both type I collagen and fibronectin are involved in the proliferation and migration of esophageal cancer cells and that knocking down these two proteins can act in synergy with chemotherapeutic drugs in reducing the growth and migration of cancer cells.

4. Materials and Methods

4.1. Clinical Tissue Collection

Twenty-one ESCC biopsy samples were collected over a period of 3 years at Groote Schuur Hospital, Cape Town, South Africa. All patients attended the oncology clinic of Groote Schuur Hospital. The biopsy samples were confirmed to be squamous cell carcinomas by a pathologist. Histological parameters were determined according to the World Health Organisation criteria. Each ESCC biopsy sample was taken together with corresponding adjacent normal tissue sample. Ethical approval was obtained from the University of Cape Town/Groote Schuur Hospital Human Research Ethics Committee (University of Cape Town, South Africa) and informed consent was obtained from all patients according to institutional guidelines. All procedures were done according to the Declaration of Helsinki guidelines. Patient biopsy samples in RNAlater solution (Qiagen, Hilden, Germany) were stored at −80 °C. RNA extraction was done as described elsewhere in the manuscript. Clinicopathological characteristics of the ESCC patients are shown in Table 1. The inclusion criteria used for tumor samples required tumor samples to contain at least 50% tumor cells.

4.2. Esophageal Cancer Cell Lines and Treatments

WHCO1, WHCO5 and WHCO6 cell lines were derived from biopsies of ESCC from South African patients [212]. KYSE180, KYSE450 and KYSE520 cell lines were derived from biopsies of ESCC from Japanese patients [213]. CT-1 fibroblasts are transformed fibroblasts obtained after WI38 fibroblasts are γ-radiated [91]. WI38 fibroblasts were obtained from American Type Culture Collection (USA).

FG_0, a normal skin fibroblasts were from the University of Cape Town. Cells were cultured in vitro at 37 °C in Dulbecco's Modified Eagle's Medium (DMEM) supplemented with 10% (*v*/*v*) fetal bovine serum (FBS), 100 U/mL penicillin and 100 µg/mL streptomycin (complete media). All cells were routinely tested for mycoplasma contamination. Preliminary data showed that the use of drug IC_{50}: 5-fluorouracil (14.1 ± 3.8 µM), cisplatin (18.5 ± 6.4 µM) and epirubicin (12.8 ± 2.3 µM) would kill a considerable amount of the cells. The IC_{50} was determined as the concentration of drug needed to kill 50% of cells over 24 h. Since we were interested in investigating early transcriptional gene expression leading up to apoptosis and the response of cancer cells to chemotherapeutic drugs, we treated the cells with less than half of the reported IC_{50}. WHCO1, WHCO5, WHCO6, KYSE180, KYSE 450 and KYSE 520 cells were grown overnight on plastic and on ECMs at the specified density and treated with the following concentrations of drugs: 3.5 µM 5-fluorouracil; 4.2 µM cisplatin, 2.5 µM Epirubicin and 0.1% DMSO (control) [214].

4.3. Preparation of Decellularised ECMs and ECM Coatings

Decellularised ECMs were prepared from transformed CT-1 fibroblasts and WHCO1 esophageal cancer cells as previously described [20,87,90,215]. All cells were cultured at 37 °C in complete media. Ascorbic acid was added at a final concentration of 50 µg/mL every alternate day. Cells were maintained up to 4 days post confluence. Decellularization was achieved by the addition of 20 mM ammonium hydroxide for 1 min. The ECMs were incubated for an hour with DNAse I (10 U/mL). The resulting ECMs were washed three times with sterile PBS. Sterilisation was achieved by exposing the dishes to UV light. Dishes coated with decellularised ECMs were used immediately or stored at 4 °C. Transformed CT1 fibroblasts produced transformed fibroblast-derived ECM (tfd-ECM), WHCO1 cancer cells produced cancer-derived ECM (cd-ECM) and co-cultured transformed CT1 fibroblasts and WHCO1 cancer cells produced combinatorial ECM (combi-ECM). Decellularised ECMs without fibronectin (ECM^{-FN}) and without Type I collagen (ECM^{-COL}) were produced by transfecting transformed CT-1 fibroblasts and WHCO1 cells with either fibronectin siRNA or COL1A1 siRNA during ECM synthesis. To maintain the knockdown of type I collagen and fibronectin during ECM synthesis, subsequent transfection of cells with fibronectin siRNA and COL1A1 siRNA was done after 3 days. To characterise the ECMs, 5 M Guanidine-HCL in buffer was added to the ECM solution and the resulting protein was run on a SDS-PAGE for an hour. Total protein was stained with Ponceau stain and Coomassie stain. Human fibronectin and type I collagen were also loaded to serve as markers.

4.4. Cell Cytotoxicity Assay

Cell growth curves or proliferation rates after plating WHCO1 on decellularised ECMs and/or treatment with cisplatin, 5-fluro-uracil and epirubicin drugs were determined using the Countess Counter (Thermo Fisher Scientific, Waltham, MA, USA). WHCO1 cells (5×10^5) were plated on the decellularised ECMs and/or treated with the drugs for the indicated time periods. Cells were trypsinised and centrifuged at 1800 rpm for 5 min. Cells were suspended in 2 mL complete media and 10 µL was mixed with Trypan Blue. In addition, WHCO1 cells were plated in 96-well plates with or without the ECMs and allowed to grow for about 48–72 h in either drug-free medium or under treatment with increasing concentrations of cisplatin, 5-fluro-uracil and epirubicin drugs. The IC_{50} for each cell population was measured using the MTT assay. Briefly, WHCO1 cells were plated in 96-well plates with or without ECMs overnight. Drugs were added and incubation continued for 24 h. The MTT reagent was added and the cells were shaken. Colour changes were read on a microplate reader.

WHCO1 cancer cell doubling time (PD) is the time it takes the population of WHCO1 cells to double and was calculated based on the following formula:

$$PD = t \times \ln 2 / \ln (FCC/SCC)$$

where t equals time in hours, ln represents the natural logarithm, FCC represents the final WHCO1 cancer cell number, and SCC represents the starting WHCO1 cancer cell number.

4.5. Quantitative Real Time RT-PCR

Fresh ESCC biopsy specimens were cut into pieces for RNA extraction using the Qiazol reagent (BioRad, Munich, Germany) and the quality of the RNA was checked by electrophoresis on a 2% agarose gel. For in vitro experiments, WHCO1 cells were treated as described above and RNA was extracted using Qiazol reagent based on the procedure of Chomczynski and Sacchi [216]. Total RNA (100–500 ng) was used to synthesise complementary DNA (cDNA) using Improm II reverse transcriptase (Promega, Madison, WI, USA). cDNA from triplicate samples were analyzed using qRT-PCR reactions and monitored using a Light Cycler 480 II machine. Thermocycling was performed under standard conditions with an initial denaturation step of 5 min at 95 °C, 30–40 cycles of denaturation, annealing and extension at 72 °C. Primers used in the study are listed in Supplemental Table S8. The $2^{-\Delta\Delta Ct}$ method was used to compute the relative gene expression for each sample by comparing to control cells [217]. Differences in gene expression for biopsy samples are shown as fold changes in tumor tissues (T) compared to the corresponding normal tissues (N) (given as 1, red line) from the same patient. GAPDH was used as a normaliser for both biopsy specimens and in vitro experiments. The Mann-Whitney test (2-tailed, non-parametric) was used to compare significance differences in gene expression between tumor and normal tissues. p value was set at $p < 0.05$ to be considered statistically significant.

4.6. Immunoblot Analysis

Immunoblot analysis was done according to standard protocols. Cell lysates were obtained by lysing cells with RIPA buffer in the presence of protease inhibitor cocktail. Total protein concentration was determined using the BCA kit and BSA as a standard. Cell lysates (50 µg) were separated by electrophoresis on a 10% polyacrylamide/SDS gels under reducing conditions (50 mM β-mercaptoethanol). Proteins were transferred to a nitrocellulose membranes for 1 h at 4 °C. Membranes were blocked with 5% fat-free milk in Tris Buffered Saline (TBS) containing Tween-20. The membranes were incubated overnight at 4 °C with the following primary antibodies: anti-Ki67 antibody, anti-PCNA antibody, anti-Cyclin D1 antibody, anti-*p*-ERK1/2 (Thr202/Tyr204), anti-ERK2, anti-Akt, anti-*p*-Akt, anti-p21, anti-p53, anti-Bcl-2, anti-Bcl-xL antibody, anti-MMP-2 antibody, anti-MMP-9 antibody, anti-ITGα2 antibody, anti-type I collagen antibody, anti-fibronectin antibody, anti- ITGα3 antibody, anti- ITGα11 antibody, anti-ITGβ1 and anti-GAPDH antibody. Three washes were done using TBS-Tween buffer and then the membranes were incubated with secondary antibodies conjugated to horse radish peroxidase (HRP). Detection was done using Lumiglo substrate (KPL, Gaithersburg, MD, USA). All experiments were done in triplicates and repeated at least twice.

4.7. Cell Cycle and Colony Formation Assay

WHCO1 cancer cells (5×10^5) were cultured on plastic and on decellularised ECMs and treated with drugs for the indicated incubation times. Cells were then dissociated from culture plates using trypsin-EDTA and processed for flow cytometry analysis. Cells were washed twice with cold PBS and fixed with 70% ethanol for 30 min at 4 °C. Washing was done twice with PBS and RNase A (10 µg/mL) was also added for 3 h at 4 °C. Cells were stained with propidium iodide solution (1 mg/mL) and analyzed with a FACScan cell sorter (BD Biosciences, Franklin Lakes, NJ, USA). Ten-thousand cells were collected and the cell cycle profiles were calculated using the Cellquest Software. For colony formation, WHCO1 cells were plated on plastic and on decellularised ECMs in 6-well plates at 500 cells per well and incubated for 10 days. Methanol (100%) was used to fix the cells and cells were stained with 0.5% crystal violet. Colonies were counted using UVP software (Upland, CA, USA) and the

numbers were plotted on a graph. Images were taken using a camera. The experiments were performed at least three times.

4.8. Annexin V/Propidium Iodide Assay for Apoptosis

WHCO1 cell apoptosis was evaluated using double staining with Annexin V conjugated to Fluorescein isothiocyanate (FITC) and Propidium Iodide (PI). After incubation, cells were washed in PBS from each treatment setup and the Annexin binding buffer was used for re-suspension. Cells were stained with Annexin V conjugated to FITC and PI following the manufacturer's instructions. Annexin binding buffer was used to wash cells and resuspension was done in 4% paraformaldehyde (PFA). Cells were incubated for 15 min at 25 °C in the dark. Flow cytometric analysis was done using a Beckman Coulter Flow Cytometer (Beckman Coulter, Life Sciences, Indianapolis, IN, USA). Data acquisition (2×10^4 events per treatment condition) was performed using the Cellquest software (Version 5.1, Becton Dickinson, Franklin Lakes, NJ, USA).

4.9. siRNA Transfection Assay

Short interfering RNAs (siRNAs) were purchased from Santa Cruz Biotechnology (Santa Cruz, CA, USA). siRNAs were dissolved in transfection diluent according to the manufacturer's protocols. Transformed CT1 fibroblasts and WHCO1 cancer cells were transfected with COL1A1 and Fibronectin siRNAs using Transfectin reagent (BioRad, Hercules, CA, USA) and ECM synthesis continued for the indicated period. To maintain knockdown efficiency, subsequent transfections were carried out every 3 days for the duration of the ECM synthesis. In a separate experiment, type I collagen knockdown was achieved by removing ascorbic acid during ECM synthesis with a similar result compared to the use of COL1A1 siRNA. Cells were cultured in 6-well plates with or without the addition of ascorbic acid and ECM synthesis was continued for the duration indicated above [218]. Confirmation of type I collagen and fibronectin knockdowns was done using immunoblot and SDS PAGE analysis.

4.10. Immunofluorescence

ECMs were synthesised on glass coverslips as described before. Cells were then plated on the ECM for the duration indicated elsewhere. Fixing of the cells was achieved using 3% paraformaldehyde solution. Permeabilisation of the cells was done using 0.1% Triton X-100 (Sigma Aldrich Chemie, Steinheim, Germany) in PBS. Blocking of cells was done using 1% BSA for 1 h at room temperature and then incubated with various primary antibodies overnight at 4 °C. Cells were then washed three times with PBS. Secondary antibodies were conjugated to FITC and Fluor 488. DAPI was added in order to visualise the nucleus. Fluorescence was observed using a Zeiss Inverted Microscope with a 20× objective. Acquisition of images was achieved using the CellSens Imaging System (Olympus, Tokyo, Japan). Proteoglycan composition within the ECMs was detected by staining the ECMs with 1% Alcian blue after preparation using a standard protocol. Briefly ECM synthesis and preparation was done on coverslips. ECMs were incubated with 1% Alcian Blue solution for 20 min and washed three times. Images were observed and photographed using a light microscope (Olympus CKX41 with SC30 camera). Images were taken at 100× magnification.

4.11. Migration Assay

Confluent cells were trypsinised and neutralised by adding DMEM supplemented with 10% FCS and Penicillin and streptomycin. Centrifugation was done at 1800 rpm for 5 min at 25 °C and cells were resuspended in DMEM. The Countess Cell Counter was used for cell counting to give a final cell density of 5000 cells per microliter. Cellular foci of 4 µL containing a total of 20,000 cells were added to plastic dishes or to the ECMs. To prevent cell death due to evaporation of media, an extra 100 µL of DMEM media was added to the cellular foci and incubation continued for 2 h. A further 3 mL of DMEM with 10% FCS was then added and incubation continued for 24 h. In a separate experiment,

cells were incubated with anti-α2 integrin blocking antibody for 30 min before plating. Images were taken at 0 h and at 24 h with a microscope. Image J (version 1.52g, National Institutes of Health; Bethesda, MD, USA) was then used to measure the area of migrating mass of cells. Migration on ECMs was normalised to that on plastic dishes.

4.12. Immunohistochemistry

Formalin-fixed, paraffin-embedded whole sections of esophageal tumor and normal samples were used to quantify type I collagen. Sections were of 4 μm thickness and standard histological analysis was carried out. Paraffin slides were deparaffinised in xylene and rehydration was achieved through the use of graded alcohols. Slides were heated in 0.01 M citrate buffer (pH 6.0) in a bath for 20 min at 97 °C for antigen retrieval. Slides were allowed to cool and were rinsed in TBS; the endogenous peroxidase was inactivated with 3% hydrogen peroxide. After protein block, incubation of slides with a primary antibody against human type I collagen was done for 1 h. TBS was used to rinse sections and incubation was done for 20 min with biotinylated secondary antibodies. Sections were rinsed with TBS and incubated with streptavidin-HRP. Peroxidase reactivity was visualised using a 3,3-diaminobenzidine (DAB). Counterstaining of sections was done with haematoxylin. Sections were mounted and images were obtained using a light microscope. Whole tissue sections from tumor and normal blocks were stained and compared by visual inspection. Results were evaluated independently by two observers.

4.13. Mass Spectrometry

The proteomic profiles of the 3D ECMs were assessed using mass spectrometry. Mass spectrometry analysis was performed on duplicate ECM samples. The samples were prepared by filter aided sample preparation (FASP) according to Wisniewski et al. [219]. Reduced and alkylated protein samples were tryptically digested at a 1:50 enzyme to sample ratio overnight for 16 h in a wet chamber at 37 °C. For each sample, 10 μg aliquots of the resulting tryptic peptides were acidified in 0.1% formic acid and desalted using in-house produced C18 stage tips. The samples were dried in a vacuum concentrator, and reconstituted in 2% acetonitrile with 0.1% formic acid prior to LC-MS/MS analysis. Samples were analysed on a Thermo Scientific Dionex Ultimate 3000 UHPLC (Thermo Fisher Scientific, Waltham, MA, USA) coupled to a Thermo Scientific Q Exactive hybrid quadrupole Orbitrap mass spectrometer. The samples were loaded onto a 2 cm Luna C18 100 μM internal diameter fused silica pre-column, packed in-house, and then separated on a 40 cm Aeris peptide C18 75 μM internal diameter analytical column, packed in-house. A total of 400 ng of each sample was analysed on a 70 min gradient from 6–40% acetonitrile with a flow rate of 400 nL/min at 40 °C. The nanoelectrospray voltage was set to 2.2 kV, and the capillary temperature was 320 °C. The Q Exactive was operated in data-dependent mode, with full scan MS spectra (m/z 300–1750) acquired in the Orbitrap analyser after accumulation to an AGC target of 3e6 or an injection time of 250 ms at a resolution of 70,000. The 10 most intense peptide ions were sequentially isolated and fragmented by HCD and acquired at a resolution of 17,500. Dynamic exclusion was enabled after 30s and for a repeat count of one. The raw files were processed using MaxQuant version 1.2.7.429 (Computational Systems Biochemistry, Martinsried, Germany) and the MS/MS spectra were searched using the Andromeda search engine against the Uniprot human protein database. The initial maximal allowed mass tolerance was set to 20 ppm for the first search and then to 4.5 ppm in the main search, and 20 ppm for fragment ions. Enzyme specificity was set to trypsin with a maximum of two missed cleavages. Carbamidomethylation of cysteine was set as a fixed modification, and oxidation of methionine and protein N-terminal acetylation were selected as variable modifications. The minimum peptide length was set to seven amino acids. Label-free protein quantification was performed using the label-free quantification (LFQ) algorithm implemented in the MaxQuant software (version 1.1.1.25, Computational Systems Biochemistry, Martinsried, Germany) with a 2 min window for matching between runs and, a maximum 1% peptide and 1% protein false discovery rate. Protein intensity values

were normalized automatically using the LFQ algorithm to identify differentially expressed proteins. Bioinformation analyses of the data were performed using Perseus v.1.2.7.4 software. Reverse and "only identified by site" entries were excluded. LFQ intensity values were log2 transformed, and the dataset was filtered to contain only entries with two minimum valid values in at least one group. Statistical significance was assessed using Student's *t*-test to identify differentially expressed proteins between the groups.

4.14. Statistical Analysis

Statistical analysis was performed using GraphPad Prism software. The Mann-Whitney test (2-tailed, non-parametric) was used to compare significance differences in gene expression between tumor and normal tissues. p value was set at $p < 0.05$ to be considered statistically significant. Evaluation of statistical significance between control cells and cells plated on plastic or ECM/treated with chemotherapeutic drugs was done using the paired Student's t test. p value was set at $p < 0.05$ to be considered statistically significant. Correlation coefficients were determined using Pearson's correlation coefficient in Microsoft Excel. Pearson's correlation coefficients were calculated to determine a point estimate of the strength of the association between the different ECM preparations.

Supplementary Materials: Supplementary Materials can be found at http://www.mdpi.com/1422-0067/19/10/2861/s1.

Author Contributions: Conceptualization, C.D., M.I.P. and K.D.; Data curation, D.A.S. and K.D.; Formal analysis, D.A.S., T.J., B.C. and K.D.; Funding acquisition, M.I.P. and K.D.; Investigation, D.A.S., D.G. and K.D.; Project administration, K.D.; Resources, A.R., N.E.T., A.W., B.C., N.C.S., J.M.B. and M.I.P.; Supervision, K.D.; Validation, D.G.; Visualization, D.M.; Writing—original draft, K.D.; Writing—review & editing, D.A.S., T.J., A.R., N.E.T., D.M., C.D., A.W., D.G., B.C., N.C.S., J.M.B. and M.I.P.

Funding: Funding for this work was from the International Centre for Genetic Engineering and Biotechnology (ICGEB), the South African Medical Research Council, the National Research Foundation (NRF) of South Africa and the University of Cape Town. M.I.P was supported by the Strategic Health Innovation Partnerships (SHIP) Unit of the South African Medical Research Council with funds received from the South African National Department of Health and the UK Medical Research Council via the Newton Fund and GlaxoSmithKline R&D.

Acknowledgments: Special mention goes to all the doctors and nurses of the oncology clinic at Groote Schuur Hospital for their help with biopsy collection. The funders had no role in the conduct of the research or the preparation of the manuscript.

Conflicts of Interest: The authors declare no conflict of interest.

Abbreviations

3D	Three dimensional
BSA	Bovine serum albumin
DNA	Deoxyribonucleic acid
DMSO	Dimethyl sulfoxide
EDTA	Ethylenediaminetetraacetate
ECM	Extracellular matrix
ESCC	Esophageal squamous cell carcinoma
FN	Fibronectin
5-FU	5-fluorouracil
ITG	Integrin
Tfd-ECM	Transformed fibroblast-derived ECM
cd-ECM	Cancer cell-derived ECM
combi-ECM	Combinatorial-ECM
MS	Mass spectrometry.
MMP	Matrix metalloprotease
PAGE	Polyacrylamide gel electrophoresis
SDS	Sodium dodecyl sulphate

References

1. Bruce, A.; Evans, R.; Mezan, R.; Shi, L.; Moses, B.S.; Martin, K.H.; Gibson, L.F.; Yang, Y. Three-dimensional microfluidic tri-culture model of the bone marrow microenvironment for study of acute lymphoblastic leukemia. *PLoS ONE* **2015**, *10*, e0140506. [CrossRef] [PubMed]
2. Guiro, K.; Patel, S.A.; Greco, S.J.; Rameshwar, P.; Arinzeh, T.L. Investigating breast cancer cell behavior using tissue engineering scaffolds. *PLoS ONE* **2015**, *10*, e0118724. [CrossRef] [PubMed]
3. Hussein, K.H.; Park, K.M.; Ghim, J.H.; Yang, S.R.; Woo, H.M. Three dimensional culture of HEPG2 liver cells on a rat decellularized liver matrix for pharmacological studies. *J. Biomed. Mater. Res. Part B Appl. Biomater.* **2016**, *104*, 263–273. [CrossRef] [PubMed]
4. Pomo, J.M.; Taylor, R.M.; Gullapalli, R.R. Influence of TP53 and CDH1 genes in hepatocellular cancer spheroid formation and culture: A model system to understand cancer cell growth mechanics. *Cancer Cell Int.* **2016**, *16*, 44. [CrossRef] [PubMed]
5. Skardal, A.; Devarasetty, M.; Forsythe, S.; Atala, A.; Soker, S. A reductionist metastasis-on-a-chip platform for in vitro tumor progression modeling and drug screening. *Biotechnol. Bioeng.* **2016**, *113*, 2020–2032. [CrossRef] [PubMed]
6. Yu, L.; Ni, C.; Grist, S.M.; Bayly, C.; Cheung, K.C. Alginate core-shell beads for simplified three-dimensional tumor spheroid culture and drug screening. *Biomed. Microdevices* **2015**, *17*, 33. [CrossRef] [PubMed]
7. Holliday, D.L. A three-dimensional in vitro model of breast cancer: Toward replacing the need for animal experiments. *Altern. Lab. Anim. ATLA* **2010**, *38* (Suppl. 1), 41–44. [PubMed]
8. Pavlov, K.; Maley, C.C. New models of neoplastic progression in barrett's oesophagus. *Biochem. Soc. Trans.* **2010**, *38*, 331–336. [CrossRef] [PubMed]
9. Priwitaningrum, D.L.; Blonde, J.G.; Sridhar, A.; van Baarlen, J.; Hennink, W.E.; Storm, G.; Le Gac, S.; Prakash, J. Tumor stroma-containing 3D spheroid arrays: A tool to study nanoparticle penetration. *J. Control. Release* **2016**, *244*, 257–268. [CrossRef] [PubMed]
10. Tan, P.H.; Aung, K.Z.; Toh, S.L.; Goh, J.C.; Nathan, S.S. Three-dimensional porous silk tumor constructs in the approximation of in vivo osteosarcoma physiology. *Biomaterials* **2011**, *32*, 6131–6137. [CrossRef] [PubMed]
11. Attieh, Y.; Vignjevic, D.M. The hallmarks of cafs in cancer invasion. *Eur. J. Cell Biol.* **2016**, *95*, 493–502. [CrossRef] [PubMed]
12. Cramer, G.M.; Jones, D.P.; El-Hamidi, H.; Celli, J.P. ECM composition and rheology regulate growth, motility, and response to photodynamic therapy in 3D models of pancreatic ductal adenocarcinoma. *Mol. Cancer Res. MCR* **2017**, *15*, 15–25. [CrossRef] [PubMed]
13. Han, W.; Chen, S.; Yuan, W.; Fan, Q.; Tian, J.; Wang, X.; Chen, L.; Zhang, X.; Wei, W.; Liu, R.; et al. Oriented collagen fibers direct tumor cell intravasation. *Proc. Natl. Acad. Sci. USA* **2016**, *113*, 11208–11213. [CrossRef] [PubMed]
14. Kalluri, R. The biology and function of fibroblasts in cancer. *Nat. Rev. Cancer* **2016**, *16*, 582–598. [CrossRef] [PubMed]
15. Sangaletti, S.; Tripodo, C.; Santangelo, A.; Castioni, N.; Portararo, P.; Gulino, A.; Botti, L.; Parenza, M.; Cappetti, B.; Orlandi, R.; et al. Mesenchymal transition of high-grade breast carcinomas depends on extracellular matrix control of myeloid suppressor cell activity. *Cell Rep.* **2016**, *17*, 233–248. [CrossRef] [PubMed]
16. Thakur, R.; Mishra, D.P. Matrix reloaded: Ccn, tenascin and sibling group of matricellular proteins in orchestrating cancer hallmark capabilities. *Pharmacol. Ther.* **2016**, *168*, 61–74. [CrossRef] [PubMed]
17. Aguado, B.A.; Caffe, J.R.; Nanavati, D.; Rao, S.S.; Bushnell, G.G.; Azarin, S.M.; Shea, L.D. Extracellular matrix mediators of metastatic cell colonization characterized using scaffold mimics of the pre-metastatic niche. *Acta Biomater.* **2016**, *33*, 13–24. [CrossRef] [PubMed]
18. Hoshiba, T.; Tanaka, M. Decellularized matrices as in vitro models of extracellular matrix in tumor tissues at different malignant levels: Mechanism of 5-fluorouracil resistance in colorectal tumor cells. *Biochim. Biophys. Acta* **2016**, *1863*, 2749–2757. [CrossRef] [PubMed]
19. Mazza, G.; Rombouts, K.; Rennie Hall, A.; Urbani, L.; Vinh Luong, T.; Al-Akkad, W.; Longato, L.; Brown, D.; Maghsoudlou, P.; Dhillon, A.P.; et al. Decellularized human liver as a natural 3D-scaffold for liver bioengineering and transplantation. *Sci. Rep.* **2015**, *5*, 13079. [CrossRef] [PubMed]

20. Scherzer, M.T.; Waigel, S.; Donninger, H.; Arumugam, V.; Zacharias, W.; Clark, G.; Siskind, L.J.; Soucy, P.; Beverly, L. Fibroblast-derived extracellular matrices: An alternative cell culture system that increases metastatic cellular properties. *PLoS ONE* **2015**, *10*, e0138065. [CrossRef] [PubMed]
21. Sholoqu, N.; Szegezdi, E.; Lowery, A.; Kerin, M.; Pandit, A.; Zeugolis, D.I. Recreating complex pathophysiologies in vitro with extracellular matrix surrogates for anticancer therapeutics screening. *Drug Discov. Today* **2016**, *21*, 1521–1531. [CrossRef] [PubMed]
22. Tiwari, A.; Tursky, M.L.; Nekkanti, L.P.; Jenkin, G.; Kirkland, M.A.; Pande, G. Expansion of human hematopoietic stem/progenitor cells on decellularized matrix scaffolds. *Curr. Protoc. Stem Cell Biol.* **2016**, *36*, 11–16.
23. Xiong, G.; Flynn, T.J.; Chen, J.; Trinkle, C.; Xu, R. Development of an ex vivo breast cancer lung colonization model utilizing a decellularized lung matrix. *Integr. Biol. Quant. Biosci. Nano Macro* **2015**, *7*, 1518–1525. [CrossRef] [PubMed]
24. Bachman, H.; Nicosia, J.; Dysart, M.; Barker, T.H. Utilizing fibronectin integrin-binding specificity to control cellular responses. *Adv. Wound Care* **2015**, *4*, 501–511. [CrossRef] [PubMed]
25. Belair, D.G.; Le, N.N.; Murphy, W.L. Design of growth factor sequestering biomaterials. *Chem. Commun.* **2014**, *50*, 15651–15668. [CrossRef] [PubMed]
26. Fan, D.; Creemers, E.E.; Kassiri, Z. Matrix as an interstitial transport system. *Circ. Res.* **2014**, *114*, 889–902. [CrossRef] [PubMed]
27. Hudalla, G.A.; Murphy, W.L. Chemically well-defined self-assembled monolayers for cell culture: Toward mimicking the natural ECM. *Soft Matter* **2011**, *7*, 9561–9571. [CrossRef] [PubMed]
28. Hudalla, G.A.; Murphy, W.L. Biomaterials that regulate growth factor activity via bioinspired interactions. *Adv. Funct. Mater.* **2011**, *21*, 1754–1768. [CrossRef] [PubMed]
29. Narayanan, K.; Leck, K.J.; Gao, S.; Wan, A.C. Three-dimensional reconstituted extracellular matrix scaffolds for tissue engineering. *Biomaterials* **2009**, *30*, 4309–4317. [CrossRef] [PubMed]
30. Schultz, G.S.; Wysocki, A. Interactions between extracellular matrix and growth factors in wound healing. *Wound Repair Regen.* **2009**, *17*, 153–162. [CrossRef] [PubMed]
31. Gobin, A.S.; West, J.L. Effects of epidermal growth factor on fibroblast migration through biomimetic hydrogels. *Biotechnol. Prog.* **2003**, *19*, 1781–1785. [CrossRef] [PubMed]
32. Kim, S.H.; Choe, C.; Shin, Y.S.; Jeon, M.J.; Choi, S.J.; Lee, J.; Bae, G.Y.; Cha, H.J.; Kim, J. Human lung cancer-associated fibroblasts enhance motility of non-small cell lung cancer cells in co-culture. *Anticancer. Res.* **2013**, *33*, 2001–2009. [PubMed]
33. Morrissey, C.; Vessella, R.L. The role of tumor microenvironment in prostate cancer bone metastasis. *J. Cell. Biochem.* **2007**, *101*, 873–886. [CrossRef] [PubMed]
34. Uchinaka, A.; Tasaka, K.; Mizuno, Y.; Maeno, Y.; Ban, T.; Mori, S.; Hamada, Y.; Miyagawa, S.; Saito, A.; Sawa, Y.; et al. Laminin alpha2-secreting fibroblasts enhance the therapeutic effect of skeletal myoblast sheets. *Eur. J. Cardiothorac. Surg.* **2016**, *51*, 457–464.
35. Wernert, N. The multiple roles of tumor stroma. *Virchows Arch. Int. J. Pathol.* **1997**, *430*, 433–443. [CrossRef]
36. Wight, T.N.; Potter-Perigo, S. The extracellular matrix: An active or passive player in fibrosis? *Am. J. Physiol. Gastrointest. Liver Physiol.* **2011**, *301*, G950–G955. [CrossRef] [PubMed]
37. Catteau, X.; Simon, P.; Buxant, F.; Noel, J.C. Expression of the glucocorticoid receptor in breast cancer-associated fibroblasts. *Mol. Clin. Oncol.* **2016**, *5*, 372–376. [CrossRef] [PubMed]
38. Domogauer, J.D.; de Toledo, S.M.; Azzam, E.I. A mimic of the tumor microenvironment: A simple method for generating enriched cell populations and investigating intercellular communication. *J. Vis. Exp. JoVE* **2016**. [CrossRef] [PubMed]
39. Leca, J.; Martinez, S.; Lac, S.; Nigri, J.; Secq, V.; Rubis, M.; Bressy, C.; Serge, A.; Lavaut, M.N.; Dusetti, N.; et al. Cancer-associated fibroblast-derived annexin A6+ extracellular vesicles support pancreatic cancer aggressiveness. *J. Clin. Investig.* **2016**, *126*, 4140–4156. [CrossRef] [PubMed]
40. McLane, J.S.; Ligon, L.A. Stiffened extracellular matrix and signaling from stromal fibroblasts via osteoprotegerin regulate tumor cell invasion in a 3-D tumor in situ model. *Cancer Microenviron.* **2016**, *9*, 127–139. [CrossRef] [PubMed]
41. Melzer, C.; Yang, Y.; Hass, R. Interaction of msc with tumor cells. *Cell Commun. Signal.* **2016**, *14*, 20. [CrossRef] [PubMed]

42. Merlino, G.; Miodini, P.; Paolini, B.; Carcangiu, M.L.; Gennaro, M.; Dugo, M.; Daidone, M.G.; Cappelletti, V. Stromal activation by tumor cells: An in vitro study in breast cancer. *Microarrays* **2016**, *5*, 10. [CrossRef] [PubMed]
43. Wang, T.; Notta, F.; Navab, R.; Joseph, J.; Ibrahimov, E.; Xu, J.; Zhu, C.Q.; Borgida, A.; Gallinger, S.; Tsao, M.S. Senescent carcinoma-associated fibroblasts upregulate IL8 to enhance pro-metastatic phenotypes. *Mol. Cancer Res. MCR* **2016**, *15*, 3–14. [CrossRef] [PubMed]
44. Zhou, L.; Yang, K.; Wickett, R.R.; Kadekaro, A.L.; Zhang, Y. Targeted deactivation of cancer-associated fibroblasts by beta-catenin ablation suppresses melanoma growth. *Tumour Biol.* **2016**, *37*, 14235–14248. [CrossRef] [PubMed]
45. Akrish, S.J.; Rachmiel, A.; Sabo, E.; Vered, M.; Ben-Izhak, O. Cancer associated fibroblasts are an infrequent finding in the microenvironment of proliferative verrucous leukoplakia associated squamous cell carcinoma. *J. Oral Pathol. Med.* **2016**, *46*, 353–358. [CrossRef] [PubMed]
46. Brechbuhl, H.M.; Finlay-Schultz, J.; Yamamoto, T.; Gillen, A.; Cittelly, D.M.; Tan, A.C.; Sams, S.B.; Pillai, M.; Elias, A.; Robinson, W.A.; et al. Fibroblast subtypes regulate responsiveness of luminal breast cancer to estrogen. *Clin. Cancer Res.* **2016**, *23*, 1710–1721. [CrossRef] [PubMed]
47. Marks, D.L.; Olson, R.L.; Fernandez-Zapico, M.E. Epigenetic control of the tumor microenvironment. *Epigenomics* **2016**, *8*, 1671–1687. [CrossRef] [PubMed]
48. McCarty, K.; Friedman, D.; Cottam, B.; Newell, P.; Gough, M.; Crittenden, M.R.; Young, K.H. Targeting cancer-associated fibroblasts in combination with radiation. *Int. J. Radiat. Oncol. Biol. Phys.* **2016**, *96*, E594–E595. [CrossRef]
49. Richards, K.E.; Zeleniak, A.E.; Fishel, M.L.; Wu, J.; Littlepage, L.E.; Hill, R. Cancer-associated fibroblast exosomes regulate survival and proliferation of pancreatic cancer cells. *Oncogene* **2016**, *36*, 1770–1778. [CrossRef] [PubMed]
50. Ohashi, S.; Miyamoto, S.; Kikuchi, O.; Goto, T.; Amanuma, Y.; Muto, M. Recent advances from basic and clinical studies of esophageal squamous cell carcinoma. *Gastroenterology* **2015**, *149*, 1700–1715. [CrossRef] [PubMed]
51. Rice, D.; Geller, A.; Bender, C.E.; Gostout, C.J.; Donohue, J.H. Surgical and interventional palliative treatment of upper gastrointestinal malignancies. *Eur. J. Gastroenterol. Hepatol.* **2000**, *12*, 403–408. [CrossRef] [PubMed]
52. Nash, C.L.; Gerdes, H. Methods of palliation of esophageal and gastric cancer. *Surg. Oncol. Clin. N. Am.* **2002**, *11*, 459–483. [CrossRef]
53. Nojilana, B.; Bradshaw, D.; Pillay-van Wyk, V.; Msemburi, W.; Laubscher, R.; Somdyala, N.I.; Joubert, J.D.; Groenewald, P.; Dorrington, R.E. Emerging trends in non-communicable disease mortality in South Africa, 1997–2010. *S. Afr. Med. J.* **2016**, *106*, 477–485. [CrossRef] [PubMed]
54. Somdyala, N.I.; Bradshaw, D.; Gelderblom, W.C.; Parkin, D.M. Cancer incidence in a rural population of South Africa, 1998–2002. *Int. J. Cancer* **2010**, *127*, 2420–2429. [CrossRef] [PubMed]
55. Best, L.M.; Mughal, M.; Gurusamy, K.S. Non-surgical versus surgical treatment for oesophageal cancer. *Cochrane Database Syst. Rev.* **2016**, *3*, CD011498. [PubMed]
56. Gao, P.; Tsai, C.; Yang, Y.; Xu, Y.; Zhang, C.; Zhang, C.; Wang, L.; Liu, H.; Wang, Z. Intraoperative radiotherapy in gastric and esophageal cancer: Meta-analysis of long-term outcomes and complications. *Minerva Med.* **2016**, *108*, 74–83. [PubMed]
57. Ge, L.; Wang, H.J.; Yin, D.; Lei, C.; Zhu, J.F.; Cai, X.H.; Zhang, G.Q. Effectiveness of 5-flurouracil-based neoadjuvant chemotherapy in locally-advanced gastric/gastroesophageal cancer: A meta-analysis. *World J. Gastroenterol.* **2012**, *18*, 7384–7393. [CrossRef] [PubMed]
58. Tamaki, Y.; Sasaki, R.; Ejima, Y.; Ogura, M.; Negoro, Y.; Nakajima, T.; Murakami, M.; Kaji, Y.; Sugimura, K. Efficacy of intraoperative radiotherapy targeted to the abdominal lymph node area in patients with esophageal carcinoma. *J. Radiat. Res.* **2012**, *53*, 882–891. [CrossRef] [PubMed]
59. Yu, W.W.; Guo, Y.M.; Zhang, Q.; Fu, S. Benefits from adjuvant intraoperative radiotherapy treatment for gastric cancer: A meta-analysis. *Mol. Clin. Oncol.* **2015**, *3*, 185–189. [CrossRef] [PubMed]
60. Chi, J.; Yang, Q.; Xie, X.F.; Yang, X.Z.; Zhang, M.Y.; Wang, H.Y.; Xu, G.L. Clinical significance and prognostic value of trim24 expression in esophageal squamous cell carcinoma. *Aging* **2016**, *8*, 2204–2221. [CrossRef] [PubMed]

61. Depypere, L.; Lerut, T.; Moons, J.; Coosemans, W.; Decker, G.; Van Veer, H.; De Leyn, P.; Nafteux, P. Isolated local recurrence or solitary solid organ metastasis after esophagectomy for cancer is not the end of the road. *Dis. Esophagus* **2017**, *30*, 1–8. [PubMed]
62. Khan, M.; Muzaffar, A.; Syed, A.A.; Khatak, S.; Khan, A.R.; Ashraf, M.I. Changes in oncological outcomes: Comparison of the conventional and minimally invasive esophagectomy, a single institution experience. *Updat. Surg.* **2016**, *68*, 343–349. [CrossRef] [PubMed]
63. Liu, S.; Anfossi, S.; Zheng, Y.; Cai, M.; Fu, J.; Qiu, B.; Yang, H.; Liu, Q.; Fu, J.; Liu, M.; et al. Clinical and biological prognostic factors for locoregional recurrence in patients with thoracic esophageal squamous cell carcinoma treated with radical 2-field lymph node dissection: Results from long-term follow-up. *Int. J. Radiat. Oncol. Biol. Phys.* **2016**, *96*, E175. [CrossRef]
64. Liu, X.; Wang, Z.; Zhang, G.; Zhu, Q.; Zeng, H.; Wang, T.; Gao, F.; Qi, Z.; Zhang, J.; Wang, R. High TRAF6 expression is associated with esophageal carcinoma recurrence and prompts cancer cell invasion. *Oncol. Res.* **2017**, *25*, 485–493. [CrossRef] [PubMed]
65. Hamano, R.; Miyata, H.; Yamasaki, M.; Kurokawa, Y.; Hara, J.; Moon, J.H.; Nakajima, K.; Takiguchi, S.; Fujiwara, Y.; Mori, M.; et al. Overexpression of mir-200c induces chemoresistance in esophageal cancers mediated through activation of the akt signaling pathway. *Clin. Cancer Res.* **2011**, *17*, 3029–3038. [CrossRef] [PubMed]
66. Wang, Y.; Zhao, Y.; Herbst, A.; Kalinski, T.; Qin, J.; Wang, X.; Jiang, Z.; Benedix, F.; Franke, S.; Wartman, T.; et al. Mir-221 mediates chemoresistance of esophageal adenocarcinoma by direct targeting of DKK2 expression. *Ann. Surg.* **2016**, *264*, 804–814. [CrossRef] [PubMed]
67. Xi, R.; Pan, S.; Chen, X.; Hui, B.; Zhang, L.; Fu, S.; Li, X.; Zhang, X.; Gong, T.; Guo, J.; et al. HPV16 E6-E7 induces cancer stem-like cells phenotypes in esophageal squamous cell carcinoma through the activation of Pi3K/AKT signaling pathway in vitro and in vivo. *Oncotarget* **2016**, *7*, 57050–57065. [CrossRef] [PubMed]
68. Yang, H.; Li, X.D.; Zhou, Y.; Ban, X.; Zeng, T.T.; Li, L.; Zhang, B.Z.; Yun, J.; Xie, D.; Guan, X.Y.; et al. Stemness and chemotherapeutic drug resistance induced by EIF5A2 overexpression in esophageal squamous cell carcinoma. *Oncotarget* **2015**, *6*, 26079–26089. [CrossRef] [PubMed]
69. Zhang, H.F.; Wu, C.; Alshareef, A.; Gupta, N.; Zhao, Q.; Xu, X.E.; Jiao, J.W.; Li, E.M.; Xu, L.Y.; Lai, R. The PI3K/AKT/C-MYC axis promotes the acquisition of cancer stem-like features in esophageal squamous cell carcinoma. *Stem Cells* **2016**, *34*, 2040–2051. [CrossRef] [PubMed]
70. Zhao, R.; Quaroni, L.; Casson, A.G. Identification and characterization of stemlike cells in human esophageal adenocarcinoma and normal epithelial cell lines. *J. Thorac. Cardiovasc. Surg.* **2012**, *144*, 1192–1199. [CrossRef] [PubMed]
71. Ha, S.Y.; Yeo, S.Y.; Xuan, Y.H.; Kim, S.H. The prognostic significance of cancer-associated fibroblasts in esophageal squamous cell carcinoma. *PLoS ONE* **2014**, *9*, e99955. [CrossRef] [PubMed]
72. Hanley, C.J.; Noble, F.; Ward, M.; Bullock, M.; Drifka, C.; Mellone, M.; Manousopoulou, A.; Johnston, H.E.; Hayden, A.; Thirdborough, S.; et al. A subset of myofibroblastic cancer-associated fibroblasts regulate collagen fiber elongation, which is prognostic in multiple cancers. *Oncotarget* **2016**, *7*, 6159–6174. [CrossRef] [PubMed]
73. Jomrich, G.; Jesch, B.; Birner, P.; Schwameis, K.; Paireder, M.; Asari, R.; Schoppmann, S.F. Stromal expression of carbonic anhydrase ix in esophageal cancer. *Clin. Transl. Oncol.* **2014**, *16*, 966–972. [CrossRef] [PubMed]
74. Kretschmer, I.; Freudenberger, T.; Twarock, S.; Yamaguchi, Y.; Grandoch, M.; Fischer, J.W. Esophageal squamous cell carcinoma cells modulate chemokine expression and hyaluronan synthesis in fibroblasts. *J. Biol. Chem.* **2016**, *291*, 4091–4106. [CrossRef] [PubMed]
75. Saito, S.; Morishima, K.; Ui, T.; Matsubara, D.; Tamura, T.; Oguni, S.; Hosoya, Y.; Sata, N.; Lefor, A.T.; Yasuda, Y.; et al. Stromal fibroblasts are predictors of disease-related mortality in esophageal squamous cell carcinoma. *Oncol. Rep.* **2014**, *32*, 348–354. [CrossRef] [PubMed]
76. Underwood, T.J.; Hayden, A.L.; Derouet, M.; Garcia, E.; Noble, F.; White, M.J.; Thirdborough, S.; Mead, A.; Clemons, N.; Mellone, M.; et al. Cancer-associated fibroblasts predict poor outcome and promote periostin-dependent invasion in oesophageal adenocarcinoma. *J. Pathol.* **2015**, *235*, 466–477. [CrossRef] [PubMed]
77. Wang, J.; Zhang, G.; Wang, J.; Wang, L.; Huang, X.; Cheng, Y. The role of cancer-associated fibroblasts in esophageal cancer. *J. Transl. Med.* **2016**, *14*, 30. [CrossRef] [PubMed]

78. Gopal, S.; Veracini, L.; Grall, D.; Butori, C.; Schaub, S.; Audebert, S.; Camoin, L.; Baudelet, E.; Radwanska, A.; Beghelli-de la Forest Divonne, S.; et al. Fibronectin-guided migration of carcinoma collectives. *Nat. Commun.* **2017**, *8*, 14105. [CrossRef] [PubMed]
79. Keeratichamroen, S.; Lirdprapamongkol, K.; Svasti, J. Mechanism of ECM-induced dormancy and chemoresistance in a549 human lung carcinoma cells. *Oncol. Rep.* **2018**, *39*, 1765–1774. [CrossRef] [PubMed]
80. Fang, M.; Yuan, J.; Peng, C.; Li, Y. Collagen as a double-edged sword in tumor progression. *Tumor Biol.* **2014**, *35*, 2871–2882. [CrossRef] [PubMed]
81. Rudnick, J.A.; Kuperwasser, C. Stromal biomarkers in breast cancer development and progression. *Clin. Exp. Metastasis* **2012**, *29*, 663–672. [CrossRef] [PubMed]
82. Voiles, L.; Lewis, D.E.; Han, L.; Lupov, I.P.; Lin, T.L.; Robertson, M.J.; Petrache, I.; Chang, H.C. Overexpression of type vi collagen in neoplastic lung tissues. *Oncol. Rep.* **2014**, *32*, 1897–1904. [CrossRef] [PubMed]
83. Xiong, G.; Deng, L.; Zhu, J.; Rychahou, P.G.; Xu, R. Prolyl-4-hydroxylase alpha subunit 2 promotes breast cancer progression and metastasis by regulating collagen deposition. *BMC Cancer* **2014**, *14*, 1. [CrossRef] [PubMed]
84. Zhu, J.; Xiong, G.; Trinkle, C.; Xu, R. Integrated extracellular matrix signaling in mammary gland development and breast cancer progression. *Histol. Histopathol.* **2014**, *29*, 1083–1092. [PubMed]
85. Troester, M.A.; Lee, M.H.; Carter, M.; Fan, C.; Cowan, D.W.; Perez, E.R.; Pirone, J.R.; Perou, C.M.; Jerry, D.J.; Schneider, S.S. Activation of host wound responses in breast cancer microenvironment. *Clin. Cancer Res.* **2009**, *15*, 7020–7028. [CrossRef] [PubMed]
86. Truong, D.; Puleo, J.; Llave, A.; Mouneimne, G.; Kamm, R.D.; Nikkhah, M. Breast cancer cell invasion into a three dimensional tumor-stroma microenvironment. *Sci. Rep.* **2016**, *6*, 34094. [CrossRef] [PubMed]
87. Dzobo, K.; Turnley, T.; Wishart, A.; Rowe, A.; Kallmeyer, K.; van Vollenstee, F.A.; Thomford, N.E.; Dandara, C.; Chopera, D.; Pepper, M.S.; et al. Fibroblast-derived extracellular matrix induces chondrogenic differentiation in human adipose-derived mesenchymal stromal/stem cells in vitro. *Int. J. Mol. Sci.* **2016**, *17*, 1259. [CrossRef] [PubMed]
88. Dzobo, K.; Vogelsang, M.; Thomford, N.E.; Dandara, C.; Kallmeyer, K.; Pepper, M.S.; Parker, M.I. Wharton's jelly-derived mesenchymal stromal cells and fibroblast-derived extracellular matrix synergistically activate apoptosis in a p21-dependent mechanism in WHCO1 and MDA MB 231 cancer cells in vitro. *Stem Cells Int.* **2016**, *2016*, 4842134. [CrossRef] [PubMed]
89. Herrmann, D.; Conway, J.R.; Vennin, C.; Magenau, A.; Hughes, W.E.; Morton, J.P.; Timpson, P. Three-dimensional cancer models mimic cell-matrix interactions in the tumor microenvironment. *Carcinogenesis* **2014**, *35*, 1671–1679. [CrossRef] [PubMed]
90. Serebriiskii, I.; Castello-Cros, R.; Lamb, A.; Golemis, E.A.; Cukierman, E. Fibroblast-derived 3D matrix differentially regulates the growth and drug-responsiveness of human cancer cells. *Matrix Biol. J. Int. Soc. Matrix Biol.* **2008**, *27*, 573–585. [CrossRef] [PubMed]
91. Namba, M.; Nishitani, K.; Kimoto, T. Effects of theophylline on the cell growth of normal and malignant human cells transformed in culture. *Gan* **1980**, *71*, 621–627. [PubMed]
92. Bao, C.H.; Wang, X.T.; Ma, W.; Wang, N.N.; Un Nesa, E.; Wang, J.B.; Wang, C.; Jia, Y.B.; Wang, K.; Tian, H.; et al. Irradiated fibroblasts promote epithelial-mesenchymal transition and hdgf expression of esophageal squamous cell carcinoma. *Biochem. Biophys. Res. Commun.* **2015**, *458*, 441–447. [CrossRef] [PubMed]
93. Petrova, V.; Annicchiarico-Petruzzelli, M.; Melino, G.; Amelio, I. The hypoxic tumour microenvironment. *Oncogenesis* **2018**, *7*, 10. [CrossRef] [PubMed]
94. Chia, P.L.; Russell, P.; Scott, A.M.; John, T. Targeting the vasculature: Anti-angiogenic agents for malignant mesothelioma. *Expert Rev. Anticancer. Ther.* **2016**, *16*, 1235–1245. [CrossRef] [PubMed]
95. Chiron, D.; Bellanger, C.; Papin, A.; Tessoulin, B.; Dousset, C.; Maiga, S.; Moreau, A.; Esbelin, J.; Trichet, V.; Chen-Kiang, S.; et al. Microenvironment-dependent proliferation and mitochondrial priming loss in mantle cell lymphoma is overcome by anti-CD20. *Blood* **2016**, *128*, 2808–2818. [CrossRef] [PubMed]
96. Crane, G.M.; Samols, M.A.; Morsberger, L.A.; Yonescu, R.; Thiess, M.L.; Batista, D.A.; Ning, Y.; Burns, K.H.; Vuica-Ross, M.; Borowitz, M.J.; et al. Tumor-infiltrating macrophages in post-transplant, relapsed classical hodgkin lymphoma are donor-derived. *PLoS ONE* **2016**, *11*, e0163559. [CrossRef] [PubMed]

97. Wilson, C.; Brown, H.; Holen, I. The endocrine influence on the bone microenvironment in early breast cancer. *Endocr. Relat. Cancer* **2016**, *23*, R567–R576. [CrossRef] [PubMed]
98. Zhang, Y.; Ma, C.; Wang, M.; Hou, H.; Cui, L.; Jiang, C.; Sun, J.; Qu, X. Prognostic significance of immune cells in the tumor microenvironment and peripheral blood of gallbladder carcinoma patients. *Clin. Transl. Oncol.* **2016**, *19*, 477–488. [CrossRef] [PubMed]
99. Hanahan, D.; Weinberg, R.A. The hallmarks of cancer. *Cell* **2000**, *100*, 57–70. [CrossRef]
100. Hanahan, D.; Weinberg, R.A. Hallmarks of cancer: The next generation. *Cell* **2011**, *144*, 646–674. [CrossRef] [PubMed]
101. Lazebnik, Y. What are the hallmarks of cancer? *Nat. Rev. Cancer* **2010**, *10*, 232–233. [CrossRef] [PubMed]
102. Tommelein, J.; Verset, L.; Boterberg, T.; Demetter, P.; Bracke, M.; De Wever, O. Cancer-associated fibroblasts connect metastasis-promoting communication in colorectal cancer. *Front. Oncol.* **2015**, *5*, 63. [CrossRef] [PubMed]
103. Wintzell, M.; Hjerpe, E.; Avall Lundqvist, E.; Shoshan, M. Protein markers of cancer-associated fibroblasts and tumor-initiating cells reveal subpopulations in freshly isolated ovarian cancer ascites. *BMC Cancer* **2012**, *12*, 359. [CrossRef] [PubMed]
104. Ohlund, D.; Handly-Santana, A.; Biffi, G.; Elyada, E.; Almeida, A.S.; Ponz-Sarvise, M.; Corbo, V.; Oni, T.E.; Hearn, S.A.; Lee, E.J.; et al. Distinct populations of inflammatory fibroblasts and myofibroblasts in pancreatic cancer. *J. Exp. Med.* **2017**, *214*, 579–596. [PubMed]
105. Bourguignon, L.Y. Matrix hyaluronan promotes specific microrna upregulation leading to drug resistance and tumor progression. *Int. J. Mol. Sci.* **2016**, *17*, 517. [CrossRef] [PubMed]
106. Bourguignon, L.Y.; Shiina, M.; Li, J.J. Hyaluronan-cd44 interaction promotes oncogenic signaling, microrna functions, chemoresistance, and radiation resistance in cancer stem cells leading to tumor progression. *Adv. Cancer Res.* **2014**, *123*, 255–275. [PubMed]
107. Bulysheva, A.A.; Bowlin, G.L.; Petrova, S.P.; Yeudall, W.A. Enhanced chemoresistance of squamous carcinoma cells grown in 3D cryogenic electrospun scaffolds. *Biomed. Mater.* **2013**, *8*, 055009. [CrossRef] [PubMed]
108. Le Calve, B.; Griveau, A.; Vindrieux, D.; Marechal, R.; Wiel, C.; Svrcek, M.; Gout, J.; Azzi, L.; Payen, L.; Cros, J.; et al. Lysyl oxidase family activity promotes resistance of pancreatic ductal adenocarcinoma to chemotherapy by limiting the intratumoral anticancer drug distribution. *Oncotarget* **2016**, *7*, 32100–32112. [CrossRef] [PubMed]
109. Payne, L.S.; Huang, P.H. The pathobiology of collagens in glioma. *Mol. Cancer Res. MCR* **2013**, *11*, 1129–1140. [CrossRef] [PubMed]
110. Rajesh, Y.; Biswas, A.; Mandal, M. Glioma progression through the prism of heat shock protein mediated extracellular matrix remodeling and epithelial to mesenchymal transition. *Exp. Cell Res.* **2017**, *359*, 299–311. [CrossRef] [PubMed]
111. Sato, N.; Kohi, S.; Hirata, K.; Goggins, M. Role of hyaluronan in pancreatic cancer biology and therapy: Once again in the spotlight. *Cancer Sci.* **2016**, *107*, 569–575. [CrossRef] [PubMed]
112. Senthebane, D.A.; Rowe, A.; Thomford, N.E.; Shipanga, H.; Munro, D.; Mazeedi, M.; Almazyadi, H.A.M.; Kallmeyer, K.; Dandara, C.; Pepper, M.S.; et al. The role of tumor microenvironment in chemoresistance: To survive, keep your enemies closer. *Int. J. Mol. Sci.* **2017**, *18*, 1586. [CrossRef] [PubMed]
113. Clementz, A.G.; Harris, A. Collagen xv: Exploring its structure and role within the tumor microenvironment. *Mol. Cancer Res. MCR* **2013**, *11*, 1481–1486. [CrossRef] [PubMed]
114. Cox, T.R.; Bird, D.; Baker, A.M.; Barker, H.E.; Ho, M.W.; Lang, G.; Erler, J.T. Lox-mediated collagen crosslinking is responsible for fibrosis-enhanced metastasis. *Cancer Res.* **2013**, *73*, 1721–1732. [CrossRef] [PubMed]
115. Eisinger-Mathason, T.S.; Zhang, M.; Qiu, Q.; Skuli, N.; Nakazawa, M.S.; Karakasheva, T.; Mucaj, V.; Shay, J.E.; Stangenberg, L.; Sadri, N.; et al. Hypoxia-dependent modification of collagen networks promotes sarcoma metastasis. *Cancer Discov.* **2013**, *3*, 1190–1205. [CrossRef] [PubMed]
116. Gilkes, D.M.; Chaturvedi, P.; Bajpai, S.; Wong, C.C.; Wei, H.; Pitcairn, S.; Hubbi, M.E.; Wirtz, D.; Semenza, G.L. Collagen prolyl hydroxylases are essential for breast cancer metastasis. *Cancer Res.* **2013**, *73*, 3285–3296. [CrossRef] [PubMed]
117. Goto, R.; Nakamura, Y.; Takami, T.; Sanke, T.; Tozuka, Z. Quantitative lc-ms/ms analysis of proteins involved in metastasis of breast cancer. *PLoS ONE* **2015**, *10*, e0130760. [CrossRef] [PubMed]

118. Raglow, Z.; Thomas, S.M. Tumor matrix protein collagen xialpha1 in cancer. *Cancer Lett.* **2015**, *357*, 448–453. [CrossRef] [PubMed]
119. Shen, Y.; Shen, R.; Ge, L.; Zhu, Q.; Li, F. Fibrillar type I collagen matrices enhance metastasis/invasion of ovarian epithelial cancer via beta1 integrin and pten signals. *Int. J. Gynecol. Cancer* **2012**, *22*, 1316–1324. [CrossRef] [PubMed]
120. Spivey, K.A.; Chung, I.; Banyard, J.; Adini, I.; Feldman, H.A.; Zetter, B.R. A role for collagen xxiii in cancer cell adhesion, anchorage-independence and metastasis. *Oncogene* **2012**, *31*, 2362–2372. [CrossRef] [PubMed]
121. Tanis, T.; Cincin, Z.B.; Gokcen-Rohlig, B.; Bireller, E.S.; Ulusan, M.; Tanyel, C.R.; Cakmakoglu, B. The role of components of the extracellular matrix and inflammation on oral squamous cell carcinoma metastasis. *Arch. Oral Biol.* **2014**, *59*, 1155–1163. [CrossRef] [PubMed]
122. Torzilli, P.A.; Bourne, J.W.; Cigler, T.; Vincent, C.T. A new paradigm for mechanobiological mechanisms in tumor metastasis. *Semin. Cancer Biol.* **2012**, *22*, 385–395. [CrossRef] [PubMed]
123. Ferguson, J.; Arozarena, I.; Ehrhardt, M.; Wellbrock, C. Combination of mek and src inhibition suppresses melanoma cell growth and invasion. *Oncogene* **2013**, *32*, 86–96. [CrossRef] [PubMed]
124. Hayashido, Y.; Kitano, H.; Sakaue, T.; Fujii, T.; Suematsu, M.; Sakurai, S.; Okamoto, T. Overexpression of integrin alphav facilitates proliferation and invasion of oral squamous cell carcinoma cells via MEK/ERK signaling pathway that is activated by interaction of integrin alphavbeta8 with type collagen. *Int. J. Oncol.* **2014**, *45*, 1875–1882. [CrossRef] [PubMed]
125. Jenkins, M.H.; Croteau, W.; Mullins, D.W.; Brinckerhoff, C.E. The BRAF(V600E) inhibitor, PLX4032, increases type I collagen synthesis in melanoma cells. *Matrix Biol. J. Int. Soc. Matrix Biol.* **2015**, *48*, 66–77. [CrossRef] [PubMed]
126. Yoshimoto, T.; Takino, T.; Li, Z.; Domoto, T.; Sato, H. Vinculin negatively regulates transcription of mt1-mmp through MEK/ERK pathway. *Biochem. Biophys. Res. Commun.* **2014**, *455*, 251–255. [CrossRef] [PubMed]
127. Alemany-Ribes, M.; Semino, C.E. Bioengineering 3D environments for cancer models. *Adv. Drug Deliv. Rev.* **2014**, *79–80*, 40–49. [CrossRef] [PubMed]
128. Benien, P.; Swami, A. 3D tumor models: History, advances and future perspectives. *Future Oncol.* **2014**, *10*, 1311–1327. [CrossRef] [PubMed]
129. Hirt, C.; Papadimitropoulos, A.; Mele, V.; Muraro, M.G.; Mengus, C.; Iezzi, G.; Terracciano, L.; Martin, I.; Spagnoli, G.C. "In vitro" 3D models of tumor-immune system interaction. *Adv. Drug Deliv. Rev.* **2014**, *79–80*, 145–154. [CrossRef] [PubMed]
130. Imamura, Y.; Mukohara, T.; Shimono, Y.; Funakoshi, Y.; Chayahara, N.; Toyoda, M.; Kiyota, N.; Takao, S.; Kono, S.; Nakatsura, T.; et al. Comparison of 2D- and 3D-culture models as drug-testing platforms in breast cancer. *Oncol. Rep.* **2015**, *33*, 1837–1843. [CrossRef] [PubMed]
131. Sung, K.E.; Beebe, D.J. Microfluidic 3D models of cancer. *Adv. Drug Deliv. Rev.* **2014**, *79–80*, 68–78. [CrossRef] [PubMed]
132. Tanner, K.; Gottesman, M.M. Beyond 3D culture models of cancer. *Sci. Transl. Med.* **2015**, *7*, 283–289. [CrossRef] [PubMed]
133. Weiswald, L.B.; Bellet, D.; Dangles-Marie, V. Spherical cancer models in tumor biology. *Neoplasia* **2015**, *17*, 1–15. [CrossRef] [PubMed]
134. Aihara, A.; Abe, N.; Saruhashi, K.; Kanaki, T.; Nishino, T. A novel 3-D cell culture system for in vitro evaluation of anticancer drugs under anchorage-independent conditions. *Cancer Sci.* **2016**, *107*, 1858–1866. [CrossRef] [PubMed]
135. Pickup, M.W.; Mouw, J.K.; Weaver, V.M. The extracellular matrix modulates the hallmarks of cancer. *EMBO Rep.* **2014**, *15*, 1243–1253. [CrossRef] [PubMed]
136. Fitzgerald, K.A.; Guo, J.; Tierney, E.G.; Curtin, C.M.; Malhotra, M.; Darcy, R.; O'Brien, F.J.; O'Driscoll, C.M. The use of collagen-based scaffolds to simulate prostate cancer bone metastases with potential for evaluating delivery of nanoparticulate gene therapeutics. *Biomaterials* **2015**, *66*, 53–66. [CrossRef] [PubMed]
137. Fraley, S.I.; Wu, P.H.; He, L.; Feng, Y.; Krisnamurthy, R.; Longmore, G.D.; Wirtz, D. Three-dimensional matrix fiber alignment modulates cell migration and MT1-MMP utility by spatially and temporally directing protrusions. *Sci. Rep.* **2015**, *5*, 14580. [CrossRef] [PubMed]
138. Talukdar, S.; Mandal, M.; Hutmacher, D.W.; Russell, P.J.; Soekmadji, C.; Kundu, S.C. Engineered silk fibroin protein 3D matrices for in vitro tumor model. *Biomaterials* **2011**, *32*, 2149–2159. [CrossRef] [PubMed]

139. Dong, Y.; Stephens, C.; Walpole, C.; Swedberg, J.E.; Boyle, G.M.; Parsons, P.G.; McGuckin, M.A.; Harris, J.M.; Clements, J.A. Paclitaxel resistance and multicellular spheroid formation are induced by kallikrein-related peptidase 4 in serous ovarian cancer cells in an ascites mimicking microenvironment. *PLoS ONE* **2013**, *8*, e57056. [CrossRef] [PubMed]
140. Loessner, D.; Rizzi, S.C.; Stok, K.S.; Fuehrmann, T.; Hollier, B.; Magdolen, V.; Hutmacher, D.W.; Clements, J.A. A bioengineered 3D ovarian cancer model for the assessment of peptidase-mediated enhancement of spheroid growth and intraperitoneal spread. *Biomaterials* **2013**, *34*, 7389–7400. [CrossRef] [PubMed]
141. Loessner, D.; Stok, K.S.; Lutolf, M.P.; Hutmacher, D.W.; Clements, J.A.; Rizzi, S.C. Bioengineered 3D platform to explore cell-ECM interactions and drug resistance of epithelial ovarian cancer cells. *Biomaterials* **2010**, *31*, 8494–8506. [CrossRef] [PubMed]
142. Soritau, O.; Tomuleasa, C.I.; Pall, E.; Virag, P.; Fischer-Fodor, E.; Foris, V.; Barbos, O.; Tatomir, C.; Kacso, G.; Irimie, A. Enhanced chemoresistance and tumor sphere formation as a laboratory model for peritoneal micrometastasis in epithelial ovarian cancer. *Rom. J. Morphol. Embryol.* **2010**, *51*, 259–264. [PubMed]
143. Hirt, C.; Papadimitropoulos, A.; Muraro, M.G.; Mele, V.; Panopoulos, E.; Cremonesi, E.; Ivanek, R.; Schultz-Thater, E.; Droeser, R.A.; Mengus, C.; et al. Bioreactor-engineered cancer tissue-like structures mimic phenotypes, gene expression profiles and drug resistance patterns observed "in vivo". *Biomaterials* **2015**, *62*, 138–146. [CrossRef] [PubMed]
144. Lv, D.; Yu, S.C.; Ping, Y.F.; Wu, H.; Zhao, X.; Zhang, H.; Cui, Y.; Chen, B.; Zhang, X.; Dai, J.; et al. A three-dimensional collagen scaffold cell culture system for screening anti-glioma therapeutics. *Oncotarget* **2016**, *7*, 56904–56914. [CrossRef] [PubMed]
145. Sarkar, J.; Kumar, A. Thermo-responsive polymer aided spheroid culture in cryogel based platform for high throughput drug screening. *Analyst* **2016**, *141*, 2553–2567. [CrossRef] [PubMed]
146. Wang, J.Z.; Zhu, Y.X.; Ma, H.C.; Chen, S.N.; Chao, J.Y.; Ruan, W.D.; Wang, D.; Du, F.G.; Meng, Y.Z. Developing multi-cellular tumor spheroid model (MCTS) in the chitosan/collagen/alginate (CCA) fibrous scaffold for anticancer drug screening. *Mater. Sci. Eng. C Mater. Biol. Appl.* **2016**, *62*, 215–225. [CrossRef] [PubMed]
147. Yan, X.; Wang, J.; Zhu, L.; Lowrey, J.J.; Zhang, Y.; Hou, W.; Dong, J.; Du, Y. A ready-to-use, versatile, multiplex-able three-dimensional scaffold-based immunoassay chip for high throughput hepatotoxicity evaluation. *Lab Chip* **2015**, *15*, 2634–2646. [CrossRef] [PubMed]
148. Reticker-Flynn, N.E.; Malta, D.F.; Winslow, M.M.; Lamar, J.M.; Xu, M.J.; Underhill, G.H.; Hynes, R.O.; Jacks, T.E.; Bhatia, S.N. A combinatorial extracellular matrix platform identifies cell-extracellular matrix interactions that correlate with metastasis. *Nat. Commun.* **2012**, *3*, 1122. [CrossRef] [PubMed]
149. Hoshiba, T.; Tanaka, M. Breast cancer cell behaviors on staged tumorigenesis-mimicking matrices derived from tumor cells at various malignant stages. *Biochem. Biophys. Res. Commun.* **2013**, *439*, 291–296. [CrossRef] [PubMed]
150. Castello-Cros, R.; Khan, D.R.; Simons, J.; Valianou, M.; Cukierman, E. Staged stromal extracellular 3D matrices differentially regulate breast cancer cell responses through PI3K and beta1-integrins. *BMC Cancer* **2009**, *9*, 94. [CrossRef] [PubMed]
151. Bissell, M. Q&A: Mina bissell on tumors as organs. *Cancer Discov.* **2013**, *3*, 7. [PubMed]
152. Bissell, M.J. Thinking in three dimensions: Discovering reciprocal signaling between the extracellular matrix and nucleus and the wisdom of microenvironment and tissue architecture. *Mol. Biol. Cell* **2016**, *27*, 3205–3209. [CrossRef] [PubMed]
153. Bissell, M.J. Goodbye flat biology-time for the 3rd and the 4th dimensions. *J. Cell Sci.* **2017**, *130*, 3–5. [CrossRef] [PubMed]
154. Nakasone, E.S.; Askautrud, H.A.; Kees, T.; Park, J.H.; Plaks, V.; Ewald, A.J.; Fein, M.; Rasch, M.G.; Tan, Y.X.; Qiu, J.; et al. Imaging tumor-stroma interactions during chemotherapy reveals contributions of the microenvironment to resistance. *Cancer Cell* **2012**, *21*, 488–503. [CrossRef] [PubMed]
155. Simian, M.; Bissell, M.J. Organoids: A historical perspective of thinking in three dimensions. *J. Cell Biol.* **2017**, *216*, 31–40. [CrossRef] [PubMed]
156. Vidi, P.A.; Bissell, M.J.; Lelievre, S.A. Three-dimensional culture of human breast epithelial cells: The how and the why. *Methods Mol. Biol.* **2013**, *945*, 193–219. [PubMed]

157. Weigelt, B.; Ghajar, C.M.; Bissell, M.J. The need for complex 3D culture models to unravel novel pathways and identify accurate biomarkers in breast cancer. *Adv. Drug Deliv. Rev.* **2014**, *69–70*, 42–51. [CrossRef] [PubMed]
158. Rintoul, R.C.; Sethi, T. The role of extracellular matrix in small-cell lung cancer. *Lancet. Oncol.* **2001**, *2*, 437–442. [CrossRef]
159. Rintoul, R.C.; Sethi, T. Extracellular matrix regulation of drug resistance in small-cell lung cancer. *Clin. Sci.* **2002**, *102*, 417–424. [CrossRef] [PubMed]
160. Sethi, T.; Ginsberg, M.H.; Downward, J.; Hughes, P.E. The small GTP-binding protein R-RAS can influence integrin activation by antagonizing a RAS/RAF-initiated integrin suppression pathway. *Mol. Biol. Cell* **1999**, *10*, 1799–1809. [CrossRef] [PubMed]
161. Sethi, T.; Rintoul, R.C.; Moore, S.M.; MacKinnon, A.C.; Salter, D.; Choo, C.; Chilvers, E.R.; Dransfield, I.; Donnelly, S.C.; Strieter, R.; et al. Extracellular matrix proteins protect small cell lung cancer cells against apoptosis: A mechanism for small cell lung cancer growth and drug resistance in vivo. *Nat. Med.* **1999**, *5*, 662–668. [CrossRef] [PubMed]
162. Sethi, T.; Woll, P.J. Growth factors and lung cancer. *Cancer Treat. Res.* **1995**, *72*, 111–130. [PubMed]
163. Janouskova, H.; Maglott, A.; Leger, D.Y.; Bossert, C.; Noulet, F.; Guerin, E.; Guenot, D.; Pinel, S.; Chastagner, P.; Plenat, F.; et al. Integrin alpha5beta1 plays a critical role in resistance to temozolomide by interfering with the p53 pathway in high-grade glioma. *Cancer Res.* **2012**, *72*, 3463–3470. [CrossRef] [PubMed]
164. Janouskova, H.; Ray, A.M.; Noulet, F.; Lelong-Rebel, I.; Choulier, L.; Schaffner, F.; Lehmann, M.; Martin, S.; Teisinger, J.; Dontenwill, M. Activation of p53 pathway by nutlin-3a inhibits the expression of the therapeutic target alpha5 integrin in colon cancer cells. *Cancer Lett.* **2013**, *336*, 307–318. [CrossRef] [PubMed]
165. Martin, S.; Janouskova, H.; Dontenwill, M. Integrins and p53 pathways in glioblastoma resistance to temozolomide. *Front. Oncol.* **2012**, *2*, 157. [CrossRef] [PubMed]
166. Goel, H.L.; Sayeed, A.; Breen, M.; Zarif, M.J.; Garlick, D.S.; Leav, I.; Davis, R.J.; Fitzgerald, T.J.; Morrione, A.; Hsieh, C.C.; et al. Beta1 integrins mediate resistance to ionizing radiation in vivo by inhibiting c-jun amino terminal kinase 1. *J. Cell. Physiol.* **2013**, *228*, 1601–1609. [CrossRef] [PubMed]
167. Hsieh, I.S.; Huang, W.H.; Liou, H.C.; Chuang, W.J.; Yang, R.S.; Fu, W.M. Upregulation of drug transporter expression by osteopontin in prostate cancer cells. *Mol. Pharmacol.* **2013**, *83*, 968–977. [CrossRef] [PubMed]
168. Hsieh, Y.T.; Gang, E.J.; Geng, H.; Park, E.; Huantes, S.; Chudziak, D.; Dauber, K.; Schaefer, P.; Scharman, C.; Shimada, H.; et al. Integrin alpha4 blockade sensitizes drug resistant PRE-B acute lymphoblastic leukemia to chemotherapy. *Blood* **2013**, *121*, 1814–1818. [CrossRef] [PubMed]
169. Hsieh, Y.T.; Gang, E.J.; Shishido, S.N.; Kim, H.N.; Pham, J.; Khazal, S.; Osborne, A.; Esguerra, Z.A.; Kwok, E.; Jang, J.; et al. Effects of the small-molecule inhibitor of integrin alpha4, TBC3486, on pre-b-all cells. *Leukemia* **2014**, *28*, 2101–2104. [CrossRef] [PubMed]
170. De, P.; Dey, N.; Terakedis, B.; Bergsagel, P.L.; Li, Z.H.; Mahadevan, D.; Garlich, J.R.; Trudel, S.; Makale, M.T.; Durden, D.L. An integrin-targeted, pan-isoform, phosphoinositide-3 kinase inhibitor, SF1126, has activity against multiple myeloma in vivo. *Cancer Chemother. Pharmacol.* **2013**, *71*, 867–881. [CrossRef] [PubMed]
171. Paiva, B.; Corchete, L.A.; Vidriales, M.B.; Puig, N.; Maiso, P.; Rodriguez, I.; Alignani, D.; Burgos, L.; Sanchez, M.L.; Barcena, P.; et al. Phenotypic and genomic analysis of multiple myeloma minimal residual disease tumor cells: A new model to understand chemoresistance. *Blood* **2016**, *127*, 1896–1906. [CrossRef] [PubMed]
172. De, P.; Carlson, J.H.; Jepperson, T.; Willis, S.; Leyland-Jones, B.; Dey, N. Rac1 GTP-ASE signals wnt-beta-catenin pathway mediated integrin-directed metastasis-associated tumor cell phenotypes in triple negative breast cancers. *Oncotarget* **2017**, *8*, 3072–3103. [PubMed]
173. Dhawan, A.; Friedrichs, J.; Bonin, M.V.; Bejestani, E.P.; Werner, C.; Wobus, M.; Chavakis, T.; Bornhauser, M. Breast cancer cells compete with hematopoietic stem and progenitor cells for intercellular adhesion molecule 1-mediated binding to the bone marrow microenvironment. *Carcinogenesis* **2016**, *37*, 759–767. [CrossRef] [PubMed]
174. Hedrick, E.; Lee, S.O.; Doddapaneni, R.; Singh, M.; Safe, S. NR4A1 antagonists inhibit beta1-integrin-dependent breast cancer cell migration. *Mol. Cell. Biol.* **2016**, *36*, 1383–1394. [CrossRef] [PubMed]

175. Li, W.; Liu, C.; Zhao, C.; Zhai, L.; Lv, S. Downregulation of beta3 integrin by mir-30a-5p modulates cell adhesion and invasion by interrupting erk/ets1 network in triple-negative breast cancer. *Int. J. Oncol.* **2016**, *48*, 1155–1164. [CrossRef] [PubMed]
176. Morozevich, G.E.; Kozlova, N.I.; Susova, O.Y.; Karalkin, P.A.; Berman, A.E. Implication of alpha2beta1 integrin in anoikis of mcf-7 human breast carcinoma cells. *Biochem. Biokhimiia* **2015**, *80*, 97–103. [CrossRef] [PubMed]
177. Sarper, M.; Allen, M.D.; Gomm, J.; Haywood, L.; Decock, J.; Thirkettle, S.; Ustaoglu, A.; Sarker, S.J.; Marshall, J.; Edwards, D.R.; et al. Loss of mmp-8 in ductal carcinoma in situ (DCIS)-associated myoepithelial cells contributes to tumor promotion through altered adhesive and proteolytic function. *Breast Cancer Res. BCR* **2017**, *19*, 33. [CrossRef] [PubMed]
178. Shao, N.; Lu, Z.; Zhang, Y.; Wang, M.; Li, W.; Hu, Z.; Wang, S.; Lin, Y. Interleukin-8 upregulates integrin beta3 expression and promotes estrogen receptor-negative breast cancer cell invasion by activating the PI3K/AKT/NF-Kappab pathway. *Cancer Lett.* **2015**, *364*, 165–172. [CrossRef] [PubMed]
179. Yao, H.; Veine, D.M.; Livant, D.L. Therapeutic inhibition of breast cancer bone metastasis progression and lung colonization: Breaking the vicious cycle by targeting alpha5beta1 integrin. *Breast Cancer Res. Treat.* **2016**, *157*, 489–501. [CrossRef] [PubMed]
180. Dickreuter, E.; Eke, I.; Krause, M.; Borgmann, K.; van Vugt, M.A.; Cordes, N. Targeting of beta1 integrins impairs DNA repair for radiosensitization of head and neck cancer cells. *Oncogene* **2016**, *35*, 1353–1362. [CrossRef] [PubMed]
181. Graham, K.; Moran-Jones, K.; Sansom, O.J.; Brunton, V.G.; Frame, M.C. Fak deletion promotes p53-mediated induction of p21, DNA-damage responses and radio-resistance in advanced squamous cancer cells. *PLoS ONE* **2011**, *6*, e27806. [CrossRef] [PubMed]
182. Huang, H.; McIntosh, J.L.; Fang, L.; Szabo, C.; Hoyt, D.G. Integrin-mediated suppression of endotoxin-induced DNA damage in lung endothelial cells is sensitive to poly(ADP-RIBOSE) polymerase-1 gene deletion. *Int. J. Mol. Med.* **2003**, *12*, 533–540. [CrossRef] [PubMed]
183. Loeffler, M.; Kruger, J.A.; Niethammer, A.G.; Reisfeld, R.A. Targeting tumor-associated fibroblasts improves cancer chemotherapy by increasing intratumoral drug uptake. *J. Clin. Investig.* **2006**, *116*, 1955–1962. [CrossRef] [PubMed]
184. Amornsupak, K.; Insawang, T.; Thuwajit, P.; O-Charoenrat, P.; Eccles, S.A.; Thuwajit, C. Cancer-associated fibroblasts induce high mobility group box 1 and contribute to resistance to doxorubicin in breast cancer cells. *BMC Cancer* **2014**, *14*, 955. [CrossRef] [PubMed]
185. Yousif, N.G. Fibronectin promotes migration and invasion of ovarian cancer cells through up-regulation of fak-pi3k/akt pathway. *Cell Biol. Int.* **2014**, *38*, 85–91. [CrossRef] [PubMed]
186. Gourley, C.; Paige, A.J.; Taylor, K.J.; Ward, C.; Kuske, B.; Zhang, J.; Sun, M.; Janczar, S.; Harrison, D.J.; Muir, M.; et al. Wwox gene expression abolishes ovarian cancer tumorigenicity in vivo and decreases attachment to fibronectin via integrin alpha3. *Cancer Res.* **2009**, *69*, 4835–4842. [CrossRef] [PubMed]
187. Lou, X.; Han, X.; Jin, C.; Tian, W.; Yu, W.; Ding, D.; Cheng, L.; Huang, B.; Jiang, H.; Lin, B. Sox2 targets fibronectin 1 to promote cell migration and invasion in ovarian cancer: New molecular leads for therapeutic intervention. *Omics* **2013**, *17*, 510–518. [CrossRef] [PubMed]
188. Pontiggia, O.; Sampayo, R.; Raffo, D.; Motter, A.; Xu, R.; Bissell, M.J.; Joffe, E.B.; Simian, M. The tumor microenvironment modulates tamoxifen resistance in breast cancer: A role for soluble stromal factors and fibronectin through beta1 integrin. *Breast Cancer Res. Treat.* **2012**, *133*, 459–471. [CrossRef] [PubMed]
189. Yuan, J.; Liu, M.; Yang, L.; Tu, G.; Zhu, Q.; Chen, M.; Cheng, H.; Luo, H.; Fu, W.; Li, Z.; et al. Acquisition of epithelial-mesenchymal transition phenotype in the tamoxifen-resistant breast cancer cell: A new role for g protein-coupled estrogen receptor in mediating tamoxifen resistance through cancer-associated fibroblast-derived fibronectin and beta1-integrin signaling pathway in tumor cells. *Breast Cancer Res. BCR* **2015**, *17*, 69. [PubMed]
190. Tomasini-Johansson, B.R.; Kaufman, N.R.; Ensenberger, M.G.; Ozeri, V.; Hanski, E.; Mosher, D.F. A 49-residue peptide from adhesin f1 of streptococcus pyogenes inhibits fibronectin matrix assembly. *J. Biol. Chem.* **2001**, *276*, 23430–23439. [CrossRef] [PubMed]
191. Holle, A.W.; Young, J.L.; Spatz, J.P. In vitro cancer cell-ECM interactions inform in vivo cancer treatment. *Adv. Drug Deliv. Rev.* **2016**, *97*, 270–279. [CrossRef] [PubMed]

192. Oskarsson, T. Extracellular matrix components in breast cancer progression and metastasis. *Breast* **2013**, *22* (Suppl. 2), S66–S72. [CrossRef] [PubMed]
193. Glinsky, G.V. Anti-adhesion cancer therapy. *Cancer Metastasis Rev.* **1998**, *17*, 177–185. [CrossRef] [PubMed]
194. Juliano, R.L.; Varner, J.A. Adhesion molecules in cancer: The role of integrins. *Curr. Opin. Cell Biol.* **1993**, *5*, 812–818. [CrossRef]
195. Carragher, N.O.; Frame, M.C. Focal adhesion and actin dynamics: A place where kinases and proteases meet to promote invasion. *Trends Cell Biol.* **2004**, *14*, 241–249. [CrossRef] [PubMed]
196. Zhao, B.; Lei, Q.; Guan, K.L. Mst out and hcc in. *Cancer Cell* **2009**, *16*, 363–364. [CrossRef] [PubMed]
197. Bommert, K.; Bargou, R.C.; Stuhmer, T. Signalling and survival pathways in multiple myeloma. *Eur. J. Cancer* **2006**, *42*, 1574–1580. [CrossRef] [PubMed]
198. Chatterjee, M.; Jain, S.; Stuhmer, T.; Andrulis, M.; Ungethum, U.; Kuban, R.J.; Lorentz, H.; Bommert, K.; Topp, M.; Kramer, D.; et al. STAT3 and MAPK signaling maintain overexpression of heat shock proteins 90alpha and beta in multiple myeloma cells, which critically contribute to tumor-cell survival. *Blood* **2007**, *109*, 720–728. [CrossRef] [PubMed]
199. Farmer, P.; Bonnefoi, H.; Anderle, P.; Cameron, D.; Wirapati, P.; Becette, V.; Andre, S.; Piccart, M.; Campone, M.; Brain, E.; et al. A stroma-related gene signature predicts resistance to neoadjuvant chemotherapy in breast cancer. *Nat. Med.* **2009**, *15*, 68–74. [CrossRef] [PubMed]
200. Liang, H.; Li, X.; Chen, B.; Wang, B.; Zhao, Y.; Zhuang, Y.; Shen, H.; Zhang, Z.; Dai, J. A collagen-binding egfr single-chain fv antibody fragment for the targeted cancer therapy. *J. Control. Release* **2015**, *209*, 101–109. [CrossRef] [PubMed]
201. Misra, S.; Hascall, V.C.; Atanelishvili, I.; Moreno Rodriguez, R.; Markwald, R.R.; Ghatak, S. Utilization of glycosaminoglycans/proteoglycans as carriers for targeted therapy delivery. *Int. J. Cell Biol.* **2015**, *2015*, 537560. [CrossRef] [PubMed]
202. Nikitovic, D.; Kouvidi, K.; Kavasi, R.M.; Berdiaki, A.; Tzanakakis, G.N. Hyaluronan/hyaladherins—A promising axis for targeted drug delivery in cancer. *Curr. Drug Deliv.* **2016**, *13*, 500–511. [CrossRef] [PubMed]
203. Sato, N.; Cheng, X.B.; Kohi, S.; Koga, A.; Hirata, K. Targeting hyaluronan for the treatment of pancreatic ductal adenocarcinoma. *Acta Pharm. Sin. B* **2016**, *6*, 101–105. [CrossRef] [PubMed]
204. Yata, T.; Lee, E.L.; Suwan, K.; Syed, N.; Asavarut, P.; Hajitou, A. Modulation of extracellular matrix in cancer is associated with enhanced tumor cell targeting by bacteriophage vectors. *Mol. Cancer* **2015**, *14*, 110. [CrossRef] [PubMed]
205. Cun, X.; Chen, J.; Ruan, S.; Zhang, L.; Wan, J.; He, Q.; Gao, H. A novel strategy through combining irgd peptide with tumor-microenvironment-responsive and multistage nanoparticles for deep tumor penetration. *ACS Appl. Mater. Interfaces* **2015**, *7*, 27458–27466. [CrossRef] [PubMed]
206. Cun, X.; Ruan, S.; Chen, J.; Zhang, L.; Li, J.; He, Q.; Gao, H. A dual strategy to improve the penetration and treatment of breast cancer by combining shrinking nanoparticles with collagen depletion by losartan. *Acta Biomater.* **2016**, *31*, 186–196. [CrossRef] [PubMed]
207. Jena, P.V.; Shamay, Y.; Shah, J.; Roxbury, D.; Paknejad, N.; Heller, D.A. Photoluminescent carbon nanotubes interrogate the permeability of multicellular tumor spheroids. *Carbon* **2016**, *97*, 99–109. [CrossRef] [PubMed]
208. Poh, S.; Chelvam, V.; Low, P.S. Comparison of nanoparticle penetration into solid tumors and sites of inflammation: Studies using targeted and nontargeted liposomes. *Nanomedicine* **2015**, *10*, 1439–1449. [CrossRef] [PubMed]
209. Villegas, M.R.; Baeza, A.; Vallet-Regi, M. Hybrid collagenase nanocapsules for enhanced nanocarrier penetration in tumoral tissues. *ACS Appl. Mater. Interfaces* **2015**, *7*, 24075–24081. [CrossRef] [PubMed]
210. Wong, C.; Stylianopoulos, T.; Cui, J.; Martin, J.; Chauhan, V.P.; Jiang, W.; Popovic, Z.; Jain, R.K.; Bawendi, M.G.; Fukumura, D. Multistage nanoparticle delivery system for deep penetration into tumor tissue. *Proc. Natl. Acad. Sci. USA* **2011**, *108*, 2426–2431. [CrossRef] [PubMed]
211. Zhang, B.; Jiang, T.; Shen, S.; She, X.; Tuo, Y.; Hu, Y.; Pang, Z.; Jiang, X. Cyclopamine disrupts tumor extracellular matrix and improves the distribution and efficacy of nanotherapeutics in pancreatic cancer. *Biomaterials* **2016**, *103*, 12–21. [CrossRef] [PubMed]
212. Veale, R.B.; Thornley, A.L. Increased single class low affinity EGF receptors expressed by human oesophageal squamous carcinoma cell lines. *S. Afr. J. Sci.* **1989**, *85*, 375–379.
213. Shimada, Y.; Imamura, M.; Wagata, T.; Yamaguchi, N.; Tobe, T. Characterization of 21 newly established esophageal cancer cell lines. *Cancer* **1992**, *69*, 277–284. [CrossRef]

214. Kaschula, C.H.; Hunter, R.; Stellenboom, N.; Caira, M.R.; Winks, S.; Ogunleye, T.; Richards, P.; Cotton, J.; Zilbeyaz, K.; Wang, Y.; et al. Structure-activity studies on the anti-proliferation activity of ajoene analogues in whco1 oesophageal cancer cells. *Eur. J. Med. Chem.* **2012**, *50*, 236–254. [CrossRef] [PubMed]
215. Dzobo, K.; Vogelsang, M.; Parker, M.I. Wnt/beta-catenin and MEK-ERK signaling are required for fibroblast-derived extracellular matrix-mediated endoderm differentiation of embryonic stem cells. *Stem Cell Rev.* **2015**, *11*, 761–773. [CrossRef] [PubMed]
216. Chomczynski, P.; Sacchi, N. Single-step method of RNA isolation by acid guanidinium thiocyanate-phenol-chloroform extraction. *Anal. Biochem.* **1987**, *162*, 156–159. [CrossRef]
217. Livak, K.J.; Schmittgen, T.D. Analysis of relative gene expression data using real-time quantitative pcr and the 2(-Delta Delta C(T)) method. *Methods* **2001**, *25*, 402–408. [CrossRef] [PubMed]
218. Dzobo, K.; Leaner, V.D.; Parker, M.I. Absence of feedback regulation in the synthesis of COL1A1. *Life Sci.* **2014**, *103*, 25–33. [CrossRef] [PubMed]
219. Wisniewski, J.R.; Zougman, A.; Nagaraj, N.; Mann, M. Universal sample preparation method for proteome analysis. *Nat. Methods* **2009**, *6*, 359–362. [CrossRef] [PubMed]

International Journal of
Molecular Sciences

MDPI

Review

The Role of Tumor Microenvironment in Chemoresistance: To Survive, Keep Your Enemies Closer

Dimakatso Alice Senthebane [1], Arielle Rowe [2], Nicholas Ekow Thomford [3], Hendrina Shipanga [1], Daniella Munro [3], Mohammad A. M. Al Mazeedi [4], Hashim A. M. Almazyadi [4], Karlien Kallmeyer [5], Collet Dandara [3], Michael S. Pepper [5], M. Iqbal Parker [1,2] and Kevin Dzobo [1,2,*]

1 Division of Medical Biochemistry and Institute of Infectious Disease and Molecular Medicine, Department of Integrative Biomedical Sciences, Faculty of Health Sciences, University of Cape Town, Cape Town 7925, South Africa; SNTDIM001@myuct.ac.za (D.A.S.); hmshipanga@gmail.com (H.S.); iqbal.parker@uct.ac.za (M.I.P.)

2 International Centre for Genetic Engineering and Biotechnology (ICGEB), Cape Town Component, Wernher and Beit Building (South), UCT Medical Campus, Anzio Road, Observatory, Cape Town 7925, South Africa; arielle.rowe@icgeb.org

3 Pharmacogenetics Research Group, Division of Human Genetics, Department of Pathology and Institute of Infectious Disease and Molecular Medicine, Faculty of Health Sciences, University of Cape Town, Cape Town 7925, South Africa; thmnic023@myuct.ac.za (N.E.T.); MNRDAN002@myuct.ac.za (D.M.); collet.dandara@uct.ac.za (C.D.)

4 Batterjee Medical College, Prince Abdullah AlFiasal St, Obhur Al-Shamaliyah, Jeddah 23819, Saudi Arabia; almazeedi.mohammad@yahoo.com (M.A.M.A.M.); hashemmazeedi@gmail.com (H.A.M.A.)

5 Institute for Cellular and Molecular Medicine, Department of Immunology and South African Medical Research Council (SAMRC) Extramural Unit for Stem Cell Research and Therapy, Faculty of Health Sciences, University of Pretoria, Pretoria 0002, South Africa; karlienkallmeyer@gmail.com (K.K.); michael.pepper@up.ac.za (M.S.P.)

* Correspondence: kd.dzobo@uct.ac.za; Tel.: +27-021-406-7689

Received: 3 July 2017; Accepted: 19 July 2017; Published: 21 July 2017

Abstract: Chemoresistance is a leading cause of morbidity and mortality in cancer and it continues to be a challenge in cancer treatment. Chemoresistance is influenced by genetic and epigenetic alterations which affect drug uptake, metabolism and export of drugs at the cellular levels. While most research has focused on tumor cell autonomous mechanisms of chemoresistance, the tumor microenvironment has emerged as a key player in the development of chemoresistance and in malignant progression, thereby influencing the development of novel therapies in clinical oncology. It is not surprising that the study of the tumor microenvironment is now considered to be as important as the study of tumor cells. Recent advances in technological and analytical methods, especially 'omics' technologies, has made it possible to identify specific targets in tumor cells and within the tumor microenvironment to eradicate cancer. Tumors need constant support from previously 'unsupportive' microenvironments. Novel therapeutic strategies that inhibit such microenvironmental support to tumor cells would reduce chemoresistance and tumor relapse. Such strategies can target stromal cells, proteins released by stromal cells and non-cellular components such as the extracellular matrix (ECM) within the tumor microenvironment. Novel in vitro tumor biology models that recapitulate the in vivo tumor microenvironment such as multicellular tumor spheroids, biomimetic scaffolds and tumor organoids are being developed and are increasing our understanding of cancer cell-microenvironment interactions. This review offers an analysis of recent developments on the role of the tumor microenvironment in the development of chemoresistance and the strategies to overcome microenvironment-mediated chemoresistance. We propose a systematic analysis of the relationship between tumor cells and their respective tumor microenvironments and our data show

that, to survive, cancer cells interact closely with tumor microenvironment components such as mesenchymal stem cells and the extracellular matrix.

Keywords: chemoresistance; tumor microenvironment; tumor heterogeneity; mesenchymal stem cells; angiogenesis; extracellular matrix; clinical oncology

1. Introduction

Cancer is a multifactorial disease and is one of the leading causes of death worldwide. It results from both genetic and epigenetic transformation of normal cells leading to abnormal proliferation. Cancer deaths outnumber the combined deaths from diseases such as HIV/AIDS, malaria and tuberculosis worldwide [1,2]. Despite the development of potent chemotherapeutics against many cancer types in recent years, durable or long lasting cure is still out of reach for many patients [3,4]. This is partly due to the development of drug/therapeutic resistance which stems from the remarkable adaptive behavior of cancer cells and is driven by both genetic and epigenetic factors. There are many distinct cancer types and these differ significantly in their genetic makeup, behavior and treatment responses [5]. Differences in cancer cells behavior stem from the dysregulation of a number of growth signals that are involved in the direct entry into and progression through the cell cycle. Due to the diverse nature of cancer, many treatment strategies have been developed and each takes advantage of a different aspect of the disease. However, most cancer drugs still target DNA replication and DNA repair mechanisms.

Cancer cells proliferate at a much higher rate than normal cells and invade nearby tissues or spread to distance organs. A number of oncogenes and tumor suppressor genes such as p53, c-Myc and transforming growth factor-β (TGF-β) are mutated in cancer cells and have been observed to play key roles in cancer cell proliferation, invasion and metastasis. Most of these oncogenes and tumor suppressor genes are considered as major contributors to drug resistance [6]. Resistance is usually accompanied by recurrence of the disease. Different cancer types respond to treatment in different ways and therefore some are better treated than others. The most common treatments for cancer are surgery, radiotherapy and chemotherapy. Surgery can successfully remove the cancerous tissue from the body and combined with chemotherapy and radiotherapy can be successful in treating any cancer [7]. Radiotherapy uses radiation to kill cancer cells. Chemotherapy remains the preferred method due in part to its effectiveness and low cost. Its lack of selectivity however hampers its success as normal cells are also killed in the process. Patients undergoing chemotherapy suffer many side-effects such as loss of hair, bleeding, nausea and death. Due to its genotoxic effects, chemotherapy induces changes in both normal and cancer cells creating further cancer cell heterogeneity and ultimately affecting the efficiency of chemotherapy [8].

A huge challenge in cancer treatment is the development of chemoresistance resulting in cancer cells that are more aggressive and able to metastasize [9]. Mechanisms that contribute to chemoresistance include tumor heterogeneity, drug inactivation, apoptosis evasion, enhanced deoxyribonucleic acid (DNA) repair, increased drug efflux, epithelial-to-mesenchymal transition and the involvement of the tumor microenvironment (TM) [8]. Though cancer cell chemoresistance is usually attributed to heterogeneity within the cancer cell population, mutations and epigenetic alterations influencing the metabolism and retention of drugs by cancer cells [10–17], additional causes could play important roles in the development of this phenomenon. Most important is the diversity within the tumor microenvironment (TM) in terms of the stromal cells present, the amount of oxygen available and the acidity of the environment [18–24]. Another important difference is the amount of the extracellular matrix (ECM) proteins around the cancer cells [25–27]. ECM proteins can create a barrier through which the drugs must pass in order to reach the cancer cells while their presence promote tumor metastasis [28–34]. As the tumor grows, it becomes difficult for chemotherapeutic

agents to reach cancer cells near the center of the tumor. All these factors can have a huge influence on how cancer cells respond to drugs.

The genetic makeup of cancer cells and cellular processes occurring within cancer cells contribute immensely to the inability of most chemotherapeutic drugs used in clinical oncology to effectively clear these cells from the body [12,14–17,35–37]. Several mutations to key genes encoding important proteins responsible for xenobiotic metabolism, as well as import and export of drugs from cells such as the ABC transporters have been identified and shown to influence how tumor cells respond to several drugs [12,14–17,35–37]. However, with remarkable advancement in technology and analytical methods seen in the last decade, attention has shifted to the TM contribution towards the development of chemoresistance [38–46]. Chemotherapeutic drugs need to access all cancer cells in a solid tumor to be effective, thus components of the tumor microenvironment become important players in the response of these cells to drugs [33,47–53]. The TM is a dynamic entity and is characterized by cellular heterogeneous, the amounts of oxygen, nutrients and ECM proteins [41,54–59]. The heterogeneous nature of cancer and stromal cells within the TM is reflected in the ECM produced by these cells. The variability of the ECM within the TM also makes targeting the ECM difficulty and might explain why therapeutic targeting of the ECM has not had much success in several clinical trials. Both cancer cells and stromal cells do deposit the ECM in a tumor [60,61]. Novel strategies need to be developed to specifically target the ECM from different cells within the tumor. In addition, understanding the response of cancer cells to the ECM at different stages of tumor development would allow for the understanding of the contribution of each ECM protein during tumor progression. Determining the most effective time point when cancer cells respond to the ECM is also necessary in the intervention to stop cancer growth. In addition several studies have shown that matrix metalloproteinases play a huge role in inducing processes such as epithelial-mesenchymal transition with the end result being malignant transformation [60–62].

This review focusses on the contribution of the TM constituents in the development of chemotherapeutic resistance especially the role played by mesenchymal stem cells and the ECM. To overcome chemoresistance, it is imperative that the TM contribution be studied and specified as only then can we attain long lasting treatment in clinical oncology.

2. Cancer Cell Chemoresistance

The accumulation of genetic aberrations over time has been recognized as the main cause of cancer [63–70]. A combination of genetic mutations and epigenetic alterations results in tumor heterogeneity [67,71–77]. Tumor heterogeneity can contribute towards chemoresistance in many ways. Tumor heterogeneity is one of the recent addition to the list of drivers of chemoresistance [78,79]. Tumors are made up of cancer cells that differ in their phenotype and therefore chemotherapeutic responses. Differences in phenotypes may also arise due to cancer cell-microenvironment interactions besides the obvious genetic differences [78,79].

The implication of intratumor heterogeneity is that cancer cells within a tumor have different responses to the same chemotherapeutic drug. Variants of cancer cells that do not respond to a drug can result in relapse. Epigenetic modifications can take the form of DNA methylation and histone modification. Hypermethylation of the multi-drug resistance protein 1 (MDR1) gene promoter has been reported to cause downregulation of certain genes involved in apoptosis. Methylation of the O(6)-methylguanine DNA methyltransferase (MGMT) gene is known to cause silencing of several genes. A small fraction of undifferentiated cancer cells have anti-drug properties. These drug-resistant cancer cells are known to be present in circulation as well as in solid tumors. In addition, solid tumors have been shown to be a complex mixture of tumor cells, stromal cells and the ECM [80–85].

Chemotherapy destroys cancer cells mostly through induction of apoptosis by damaging DNA and inhibiting cell cycle progression [5,86,87]. Over time, cancer cells can acquire diverse strategies that decrease the efficacy of many therapeutic agents leading to chemoresistance [88]. Resistance to therapy occurs either as de novo or acquired. Acquired resistance occur when changes in the genetic makeup

of cells over time result in therapy-resistant cells. De novo drug resistance can either be soluble-factor mediated drug resistance or cell-adhesion mediated drug resistance. Chemokines, growth factors and cytokines are known to induce the soluble factor mediated drug resistance. The interaction of cancer cells and stromal components such as fibroblasts and the ECM via surface receptors such as integrins induce cell-adhesion mediated drug resistance.

The bi-directional communication between cancer and stromal cells is much more complex than initially perceived. Our data and that from others have shown that the cancer cell-stromal cell relationship is transient and ever changing [27,55,89,90]. Both tumor cells and stromal cells within the TM are exposed to different conditions over time including different concentrations of drugs. Eventually cancer and stromal cells develop a cooperative relationship that appear to benefit cancer cells. Through the release of soluble factors and the ECM, stromal cells determine the conditions within the TM. Stromal cells such as fibroblasts and mesenchymal stem cells have been the subject of many drug resistance studies to date. A summary of the various mechanisms known to be involved in cancer cell chemoresistance is shown in Figure 1. These mechanisms include enhanced survival signaling, enhanced drug inactivation, reduced drug uptake, enhanced DNA repair processes and inhibition of apoptosis [91].

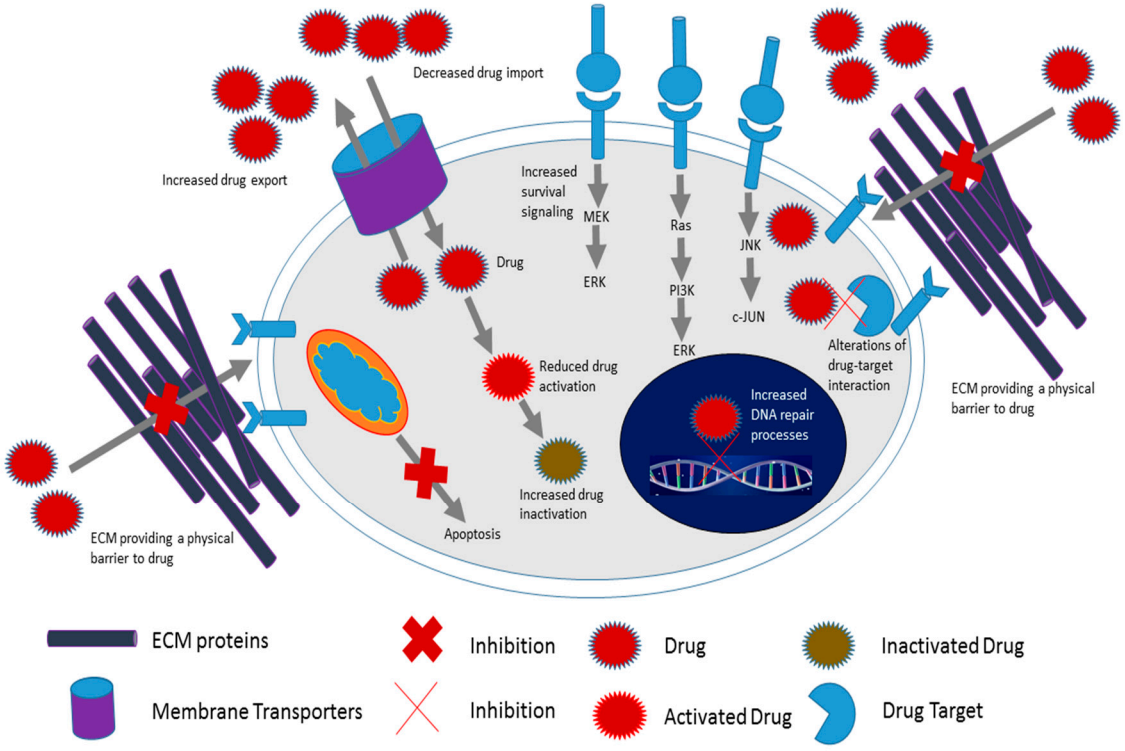

Figure 1. Schematic representation of processes that have been implicated in the development of chemoresistance. Some of these processes include enhanced survival signaling, enhanced drug inactivation, enhanced drug export, reduced drug uptake, inhibition of apoptosis, and increased production of extracellular matrix (ECM) proteins and inhibition of cytoskeleton organization (adapted from [92]).

3. Tumor Microenvironment

The dynamic nature of the TM during malignant progression underscores the need to study its role in disease progression. Importantly, the role of the cellular and non-cellular components in tumor initiation and progression needs to be investigated. Solid tumors are more than just a lump of cancer cells. Beside stromal cells, non-cellular components of the TM include the ECM and soluble growth factors [93–98]. The interaction between cells and their respective microenvironment is key

for cellular growth and the maintenance of homeostasis. So it is for tumor growth. Though the gradual accumulation of genetic lesions creates the initial 'spark' necessary for disease initiation it is widely acknowledged that the TM play a critical role at every stage of malignant progression. Cancer cell-microenvironment interactions impacts on disease initiation, development and ultimately metastasis. Understanding the role of the TM in disease progression and chemotherapy is now considered central to cancer eradication. Initially thought to be only due to genetic lesions in cancer cells, the heterogeneous nature of tumors is now understood to be of microenvironmental origin as well. Both cellular and non-cellular components of the TM contribute towards the tumor heterogeneity observed in solid tumors. By contributing towards the tumor heterogeneity the TM components ultimately play a part in the development of chemoresistance. The crosstalk between tumor cells and their microenvironment makes this relationship very complex. However, the plasticity of the tumor stroma affords scientists an opportunity to devise therapeutic strategies that can allow most TM members to acquire anti-tumorigenic properties. It is also possible to convert pro-tumorigenic TM constituent members to become anti-tumorigenic.

In normal tissues a homeostatic environment is maintained with most cells maintaining their differentiated states and well defined boundaries between tissue compartments. Tumor initiation and progression is associated with disruption of tissue architecture and organization [99–101]. An environment that was tumor inhibiting becomes permissive and supportive to tumor growth and metastasis [80,83,90,102–104]. The TM (Figure 2) is now identified as a leading factor that influences cancer cell proliferation, metastasis and anticancer drug efficacy [105–107]. Normal cellular processes and tissue homeostasis are reversed in tumors, as tumor cells bypass or override necessary homeostatic control measures. Cellular mechanisms of surrounding cells and the effect of non-cellular components is basically hijacked by cancer cells with the ultimate goal of ensuring cancer cells survival. Several anti-tumorigenic cells such as fibroblasts and macrophages are converted into tumor-promoting cells, releasing soluble factors such as growth factors and proteases needed by tumor cells to burrow through the ECM and support accelerated tumor cell growth [60,108]. Fibroblasts and macrophages are converted to cancer associated fibroblasts (CAFs) and tumor associated macrophages (TAMs) via the action of tumor-released factors such as TGF-β and platelet derived growth factor (PDGF). Both tumor-associated fibroblasts and macrophages are known to participate in this pro-tumorigenic process. Importantly CAFs are known to synthesize and deposit large quantities of thick ECM fibers, thus contributing to deregulated homeostasis. CAFs also contribute towards cancer cell invasion and metastasis through synthesis of metastasis-promoting ECM proteins such as fibronectin and periostin and the release of matrix metalloproteases. This allows tumor cells to lose their attachment to the ECM and acquire mesenchymal behavior. The origin of CAFs in solid tumor is controversial. The most straight forward suggestion is that they are of fibroblast origin. Through the action of tumor-derived factors normal fibroblasts are converted into 'activated fibroblasts' also termed CAFs with the function of bidding for tumor cell survival. Several studies have suggested that they are of endothelial origin. Yet other studies appear to show that mesenchymal stem cells can be converted to CAFs. Our studies support this suggestion. Tumor-released TGF-β appears to contribute to mesenchymal stem cells conversion to α-smooth muscle producing CAFs.

TAMs are known to locate to the leading edge of tumors where they release matrix metalloproteases needed to degrade the ECM. TAMs also contribute to the increased levels of growth factors such as EGF leading to tumor cell migration. The plasticity of macrophages allows them to act both as pro-tumorigenic and anti-tumorigenic depending on the surrounding environments and existing conditions. Through the release of pro-inflammatory cytokines, macrophages present antigens and play an anti-tumorigenic role in the TM. However, activated macrophages can be pro-tumorigenic through production of type II cytokines. Macrophages also help tumor cells intravasate into blood vessels. TM conditions such as hypoxia and acidity play significant roles in the activation of macrophages, with macrophages appearing to be attracted to regions of low oxygen tension. Localized selective pressures such as hypoxia and acidity select for stromal cells that ensure the survival of cancer

cells. Several reports have also shown that the presence of growth factors and micro RNAs can drive activated macrophages back to normal leading to tumor regression. Thus resident macrophages can be targeted in the TM to have anti-tumorigenic properties. Due to the presence of several components within the TM, tumor cells are exposed to chemotherapeutic drugs in a gradient fashion. The ECM by forming thick fibers within the tumor present a physical barrier to diffusion of chemotherapeutic drugs [109–114].

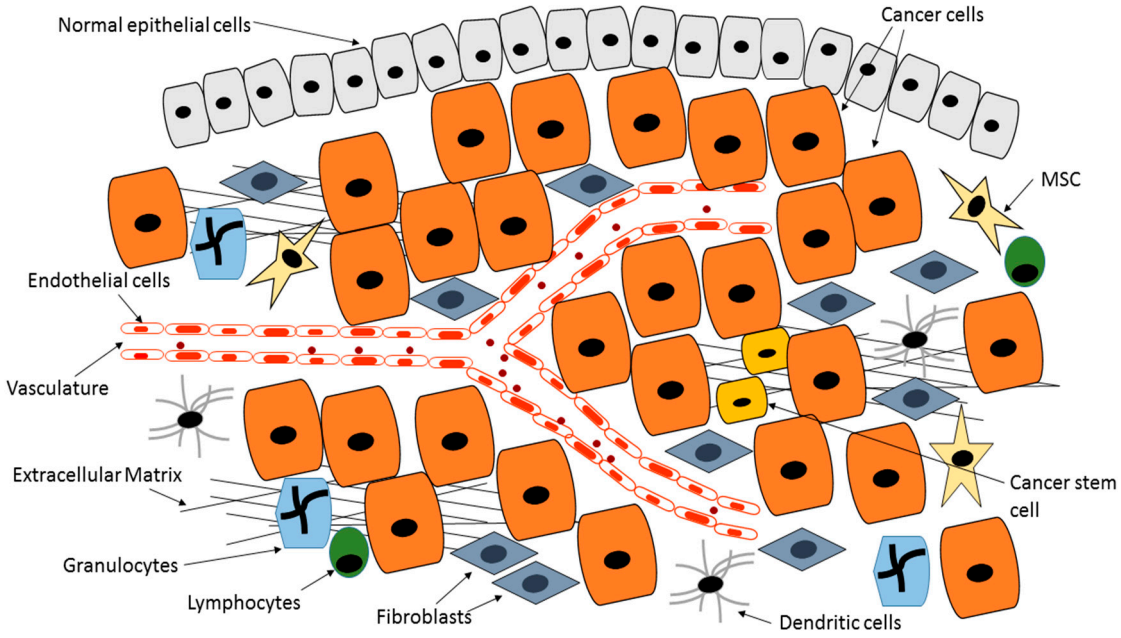

Figure 2. Tumor Microenvironment. The tumor microenvironment consists of several cells including cancer cells, mesenchymal stem cells (MSCs), endothelial cells, fibroblasts, cancer stem cells (CSC), bone marrow-derived cells (BMDC) as well as Extracellular matrix (ECM). All the cells in the tumor microenvironment (TM) contribute to tumor progression.

The invasive nature of cancer cells cannot be exhibited without the interplay between tumor cells and their microenvironment. With an increase in our knowledge of molecular targets and medicine, clinical therapeutic targets have increased to include components of the TM [28,54,89]. The crosstalk between stromal and tumor cells involves growth factors, chemokines and cytokines as well as ECM and can affect the sensitivity of anticancer drugs and pathways involved in apoptosis [115,116]. Tumors depend on the formation of new blood vessels, through a process called angiogenesis, in order to increase in size as tumor cells need a constant supply of oxygen and nutrients [117–119]. Due to tissue disorganization associated with tumors, they tend to have lower blood flow and therefore less drugs reaches the tumor cells than is administered.

For chemotherapeutic drugs to reach tumor cells in vivo, they have to travel through the blood vessels [120–123]. Blood flow through a solid tumor is varied and disorganized [124,125]. Most blood vessels in tumors are dilated and "leaky" compared to those in normal tissues. Thus the vasculature also influences the response of tumor cells to drugs. The compactness of a solid tumor increases blood flow resistance and this causes gradients of nutrients and oxygen, meaning that there are different proliferation rates in different regions of the tumor [126–131]. Nutrient deprivation is also a result of blood flow resistance. Most chemotherapeutic drugs are designed against highly proliferating cells and not quiescent cells [132–135]. Thus having tumor cells proliferating at different rates has a major impact on the effectiveness of chemotherapy. Due to impaired blood flow the clearance of breakdown products within the tumor can lead to a toxic microenvironment [136–138].

The compactness of a solid tumor and the reduced blood flow leads to either temporary or chronic hypoxia [139–145]. Cells in hypoxic conditions tends to divide slowly, making them unresponsive to chemotherapeutic reagents. Hypoxia can result in the activation of genes associated with angiogenesis and cell survival [146–148]. Many chemotherapeutic drugs cause DNA damage through generating free radicals [149–151]. Without oxygen however, the cytotoxicity of several chemotherapeutic drugs whose activity depends on generating free radicals is reduced. In addition, it has been shown that cancer stem cells (CSCs) tend to be located at the center of a solid tumor [152–157]. These CSCs are able to withstand lower oxygen levels than the general population of cancer cells [18,80]. Thus the inability of drugs to reach the center of the solid tumor can result in recurrence of the tumor even after an apparent successful treatment. It has also been observed that hypoxia can lead to increased expression of P glycoprotein, which is involved in drug inactivation, resulting in drug resistance [158]. Hypoxia inducible factor (HIF)-1 is stimulated under low oxygen conditions and this transcription factor controls many genes involved in survival mechanisms such as angiogenesis and apoptosis. Several pro-drugs have been developed to be activated under complete or partial hypoxic conditions. For example, Tirapazamine (TPZ) is activated over a range of oxygen levels. Due to the varying amounts of oxygen in solid tumors, TPZ activation over time. Thus at some point tumor cells are exposed to sub-lethal levels of TPZ with the consequent development of chemoresistance. The pH in the TM can affect the cytotoxicity of anticancer drugs. An acidic microenvironment can inhibit the activation of many chemotherapeutic drugs [159,160]. Changes in pH inside and outside of cancer cells can have a lasting effect on chemotherapeutic drugs. The pressure gradient that exists within the microenvironment also influences the distribution of many anticancer drugs. The ability of cancer cells to manipulate their microenvironment enables them to acquire important hallmark properties that are necessary for tumor growth and development.

3.1. Cancer-Associated Fibroblasts (CAFs)

Cancer-associated fibroblasts (CAFs) are activated fibroblasts found in association with cancer cells. CAFs are the most abundant cells within the TM and are involved in tumor initiation, by activating signals involve in growth and differentiation, and evade cancer therapy [161,162]. CAFs secrete growth factors, such as hepatocyte growth factor (HGF), epidermal growth factor (EGF), and cytokines such as stromal cell-derived factor 1 (SDF-1) and IL-6. Wang et al. showed that secretion of HGF by CAFs induced resistance to EGF-tyrosine kinase inhibitors in lung cancer cells [163]. Secretion of chemokines and cytokine by CAFs can lead to immune cells infiltration which contribute to angiogenesis and metastasis [164]. CAFs are known to stimulate the growth of new blood vessels through the release of growth factors such as vascular endothelial growth factor. Enhanced invasion of pancreatic cancer cells was observed in the presence of fibroblast-derived SDF-1 and IL-8 was also found to induce angiogenesis in vitro [165]. CAFs can regulate ECM composition via expression of matrix metalloproteinases (MMPs), which allows cancer cell adhesion and migration as well as inhibition of apoptosis by activating PI3K-Akt/PKB as seen in breast cancer models [158]. The presence of CAFs or transformed fibroblasts is known to activate migratory behavior in cancer cells through upregulation of integrin expression and cell survival signaling pathways such as the MEK-ERK and the PI3K-Akt pathways. In prostate cancer, increased secretion of MMP-2 and MMP-9 by CAFs was associated with the induction of epithelial-mesenchymal transition (EMT), known to be involve in cancer cell invasion and metastasis [166]. CAFs also secrete IL-6, which promotes cancer metastasis and chemoresistance through induction of EMT [167]. A study by Conze and colleagues showed that IL-6 is overexpressed in multidrug resistant breast cancer [168]. In vitro and in vivo studies have shown that CAFs derived from breast cancer induced tamoxifen resistance through decreasing estrogen receptor-α (ER-α) levels and IL-6 secretion [169].

3.2. Mesenchymal Stromal/Stem Cells (MSCs)

MSCs have received a lot of attention in cancer biology partly because of their primitive nature and their ability to generate several other cells types. Through the action of tumor cell-derived factors, MSCs are recruited to the tumor site where they produce factors needed by cancer cells. MSCs are found in many adult tissues including bone marrow and adipose tissues [170]. MSCs can self-renew and differentiate into specialized tissue-specific cell types such as adipocytes, chondrocytes, fibroblasts and osteoblast [167,170–172]. MSCs are also found in the TM and are known to play an important role in tumor progression and chemoresistance [172]. MSCs promote tumor growth either by the secretion of growth factors, or by differentiating into tumor associated fibroblasts (TAFs) [55,170,173,174]. The origin of TAFs or CAFs in the TM is still debatable. TAFs are a heterogeneous cell population and are commonly identified by α-smooth muscle actin (α-SMA) and vimentin expression which is indicative of an 'activated' myofibroblast-like phenotype [175,176]. One source of TAFs that has been touted is MSCs present in the tumor stroma [175,176]. We present data from an extension of our previous publication [90], showing that long term co-culture of esophageal WHCO1 and breast cancer MDA MB 231 cells with human MSCs trigger hMSCs differentiation into 'tumor associated fibroblasts' via the TGF-β/Smad signaling pathway.

In our study, we evaluated the effect of esophageal WHCO1 and breast MDA MB 231 cancer cells on Wharton's Jelly-derived mesenchymal stromal/stem cells (WJ-MSCs) gene expression over 24 days of co-culture. The expression of α-SMA, the most reliable marker of tumor associated fibroblasts (TAFs) and vimentin showed a clear and gradual increase in WJ-MSCs up to a maximum at day 16 in our co-culture system (Figure 3A,B). TGF-β is one of the growth factors released by cancer cells in order to evade immune detection in vivo and can increase expression of proteins such as α-SMA and vimentin. Treatment of WJ-MSCs with 1 μM 5-azacytidine resulted in their differentiation into myofibroblastic lineages expressing increased levels of α-SMA and type I collagen. Addition of exogenous TGF-β (10 μM) and treatment of naïve MSCs with 5-azacytidine (1 μM) up to 48 h resulted in increased levels of α-SMA and type I collagen similar to MSCs co-cultured for 16 days (Figure 3C–F). Our observations show that over time MSCs exposed to esophageal and breast cancer cells differentiate and express markers of the myofibroblastic lineage. Many studies have shown that ACTA2 (α-SMA) gene transcription is regulated through the interactions of several signaling pathways. To substantiate these results, the TGF-β inhibitor SB 431542 (10 nM) was added to the co-culture media. Addition of SB 431542 decreased the α-SMA protein levels in MSCs exposed to WHCO1 and MDA MB 231 cells (Figure 4A,B). As an orthogonal approach, suppression of TGF-β expression in co-cultured MSCs through the use of TGF-β siRNA resulted in decreased α-SMA protein levels (Figure 4C,D). In addition, TGF-β knockdown in both WHCO1 and MDA MB 231 cells during co-culture decreased α-SMA protein levels in MSCs (Figure 4E,F). We also observed that Smad2 increased in WJ-MSCs cocultured with WHCO1 and MDA MB 231 cells (data not shown). These results demonstrate that the TGF-β/Smad signaling pathway is involved in the differentiation of MSCs into TAFs and that TGF-β probably is probably produced by both MSCs and cancer cells.

Thus it is possible that cancer cells can attract MSCs to the tumor site and the MSCs can become part of the TM as TAFs. However other cells can also be a source of TAFs. TAFs are known as accomplices in increased tumor growth, metastasis and chemoresistance [177,178]. MSCs can also promote drug resistance both by secreting protective cytokines, and by preventing cancer cell apoptosis [177]. Our data show that MSCs can be transformed to CAFs by cancer cells through release of growth factors such as TGF-β (Figure 5). Importantly, both WHCO1 and MDA MB 231 cells co-cultured with "cancer cell activated" WJ-MSCs survive treatment with paclitaxel and cisplatin better than WHCO1 and MDA MB 231 cancer cells alone (Figure 6).

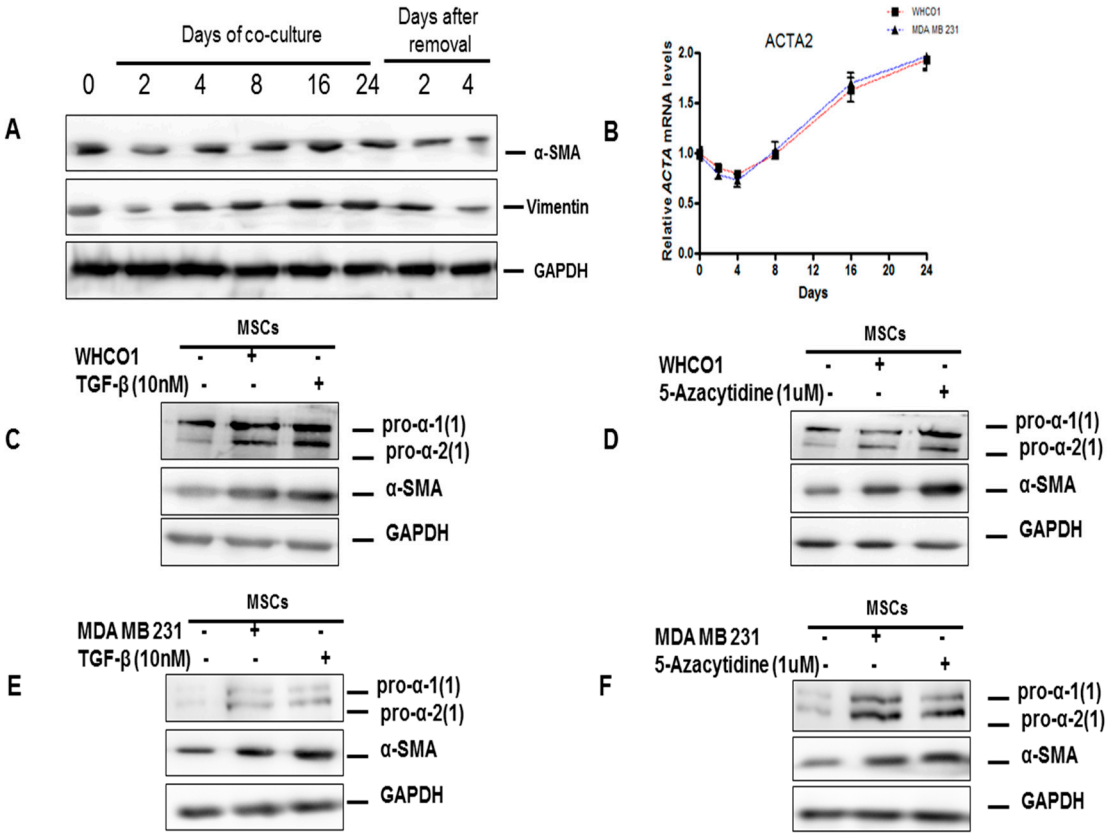

Figure 3. Cancer cells trigger MSCs differentiation into tumor associated fibroblasts via the transforming growth factor-β (TGF-β) /Smad signaling pathway. For the co-culture experiments cells were co-cultured in 6-transwell plates (size of pore: 0.4 μm, Polycarbonate membrane, Costar, Corning, Cambridge, MA, USA). Mesenchymal stem cells (5×10^5 cells) were cultured in the upper insert and cancer cells (WHCO1 and MDA MB 231) (5×10^5 cells) were cultured in the lower compartment. Empty inserts were used for the control group (no cells) and a mixture of MSCs medium and cancer cell medium (1:1) was used. Medium was changed every 3 days for longer incubation periods and fresh TGF-β and reagents were added. TGF-β and all reagents were added to the media to the final concentrations as shown. At specific time points or at the end of the experiment, cells (cancer cells and MSCs) were harvested and used in various analyses. (**A**) Western blot analysis of lysates from MSCs co-cultured with WHCO1 cells for 24 days showing α-smooth muscle actin (α-SMA) and vimentin protein levels. Glyceraldehyde 3-phosphate dehydrogenase (GAPDH) was used as a loading control. (**B**) Real time quantitative reverse transcription polymerase chain reaction (RT-qPCR) analysis was performed to assess the expression of Actin, alpha2, smooth muscle, aorta (ACTA2) (α-SMA gene) in MSCs co-cultured with WHCO1 and MDA MB 231 cancer cells over a 24 day period; (**C**,**D**) western blot analysis of lysates from MSCs co-cultured with WHCO1 cells for 16 days or after the addition of 10 nM TGF-β (**C**) or 1 μM 5-azacytidine (**D**) for 48 h showing the expression of type I collagen and α-SMA; (**E**,**F**) western blot analysis of lysates from MSCs co-cultured with MDA MB 231 cells for 16 days or after the addition of 10 nM TGF-β (**E**) or the addition of 1 μM 5-azacytidine (**F**) for 48 h showing the expression of type I collagen and α-SMA.

Both WHCO1 and MDA MB 231 cancer cells co-cultured with the above WJ-MSCs for 16 days survived treatment with cisplatin and paclitaxel better than WHCO1 and MBA MB 231 cell alone (Figure 6). It is evident that the presence of WJ-MSCs, possibly through the release of protein factors, protected the cancer cells from the effect of the drugs used.

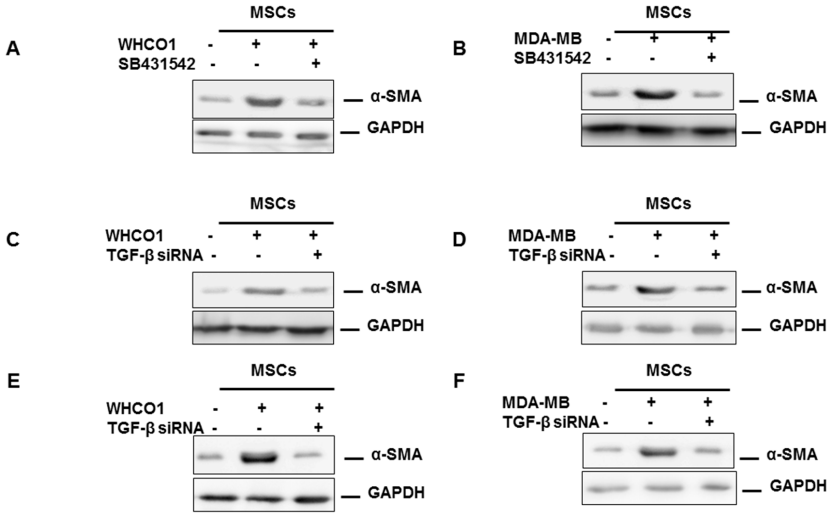

Figure 4. WHCO1, MDA MB 231 cells and MSCs secrete TGF-β. Mesenchymal stem cells (5×10^5 cells) were cultured in the upper insert and cancer cells (WHCO1 and MDA MB 231) (5×10^5 cells) were cultured in the lower compartment as described in Figure 3. At specific time points or at the end of the experiment, cells (cancer cells and MSCs) were harvested and used in various analyses. (**A**,**B**) TGF-β inhibitor SB431542 was added to the co-culture media to a final concentration of 10 μM. Co-culture was continued for 16 days after which α-SMA protein levels was determined by western blot analysis. Glyceraldehyde 3-phosphate dehydrogenase (GAPDH) was used as a loading control. (**C**,**D**) MSCs were treated with TGF-β siRNA to a final concentration of 100 nM and co-culture was continued for 16 days. To maintain knockdown of TGF-β, subsequent transfections were done every other three days till the end of the experiment. Western blot analysis was performed to evaluate the α-SMA protein levels in MSCs lysates; (**E**,**F**) WHCO1 and MDA MB 231 cells were treated with TGF-β siRNA to a final concentration of 100 nM and co-culture was continued for 16 days. To maintain knockdown of TGF-β, subsequent transfections were done every other three days till the end of the experiment. Western blot analysis was performed to evaluate the α-SMA protein levels in MSCs lysates.

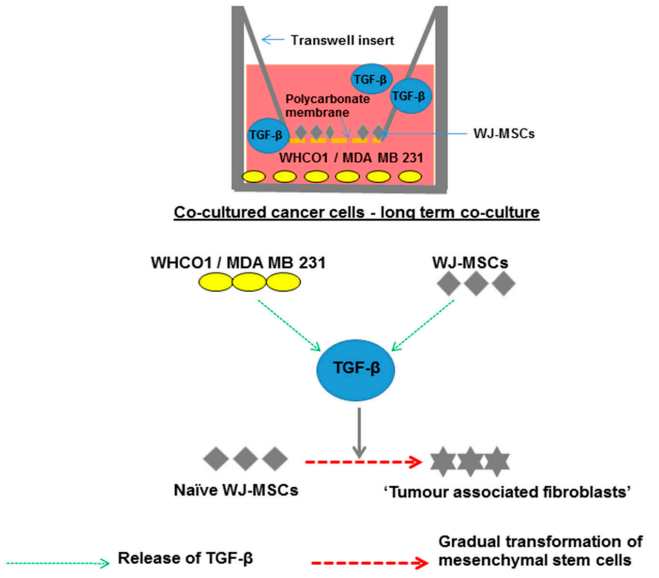

Figure 5. Our co-culture experiments have shown that TGF-β plays an important role in the interaction between cancer cells and MSCs. Our data show that in the long term, WHCO1 and MDA MB 231 cancer cell exposed-Wharton's Jelly derived-MSCs differentiate into tumor associated fibroblasts (TAFs) through a TGF-β/Smad-mediated process.

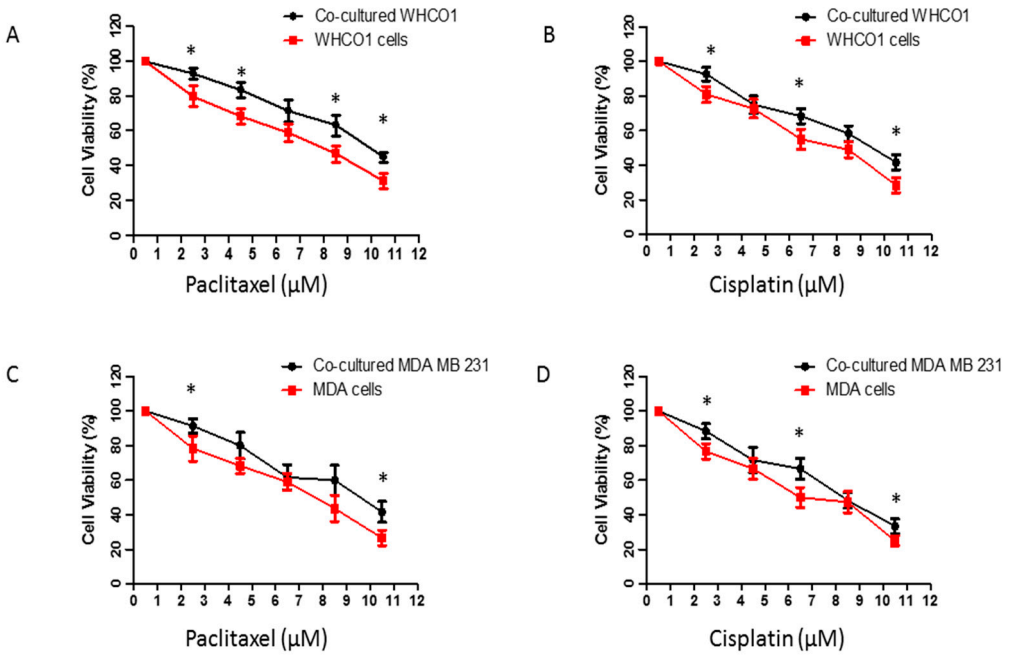

Figure 6. Co-cultured cancer cells survive treatment with cisplatin and paclitaxel better than WHCO1 and MDA MB 231 cells alone. WHCO1 and MDA MB 231 cancer cells (5×10^5) were cultured alone or co-cultured with WJ-MSCs for 16 days as described in Figure 3. Empty inserts were used for the control group (no MSCs) and a mixture of MSCs medium and cancer cell medium (1:1) was used. Medium was changed every 3 days for longer incubation periods. At the end of the incubation, the same number of WHCO1 and MDA MB 231 cancer cells were treated with increasing concentrations of paclitaxel and cisplatin for 48 h as shown above. After 48 h, cells were counted with a Countess Cell counter using the Trypan Blue exclusion method. Cells were expressed as a percentage of cells treated with 0.1% DMSO (control). Experiments were repeated three times. * $p < 0.05$.

3.3. The Role of the Extracellular Matrix in Chemotherapeutic Resistance

The ECM is the crucial non-cellular component of the TM and consists of mainly glycoproteins, proteins and proteoglycans [179]. The ECM plays key roles in tissue maintenance and function. The ECM regulates cellular behavior directly and indirectly [179]. Due to the crucial roles the ECM plays in vivo, a number of mechanisms are involved in the regulation of ECM production, degradation and remodeling [180]. Perturbation of these mechanisms can promote pathological conditions such as fibrosis and cancer [179,181]. The physical properties of the ECM determines its role as a scaffolding to maintain tissue structure and function [179]. It also controls the behavior of cells through proliferation, differentiation and signaling pathways [182,183]. The signaling abilities of the ECM's biochemical properties permits interactions between cells and their environment [179]. The composition and structure of the ECM is precisely tuned according to the needs of the surrounding cells. This is achieved through the release of soluble factors such as growth factors and chemokines. Besides serving as a physical scaffold onto which cells are anchored, the ECM provides signals necessary for cellular growth, migration and differentiation. Both physical and chemical properties of the ECM can influence cellular behaviors and these properties can be altered in cancer. ECM remodeling involves many enzymes, including matrix degrading enzymes including MMPs, lysyl oxidase (LOX), tissue inhibitors of metalloproteinases (TIMPs) and cathepsins [60]. Thus the composition of the ECM in cancer is a very important factor in deciding the efficacy of many drugs. Most cancer cell behavior is affected by the surrounding ECM. Effective cancer treatment requires knowledge of the cancer-ECM interactions in addition to the interactions with other TM components.

Due to its plasticity, the ECM has been ascribed both pro-tumorigenic and anti-tumorigenic properties. Initially thought to be a passive bystander, the ECM is emerging as a key player in malignant initiation, progression and chemoresistance. It is likely that the ECM inhibits early tumor growth and at later stages becomes pro-tumorigenic. Several studies have shown that the ECM present in the TM influence disease progression and is a major indicator of clinical prognosis. High levels of protease inhibitors within the ECM is associated with a good clinical outcome whilst high levels of surface receptors such as integrins and MMPs are associated with a poor outcome and relapse of disease. The ECM and its associated proteins, now referred to as the 'matrisome', is synthesized by different types of cells within the TM. The manipulation of the ECM and its ligands offers an attractive therapeutic avenue to eradicate cancer. Many studies have shown that matrix stiffness can influence cellular adhesion to surfaces, migration, differentiation and even proliferation [27,89,184–186]. Cells migrating to other regions have been shown to be softer and more pliable than benign cells. In general the tumor surrounding-ECM has been found to be stiffer than the ECM surrounding healthy tissues [23,51,186–191]. The stiffening observed in cancer is thought to be linked to fibrosis and deposition of collagen as shown in breast cancer [139,192–195]. Studies have showed that a stiff microenvironment induces tumor progression and malignancy through integrin signaling as a result of ECM tumor-associated remodeling [106,107,179,196]. Several studies have reported that tumor metastasis is promoted by ECM stiffening through the action of lysyl oxidase and the increased deposition of collagens and fibronectin. Stiffened ECM downregulates the expression of genes associated with cell cycle inhibition. MicroRNAs are reportedly induced by matrix stiffening and these microRNAs downregulates the expression of PTEN, a tumor suppressor protein. This has the effect of increasing PI3K-Akt activity, a survival pathway implicated in tumor growth and metastasis. Inhibition of lysyl oxidase (LOX) softens the ECM [197]. ECM abnormality is known to result in cancer cell growth, survival, migration and anticancer drug resistance [179]. However, the ECM is composed of many constituents and as such it is difficult to pinpoint the role of each component on tumor progression. It is likewise difficult to recapitulate the in vivo situation in an in vitro setting in order to study the effect of each individual TM component on tumor progression and chemoresistance.

Several ECM proteins have been associated with resistance to chemotherapy. Fibronectin has been associated with increased migration of several cancer cells [198–201]. Changes in ECM elasticity and stiffness are some of the factors known to affect drug delivery to cancer cells. ECM stiffness has been associated with tumor initiation in many cancer types. Dysregulation of ECM remodeling can result in the evasion of apoptosis by mutant cells, enlargement of CSC pool and disruption of tissue polarity [179]. Like normal cells, tumor cells need nutrients, oxygen and waste exchange [179]. These needs are met by angiogenesis, which results in increase in tumor size, and by lymphangiogenesis, the growth of lymphatic blood vessels [179]. Diffusion and pressure are associated with drug delivery in the interstitial spaces. ECM remodeling promotes drug resistance in the form of physical barrier that dissolve or delay drug delivery [202]. Interaction of the ECM with other cells has been considered to be involved in the promotion of chemoresistance through the activation of survival proteins [203]. These survival pathways include PI3K/AKT, p53 and MAPK which have been demonstrated to be activated upon the binding to ECM. Cancer should no longer be viewed as a disease of mis-regulated or mutated genomes. That tumors are like organs is illustrated more by their dependent on angiogenesis. The tumor's need for nutrients and oxygen, supplied via the bloodstream, makes angiogenesis a necessity for tumor growth. Several factors are released by stromal cells within the TM to initiate and to allow tumor vascularization to occur.

3.3.1. Collagen

Collagen is the main ECM protein synthesized in several tissues. Collagen is known to promote cancer cell clustering and invasiveness. Collagen is an ECM protein for scaffolding and provides tissue strength and support. The structural organization and level of collagens within tissues can indirectly influence drug efficacy. Type I and IV collagen can promote drug resistance through the interaction

with integrins on cancer cells [204,205]. An environment rich in collagen is known to activate several signaling pathways such as MEK-ERK and the Wnt/B-catenin pathways. Increased expression of ECM proteins such as collagen by cancer cells further limits the diffusion of chemotherapeutic drugs into cancer tissues [206–208]. Drug delivery is significantly limited by tortuous and dense tumor ECM [207,208]. The expression of collagen play a crucial role in both drug resistance at the cellular level and tissue mediated drug resistance [206]. Interaction of ECM proteins including collagens with cancer cells can alter the cancer cell response to the presence of chemotherapeutic reagents [206,209]. Several studies have shown that high levels of expression of collagen genes was associated with drug resistance in ovarian and breast cancer cell lines [206,210]. The time needed for drugs to penetrate through collagen fibers before reaching cancer cells is lengthened, which can result in drug resistance [211].

ECM that contains large amount of collagen enhances tumor progression and invasiveness [204,210,212]. Pancreatic ductal adenocarcinoma (PDA) is one of the most aggressive human malignancies and a leading cause of cancer mortality. A unique molecular hallmark associated with PDA is the presence of dense collagen-rich fibrosis [213]. Increased expression of type I collagen has been associated with increased risk of metastasis in several cancer types [213–215]. Pancreatic cancer cells cultured in 3D collagen showed decreased sensitivity to gemcitabine therapy and increased proliferation despite drug treatment [213,216]. Collagen type XI α1 (COL11A1) is a member of collagen family, which is the important component of the interstitial ECM. Overexpression of COL11A1 is associated with progression of several cancers and poor survival [177,178,217]. COL11A1 expression has been demonstrated to be high in cisplatin-resistance ovarian cancer cells [218,219]. In addition, COL11A1 promotes ovarian cancer cell chemoresistance through the activation of signaling pathways such Akt and PDK1 pathways [219]. The deposition of collagens, expression of LOX and increased ECM stiffness in breast cancer resulted in increased adhesion and PIK3 activity [197]. These findings suggest that the TM induces chemo-protection and increases cancer cell survival through remodeling of components in the ECM.

3.3.2. Laminin

Laminin constitutes a major family of the ECM proteins in the basal lamina and is known to affect cellular processes such as differentiation, adhesion and migration [220,221]. This family of ECM proteins plays a key role in the invasive behavior of several cancer cells. Laminin-332 (LN-332) is a heterotrimer made of β3, α3 and γ2 chains that has been shown to be key in cell adhesion and cancer metastasis [220–223]. Laminin-332 is involved in maintaining the self-renewal abilities of CSCs and has been implicated in resistance to sorafenib and doxorubicin [223]. Laminin β3 chain expression is associated with poor outcome in colorectal cancer and is related to chemoresistance to 5-FU-based chemotherapy regimens [222]. Another family member, Laminin β1 (LAMB1), is increased in paclitaxel-resistance cell lines [220].

LN-332 can bind the integrin α3β1 receptor which is reported to be enhanced in gefitinib resistance in hepatocellular carcinomas (HCCs) [224]. LN-integrin interactions increase cell survival and chemoresistance through the activation of mTOR [223,225]. It was demonstrated that LN-332 does not only protect hepatic cancer cells against therapeutic drugs but it promotes cell proliferation upon sorafenib exposure [223]. LN-332 and its γ2-chain play a key role in CSC self-renewal and differentiation and in maintaining and supporting quiescence as part of the human hepatic cancer stem cell niche [223]. LN protects pancreatic cells from gemcitabine induced apoptosis and cytotoxicity [226]. The protection of pancreatic cells by LN is a result of the activation of focal adhesion kinase (FAK), itself a result gemcitabine resistance induced apoptosis [226].

3.3.3. Fibronectin

Fibronectin (FN) plays a crucial role in growth, differentiation, adhesion and migration [227]. Fibronectins are glycoproteins that attach cells to collagen fibers in the ECM, facilitating movement

of cells through the ECM [227]. Fibronectin binds to cell surface integrins and collagen resulting in reorganization of the cell's cytoskeleton allowing movement of cells. Fibronectin has been found to be key in wound healing and in cancer initiation and progression [200]. Increased tumorigenicity and resistance to apoptosis-inducing therapeutic drugs in lung cancer is achieved when lung carcinoma cells adhere to FN [228]. Overexpression of FN at the invasion front and in tumor stroma is observed in head and neck squamous cell carcinomas (HNSCCs) [229]. Increased expression of FN in HSCC is associated with decreased survival of patients [200]. FN induced migration of carcinoma collectives through αvβ6 and α9β1 integrins [200]. Small-cell lung cancer cells (SCLC) that adhered to laminin, collagen and fibronectin were found to be protected from apoptosis induced by chemotherapeutic drugs compared to those that were grown on plastic [228]. FN facilitated non-small cell lung carcinoma cell (NSCLC) growth and reduced apoptosis through induction of cyclooxygenase-2 (COX-2) and activation of integrin α5β1 [230]. These effects were correlated with activation of many kinase signaling pathways such as MEK-ERK and Rho kinase signaling pathways [231]. FN adhesion led to protection of tumor cells against docetaxel-induced apoptosis [223,231,232].

3.3.4. Periostin

Periostin, a secretory protein also known as osteoblast-specific factor 2, is expressed as an extracellular matrix protein [233,234]. It is a cell adhesion protein that plays important roles in tooth and bone tissue homeostasis and development. It has also been found to be key in cardiac development and healing [220,233,234]. Overexpression of periostin has been implicated in many types of cancer such as gastric, colon, esophageal, ovarian, thyroid, lung, breast and head and neck carcinomas [233,234]. It regulates cell-matrix interactions through binding to fibronectin, type I/V collagen and tenascin C [234]. Periostin is a ligand for integrins such as αvβ3, αvβ5 and α6β4 [235]. It interacts with several signaling pathways such as Notch 1 and B-catenin signaling. It has been demonstrated that periostin in normal esophagus is significantly lower than in esophageal squamous cell carcinoma (ESCC) [234,235]. Periostin induces the PI3K-Akt signaling pathway by binding as a ligand to αvβ3 and αvβ5 integrins in esophageal cancer [176]. Periostin also increases cancer cell proliferation and EMT in nicotine-induced gastric cancer [176]. Periostin is overexpressed in gastric cancer cells that are resistance to cisplatin and 5-fluorouracil (5-FU) [234]. It was shown that periostin levels correlated with tumor angiogenesis and tumor recurrence [236]. In epithelial ovarian carcinoma, periostin induced Akt phosphorylation to increase resistance to paclitaxel [237]. Periostin not only serves as a prognostic factor for clinical outcome but also plays a role in resistance in several tumor cell types [238].

4. Strategies to Overcome Chemoresistance

To date most remedies for cancer have tended to focus directly on intrinsic characteristics of cancer cells. This is despite the fact that a tumor is a heterogeneous mixture of cancer cells, stromal cells and the extracellular matrix. Indeed, heterogeneity occurs at every level in cancer cells. Targeting stable stromal cells, with less or no genetic mutations, therefore is appealing. Stromal cells, due to their stable genetic makeup, are less likely to develop resistance to therapeutic agents. Perturbing or removing all the supporting cells and non-cellular components in the TM should ultimately lead to tumor regression or tumor cell reversion. Most stromal components can be engineered to be anti-tumorigenic due to their pliable behaviors. Given the heterogeneity evident in all cancers, it is imperative to study the TM as a possible avenue for cancer treatment. Indeed, several reports on combination therapies against both cancer and stromal cells appear to show promising outcomes in animal studies and in early phases of clinical trials. Several important aspects of TM-directed therapies need to be researched further. For example, the use of MSCs in cancer treatment needs to be studied further as several studies have shown that over time MSCs can be converted to 'cancer associated fibroblasts'. Thus benefits derived from MSCs might be negated in the long run if MSCs are converted to CAFs. We advocate for the inclusion of TM components in in vitro experimental systems in order to delineate the role of TM

components on cancer cell growth and metastasis. Novel animal models that are able to initiate tumors within native tissues will advance our understanding of the involvement of the TM in malignant initiation and development.

The efficacy of chemotherapeutic drugs may be impaired in several ways including limited delivery of drugs, cell death inhibition, drug inactivation, drug target alteration, EMT, the involvement of the TM or any combination of these factors. Therefore, combination therapy appear to be a reasonable solution to prevent drug resistance in many cancer types. Several novel ways have been suggested to overcome drugs resistance due to microenvironmental factors. Before treatment, administration of antiangiogenic therapy can help to remove extra capillaries and abnormal blood vessels leading to a reduction in the pressure of the interstitial fluid [239–242]. Other suggestions include damaging already existing blood vessels leading to solid tumor vessel permeability and increased drug delivery [184,243–245]. It should be recalled however that several strategies that target tumors inadvertently affect normal tissues as well.

Another effective way to improve drug penetration and efficacy is to inhibit sequestrations of drugs in cellular compartments such as endosomes [246–251]. Yet another strategy involve modifying the ECM to enable enhanced penetration of drugs into solid tumors [187,252–254]. Caution must be exercised however as ECM modification can promote cancer metastasis [255–258]. Modifying or degrading even part of the ECM might create a highway through which cancer cells can migrate to other tissues or organs [257,259–261].

The ABC transporters are an important mechanism for drug resistance. As mentioned above, ABC transporters play a role in protecting tissues from toxins but they also play a role in the uptake of drugs and delivery to their target molecules. As a result, targeting ABC transporters could be used in the treatment of cancer in future. Great interest has been shown towards the manufacture of anti-ABC drugs. Inhibitors against P glycoprotein may be considered to be the best treatment of cancer and prevention of MDR. Additionally, Chen et al. showed that activation protein kinase D isoform 2 (PKD2) is an important modulator of MDR and P-glycoprotein expression in paclitaxel-treated breast cancer cell lines [262]. The same study also demonstrated that shRNA knockdown of PDK2 in breast cancer cell lines resulted in significant decrease in resistance to anticancer agent paclitaxel [262]. These results suggest that inhibition of MDR and P-gp through the inactivation of PKD2 might be a potential strategy to overcome chemoresistance. However, due to the specificity of the anti-ABC drugs, each patient's ABC profile and expression levels will need to be determined before treatment using these drugs. The use of antibodies has been successful in increasing the efficacy of anticancer drugs and reducing growth factors which are overexpressed in breast cancer. The use of trastuzumab against the human epidermal growth factor receptor 2 (HER2), a protein involved in the development of breast cancer, was found to increase the efficacy of chemotherapy in metastatic breast cancer that overexpresses HER2 [263]. Another example is the monoclonal antibody cetuximab, which specifically blocks EGFR that is overexpressed in several cancers. Cetuximab is effective in patients who were resistant to treatment with fluorouracil and irinotecan in colorectal cancer [264].

Epithelial-to-mesenchymal transition (EMT) is one of the factors that contributes to chemoresistance and therefore future drug discovery targeting EMT should be considered [62]. Drugs targeting the TM are better potential strategies to overcome chemoresistance. More especially by targeting the hypoxic regions of tumors to improve drug delivery. Using combinational therapies targeting different stromal cells (such as MSCs, CAFs, ECM) found in the TM can enhance the efficacy of many antitumor agents. This can be achieved by understanding the mechanisms of cell-ECM interactions and using drugs that inhibit components involved in ECM remodeling. How chemotherapy affects the TM stromal components is only now becoming clear. Several strategies targeting stroma-initiated signaling are being explored to combat drug resistance. Very few studies, however, have focused on how stromal components respond to chemotherapy and how this contribute to chemoresistance. Recent studies have shown that stroma cells develop drug resistance in the same way as cancer cells, and that stromal cell-drug resistance is vital for cancer cell drug resistance.

Targeting the TM and stroma-initiated signaling might be effective ways of killing cancer cells if done in combination with conventional therapy. The protective effect provided by stromal cells to cancer cells can be blocked through selective inhibition of specific receptors.

Lastly, many in vitro models utilized during drug development do not recapitulate the in vivo tumor environment. Most drug development assays are done on 2D cancer cell monolayer cultures where cancer cells are fully exposed to chemotherapeutic reagents do not show drug resistance. Of late, several 3D models have been developed to study cancer cell behavior in vitro. Multicellular tumor spheroids are being used as in vitro tumors and novel information is being obtained. While 3D culture of cancer cells recapitulate the in vivo tumor environment better than 2D culture, cancer cell drug resistance in 3D culture is not only due to cellular changes. Drug distribution in 3D is affected by many other factors such as the presence of ECM components and soluble factors within the microenvironment milieu. The involvement of biomedical engineers in the development of 3D culture models is important since many of these models take into account ECM biophysical properties and controllability in designing the best model. Finally, to fully recapitulate the 3D setting it will be important to include a vascular component such as endothelial cells.

5. Conclusions

The future success of cancer therapy is dependent in part on the ability to identify and target mechanisms and pathways involved in chemotherapy resistance. Several targeted strategies including the use of monoclonal antibodies still require a proper understanding of chemoresistance before successful treatment is achieved. Strategies to inhibit processes such as EMT and the removal of supporting stromal cells and the ECM are some of the ways being envisaged to treat cancer in the future. Importantly, the role of the TM components in tumor development and metastasis is now under greater scrutiny. The efficacy of chemotherapy is impaired by reduced delivery of drugs to tumor cells leading to resistance of many anticancer agents. Drug inactivation, inhibition of apoptosis, EMT and the TM play an essential role in events leading to drug resistance and relapse. Tumor associated ECM also plays a role in chemoresistance by providing an environment that stimulates survival pathways. Unlike tumor cells, the components of the TM do not harbor genetic mutations. TM- or stromal directed therapies appear to be gaining ground as they can be used in combination with conventional therapies to control malignant progression. Unfortunately, as many studies have shown, several therapeutic targets identified in stromal cells are common to tumor cells as well, presenting a huge conundrum to scientists. Clinical trials targeting a dysregulated TM show some avenues that can be taken to engineer stromal cells to modulate conventional therapeutic efficacy. Therefore, multiple drugs targeting the TM and inhibiting tumor-stroma interactions may be important strategies to overcome chemoresistance and improve cancer treatment.

Acknowledgments: The funding for this research was provided by the National Research Foundation (NRF) of South Africa (Grant Number: 91457: RCA13101656402), International Centre for Genetic Engineering and Biotechnology (ICGEB) (Grant Number: 2015/0001), the South African Medical Research Council in terms of the MRC's Flagships Awards Project SAMRC-RFA-UFSP-01-2013/STEM CELLS, the SAMRC Extramural Unit for Stem Cell Research and Therapy Unit, the National Research Foundation and the Institute for Cellular and Molecular Medicine of the University of Pretoria and the University of Cape Town.

Author Contributions: Dimakatso Alice Senthebane and Kevin Dzobo performed all experiments and analyzed the data. Kevin Dzobo, Collet Dandara, Michael S. Pepper, and M. Iqbal Parker developed the experimental design. All authors proofread and corrected the manuscript. Dimakatso Alice Senthebane and Kevin Dzobo wrote the main body of the manuscript.

Conflicts of Interest: The authors declare no conflict of interest.

References

1. Lemoine, M.; Girard, P.M.; Thursz, M.; Raguin, G. In the shadow of hiv/aids: Forgotten diseases in sub-Saharan Africa: Global health issues and funding agency responsibilities. *J. Public Health Policy* **2012**, *33*, 430–438. [CrossRef] [PubMed]

2. Levitt, N.S.; Steyn, K.; Dave, J.; Bradshaw, D. Chronic noncommunicable diseases and hiv-aids on a collision course: Relevance for health care delivery, particularly in low-resource settings—Insights from South Africa. *Am. J. Clin. Nutr.* **2011**, *94*, 1690S–1696S. [CrossRef] [PubMed]
3. Lipson, E.J.; Sharfman, W.H.; Drake, C.G.; Wollner, I.; Taube, J.M.; Anders, R.A.; Xu, H.; Yao, S.; Pons, A.; Chen, L.; et al. Durable cancer regression off-treatment and effective reinduction therapy with an anti-pd-1 antibody. *Clin. Cancer Res.* **2013**, *19*, 462–468. [CrossRef] [PubMed]
4. Philips, G.K.; Atkins, M. Therapeutic uses of anti-pd-1 and anti-pd-l1 antibodies. *Int. Immunol.* **2015**, *27*, 39–46. [CrossRef] [PubMed]
5. Wilson, T.R.; Longley, D.B.; Johnston, P.G. Chemoresistance in solid tumours. *Ann. Oncol.* **2006**, *17*, x315–x324. [CrossRef] [PubMed]
6. Hanahan, D.; Weinberg, R.A. Hallmarks of cancer: The next generation. *Cell* **2011**, *144*, 646–674. [CrossRef] [PubMed]
7. You, Y.N.; Lakhani, V.T.; Wells, S.A. The role of prophylactic surgery in cancer prevention. *World J. Surg.* **2007**, *31*, 450–464. [CrossRef] [PubMed]
8. Luqmani, Y.A. Mechanisms of drug resistance in cancer chemotherapy. *Med. Princ. Pract. Int. J. Kuwait Univ. Health Sci. Cent.* **2005**, *14*, 35–48. [CrossRef] [PubMed]
9. Thomas, M.; Coyle, K.; Sultan, M.; Vaghar-Kashani, A.; Marcato, P. Chemoresistance in cancer stem cells and strategies to overcome resistance. *Chemotherapy* **2014**, *3*, 2.
10. Bilen, M.A.; Hess, K.R.; Campbell, M.T.; Wang, J.; Broaddus, R.R.; Karam, J.A.; Ward, J.F.; Wood, C.G.; Choi, S.L.; Rao, P.; et al. Intratumoral heterogeneity and chemoresistance in nonseminomatous germ cell tumor of the testis. *Oncotarget* **2016**, *7*, 86280–86289. [PubMed]
11. Brown, F.C.; Cifani, P.; Drill, E.; He, J.; Still, E.; Zhong, S.; Balasubramanian, S.; Pavlick, D.; Yilmazel, B.; Knapp, K.M.; et al. Genomics of primary chemoresistance and remission induction failure in paediatric and adult acute myeloid leukaemia. *Br. J. Haematol.* **2017**, *176*, 86–91. [CrossRef] [PubMed]
12. Fletcher, N.M.; Belotte, J.; Saed, M.G.; Memaj, I.; Diamond, M.P.; Morris, R.T.; Saed, G.M. Specific point mutations in key redox enzymes are associated with chemoresistance in epithelial ovarian cancer. *Free Radic. Biol. Med.* **2017**, *102*, 122–132. [CrossRef] [PubMed]
13. Guryanova, O.A.; Shank, K.; Spitzer, B.; Luciani, L.; Koche, R.P.; Garrett-Bakelman, F.E.; Ganzel, C.; Durham, B.H.; Mohanty, A.; Hoermann, G.; et al. DNMT3A mutations promote anthracycline resistance in acute myeloid leukemia via impaired nucleosome remodeling. *Nat. Med.* **2016**, *22*, 1488–1495. [CrossRef] [PubMed]
14. Hu, X.; Baytak, E.; Li, J.; Akman, B.; Okay, K.; Hu, G.; Scuto, A.; Zhang, W.; Kucuk, C. The relationship of rel proto-oncogene to pathobiology and chemoresistance in follicular and transformed follicular lymphoma. *Leuk. Res.* **2017**, *54*, 30–38. [CrossRef] [PubMed]
15. Janczar, S.; Janczar, K.; Pastorczak, A.; Harb, H.; Paige, A.J.; Zalewska-Szewczyk, B.; Danilewicz, M.; Mlynarski, W. The role of histone protein modifications and mutations in histone modifiers in pediatric b-cell progenitor acute lymphoblastic leukemia. *Cancers* **2017**, *9*, 2. [CrossRef] [PubMed]
16. Takada, M.; Nagai, S.; Haruta, M.; Sugino, R.P.; Tozuka, K.; Takei, H.; Ohkubo, F.; Inoue, K.; Kurosumi, M.; Miyazaki, M.; et al. BRCA1 alterations with additional defects in DNA damage response genes may confer chemoresistance to BRCA-like breast cancers treated with neoadjuvant chemotherapy. *Genes Chromosomes Cancer* **2017**, *56*, 405–420. [CrossRef] [PubMed]
17. Taylor-Weiner, A.; Zack, T.; O'Donnell, E.; Guerriero, J.L.; Bernard, B.; Reddy, A.; Han, G.C.; AlDubayan, S.; Amin-Mansour, A.; Schumacher, S.E.; et al. Genomic evolution and chemoresistance in germ-cell tumours. *Nature* **2016**, *540*, 114–118. [CrossRef] [PubMed]
18. Chan, R.; Sethi, P.; Jyoti, A.; McGarry, R.; Upreti, M. Investigating the radioresistant properties of lung cancer stem cells in the context of the tumor microenvironment. *Radiat. Res.* **2016**, *185*, 169–181. [CrossRef] [PubMed]
19. Conrad, C.A.; Fueyo, J.; Gomez-Manzano, C. Intratumoral heterogeneity and intraclonal plasticity: From warburg to oxygen and back again. *Neuro Oncol.* **2014**, *16*, 1025–1026. [CrossRef] [PubMed]
20. Gentric, G.; Mieulet, V.; Mechta-Grigoriou, F. Heterogeneity in cancer metabolism: New concepts in an old field. *Antioxid. Redox Signal.* **2016**, *26*, 462–485. [CrossRef] [PubMed]
21. Hida, K.; Maishi, N.; Torii, C.; Hida, Y. Tumor angiogenesis—Characteristics of tumor endothelial cells. *Int. J. Clin. Oncol.* **2016**, *21*, 206–212. [CrossRef] [PubMed]

22. Martin, J.D.; Fukumura, D.; Duda, D.G.; Boucher, Y.; Jain, R.K. Reengineering the tumor microenvironment to alleviate hypoxia and overcome cancer heterogeneity. *Cold Spring Harb. Perspect. Med.* **2016**, *6*, a027094. [CrossRef] [PubMed]
23. Mumenthaler, S.M.; Foo, J.; Choi, N.C.; Heise, N.; Leder, K.; Agus, D.B.; Pao, W.; Michor, F.; Mallick, P. The impact of microenvironmental heterogeneity on the evolution of drug resistance in cancer cells. *Cancer Inform.* **2015**, *14*, 19–31. [PubMed]
24. Pucciarelli, D.; Lengger, N.; Takacova, M.; Csaderova, L.; Bartosova, M.; Breiteneder, H.; Pastorekova, S.; Hafner, C. Hypoxia increases the heterogeneity of melanoma cell populations and affects the response to vemurafenib. *Mol. Med. Rep.* **2016**, *13*, 3281–3288. [CrossRef] [PubMed]
25. Guerra, L.; Odorisio, T.; Zambruno, G.; Castiglia, D. Stromal microenvironment in type VII collagen-deficient skin: The ground for squamous cell carcinoma development. *Matrix Biol. J. Int. Soc. Matrix Biol.* **2017**. [CrossRef] [PubMed]
26. Fuzer, A.M.; Lee, S.Y.; Mott, J.D.; Cominetti, M.R. [10]-Gingerol reverts malignant phenotype of breast cancer cells in 3d culture. *J. Cell. Biochem.* **2017**, *118*, 2693–2699. [CrossRef] [PubMed]
27. Tadeo, I.; Berbegall, A.P.; Navarro, S.; Castel, V.; Noguera, R. A stiff extracellular matrix is associated with malignancy in peripheral neuroblastic tumors. *Pediatr. Blood Cancer* **2017**. [CrossRef] [PubMed]
28. Affo, S.; Yu, L.; Schwabe, R.F. The role of cancer-associated fibroblasts and fibrosis in liver cancer. *Annu. Rev. Pathol.* **2017**, *24*, 153–186. [CrossRef] [PubMed]
29. Gjorevski, N.; Sachs, N.; Manfrin, A.; Giger, S.; Bragina, M.E.; Ordonez-Moran, P.; Clevers, H.; Lutolf, M.P. Designer matrices for intestinal stem cell and organoid culture. *Nature* **2016**, *539*, 560–564. [CrossRef] [PubMed]
30. Kopanska, K.S.; Alcheikh, Y.; Staneva, R.; Vignjevic, D.; Betz, T. Tensile forces originating from cancer spheroids facilitate tumor invasion. *PLoS ONE* **2016**, *11*, e0156442. [CrossRef] [PubMed]
31. McLane, J.S.; Ligon, L.A. Stiffened extracellular matrix and signaling from stromal fibroblasts via osteoprotegerin regulate tumor cell invasion in a 3-d tumor in situ model. *Cancer Microenviron.* **2016**, *9*, 127–139. [CrossRef] [PubMed]
32. Park, J.; Kim, D.H.; Kim, H.N.; Wang, C.J.; Kwak, M.K.; Hur, E.; Suh, K.Y.; An, S.S.; Levchenko, A. Directed migration of cancer cells guided by the graded texture of the underlying matrix. *Nat. Mater.* **2016**, *15*, 792–801. [CrossRef] [PubMed]
33. Romero-Lopez, M.; Trinh, A.L.; Sobrino, A.; Hatch, M.M.; Keating, M.T.; Fimbres, C.; Lewis, D.E.; Gershon, P.D.; Botvinick, E.L.; Digman, M.; et al. Recapitulating the human tumor microenvironment: Colon tumor-derived extracellular matrix promotes angiogenesis and tumor cell growth. *Biomaterials* **2017**, *116*, 118–129. [CrossRef] [PubMed]
34. Shin, J.W.; Mooney, D.J. Extracellular matrix stiffness causes systematic variations in proliferation and chemosensitivity in myeloid leukemias. *Proc. Natl. Acad. Sci. USA* **2016**, *113*, 12126–12131. [CrossRef] [PubMed]
35. Dave, B.; Gonzalez, D.D.; Liu, Z.B.; Li, X.; Wong, H.; Granados, S.; Ezzedine, N.E.; Sieglaff, D.H.; Ensor, J.E.; Miller, K.D.; et al. Role of RPL39 in metaplastic breast cancer. *J. Natl. Cancer Inst.* **2017**. [CrossRef] [PubMed]
36. Jahani, M.; Azadbakht, M.; Norooznezhad, F.; Mansouri, K. L-arginine alters the effect of 5-fluorouracil on breast cancer cells in favor of apoptosis. *Biomed. Pharmacother. Biomed. Pharmacother.* **2017**, *88*, 114–123. [CrossRef] [PubMed]
37. Spitschak, A.; Meier, C.; Kowtharapu, B.; Engelmann, D.; Putzer, B.M. MiR-182 promotes cancer invasion by linking ret oncogene activated NF-κB to loss of the hes1/notch1 regulatory circuit. *Mol. Cancer* **2017**, *16*, 24. [CrossRef] [PubMed]
38. Avnet, S.; Di Pompo, G.; Chano, T.; Errani, C.; Ibrahim-Hashim, A.; Gillies, R.J.; Donati, D.M.; Baldini, N. Cancer-associated mesenchymal stroma fosters the stemness of osteosarcoma cells in response to intratumoral acidosis via nf-kappab activation. *Int. J. Cancer* **2017**, *140*, 1331–1345. [CrossRef] [PubMed]
39. Cortini, M.; Massa, A.; Avnet, S.; Bonuccelli, G.; Baldini, N. Tumor-activated mesenchymal stromal cells promote osteosarcoma stemness and migratory potential via IL-6 secretion. *PLoS ONE* **2016**, *11*, e0166500. [CrossRef] [PubMed]
40. Cramer, G.M.; Jones, D.P.; El-Hamidi, H.; Celli, J.P. Ecm composition and rheology regulate growth, motility, and response to photodynamic therapy in 3d models of pancreatic ductal adenocarcinoma. *Mol. Cancer Res. MCR* **2017**, *15*, 15–25. [CrossRef] [PubMed]

41. Dauer, P.; Nomura, A.; Saluja, A.; Banerjee, S. Microenvironment in determining chemo-resistance in pancreatic cancer: Neighborhood matters. *Pancreatology* **2016**. [CrossRef] [PubMed]
42. Liu, Y.; Li, F.; Gao, F.; Xing, L.; Qin, P.; Liang, X.; Zhang, J.; Qiao, X.; Lin, L.; Zhao, Q.; et al. Periostin promotes the chemotherapy resistance to gemcitabine in pancreatic cancer. *Tumour Biol.* **2016**, *37*, 15283–15291. [CrossRef] [PubMed]
43. Majidinia, M.; Yousefi, B. Breast tumor stroma: A driving force in the development of resistance to therapies. *Chem. Biol. Drug Des.* **2017**, *89*, 309–318. [CrossRef] [PubMed]
44. Rao, C.V.; Janakiram, N.B.; Mohammed, A. Molecular pathways: Mucins and drug delivery in cancer. *Clin. Cancer Res.* **2017**, *23*, 1373–1378. [CrossRef] [PubMed]
45. Song, Y.; Kim, S.H.; Kim, K.M.; Choi, E.K.; Kim, J.; Seo, H.R. Activated hepatic stellate cells play pivotal roles in hepatocellular carcinoma cell chemoresistance and migration in multicellular tumor spheroids. *Sci. Rep.* **2016**, *6*, 36750. [CrossRef] [PubMed]
46. Zhang, H.; Xie, C.; Yue, J.; Jiang, Z.; Zhou, R.; Xie, R.; Wang, Y.; Wu, S. Cancer-associated fibroblasts mediated chemoresistance by a FOXO1/TGFβ1 signaling loop in esophageal squamous cell carcinoma. *Mol. Carcinog.* **2017**, *56*, 1150–1164. [CrossRef] [PubMed]
47. Afik, R.; Zigmond, E.; Vugman, M.; Klepfish, M.; Shimshoni, E.; Pasmanik-Chor, M.; Shenoy, A.; Bassat, E.; Halpern, Z.; Geiger, T.; et al. Tumor macrophages are pivotal constructors of tumor collagenous matrix. *J. Exp. Med.* **2016**, *213*, 2315–2331. [CrossRef] [PubMed]
48. Kaushik, S.; Pickup, M.W.; Weaver, V.M. From transformation to metastasis: Deconstructing the extracellular matrix in breast cancer. *Cancer Metastasis Rev.* **2016**, *35*, 655–667. [CrossRef] [PubMed]
49. Lim, E.J.; Suh, Y.; Yoo, K.C.; Lee, J.H.; Kim, I.G.; Kim, M.J.; Chang, J.H.; Kang, S.G.; Lee, S.J. Tumor-associated mesenchymal stem-like cells provide extracellular signaling cue for invasiveness of glioblastoma cells. *Oncotarget* **2017**, *8*, 1438–1448. [CrossRef] [PubMed]
50. Mellone, M.; Hanley, C.J.; Thirdborough, S.; Mellows, T.; Garcia, E.; Woo, J.; Tod, J.; Frampton, S.; Jenei, V.; Moutasim, K.A.; et al. Induction of fibroblast senescence generates a non-fibrogenic myofibroblast phenotype that differentially impacts on cancer prognosis. *Aging* **2016**, *9*, 114–132. [CrossRef] [PubMed]
51. Miroshnikova, Y.A.; Mouw, J.K.; Barnes, J.M.; Pickup, M.W.; Lakins, J.N.; Kim, Y.; Lobo, K.; Persson, A.I.; Reis, G.F.; McKnight, T.R.; et al. Tissue mechanics promote IDH1-dependent HIF1α-tenascin c feedback to regulate glioblastoma aggression. *Nat. Cell Biol.* **2016**, *18*, 1336–1345. [CrossRef] [PubMed]
52. Mongiat, M.; Andreuzzi, E.; Tarticchio, G.; Paulitti, A. Extracellular matrix, a hard player in angiogenesis. *Int. J. Mol. Sci.* **2016**, *17*, 1822. [CrossRef] [PubMed]
53. Suzuki, S.; Itakura, S.; Matsui, R.; Nakayama, K.; Nishi, T.; Nishimoto, A.; Hama, S.; Kogure, K. Tumor microenvironment-sensitive liposomes penetrate tumor tissue via attenuated interaction of the extracellular matrix and tumor cells and accompanying actin depolymerization. *Biomacromolecules* **2017**, *18*, 535–547. [CrossRef] [PubMed]
54. Affolter, A.; Hess, J. Preclinical models in head and neck tumors: Evaluation of cellular and molecular resistance mechanisms in the tumor microenvironment. *HNO* **2016**, *64*, 860–869. [CrossRef] [PubMed]
55. Eiro, N.; Fernandez-Gomez, J.; Sacristan, R.; Fernandez-Garcia, B.; Lobo, B.; Gonzalez-Suarez, J.; Quintas, A.; Escaf, S.; Vizoso, F.J. Stromal factors involved in human prostate cancer development, progression and castration resistance. *J. Cancer Res. Clin. Oncol.* **2017**, *143*, 351–359. [CrossRef] [PubMed]
56. Fujimura, T.; Kakizaki, A.; Furudate, S.; Kambayashi, Y.; Aiba, S. Tumor-associated macrophages in skin: How to treat their heterogeneity and plasticity. *J. Dermatol. Sci.* **2016**, *83*, 167–173. [CrossRef] [PubMed]
57. Mitrofanova, I.; Zavyalova, M.; Telegina, N.; Buldakov, M.; Riabov, V.; Cherdyntseva, N.; Kzhyshkowska, J. Tumor-associated macrophages in human breast cancer parenchyma negatively correlate with lymphatic metastasis after neoadjuvant chemotherapy. *Immunobiology* **2017**, *222*, 101–109. [CrossRef] [PubMed]
58. Parajuli, H.; Teh, M.T.; Abrahamsen, S.; Christoffersen, I.; Neppelberg, E.; Lybak, S.; Osman, T.; Johannessen, A.C.; Gullberg, D.; Skarstein, K.; et al. Integrin α11 is overexpressed by tumour stroma of head and neck squamous cell carcinoma and correlates positively with α smooth muscle actin expression. *J. Oral Pathol. Med.* **2017**, *46*, 267–275. [CrossRef] [PubMed]
59. Prime, S.S.; Cirillo, N.; Hassona, Y.; Lambert, D.W.; Paterson, I.C.; Mellone, M.; Thomas, G.J.; James, E.N.; Parkinson, E.K. Fibroblast activation and senescence in oral cancer. *J. Oral Pathol. Med.* **2017**, *46*, 82–88. [CrossRef] [PubMed]

60. Bissell, M.J.; Kenny, P.A.; Radisky, D.C. Microenvironmental regulators of tissue structure and function also regulate tumor induction and progression: The role of extracellular matrix and its degrading enzymes. *Cold Spring Harb. Symp. Quant. Biol.* **2005**, *70*, 343–356. [CrossRef] [PubMed]
61. Bizzarri, M.; Cucina, A.; Conti, F.; D'Anselmi, F. Beyond the oncogene paradigm: Understanding complexity in cancerogenesis. *Acta Biotheor.* **2008**, *56*, 173–196. [CrossRef] [PubMed]
62. Bizzarri, M.; Cucina, A.; Proietti, S. Tumor reversion: Mesenchymal-epithelial transition as a critical step in managing the tumor-microenvironment cross-talk. *Curr. Pharm. Des.* **2017**. [CrossRef]
63. Aihara, K.; Mukasa, A.; Nagae, G.; Nomura, M.; Yamamoto, S.; Ueda, H.; Tatsuno, K.; Shibahara, J.; Takahashi, M.; Momose, T.; et al. Genetic and epigenetic stability of oligodendrogliomas at recurrence. *Acta Neuropathol. Commun.* **2017**, *5*, 18. [CrossRef] [PubMed]
64. Antonucci, I.; Provenzano, M.; Sorino, L.; Rodrigues, M.; Palka, G.; Stuppia, L. A new case of "de novo" brca1 mutation in a patient with early-onset breast cancer. *Clin. Case Rep.* **2017**, *5*, 238–240. [CrossRef] [PubMed]
65. Cheema, P.K.; Raphael, S.; El-Maraghi, R.; Li, J.; McClure, R.; Zibdawi, L.; Chan, A.; Victor, J.C.; Dolley, A.; Dziarmaga, A. Rate of EGFR mutation testing for patients with nonsquamous non-small-cell lung cancer with implementation of reflex testing by pathologists. *Curr. Oncol.* **2017**, *24*, 16–22. [CrossRef] [PubMed]
66. Dolatkhah, R.; Somi, M.H.; Kermani, I.A.; Farassati, F.; Dastgiri, S. A novel kras gene mutation report in sporadic colorectal cancer, from northwest of Iran. *Clin. Case Rep.* **2017**, *5*, 338–341. [CrossRef] [PubMed]
67. Jiangdian, S.; Di, D.; Yanqi, H.; Yali, Z.; Zaiyi, L.; Jie, T. Association between tumor heterogeneity and progression-free survival in non-small cell lung cancer patients with EGFR mutations undergoing tyrosine kinase inhibitors therapy. In Proceedings of the 2016 IEEE 38th Annual International Conference of the Engineering in Medicine and Biology Society (EMBC), Orlando, FL, USA, 16–20 August 2016; pp. 1268–1271.
68. Mahalakshmi, R.; Husayn Ahmed, P.; Mahadevan, V. HDAC inhibitors show differential epigenetic regulation and cell survival strategies on p53 mutant colon cancer cells. *J. Biomol. Struct. Dyn.* **2017**. [CrossRef]
69. Tan, R.Y.; Walsh, M.; Howard, A.; Winship, I. Multiple cutaneous leiomyomas leading to discovery of novel splice mutation in the fumarate hydratase gene associated with HLRCC. *Australas. J. Dermatol.* **2017**. [CrossRef] [PubMed]
70. Walton, S.J.; Frayling, I.M.; Clark, S.K.; Latchford, A. Gastric tumours in FAP. *Fam. Cancer* **2017**, *16*, 363–369. [CrossRef] [PubMed]
71. Alderton, G.K. Tumour evolution: Epigenetic and genetic heterogeneity in metastasis. *Nat. Rev. Cancer* **2017**, *17*, 141. [CrossRef] [PubMed]
72. Brown, D.V.; Filiz, G.; Daniel, P.M.; Hollande, F.; Dworkin, S.; Amiridis, S.; Kountouri, N.; Ng, W.; Morokoff, A.P.; Mantamadiotis, T. Expression of cd133 and cd44 in glioblastoma stem cells correlates with cell proliferation, phenotype stability and intra-tumor heterogeneity. *PLoS ONE* **2017**, *12*, e0172791. [CrossRef] [PubMed]
73. Carmona-Fontaine, C.; Deforet, M.; Akkari, L.; Thompson, C.B.; Joyce, J.A.; Xavier, J.B. Metabolic origins of spatial organization in the tumor microenvironment. *Proc. Natl. Acad. Sci. USA* **2017**, *114*, 2934–2939. [CrossRef] [PubMed]
74. Lapa, C.; Schirbel, A.; Samnick, S.; Luckerath, K.; Kortum, K.M.; Knop, S.; Wester, H.J.; Buck, A.K.; Schreder, M. The gross picture: Intraindividual tumour heterogeneity in a patient with nonsecretory multiple myeloma. *Eur. J. Nucl. Med. Mol. Imaging* **2017**, *44*, 1097–1098. [CrossRef] [PubMed]
75. Mehta, R.S.; Song, M.; Nishihara, R.; Drew, D.A.; Wu, K.; Qian, Z.R.; Fung, T.T.; Hamada, T.; Masugi, Y.; da Silva, A.; et al. Dietary patterns and risk of colorectal cancer: Analysis by tumor location and molecular subtypes. *Gastroenterology* **2017**, *152*, 1944–1952. [CrossRef] [PubMed]
76. Yang, Z.; Sun, Y.; Xu, X.; Zhang, Y.; Zhang, J.; Xue, J.; Wang, M.; Yuan, H.; Hu, S.; Shi, W.; et al. The assessment of estrogen receptor status and its intratumoral heterogeneity in breast cancer patients by using 18 f-fluoroestradiol pet/ct. *Clin. Nucl. Med.* **2017**, *42*, 421–427. [CrossRef] [PubMed]
77. Zhai, W.; Lim, T.K.; Zhang, T.; Phang, S.T.; Tiang, Z.; Guan, P.; Ng, M.H.; Lim, J.Q.; Yao, F.; Li, Z.; et al. The spatial organization of intra-tumour heterogeneity and evolutionary trajectories of metastases in hepatocellular carcinoma. *Nat. Commun.* **2017**, *8*, 4565. [CrossRef] [PubMed]
78. Saunders, N.A.; Simpson, F.; Thompson, E.W.; Hill, M.M.; Endo-Munoz, L.; Leggatt, G.; Minchin, R.F.; Guminski, A. Role of intratumoural heterogeneity in cancer drug resistance: Molecular and clinical perspectives. *EMBO Mol. Med.* **2012**, *4*, 675–684. [CrossRef] [PubMed]

79. Gerlinger, M.; Horswell, S.; Larkin, J.; Rowan, A.J.; Salm, M.P.; Varela, I.; Fisher, R.; McGranahan, N.; Matthews, N.; Santos, C.R.; et al. Genomic architecture and evolution of clear cell renal cell carcinomas defined by multiregion sequencing. *Nat. Genet.* **2014**, *46*, 225–233. [CrossRef] [PubMed]
80. Burmakin, M.; van Wieringen, T.; Olsson, P.O.; Stuhr, L.; Ahgren, A.; Heldin, C.H.; Reed, R.K.; Rubin, K.; Hellberg, C. Imatinib increases oxygen delivery in extracellular matrix-rich but not in matrix-poor experimental carcinoma. *J. Transl. Med.* **2017**, *15*, 47. [CrossRef] [PubMed]
81. Gomez-Chou, S.; Swidnicka-Siergiejko, A.; Badi, N.; Chavez-Tomar, M.; Lesinski, G.B.; Bekaii-Saab, T.; Farren, M.R.; Mace, T.A.; Schmidt, C.; Liu, Y.; et al. Lipocalin-2 promotes pancreatic ductal adenocarcinoma by regulating inflammation in the tumor microenvironment. *Cancer Res.* **2017**, *77*, 2647–2660. [CrossRef] [PubMed]
82. Lee, J.S.; Yoo, J.E.; Kim, H.; Rhee, H.; Koh, M.J.; Nahm, J.H.; Choi, J.S.; Lee, K.H.; Park, Y.N. Tumor stroma with senescence-associated secretory phenotype in steatohepatitic hepatocellular carcinoma. *PLoS ONE* **2017**, *12*, e0171922. [CrossRef] [PubMed]
83. Nordby, Y.; Richardsen, E.; Rakaee, M.; Ness, N.; Donnem, T.; Patel, H.R.; Busund, L.T.; Bremnes, R.M.; Andersen, S. High expression of pdgfr-β in prostate cancer stroma is independently associated with clinical and biochemical prostate cancer recurrence. *Sci. Rep.* **2017**, *7*, 43378. [CrossRef] [PubMed]
84. Ramamonjisoa, N.; Ackerstaff, E. Characterization of the tumor microenvironment and tumor-stroma interaction by non-invasive preclinical imaging. *Front. Oncol.* **2017**, *7*, 3. [CrossRef] [PubMed]
85. Szebeni, G.J.; Vizler, C.; Kitajka, K.; Puskas, L.G. Inflammation and cancer: Extra- and intracellular determinants of tumor-associated macrophages as tumor promoters. *Mediat. Inflamm.* **2017**, *2017*, 9294018. [CrossRef] [PubMed]
86. Chang, A. Chemotherapy, chemoresistance and the changing treatment landscape for nsclc. *Lung Cancer* **2011**, *71*, 3–10. [CrossRef] [PubMed]
87. Zahreddine, H.; Borden, K.L. Mechanisms and insights into drug resistance in cancer. *Front. Pharmacol.* **2013**, *4*, 28. [CrossRef] [PubMed]
88. Tredan, O.; Galmarini, C.M.; Patel, K.; Tannock, I.F. Drug resistance and the solid tumor microenvironment. *J. Natl. Cancer Inst.* **2007**, *99*, 1441–1454. [CrossRef] [PubMed]
89. Acerbi, I.; Cassereau, L.; Dean, I.; Shi, Q.; Au, A.; Park, C.; Chen, Y.Y.; Liphardt, J.; Hwang, E.S.; Weaver, V.M. Human breast cancer invasion and aggression correlates with ECM stiffening and immune cell infiltration. *Integr. Biol.* **2015**, *7*, 1120–1134. [CrossRef] [PubMed]
90. Dzobo, K.; Vogelsang, M.; Thomford, N.E.; Dandara, C.; Kallmeyer, K.; Pepper, M.S.; Parker, M.I. Wharton's jelly-derived mesenchymal stromal cells and fibroblast-derived extracellular matrix synergistically activate apoptosis in a p21-dependent mechanism in whco1 and MDA MB 231 cancer cells in vitro. *Stem Cells Int.* **2016**, *2016*, 4842134. [CrossRef] [PubMed]
91. Kerbel, R.S.; Rak, J.; Kobayashi, H.; Man, M.S.; St Croix, B.; Graham, C.H. Multicellular resistance: A new paradigm to explain aspects of acquired drug resistance of solid tumors. *Cold Spring Harb. Symp. Quant. Biol.* **1994**, *59*, 661–672. [CrossRef] [PubMed]
92. Fodale, V.; Pierobon, M.; Liotta, L.; Petricoin, E. Mechanism of cell adaptation: When and how do cancer cells develop chemoresistance? *Cancer J.* **2011**, *17*, 89–95. [CrossRef] [PubMed]
93. Asimakopoulos, F.; Hope, C.; Johnson, M.G.; Pagenkopf, A.; Gromek, K.; Nagel, B. Extracellular matrix and the myeloid-in-myeloma compartment: Balancing tolerogenic and immunogenic inflammation in the myeloma niche. *J. Leukoc. Biol.* **2017**. [CrossRef] [PubMed]
94. Chen, B.; Dai, W.; He, B.; Zhang, H.; Wang, X.; Wang, Y.; Zhang, Q. Current multistage drug delivery systems based on the tumor microenvironment. *Theranostics* **2017**, *7*, 538–558. [CrossRef] [PubMed]
95. La Porta, C.A.; Zapperi, S. Complexity in cancer stem cells and tumor evolution: Toward precision medicine. *Semin. Cancer Biol.* **2017**. [CrossRef] [PubMed]
96. Nettersheim, D.; Schorle, H. The plasticity of germ cell cancers and its dependence on the cellular microenvironment. *J. Cell. Mol. Med.* **2017**. [CrossRef] [PubMed]
97. Yang, L.; Zhang, Y. Tumor-associated macrophages: From basic research to clinical application. *J. Hematol. Oncol.* **2017**, *10*, 58. [CrossRef] [PubMed]
98. Zhang, Y.S.; Duchamp, M.; Oklu, R.; Ellisen, L.W.; Langer, R.; Khademhosseini, A. Bioprinting the cancer microenvironment. *ACS Biomater. Sci. Eng.* **2016**, *2*, 1710–1721. [CrossRef] [PubMed]

99. Kabeer, M.H.; Loudon, W.G.; Dethlefs, B.A.; Li, Z.; Zhong, J.F.; Luo, J.J.; Vu, L.T.; Li, S.C. Tissue elasticity bridges cancer stem cells to the tumor microenvironment through micrornas: Implications for a "watch-and-wait" approach to cancer. *Curr. Stem Cell Res. Ther.* **2017**. [CrossRef] [PubMed]
100. Maturu, P.; Jones, D.; Ruteshouser, E.C.; Hu, Q.; Reynolds, J.M.; Hicks, J.; Putluri, N.; Ekmekcioglu, S.; Grimm, E.A.; Dong, C.; et al. Role of cyclooxygenase-2 pathway in creating an immunosuppressive microenvironment and in initiation and progression of wilms' tumor. *Neoplasia* **2017**, *19*, 237–249. [CrossRef] [PubMed]
101. Wang, G.Y.; Wood, C.N.; Dolorito, J.A.; Libove, E.; Epstein, E.H., Jr. Differing tumor-suppressor functions of arf and p53 in murine basal cell carcinoma initiation and progression. *Oncogene* **2017**, *36*, 3772–3780. [CrossRef] [PubMed]
102. Fuhrmann, A.; Banisadr, A.; Beri, P.; Tlsty, T.D.; Engler, A.J. Metastatic state of cancer cells may be indicated by adhesion strength. *Biophys. J.* **2017**, *112*, 736–745. [CrossRef] [PubMed]
103. Ring, K.L.; Yemelyanova, A.V.; Soliman, P.T.; Frumovitz, M.M.; Jazaeri, A.A. Potential immunotherapy targets in recurrent cervical cancer. *Gynecol. Oncol.* **2017**, *143*, 462–468. [CrossRef] [PubMed]
104. Dzobo, K.; Senthebane, D.A.; Rowe, A.; Thomford, N.E.; Mwapagha, L.M.; Al-Awwad, N.; Dandara, C.; Parker, M.I. Cancer stem cell hypothesis for therapeutic innovation in clinical oncology? Taking the root out, not chopping the leaf. *Omics* **2016**, *20*, 681–691. [CrossRef] [PubMed]
105. Castells, M.; Thibault, B.; Delord, J.-P.; Couderc, B. Implication of tumor microenvironment in chemoresistance: Tumor-associated stromal cells protect tumor cells from cell death. *Int. J. Mol. Sci.* **2012**, *13*, 9545–9571. [CrossRef] [PubMed]
106. Sung, S.Y.; Hsieh, C.L.; Wu, D.; Chung, L.W.; Johnstone, P.A. Tumor microenvironment promotes cancer progression, metastasis, and therapeutic resistance. *Curr. Probl. Cancer* **2007**, *31*, 36–100. [CrossRef] [PubMed]
107. Whatcott, C.J.; Han, H.; Posner, R.G.; Hostetter, G.; Von Hoff, D.D. Targeting the tumor microenvironment in cancer: Why hyaluronidase deserves a second look. *Cancer Discov.* **2011**, *1*, 291–296. [CrossRef] [PubMed]
108. Whiteside, T.L. The tumor microenvironment and its role in promoting tumor growth. *Oncogene* **2008**, *27*, 5904–5912. [CrossRef] [PubMed]
109. Ahmadzadeh, H.; Webster, M.R.; Behera, R.; Jimenez Valencia, A.M.; Wirtz, D.; Weeraratna, A.T.; Shenoy, V.B. Modeling the two-way feedback between contractility and matrix realignment reveals a nonlinear mode of cancer cell invasion. *Proc. Natl. Acad. Sci. USA* **2017**, *114*, E1617–E1626. [CrossRef] [PubMed]
110. Lee, S.; Han, H.; Koo, H.; Na, J.H.; Yoon, H.Y.; Lee, K.E.; Lee, H.; Kim, H.; Kwon, I.C.; Kim, K. Extracellular matrix remodeling in vivo for enhancing tumor-targeting efficiency of nanoparticle drug carriers using the pulsed high intensity focused ultrasound. *J. Control. Release* **2017**. [CrossRef] [PubMed]
111. Logun, M.T.; Bisel, N.S.; Tanasse, E.A.; Zhao, W.; Gunasekera, B.; Mao, L.; Karumbaiah, L. Glioma cell invasion is significantly enhanced in composite hydrogel matrices composed of chondroitin 4- and 4,6-sulfated glycosaminoglycans. *J. Mater. Chem. B* **2016**, *4*, 6052–6064. [CrossRef] [PubMed]
112. Maddaly, R.; Subramaniyan, A.; Balasubramanian, H. Cancer cytokines and the relevance of 3d cultures for studying those implicated in human cancers. *J. Cell. Biochem.* **2017**, *118*, 2544–2558. [CrossRef] [PubMed]
113. Pinto, M.L.; Rios, E.; Silva, A.C.; Neves, S.C.; Caires, H.R.; Pinto, A.T.; Duraes, C.; Carvalho, F.A.; Cardoso, A.P.; Santos, N.C.; et al. Decellularized human colorectal cancer matrices polarize macrophages towards an anti-inflammatory phenotype promoting cancer cell invasion via ccl18. *Biomaterials* **2017**, *124*, 211–224. [CrossRef] [PubMed]
114. Tourell, M.C.; Shokoohmand, A.; Landgraf, M.; Holzapfel, N.P.; Poh, P.S.; Loessner, D.; Momot, K.I. The distribution of the apparent diffusion coefficient as an indicator of the response to chemotherapeutics in ovarian tumour xenografts. *Sci. Rep.* **2017**, *7*, 42905. [CrossRef] [PubMed]
115. Binder, M.J.; McCoombe, S.; Williams, E.D.; McCulloch, D.R.; Ward, A.C. The extracellular matrix in cancer progression: Role of hyalectan proteoglycans and adamts enzymes. *Cancer Lett.* **2017**, *385*, 55–64. [CrossRef] [PubMed]
116. Di Marzo, L.; Desantis, V.; Solimando, A.G.; Ruggieri, S.; Annese, T.; Nico, B.; Fumarulo, R.; Vacca, A.; Frassanito, M.A. Microenvironment drug resistance in multiple myeloma: Emerging new players. *Oncotarget* **2016**, *7*, 60698–60711. [CrossRef] [PubMed]
117. Ribatti, D. Epithelial-mesenchymal transition in morphogenesis, cancer progression and angiogenesis. *Exp. Cell Res.* **2017**, *353*, 1–5. [CrossRef] [PubMed]

118. Riechelmann, R.; Grothey, A. Antiangiogenic therapy for refractory colorectal cancer: Current options and future strategies. *Ther. Adv. Med. Oncol.* **2017**, *9*, 106–126. [CrossRef] [PubMed]
119. Simone, V.; Brunetti, O.; Lupo, L.; Testini, M.; Maiorano, E.; Simone, M.; Longo, V.; Rolfo, C.; Peeters, M.; Scarpa, A.; et al. Targeting angiogenesis in biliary tract cancers: An open option. *Int. J. Mol. Sci.* **2017**, *18*, 418. [CrossRef] [PubMed]
120. Epshtein, M.; Korin, N. Shear targeted drug delivery to stenotic blood vessels. *J. Biomech.* **2017**, *50*, 217–221. [CrossRef] [PubMed]
121. Saber, M.M.; Bahrainian, S.; Dinarvand, R.; Atyabi, F. Targeted drug delivery of sunitinib malate to tumor blood vessels by crgd-chiotosan-gold nanoparticles. *Int. J. Pharm.* **2017**, *517*, 269–278. [CrossRef] [PubMed]
122. Wenes, M.; Shang, M.; Di Matteo, M.; Goveia, J.; Martin-Perez, R.; Serneels, J.; Prenen, H.; Ghesquiere, B.; Carmeliet, P.; Mazzone, M. Macrophage metabolism controls tumor blood vessel morphogenesis and metastasis. *Cell Metab.* **2016**, *24*, 701–715. [CrossRef] [PubMed]
123. Wong, P.P.; Bodrug, N.; Hodivala-Dilke, K.M. Exploring novel methods for modulating tumor blood vessels in cancer treatment. *Curr. Biol.* **2016**, *26*, R1161–R1166. [CrossRef] [PubMed]
124. Haldorsen, I.S.; Stefansson, I.; Gruner, R.; Husby, J.A.; Magnussen, I.J.; Werner, H.M.; Salvesen, O.O.; Bjorge, L.; Trovik, J.; Taxt, T.; et al. Increased microvascular proliferation is negatively correlated to tumour blood flow and is associated with unfavourable outcome in endometrial carcinomas. *Br. J. Cancer* **2014**, *110*, 107–114. [CrossRef] [PubMed]
125. Tsafnat, N.; Tsafnat, G.; Lambert, T.D. A three-dimensional fractal model of tumour vasculature. In Proceedings of the 26th Annual International Conference of the IEEE Engineering in Medicine and Biology Society, San Francisco, CA, USA, 1–5 September 2004; pp. 683–686.
126. Choi, S.H.; Park, J.Y. Regulation of the hypoxic tumor environment in hepatocellular carcinoma using RNA interference. *Cancer Cell Int.* **2017**, *17*, 3. [CrossRef] [PubMed]
127. Daniell, K.; Nucera, C. Effect of the micronutrient iodine in thyroid carcinoma angiogenesis. *Aging* **2016**, *8*, 3180–3184. [CrossRef] [PubMed]
128. Liu, Y.; Gao, F.; Song, W. Periostin contributes to arsenic trioxide resistance in hepatocellular carcinoma cells under hypoxia. *Biomed. Pharmacother.* **2017**, *88*, 342–348. [CrossRef] [PubMed]
129. Lu, Y.; Ji, N.; Wei, W.; Sun, W.; Gong, X.; Wang, X. Mir-142 modulates human pancreatic cancer proliferation and invasion by targeting hypoxia-inducible factor 1 (HIF-1α) in the tumor microenvironments. *Biol. Open* **2017**, *6*, 252–259. [CrossRef] [PubMed]
130. Semenza, G.L. Hypoxia-inducible factors: Coupling glucose metabolism and redox regulation with induction of the breast cancer stem cell phenotype. *EMBO J.* **2017**, *36*, 252–259. [CrossRef] [PubMed]
131. Tarrado-Castellarnau, M.; de Atauri, P.; Cascante, M. Oncogenic regulation of tumor metabolic reprogramming. *Oncotarget* **2016**, *7*, 62726–62753. [CrossRef] [PubMed]
132. Demaria, M.; O'Leary, M.N.; Chang, J.; Shao, L.; Liu, S.; Alimirah, F.; Koenig, K.; Le, C.; Mitin, N.; Deal, A.M.; et al. Cellular senescence promotes adverse effects of chemotherapy and cancer relapse. *Cancer Discov.* **2016**. [CrossRef] [PubMed]
133. Luna, J.I.; Grossenbacher, S.K.; Murphy, W.J.; Canter, R.J. Targeting cancer stem cells with natural killer cell immunotherapy. *Expert Opin. Biol. Ther.* **2016**. [CrossRef] [PubMed]
134. Pearl Mizrahi, S.; Gefen, O.; Simon, I.; Balaban, N.Q. Persistence to anti-cancer treatments in the stationary to proliferating transition. *Cell Cycle* **2016**, *15*, 3442–3453. [CrossRef] [PubMed]
135. Wu, X.; Wu, M.Y.; Jiang, M.; Zhi, Q.; Bian, X.; Xu, M.D.; Gong, F.R.; Hou, J.; Tao, M.; Shou, L.M.; et al. TNF-α sensitizes chemotherapy and radiotherapy against breast cancer cells. *Cancer Cell Int.* **2017**, *17*, 13. [CrossRef] [PubMed]
136. Dart, A. Tumour metabolism: Packed full of protein! *Nat. Rev. Cancer* **2017**, *17*, 77. [CrossRef] [PubMed]
137. Kremer, J.C.; Prudner, B.C.; Lange, S.E.; Bean, G.R.; Schultze, M.B.; Brashears, C.B.; Radyk, M.D.; Redlich, N.; Tzeng, S.C.; Kami, K.; et al. Arginine deprivation inhibits the warburg effect and upregulates glutamine anaplerosis and serine biosynthesis in ass1-deficient cancers. *Cell Rep.* **2017**, *18*, 991–1004. [CrossRef] [PubMed]
138. Schwartz, L.; Seyfried, T.; Alfarouk, K.O.; Da Veiga Moreira, J.; Fais, S. Out of warburg effect: An effective cancer treatment targeting the tumor specific metabolism and dysregulated ph. *Semin. Cancer Biol.* **2017**. [CrossRef] [PubMed]

139. Cui, L.; Tse, K.; Zahedi, P.; Harding, S.M.; Zafarana, G.; Jaffray, D.A.; Bristow, R.G.; Allen, C. Hypoxia and cellular localization influence the radiosensitizing effect of gold nanoparticles (aunps) in breast cancer cells. *Radiat. Res.* **2014**, *182*, 475–488. [CrossRef] [PubMed]
140. Michiels, C.; Tellier, C.; Feron, O. Cycling hypoxia: A key feature of the tumor microenvironment. *Biochim. Biophys. Acta* **2016**, *1866*, 76–86. [CrossRef] [PubMed]
141. Muller-Edenborn, K.; Leger, K.; Glaus Garzon, J.F.; Oertli, C.; Mirsaidi, A.; Richards, P.J.; Rehrauer, H.; Spielmann, P.; Hoogewijs, D.; Borsig, L.; et al. Hypoxia attenuates the proinflammatory response in colon cancer cells by regulating ikappab. *Oncotarget* **2015**, *6*, 20288–20301. [CrossRef] [PubMed]
142. Sun, Q.; Li, X. Targeting cyclic hypoxia to prevent malignant progression and therapeutic resistance of cancers. *Histol. Histopathol.* **2015**, *30*, 51–60. [PubMed]
143. Vaupel, P.; Mayer, A. Hypoxia in tumors: Pathogenesis-related classification, characterization of hypoxia subtypes, and associated biological and clinical implications. *Adv. Exp. Med. Biol.* **2014**, *812*, 19–24. [PubMed]
144. Vaupel, P.; Mayer, A. Tumor hypoxia: Causative mechanisms, microregional heterogeneities, and the role of tissue-based hypoxia markers. *Adv. Exp. Med. Biol.* **2016**, *923*, 77–86. [PubMed]
145. Zhang, C.; Cao, S.; Toole, B.P.; Xu, Y. Cancer may be a pathway to cell survival under persistent hypoxia and elevated ros: A model for solid-cancer initiation and early development. *Int. J. Cancer* **2015**, *136*, 2001–2011. [CrossRef] [PubMed]
146. Hu, Z.; Dong, N.; Lu, D.; Jiang, X.; Xu, J.; Wu, Z.; Zheng, D.; Wechsler, D.S. A positive feedback loop between ros and mxi1–0 promotes hypoxia-induced vegf expression in human hepatocellular carcinoma cells. *Cell. Signal.* **2017**, *31*, 79–86. [CrossRef] [PubMed]
147. Lu, Y.; Yu, S.S.; Zong, M.; Fan, S.S.; Lu, T.B.; Gong, R.H.; Sun, L.S.; Fan, L.Y. Glucose-6-phosphate isomerase (G6PI) mediates hypoxia-induced angiogenesis in rheumatoid arthritis. *Sci. Rep.* **2017**, *7*, 40274. [CrossRef] [PubMed]
148. Zhang, Y.; Xu, Y.; Ma, J.; Pang, X.; Dong, M. Adrenomedullin promotes angiogenesis in epithelial ovarian cancer through upregulating hypoxia-inducible factor-1α and vascular endothelial growth factor. *Sci. Rep.* **2017**, *7*, 40524. [CrossRef] [PubMed]
149. Da Silva, E.F.; Krause, G.C.; Lima, K.G.; Haute, G.V.; Pedrazza, L.; Mesquita, F.C.; Basso, B.S.; Velasquez, A.C.; Nunes, F.B.; de Oliveira, J.R. Rapamycin and fructose-1,6-bisphosphate reduce the HEPG2 cell proliferation via increase of free radicals and apoptosis. *Oncol. Rep.* **2016**, *36*, 2647–2652. [CrossRef] [PubMed]
150. Fong, C.W. Platinum based radiochemotherapies: Free radical mechanisms and radiotherapy sensitizers. *Free Radic. Biol. Med.* **2016**, *99*, 99–109. [CrossRef] [PubMed]
151. Guo, P.; Wang, S.; Liang, W.; Wang, W.; Wang, H.; Zhao, M.; Liu, X. Salvianolic acid b reverses multidrug resistance in HCT8/VCR human colorectal cancer cells by increasing ROS levels. *Mol. Med. Rep.* **2017**, *15*, 724–730. [PubMed]
152. Cao, Z.; Scandura, J.M.; Inghirami, G.G.; Shido, K.; Ding, B.S.; Rafii, S. Molecular checkpoint decisions made by subverted vascular niche transform indolent tumor cells into chemoresistant cancer stem cells. *Cancer Cell* **2017**, *31*, 110–126. [CrossRef] [PubMed]
153. Garcia-Mazas, C.; Csaba, N.; Garcia-Fuentes, M. Biomaterials to suppress cancer stem cells and disrupt their tumoral niche. *Int. J. Pharm.* **2017**, *523*, 490–505. [CrossRef] [PubMed]
154. Lee, G.; Hall, R.R., 3rd; Ahmed, A.U. Cancer stem cells: Cellular plasticity, niche, and its clinical relevance. *J. Stem Cell Res. Ther.* **2016**, *6*, 363. [CrossRef] [PubMed]
155. Oei, A.L.; Vriend, L.E.; Krawczyk, P.M.; Horsman, M.R.; Franken, N.A.; Crezee, J. Targeting therapy-resistant cancer stem cells by hyperthermia. *Int. J. Hyperth.* **2017**. [CrossRef] [PubMed]
156. Picco, N.; Gatenby, R.A.; Anderson, A.R. Stem cell plasticity and niche dynamics in cancer progression. *IEEE Trans. Biomed. Eng.* **2016**. [CrossRef] [PubMed]
157. Shahriyari, L.; Mahdipour Shirayeh, A. Modeling dynamics of mutants in heterogeneous stem cell niche. *Phys. Biol.* **2017**. [CrossRef] [PubMed]
158. Comerford, K.M.; Wallace, T.J.; Karhausen, J.; Louis, N.A.; Montalto, M.C.; Colgan, S.P. Hypoxia-inducible factor-1-dependent regulation of the multidrug resistance (mdr1) gene. *Cancer Res.* **2002**, *62*, 3387–3394. [PubMed]
159. Cowan, D.S.; Tannock, I.F. Factors that influence the penetration of methotrexate through solid tissue. *Int. J. Cancer* **2001**, *91*, 120–125. [CrossRef]

160. Mahoney, B.P.; Raghunand, N.; Baggett, B.; Gillies, R.J. Tumor acidity, ion trapping and chemotherapeutics. I. Acid pH affects the distribution of chemotherapeutic agents in vitro. *Biochem. Pharmacol.* **2003**, *66*, 1207–1218. [CrossRef]
161. Abulaiti, A.; Shintani, Y.; Funaki, S.; Nakagiri, T.; Inoue, M.; Sawabata, N.; Minami, M.; Okumura, M. Interaction between non-small-cell lung cancer cells and fibroblasts via enhancement of tgf-β signaling by il-6. *Lung Cancer* **2013**, *82*, 204–213. [CrossRef] [PubMed]
162. Mukaida, N.; Sasaki, S. Fibroblasts, an inconspicuous but essential player in colon cancer development and progression. *World J. Gastroenterol.* **2016**, *22*, 5301–5316. [CrossRef] [PubMed]
163. Wang, W.; Li, Q.; Yamada, T.; Matsumoto, K.; Matsumoto, I.; Oda, M.; Watanabe, G.; Kayano, Y.; Nishioka, Y.; Sone, S.; et al. Crosstalk to stromal fibroblasts induces resistance of lung cancer to epidermal growth factor receptor tyrosine kinase inhibitors. *Clin. Cancer Res.* **2009**, *15*, 6630–6638. [CrossRef] [PubMed]
164. De Veirman, K.; Rao, L.; De Bruyne, E.; Menu, E.; Van Valckenborgh, E.; Van Riet, I.; Frassanito, M.A.; Di Marzo, L.; Vacca, A.; Vanderkerken, K. Cancer associated fibroblasts and tumor growth: Focus on multiple myeloma. *Cancers* **2014**, *6*, 1363–1381. [CrossRef] [PubMed]
165. Matsuo, Y.; Ochi, N.; Sawai, H.; Yasuda, A.; Takahashi, H.; Funahashi, H.; Takeyama, H.; Tong, Z.; Guha, S. CXCL8/Il-8 and CXCL12/SDF-1α co-operatively promote invasiveness and angiogenesis in pancreatic cancer. *Int. J. Cancer. J. Int. Cancer* **2009**, *124*, 853–861. [CrossRef] [PubMed]
166. Park, J.E.; Lenter, M.C.; Zimmermann, R.N.; Garin-Chesa, P.; Old, L.J.; Rettig, W.J. Fibroblast activation protein, a dual specificity serine protease expressed in reactive human tumor stromal fibroblasts. *J. Biol. Chem.* **1999**, *274*, 36505–36512. [CrossRef] [PubMed]
167. Bharti, R.; Dey, G.; Mandal, M. Cancer development, chemoresistance, epithelial to mesenchymal transition and stem cells: A snapshot of il-6 mediated involvement. *Cancer Lett.* **2016**, *375*, 51–61. [CrossRef] [PubMed]
168. Conze, D.; Weiss, L.; Regen, P.S.; Bhushan, A.; Weaver, D.; Johnson, P.; Rincon, M. Autocrine production of interleukin 6 causes multidrug resistance in breast cancer cells. *Cancer Res.* **2001**, *61*, 8851–8858. [PubMed]
169. Sun, X.; Mao, Y.; Wang, J.; Zu, L.; Hao, M.; Cheng, G.; Qu, Q.; Cui, D.; Keller, E.T.; Chen, X.; et al. Il-6 secreted by cancer-associated fibroblasts induces tamoxifen resistance in luminal breast cancer. *Oncogene* **2014**. [CrossRef] [PubMed]
170. Houthuijzen, J.M.; Daenen, L.G.; Roodhart, J.M.; Voest, E.E. The role of mesenchymal stem cells in anti-cancer drug resistance and tumour progression. *Br. J. Cancer* **2012**, *106*, 1901–1906. [CrossRef] [PubMed]
171. Sun, Z.; Wang, S.; Zhao, R.C. The roles of mesenchymal stem cells in tumor inflammatory microenvironment. *J. Hematol. Oncol.* **2014**, *7*, 14. [CrossRef] [PubMed]
172. Roodhart, J.M.; Daenen, L.G.; Stigter, E.C.; Prins, H.J.; Gerrits, J.; Houthuijzen, J.M.; Gerritsen, M.G.; Schipper, H.S.; Backer, M.J.; van Amersfoort, M.; et al. Mesenchymal stem cells induce resistance to chemotherapy through the release of platinum-induced fatty acids. *Cancer Cell* **2011**, *20*, 370–383. [CrossRef] [PubMed]
173. Erdogan, B.; Webb, D.J. Cancer-associated fibroblasts modulate growth factor signaling and extracellular matrix remodeling to regulate tumor metastasis. *Biochem. Soc. Trans.* **2017**, *45*, 229–236. [CrossRef] [PubMed]
174. Gascard, P.; Tlsty, T.D. Carcinoma-associated fibroblasts: Orchestrating the composition of malignancy. *Genes Dev.* **2016**, *30*, 1002–1019. [CrossRef] [PubMed]
175. Kalaszczynska, I.; Ferdyn, K. Wharton's jelly derived mesenchymal stem cells: Future of regenerative medicine? Recent findings and clinical significance. *BioMed Res. Int.* **2015**, *2015*, 430847. [CrossRef] [PubMed]
176. Underwood, T.J.; Hayden, A.L.; Derouet, M.; Garcia, E.; Noble, F.; White, M.J.; Thirdborough, S.; Mead, A.; Clemons, N.; Mellone, M.; et al. Cancer-associated fibroblasts predict poor outcome and promote periostin-dependent invasion in oesophageal adenocarcinoma. *J. Pathol.* **2015**, *235*, 466–477. [CrossRef] [PubMed]
177. Chong, I.W.; Chang, M.Y.; Chang, H.C.; Yu, Y.P.; Sheu, C.C.; Tsai, J.R.; Hung, J.Y.; Chou, S.H.; Tsai, M.S.; Hwang, J.J.; et al. Great potential of a panel of multiple hMTH1, SPD, ITGA11 and COL11A1 markers for diagnosis of patients with non-small cell lung cancer. *Oncol. Rep.* **2006**, *16*, 981–988. [CrossRef] [PubMed]
178. Wu, Y.H.; Chang, T.H.; Huang, Y.F.; Huang, H.D.; Chou, C.Y. Col11a1 promotes tumor progression and predicts poor clinical outcome in ovarian cancer. *Oncogene* **2014**, *33*, 3432–3440. [CrossRef] [PubMed]
179. Lu, P.; Weaver, V.M.; Werb, Z. The extracellular matrix: A dynamic niche in cancer progression. *J. Cell Biol.* **2012**, *196*, 395–406. [CrossRef] [PubMed]

180. Page-McCaw, A.; Ewald, A.J.; Werb, Z. Matrix metalloproteinases and the regulation of tissue remodelling. *Nat. Rev. Mol. Cell Biol.* **2007**, *8*, 221–233. [CrossRef] [PubMed]
181. Cox, T.R.; Erler, J.T. Remodeling and homeostasis of the extracellular matrix: Implications for fibrotic diseases and cancer. *Dis. Models Mech.* **2011**, *4*, 165–178. [CrossRef] [PubMed]
182. Paszek, M.J.; Weaver, V.M. The tension mounts: Mechanics meets morphogenesis and malignancy. *J. Mammary Gland Biol. Neoplasia* **2004**, *9*, 325–342. [CrossRef] [PubMed]
183. Kass, L.; Erler, J.T.; Dembo, M.; Weaver, V.M. Mammary epithelial cell: Influence of extracellular matrix composition and organization during development and tumorigenesis. *Int. J. Biochem. Cell Biol.* **2007**, *39*, 1987–1994. [CrossRef] [PubMed]
184. Bordeleau, F.; Mason, B.N.; Lollis, E.M.; Mazzola, M.; Zanotelli, M.R.; Somasegar, S.; Califano, J.P.; Montague, C.; LaValley, D.J.; Huynh, J.; et al. Matrix stiffening promotes a tumor vasculature phenotype. *Proc. Natl. Acad. Sci. USA* **2017**, *114*, 492–497. [CrossRef] [PubMed]
185. Hui, L.; Zhang, J.; Ding, X.; Guo, X.; Jiang, X. Matrix stiffness regulates the proliferation, stemness and chemoresistance of laryngeal squamous cancer cells. *Int. J. Oncol.* **2017**, *50*, 1439–1447. [CrossRef] [PubMed]
186. Hoon, J.L.; Tan, M.H.; Koh, C.G. The regulation of cellular responses to mechanical cues by Rho GTPases. *Cells* **2016**, *5*, 17. [CrossRef] [PubMed]
187. Grantab, R.H.; Tannock, I.F. Penetration of anticancer drugs through tumour tissue as a function of cellular packing density and interstitial fluid pressure and its modification by bortezomib. *BMC Cancer* **2012**, *12*, 214. [CrossRef] [PubMed]
188. Harisi, R.; Jeney, A. Extracellular matrix as target for antitumor therapy. *OncoTargets Ther.* **2015**, *8*, 1387–1398.
189. Holle, A.W.; Young, J.L.; Spatz, J.P. In vitro cancer cell-ecm interactions inform in vivo cancer treatment. *Adv. Drug Deliv. Rev.* **2016**, *97*, 270–279. [CrossRef] [PubMed]
190. Mittal, V.; El Rayes, T.; Narula, N.; McGraw, T.E.; Altorki, N.K.; Barcellos-Hoff, M.H. The microenvironment of lung cancer and therapeutic implications. *Adv. Exp. Med. Biol.* **2016**, *890*, 75–110. [PubMed]
191. Nieponice, A.; McGrath, K.; Qureshi, I.; Beckman, E.J.; Luketich, J.D.; Gilbert, T.W.; Badylak, S.F. An extracellular matrix scaffold for esophageal stricture prevention after circumferential EMR. *Gastrointest. Endosc.* **2009**, *69*, 289–296. [CrossRef] [PubMed]
192. Barcus, C.E.; Holt, E.C.; Keely, P.J.; Eliceiri, K.W.; Schuler, L.A. Dense collagen-I matrices enhance pro-tumorigenic estrogen-prolactin crosstalk in MCF-7 and T47D breast cancer cells. *PLoS ONE* **2015**, *10*, e0116891. [CrossRef] [PubMed]
193. Barcus, C.E.; O'Leary, K.A.; Brockman, J.L.; Rugowski, D.E.; Liu, Y.; Garcia, N.; Yu, M.; Keely, P.J.; Eliceiri, K.W.; Schuler, L.A. Elevated collagen-I augments tumor progressive signals, intravasation and metastasis of prolactin-induced estrogen receptor α positive mammary tumor cells. *Breast Cancer Res.* **2017**, *19*, 9. [CrossRef] [PubMed]
194. Brechbuhl, H.M.; Finlay-Schultz, J.; Yamamoto, T.; Gillen, A.; Cittelly, D.M.; Tan, A.C.; Sams, S.B.; Pillai, M.; Elias, A.; Robinson, W.A.; et al. Fibroblast subtypes regulate responsiveness of luminal breast cancer to estrogen. *Clin. Cancer Res.* **2016**, *23*, 1710–1721. [CrossRef] [PubMed]
195. Cun, X.; Ruan, S.; Chen, J.; Zhang, L.; Li, J.; He, Q.; Gao, H. A dual strategy to improve the penetration and treatment of breast cancer by combining shrinking nanoparticles with collagen depletion by losartan. *Acta Biomater.* **2016**, *31*, 186–196. [CrossRef] [PubMed]
196. Mbeunkui, F.; Johann, D.J. Cancer and the tumor microenvironment: A review of an essential relationship. *Cancer Chemother. Pharmacol.* **2009**, *63*, 571–582. [CrossRef] [PubMed]
197. Levental, K.R.; Yu, H.; Kass, L.; Lakins, J.N.; Egeblad, M.; Erler, J.T.; Fong, S.F.; Csiszar, K.; Giaccia, A.; Weninger, W.; et al. Matrix crosslinking forces tumor progression by enhancing integrin signaling. *Cell* **2009**, *139*, 891–906. [CrossRef] [PubMed]
198. Villegas-Pineda, J.C.; Toledo-Leyva, A.; Osorio-Trujillo, J.C.; Hernandez-Ramirez, V.I.; Talamas-Rohana, P. The translational blocking of α5 and α6 integrin subunits affects migration and invasion, and increases sensitivity to carboplatin of SKOV-3 ovarian cancer cell line. *Exp. Cell Res.* **2017**, *351*, 127–134. [CrossRef] [PubMed]
199. Meenakshi Sundaram, D.N.; Kucharski, C.; Parmar, M.B.; Kc, R.B.; Uludag, H. Polymeric delivery of sirna against integrin-β1 (CD29) to reduce attachment and migration of breast cancer cells. *Macromol. Biosci.* **2017**. [CrossRef] [PubMed]

200. Gopal, S.; Veracini, L.; Grall, D.; Butori, C.; Schaub, S.; Audebert, S.; Camoin, L.; Baudelet, E.; Radwanska, A.; Beghelli-de la Forest Divonne, S.; et al. Fibronectin-guided migration of carcinoma collectives. *Nat. Commun.* **2017**, *8*, 14105. [CrossRef] [PubMed]
201. Gehler, S.; Compere, F.V.; Miller, A.M. Semaphorin 3a increases FAK phosphorylation at focal adhesions to modulate MDA-MB-231 cell migration and spreading on different substratum concentrations. *Int. J. Breast Cancer* **2017**, *2017*, 9619734. [CrossRef] [PubMed]
202. Morin, P.J. Drug resistance and the microenvironment: Nature and nurture. *Drug Resist. Updat.* **2003**, *6*, 169–172. [CrossRef]
203. Sato, N.; Kohi, S.; Hirata, K.; Goggins, M. Role of hyaluronan in pancreatic cancer biology and therapy: Once again in the spotlight. *Cancer Sci.* **2016**, *107*, 569–575. [CrossRef] [PubMed]
204. Armstrong, T.; Packham, G.; Murphy, L.B.; Bateman, A.C.; Conti, J.A.; Fine, D.R.; Johnson, C.D.; Benyon, R.C.; Iredale, J.P. Type I collagen promotes the malignant phenotype of pancreatic ductal adenocarcinoma. *Clin. Cancer Res.* **2004**, *10*, 7427–7437. [CrossRef] [PubMed]
205. Sethi, T.; Rintoul, R.C.; Moore, S.M.; MacKinnon, A.C.; Salter, D.; Choo, C.; Chilvers, E.R.; Dransfield, I.; Donnelly, S.C.; Strieter, R.; et al. Extracellular matrix proteins protect small cell lung cancer cells against apoptosis: A mechanism for small cell lung cancer growth and drug resistance in vivo. *Nat. Med.* **1999**, *5*, 662–668. [CrossRef] [PubMed]
206. Januchowski, R.; Swierczewska, M.; Sterzynska, K.; Wojtowicz, K.; Nowicki, M.; Zabel, M. Increased expression of several collagen genes is associated with drug resistance in ovarian cancer cell lines. *J. Cancer* **2016**, *7*, 1295–1310. [CrossRef] [PubMed]
207. Chauhan, V.P.; Stylianopoulos, T.; Boucher, Y.; Jain, R.K. Delivery of molecular and nanoscale medicine to tumors: Transport barriers and strategies. *Annu. Rev. Chem. Biomol. Eng.* **2011**, *2*, 281–298. [CrossRef] [PubMed]
208. Jain, R.K. Transport of molecules in the tumor interstitium: A review. *Cancer Res.* **1987**, *47*, 3039–3051. [PubMed]
209. St Croix, B.; Kerbel, R.S. Cell adhesion and drug resistance in cancer. *Curr. Opin. Oncol.* **1997**, *9*, 549–556. [CrossRef] [PubMed]
210. Iseri, O.D.; Kars, M.D.; Arpaci, F.; Gunduz, U. Gene expression analysis of drug-resistant MCF-7 cells: Implications for relation to extracellular matrix proteins. *Cancer Chemother. Pharmacol.* **2010**, *65*, 447–455. [CrossRef] [PubMed]
211. Netti, P.A.; Berk, D.A.; Swartz, M.A.; Grodzinsky, A.J.; Jain, R.K. Role of extracellular matrix assembly in interstitial transport in solid tumors. *Cancer Res.* **2000**, *60*, 2497–2503. [PubMed]
212. Berchtold, S.; Grunwald, B.; Kruger, A.; Reithmeier, A.; Hahl, T.; Cheng, T.; Feuchtinger, A.; Born, D.; Erkan, M.; Kleeff, J.; et al. Collagen type V promotes the malignant phenotype of pancreatic ductal adenocarcinoma. *Cancer Lett.* **2015**, *356*, 721–732. [CrossRef] [PubMed]
213. Shields, M.A.; Dangi-Garimella, S.; Redig, A.J.; Munshi, H.G. Biochemical role of the collagen-rich tumour microenvironment in pancreatic cancer progression. *Biochem. J.* **2012**, *441*, 541–552. [CrossRef] [PubMed]
214. Provenzano, P.P.; Eliceiri, K.W.; Campbell, J.M.; Inman, D.R.; White, J.G.; Keely, P.J. Collagen reorganization at the tumor-stromal interface facilitates local invasion. *BMC Med.* **2006**, *4*, 38. [CrossRef] [PubMed]
215. Tavazoie, S.F.; Alarcon, C.; Oskarsson, T.; Padua, D.; Wang, Q.; Bos, P.D.; Gerald, W.L.; Massague, J. Endogenous human microrna that suppress breast cancer metastasis. *Nature* **2008**, *451*, 147–152. [CrossRef] [PubMed]
216. Sahai, V.; Dangi-Garimella, S.; Ebine, K.; Kumar, K.; Munshi, H.G. Promotion of gemcitabine resistance in pancreatic cancer cells by three-dimensional collagen I through HMGA2-dependent histone acetyltransferase expression. *J. Clin. Oncol.* **2013**, *31*, 172. [CrossRef]
217. Li, J.; Wood, W.H., 3rd; Becker, K.G.; Weeraratna, A.T.; Morin, P.J. Gene expression response to cisplatin treatment in drug-sensitive and drug-resistant ovarian cancer cells. *Oncogene* **2007**, *26*, 2860–2872. [CrossRef] [PubMed]
218. Teng, P.N.; Wang, G.; Hood, B.L.; Conrads, K.A.; Hamilton, C.A.; Maxwell, G.L.; Darcy, K.M.; Conrads, T.P. Identification of candidate circulating cisplatin-resistant biomarkers from epithelial ovarian carcinoma cell secretomes. *Br. J. Cancer* **2014**, *110*, 123–132. [CrossRef] [PubMed]

219. Wu, Y.H.; Chang, T.H.; Huang, Y.F.; Chen, C.C.; Chou, C.Y. Col11a1 confers chemoresistance on ovarian cancer cells through the activation of Akt/c/EBPβ pathway and PDK1 stabilization. *Oncotarget* **2015**, *6*, 23748–23763. [CrossRef] [PubMed]
220. Januchowski, R.; Zawierucha, P.; Ruciński, M.; Nowicki, M.; Zabel, M. Extracellular matrix proteins expression profiling in chemoresistant variants of the A2780 ovarian cancer cell line. *BioMed Res. Int.* **2014**, *2014*, 365867. [CrossRef] [PubMed]
221. Timpl, R.; Rohde, H.; Robey, P.G.; Rennard, S.I.; Foidart, J.M.; Martin, G.R. Laminin—A glycoprotein from basement membranes. *J. Biol. Chem.* **1979**, *254*, 9933–9937. [PubMed]
222. Fukazawa, S.; Shinto, E.; Tsuda, H.; Ueno, H.; Shikina, A.; Kajiwara, Y.; Yamamoto, J.; Hase, K. Laminin β3 expression as a prognostic factor and a predictive marker of chemoresistance in colorectal cancer. *Jpn. J. Clin. Oncol.* **2015**, *45*, 533–540. [PubMed]
223. Govaere, O.; Wouters, J.; Petz, M.; Vandewynckel, Y.P.; van den Eynde, K.; van den Broeck, A.; Verhulst, S.; Dolle, L.; Gremeaux, L.; Ceulemans, A.; et al. Laminin-332 sustains chemoresistance and quiescence as part of the human hepatic cancer stem cell niche. *J. Hepatol.* **2016**, *64*, 609–617. [CrossRef] [PubMed]
224. Giannelli, G.; Azzariti, A.; Fransvea, E.; Porcelli, L.; Antonaci, S.; Paradiso, A. Laminin-5 offsets the efficacy of gefitinib ('iressa') in hepatocellular carcinoma cells. *Br. J. Cancer* **2004**, *91*, 1964–1969. [CrossRef] [PubMed]
225. Tsurutani, J.; West, K.A.; Sayyah, J.; Gills, J.J.; Dennis, P.A. Inhibition of the phosphatidylinositol 3-kinase/Akt/mammalian target of rapamycin pathway but not the MEK/ERK pathway attenuates laminin-mediated small cell lung cancer cellular survival and resistance to imatinib mesylate or chemotherapy. *Cancer Res.* **2005**, *65*, 8423–8432. [CrossRef] [PubMed]
226. Huanwen, W.; Zhiyong, L.; Xiaohua, S.; Xinyu, R.; Kai, W.; Tonghua, L. Intrinsic chemoresistance to gemcitabine is associated with constitutive and laminin-induced phosphorylation of FAK in pancreatic cancer cell lines. *Mol. Cancer* **2009**, *8*, 125. [CrossRef] [PubMed]
227. Pankov, R.; Yamada, K.M. Fibronectin at a glance. *J. Cell Sci.* **2002**, *115*, 3861–3863. [CrossRef] [PubMed]
228. Rintoul, R.C.; Sethi, T. Extracellular matrix regulation of drug resistance in small-cell lung cancer. *Clin. Sci.* **2002**, *102*, 417–424. [CrossRef] [PubMed]
229. Kosmehl, H.; Berndt, A.; Strassburger, S.; Borsi, L.; Rousselle, P.; Mandel, U.; Hyckel, P.; Zardi, L.; Katenkamp, D. Distribution of laminin and fibronectin isoforms in oral mucosa and oral squamous cell carcinoma. *Br. J. Cancer* **1999**, *81*, 1071–1079. [CrossRef] [PubMed]
230. Han, S.; Sidell, N.; Roser-Page, S.; Roman, J. Fibronectin stimulates human lung carcinoma cell growth by inducing cyclooxygenase-2 (COX-2) expression. *Int. J. Cancer* **2004**, *111*, 322–331. [CrossRef] [PubMed]
231. Han, S.; Sidell, N.; Roman, J. Fibronectin stimulates human lung carcinoma cell proliferation by suppressing p21 gene expression via signals involving Erk and rho kinase. *Cancer Lett.* **2005**, *219*, 71–81. [CrossRef] [PubMed]
232. Xing, H.; Weng, D.; Chen, G.; Tao, W.; Zhu, T.; Yang, X.; Meng, L.; Wang, S.; Lu, Y.; Ma, D. Activation of fibronectin/PI-3K/Akt2 leads to chemoresistance to docetaxel by regulating survivin protein expression in ovarian and breast cancer cells. *Cancer Lett.* **2008**, *261*, 108–119. [CrossRef] [PubMed]
233. Horiuchi, K.; Amizuka, N.; Takeshita, S.; Takamatsu, H.; Katsuura, M.; Ozawa, H.; Toyama, Y.; Bonewald, L.F.; Kudo, A. Identification and characterization of a novel protein, periostin, with restricted expression to periosteum and periodontal ligament and increased expression by transforming growth factor β. *J. Bone Miner. Res.* **1999**, *14*, 1239–1249. [CrossRef] [PubMed]
234. Moniuszko, T.; Wincewicz, A.; Koda, M.; Domysławska, I.; Sulkowski, S. Role of periostin in esophageal, gastric and colon cancer. *Oncol. Lett.* **2016**, *12*, 783–787. [CrossRef] [PubMed]
235. Gillan, L.; Matei, D.; Fishman, D.A.; Gerbin, C.S.; Karlan, B.Y.; Chang, D.D. Periostin secreted by epithelial ovarian carcinoma is a ligand for α(v)β(3) and α(v)β(5) integrins and promotes cell motility. *Cancer Res.* **2002**, *62*, 5358–5364. [PubMed]
236. Zhu, M.; Fejzo, M.S.; Anderson, L.; Dering, J.; Ginther, C.; Ramos, L.; Gasson, J.C.; Karlan, B.Y.; Slamon, D.J. Periostin promotes ovarian cancer angiogenesis and metastasis. *Gynecol. Oncol.* **2010**, *119*, 337–344. [CrossRef] [PubMed]
237. Tumbarello, D.A.; Temple, J.; Brenton, J.D. β3 integrin modulates transforming growth factor β induced (TGFBI) function and paclitaxel response in ovarian cancer cells. *Mol. Cancer* **2012**, *11*, 36. [CrossRef] [PubMed]

238. Sung, P.-L.; Jan, Y.-H.; Lin, S.-C.; Huang, C.-C.; Lin, H.; Wen, K.-C.; Chao, K.-C.; Lai, C.-R.; Wang, P.-H.; Chuang, C.-M.; et al. Periostin in tumor microenvironment is associated with poor prognosis and platinum resistance in epithelial ovarian carcinoma. *Oncotarget* **2016**, *7*, 4036–4047. [PubMed]
239. Abdel-Qadir, H.; Ethier, J.L.; Lee, D.S.; Thavendiranathan, P.; Amir, E. Cardiovascular toxicity of angiogenesis inhibitors in treatment of malignancy: A systematic review and meta-analysis. *Cancer Treat. Rev.* **2016**, *53*, 120–127. [CrossRef] [PubMed]
240. Cantelmo, A.R.; Pircher, A.; Kalucka, J.; Carmeliet, P. Vessel pruning or healing: Endothelial metabolism as a novel target? *Expert Opin. Ther. Targets* **2017**, *21*, 239–247. [CrossRef] [PubMed]
241. Chen, L.T.; Oh, D.Y.; Ryu, M.H.; Yeh, K.H.; Yeo, W.; Carlesi, R.; Cheng, R.; Kim, J.; Orlando, M.; Kang, Y.K. Anti-angiogenic therapy in patients with advanced gastric and gastroesophageal junction cancer: A systematic review. *Cancer Res. Treat.* **2017**. [CrossRef] [PubMed]
242. Torok, S.; Rezeli, M.; Kelemen, O.; Vegvari, A.; Watanabe, K.; Sugihara, Y.; Tisza, A.; Marton, T.; Kovacs, I.; Tovari, J.; et al. Limited tumor tissue drug penetration contributes to primary resistance against angiogenesis inhibitors. *Theranostics* **2017**, *7*, 400–412. [CrossRef] [PubMed]
243. Ikeda, Y.; Hisano, H.; Nishikawa, Y.; Nagasaki, Y. Targeting and treatment of tumor hypoxia by newly designed prodrug possessing high permeability in solid tumors. *Mol. Pharm.* **2016**, *13*, 2283–2289. [CrossRef] [PubMed]
244. Lee, K.Y.; Lee, G.Y.; Lane, L.A.; Li, B.; Wang, J.; Lu, Q.; Wang, Y.; Nie, S. Functionalized, long-circulating, and ultrasmall gold nanocarriers for overcoming the barriers of low nanoparticle delivery efficiency and poor tumor penetration. *Bioconjug. Chem.* **2017**, *28*, 244–252. [CrossRef] [PubMed]
245. Zhang, K.; Li, P.; He, Y.; Bo, X.; Li, X.; Li, D.; Chen, H.; Xu, H. Synergistic retention strategy of RGD active targeting and radiofrequency-enhanced permeability for intensified RF & chemotherapy synergistic tumor treatment. *Biomaterials* **2016**, *99*, 34–46. [PubMed]
246. Jin, J.; Pastrello, D.; Penning, N.A.; Jones, A.T. Clustering of endocytic organelles in parental and drug-resistant myeloid leukaemia cell lines lacking centrosomally organised microtubule arrays. *Int. J. Biochem. Cell Biol.* **2008**, *40*, 2240–2252. [CrossRef] [PubMed]
247. Kitatani, K.; Idkowiak-Baldys, J.; Hannun, Y.A. Mechanism of inhibition of sequestration of protein kinase C α/βII by ceramide. Roles of ceramide-activated protein phosphatases and phosphorylation/dephosphorylation of protein kinase C α/βII on threonine 638/641. *J. Biol. Chem.* **2007**, *282*, 20647–20656. [CrossRef] [PubMed]
248. Lee, C.M.; Tannock, I.F. Inhibition of endosomal sequestration of basic anticancer drugs: Influence on cytotoxicity and tissue penetration. *Br. J. Cancer* **2006**, *94*, 863–869. [CrossRef] [PubMed]
249. Seebacher, N.A.; Lane, D.J.; Jansson, P.J.; Richardson, D.R. Glucose modulation induces lysosome formation and increases lysosomotropic drug sequestration via the p-glycoprotein drug transporter. *J. Biol. Chem.* **2016**, *291*, 3796–3820. [CrossRef] [PubMed]
250. Williams, M.; Catchpoole, D. Sequestration of AS-DACA into acidic compartments of the membrane trafficking system as a mechanism of drug resistance in rhabdomyosarcoma. *Int. J. Mol. Sci.* **2013**, *14*, 13042–13062. [CrossRef] [PubMed]
251. Zhao, H.; Vaananen, H.K. Pharmacological sequestration of intracellular cholesterol in late endosomes disrupts ruffled border formation in osteoclasts. *J. Bone Miner. Res.* **2006**, *21*, 456–465. [CrossRef] [PubMed]
252. Parodi, A.; Haddix, S.G.; Taghipour, N.; Scaria, S.; Taraballi, F.; Cevenini, A.; Yazdi, I.K.; Corbo, C.; Palomba, R.; Khaled, S.Z.; et al. Bromelain surface modification increases the diffusion of silica nanoparticles in the tumor extracellular matrix. *ACS Nano* **2014**, *8*, 9874–9883. [CrossRef] [PubMed]
253. Zhang, B.; Shen, S.; Liao, Z.; Shi, W.; Wang, Y.; Zhao, J.; Hu, Y.; Yang, J.; Chen, J.; Mei, H.; et al. Targeting fibronectins of glioma extracellular matrix by CLT1 peptide-conjugated nanoparticles. *Biomaterials* **2014**, *35*, 4088–4098. [CrossRef] [PubMed]
254. Zhou, H.; Fan, Z.; Deng, J.; Lemons, P.K.; Arhontoulis, D.C.; Bowne, W.B.; Cheng, H. Hyaluronidase embedded in nanocarrier peg shell for enhanced tumor penetration and highly efficient antitumor efficacy. *Nano Lett.* **2016**, *16*, 3268–3277. [CrossRef]
255. Fink, K.; Boratynski, J. The role of metalloproteinases in modification of extracellular matrix in invasive tumor growth, metastasis and angiogenesis. *Postepy Hig. Med. Dosw.* **2012**, *66*, 609–628. [CrossRef]
256. Kotula, E.; Berthault, N.; Agrario, C.; Lienafa, M.C.; Simon, A.; Dingli, F.; Loew, D.; Sibut, V.; Saule, S.; Dutreix, M. DNA-PKcs plays role in cancer metastasis through regulation of secreted proteins involved in migration and invasion. *Cell Cycle* **2015**, *14*, 1961–1972. [CrossRef]

257. Ortiz, R.; Diaz, J.; Diaz, N.; Lobos-Gonzalez, L.; Cardenas, A.; Contreras, P.; Diaz, M.I.; Otte, E.; Cooper-White, J.; Torres, V.; et al. Extracellular matrix-specific caveolin-1 phosphorylation on tyrosine 14 is linked to augmented melanoma metastasis but not tumorigenesis. *Oncotarget* **2016**, *7*, 40571–40593. [CrossRef]
258. Rucci, N.; Sanita, P.; Angelucci, A. Roles of metalloproteases in metastatic niche. *Curr. Mol. Med.* **2011**, *11*, 609–622. [CrossRef] [PubMed]
259. Chen, Y.; Guo, H.; Terajima, M.; Banerjee, P.; Liu, X.; Yu, J.; Momin, A.A.; Katayama, H.; Hanash, S.M.; Burns, A.R.; et al. Lysyl hydroxylase 2 is secreted by tumor cells and can modify collagen in the extracellular space. *J. Biol. Chem.* **2016**, *291*, 25799–25808. [CrossRef] [PubMed]
260. Nielsen, M.F.; Mortensen, M.B.; Detlefsen, S. Key players in pancreatic cancer-stroma interaction: Cancer-associated fibroblasts, endothelial and inflammatory cells. *World J. Gastroenterol.* **2016**, *22*, 2678–2700. [CrossRef]
261. Spicer, G.L.; Azarin, S.M.; Yi, J.; Young, S.T.; Ellis, R.; Bauer, G.M.; Shea, L.D.; Backman, V. Detection of extracellular matrix modification in cancer models with inverse spectroscopic optical coherence tomography. *Phys. Med. Biol.* **2016**, *61*, 6892–6904. [CrossRef] [PubMed]
262. Chen, J.; Lu, L.; Feng, Y.; Wang, H.; Dai, L.; Li, Y.; Zhang, P. PKD2 mediates multi-drug resistance in breast cancer cells through modulation of P-glycoprotein expression. *Cancer Lett.* **2011**, *300*, 48–56. [CrossRef]
263. Slamon, D.J.; Leyland-Jones, B.; Shak, S.; Fuchs, H.; Paton, V.; Bajamonde, A.; Fleming, T.; Eiermann, W.; Wolter, J.; Pegram, M.; et al. Use of chemotherapy plus a monoclonal antibody against HER2 for metastatic breast cancer that overexpresses HER2. *N. Engl. J. Med.* **2001**, *344*, 783–792. [CrossRef] [PubMed]
264. Cunningham, D.; Humblet, Y.; Siena, S.; Khayat, D.; Bleiberg, H.; Santoro, A.; Bets, D.; Mueser, M.; Harstrick, A.; Verslype, C.; et al. Cetuximab monotherapy and cetuximab plus irinotecan in irinotecan-refractory metastatic colorectal cancer. *N. Engl. J. Med.* **2004**, *351*, 337–345. [CrossRef] [PubMed]